DECIPHERING THE ROLE OF MESENCHYMAL STEM CELLS (MSCS) IN CUTANEOUS WOUND HEALING

Moyassar Basil Hadi Al-Shaibani (M.Sc.)

Submitted in partial fulfilment of the requirements for the degree of Doctor of Philosophy

Haematological Sciences

Institute of Cellular Medicine

The Faculty of Medical Sciences

University of Newcastle upon Tyne

October, 2018

ABSTRACT

MSCs (N=9) were isolated from the bone marrow of patients who had received hip replacement therapy. MSC-serum free conditioned media (MSC-CM) were collected at different time points during MSC passage and analysed for protein content using enzyme linked immunosorbent assay (ELISA). The effect of MSC-CM was tested on migration and proliferation of human skin cells (HaCat cell line, primary fibroblast and primary keratinocytes) (N=4) using a 2D scratch assay and tetrazolium salt proliferation assay respectively. For primary keratinocyte experiments, MSC-CM were collected in keratinocyte growth media containing low calcium levels (0.04 mM/L) (LC-CM). The effect of LC-CM was tested on migration and proliferation of primary keratinocytes during different testing conditions; normoxia (N=4), hypoxia (N=4), blocking of stromal derived factor-1α (SDF-1α) (N=4) and inhibition of proliferation (N=4). MSCs were tested for their ability to differentiate into epidermal like cells (ELCs) using both 2D and 3D cultures. A human 3D skin model was developed for wound healing and micro RNA profiling studies. All MSCs met the criteria stipulated by the International Society for Cellular Therapy (ISCT). MSC-CM contained growth factors e.g. keratinocyte growth factor (KGF), hepatocyte growth factor (HGF), platelet derived growth factor-AB (PDGF-AB), transforming growth factor-β1 (TGF-β), macrophage stimulating protein-1 (MSP-1) and SDF-1α and RT qPCR analysis demonstrated receptors of these growth factors e.g. FGFR2, c-MET, PDGFRA, TGFβ-R1, RON and CXCR4 respectively on both scratched and non-scratched primary keratinocytes. The main findings from this study showed that MSCs could differentiate into ELCs and MSC-CM were shown to have a positive effect on migration and proliferation of skin cells in 2D and 3D culture. MSC secretions collected at early time points were more effective on cell migration than those collected at later time points during MSC expansion. 2D and 3D studies also showed that cell migration was the first and the major mechanism evoked by MSC-CM followed by proliferation and differentiation. Additionally, the 3D skin model developed in this study could be used as a skin replica for wound healing studies at the cellular and molecular level including the use of microRNA profiling. These microRNAs were regulated at different time points during the wound repair suggesting their participation in the different phases of the healing process. In conclusion, MSCs play a multifunctional role in the cellular and molecular mechanisms of the healing process and enhance the healing process via two mechanisms; cell mediated repair by differentiation into ELCs and secretory mediated repair by cytokines.

AUTHOR'S DECLARATION

I declare that this thesis is my own work and that I have correctly acknowledged the work of others. I certify that no part of the material offered has been previously submitted by me for a degree or other qualification in this or any other University.

Moyassar Al-Shaibani (M.Sc.)

October, 2018

DEDICATION

To the source of my inspiration

The spirits of my parents

To my life companion

My wife (my love)

To my darlings

My children

To the candle of my life during darkness

My sister and brothers

To my right-hand women in my research

My supervisors

I dedicate all of you this thesis with respect and appreciation.

Moyassar

ACKNOWLEDGMENTS

All praise to be to Allah who is deserving the thanks. The prayers and the peace to be upon our Prophet, Mohammed, the final prophet and messenger. And the peace to be upon his kind family and his preferable companions.

There are no words other than introducing thankfulness and grateful to everybody has supported me during my research journey. First of all, I introduce my special thanks to my principal supervisor Professor Anne M Dickinson for being confident in me and accepting me to complete my PhD study and gave me a chance to share knowledge here with great people. I am also very thankful to my other supervisors Professor Penny E Lovat and Dr Xiao-nong Wang for their advices, support and cooperation since the first moments until finishing this work. Many thanks to my supervisors for being there in both happy and hard moments that I had and being aware about the difficulties I faced during my research. I'll never forget your support. My special thanks to my financial sponsors; the Higher Committees for Education Development in Iraq (HCED) and Al-Nahrain University for funding and supporting me throughout my study.

I introduce my thanks to the people who showed assistance every time I need in particular, Dr Clare Lendrem, Dr Lindsay Nicholson, Dr Rachel Crossland, Dr Asif Tulah, Dr Kim Pearce, Mrs Katie Gray, Mrs Elizabeth A Douglas and Mrs Jamie Williamson / academic haematology, Dr David Hill, Dr Stamatina Verykiou and Dr Ashleigh McConnell Department of Dermatology, Dr Rachel Dickinson, Mrs Sarah Pagan and Ms Anastasia Resteu / Dendritic cell laboratory, Dr Alex Laude, Dr Trevor Booth and Dr Ashleigh Herriott / The Bioimaging Unit, Dr Andrew Fuller / Flow Cytometry Core, Newcastle University. Also, my thanks to the members of the annual assessment panel Professor Mark Birch-Machin / Dermatology Department / Newcastle University and Dr Andrew Gennery / The Great North Children's Hospital. Thanks to IT-ICM service in particular, David Graham, Wendy Craig, Mark Warwick and Nancy Woadden. I am really grateful for being a member of this grate university, University of Newcastle upon Tyne, and using its facilities and laboratories. A special thanks with love to the person who spent nights and days to make everything easy to me, my lovely wife (Hiba Al-Mafrachi) and my lovely children. A huge thank with respect and appreciation to my sisters and brothers who were supporting me overseas.

At the end, a big thank to all patients and healthy volunteers who donated cells for this research.

Last but not the least, I thank everyone who ministered me during this work, and wishing success for all, always and forever.

LIST OF ABBREVIATIONS

Abbreviations	Terms
2DCC	Two-Dimensional Cell Culture
3'UTR	3'-Untranslated Region
3DCC	Three-Dimensional Cell Culture
3D-SEM	3D Skin Equivalent Model
Akt	Alpha Serine/Threonine Kinase
ALCAM	Activated Leukocyte-Cell Adhesion Molecule
ALK	Activin Like Kinase
ALP	Alkaline Phosphatase
AMM	Annealing Master Mix
ANGPT	angiopoietin
ANOVA	Analysis of Variance
APC	Allophycocyanin (Fluorescence Stain)
APC	Acid–Phenol-Chloroform (Chemical substance_Toxic)
APC	Antigen Presenting Cell
APC	Adenomatous Olyposis Coli (gene)
APSS	Alkaline Phosphate Substrate Solution
AT	Antiguagulant
AT-MSCs	Adipose Tissue derived Mesenchymal Stem Cells
BC	Blocking Conditions
BF	Bright Field
bFGF	basic Fibroblast Growth Factor
BM-40	Basement-Membrane Protein 40
BME	Basal Membrane Extract
BM-MSCs	Bone Marrow derived Mesenchymal Stem Cells
BrdU	5-bromo-2'-deoxyuridine
BSA	Bovine Serum Albumin
CALPAIN	Calcium-dependent, non-lysosomal Cysteine Proteases
CAP-18	Cathelicidin Antimicrobial Peptide-18 kDa
CCL	C-C motif Chemokine Ligand
CCR	C-C motif Chemokine Receptor
CD	Cluster of Differentiation
CDM	Chondrogenic Differentiation Medium
cDNA	Complementary DNA
CFU-f	Colony-Forming Unit-fibroblasts
CM	Conditioned Media
CM24	MSC secretions collected after 24 hours of growth in *in vitro* culture
CM48	MSC secretions collected after 48 hours of growth in *in vitro* culture
CM72	MSC secretions collected after 72 hours of growth in *in vitro* culture
COX2	Cytochrome c Oxidase subunit 2
CRABP1	Cellular Retinoic Acid-Binding Protein 1
CTGF	Connective Tissue Growth Factor
CXCL	C-X-C motif Ligand
DAPI	4,6-Diamidino-2-phenylindole
DCs	Dendritic Cells
DDW	Deionized (or Double) Distilled Water
DEPC	Diethyl Pyrocarbonate
DMEM	Dulbecco's Modified Eagle's Medium
DMEM-FCS	DMEM supplemented with 10% Foetal Calf Serum
DMSO	Dimethyl sulfoxide

DNA	Deoxyribonucleic Acid
DPX	Dibutylphthalate Polystyrene Xylene
dsRNA	double stranded RNA
DT	Doubling Time
DW	Distilled Water
ECM	Extra Cellular Matrix
ECs	Endothelial Cells
EDM	Epidermal Differentiation Media
EDNRB	Endothelin Receptor type B
EDTA	Ethylenediaminetetraacetic acid
EGF	Epidermal Growth Factor
EHMT1	Euchromatic Histone-Lysine N-Methyltransferase 1
EIA	Enzyme Immunoassay
ELCs	Epidermal like Cells
ELISA	Enzyme-linked Immunosorbent Assay
ELS	Epidermal like Structure
EMP-1	Epithelial Membrane Protein-1
EMT	epithelial-mesenchymal transition
EMT	Epithelial-Mesenchymal Transition
ER	Epithelialization Rate
ERK	Extracellular Signal-Regulated Kinase
ESCs	Embryonic Stem Cells
FACS	Fluorescence Activated Cell Sorting
FaX	Factor X
FB	Flow Buffer
FBS	Foetal Bovine Serum
FCFU	Fibroblastoid Colony-Forming Unit
FCS	Foetal Calf Serum
FGA, *FGB* and *FGG*	*Fibrinogen A, Fibrinogen B and Fibrinogen G*
FGF	Fibroblast Growth Factor
FGFR-2	Fibroblast Growth Factor Receptor-2
FHR	Final Hybridization Reaction
FITC	Fluorescein Isothiocyanate
FLII	Protein Flightless-1 homolog
GAPDH	Glyceraldehyde 3-phosphate dehydrogenase
G-CSF	Granulocyte Colony-Stimulating Factor
GDM	Gel-Dye Mix
GFP	Green Fluorescent Protein
GM-CSF	Granulocyte-Macrophage Colony-Stimulating Factor
GPCRs	G-Protein Coupled Receptors
GTP	Guanosine-5'-triphosphate
GvHD	Graft-versus-Host Disease
HaCat	Human keratinocyte Cell Line
HB-EGF	Heparin-Binding Epidermal Growth Factor
HC-CM	High Calcium Conditioned Media
HCL	High Calcium Level
HC-Media	High Calcium-Media
HeLa	Cancer Cell Line Isolated from a lady her name (Henrietta Lacks)
HGF	Hepatocyte Growth Factor
HGFL	Hepatocyte Growth Factor Like Protein
HIF	Hypoxia Inducible Factor

HIPK1	Homeodomain-Interacting Protein Kinase 1
HKGS	Human Keratinocyte Growth Supplement
HLA	Human Leukocyte Antigen
HMECs	Human Mammary Epithelial Cells
HMGA2	high-mobility group AT-hook 2
h-MSCs	human Mesenchymal Stem Cells
HMW	High Molecular Weight
HPCs	Haematopoietic Progenitor Cells
HR	Healing Rate
HSCs	Haematopoietic Stem Cells
ICAM-1	Intercellular Adhesion Molecule-1
IF	Immunofluorescence
IFN-γ	Interferon-gamma
IGF	Insulin-Like Growth Factor
IGF-1	Insulin like Growth Factor-1
IgG	Immunoglobulin G
IL	Interleukin
IP	Inhibited proliferation
IRAK-1	Interleukin-1 Receptor-Associated Kinase-1
ISCT	International Society for Cellular Therapy
ITS	Insulin-Transferrin-Selenium
K10	Keratin 10
K14	Cytokeratin K14 or Keratin 14
KGF	Keratinocyte Growth Factor
KGM	Keratinocyte Growth Media
KLF5	Kruppel-Like Factor 5
KMT2D	Histone-lysine N-methyltransferase 2D
KRT5	Keratin 5 gene
KSP	Keratinocyte Specific Protein
LB	Lysis Buffer
LC-CM	Low Calcium Conditioned Media
LCL	Low Calcium Level
LC-Media	Low Calcium-Media
LET	Length of Epidermal Tongue
LMAT	Leukocyte Migration Agarose Technique
LMM	Ligation Master Mix
LPS	lipopolysaccharides
MCF7	Breast Cancer Cells Line
MCP-1	Macrophage Chemoattractant Protein-1
MHC-II	Major Histocompatibility Complex class II
MIP-1α and MIP-1β	Macrophage Inflammatory Protein-1 alpha and beta
miRNA	Micro Ribonucleic Acid
MMC	Mitomycin C
MMP	Matrix Metalloproteinase
MNC	Mononuclear Cells
MPCs	Mesodermal Precursor Cells
mRNA	Messenger RNA
MSC-CM	Mesenchymal Stem Cell-Conditioned Media
MSCs	Mesenchymal Stem Cells
MSP	Macrophage-Stimulating Protein
NADPH	Nicotinamide Adenine Dinucleotide Phosphate

NBC	Non-Blocking Conditions
NDRG2	N-Myc Downstream Regulated Gene 2
NF-κB	Nuclear Factor kappa-light-chain-enhancer of activated B cells
NGF	Nerve Growth Factor
NHM	Non-haematopoietic Medium
NHS	National Health Service
NIP	Non-inhibited Proliferation
NKCs	Natural Killer Cells
NS	No Scratch
OD	Optical Density
ODM	Osteogenic Differentiation Medium
OTUB1	Otubain-1
PAI-1	Plasminogen Activator Inhibitor-1
PB-MSCs	Peripheral Blood derived Mesenchymal Stem Cells
PBS	Phosphate Buffered Saline
PCR-RM	PCR Reaction Mix
PD	Population Doubling
PDCD-4	Programmed Cell Death Protein-4
PDGF	Platelet Derived Growth Factor
PE	Phycoerythrin
perCPC	Peridinin Chlorophyll Protein
PFA	Paraformaldehyde
PL-MSCs	Placenta derived Mesenchymal Stem Cells
pre-miRNA	Premature micro RNA
PRGF	Plasminogen-Related Growth Factor
pri-miRNA	Primary micro RNA
PS	Protein S (Protein)
PS	Penicillin–Streptomycin (Antibiotics used in culture media)
PS	Primitive Streak (transient structure at week 15 during human development indicates start of gastrulation)
PSA	Penicillin–Streptomycin–Amphotericin B
PTEN	Phosphatase And Tensin Homolog
qPCR	Quantitative Polymerase Chain Reaction
RAN	RAs-related nuclear protein
RAPH-1	Ras-Associated and Pleckstrin Homology domains-containing protein 1
RIN	RNA Integrity Number
RISC	miRNA-Induced-Silencing-Complex
RNA	Ribonucleic Acid
ROCK-1	Rho-Associated, Coiled-Coil-Containing Protein Kinase-1
RON	Recepteur d'Origine Nantais) named after the French city in which it was discovered
ROS	Reactive Oxygen Species
RPMI	Roswell Park Memorial Institute medium
RT-MM	Reverse Transcriptase Master Mix
RT-PCR	Reverse Transcription Polymerase Chain Reaction
RT-qPCR	Quantitative Reverse Transcription Polymerase Chain Reaction
SA	Scratch Assay
SCC	Standard Culture Conditions (37^{o}C, ≈20% O_2 and 5% CO_2.)
SDF-1 α	Stromal-Derived Factor-1 alpha
SDS	Sodium Dodecyl Sulfate
SERPINC1	Serine Peptidase Inhibitor Clade 1

SF	Synovial Fluid
SF	Serum Free
SFs	Scatter Factors
SGCs	Sweat Gland Cells
SHIP1	SH2-containing inositol-5'-phosphatase-1
S-MSCs	Synovium derived Mesenchymal Stem Cells
SMAD	SmaII Mothers Against Decapentaplegic
SNT	Scratched non-treated
SOCS-1	Suppressor Of Cytokine Signalling-1
SPARC	Secreted Protein Acidic and Rich in Cysteine
SS	Starter Standard
SSEA4	Stage-Specific Embryonic Antigen-4
STAT 3	Signal Transducer and Activator of Transcription 3
ST-CM	Scratched treated with MSC-CM
SVF	Stromal Vascular Fraction
TAGLN	Transgelin gene
TBS	Tris Buffered Saline
TET	Thickness of Epidermal Tongue
TF	Tissue Factor
TGF-ß1	Transforming Growth Factor Beta-1
TLR-2	Toll-like Receptor 2
TMB	Tetramethylbenzidine
TN-C	Tenascin C
TNF-α	Tumor Necrosis Factor-alpha
TP53	Tumour Protein 53
T-reg	Regulatory-T Cells
TRIM11	Tripartite Motif-Containing Protein 11
UBE3C	Ubiquitin-protein ligase E3C
UCB	Umbilical Cord Blood
VAMP-8	Vesicle-associated Membrane Protein 8
VCAM-1	Vascular Cell Adhesion Molecule-1
VEGF	Vascular Endothelial Growth Factor
VEGF-A	Aascular Endothelial Growth Factor A
vWF	von Willebrand Factor

LIST OF CONTENTS

Abstract i
Author's Declaration ii
Dedication iii
Acknowledgments iv
List of Abbreviations v
List of Contents x
List of Tables xv
List of Figures xvii
List of Equations xxi
List of Publications / Posters and Awards xxii
CHAPTER 1 LITERATURE REVIEW AND AIMS OF THE STUDY 1
1.1 Introduction 2
1.2 Mesenchymal Stem Cells (MSCs): Historic View and Definition 3
1.3 Main Sources of Mesenchymal Stem Cells 4
1.3.1 Bone Marrow 4
1.3.2 Umbilical Cord Blood and Placenta 5
1.3.3 Adipose Tissue 6
1.3.4 Peripheral Blood 7
1.3.5 Other Sources 7
1.4 Identifying Characteristics of Mesenchymal Stem Cells 8
1.4.1 Morphology 9
1.4.2 In vitro Characteristics 9
1.4.3 Phenotypic Markers of Mesenchymal Stem Cells 10
1.5 Differentiation Potential of Mesenchymal Stem Cells 14
1.6 Biologically Active Substances Secreted by Mesenchymal Stem Cells 15
1.6.1 Growth factors 16
1.6.2 Cytokines 17
1.6.3 Chemokines 18
1.6.4 Exosomes (MSC-EXOSOME) 19
1.7 Clinical Application of Mesenchymal Stem Cells 20
1.7.1 Mesenchymal Stem Cells in Skin Regeneration 21
1.7.2 Utilisation and Mode of Action of Mesenchymal Stem Cells in Wound Healing 22
1.8 Benefits of the Use of Mesenchymal Stem Cells in Treating Wounds 26
1.8.1 Immunomodulatory Features of MSCs 26
1.8.2 Migration and Engraftment Capacity 27
1.8.3 Wound Closure Acceleration 27

1.8.4 Antimicrobial Activity 28
1.8.5 Prevent Chronic Condition 28
1.8.6 Attenuation of Scar Formation 28
1.8.7 Neutralizing the Reactive Oxygen Species (ROS) 28
1.8.8 Producing Anti-fibrotic Factors 29
1.8.9 Enhancing Dermal Fibroblast Function 29
1.8.10 Promoting Angiogenesis and Vascular Stability 30
1.9 Human Skin 30
1.9.1 Human Skin Layers 30
1.9.2 Skin Glands 33
1.9.3 Skin Proteins 33
1.9.4 Other Skin Components 34
1.10 Cells Involved in Skin Regeneration and Wound Healing 34
1.10.1 Keratinocytes 34
1.10.2 Fibroblasts 34
1.10.3 Immune cells 35
1.11 Types of Skin Wounds 36
1.11.1 Acute Skin Wounds 36
1.11.2 Chronic Skin Wounds 36
1.12 Phases of the Healing Process of Skin Wounds 37
1.12.1 Haemostasis Phase (Coagulation) 38
1.12.2 Inflammatory Phase 39
1.12.3 Proliferation Phase 40
1.12.4 Contraction Phase 40
1.12.5 Remodelling Phase (Resolution) 41
1.13 Roles of Micro Ribonucleic Acids (MicroRNAs) in Wound Healing 42
1.13.1 Biogenesis of MicroRNA 43
1.13.2 Roles of MicroRNAs in Skin Development and Morphogenesis 45
1.13.3 Roles of MicroRNAs in Wound Healing 46
1.14 Receptors of Growth Factors and Cytokines and Their Roles in Wound Healing ... 51
1.14.1 c-MET: HGF Receptor 52
1.14.2 PDGFR: Receptor of PDGFA, PDGFB, PDGFAB, PDGFCC. 53
1.14.3 FGFR2: KGF Receptor 54
1.14.4 TGFß-R1: TGFß-1 Receptor 54
1.14.5 MSTR1: MSP-1 Receptor (Also Known as RON; PTK8; CD136; CDw136) 55
1.14.6 CXCR4: SDF-1α Receptor 56
1.15 Two-Dimensional and Three-Dimensional Cell Culture 56

1.16 Skin Equivalent Model 58
1.17 Aims of the Study 59
1.17.1 The Problem 59
1.17.2 Hypotheses 59
1.17.3 Aims of the Study 60
CHAPTER 2 MATERIALS AND METHODS 61
2.1 Ethics and Consent 62
2.2 Materials and Equipment 62
2.2.1 Culture Media 62
2.2.2 MSC Phenotypic Characterisation Kit 62
2.2.3 ELISA Kits 63
2.2.4 Immunofluorescence Antibodies and Stains 63
2.2.5 Materials and Reagents of Gene Expression 63
2.2.6 MicroRNA Profiling Kits 64
2.2.7 Stains and Staining Reagents 64
2.2.8 General Reagents 65
2.2.9 Equipment and Machines 65
2.2.10 Plastic and Glass Wares 66
2.2.11 Other Tools 66
2.2.12 Bioimaging Machines 67
2.2.13 Preparation of Culture Media 67
2.3 Methods 72
2.3.1 General Protocols of Cell Culture 72
2.3.2 Isolation of MSCs from Bone Marrow (Primary Culture) 73
2.3.3 Expansion of MSCs in vitro 73
2.3.4 Cryopreservation of MSCs 74
2.3.5 Characterisation of MSCs 74
2.3.6 Preparation of MSC Conditioned Media (MSC-CM) 79
2.3.7 Human Skin Primary Cells and Cell Lines 84
2.3.8 Assessment of Cell Migration 86
2.3.9 Detection of Proliferation Markers 87
2.3.10 Viability and Proliferation Assay 89
2.3.11 Differentiation of MSCs into Epidermal-like Cells 90
2.3.12 Immunofluorescence of Slide Fixed Cells 91
2.3.13 Detection of Growth Factor Receptors in Primary Keratinocytes 91
2.3.14 Construction of 3D Skin Equivalent Model (3D-SEM) 98
2.3.15 Differentiation of MSCs into Epidermal-like Structure in 3D Culture 99

2.3.16 Developing a Prototype 3D Skin Equivalent Model (3D-SEM) for Wound Healing Studies 100
2.3.17 Evaluation of Wound Healing 102
2.3.18 Immunofluorescence Staining of the 3D Skin Equivalent Model (3D-SEM) 102
2.3.19 MicroRNA Profiling During Wound Healing Using 3D-SEM 103
2.4 Data Collection and Statistical Analysis 111
2.4.1 Data Types and choosing of Statistical Test 111
2.4.2 Statistical Analysis of MicroRNA Profiling 112
CHAPTER 3 CHARACTERISTICS OF MESENCHYMAL STEM CELLS AND DEFINING THEIR SECRETIONS 113
3.1 Introduction 114
3.2 Specific Aims of Chapter Three 116
3.3 Results 117
3.3.1 Donors and Sample Collection 117
3.3.2 Characteristics of Human MSCs 118
3.4 Discussion 132
CHAPTER 4 EFFECT OF MSC-CM ON MIGRATION OF SKIN CELLS 139
4.1 Introduction 140
4.2 Specific Aims of Chapter Four 142
4.3 Results 143
4.3.1 Skin Cells 143
4.3.2 Effect of MSC-CM on Migration of Skin Cells 146
4.3.2.1 Optimisation of 2D Scratch Assay Using HaCat Cell Line 146
4.3.2.2 Effect of High Calcium-CM (HC-CM) on Migration of Primary Keratinocytes 148
4.3.2.3 Effect of Low Calcium-CM (LC-CM) on Migration of Primary Keratinocytes 151
4.3.2.4 Effect of LC-CM on Migration of Primary Keratinocytes in Hypoxic Conditions 154
4.3.2.5 Effect of MSC-CM on Migration of Primary Keratinocytes During Blocking SDF-1α Receptor (CXCR4) 156
4.3.2.6 Effect of MSC-CM on Migration of Primary Fibroblasts 163
4.4 Discussion 166
CHAPTER 5 EFFECT OF MSC-CM ON PROLIFERATION OF SKIN CELLS 173
5.1 Introduction 174
5.2 Specific Aims of Chapter Five 175
5.3 Results 176
5.3.1 Effect of MSC-CM on Proliferation of Skin Cells 176
5.3.1.1 Optimisation of MTS Proliferation Assay Using the HaCat Cell Line 176

5.3.2 Determining Migrating and Proliferating Cells During Wound Closure 182
5.4 Discussion 209
CHAPTER 6 DEVELOPING A PROTOTYPE 3D SKIN EQUIVALENT MODEL (3D-SEM) AND ROBUST PROTOCOL FOR WOUND HEALING STUDIES 214
6.1 Introduction 215
6.2 Specific Aims of Chapter Six 217
6.3 Results 218
6.3.1 Validation of the Reproduced 3D Skin Equivalent Model 218
6.3.2 Developing a Prototype 3D Skin equivalent Model (3D-SEM) for Wound Healing Studies 222
6.3.3 MSCs Differentiate into 3D Epidermal-like Structures When incorporated Over Dermal Fibroblast Layers Using The alvetex® Scaffold 244
6.4 Discussion 248
6.4.1 Creating and Characterising the 3D-SEM for Wound Healing 248
6.4.2 Investigating the Role of MSC-CM on Wound Healing Using the Developed 3D-SEM 253
CHAPTER 7 THE MOLECULAR BIOLOGY OF WOUND HEALING 257
7.1 Introduction 258
7.2 Specific Aims of Chapter Seven 262
7.3 Results 263
7.3.1 Characterisation of the 3D Skin Model -MicroRNA Expression Profiles 263
7.3.2 Differentially Expressed MicroRNAs by the 3D Skin Model During Wound Healing 269
7.3.3 Detection of Growth Factor Receptors Using Gene Expression 290
7.4 Discussion 294
CHAPTER 8 GENERAL DISCUSSION AND CONCLUDING REMARKS 307
8.1 Introduction 308
8.2 General Discussion 308
8.3 Conclusion 312
8.4 Limitations of Using MSCs in Wound Treatment 313
8.5 Future Work 313
Ethics Approval 315
References 318

LIST OF TABLES

Table 1.1 Positive and negative markers of MSCs. 13
Table 1.2 Growth factors secreted by MSCs and their roles in wound healing. 17
Table 1.3 Cytokines secreted by MSCs and their roles in wound healing. 18
Table 1.4 Chemokines secreted by MSCs and their roles in wound healing. 19
Table 1.5 The main phases and events of the wound healing process. 42
Table 2.1 Types of media used for culturing different cell types. 62
Table 2.2 Antibodies and isotypes used for phenotypic assay of MSCs. 63
Table 2.3 ELISA kits used to measure the concentrations of growth factors and cytokines in MSC-CM. 63
Table 2.4 Primary and secondary antibodies and other reagents used for immunofluorescence staining. 63
Table 2.5 Reagent and substances used for gene expression assay. 64
Table 2.6 Kits and reagents used for microRNA analysis. 64
Table 2.7 Stains and reagents used during the different staining protocols. 64
Table 2.8 General reagents and materials used during the study. 65
Table 2.9 Systems and machines used to carry out experiments during the study. 66
Table 2.10 Consumables used for general techniques throughout the study. 66
Table 2.11 Other tools used for different lab purposes. 66
Table 2.12 Microscopes used to image the live cells, dead stained cells and 3D skin models. 67
Table 2.13 Components of standard culture media. 68
Table 2.14 Constituents of MCDB media. 68
Table 2.15 Types of media used to collect MSC secretions. 69
Table 2.16 Ingredients of epidermal differentiation media. 69
Table 2.17 Components of dermal layer feeding media (media B). 70
Table 2.18 Constituents of keratinocyte chelating media (Media C). 70
Table 2.19 Ingredients of air-liquid interphase media (Media D). 71
Table 2.20 Freezing solutions of different cell types. 71
Table 2.21 Summary of MSC phenotyping assay. 76
Table 2.22 Summary of MSC differentiation assays. 79
Table 2.23 An example of an ELISA kit and reagent preparation. 80
Table 2.24 Concentrations of standards differ depending on growth factors. 81
Table 2.25 Content of RNeasy micro kit and their preparation. 93
Table 2.26 Content of high capacity cDNA reverse transcription kit and their preparations. 94
Table 2.27 Conditions of the thermal cycler for reverse transcriptase PCR. 95
Table 2.28 The components of PCR master mix and their preparations. 96
Table 2.29 Conditions of RT-PCR system required for TaqMan gene expression 98

Table 2.30 Contents of microRNA isolation kit (mirVana™) 103
Table 2.31 Content and reagents of Agilent RNA 6000 Nano kit. 105
Table 2.32 Temperature setting of the thermocycler for annealing, ligation and purification protocols during microRNA profiling technique using NanoString technology. 109
Table 3.1 Information about MSCs used in the study. 117
Table 3.2 Information about MSC secretions in different media. 128
Table 4.1 Human epidermal keratinocytes and HaCat cell line obtained as frozen cells. 144
Table 4.2 Human dermal fibroblasts obtained as frozen cells. 144
Table 4.3 Skin samples and biopsies used to isolate human primary skin cells. 145
Table 5.1 Numbers and percentages of migrating and proliferating cells in the scratch area during wound healing. 192
Table 5.2 Numbers and ratios of migrating and proliferating MMC-treated cells in the scratch area during wound healing. 205
Table 7.1 Further details of differentially expressed microRNAs by real skin and their derived 3D skin model equivalents (3D-SEM). 269
Table 7.2 Further details of differentially expressed microRNAs between intact 3D-SEM and wounded 3D-SEM after 2 hours of initiating the healing process. 273
Table 7.3 Further details of differentially expressed microRNAs between intact 3D-SEM and wounded 3D-SEM after 4 hours of initiating the healing process. 276
Table 7.4 Further details of differentially expressed microRNAs between intact 3D-SEM and wounded 3D-SEM after 24 hours of initiating the healing process. 279
Table 7.5 Further details of differentially expressed microRNAs between intact 3D-SEM and wounded 3D-SEM after 72 hours of initiating the healing process. 282
Table 7.6 Further details of differentially expressed microRNAs between intact 3D-SEM and wounded 3D-SEM after 1 week of initiating the healing process. 285
Table 7.7 Common differentially expressed microRNAs at different time points during the wound healing process. 286
Table 7.8 Target genes of overlapping microRNAs during the healing process. 288
Table 7.9 MicroRNAs upregulated in wounded 3D-SEM compared to intact 3D-SEM at only one time point during the entire healing process. 289
Table 7.10 MicroRNAs that are predicted to target cell surface receptors. 293

LIST OF FIGURES

Figure 1.1 Identifying characteristics of MSCs using the ISCT criteria. 9
Figure 1.2 Differentiation Potential of MSCs. 15
Figure 1.3 Potential applications of MSCs in wound healing. 23
Figure 1.4 Participation of MSC secretions in wound healing phases and events. 25
Figure 1.5 Simplified structure of human skin. 31
Figure 1.6 Simplified structure of human epidermis. 32
Figure 1.7 Biogenesis of microRNA. 44
Figure 1.8 Interaction between growth factors and their receptors expressed by primary keratinocytes. 52
Figure 2.1 Preparation of ELISA standards. 80
Figure 2.2 Explanatory scheme of ELISA protocol. 82
Figure 2.3 Standards curves of growth factors and cytokines. 83
Figure 2.4 HeLa cell line in culture at different densities (Adopted from ATCC). 85
Figure 2.5 Design of scratch assay. 87
Figure 2.6 Design of proliferation assay. 90
Figure 2.7 Conditions applied to primary keratinocytes for further gene expression of growth factor receptors. 92
Figure 2.8 Steps of gene expression assay. 92
Figure 2.9 Explanatory images of assessing nucleic acid purity. 96
Figure 2.10 Flowchart of preparing RT-PCR reaction and PCR plate. 97
Figure 2.11 Generation of a 3D skin equivalent model (3D-SEM) using the Alvetex®. 99
Figure 2.12 The developed protocol for wound healing using a fully humanised 3D kin equivalent model (3D-SEM). 101
Figure 2.13 Summary of protocol for determining microRNA integrity number. 106
Figure 2.14 Evaluation of microRNAs using bioanalyzer. 108
Figure 3.1 Morphology and shapes of MSCs at different time points and different growth conditions. 119
Figure 3.2 Expansion indices of MSCs. 120
Figure 3.3 Phenotypic characteristics of MSCs at standard (high) calcium media (HC-Media). 122
Figure 3.4 Phenotypic characteristics of human MSCs at low calcium media (LC-Media). 123
Figure 3.5 Comparison between MSC phenotypic markers expressed at standard high calcium media (HC-Media) and low calcium media (LC-Media). 124
Figure 3.6 Differentiation potential of MSCs into tri-lineages. 125
Figure 3.7 Morphology of MSCs in EDM at different time points. 126
Figure 3.8 Differentiation potential of MSCs into epidermal like cells (ELCs). 127
Figure 3.9 Growth factors present in MSC-CM. 129

Figure 3.10 Concentrations of growth factors and cytokines present in MSC-CM collected at different conditions. 131
Figure 4.1 Human skin cells used in the study. 143
Figure 4.2 Scratch assay of HaCat cell line. 147
Figure 4.3 Kinetics of scratch closure of HaCat cells. 148
Figure 4.4 The effect of HC-CM on migration of primary keratinocytes. 150
Figure 4.5 Kinetics of scratch closure of primary keratinocytes treated with HC-CM. 150
Figure 4.6 Effect of LC-CM on migration of primary keratinocytes using scratch assay. 152
Figure 4.7 Kinetics of migration of primary keratinocytes treated with LC-CM. 152
Figure 4.8 Comparison between the effect of LC-CM and HC-CM on migration of primary keratinocytes. 154
Figure 4.9 Migration of primary keratinocytes treated with LC-CM in hypoxic conditions. 155
Figure 4.10 Kinetics of the effect of LC-CM on migration of primary keratinocytes in hypoxic conditions. 156
Figure 4.11 Migration of primary keratinocytes treated with LC-CM during SDF-1α non-blocking conditions. 158
Figure 4.12 Kinetics of the effect of LC-CM on migration of primary keratinocytes during non-blocking of SDF-1α. 159
Figure 4.13 Migration of primary keratinocytes treated with LC-CM during SDF-1α blocking. 160
Figure 4.14 Kinetics of the effect of LC-CM on migration of primary keratinocytes during blocking SDF-1α. 161
Figure 4.15 Kinetics the effects of different substances on migration of primary keratinocytes during blocking and non-blocking of SDF-1α. 163
Figure 4.16 Migration of primary dermal fibroblasts after treatment with HC-CM. 164
Figure 4.17 Kinetics of the effect of HC-CM on migration of primary fibroblasts. 165
Figure 5.1 Statistical analysis of the effect of MSC-CM on proliferation of HaCat cells using MTS assay. 177
Figure 5.2 Statistical analysis of the effect of high calcium-conditioned media (HC-CM) on proliferation of primary keratinocytes using MTS assay. 178
Figure 5.3 Statistical analysis of the effect of low calcium-conditioned media (LC-CM) on proliferation of primary keratinocytes using MTS assay. 179
Figure 5.4 Comparison between the effect of LC-CM and HC-CM on proliferation of primary keratinocytes using MTS assay. 180
Figure 5.5 Statistical analysis of the effect of MSC-CM (HC-CM) on proliferation of primary fibroblasts using MTS assay. 182
Figure 5.6 Proliferating HeLa cells express the proliferation marker (BrdU). 184
Figure 5.7 Proliferating primary keratinocytes express the proliferation marker (BrdU). 186

Figure 5.8 Migrating and proliferating cells during wound closure in sample S1212K..... 188
Figure 5.9 Migrating and proliferating cells during wound closure in sample S1214K..... 190
Figure 5.10 Migrating and proliferating cells during wound closure in sample S1216K..... 192
Figure 5.11 Numbers and ratios of migrating and proliferating cells during wound closure. 194
Figure 5.12 Migration of primary keratinocytes treated with MMC using a 2D scratch assay. 196
Figure 5.13 Statistical analysis of the effect of LC-CM on migration of primary keratinocytes treated with MMC. 197
Figure 5.14 Migrating and proliferating MMC-treated cells during wound closure using sample S1212K. 200
Figure 5.15 Migrating and proliferating MMC-treated cells during wound closure using sample S1214K. 202
Figure 5.16 Migrating and proliferating MMC-treated cells of inhibited proliferation during wound closure using sample S1216K. 204
Figure 5.17 Numbers and ratios of migrating and proliferating keratinocytes treated with MMC inhibited proliferation (IP) during wound closure. 206
Figure 5.18 Statistical comparison between numbers of migrating keratinocytes treated with MMC (inhibition of proliferation (IP) and untreated keratinocytes (non-inhibition of proliferation (NIP) during wound closure. 207
Figure 5.19 Comparison between proliferating cells with inhibited (IP) and non-inhibited proliferation (NIP) during wound closure. 208
Figure 6.1 Haematoxylin-Eosin (H-E) image of constructed 3D skin model equivalent (3D-SEM)..... 218
Figure 6.2 Epidermal differentiation markers expressed by human skin. 219
Figure 6.3 Epidermal Differentiation and Dermal markers expressed by a reconstructed 3D skin equivalent model (3D-SEM). 221
Figure 6.4 Multiple immunofluorescence staining of 3D skin equivalent model (3D-SEM). 222
Figure 6.5 MSC-CM enhances wound healing in 3D skin equivalents model (3D-SEM). .. 225
Figure 6.6 Schematic figure of the healing process in in vitro 3D skin equivalent model (3D-SEM)..... 226
Figure 6.7 Schematic figure indicating the adopted process to quantify the healing progress and epithelialisation rate. 227
Figure 6.8 Explanatory geometric figure of the newly formed epidermal sheet. 230
Figure 6.9 MSC-CM promotes epithelialisation and wound healing rates in 3D skin equivalent models (3D-SEM). 233
Figure 6.10 MSC-CM promotes re-epithelialisation in a punched 3D skin equivalent model (3D-SEM)..... 234

Figure 6.11 MSC-CM promotes expression of K14 by the epidermal layer at different times during the healing process. 237
Figure 6.12 MSC-CM promotes expression of K10 by the epidermal layer at different time points during the healing process. 239
Figure 6.13 MSC-CM mediated expression of involucrin by the epidermal layer at different time points during the healing process. 241
Figure 6.14 MSC-CM promotes Expression of loricrin by the epidermal layer at different time points during the wound healing process. 243
Figure 6.15 MSC-CM promotes expression of collagen IV (column A) and collagen III (column B) by the dermal layer during the healing process. 244
Figure 6.16 MSCs differentiate into epidermal like structure when incorporated onto dermal fibroblast layer on Alvetex® scaffold. 245
Figure 6.17 MSCs express full panel of epidermal differentiation markers and dermal markers when fed with epidermal differentiation media. 247
Figure.7.1 Ligation of specific tags to target microRNAs. 259
Figure 7.2 Hybridisation of specific tags to the target microRNAs. 261
Figure 7.3 Correlation between microRNA expression in real skin and the derived 3D skin models. 265
Figure 7.4 Differential microRNA expression between real skin and their derived 3D skin equivalent models (3D-SEM). 267
Figure 7.5 Differentially expressed microRNAs between intact 3D skin equivalent model (3D-SEM) and wounded 3D-SEM after 2 hours of initiating the healing process. 272
Figure 7.6 Differentially expressed microRNAs between intact 3D-SEM and wounded 3D-SEM after 4 hours of initiating the healing process. 275
Figure 7.7 Differentially expressed microRNAs between intact 3D-SEM and wounded 3D-SEM after 24 hours of initiating the healing process. 278
Figure 7.8 Differentially expressed microRNAs between intact 3D-SEM and wounded 3D-SEM after 72 hours of initiating the healing process. 281
Figure 7.9 Differentially expressed microRNAs between intact 3D-SEM and wounded 3D-SEM after 1 week of initiating the healing process. 284
Figure 7.10 Fold change of overlapping microRNAs at different time points during the healing process. 287
Figure 7.11 Receptors expressed by primary keratinocytes. 292

LIST OF EQUATIONS

Equation 2.1 67
Equation 2.2 67
Equation 2.3 72
Equation 2.4 72
Equation 2.5 74
Equation 2.6 74
Equation 2.7 98
Equation 2.8 98
Equation 6.1 228
Equation 6.2 228
Equation 6.3 228
Equation 6.4 228
Equation 6.5 229
Equation 6.6 229
Equation 6.7 229
Equation 6.8 231
Equation 6.9 231
Equation 6.10 231

LIST OF PUBLICATIONS / POSTERS AND AWARDS

1. Book Chapter

Moyassar B. H. Al-Shaibani, Xiao-nong Wang, Penny E. Lovat and Anne M. Dickinson (2016). Cellular Therapy for Wounds: Applications of Mesenchymal Stem Cells in Wound Healing, Wound Healing - New insights into Ancient Challenges, Dr. Vlad Alexandrescu (Ed.), InTech, Ch.5: 99-131. DOI: 10.5772/63963

2. Conference Posters

Al-Shaibani, M. B., A. Dickinson, X. Nong-Wang, A. S. Tulah and P. E. Lovat (2017). Effect of conditioned media from mesenchymal stem cells (MSC-CM) on wound healing using a prototype of a fully humanised 3D skin model. *Cytotherapy* **19**(5): e23-e24.

Al-Shaibani MBH, Wang XN, Lovat PE, Tulah A, Dickinson AM (2017). Conditioned Media from Allogenic Mesenchymal Stem Cell Culture (MSC-CM) Enhances Wound Healing in an Allogenic 3D Skin Model. Bone Marrow Transplantation. 52: S152-S152.

Al-Shaibani M, Wang X, Lovat P, Dickinson A (2016). Mesenchymal stem cells promote wound healing via differentiation into epidermal keratinocyte-like cells. British Journal of Dermatology, 174, (5): E71-E71.

Al-Shaibani MBH, Wang XN, Lovat PE, Dickinson AM (2015). Deciphering the Role of Mesenchymal Stem Cells Paracrine in Wound Closure Acceleration. Bone Marrow Transplantation, 50: S315-S315. DOI:10.1038/bmt.2015.30.

3. Awards

Farber Award Winner (Eugene M. Farber Travel Awards for Young Investigators-2015). http://www.montagnasymposium.org/pdfs/15TravelAwardees.pdf

CHAPTER 1 LITERATURE REVIEW AND AIMS OF THE STUDY

CHAPTER ONE: LITERATURE REVIEW AND AIMS OF THE STUDY

1.1 INTRODUCTION

Chronic wounds significantly affect millions of people and impair their quality of life and represent the most challenging disease in modern pathological medicine requiring modern effective therapies (Morimoto *et al.*, 2015; Tenci *et al.*, 2016). In the UK, in 2003, approximately 200,000 patients experience a chronic wound of varying types, ranging from ulcerations, scars, trauma and burns. Unfortunately, patient morbidity and in some cases mortality may result from such injuries for which chronic ulceration is a major factor (Franks and Morgan, 2003; White, 2009). Consequently, both society and the health sector are affected by the burden of chronic wounds. One of which is the reduced contribution to society by individuals suffering from chronic wounds due to their inability to work (White, 2009). In the context of healthcare treatment and hospitalization, chronic wounds are very costly in both treatment time and nurse time (Posnett and Franks, 2008). In 2005 and 2006, the nursing care of patients with a chronic wound cost the NHS approximately £2.3bn–£3.1bn a year, £6.08 million in England alone (Drew *et al.*, 2007). In 2012 and 2013, the annual cost of management of chronic wounds increased from £4.5 to 5.1 billion (Guest *et al.*, 2015) indicating that wound management is a growing costly problem. Furthermore, infection is inevitable, which not only negatively affects wound healing but is also life threatening (Butcher, 2013), requiring further hospitalisation and increased healthcare expenditure (Cook and Ousey, 2011).

Moreover, despite great progress in wound treatment, including the implementation of growth factors and biologically engineered skin equivalents, present treatment options for burns and non-healing chronic wounds are limited and not always effective (Hocking, 2012). Engineered skin models are limited by their construction from substances that are difficult to degrade, and do not always result in complete integration into normal uninjured skin. Furthermore, complete renewal of this model requires the alteration of immune responses to reduce fibrotic reactions in order to diminish scar production (Metcalfe and Ferguson, 2007). Therefore, there is an urgent need for new therapies for wounds with delayed healing (Hocking, 2012). Specific extra cellular matrix (ECM) proteins equivalent to the skin, specific growth factors, mesenchymal stem cells (MSCs), fibroblasts or viable epithelial cells may however impact on the wound healing process and their addition to

potential wound healing treatments may improve the efficacy of current therapeutic strategies (Maxson *et al.*, 2012). MSCs are generally defined as self-renewable, multi-potent progenitor adult stem cells. *In vivo*, they have the ability to differentiate widely into many mesenchymal lineages such as cartilage, bone, muscle and adipose tissues (Kadir *et al.*, 2012). Furthermore, MSCs have the ability to migrate from bone marrow to an injured site and differentiate into functional skin cells (Badiavas *et al.*, 2003; Sasaki *et al.*, 2008). *In vitro*, MSC's can be defined as fibroblast-like cells capable of self-renewal with the ability to adhere to plastic and subsequently differentiate into adipose, bone, cartilage tissue (Dominici *et al.*, 2006) as well as a multi-layered epidermis-like structures (Ma *et al.*, 2009).

The availability of MSCs in human skin (Hoogduijn and Dor, 2013) and their vital function in wound healing, suggests in particular the exogenous application of such cells may represent a promising solution for treatment of non-healing wounds (Paquet-Fifield *et al.*, 2009).

MSCs are potentially recognized as a promising strategy not only to treat non healing wounds but also to accelerate wound closure, prevent infection and restrain wounds from reaching a chronic state. Given the ability of MSCs to differentiate into skin like cells *in vitro* this project will explore the potential molecular, cellular and extracellular mechanisms of MSCs in wound healing and their potential therapeutic application for the treatment of cutaneous wounds.

1.2 Mesenchymal Stem Cells (MSCs): Historic View and Definition

In 1968, Alexander Friedenstein and colleagues were the first to discover that, besides haematopoietic stem cells (HSC), bone marrow harbours adherent fibroblast-like cells referred to as colony-forming unit-fibroblasts (CFU-f). In 1994, Caplan and collaborators termed these cells mesenchymal stem cells (MSCs) (Caplan, 1994). In 1999, these cells were described by Pittenger and co-workers as multipotent stem cells capable of differentiating into other cells from mesenchymal tissues (Pittenger *et al.*, 1999). They have also been termed marrow stromal cells, or fibroblastoid colony-forming units (FCFU) (Gregory *et al.*, 2005). MSCs first defined by Song *et al*. in 2007 as a type of stem cell population capable of self-renewing and differentiating into different cell types with pluripotent potential (Song *et al.*, 2007). They were defined as a heterogeneous

population of non-haematopoietic stem cells with the potential capacity to differentiate into various somatic lineages and tissues of both mesenchymal and non-mesenchymal origin (Rastegar *et al.*, 2010). They were also termed mesenchymal stem cells, multipotent mesenchymal stromal cells or stromal progenitor cells (Hocking and Gibran, 2010) and characterised by their ability to differentiate into bone (Rastegar *et al.*, 2010; Wang *et al.*, 2012a) with clonogenic properties *in vitro* (Semedo *et al.*, 2009). Interestingly, they can be isolated from a variety of tissue sources from the adult human body (Hass *et al.*, 2011).

1.3 MAIN SOURCES OF MESENCHYMAL STEM CELLS

Diverse tissues of the adult organism harbour MSCs capable of generating and renewing cell types specific for these tissues (Tuan *et al.*, 2003). Primarily, bone marrow, adipose tissue, peripheral blood, umbilical cord and cord blood and placenta are primary sources of MSCs. They are also found in other tissues and organs such as liver, synovial fluid, muscle and dental pulp (Tuan *et al.*, 2003; Yoshimura *et al.*, 2007; Huang and Burd, 2012; Yalvac *et al.*, 2013). Moreover, dermis, pericytes, synovial membrane and trabecular bone are identified as tissues harbouring MSCs (Tuan *et al.*, 2003).

1.3.1 *BONE MARROW*

Stromal cells, haematopoietic stem cells and endothelial cells are the main three cell types contained in the bone marrow. Bone marrow stroma is considered to be the common harbor of multi-potent cells; thereby, key in maintaining the microenvironment of the bone marrow (Tuan *et al.*, 2003; Barry and Murphy, 2004; Gimble *et al.*, 2008; Hua *et al.*, 2009). MSCs constitute approximately 0.01–0.001% of cell populations in the bone marrow (Rastegar *et al.*, 2010; Akiyama *et al.*, 2012). Although a small ratio is represented by this subtype of the cells, they are capable of proliferating and differentiating into osteoblastic, adipogenic, chondrogenic and neurogenic lineages (Akiyama *et al.*, 2012). Tuan and colleagues thought that these heterogeneous cells possessed the ability to circulate and gain access to different tissues and participate in maintaining and repairing these tissues (Tuan *et al.*, 2003). BM-MSCs are characterised by expressing cluster of differentiation (CD) markers such as CD73 (SH3), CD90 (Thy1), and CD105 (endoglin “SH2”) (Griffiths *et al.*, 2005; Tondreau *et al.*, 2005; Gang *et al.*, 2007; Greco *et al.*, 2007; Hass *et al.*, 2011; Akiyama *et al.*, 2012; Jin *et al.*, 2013a). Moreover, other reports have showed that BM-

MSCs can express more CD markers such as CD13, STRO-1, Octamer-4 (Oct4), and stage-specific embryonic antigen-4 (SSEA4) (Gang *et al.*, 2007; Greco *et al.*, 2007; Akiyama *et al.*, 2012), STRO-1 (Gang *et al.*, 2007; Greco *et al.*, 2007; Hass *et al.*, 2011; Akiyama *et al.*, 2012) CD44, CD166 (Gang *et al.*, 2007; Greco *et al.*, 2007; Hass *et al.*, 2011; Akiyama *et al.*, 2012; Jin *et al.*, 2013a) and human leukocyte antigen (HLA)-ABC (Jin *et al.*, 2013a).

On the other hand, BM-MSCs lack the expression of monocytes/macrophage CD markers (CD14), lymphocyte marker (CD11a), endothelial cell marker (CD31) (Deans and Moseley, 2000), the primitive haematopoietic stem cell (HSCs) marker (CD34) and a marker of all haematopoietic cells (CD45) (Griffiths *et al.*, 2005; Gang *et al.*, 2007; Greco *et al.*, 2007; Kolf *et al.*, 2007; Hass *et al.*, 2011; Akiyama *et al.*, 2012; Jin *et al.*, 2013a). Furthermore, BM-MSCs do not express other markers for example, CD11b (an immune cell marker ”myeloid”) (Kolf *et al.*, 2007; Jin *et al.*, 2013a), glycophorin-A (an erythroid lineage marker), CD14 (a myeloid biomarker), CD79a, and HLA-DR. Isolation of MCSs from bone marrow is characterised by two main advantages; (1) a large number of cells can be collected and (2) a low number of T-cells, while there are two disadvantages; (1) it requires a painful procedure with (2) risk of infection (Hass *et al.*, 2011).

1.3.2 *Umbilical Cord Blood and Placenta*

Umbilical cord blood (UCB) is a typical source of MSCs because their isolation is free from ethical concerns, and is carried out in a non-invasive manner (Jin *et al.*, 2013a). Depending on the morphological phenotypes, two subsets of MSC populations can be recognized in umbilical cord blood; the first group is spindle-shaped fibroblasts which can express CD90 with more capacity for adipogenesis compared with other types of cells which are flattened fibroblasts and negative for CD90 showing less capacity for adipogenesis (Arufe *et al.*, 2011). However, all UCB-MSCs share the same typical MSC criteria; for example, they are capable of self-renewing, differentiating into diverse cell linages such as bone, cartilage and adipose tissue *in vitro* and expressing cell surface markers with high levels of CD73, CD90 and CD105 while they are negative for CD14, CD34 and CD45 (Dominici *et al.*, 2006; Hass *et al.*, 2011; Jin *et al.*, 2013a). On the other hand, Jin and colleagues state that UCB-MSCs can express CD29, CD44, CD166 and human leukocyte antigen (HLA) while lack the expression of CD11b, CD14, CD79a, and

HLA-DR (Jin *et al.*, 2013a). Placental tissue is also considered as a great source of MSCs which could be utilised for translational research and regenerative medicine (Kadam *et al.*, 2010). Placenta-derived mesenchymal stem cells (PL-MSCs) characterised by their plasticity, ease of isolation, high yields and *in vitro* rapid expansion, retain both morphological and functional features (Hass *et al.*, 2011). These cells could be induced to give different cell linages such as neural-like cells, cartilage, hepatocyte and vascular endothelial cells (Matikainen and Laine, 2005; Kadam *et al.*, 2010; Portmann-Lanz *et al.*, 2010).

In general, neonatal tissues, as an MSC source, have significant benefits due to their availability and also potentially additional differentiation capacities when compared with MSCs obtained from adult tissues (Hass *et al.*, 2011). For example, high yields of MSCs could be obtained from UCB, with immunosuppressive functions making them an attractive candidate for use in allogenic transplantation (Jin *et al.*, 2013a).

1.3.3 *ADIPOSE TISSUE*

In comparison to other sources, adipose tissue is considered an ubiquitously available source, yielding high levels of MSCs, essential for tissue engineering and cell based therapies (Barry and Murphy, 2004; Gimble *et al.*, 2008). In addition, one gram of stromal vascular fraction (SVF) obtained from adipose tissue contains approximately five hundred times more MSCs than BM-MSCs (Strem *et al.*, 2005; Astori *et al.*, 2007; Varma *et al.*, 2007). Functionally, adipose tissue derived MSCs (AT-MSCs) and BM-MSCs are similar yet, some differences occur (Estes *et al.*, 2006; da Silva Meirelles *et al.*, 2009). At the level of CD marker expression, adipose tissue MSCs (AT-MSCs) are positive for CD73 (SH3), CD90 and CD105 (SH2) while they are negative for CD19 (a lymphoid biomarker), CD34 and CD45 (Zuk *et al.*, 2002; Schaffler and Buchler, 2007; Hass *et al.*, 2011; Jin *et al.*, 2013a). Other studies show that AT-MSCs possess the ability to express other CD markers such as CD9, CD13, CD54, CD106, CD146, HLA I, STRO-1 (Zuk *et al.*, 2002; Schaffler and Buchler, 2007; Hass *et al.*, 2011), CD29, CD44, CD166 (Hass *et al.*, 2011; Jin *et al.*, 2013a) and HLA ABC (Jin *et al.*, 2013a). On the other hand, AT-MSCs lack expression of specific CD markers such as CD19, CD34, and CD45 (Zuk *et al.*, 2002; Schaffler and Buchler, 2007; Hass *et al.*, 2011; Jin *et al.*, 2013a). Additionally, AT-MSCs express other markers for example, CD11b, CD14, CD 45, CD79α (a lymphoid

biomarker), HLA-DR (Hass *et al.*, 2011; Jin *et al.*, 2013a), CD31, CD133 and CD144 (Hass *et al.*, 2011). Adipose tissues are characterised by ease of access, non-invasive cell harvesting technique and high collection yields of MSCs (Baer and Geiger, 2012). Additionally, AT-MSCs are functionally similar to BM-MSC with mild differences such as AT-MSCs have higher proliferative potential while BM-MSCs have greater capacity to commit osteogenic and chondrogenic differentiation (Li *et al.*, 2015a).

1.3.4 *PERIPHERAL BLOOD*

Peripheral blood of normal individuals harbor MSCs (PB-MSCs) that share features and capacities of differentiation similar to these of BM-MSCs where they can differentiate into osteoblastic, chondrogenic, and adipogenic lineages. These cells therefore could serve as good candidates for repairing damaged cartilage. PB-MSCs are also capable of self-renewing and rapid proliferation *in vitro* (Zvaifler *et al.*, 2000). The surface of PB-MSCs are characterised by their ability to express CD44, CD54, CD105 (SH2) and CD166 (Cao and Dong, 2005; Tondreau *et al.*, 2005; Kuhbier *et al.*, 2010; Hass *et al.*, 2011). While they lack the expression of CD14, CD34, CD45 and CD31 (Cao and Dong, 2005; Tondreau *et al.*, 2005; Kuhbier *et al.*, 2010; Hass *et al.*, 2011). However, not all MSCs devoid of CD34 (Chong *et al.*, 2012). Kassis and colleagues have isolated PB-MSC and described them as positive for CD90 and CD105 (SH2) and negative for CD45 and CD34 (Kassis *et al.*, 2006). Trivanović and others found that PB-MSCs were negative for CD11a, CD33, CD45 and Glycophorin-CD235a (Trivanovic *et al.*, 2013). The main advantages of collecting PB-MSCs is the ease of isolation with multiple collections possible, while the drawback of this source is that the amount of isolated cells is limited and the donor requires treatment with granulocyte colony-stimulating factor (G-CSF) to mobilise the cells from the bone marrow (Kassis *et al.*, 2006).

1.3.5 *OTHER SOURCES*

Although the bone marrow is the original source of MSCs, other sources have been described since 1999 (Gabbay *et al.*, 2006) and many tissues have been successfully used to harvest MSCs (Rastegar *et al.*, 2010). Almost, all adult tissues contain MSCs but in low numbers such as periosteum, trabecular bone, synovium, skeletal muscle, deciduous teeth (Barry and Murphy, 2004), liver (Kassis *et al.*, 2006), spleen, cartilage,

tendon (Gimble *et al.*, 2008), dermis (Hua *et al.*, 2009), brain, periosteum and hair follicles (Zuk *et al.*, 2001; Amoh *et al.*, 2005a; Rastegar *et al.*, 2010). MSCs are also found in kidney (Bussolati *et al.*, 2005), dental pulp (Gabbay *et al.*, 2006), amniotic fluid (Perin (Perin *et al.*, 2008), limbus (Polisetty *et al.*, 2008), amniotic membrane (Diaz-Prado *et al.*, 2010) and adenoid tissues (Lee *et al.*, 2013). Also, Semedo and colleagues have reported that multipotent MSCs are found in almost every single tissue in the body and they could be isolated from these tissues and expanded *in vitro* keeping their ability of self-renew and differentiate into different linages of mesodermal origin (Semedo *et al.*, 2009). Furthermore, postnatal tissues and organs have been described as sources for MSCs; for example, articular cartilage, trabecular bone, deciduous teeth, muscle, adipose, periosteum, pericytes, synovial fluid (SF), synovial membrane, dermis and infrapatellar fat pad (Bianco *et al.*, 2008). Moreover, fetal organs for instance, lung (Hua *et al.*, 2009), pancreas, first-trimester blood (Kassis *et al.*, 2006), kidney, liver, bone marrow and the circulating blood preterm foetuses harbour MSCs (Miao *et al.*, 2006).

Although MSCs can be isolated from different tissues, they share the major criteria defining MSCs with minor differences related to their differentiation capacity and cell surface expression profile (Wagner *et al.*, 2005; Rastegar *et al.*, 2010). These differences were challenging to the scientists characterising MSCs (Dominici *et al.*, 2006).

1.4 IDENTIFYING CHARACTERISTICS OF MESENCHYMAL STEM CELLS

The International Society for Cellular Therapy (ISCT) has suggested minimal criteria defining human MSCs in an attempt to resolve this challenge (Hocking and Gibran, 2010). Three minimal criteria have been agreed to become consensus characteristics shared by human MSCs and many scientists (Oswald *et al.*, 2004; Dominici *et al.*, 2006; Hocking and Gibran, 2010; Blaber *et al.*, 2012; Wang *et al.*, 2012a) have referred to them in their research (Figure 1.1). These criteria are:

1. The isolated MSCs should possess plastic adherence ability.
2. More than 95 % of the isolated MSCs must express CD73 (SH3), CD90 and CD105 (HS2) and more than 98 % of the isolated MSCs do not express CD14, D19, CD34, CD45, CD11b, CD79a and HLA-DR surface molecules.
3. The isolated MSCs have the capacity to differentiate into osteoblastic, chondrogenic, and adipogenic lineages under *in vitro* standard differentiation conditions.

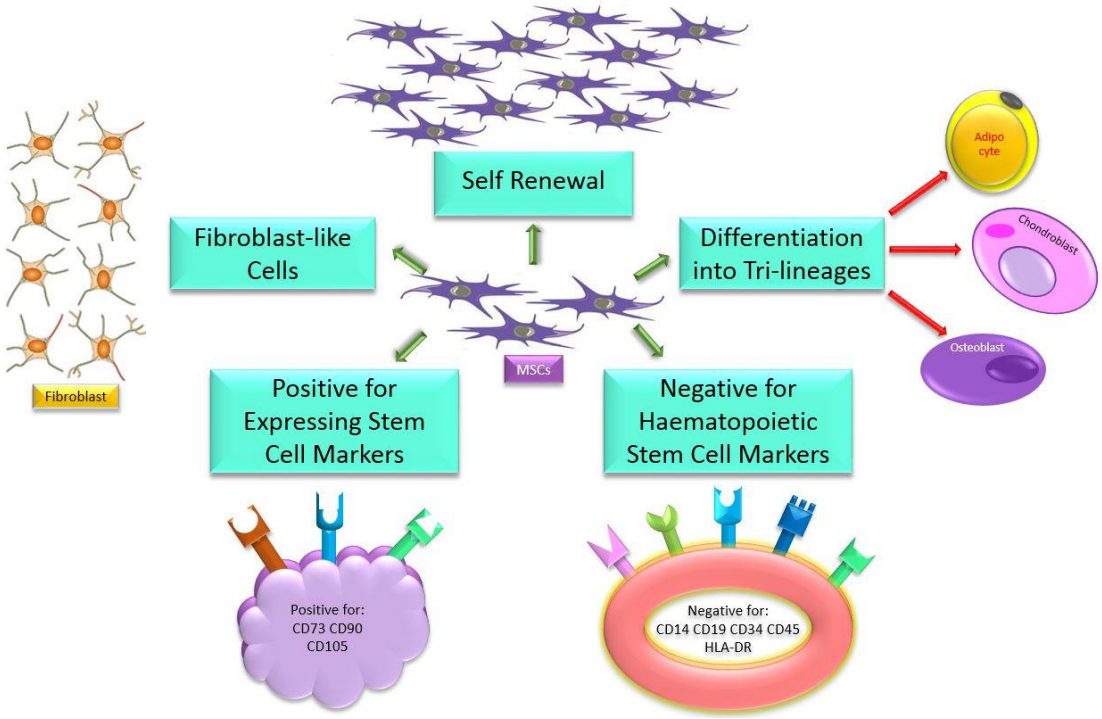

Figure 1.1 Identifying characteristics of MSCs using the ISCT criteria.

MSCs are fibroblast like cells able to re-new themselves in vitro*. They are positive for stem cell markers such as CD73, CD90 and CD105, while negative for markers of haematopoietic stem cell such as CD14, CD19, CD34, CD45 and HLA-DR. They also differentiate into three lineages; adipocyte, chondroblast and osteoblast.*

1.4.1 *MORPHOLOGY*

Morphologically, MSCs are characterised by a small longitudinal, thin body provided with long and thin appendages. Like other human cells, MSCs contain a round large nucleus with an obvious nucleolus surrounded by fine chromatin particles. Additionally, polyribosomes, mitochondria, rough endoplasmic reticulum and Golgi apparatus are present. Their extracellular matrix is filled with a few reticular fibrils while free of the other types of collagen fibrils (Brighton and Hunt, 1991). MSCs have also been described as spindle-shaped fibroblastic cells or polygonal with long processes and one nucleus and have the ability to form colonies after 7-10 days of *in vivo* plating (Xu *et al.*, 2004; Zhu *et al.*, 2006).

1.4.2 *IN VITRO CHARACTERISTICS*

MSCs look like spindle-shaped fibroblastic cells and start to form colonies, while after the second passage, they either keep the spindle-shaped cells or develop polygonal long

processes (Xu *et al.*, 2004; Zhu *et al.*, 2006). Digirolamo and colleagues reported that MSCs expand heterogeneously *in vitro*, even when using different samples from the same patient (Digirolamo *et al.*, 1999). MSCs can also be propagated keeping their differentiation potential into osteocytic, adipocytic and chondrocytic linages *in vitro* (Maxson *et al.*, 2012). In an attempt to investigate the *in vivo* characteristics of MSCs, most scientists cultured MSCs *in vitro*. However, the markers expressed under these conditions are determined by the culture conditions instead of the original characteristics of MSCs *in situ*. Therefore, it is difficult to characterise, track and detect the phenotype of MSCs *in vivo*; consequently, there are no agreed phenotypic characteristics to identify MSCs *in vivo* (Si *et al.*, 2011). Many researchers have shown that tissues play a role in determining the specific biomarkers of MSCs *in vivo*. For example, MSCs in bone marrow are enriched with Stage-Specific Embryonic Antigen-1 (SSEA-1) and SSEA-4 or enriched with CD133 from peripheral and umbilical cord blood (Tondreau *et al.*, 2005; Gang *et al.*, 2007; Si *et al.*, 2011).

1.4.3 *PHENOTYPIC MARKERS OF MESENCHYMAL STEM CELLS*

Considerable studies have been conducted aiming to identify certain MSC markers for detection, isolation, characterisation and evaluation of human MSCs populations. Amongst these efforts is the rise of monoclonal antibodies as reagents for detecting and isolation of human MSCs. An example of these antibodies is Stro-1 a monoclonal antibody which can react with non-haematopoietic progenitor stromal cells derived from human bone marrow (Simmons and Torok-Storb, 1991). Also, the differentiation potential of MSCs is consistent with Stro-1 since MSCs positive for this marker become osteocyte, adipocyte, chondrocyte, smooth muscle cells and HSC-supporting fibroblasts (Kolf *et al.*, 2007). However, Gronthos *and colleagues* suggested Stro-1 is an unlikely generic MSCs biomarker for two main reasons: first; it is not secreted by MSCs exclusively, second; it is gradually lost during MSC *in vitro* expansion (Gronthos *et al.*, 2003). Therefore, Stro-1 expression as an MSC identification marker should be in conjunction with other markers such as vascular cell adhesion molecule-1 (VCAM-1) which is involved in MSC chemotaxis, adhesion, and signal transduction (Carter and Wicks, 2001) and CD106 which could be an indicator for increasing frequency of CFU-F (Gronthos *et al.*, 2003). Another example of reagents for MSC detection are the SH-2n SH3 and SH4 antibodies

which do not react with haematopoietic cells (Haynesworth *et al.*, 1992; Kolf *et al.*, 2007). A further example is the SB-10 antibody which reacts specifically with CD166 (activated leukocyte-cell adhesion molecule, ALCAM). In addition, SB-10 can react with an antigen expressed on undifferentiated MSC cells and once these undifferentiated MSCs initiate osteogenesis, this antigen disappears and is replaced by alkaline phosphatase (Bruder *et al.*, 1998). For more details about MSC positive markers, see (Table 1.1).

1.4.3.1 *POSITIVE MARKERS*

The International Society for Cellular Therapy (ISCT) has minimised the criteria for defining human MSCs to be positive for CD73 (SH3/4), CD90 and CD105 (SH2) (Oswald *et al.*, 2004; Dominici *et al.*, 2006; Gimble *et al.*, 2008; Hocking and Gibran, 2010; Blaber *et al.*, 2012; Wang *et al.*, 2012a). However, other CD marker profile have been expressed by MSCs such as CD106, CD120a, CD124 (Baron and Storb, 2012), CD29 (b1-integrin), CD13, CD44, CD71 (Oswald *et al.*, 2004; Honczarenko *et al.*, 2006; Wu *et al.*, 2007; Motaln *et al.*, 2010; Parekkadan and Milwid, 2010; Baron and Storb, 2012), CD166 (ALCAM) (Motaln *et al.*, 2010; Parekkadan and Milwid, 2010; Baron and Storb, 2012), CD146, CD58, CD54 (intercellular adhesion molecule-1 [ICAM]-1), CD49e (a5-integrin) and CD10 (Motaln *et al.*, 2010; Parekkadan and Milwid, 2010) and CD271 (Quirici *et al.*, 2002; Motaln *et al.*, 2010; Parekkadan and Milwid, 2010). Also, MSCs strongly express typical surface antigens such as stem cells antigen-1 (Sca-1) (Wu et al., 2007), HLA class I (HLA-I) and they can be induced by IFN-γ to express HLA-II (Baron and Storb, 2012). Additionally, they can express combination of chemokine receptors for example, CXCR 1, 2, 3, 4 and 5, CCR 1, 4, 7, 9 and 10 and CX3CR1 (Patel *et al.*, 2013). It is therefore difficult to identify human MSCs with the use of specific markers.

1.4.3.2 *NEGATIVE MARKERS*

As per the ISCT, the minimal criteria for defining h-MSCs pertaining the negative markers are CD14, D19, CD34, CD45, CD11b, CD79 alpha and HLA-DR (Oswald *et al.*, 2004; Dominici *et al.*, 2006; Gimble *et al.*, 2008; Hocking and Gibran, 2010; Blaber *et al.*, 2012; Wang *et al.*, 2012a). Yet, there is an agreement that h-MSCs do not express CD3 (Oswald *et al.*, 2004; Wu *et al.*, 2007), CD14, CD34, CD45 (Baron and Storb, 2012), CD31, an endothelial and haematopoietic cells marker and CD117, a haematopoietic stem/progenitor cell biomarker (Kolf *et al.*, 2007; Motaln *et al.*, 2010; Parekkadan and

Milwid, 2010; Torsvik *et al.*, 2010), CD15, CD33 (Oswald *et al.*, 2004; Motaln *et al.*, 2010; Parekkadan and Milwid, 2010), CD38 (Oswald *et al.*, 2004), CD40 (Rastegar *et al.*, 2010), CD80, CD86 (Motaln *et al.*, 2010; Parekkadan and Milwid, 2010; Rastegar *et al.*, 2010). Moreover, h-MSCs do not express CD106 (vascular cell adhesion molecule [VCAM]-1), CD62E, CD62L, CD62P, CD50, CD49b, CD49d, CD49f, CD25, CD16, CD11a, CD8, glycophorin A and cadherin V (Motaln *et al.*, 2010; Parekkadan and Milwid, 2010). Accordingly, the criteria mentioned by Rastegar and colleagues that MSCs negative for CD40, CD80, CD86 and MHC II make these cells attractive candidate for treating human diseases especially allogenic stem cell transplantation without immunosuppression (Rastegar *et al.*, 2010).

1.4.3.3 *CONTROVERSIAL MARKERS*

Human MSCs populations express considerable variability in their cell surface markers. There is therefore no unique surface antigen specific to MSCs (Quirici *et al.*, 2002; Hocking and Gibran, 2010). Mabuchi and others (Mabuchi *et al.*, 2013) reported that most CD markers expressed by h-MSCs such as CD49a, CD73, CD105, CD106, CD271, MSC antigen-1, Stro-1, and SSEA-4 are not specific for MSCs; rather, they are widely expressed in stromal cells. CD106 is also considered as a positive marker for h-MSCs while other researchers have shown that h-MSC do not express CD106 (Motaln *et al.*, 2010; Parekkadan and Milwid, 2010; Baron and Storb, 2012). Additionally, other CD markers such as CD271/NGFR (Quirici *et al.*, 2002), CD10, CD13, CD29, CD44, CD90/Thy-1, CD105, foetal liver kinase 1 (Flk-1) /CD309 and Sca-1 (Honczarenko *et al.*, 2006) are often expressed on the MSC cell surface, but they lack specificity or consistent expression. Researchers have therefore reported an enormous variation in positive markers and each group of co-workers have used different subsets of markers. The lack of specific markers for h-MSCs represents the challenge of MSC identification (Kolf *et al.*, 2007) and attempts to investigate the true identity and function of these cells is still problematic (Mabuchi *et al.*, 2013).

<table>
<tr><th>Positive Markers</th><th>References</th><th>Negative Markers</th><th>References</th></tr>
<tr><td>CD73
CD90
CD105</td><td>(Oswald et al., 2004;
Dominici et al., 2006;
Gimble et al., 2008;
Hocking and Gibran, 2010;
Blaber et al., 2012;
Wang et al., 2012)</td><td>CD14
CD34
CD45</td><td>(Oswald et al., 2004;
Dominici et al., 2006;
Gimble et al., 2008;
Hocking and Gibran, 2010;
Baron and Storb, 2012;
Blaber et al., 2012;
Wang et al., 2012)</td></tr>
<tr><td>CD13</td><td>(Oswald et al., 2004;
Honczarenko et al., 2006;
Wu et al., 2007;
Motaln et al., 2010;
Parekkadan and Milwid, 2010)</td><td>D19
CD11b
CD79a
HLA-DR</td><td>(Oswald et al., 2004;
Dominici et al., 2006;
Gimble et al., 2008;
Hocking and Gibran, 2010;
Blaber et al., 2012;
Wang et al., 2012)</td></tr>
<tr><td rowspan="3">CD29
CD44
CD71</td><td rowspan="3">(Oswald et al., 2004;
Honczarenko et al., 2006;
Wu et al., 2007;
Motaln et al., 2010;
Parekkadan and Milwid, 2010;
Baron and Storb, 2012)</td><td>CD31
CD117</td><td>(Kolf et al., 2007;
Motaln et al., 2010;
Parekkadan and Milwid, 2010)</td></tr>
<tr><td>CD38</td><td>(Oswald et al., 2004)</td></tr>
<tr><td>CD40</td><td>(Rastegar et al., 2010)</td></tr>
<tr><td rowspan="2">CD106
CD120a
CD124
HLA-I
HLA-II</td><td rowspan="2">(Baron and Storb, 2012)</td><td>CD15
CD33</td><td>(Oswald et al., 2004;
Motaln et al., 2010;
Parekkadan and Milwid, 2010;</td></tr>
<tr><td>CD3</td><td>Oswald et al., 2004;
Wu et al., 2007)</td></tr>
<tr><td>CD166</td><td>(Motaln et al., 2010;
Parekkadan and Milwid, 2010;
Baron and Storb, 2012)</td><td rowspan="6">CD106
CD62E
CD62L
CD62P
CD50
CD49b
CD49d
CD49f
CD25
CD16
CD11a
CD8
glycophorin A
cadherin V</td><td rowspan="6">(Motaln et al., 2010;
Parekkadan and Milwid, 2010)</td></tr>
<tr><td>CD146
CD58
CD54
CD49e
CD10</td><td>(Motaln et al., 2010;
Parekkadan and Milwid, 2010)</td></tr>
<tr><td>CD271</td><td>(Quirici et al., 2002;
Motaln et al., 2010;
Parekkadan and Milwid,2010)</td></tr>
<tr><td>Sca-1</td><td>(Wu et al., 2007)</td></tr>
<tr><td colspan="2">Chemokine Receptors</td></tr>
<tr><td>CXCR1, CXCR2,
CXCR3, CXCR4,
CXCR5, CCR1,
CCR4, CCR7,
CCR9, CCR10,
CX3CR1</td><td>(Patel et al., 2013)</td><td>CD80
CD86</td><td>(Motaln et al., 2010;
Parekkadan and Milwid, 2010;
Rastegar et al., 2010)</td></tr>
</table>

Table 1.1 Positive and negative markers of MSCs.

MSCs are able to express a wide range of cluster of differentiation (CD) markers and many chemokine receptors. These markers enable MSCs to bind to a variety of growth factors, cytokine and chemokines and their activating ligands thereby MSCs participate in a wide range of cellular activities and treating many pathological conditions. On the other hand, MSCs determined as negative haematopoietic stem cell markers.

In addition to the phenotypic characterisation of MSCs, they could be characterised according to their differentiation potential.

1.5 DIFFERENTIATION POTENTIAL OF MESENCHYMAL STEM CELLS

It has been well documented that MSCs possess the ability to remain undifferentiated for long periods keeping, concurrently, their differentiation potency along unipotent (one lineage), multipotent (multiple lineages) or pluripotent (all three germ lineages) (Young, 2004; Hua *et al.*, 2009; Rastegar *et al.*, 2010) have described MSCs as progenitor cells with multipotency with the ability to differentiate into several types of cells. Other researchers have suggested that MSCs can differentiate into keratinocytes in epidermis, pericytes and endothelial cells *in vivo* (Li *et al.*, 2006; Hocking and Gibran, 2010). They can also differentiate into a multi-layered epidermis-like structure (Ma *et al*., 2009) and skin cells (Hua *et al.*, 2009). Additionally, MSCs in the skin adjacent to the wound, can differentiate into sebocytes of the sebaceous glands. Moreover, it has been reported that MSCs are capable of differentiating into tri-mesenchymal lineages, osteocyte, adipocytes and chondrocytes, under both *in vivo* conditions and *in vitro* culture (Deans and Moseley, 2000; Oswald *et al.*, 2004; Dan *et al.*, 2006; Dominici *et al.*, 2006; Rea *et al.*, 2009; Wang *et al.*, 2012a). Furthermore, BM-MSCs can differentiate into fibroblasts, and keratinocytes (Rea *et al.*, 2009), tendonogenic lineages (Majumdar et al., 2000), cartilage, bone, muscle, adipose tissues (Kadir et al., 2012), cardiomyogenic and neuronal lineages (Jackson *et al.*, 2007; Rastegar *et al.*, 2010). Figure 1.2 illustrates the differentiation potential of MSCs.

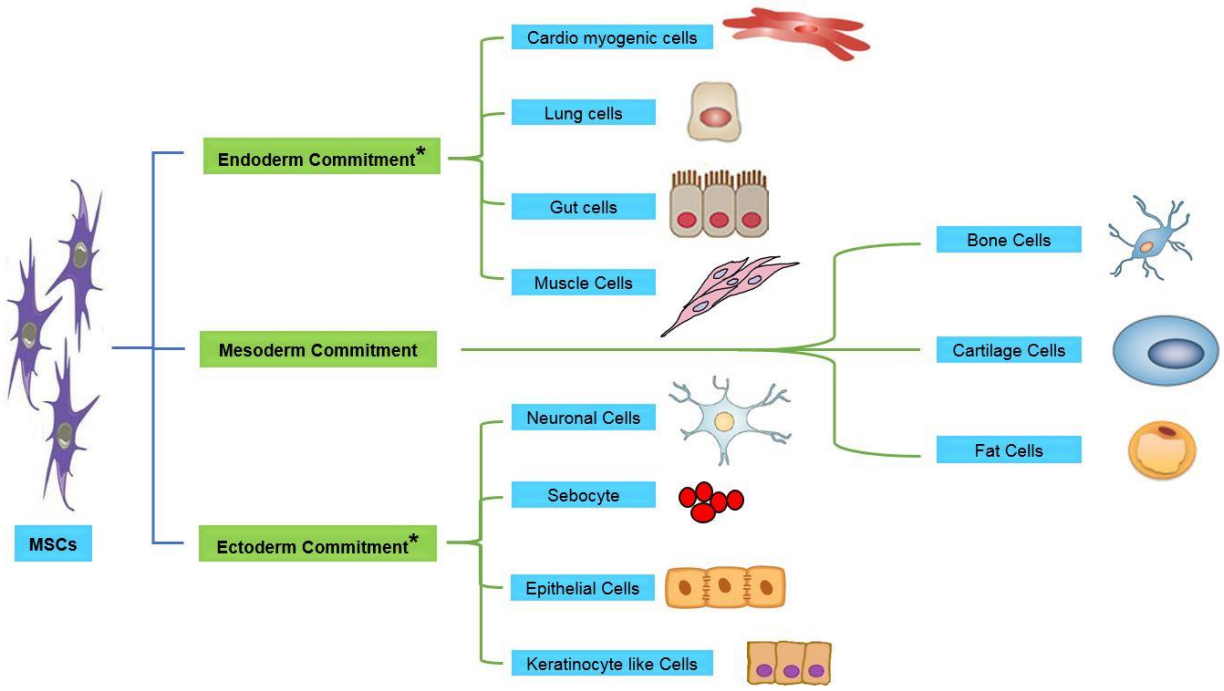

Figure 1.2 Differentiation Potential of MSCs.

MSCs are pluripotent stem cells and have the ability to differentiate into different cell types of all the germ layers, i.e., it is well documented that MSCs possess mesodermal commitment and differentiate into bone, cartilage and fat cells. * *The ability of MSCs to possess endodermal commitment, such as cardiosmyocyte, lung cells, gut cells and muscle cells and ectodermal cells including neurons, sebocytes, epithelial cells and keratinocyte like cells is still controversial and more studies are required to confirm these claims.*

In addition to their differentiation potential, MSCs are a promising target for cellular therapy because they secrete a wide range of biomolecules.

1.6 Biologically Active Substances Secreted by Mesenchymal Stem Cells

The potential of MSCs in regenerative medicine and wound healing has been illustrated by their secretion of biomolecules including growth factors, cytokines and chemokines (Chen and Tuan, 2008; Gnecchi *et al.*, 2008; Tamama and Kerpedjieva, 2012). Some 36 cytokines have been reported to be released by MSCs which act in concert to promote the wound healing process (Hwang *et al.*, 2009).

1.6.1 *GROWTH FACTORS*

Human MSCs secrete a wide range of growth factors that play a significant role in the wound healing process. These are; angiopoietins (ANGPT), connective tissue growth factors (CTGFs), epidermal growth factor (EGF), fibroblast growth factors (FGFs), insulin-like growth factors (IGF), keratinocyte growth factor (KGF), nerve growth factor (NGF), platelet derived growth factor (PDGF), transforming growth factor (TGF), vascular endothelial growth factor (VEGF) and scatter factors (SF) which are a family of growth factors also known as plasminogen-related growth factors (PRGFs), which include two members: hepatocyte growth factor (HGF) also referred to as plasminogen-related growth factor-1 (PRGF-1) and macrophage-stimulating protein (MSP) which is also known as scatter factor-2 (SF-2) or hepatocyte growth factor like protein (HGFL) (Table 1.2).

Growth Factors	Function(s)	Reference
ANGPT	ANGPT-1 is responsible for the stabilization of blood vessels and promotes wound closure	(Barrientos *et al.*, 2008b) (Chen *et al.*, 2008)
	ANGPT-2 causes vessel destabilization and remodelling	(Werner and Grose, 2003)
CTGFs	Stimulation of chemotaxis, proliferation of fibroblasts, and the induction of extracellular matrix proteins including fibronectin and collagen type I	(Werner and Grose, 2003)
	Promote endothelial angiogenesis, survival, migration, proliferation, and adhesion.	(Shimo *et al.*, 1999)
EGF	Reepithelialisation of skin wounds	(Alfaro *et al.*, 2013)
	Promotion of wound closure	(Werner and Grose, 2003)
FGFs	Exert a cytoprotective function in would repair , supporting cell survival under stress conditions	(Wang *et al.*, 2012a)
	Promotes mitogenic activity for keratinocytes and fibroblasts at the wound site. FGF1 and FGF2 stimulate angiogenesis. basic fibroblast growth factor (bFGF) enhances the proliferation of endothelial cells and smooth muscle cells.	
IGF	In association with heparin-binding epidermal growth factor (HB-EGF), IGF enhances the proliferation of keratinocyte in vitro. Mitogenesis and survival of many cells is stimulated by IGF-I and IGF-II promoting wound closure.	(Werner and Grose, 2003)
KGF	Promotes wound closure in two ways;	van de Kamp et al., 2013
	(1) it serves as a transporter for alveolar epithelial fluid	(Werner and Grose, 2003)
	(2) Play a role in tissue remodeling.	
NGF	Involved in fibroblast migration, increasing expression of actin by smooth muscle and collagen gel contraction by these cells	(Wang *et al.*, 2012a)
	Performs two functions in wound healing; (1) stimulation of keratinocyte proliferation and inhibiting apoptosis in vitro, (2) supporting the proliferation of human dermal microvascular endothelial cells and their adherence molecule expression.	(Maxson *et al.*, 2012)

PDGF	Stimulates DNA synthesis, attracting fibroblasts to wound sites, enhancing their production of collagenase, collagen and glycosaminoglycan	(Micera *et al.*, 2001)
	The first chemotactic growth factor participating in migration of fibroblasts, monocytes, and neutrophils into the skin wound, subsequently stimulating the production of extracellular matrix and the induction of a myofibroblast phenotype.	(Werner and Grose, 2003)
HGF or PRGF-1	It inhibits fibrosis and promotes re-epithelialisation	(Maxson *et al.*, 2012)
	Enhances keratinocytes to migrate, proliferate and produce matrix metalloproteinase and stimulates new blood vessel formation	
MSP	Accelerates cell migration and proliferation with regulation of proliferation and differentiation of keratinocytes and macrophages. plays an integral role in inflammation, proliferation and the remodelling phases of the healing process	(Werner and Grose, 2003)
TGF	Enhances proliferation of epithelial cells, expression of antimicrobial peptides and release of chemotactic cytokines	(Alfaro *et al.*, 2013)
	TGF-β1 activates keratinocytes and macrophages, while suppressing T-lymphocytes	(Werner and Grose, 2003)
	TGF-β3 stimulates remodelling	
	Activins which are members of TGF-β family act as enhancers for granulation tissue fibroblasts and the induction of extracellular matrix deposition	(Wang *et al.*, 2012a)
	Activin B supports wound repair and regeneration of hair follicles; promoting wound closure	(Maxson *et al.*, 2012)
VEGF	Regulates angiogenesis	(Zhang *et al.*, 2013)
	VEGF-α promotes wound closure	Werner and Grose, 2003 (Caplan, 2009)
	Promotes proliferation of endothelial cells	(Barrientos *et al.*, 2008b) (Chen *et al.*, 2008) (Maxson *et al.*, 2012)

Table 1.2 Growth factors secreted by MSCs and their roles in wound healing.

MSCs secrete a wide spectrum of growth factors. These biological substances participate in wound healing from early stages starting with haemostasis and coagulation and ending with remodelling. These growth factors promote angiogenesis, accelerate proliferation and also migration of endothelial cells. In addition, they are involved in the contraction phase, ending at the last stages of remodelling, leading to wound healing in the absence of scar formation.

1.6.2 *CYTOKINES*

Cytokines are small proteins secreted by many cell types which affect the activity of other cells including immune cells; they include interleukins, lymphokines and other signalling biomolecules including, prostaglandin E2 (PGE2) (Jackson *et al.*, 2012a), cathelicidin antimicrobial peptide, 18 kDa (CAP-18) (Krasnodembskaya *et al.*, 2010), granulocyte-macrophage colony-stimulating factor (GM-CSF) (Hocking, 2012), interferons and tumour necrosis factor (TNF) (Werner and Grose, 2003). Here, they are categorised into groups depending on their role in the wound healing process (Table 1.3).

Cytokine	Pro-inflammatory Cytokines Function(s)	Reference
IL-1α IL-1β IL-6 TNF-β	Stimulate proliferation of fibroblast and keratinocyte Enhance synthesis and breakdown of extracellular matrix proteins Control fibroblast chemotaxis Regulate immune response	(Grellner, 2002); Werner and Grose, 2003)
Cytokine	**Anti-inflammatory cytokines Function(s)**	**Reference**
PGE2	Possess multiple fibro-regulatory activities on the wound	(Jackson *et al.*, 2012a)
IL-1	Anti-inflammatory	(Ortiz *et al.*, 2007)
IL-4	Anti-inflammatory	(Blaber *et al.*, 2012) (Maxson *et al.*, 2012)
IL-13	Anti-inflammatory	(Blaber *et al.*, 2012)
CPA-18	Anti-microbial peptide Reduces inflammation	(Krasnodembskaya *et al.*, 2010)
Cytokine	**Proliferative cytokines Function(s)**	**Reference**
IL-10	limitation and termination of inflammatory responses	(Werner and Grose, 2003; (Nemeth *et al.*, 2009) (Maxson *et al.*, 2012)
	regulates differentiation and/or growth of keratinocytes and endothelial and various immune cells	(Moore *et al.*, 2001)
	It regulates infiltration of macrophages neutrophils into the wound site Promotes expression of pro-inflammatory cytokines Reduces matrix deposition Inhibits scar formation	(Werner and Grose, 2003)
IL-6	Regulates cellular responses	(Hocking, 2012)
	Promotes epithelial cell migration	(Tamama and Kerpedjieva, 2012)
	Angiogenesis formation	(Hocking, 2012) (Tamama and Kerpedjieva, 2012)
GM-CSF	Possess mitogenic activity for keratinocytes Stimulation of proliferation and migration of endothelial cells	(Werner and Grose, 2003)
	Regulates angiogenesis formation, cellular responses, and tissue remodelling	(Hocking, 2012)

Table 1.3 Cytokines secreted by MSCs and their roles in wound healing.

MSCs secrete a wide range of cytokines. These secretions initiate and terminate the inflammatory phase and accelerate proliferation and also migration of endothelial cells. In addition, they are involved in the contraction phase, ending at the last stages of remodelling, leading to wound healing in the absence of scar formation.

1.6.3 *CHEMOKINES*

Chemokines are a large family of small cytokines (8–10 kDa) (Rees *et al.*, 2015) responsible for stimulating chemotaxis and extravasation of leukocytes; hence referred to as so, they are called chemotactic cytokines (Werner and Grose, 2003). They could also be classified based on their functions; for example, inflammatory, homeostatic, or even

both (Rees *et al.*, 2015). Chemokine receptors are G-protein coupled receptors (GPCRs) spanning the lipid bilayer of the cell membrane of the target cell and possess both extracellular and intracellular domains (Mellado *et al.*, 2001). Upon binding to their receptors, chemokines exert their effect on the target cell, they stimulate a cytoplasmic signaling cascade and initiate several physiological processes such as migration, degranulation, and trafficking of leukocyte, myofibroblast recruitment, cell differentiation and angiogenesis (Rees *et al.*, 2015). Human MSCs release several chemokines that participate in wound healing, such as IL-8 and its receptor (CXCL8), macrophage chemoattractant protein-1 (MCP-1) ant its receptor (CCL2), macrophage inflammatory protein-1 alpha and beta (MIP-1α and MIP-1β) and stromal-derived factor 1 (SDF-1) (Table 1.4).

	Chemokine	Function	Reference
1	IL-8	Increase proliferation of keratinocyte Act as chemoattractant for neutrophils	(Rennekampff *et al.*, 2000)
		Enhances migration of epithelial cells	(Yew *et al.*, 2011; Tamama and Kerpedjieva, 2012)
2	MCP-1	Involved in macrophage infiltration	
		Act as inflammation regulatory	(Werner and Grose, 2003)
3	MIP-1α and MIP-1β	Promote wound closure	(Barrientos *et al.*, 2008b; Chen *et al.*, 2008)
		Increases macrophage trafficking	(Blaber *et al.*, 2012)
4	SDF-1	Regulates skin homeostasis and tissue remodelling	(Werner and Grose, 2003)
		Promotes wound closure	(Barrientos *et al.*, 2008b; Chen *et al.*, 2008)
		Induces cell migration	(Patel *et al.*, 2013)

Table 1.4 Chemokines secreted by MSCs and their roles in wound healing.

MSCs secrete chemokines. These biological substances participate in wound healing from early stages starting with haemostasis and coagulation and ending with remodelling. They also participate in the inflammatory phase and accelerate proliferation and also migration of endothelial cells. In addition, they are involved in the contraction phase, ending at the last stages of remodelling, leading to wound healing in the absence of scar formation.

1.6.4 *EXOSOMES (MSC-EXOSOME)*

Exosomes are tiny vesicles (30 or 40-100 nm in diameter) present in blood and urine and perhaps all other biological fluids that can be collected from *in vitro* cell culture (Booth *et al.*, 2006; Lai *et al.*, 2015; Zhang *et al.*, 2015b). They are Originated from the endosomal compartment and released from the plasma membrane into the extracellular environment to participate in coagulation, intracellular signalling communication and cytoplasmic

cleaning (Booth *et al.*, 2006; Muralidharan-Chari *et al.*, 2010; Lai *et al.*, 2015; Zhang *et al.*, 2015a). Like other exosomes, the main physiological role of MSC derived exosomes is communication through maintaining a dynamic and homeostatic niche for MSCs to communicate with multiple cell types and evoke cellular responses (Lai *et al.*, 2015). Collectively, these criteria make MSCs good candidates for a variety of clinical applications (Hocking, 2012) as discussed in the next section.

1.7 Clinical Application of Mesenchymal Stem Cells

As previously stated MSCs possess stem cell-like features including differentiation potential with multipotency and self-renewal capacities (Hass *et al.*, 2011; Hocking, 2012). Also, they activate a protective mechanism and stimulate endogenous regeneration (Caplan and Dennis, 2006). They can be found in nearly all body tissues (Amoh *et al.*, 2005b; Rastegar *et al.*, 2010; Hass *et al.*, 2011). Furthermore, they are characterised by their homing ability and a wide range of secreting profiles of bioactive molecules important for wound healing, tissue regeneration and certain cancers (Hass *et al.*, 2011). Moreover, the easy procedure of harvesting MSCs and their great plasticity are important characteristics for allogeneic and autologous cell mediated therapies (Song *et al.*, 2007). Finally and fortunately, MSCs have been considered as safe, with respect to therapeutics since no critical adverse side effects of MSCs have been detected during therapy (Patel *et al.*, 2013). Collectively, these characteristics and functions underlie the importance of MSCs in clinical application making them good candidates for regenerative medicine and tissue engineering (Hocking, 2012; Tamama and Kerpedjieva, 2012). MSCs are also characterised by proliferation and senescence which are very important concepts for researchers looking for new therapeutic strategies (Jin *et al.*, 2013a). The most popular application of MSCs in regenerative medicine is utilising them in wound healing and skin regeneration (Yeum *et al.*, 2013). However, MSCs have more clinical applications including ameliorating tissue damage in nearly all the major organs of the body such as skin regeneration, cardiac therapy, hepatic cirrhosis (Lau *et al.*, 2009; Hocking and Gibran, 2010; Si *et al.*, 2011), brain, lung, kidney and eye (Lau *et al.*, 2009; Hocking and Gibran, 2010). Additional applications of MSCs are pancreatic regeneration, neurological defects, limb ischemia, graft-versus-host disease (GvHD), rheumatoid arthritis, osteoarthritis (OA) and other bone and cartilage disorders (Si *et al.*, 2011).

1.7.1 *MESENCHYMAL STEM CELLS IN SKIN REGENERATION*

Wounding in higher organisms will evoke two types of biological responses; tissue regeneration and wound repair. MSCs leave their niche to the affected tissues and participate mainly in both responses (Fu and Li, 2009). Recently, skin regeneration especially cutaneous regeneration via MSC engraftment to heal wounds has significantly progressed because they can accelerate wound closure as well as re-epithelialization and angiogenesis. Notably, BM-MSCs transplanted into the injury site express keratinocyte specific protein (KSP) and form glandular structures (Wu *et al.*, 2007). One successful therapy was the induction of BM-MSCs, expressing the phenotypic characteristics of sweat gland cells (SGCs) *in vitro* and transplanting these cells into fresh wounds of deep burns. In five patients recovery of functional sweat glands with perspiration function occurred within 2–12 months follow up after the procedure, indicating that SGCs derived from MSCs were involved in the recovery of functional sweat glands (Sheng *et al.*, 2009). Another study focusing on chronic diabetic foot ulcers showed that injection of a biograft, consisting of a combination of MSCs and autologous skin fibroblasts, increased both the thickness and the vascularity of the dermis and reduced wound size when applied directly to the wound site (Vojtassak *et al.*, 2006; Fu and Li, 2009). Another study has investigated the differentiation potential of MSCs in skin regeneration and showed that MSCs acquire phenotypic characteristics of epidermal cells or vascular endothelial cells after *in vitro* culture in media supplemented with EGF or VEGF, respectively (Fu and Li, 2009). Finally, MSCs undergo transdifferentiation into keratinocytes enabling them to interact with original epidermal cells suggesting that MSCs can participate directly in tissue regeneration of both dermal and epidermal cells (Jackson *et al.*, 2012a). These characteristics, collectively, reveal the plasticity of MSCs making them a promising cellular source to regenerate skin; consequently, their potential use as a therapeutic technology for wound healing (Sheng *et al.*, 2009). However, more information is required about the use of MSCs before applying them as a therapeutic option, such as the MSC niche and factors required for MSC differentiation. In addition, the use of MSCs in the clinic is still challenging since it requires proof of concept MSC-therapy multi-centre large scale clinical trials (Si *et al.*, 2011).

1.7.2 *Utilisation and Mode of Action of Mesenchymal Stem Cells in Wound Healing*

MSCs are the pivotal player for coordinating the repair process by differentiation and secreting biologically active substances thereby recruiting other host cells. They are therefore involved in all phases of the healing process (Maxson *et al.*, 2012; Zahorec *et al.*, 2015). For instance, MSCs modulate the immune response (Yagi *et al.*, 2010; Blaber *et al.*, 2012) by enhancing the synthesis of anti-inflammatory cytokines including IL-10 and IL-4. They are also supress the production of pro-inflammatory cytokines such as tumor necrosis factor-alpha (TNF-α) and interferon-gamma (IFN-γ) (Aggarwal and Pittenger, 2005). Additionally, MSCs can evoke several mechanisms (see 1.8.1) which result in escaping the immune surveillance during immunosuppressive therapies (Sasaki *et al.*, 2008). Moreover, MSCs produce bioactive substances to act as inhibitors for fibrosis and apoptosis and to act as inducers for angiogenesis, mitosis and / or differentiation of progenitor cells, activating target cells or neighbouring cells to release biologically active substances (Caplan and Dennis, 2006). All in all, MSCs impact the whole phases of wound healing; inflammation, proliferation and tissue remodelling (Hocking and Gibran, 2010) including the cutaneous wound healing process (Rea *et al.*, 2009). Many recent studies suggest that MSCs are the main candidates for cell mediated therapies and tissue regeneration (Sasaki *et al.*, 2008) not only for their differentiation ability but also for their ability to produce active biomolecules (Caplan and Dennis, 2006). Therefore, differentiation and paracrine signalling have both been implicated as mechanisms by which MSCs recruit other host cells in all steps of the healing process to improve tissue repair (Hocking and Gibran, 2010). To better understand the role of MSCs in wound healing, their participation in repair can be divided into two major mechanisms; (1) cell mediated repair and (2) secretory mediated repair as illustrated in (Figure 1.3).

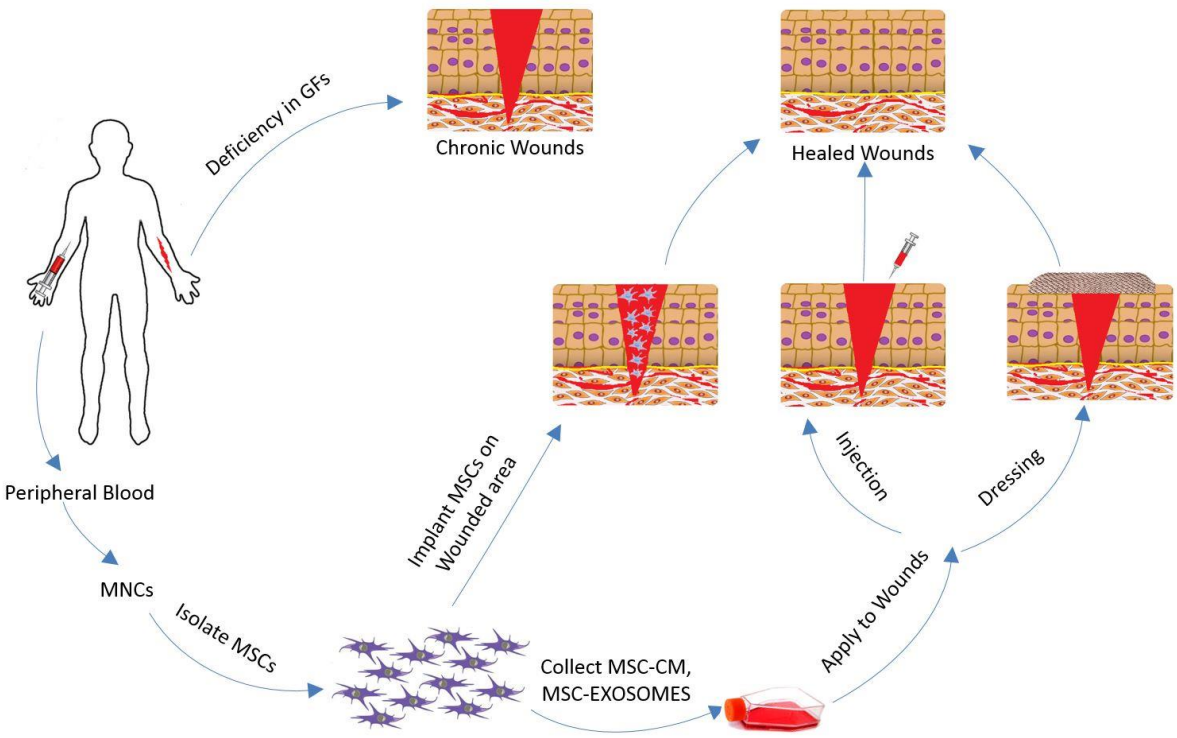

Figure 1.3 Potential applications of MSCs in wound healing.

MSC therapy contributes to skin wound healing via two mechanisms: (1) Differentiation into skin-like cells (SLCs), thereby compensating for the loss of cells due to damaged tissue. (2) Promote proliferation and migration of skin cells into the injury site by secreting soluble factors and macrovesicles. MSC secretions represented by MSC-CM and MSC-EXOSOME can be either injected onto the wounded skin area or applied on the skin wound using biofilm dressings.

1.7.2.1 *CELL MEDIATED REPAIR*

In vitro studies have shown that MSCs possess phenotypic properties resembling native dermal fibroblasts or myoblasts (Yamaguchi *et al.*, 2005). Furthermore, BM-MSCs may accelerate wound closure by differentiating into epidermal keratinocytes and other skin cells (Alfaro *et al.*, 2008; Hocking and Gibran, 2010). Recent studies have shown that MSCs undergo transdifferentiation into keratinocytes, epidermal cells and microvascular endothelial cells when cultured under defined culture conditions (Jackson *et al.*, 2012a) and express keratinocyte specific protein keratin (KSP) (Chen *et al.*, 2009; Chen *et al.*, 2015). MSCs therefore could be utilised for wound healing by transplanting aggregated MSCs into the injured tissue to increase collagen deposition and improve epithelisation (An *et al.*, 2015). They can also differentiate into other skin cells such as endothelial cells, keratin-14-positive cells and pericytes (Sasaki *et al.*, 2008), and when localised to blood vessels and dermis, sebaceous glands and hair follicles (Hocking and Gibran, 2010).

1.7.2.2 *SECRETORY MEDIATED REPAIR: ROLE OF MSC-CM*

Paracrine signalling of BM-MSC is the major mechanism by which these cells contribute to wound repair, where their secretory products impact on inflammation, fibrotic proliferation and angiogenesis (Gnecchi *et al.*, 2008). Many studies have reported that MSC-conditioned medium (MSC-CM) significantly promotes wound healing by affecting the pivotal steps of the repair process. The components of MSC-CM have accelerated epithelialization, and via chemotaxis recruited endothelial cells and macrophages to the injured site *in vivo* (Chen *et al.*, 2008). The MSC-CM recruits both epidermal keratinocytes and dermal fibroblasts to the wound site *in vitro* (Chen and Tuan, 2008; Hocking and Gibran, 2010). As well as its activity as a chemo-attractant, MSC paracrine secretions serve as regulators of cell migration in response to wounding leading to faster wound closure by regulating dermal fibroblast migration (Smith *et al.*, 2010). MSC secretory mitogens stimulate the proliferation of keratinocytes, dermal fibroblasts and endothelial cells (Kim *et al.*, 2007). MSC-CM contains all the effector biomolecules for tissue regeneration and wound healing by promoting migration, proliferation and differentiation of human skin cells such as fibroblasts and keratinocytes. Collectively, these data suggest that MSC-CM may represent a novel therapeutic strategy for wound therapy (Tamama and Kerpedjieva, 2012). Figure 1.4 summarises the participation of MSC secretions in wound healing.

1.7.2.3 *SECRETORY MEDIATED REPAIR: ROLE OF MSC-EXOSOMES*

It has been reported that MSC-EXOSOMES repair renal injury indicating that MSC-EXOSOMES are a potential mechanism which could be harnessed for wound healing (Li *et al.*, 2013; Zhang *et al.*, 2015a; Zhang *et al.*, 2015b). With respect to wound healing, MSC-EXOSOMES play an important role in collagen synthesis, the acceleration of cell migration and proliferation and in the formation of new and mature blood vessels (Zhang *et al.*, 2015b). Exosome healing action could be attributed to its ability to transfer RNA, microRNA and proteins into the injured tissues, participating in skin repair by promoting re-epithelialization and cell proliferation as well as activation of β-catenin, which plays a pivotal role in skin development and wound healing (Li *et al.*, 2013). Additionally, MSC-EXOSOMS have been shown to accelerate wound repair by mediating signalling cascades of some genes such as alpha serine/threonine kinase (Akt), extracellular signal-

regulated kinase (ERK), and signal transducer and activator of transcription 3 (STAT3) as well as by enhancing the expression of important growth factors i.e., HGF, IGF-1, NGF and SDF-1 which collectively accelerate migration and proliferation of fibroblasts in normal and diabetic wounds (Shabbir *et al.*, 2015). Moreover, MSC-EXOSOME reduces the levels of pro-apoptotic Bax gene, therefore inhibiting apoptosis of skin cells such keratinocytes and fibroblasts (Rani and Ritter, 2015; Zhang *et al.*, 2015a). Collectively, these data suggest the MSC-EXOSOMES play a significant role in wound healing.

The application of MSC-CM or MSC-EXOSOMES onto chronic wounds either by direct injection or by designing biological dressings enriched with MSC-CM or MSC-EXOSOMES, collected from autologous MSCs, may therefore provide a valuable therapeutic strategy.

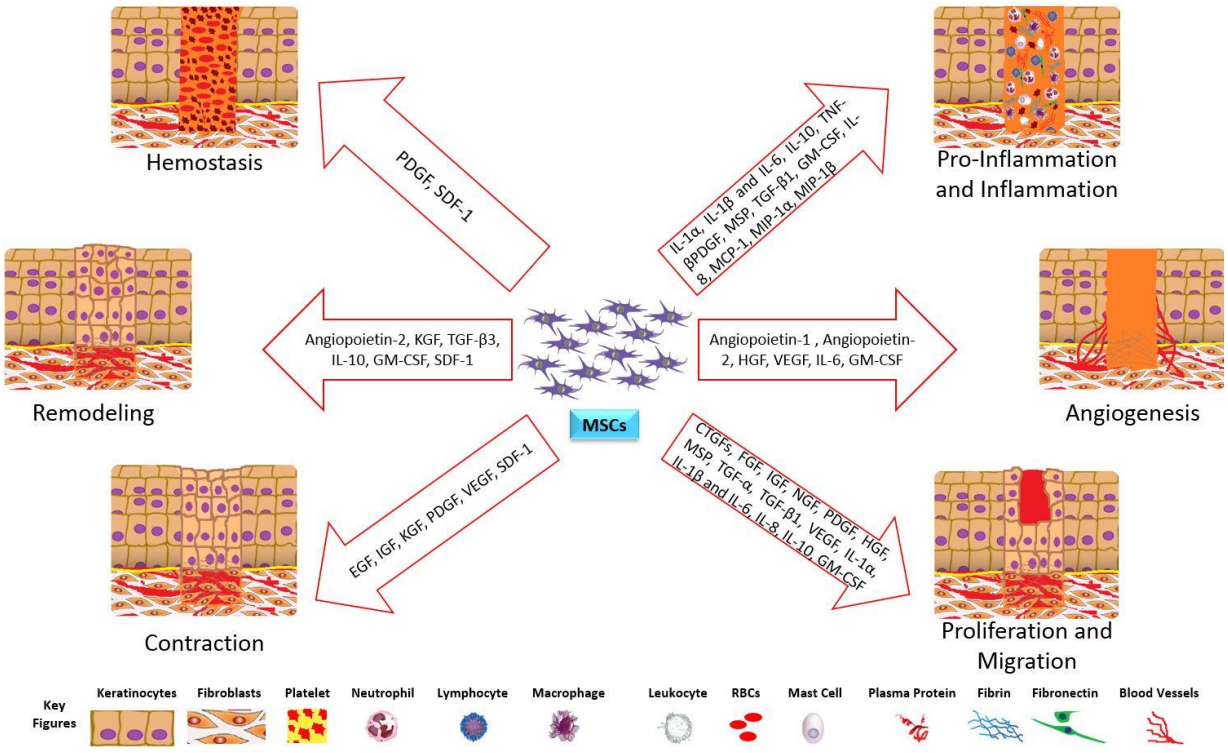

Figure 1.4 Participation of MSC secretions in wound healing phases and events.

MSCs secrete a wide spectrum of growth factors, cytokines and chemokines. These biological substances participate in wound healing from early stages, starting with haemostasis and coagulation and ending with remodelling. These secretions initiate and terminate the inflammatory phase and promote angiogenesis, accelerate proliferation and also migration of endothelial cells. In addition, they are involved in the contraction phase, ending at the last stages of remodelling, leading to wound healing in the absence of scar formation.

1.8 BENEFITS OF THE USE OF MESENCHYMAL STEM CELLS IN TREATING WOUNDS

1.8.1 *IMMUNOMODULATORY FEATURES OF MSCS*

In 2000, Liechty *et al.* were the first to recognise that MSCs possess unique immunologic features allowing them to persist in a xenogeneic environments and modulate the immune response (Liechty *et al.*, 2000). They have the potential to reduce inflammation and enhance wound repair (Nuschke, 2014). The exact mechanism by which MSCs modulate the immune system is not fully understood. The potential mechanism includes cell to cell direct contact, secretion of immune suppressive factors and interaction with other immune cells such as T-lymphocytes, B- lymphocytes, dendritic cells (DC) and natural killer (NK) cells (Popp *et al.*, 2008). In 2013 Patel and colleagues reported that MSCs suppress both the activation and proliferation of lymphocytes, in response to allogeneic antigens, as well as enhancing the development of CD8+ regulatory-T cells (T-reg) in suppressing an allogeneic lymphocyte response (Patel *et al.*, 2013). Additional immune suppressive activities of MSC include inhibition of differentiation of peripheral blood monocyte progenitor cells and CD34+ haemopoietic progenitor cells (HPC) into antigen presenting cells (APCs) (Djouad *et al.*, 2007). MSCs also inhibit the proliferation of NK cells mediated by IL-2 or IL-15 (Sotiropoulou *et al.*, 2006). MSCs have been shown to exert other immunomodulatory activities including altering the proliferation and activation of B-cells, IgG production, antibody secretion, chemoattractant behaviour, and reducing the expression of CD40, and CD86 and major histocompatibility complex class II (MHC-II) (Petrie Aronin and Tuan, 2010).

The ability of MSCs to modulate T-cell proliferation (Chamberlain *et al.*, 2007) and suppress the proliferation of B-cells (Corcione *et al.*, 2006) and NK cells (Sotiropoulou *et al.*, 2006) is well documented. By attenuating the function of these cells, MSCs reduce the pro-fibrotic process (Redd *et al.*, 2004). Importantly, by the secretion of prostaglandin E2 (PEG2) (Foraker et al., 2011) and IL-10 (Nemeth *et al.*, 2009; Maxson *et al.*, 2012). MSCs also regulate macrophage and lymphocyte function (Jackson *et al.*, 2012a). For instance, PGE2 attenuate mitogenesis and proliferation of T-cells in the wound (Djouad *et al.*, 2007) acting as co-operator in regulating the transition from Th1 cells into Th2 cells (Zanone *et al.*, 2010). On the other hand, IL-10 prevents the deposition of excessive collagen and inhibits the invasion of neutrophils into the wound and their release of

reactive oxygen species (ROS), which collectively participate in the prevention of scar tissue formation (Jackson *et al.*, 2012a).

1.8.2 *Migration and Engraftment Capacity*

Various studies have reported the capability of MSCs to selectively migrate to and engraft into the wound site and exert local functional effects on inflammatory reactions regardless of tissue type (Jackson *et al.*, 2012a; Wang *et al.*, 2012a). In this context, murine studies have shown that MSCs can home to the lung, adopting phenotypic characteristics of epithelium like cells and reducing inflammation in response to injury (Ortiz *et al.*, 2003). Another study in mdx mice, a strain of mice arising from a spontaneous mutation (mdx) in inbred C57BL mice, showed that MSCs may migrate to muscle tissues (Liu *et al.*, 2007). MSC migration has been shown to be regulated by a multitude of signals (Spaeth *et al.*, 2008) ranging from growth factors such as platelet derived growth factor (PDGF) insulin like growth factor-1 (IGF-1) and cytokines such as SDF-1, chemokines such as CCL5 and C-C motif chemokine receptors including; CCR2, CCR3 and CCR4 (Yagi *et al.*, 2010; Wang *et al.*, 2012a).

1.8.3 *Wound Closure Acceleration*

MSCs play a role not only in wound healing but also in accelerating the healing process by increasing the tensile strength of the healing wound (the ability of the healing wound to resist the tension) (Ireton *et al.*, 2013) and by reducing scaring (Hocking and Gibran, 2010). The effects of MSCs during wound healing include acceleration of epithelialization, an increase in angiogenesis and the formation of granulation tissue (Maxson *et al.*, 2012). These activities are attributed to the ability of MSCs to produce biologically active substances capable of accelerating the regeneration process (Mishra and Banerjee, 2012) including interlukin-8 (IL-8) and C-X-C motif ligand 1 (CXCL1), responsible for stimulating the migration of epithelial cells and accelerating wound closure (Yew *et al.*, 2011).

1.8.4 *ANTIMICROBIAL ACTIVITY*

Secretions of MSCs (MSC-CM) is capable of inhibiting bacterial growth. MSCs produce and release substantial amounts of the anti-bacterial substance known as human cathelicidin peptide-18 (hCAP-18) produced by the gene LL-37, characterised by itsability to retard *in vitro* growth of *P. aeruginosa* and *E. coli* (Krasnodembskaya *et al.*, 2010), thus, avoiding wound contamination and infectious complications which exacerbate the healing process (Guo and DiPietro, 2010).

1.8.5 *PREVENT CHRONIC CONDITION*

Besides having immunomodulatory activities, the effective biomolecules secreted by MSCs can prevent wounds from reaching a chronic state by their angiogenic and anti-apoptotic characteristics (Blaber *et al.*, 2012). For instance, transplantation of human MSCs intramyocardially, have the ability to improve cardiac function via enhancing myogenesis and angiogenesis in the ischemic myocardium (Liu *et al.*, 2008). MSCs also, enable a wound to progress to healing beyond the inflammation stage and not regress into a chronic state (Maxson *et al.*, 2012).

1.8.6 *ATTENUATION OF SCAR FORMATION*

The tissues in the scar have many disadvantages, including their undesirable visual appearance and lack of structures that are present in the native skin such as hair follicles, sebaceous glands and sensory nerve receptors (Jackson *et al.*, 2012a). In addition, scar tissue weakens the skin making it more susceptible to re-injury (Buchanan *et al.*, 2009). MSCs have been shown to overcome these disadvantages via attenuating scar formation (Jackson *et al.*, 2012b).

1.8.7 *NEUTRALIZING THE REACTIVE OXYGEN SPECIES (ROS)*

Although IL-10 participates in preventing the invasion of neutrophils into the site of tissue injury and the enhancement of collagen deposition, the penetrations of some populations results in the release of reactive oxygen species (ROS), which are oxygen molecules with unpaired electrons making them extremely reactive. These include superoxide, hydrogen peroxide and alkyl peroxides (Poli, 2000).

Many tissues are susceptible to attack by ROS contributing to dangerous diseases including heart disease and cancer. Also, prolonged persistence of ROS induces fibrogenesis and the accumulation of fibrotic tissues (Jackson *et al.*, 2012a). To counter such effects, MSCs significantly up-regulate the expression of nitric oxide synthase (Sato *et al.*, 2007) which alters the ROS balance eand prevents the formation of fibrotic tissues (Ferrini *et al.*, 2002).

1.8.8 *PRODUCING ANTI-FIBROTIC FACTORS*

MSCs release growth factors and cytokines characterised by their anti-fibrotic activities such as hepatocyte growth factor (HGF) and IL-10 (Li *et al.*, 2009). HGF has been shown to down-regulate the expression of collagen type I and type III by fibroblasts therefore attenuating fibrosis and scar formation (Mou *et al.*, 2009). Moreover, HGF impacts on the keratinocyte behaviour by promoting their migration, proliferation and expression of vascular endothelial growth factor A (VEGF-A), thereby generating a well granulated tissue with a high degree of vascularization and re-epithelialization (Jackson *et al.*, 2012a).

1.8.9 *ENHANCING DERMAL FIBROBLAST FUNCTION*

In response to the wounding process, fibroblasts present at the injury site produce additional quantities of extracellular matrix (ECM) to restore the integrity of the skin leading to scarred tissue (McAnulty, 2007). Also, many endothelial cells undergo epithelial-to-mesenchymal transition (EMT) under the effect of transforming growth factor beta 1 (TGF-β1) and become wound healing myofibroblasts (Jackson *et al.*, 2012b). Both of these actions affect the function of dermal fibroblasts. Therefore, MSCs present in the wound site enhance dermal fibroblast function by producing HGF and PGE2 which both play a role in inhibiting epithelial-mesenchymal transition (EMT) (Zhang *et al.*, 2006); and secrete biomolecules promoting the function of dermal fibroblast in wound healing (Smith *et al.*, 2010). MSCs therefore enable the cells present in the wound site to release ECM, similar to those produced by neighbouring dermal cells (Jackson *et al.*, 2012a).

1.8.10 *Promoting Angiogenesis and Vascular Stability*

It has been well documented that BM-MSCs play a major role in angiogenesis and microvascularisation via promoting proliferation, migration and differentiation of microvascular endothelial cells by producing basic Fibroblast Growth Factor (FGF) and VEGF-A (Renault *et al.*, 2009).

In the same way, more information about the skin and its structure is necessary in order for a better understanding of the healing process as discussed below.

1.9 Human Skin

Human skin represents the largest organ of human body since it constitutes approximately 15 % of the total adult body weight (Kanitakis, 2002). It serves many vital roles, such as protection against foreign invader microbes, thermal insulation, sensation, as well as homeostasis regulation. Therefore, a body with injured or damaged skin cannot perform such important functions and consequently, will be at risk of numerous complications including infection and fluid loss (Kanitakis, 2002; Xie *et al.*, 2010).

1.9.1 *Human Skin Layers*

Human adult skin is composed basically of three layers; epidermis, dermis, and hypodermis (subcutaneous) (Kanitakis, 2002; Banerjee and Sen, 2013) (Figure 1.5).

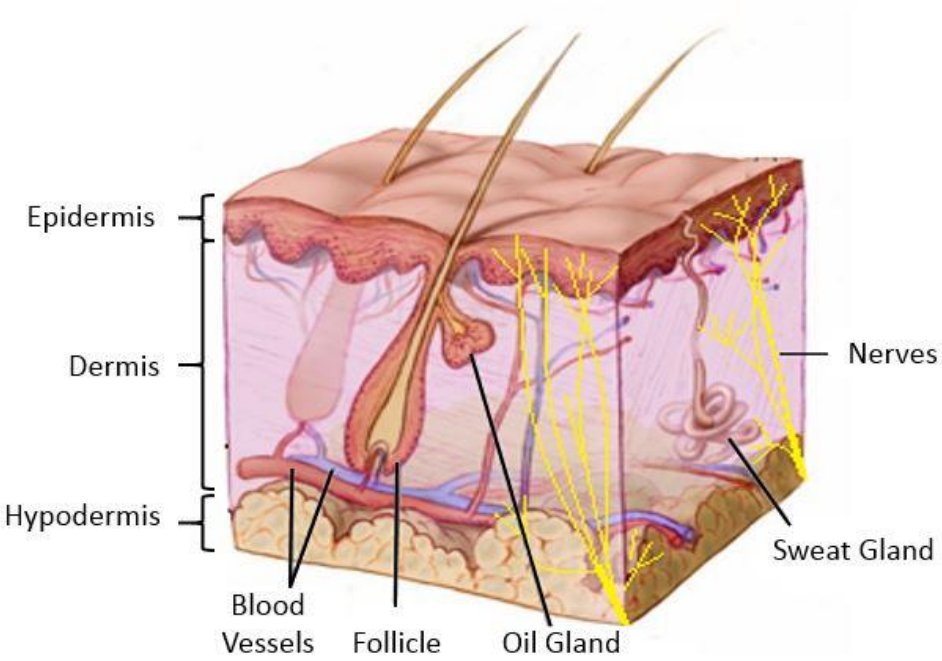

Figure 1.5 Simplified structure of human skin.

Human skin is composed of three cellular layers; epidermis and dermis separated by the basement membrane; and a lower subcutaneous layer. The skin also contains glands such as sebaceous (oil) glands and sweat glands; in addition to blood vessels, hair follicles and nerves. (Adapted from www.thinglink.com with some amendments).

1.9.1.1 *EPIDERMIS*

The epidermis consists of four stratum layers, the skin surface, basal, spinosum, granulosum and stratum corneum (Banerjee *et al.*, 2011) (Figure 1.6). Collectively, these layers constitute the epidermis, which represents the outer barrier of the human body. The keratinized stratified tissues provide a waterproof integral part of the body (Martin, 1997). The main cells present in the epidermis are keratinocytes, melanocytes, Langerhans cells and Merkel cells. Keratinocytes represent the dominant cell type in the epidermis since they constitute the vast majority of cells in the four epidermal sublayers. Keratinocytes in each layer express a panel of differential proteins which are used as biomarkers to detect keratinocyte differentiation. In the basal layer, basal keratinocytes express keratin 5 (K5), K14 and K15. During usual skin renewal, basal cells proliferate and differentiate into a spinous layer and express a different panel of proteins such as transglutaminase 1 & 5. The cells of spinous layer continue differentiating into a granular layer when cells express early differentiation markers such as K1, K2, K10, profilaggrin & transglutaminase 3.

Stratum corneum or the cornified layer is the late differentiating layer of epidermis. Cells in this layer express late differentiation markers such as loricrin, involucrin, trichohyalin, S100 proteins and small-molecules rich in protein (Chu and Weiss, 2002; Chu, 2008; Banerjee and Sen, 2013).

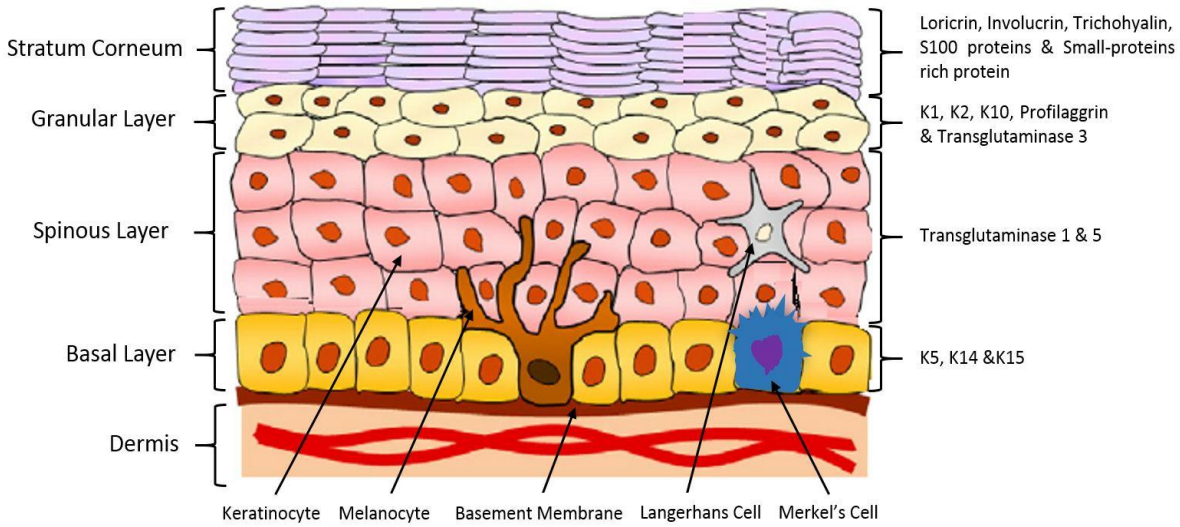

Figure 1.6 Simplified structure of human epidermis.

The epidermal layer is composed of four cell types; keratinocytes, melanocytes, Langerhans cells and Markel's cells. However, the epidermis does not contain blood vessels. [Adapted from (Visscher and Narendran, 2014) with some amendments].

1.9.1.2 *DERMIS*

The dermis represents the second supportive layer of the skin located beneath the epidermis and connected to each other by the basal membrane (Chu, 2008). Connective tissues, collagen and elastic fibres are the primarily components of the dermis, which support the skin against stress and strain (Martin, 1997). Another supportive component of the dermis is its base which is made of a glycosaminoglycan-proteoglycan fraction which in turn is composed of macromolecules (polysaccharides and protein) which play a vital role in tissue remodelling and wound repair (Banerjee and Sen, 2013). The main dominant cell types in the dermis are fibroblasts, mast cells, macrophages and lymphocytes (Banerjee *et al.*, 2011) in addition to blood and lymphatic vessels and hair follicles (Chu, 2008).

1.9.1.3 *HYPODERMIS*

The hypodermis is also termed subcutaneous tissue. It consists of elastin, connective tissue (mainly loose connective tissue) and fat which represent 50 % of the body's fat. The primarily cells available in this layer are fibroblasts, adipocytes and macrophages (Chu, 2008).

1.9.1.4 *BASEMENT MEMBRANE*

The basement membrane is a type of extracellular matrix composed mainly of proteoglycans, glycosaminoglycans, collagen IV, and laminin, in addition to a wide spectrum of growth factors which regulate several cellular activities (Mao *et al.*, 2015). It represents a junction between the dermis and the epidermis and binds to a variety of growth factors and cytokines to control the trafficking in both directions. It is therefore significantly involved during repair and remodelling (Iozzo, 2005).

1.9.2 *SKIN GLANDS*

Sebaceous glands are located all over the body, in the base of hair follicles, except the hands palms soles of the feet (Ro and Dawson, 2005). Their main function is thermoregulatory, when the skin is under cool or hot conditions keeping it emulsified by the action of sebum secreted by the glands (Porter, 2001). Sweat glands, primarily eccrine sweat glands are distributed all over the human body and concentrated mainly in the forehead, palms, soles of the feet and underarms. They contribute in re epithelialisation of wounded skin by generating outgrowths of keratinocytes which form a new epidermis (Rittie *et al.*, 2013).

1.9.3 *SKIN PROTEINS*

The most abundant protein present in human skin is collagen, constituting up to 75% of human skin. It contributes to anti-ageing by fighting wrinkles and lines. Unfortunately, collagen production is affected by many factors such as ageing and environmental conditions (Igarashi *et al.*, 1996; Tsukahara *et al.*, 2002). Elastin is related to skin wrinkling and sagging and provides structure for skin and organs in association with collagen in the dermis (Igarashi *et al.*, 1996; Tsukahara *et al.*, 2002). Another skin protein is keratin, which provides skin rigidity and is the strongest protein in the skin (Igarashi *et al.*, 1996).

1.9.4 *Other Skin Components*

Blood vessels besides their function in keeping our bodies at stable temperature, also play a significant role in maintaining tissue and repairing wounds (Amoh *et al.*, 2004). Hair follicles originate from fatty layers located in subcutaneous tissue and give rise to blood vessels thereby contributing to skin regeneration (Amoh *et al.*, 2005b). Nerves of the skin are mainly, related to skin sensation. They consist of unmyelinated small sensory fibres. During nerve formation, the number of the axons decreases and the somatic fibres become myelinated (Chu, 2008). The skin pigments melanin and haemoglobin are able to absorb sunlight and are the main chromophores responsible for skin colour. Melanin is produced by specific cells located in the epidermis called melanocytes and their main function is protecting the skin by absorbing and dispersing UV light (Igarashi *et al.*, 1996). In addition to skin cells, other cell types participate in the healing process as described below.

1.10 Cells Involved in Skin Regeneration and Wound Healing

1.10.1 *Keratinocytes*

The majority of cellular component of human epidermis are keratinocytes since they constitute 95 % of epidermal cells. They are found in the different layers of epidermis and referred to as the same name as the layer such as the basal keratinocytes. They are also found in the mucosa of the mouth and oesophagus and referred to as squamous keratinocytes. They tighten the nerves of the skin and serve as a junction between the epidermis and the dermis, keeping the epidermal Langerhans and the dermal lymphocytes in place (Pastar *et al.*, 2014). In wounded skin, keratinocytes have several critical roles and are involved in the complicated mechanisms of inception, maintenance and healing. In chronic wounds, healthy keratinocytes cross-talk with other cell types, and remove and replace unhealthy cells from a quiescent wound edge (Santoro and Gaudino, 2005).

1.10.2 *Fibroblasts*

Fibroblasts are a type of cells mainly present in the connective tissue of the body and responsible for producing ECM and collagen which together form the framework structure

of many tissues and play a pivotal role in tissue repair (Darby *et al.*, 2014). These types of cells present in two alternative states, as inactive fibrocyte and active fibroblasts (Mine *et al.*, 2009). The main function of the fibroblast is supporting the connective tissue and maintaining the integrity of tissue structures by secreting collagen, extracellular precursors and fibers (Eyden, 2005). Meanwhile, during angiogenesis, fibroblasts start migrating towards the wound site as the inflammatory phase terminates (two to five days post-wounding) and become the most dominant cell type at the injury site (Hinz and Gabbiani, 2003). Fibroblasts are important cells supporting the healing process and are involved in the main events such breaking down the fibrin clot, producing a new collagen structure and ECM to support other cells involved in the healing process and finally, in wound contraction (Darby *et al.*, 2014).

1.10.3 *IMMUNE CELLS*

Immune cells (mast cells, neutrophils, macrophages and lymphocytes) play important roles in the healing process of both normal and pathological repair. The immune system is activated immediately after the injury and immune-inflammatory cells are recruited from the blood circulation, and start the inflammatory response (Zhang and Mosser, 2008; Abbas and Lichtman, 2010). The first immune response is the arrival of mast cells to the wound site. Mast cells are a type of granular white blood cells, which have originated from myeloid stem cells and perform several roles including defence against pathogens, participate in immune-tolerance and involved ultimately in wound healing and angiogenesis (da Silva *et al.*, 2014; Polyzoidis *et al.*, 2015). However, circulating neutrophils infiltrate the wound quicker than other cells and become the most abundant immune cells at the injury site during the first two days post wounding (Eming *et al.*, 2007a; Wright *et al.*, 2010). Concurrently, circulating monocytes infiltrate into the wound site and start to differentiate into mature macrophages which in turn start phagocytic activity against the pathogens and cell debris, in addition to secreting collagenases and elastases to break down the damaged tissues (Ariel *et al.*, 2012). These macrophages also secrete mediators important to inflammation which activate many signals and act as chemoattractant to enhance leukocyte migration to the wound site (Sen *et al.*, 2009b). The late inflammatory response includes T lymphocytes which appear at the injury site while the number of other immune cells diminish, indicating the end of the inflammatory

phase and the start of the remodelling and resolution phase of the healing process (Martin and Leibovich, 2005). The activities of immune cells due to the inflammatory roles and promoting cellular cross-talk via secretion of cytokines (Strbo *et al.*, 2014) may have profound effects on the outcome of wound healing; in particular, fibrosis and scar formation (Martin and Leibovich, 2005). Understanding different wound types is also important for successful wound repair.

1.11 TYPES OF SKIN WOUNDS

Generally, wounds are classified on the basis of location, depth and tissue loss into three categories; superficial wounds where damage affects the epidermis only, partial thickness wounds when both the epidermis and dermis are involved, and full thickness wounds which involve the dermis, subcutaneous fats and sometimes, bone. However, depending on the normal healing trajectory there are two principal categories of skin wounds; acute and chronic (Monaco and Lawrence, 2003; Whitney, 2005).

1.11.1 *ACUTE SKIN WOUNDS*

Acute wounds arise either as a result of surgical incision or following traumatic accidents including abrasions, superficial burns, and partial thickness injuries with significant loss of tissues. Irrespective to their causes, the healing process of acute wounds is complex and utilises different types of cells and cytokines (Monaco and Lawrence, 2003).

1.11.2 *CHRONIC SKIN WOUNDS*

Wounds are defined as chronic when they fail to heal during one or all of the phases of the healing process causing an injury that cannot be repaired within the expected time period of normal wound repair (Maxson *et al.*, 2012). Chronic wounds mainly accompany disorders such as pressure ulcers, diabetes, burns, vascular insufficiency and vasculitis (Sen *et al.*, 2009b). The chronic state of non-healing wounds is exacerbated by many factors including tissue hypoxia, microbial infection, necrosis, exudates, and an elevated ratio of inflammatory cytokines during the different healing stages (Guo and DiPietro, 2010). Neutrophils also contribute by releasing excessive amounts of collagenase which leads to break down of the ECM (Diegelmann and Evans, 2004) and enzyme elastase

destroying important healing factors such as platelet-derived growth factor (PDGF) and TGF-β. Chronic wounds do not respond to therapy unless the prolonged inflammation is targeted (Maxson *et al.*, 2012). Consequently, human skin, with its limited abilities, will fail to heal itself in cases of wounds penetrating the epidermis (Jackson *et al.*, 2012a) due to the deficiency in growth factors and cytokines which are depleted during the healing process (Schönfelder *et al.*, 2005). The mechanisms of wound repair, phases of the healing process, and types of wounds are discussed below.

1.12 Phases of the Healing Process of Skin Wounds

Each wound undergoes a series of successive events for repairing and healing. These processes take from several minutes such as coagulation, several days such as inflammation to several months or years such as remodelling and can be divided into three, four or five overlapping phases and stages. Monaco and Lawrence stated that the wound healing process consisted of five distinct phases; (a) haemostasis, (b) inflammation, (c) cellular migration and proliferation, (d) protein synthesis and wound contraction, and (e) remodelling (Monaco and Lawrence, 2003). Others described the healing process as consisting of four highly integrated and overlapping phases: (a) haemostasis, (b) inflammation, (c) proliferation, and (d) tissue remodelling or resolution (Zhou *et al.*, 2013; Marfia *et al.*, 2015). Other scientists defined the normal wound healing mechanism is a dynamic and complex process involving a series of coordinated events, including (a) bleeding and coagulation, (b) acute inflammation, (c) cell migration, (d) proliferation, (e) differentiation, (f) angiogenesis, re-epithelialization and (g) synthesis and remodelling of ECM. Conversely, Maxson and colleagues reported that the healing process is a complex event occurring in three overlapping phases: (a) inflammatory, (b) proliferative, and (c) remodelling (Maxson *et al.*, 2012). These phases and their bio-physiological functions must occur in the proper sequence, at a specific time, and continue for a specific duration and intensity (Mathieu *et al.*, 2006). There are many factors that can affect wound healing which interfere with one or more phases in this process, thus causing improper or impaired tissue repair (Guo and DiPietro, 2010). All in all, a successful healing process cannot be accomplished without any one of these processes; haemostasis, inflammation, angiogenesis, proliferation, contraction, re-epithelialization

and remodelling (Jorgensen, 2003). To better understand the healing process, the five phases are further discussed together with how they overlap.

1.12.1 *Haemostasis Phase (Coagulation)*

During blood circulation in an intact blood vessel, endothelial cells of the blood vessel secrete coagulation and aggregation inhibitors i.e. they release heparin like molecules to prevent blood coagulation and thrombomodulin to prevent platelet aggregation. Prostacyclin and nitric oxide are also involved in this process (Mendonça and Coutinho-Netto, 2009). In contrast, the endothelial cells of broken blood vessels replace the secretions of clot inhibitors with a blood glycoprotein called von Willebrand Factor (vWF) which initiates haemostasis (Rasche, 2001; Mendonça and Coutinho-Netto, 2009).

Haemostasis is the first phase of wound healing and consists of three successive steps; vasoconstriction, blockage of the wound by platelet aggregation and blood coagulation. When skin is injured, a blood extravasation begins to fill the injured site. Immediately after the skin injury and bleeding, the blood vessel contracts and reduces the blood flow to the wounded site thereby keeping the blood within the damaged vessel and causing bleeding to stop (Rasche, 2001; Versteeg *et al.*, 2013). Not only do vessel contractions stop haemorrhage, but also, blood changing from a liquid phase to a gel phase forming a blood clot (coagulation) and platelet aggregation generates a haemostatic buffer (plasma) which is rich in fibrin, thereby stopping the haemorrhage and restoring a barrier protecting the wound from infection by invading microorganisms. This process constitutes a matrix that encourages cell migration (Eming *et al.*, 2007b). In this phase, the role of platelets is not only restricted to blocking the damaged area and in clot formation, but also in the formation of a transient extracellular matrix by secreting adhesion molecules such as fibronectin and thrombospondin, as well as, growth factors such as epidermal growth factor (EGF), PDGF, TGF-α and TGF-β, and vascular endothelial growth factor (VEGF) (Streit *et al.*, 2000). This matrix serves as a reservoir for growth factors and cytokines critical to the subsequent healing phases (Eming *et al.*, 2007b). Collectively, the matrix, activated cascade coagulation, and parenchymatous cells make the injured vessel a chemotactic environment to attract inflammatory cells at the wound site and initiate the start of the inflammatory phase (Clark, 1996).

1.12.2 *INFLAMMATORY PHASE*

An inflammatory reaction begins soon after the haemorrhage stops at the site of injury. This reaction promotes mobility of various cells toward the injured tissue giving rise to a multitude of complicated and successive series of reactions ending with rebuilding of a tissue like structure (Midwood *et al.*, 2004). The main advantages of this phase are isolating the injured tissues from the surrounding contaminated environment, cleaning out cell debris and damaged tissues and the initiation of the healing process (Abbas and Lichtman, 2010). The main reactivity observed in this phase is an increased migration of inflammatory cells from intravascular tissue towards the extracellular wound site due to increased vascular permeability. This permeability increases due to vasodilation when both fibrin and thrombin are activated by the coagulation cascade. Meanwhile, clot formation and their stimuli are dissipated and plasminogen converted to plasmin (Sherwood and Toliver-Kinsky, 2004). Three main cell types are involved in the inflammatory phase, neutrophils, macrophages, and lymphocytes whose activity is initiated within hours of injury (Midwood *et al.*, 2004; Abbas and Lichtman, 2010). Neutrophils seem to be the most dominant cell type during the first 48 hours, cleaning the wound site from bacteria, cell debris and damaged tissue by releasing free radicals. However, they are not essential for the healing process (Eming *et al.*, 2007b; Wright *et al.*, 2010). Approximately 48 hours following the injury, stimuli for neutrophils no longer persist and neutrophil numbers cease when macrophages (monocyte-derived macrophages) penetrate the wound site via the blood and become the dominant cellular component of the inflammatory phase by phagocytosing cell debris and bacteria including expended neutrophils. Macrophages also secrete collagenases and elastases to break down the damaged tissues (Ariel *et al.*, 2012). In contrast to neutrophils, the role of macrophages is not restricted to cleaning of the tissues, as they also play a crucial role in the healing process by secreting prostaglandins, which act as vasodilators increasing microvessel permeability and attracting other inflammatory cells into the wounded site (Tonnesen *et al.*, 2000; Eming *et al.*, 2007b). In addition, macrophages secrete fibroblast growth factors (FGF), PDGF, TGF-α, and VEGF which are important for proliferation and migration of fibroblasts as well as cytokines, which attract endothelial cells to the injury site promoting their proliferation and the development of a tissue (Swirski *et al.*, 2009; Ariel *et al.*, 2012). Within three days of the inflammatory phase, T-lymphocytes home to

the injury site by the activity of interlukin-1 and secret lymphokines such heparin-binding epidermal growth factor (HB-EGF) and basic fibroblast growth factor (bFGF), promoting fibroblast proliferation (Ross, 1994).

1.12.3 *PROLIFERATION PHASE*

The proliferation phase (epithelial proliferation phase) represents the main phase responsible for actual wound closure. In the case of skin wounds, endothelial non inflammatory cells such as keratinocytes and fibroblasts start to proliferate and migrate towards the edges of the wound producing collagen for the development of new tissues (Santoro and Gaudino, 2005; Bellayr *et al.*, 2010). Within a few hours (between 6 and 24 hours) of injury, TGF-ß and EGF act as mitogenic and chemotactic stimulators attracting keratinocytes which migrate towards the wound and start epithelialization (Usui *et al.*, 2008a). Fibroblasts are activated and start to differentiate into myofibroblasts which participate in reducing the wound size by contracting and secreting ECM proteins giving rise to healing of the connective tissue (Li and Wang, 2011; Li *et al.*, 2011b). Meanwhile angiogenesis progresses, co-ordinating the transfer of nutrients and oxygen from newly formed capillaries to the wound site enhancing metabolic activity (Dvorak, 2002). Epithelisation, fibroplasia and angiogenesis collectively comprise granulation tissue which covers the damaged tissues within four days of injury (Bellayr *et al.*, 2010).

1.12.4 *CONTRACTION PHASE*

Wound contraction could be defined as mobility of the wound margins towards the wound core to facilitate closure. This phase begins when fibroblasts stop proliferating and undergo apoptosis within 5-15 days post injury which occurs concurrently with collagen synthesis (Eichler and Carlson, 2006; Hinz, 2006). The rate of movement of wound edges depends on tissue laxity and wound shape. For instance, the looser tissues tend to contract more rapidly than the compact tissues and squared wounds contract more quickly than rounded wounds. The contraction rate also depends on the availability of myofibroblasts and their proliferation and connection to the surrounding extracellular matrix (Newton *et al.*, 2004).

1.12.5 *REMODELLING PHASE (RESOLUTION)*

Remodelling or resolution is the last phase of the wound healing process. The biological processes observed in this step involve gradual resolution of the inflammatory phase, collagen deposition, complete coverage of the injured site by the new tissues and formation of scar tissue (Mora and Pessin, 2002). Successful remodelling requires stable collagen content, therefore, the important step in this phase is controlling collagen remodelling (Zhou *et al.*, 2013). Although collagen synthesis is continuing during this phase, its level is restricted due to the activity of collagenases and metalloproteinases which aid in removing the excess collagen (Greenhalgh, 1998; Ruszczak, 2003). For optimal remodelling, collagen levels need to be balanced by the activity of metalloproteinases inhibitors secreted by tissue and which arrest the collagen lytic enzymes and balance the production of new collagen with that of the removed old collagen (Ruszczak, 2003). The outcome of this process is that collagen type III is replaced by collagen type I, hence replacing both hyaluronic acid and glycosaminoglycans by proteoglycans and the disappearance of fibronectin as well as resorbing water from scar tissues. These events start approximately 3 weeks after the injury and may last indefinitely as collagen fibres stack closer to each other decreasing scar thickness and increasing wound bursting strength “resistance to rupture” (McDougall *et al.*, 2006).

As described above, the main issues in the wound healing process are how cells are attracted to the site of injury and how their proliferation and differentiation is enhanced at the wounded region. These cells include inflammatory cells (neutrophils, macrophages and lymphocytes) and epithelial cells (fibroblasts and keratinocytes). All these activities are mainly regulated by growth factors and cytokines. In many cases these cells fail to migrate, proliferate and differentiate due to deficiency in growth factors and cytokines; consequently, the healing process will be impaired and chronic wounds will arise (Usui *et al.*, 2008a). Therefore, in order to improve wound healing, there is a need for an alternative source of healing cytokines and growth factors to enrich the injury site. MSC-CM acts as a rich source of 36 growth factors, cytokines and chemokines which, collected from MSC *in vitro* under good manufacturing practice (GMP) could be used as therapy for wounds in the future (Hwang *et al.*, 2009). For further detail about the phases and events of the healing process see (Table 1.5).

Phase	Haemostasis	Inflammation	Proliferation Migration	Contraction	Remodelling
Starts post injury	Immediately	First hours	Day 4	Day 5	Day 20
Duration	(minutes-hour)	(3 days-14 days)	(3 weeks)	(10 days- 20 days)	(Months-2 years)
Events	Haemorrhage	Phagocytosis	Endothelial cells migration	Fibroblast apoptosis	Collagen control remodelling
	Vasoconstriction	Growth factors secretion	Epithelialization	Wound edges pull	Replacing collagen type III by type I
	Platelet aggregation	Cytokines secretion	Fibroblast differentiate into myofibroblasts	Wound Closure	Disappearance of fibronectin
	Blood coagulation	Synthesis of preliminary ECM	ECM Production	Scar maturation	
		Immuno-modulation by T-lymphocytes	Angiogenesis	Collagen fiber cross linking	
	Migration of inflammatory cells		Collagen production		
	Activation of coagulation cascade		Granulation		
		Fibroblast migration			
		Fibroblasia			
Healing Progress	(A) Wound initiated	(B) Healing not initiated	(C) Progressive Healing	(D) Healed	(E) Healing Complete

Table 1.5 The main phases and events of the wound healing process.

Main phases and events of the wound healing process which are divided into five overlapping phases. (A) The wound is not healed and there is a possibility to reach a chronic state if the coagulation phase fails. (B) The wound is still not healed but it is progressing towards healing; however, if inflammation is not terminated, a chronic condition has a chance to be initiated. (C) The active healing process has been initiated. (D) Development of the healing process with less chance of progression to a chronic condition. (E) Complete healing and remodelling.

In addition to the cellular components of wound repair, micro molecules are also vital for the healing process, in particular, micro ribonucleic acids (microRNAs).

1.13 Roles of Micro Ribonucleic Acids (MicroRNAs) in Wound Healing

Micro RNAs are single stranded, short sequence (19-24) nucleotides (ntds) in length originated from endogenous non-coding RNA genes. They target the 3′-untranslated region (3′UTR) of messenger RNA (mRNA) and suppress the expression of proteins produced by these coding genes (Aberdam *et al.*, 2008; Banerjee *et al.*, 2011; Schneider, 2012; Mills *et al.*, 2013). MicroRNAs were first discovered by (Wightman, et al, 1993) when they found that small sequences of lin-4 RNAs (miRNA-lin14) pairs to sites in the 3′UTR of *lin-14* gene, formed multiple RNA duplexes and terminated the translation process

resulting in downregulation of the expression of the gene lin-14 in *Caenorhabditis elegans*. MicroRNAs are the major group of non-coding RNAs; approximately, 1000 microRNAs regulate gene expression of almost 33 % of the coding genes (Pritchard *et al.*, 2012; Mills *et al.*, 2013). These small sequences can regulate gene expression post-transcription by binding to their target mRNA resulting either in mRNA degradation or translation suppression or both (Wei *et al.*, 2010; Banerjee *et al.*, 2011). They may even suppress gene activation (Moura et al., 2014). Interestingly, more than one gene could be regulated by an individual microRNA and similarly, more than one microRNA could affect one gene (Li *et al.*, 2015e). The main function of these highly conserved microRNAs is regulation of gene expression post transcription, therefore, they have been involved in many biological process such pathogenesis of disease and considered as promising therapeutic strategies and demonstrating great potential as diagnostic biomarkers for diseases (Moura *et al.*, 2014). In the field if dermatology, microRNA research is promising and the early findings are suggesting new strategies for developing effective therapies and providing novel opportunities for treating skin diseases and addressing major global health concerns such as chronic wounds (Sen and Roy, 2008; Banerjee *et al.*, 2011). Moreover, microRNAs have been reported to serve as critical regulators in wound repair and skin regeneration by controlling cell division, differentiation and apoptosis of skin cells (Mills *et al.*, 2013). However, investigating the key microRNAs in wound healing and their activities is still in its early stages and more studies are required to develop this field (Li *et al.*, 2015e).

1.13.1 *Biogenesis of MicroRNA*

MicroRNA synthesis is a highly regulated process with remarkably well coordinated steps which start at the nucleus and terminates in the cytoplasm by producing mature-microRNAs (Kim *et al.*, 2004). As shown in (Figure 1.7), RNA polymerase III binds to microRNA coding genes, present in the human genome and transcribe long capped and polyadenylated fragments consisting of several kilobytes of nucleotides termed to primary microRNA (pri-miRNA). Drosha and two other microprocessor enzymes (RNase III and DGCR8) cleave the pri-microRNA into smaller sequences (approximately 70 nucleotides in length) referred to as premature microRNA (pre-microRNA). The export system transports this pre-microRNA from the nucleus to the cytoplasm by the action of Ran-GTP-dependent nuclear export factor (exportin-5) where the Dicer, an RNA polymerase

enzyme, cleaves the pre-microRNA into shorter sequences (18-24 nucleotides in length) of double stranded RNA (dsRNA). Then, a microRNA-induced-silencing-complex (RISC) associates with dsRNA and degrades one of its strands resulting in single stranded RNA which is the mature microRNA (microRNA). This microRNA starts its activity to target specific mRNAs by binding to a complementary sequence at a certain site known as a seed sequence or 3'UTR (Ha and Kim, 2014; Melo and Melo, 2014). The outcome of this binding will be either mRNA degradation, translation inhibition or suppression of chromosome assembly, consequently, suppressing gene expression (Ha and Kim, 2014; Melo and Melo, 2014; Moura *et al.*, 2014).

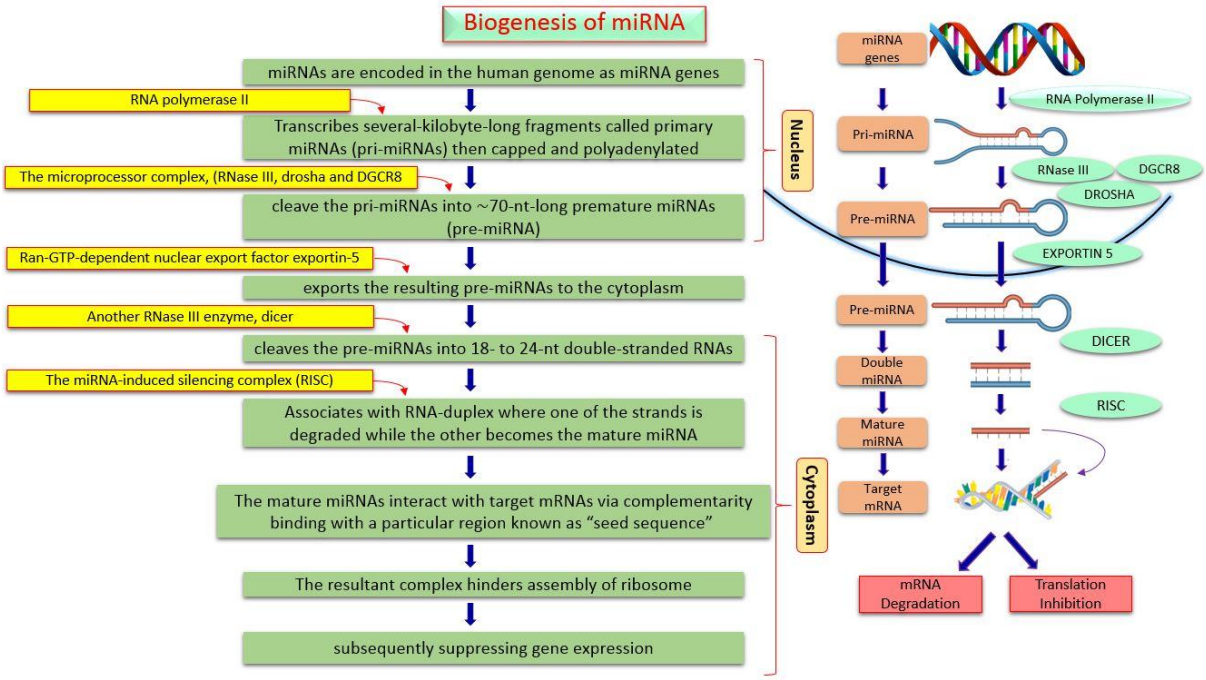

Figure 1.7 Biogenesis of microRNA.

This diagram explains microRNA biogenesis. In the nucleus, RNA polymerase III binds to microRNA coding genes and transcribes long fragments called primary microRNA (pri-microRNA). A group of three enzymes (RNase III, DROSHA and DGCR8) cleave the pri-microRNA into shorter sequences (~70-nts-long) to form the pre-mature microRNA (pre-microRNA). Then exportin-5 transport the pre-microRNA into the cytoplasm when another RNase enzyme called DICER split it into smaller double stranded RNAs (18-24 -ntds-long). The RISC associates with these double stranded RNAs and degrades one strand, while the other strand become the mature microRNA. These microRNAs start their activity by binding to a complimentary specific sequence called "seed sequence" on the target mRNAs and prevent ribosome assembly resulting in either degradation of mRNA or inhibition of translation, or both.

1.13.2 *Roles of MicroRNAs in Skin Development and Morphogenesis*

It has been well documented that microRNAs are responsible for regulating gene expression during skin development. Subsequently, they are important in development and maintenance of human skin including epidermis, dermis and adult skin stem cells (Pastar *et al.*, 2012; Banerjee and Sen, 2013). Notably, Dicer, the main microRNA processing enzyme, is found in the epidermal layer and the hair follicle (Andl *et al.*, 2006; Pastar *et al.*, 2012). It has been found that mice lacking Dicer will die early to a lack of skin development (Schneider, 2012). Other evidence suggests that microRNAs play significant roles in skin morphogenesis, starting with organizing renewal of skin stem cells and their differentiation into basal epidermal cells and migration of these cells from the basal membrane to differentiate into other epidermal layers (Fuchs, 2008; Blanpain and Fuchs, 2009). The most highly expressed microRNAs in human skin are miR-16, miR-21, miR-27a, miR-27b, miR-30b, miR-34a, miR-125a, miR-125b, miR-126, miR-143, miR-152, miR-191, miR-203, miR-205, miR-214; miR-19/-20 family including (miR-19b, miR-20, miR-17-5p and miR-93); miR-199 family including (miR-199a and miR-199b) and miR-200 family including (miR-200a, miR-200b, miR-200c, miR-141, and miR-429) (Banerjee *et al.*, 2011). Many microRNAs have been shown to play a crucial role in skin development and morphogenesis. For example, miR-125b represses stem cell differentiation through silencing both B lymphocyte induced maturation protein 1 (Blimp1) and Vitamin D Receptor (VDR) (Zhang *et al.*, 2011a). miR-125b has shown to play an important role in the development of stem cell progenitors, during the differentiation of epidermal cells, oil-glands and hair-follicles (Yi *et al.*, 2008). Another microRNA, miR-203 plays an important role in the differentiation of a single-layered epithelium into a stratified epidermal layer by suppressing p63 post-transcriptionally. It also maintains the proliferation potential of basal keratinocytes (Schneider, 2012; Lai and Siu, 2014). Interestingly, miR-203 performs the same functions both in zebrafish and man indicating its consistency and performance of a conserved function regardless of the species (Wienholds *et al.*, 2005; Wei *et al.*, 2010). On the other hand, overexpression of miR-203 in the epidermal basal layer of transgenic mice leads to formation of a thin epidermal layer with depletion in keratin 5 positive cells and frequent death shortly after birth (Yi *et al.*, 2008; Wei *et al.*, 2010). Therefore, the main function of miR-203 is thought to be to limit the proliferation potential of progenitor cells when they differentiate from the basal to the suprabasal layer by targeting the transcription

factor p63, shown to be the key player in maintaining stem cells in stratified tissues (Senoo *et al.*, 2007). Interestingly, p63 regulates cell division and differentiation of keratinocytes by repressing miR-34 family members (Antonini *et al.*, 2010). In addition, nine microRNAs have been shown to regulate differentiation of human keratinocytes and these include (miR-23b, miR-26a, miR-27b, miR-95, miR-200a, miR-210, miR-224, miR-328, and miR-376a) (Banerjee *et al.*, 2011; Hildebrand *et al.*, 2011). In that case, microRNAs play different important roles during the healing process.

1.13.3 *Roles of MicroRNAs in Wound Healing*

The significant roles played by microRNAs during skin morphogenesis and development, suggest that microRNAs are associated with skin pathologies, including cancer, and wound healing. They have therefore been considered as valuable regulators in wound healing (Banerjee *et al.*, 2011; Pastar *et al.*, 2012). Specific microRNAs have been reported to have changes in their expression during the cutaneous wound healing process. Up- and or down-regulation of these specific microRNAs may therefore play a crucial role in delayed wound healing (Shilo *et al.*, 2007). In a mouse model study, microRNAs have been demonstrated to play significant roles in dermal wound healing, since down-regulation of specific microRNAs such as those of the miR-99 family including (miR-99a, miR-99b and miR-100) (Jin *et al.*, 2013b) resulted in delayed wound healing. MicroRNAs could be involved in different phases of the healing process, participating from the early stages until the final phase.

1.13.3.1 *Role of MicroRNAs in The Coagulation Phase*

MicroRNAs have been shown to play important roles during the haemostasis phase of the healing process. They can influence the main steps and events of the coagulation cascade including; platelet biogenesis and function, coagulation and anti-coagulation factors, and fibrinolysis (Teruel-Montoya *et al.*, 2015). Landry and colleagues suggest that miR-223 regulate the expression of platelet surface protein known as (P2Y12) which is very important in coagulation (Landry *et al.*, 2009). In contrast, Leierseder and others explained that the role of miR-223 is restricted and minor during coagulation because the platelets of miR-223 deficient mice show normal reactivity and function (Leierseder *et al*., 2013). Another microRNA, miR-96 has been involved in regulation of vesicle-associated

membrane protein 8 (VAMP-8), which is a critical receptor involved in secretion of platelet granule (Shi *et al*., 2013). Also, miR-107, miR-200b and miR-495 possess suppressive activity on the proteins Circadian Locomotor Output Cycles Kaput (CLOCK), protein kinase type II-beta regulatory subunit (PRKAR2B) and Kelch Like Family Member 5 (KLHL5) respectively (Nagalla *et al*., 2011). With respect to haemostatic factors, fibrinogen is the first coagulation factor targeted by microRNAs. Fibrinogen (FG) is composed of three nodules (Aα, Bβ and γ chains) encoded by three different genes (FGA, FGB and FGG) respectively. miR-409-3p targets *FGB*, while *miR*-29c targets FGA-Ae. Whereas the miR-29 family including (miR-29a, miR-29b and miR-29c) target the three transcripts indirectly (Hatziapostolou *et al.*, 2011; Fish and Neerman-Arbez, 2012). Moreover, members of miR-29 family play important role in fibrosis by targeting other coagulation factors such as collagen, elastin and fibrillin (van Rooij *et al.*, 2008). Another coagulation factor, tissue factor (TF), the main initiator of blood coagulation, is encoded by the F3 gene which is by microRNAs. In *in vitro* studies miR-19 has been shown to bind to 3′-UTR of F3 while miR-20a and miR-106b bind to different sites of F3 and cause severe inhibition of TF in the breast cancer cell line and monocytic leukemia cell line, consequently, affecting the procoagulation activity of these cells (Teruel *et al.*, 2011b). *Regarding anticoagulation factors,* miR-18a and miR-19b significantly affect the serine peptidase inhibitor clade 1 (*SERPINC1) gene which encode* the most important anticoagulant AT, thereby inhibiting both thrombin and Factor X (FaX) (Teruel *et al.*, 2011a). Another anticoagulant protein S (PS) which is critical during thrombosis of pregnancy is regulated by miR-494. miR-494 regulates PS expression by binding to its gene *PROS1* (Tay *et al*., 2013)*. Moreover, miR-133a directly regulates* anticoagulant targets in liver such as VKORC1 (vitamin-K 2,3-epoxide reductase complex subunit-1) (Teruel-Montoya *et al.*, 2015). Many microRNAs also play important roles in the regulation of fibrinolysis. For example, plasminogen activator inhibitor-1 (PAI-1) encoded by serine peptidase inhibitor E1 (*SERPINE1) is* the primary inhibitor of the fibrinolytic cascade by targeting and inhibiting the activators of both tissue and uro-kinase type plasminogen (Iwaki *et al.*, 2012). Both miR-30c and miR-421 directly inhibit PAI-1 by binding to the 3’ UTR of *SERPINE1* mRNA (Marchand *et al.*, 2012).

1.13.3.2 *ROLE OF MICRORNAS IN THE INFLAMMATION PHASE*

As mentioned before, initiation and termination of successful inflammation is important for wound healing. The inflammatory response is highly regulated by pro-inflammatory and anti-inflammatory signals and cytokines (Banerjee and Sen, 2013). Many microRNAs mediate the inflammatory response during the course of wound healing and have shown significant regulatory roles during wound repair (Zhu *et al.*, 2011; Ryan *et al.*, 2012). Any failure in microRNA biogenesis will have a severe impact on the immune response leading to chronic non-healing wounds (Roy and Sen, 2012). Some studies have reported that miR-21, miR-146a, miR-146b, and miR-155 exert multi-axial roles and orchestrate the inflammatory response (Roy and Sen, 2012). Sonkoly and colleagues showed that some microRNAs serve as main regulators in human skin inflammation such as psoriasis and atopic eczema (Sonkoly *et al.*, 2008). For example, miR-203 is highly expressed in the skin epithelium of psoriasis patients. miR-146a targets TNF-α and regulates innate immune responses during psoriasis. Also, miR-125b is involved in theTNF-α pathway during psoriasis and atopic eczema (Sonkoly *et al.*, 2008). Additionally, miR-424 regulates the proliferation and differentiation of human monocyte and macrophages during inflammation via targeting the genes of the transcription factors unit protKB (*PU.1)* and nuclear factor IA (*NFIA)* (Lai and Siu, 2014). Also, miR-21 targets some inflammatory mediators including phosphatase and tensin homolog gene (PTEN) and programmed cell death protein-4 (PDCD-4) genes. Moreover, miR-146 targets interleukin-1 receptor-associated kinase-1 (IRAK-1) and Cytochrome c oxidase subunit 2 (COX2), while miR-155 targets the gene that encodes the multifunctional protein called SH2-containing inositol-5'-phosphatase-1 (SHIP1) which plays many roles in haematopoiesis of blood cells including their activation, proliferation and survival (Roy and Sen, 2012; Fernandes *et al.*, 2013). Additionally; miR-155 targets suppressor of cytokine signalling (SOCS-1) and (IL-12) (Roy and Sen, 2012). Also, miR-105 serves as an inflammatory regulator in human oral keratinocytes by targeting and suppressing Toll-like receptor 2 (TLR-2) (Benakanakere *et al.*, 2009). On the other hand, miR-147 may have anti-inflammatory activity and prevent excessive inflammatory events by terminating the inflammatory phase by targeting the gene that encodes the Toll-like receptors (TLRs) during the healing process (Lai and Siu, 2014).

1.13.3.3 *ROLE OF MICRORNAS IN EPITHELIALISATION PHASE*

Epithelialisation also called re-epithelialization is a key phase during wound healing and the wound will be considered as non-healing if the tissues fail to re-epithelialise. As previously mentioned, re-epithelialization of a wound is an outcome of three overlapping biological process related to keratinocytes which are migration, proliferation and differentiation (Banerjee and Sen, 2013). Switching to the proliferative phase from the inflammatory phase is a critical step during the healing process and controlling this event and kinetics is very important to progress towards healing (Reinke and Sorg, 2012; Banerjee and Sen, 2013). It has been shown that miR-132 is highly expressed during the inflammatory phase and regulates many genes related to several immune responses such as the immune cell cycle. During the proliferative phase, miR-132 expression is predominant in epidermal keratinocytes and suppresses the nuclear factor kappa light chain enhancer of activated B cells (NF-κB) signalling pathway and increase the activities of both extracellular-signal-regulated kinase (ERK) and signal transducer and activator of transcription 3 (STAT3) signalling pathways. Silencing miR-132 in mouse and human *ex vivo* wounds results in delayed wound healing with a severe prolonged inflammatory phase suggesting that this microRNA is a pivotal regulator in transition from the inflammatory phase to the proliferative phase during wound healing (Landén *et al.*, 2016). miR-21 is upregulated during wound healing and promotes keratinocyte migration via regulating the TGF-β1 signalling pathway since keratinocyte migration induced by TGF-β1 is significantly attenuated when miR-21is knocked (Yang *et al.*, 2011; Wang *et al.*, 2012b). miR-21 also regulates cell proliferation through the phosphatase and tensin homolog / phosphoinositide-3 kinase / alpha serine-threonine protein kinase (PTEN/PI-3 K/Akt) signalling pathways (Li *et al.*, 2015e) and showed that miR-21 is gradually overexpressed during wound healing when compared to intact skin, resulting in increased proliferation and migration of keratinocytes via direct targeting of the epithelial membrane protein 1 (EMP-1) gene. Another microRNA, miR-203, has a positive effect on migration and proliferation of keratinocytes via targeting two mRNA sequences which encode Ras-related nuclear protein (RAN) and Ras-associated and pleckstrin homology domains-containing protein 1 (RAPH-1), important for cell migration and proliferation. Therefore, miR-203 plays a pivotal role in epidermal wound re-epithelialization and haemostasis and hence re-establishing the injured skin (Viticchie *et al.*, 2012). Additionally, miR-203

support the proliferative capacity of basal keratinocytes and maintains the stratification potential of epithelial cells (Banerjee *et al.*, 2011).

1.13.3.4 *ROLE OF MICRORNAS IN ANGIOGENESIS*

Many studies have investigated the role of microRNAs in regulating angiogenesis and have shown that depletion of Dicer arrests microRNA biogenesis, resulting in arrested or incomplete formation of blood vessels (Sen *et al.*, 2009a). One of the issues controlled by microRNAs in wound healing angiogenesis is regulating nicotinamide adenine dinucleotide phosphate (NADPH) oxidase to produce reactive oxygen species (ROS) (Shilo *et al.*, 2008). miR-200b is a hypoxia-sensitive microRNA which plays a crucial role in angiogenesis during hypoxic conditions of wounds by targeting *ETS-1* gene which encodes the transcription protein C-ets-1 in human mammary epithelial cells (HMEC) (Chan *et al.*, 2011; Roy and Sen, 2012). Other microRNAs shown to target specific genes and regulate angiogenesis proteins include miR-17-5p which regulates tissue inhibitor of metalloproteinases (TIMP-1) (Otsuka *et al.*, 2008), miR-17/miR-92 (TSP-1) (Dews *et al.*, 2006), miR-20a (VEGF) a potent regulator of angiogenesis (Hua *et al.*, 2006), miR-92a (ITGB-5) which encodes Integrin beta-5 (Bonauer *et al.*, 2009), miR-126 which encodes Sprouty-related, EVH1 domain-containing protein 1 (SPRED-1) (Fish *et al.*, 2008) and miR-221/miR-222 (c-KIT or CD177) which play important roles in cell survival, proliferation, and differentiation (Poliseno *et al.*, 2010). Additionally, there are many microRNAs such as miR-15a, miR-16 (Sun *et al.*, 2013), miR-20b (Cascio *et al.*, 2010), miR-101 (Zhao *et al.*, 2015), and miR-206 (Zhang *et al.*, 2011b) that increase the angiogenic activity through regulating VEGF in cancer cells. Therefore controlling these microRNAs may be of importance in regulating VEGF and promoting angiogenesis during wound repair (Lai and Siu, 2014).

1.13.3.5 *ROLE OF MICRORNAS IN THE CONTRACTION AND REMODELLING PHASE*

As previously mentioned, collagen deposition is a critical step for the remodelling phase during wound healing. Many microRNAs have been shown to regulate collagen deposition such as miR-21 (Lai and Siu, 2014), miR-29a, miR-29b, miR-29c and miR-192 (Cheng *et al.*, 2010). Both miR-29b and miR-29c target and silence specific genes responsible for producing many extracellular matrix proteins such as anti-fibrotic TGF-β, β-catenin and small mother against decapentaplegic (SMAD) like proteins which are involved in collagen

regulatory signalling pathways during remodelling (van Rooij *et al.*, 2008). Whereas, miR-129 targets smad interacting protein-1 (SIP-1) which encodes the expression of both collagen type I and type II (Kato *et al.*, 2007). Additionally, miR-21 is involved in wound contraction via mediating the TGF-β-signalling pathway (Wang *et al.*, 2012b; Lai and Siu, 2014).

Based on the observations mentioned above, regulation of microRNA levels at the wound site makes microRNAs attractive candidates for treating non-healing wounds via novel strategies (microRNA-therapies) to overcome this global burden. The unique concept that microRNA-therapies could regulate more than one gene in the pathway gives them advantage over the conventional gene therapy (Banerjee and Sen, 2013).

Conversely, Pastar and others explained that some microRNAs affect wound healing negatively (Pastar *et al.*, 2012). For example, miR-210 inhibits wound healing in ischemic wounds of a murine model, by repressing keratinocyte proliferation (Biswas *et al.*, 2010). Other microRNAs expressed differentially during rat and human venous ulcers can delay the healing process such miR-16, miR-20a, miR-21, miR-106a, miR-130a, and miR-203 since these microRNAs target growth factor signalling and suppress the re-epithelialisation process and formation of granulation tissue (Pastar *et al.*, 2012). Also, miR-125b reduces the proliferative ability of keratinocytes via regulation of fibroblast growth factor-2 receptor (FGFR2) (Schneider, 2012)**.** Additionally, miR-198 significantly prevents keratinocyte migration and re-epithelialisation resulting in chronic wounds (Sundaram *et al.*, 2013).

Recently, it has been shown that cellular receptors are important for granulation tissue formation, appropriate tissue regeneration and wound repair (Feoktistov *et al.*, 2009).

1.14 Receptors of Growth Factors and Cytokines and Their Roles in Wound Healing

The potential to recognize tissue damage and initiate a proper repair mechanism is carried out by biological molecules that mediate signal transduction and make structural changes in the cellular environment, enhancing the cellular response and restoring function such as inflammation and wound healing. These molecules are termed recognition receptors (Dasu and Rivkah Isseroff, 2012). Interestingly, cell receptors such as Toll-like receptors can recognize pathogens upon injury, trigger immune responses (Jiang *et al.*, 2005) and

induce inflammation (Sims *et al.*, 2010). Secretion of these receptors is not only restricted to the immune cells, but they are also present on non-myeloid cells such as endothelial and epithelial cells and thus involve them in the wound healing process (Grote *et al.*, 2011).

Upon binding of growth factors or cytokines to receptors on the target cell, many signalling pathways are activated and several cellular responses evoked, such as cell division, proliferation, migration, differentiation, survival or apoptosis and many other cellular functions (Manavalan *et al.*, 2011) (Figure 1.8).

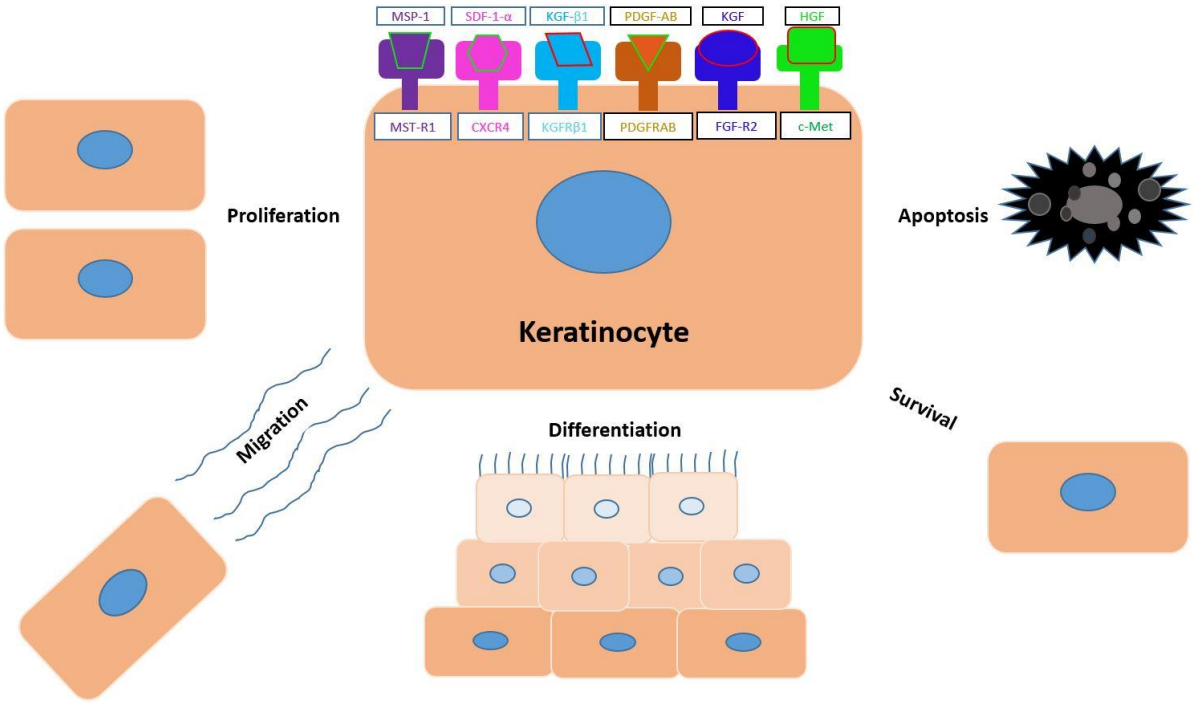

Figure 1.8 Interaction between growth factors and their receptors expressed by primary keratinocytes.

Upon binding of one or more growth factors and cytokines to their particular receptor on the target cell, specific signaling pathways will be evoked leading to activation of the cell response such as cell division and proliferation, migration, differentiation and apoptosis.

1.14.1 *c-MET: HGF RECEPTOR*

c-Met is the receptor of HGF and scatter factors (SFs) and participates in signalling pathways enhancing proliferation and mobility of epithelial cells (Bottaro *et al.*, 1991; Birchmeier *et al.*, 2003). The signalling pathway mediated by HGF and its tryrosine kinase proto-oncogene receptor (c-Met) is very important for vertebrate embryogenesis since

these mediators control several cellular activities including formation of the placenta as well as proliferation and survival of hepatocytes (Dietrich *et al.*, 1999). Therefore, c-Met is essential for liver repair and regeneration (Borowiak *et al.*, 2004; Taub, 2004). Interestingly, c-Met expression is increasingly observed after injury of other tissues such as heart, kidney and skin (Cowin *et al.*, 2001). Therefore, expression of HGF, SFs and c-Met could be upregulated during response to tissue damage and repair by the activity of IL-1 and IL-6, when both are activated via transcription of HGF and SFs (Michalopoulos and DeFrances, 1997). Interestingly, c-Met in the epidermis of mutant mice are unable to participate in re-epithelialization of skin wounds and wound closure is slightly attenuated since the closure process is enhanced only by the few keratinocytes which escaped the mutation. Additionally, c-Met mutant primary keratinocytes grown *in vitro* failed to close the scratched area and only c-Met positive cells that escaped the mutation participated in wound healing suggesting that c-Met is an important signalling pathway not only for cell growth and migration but also for proliferation and regeneration of skin during wound healing (Chmielowiec *et al.*, 2007).

1.14.2 *PDGFR: RECEPTOR OF PDGFA, PDGFB, PDGFAB, PDGFCC.*

PDGF is the primary growth factor that appears at the injury site and is secreted by the platelets (Martin, 1997). It presents in three classic isoforms, which are composed of polypeptide A and B units, forming two homodimers PDGF-AA, PDGF-BB and one heterodimer PDGF-AB (Heldin and Westermark, 1999). The physiological action of these three isoforms of PDGF are evoked by binding to two specific tyrosine kinases cell surface receptors (α and β) (Heldin *et al.*, 1988). Additionally, two homodimers of PDGF have been recognized; PDGF-CC and PDGF-DD (Bergsten *et al.*, 2001). The α receptor has the ability to bind to PDGF-AA, PDGF-BB, PDGF-AB and PDGF-CC isoforms, whereas the β receptor can bind to PDGF BB and PDGF-DD isoforms (Heldin and Westermark, 1999; Bergsten *et al.*, 2001). Genetic studies showed that the PDGFR-α signalling pathway is important for palatogenesis, somites formation and patterning of mesodermal tissue (Ding *et al.*, 2004). Additionally, both PDGF-α and -β receptors trigger mitogenic signals and enhance cell motility and actin filament production. Mutations in PDGF-B- and its receptor (PDGFR-β) results in failure to recruit pericytes and smooth muscle cells to initiate primary blood vessels leading to widespread haemorrhaging and death *in utero* (a

term used to describe the state of the foetus in the womb). Moreover, PDGFR-β inhibition leads to delayed wound healing and reduced wound closure which is accompanied by significant reduction in myofibroblast recurrence, fibronectin expression, collagen type I synthesis and distribution of collagen-producing cells at the edges of the wound, arresting proliferation and migration of fibroblast and inhibition of pericyte proliferation and migration *in vitro* at the early stages of the wound healing process (Rajkumar *et al.*, 2006).

1.14.3 *FGFR2: KGF RECEPTOR*

Fibroblast growth factor receptor-2 (FGFR-2) also known by other names such as keratinocyte growth factor receptor (KGFR) and CD332, is a transmembrane receptor tyrosine kinase encoded by the *FGFR2* gene (Abuharbeid *et al.*, 2006). There are many slight differences in FGFR-2 isoforms such as FGFR-1, FGFR-2, FGFR-3, FGFR-4, FGFR-7 and FGFR-10 which spread around the different tissue types in the body and change during growth and development (Ornitz and Itoh, 2001). It is involved in many important cell activities including division, growth and maturation of the cell, formation of blood vessels, embryogenesis, healing of chronic wounds and tissue repair. Lack of binding to their transmembrane receptor, causes the FGF family including KGF unable to regulate proliferation, migration, survival and differentiation of many cell types in both normal and wounded skin (Gartside *et al.*, 2009; Werner, 2011). Structurally, FGFR-2 is composed of two domains, one remains inside the cell and the other spans the cell membrane, to allow the receptor to bind and interact with specific ligands and growth factors outside the cells triggering a cell response to the extracellular environment. For instance, when a growth factor binds to the FGFR2 protein, the receptor acts as a signal transducer and initiates a series of chemical reactions that evoke signalling cascades inside the cell which in turn inform the cell to perform special functions such as growth, migration, proliferation and differentiation or participate in the development of embryonic cells to become more specialized cells of other tissues (Gartside *et al.*, 2009).

1.14.4 *TGFß-R1: TGFß-1 RECEPTOR*

Transforming growth factor beta in its three isoforms (TGF-β1, TGF-β2, and TGF-β3) are members of a superfamily of cytokines. All three isoforms participate in the wound healing process; however, TGFβ-1 is the most influential and dominant isoform since it is secreted

by many cell types such as platelets, monocytes and macrophages to initiate the inflammatory response. It is also secreted by keratinocytes and fibroblasts to enhance granulation tissue formation (Barrientos *et al.*, 2008b). Receptors of TGF-β are transmembrane receptors characterised by dual specificity, firstly, they are unique in their ability in man to strongly bind to serine/threonine kinases (Huminiecki *et al.*, 2009). Secondly, they weakly bind to tyrosine kinases (Heldin *et al.*, 2009; Huminiecki *et al.*, 2009). They could be divided into three types; (TGFβ-1R; which is also known as activin like kinase /ALK), TGFβ-2R) and TGFβ-3R). All TGFs-β cannot perform their functions in the target cell independently without binding to their specific receptors. First of all, TGFβ is released and its ligand binds to the active TGFβ-2R which then binds to TGFβ-1R (Goumans *et al.*, 2009) and forms TGFβ-1R phosphorylate (Heldin *et al.*, 2009). Then, TGFβ-3R regulates the receptor activity by mediating the binding of specific TGF-β isoforms (Moustakas and Heldin, 2009). After activation, the ligand-receptor complex evokes intracellular cascades and activates canonical and non-canonical signalling pathways including both R-Smad dependent pathways (Smad2/3), and R-Smad independent pathways (ERK1/2) which are well documented to enhance epidermal and dermal cell migration during the wound healing process (Bandyopadhyay *et al.*, 2011) as well as their important roles in angiogenesis and fibrosis (Maring *et al.*, 2012).

1.14.5 *MSTR1: MSP-1 Receptor (Also Known as RON; PTK8; CD136; CDw136)*

MSTR1 is a tyrosine kinase receptor which binds to extracellular signals and transfers them through the cell membrane into the cytoplasm and induces RON (Recepteur d'Origine Nantais) auto-phosphorylation to initiate intracellular cascades and enhance physiological process such as cell survival, proliferation, migration and differentiation of epithelial cells into the wound site. Additionally, RON restores downstream signaling molecules which regulate macrophage migration and phagocytic activities involved in the immune response (Côté *et al.*, 2007; Feres *et al.*, 2008). It has been shown that RON possess anti-inflammatory activity, since it mediates the transduction of signals that suppress the production of inflammatory mediators by the NF-kβ pathway by blocking lipopolysaccharides (LPS) (Wang *et al.*, 2002; Kretschmann *et al.*, 2010). In addition, MSP/RON signalling are strongly involved in the different steps of the healing process and are significantly increased during the first 7 and 21 days. Interestingly, in RON deficient

mice suffering from lung injury the wounds become significantly chronic and lead to poor survival (Kretschmann *et al.*, 2010).

1.14.6 *CXCR4: SDF-1A RECEPTOR*

Cellular migration is generally regulated by chemokines (Gillitzer and Goebeler, 2001). It has been shown that the CXCR4/SDF-1 signalling pathway is implicated in many disorders such as skin wound healing, tumour angiogenesis, basal cell carcinoma and systemic lupus erythematosus (Bollag and Hill, 2013). SDF-1α and its receptor CXCR4 represent the most effective chemotactic pathway for cellular mobility of MSCs and monocytes towards the damaged tissue (Ding *et al.*, 2011; Sánchez-Martín *et al.*, 2011). Therefore, SDF-1α/CXCR4 signalling pathway not only facilitate MSC migration from the bone marrow towards the wound site, but also represent the crucial migratory mechanism during the inflammation and proliferation phase of the healing process (Hu *et al.*, 2013; Campeau *et al.*, 2015). CXCR4 expressing cells are attracted by SDF-1α (CXCL12) and migrate to the peripheral tissue and initiate the CXCR4 dependent signalling pathway (Miller *et al.*, 2008; Campeau *et al.*, 2015). It has been reported that SDF-1 and/or CXCR4 are up-regulated during burns and excisional wounds in skin epidermis indicating their involvement in the wound healing process (Avniel *et al.*, 2006; Toksoy *et al.*, 2007). Avniel et al reported that CXCR4 and its ligand SDF-1α are upregulated in skin burns of man, pigs and rats where SDF-1α was mainly released by dermal fibroblasts but not the keratinocytes which instead secreted its receptor CXCR4 (Avniel *et al.*, 2006). Several cell types are shown to express CXCR4 at the wound site including vascular endothelial cells and infiltrating immune cells (Avniel *et al.*, 2006; Bollag and Hill, 2013) as well as embryonic and adult stem cells (Miller *et al.*, 2008).

To date, the vast majority of cell based assays are tested in traditional two-dimensional cell culture (2DCC), however, new techniques have been developed that mimic the *in vivo* environment by growing the cells in a three-dimensional cell culture (3DCC) (Edmondson *et al.*, 2014).

1.15 TWO-DIMENSIONAL AND THREE-DIMENSIONAL CELL CULTURE

The majority of biological studies on experimental skin have been conducted in standard two-dimensional cell culture (2DCC), whereas, accumulating evidence has suggested that

the behaviour of the cells in the 2DCC is quite different from their behaviour when they are grown in three-dimensional cell culture (3DCC) (Li *et al.*, 2011a). Therefore, *in vitro* cell culture has recently developed from 2DCC to 3DCC, characterised by cultured cells with an environment which significantly mimics the *in vivo* niche by growing the cells as a floating mass (Wozniak and Keely, 2005). The 3DCC design is provided by a collagen matrix and emulates the ECM, and mimics a natural environment for cell growth.(Wozniak and Keely, 2005). Recently, scientists have developed 3D human skin constructs consisting of epidermis represented by stratified, differentiated keratinocytes, dermis composed of fibroblasts embedded in a collagen I matrix and functional basement membrane separating the two layers thus, enabling investigations into the interactions between different cell types and cell matrix compositions. Moreover, in other research experiments, the constructed skin has contained melanocytes located in the basement membrane as shown *in vivo* (Li *et al.*, 2011a). Recently, applications of 3D culture has involved developing 3D skin models for a variety of purposes, including wound healing studies and drug screening investigations. The majority of drug testing assays including drug discovery, cytotoxicity and wound healing assays, rely on 2D culture-based techniques involving the seeding of cells on naked or coated plastic and glass flat surfaces in tissue culture plates. Although, these assays are advantageous in terms of simplicity, quick, and inexpensive when compared to large-scale cell culture, they still have many disadvantages when compared to 3D culture (Edmondson *et al.*, 2014). For instance, cells in 2D culture differ morphologically and physiologically from cells in 3D culture (Baharvand *et al.*, 2006). Also, cells in 2D culture lack the criteria of being surrounded by cellular elements and extracellular matrix as in an *in vivo* environment, whereas 3D culture mimics this habitat and offers the cultured cells, to some extent, an environment mimicking *in vivo* conditions including the growth of cells floating in culture media (Bhadriraju and Chen, 2002). Additionally, 2D culture does not enable adequate exposure of the cells to the tested drug or substance of interest resulting in false, non-predictive and misleading data (Birgersdotter *et al.*, 2005). Moreover, wound healing studies require testing the ability of the compound to enhance the motility of cell mass or cell sheets in the damaged area as in an epithelial wound which cannot be performed in 2D culture since the cells may migrate as single cells in two dimensions (Poujade *et al.*, 2007). Furthermore, to mimic cutaneous wounding, cultured skin equivalents require exposure to the air-liquid interface, which is

not applicable to 2D culture. In addition, some experiments require a shrinkable substrate to form an even organotypic culture, which is again not applicable to 2D culture (Laco *et al.*, 2009; Ma *et al.*, 2009) while it is easily achieved in 3D culture through the use scaffolds such as the Alvetex® scaffold.

1.16 Skin Equivalent Model

Due to the limitations and lack of knowledge in understanding of the biological mechanisms involved in wound repair and for furthering human skin research, significant efforts have been made to establish *in vitro* and *ex vivo* skin models (Xie *et al.*, 2010). In the early 1980s, the first human skin-like structure was developed by Bell and colleagues (Bell *et al.*, 1981) when they attempted to treat burns and chronic wounds. Although, all constructed skin models are based on the same protocols and principles, some modifications have been made and a skin model consisting of fibroblasts and collagen matrix overlaid with epidermal keratinocytes has been constructed (Carlson *et al.*, 2008). Recently, skin constructs have been improved and developed models have been produced such as pigmented, vascularised, innervated skin and immune competent-containing skin (Roggenkamp *et al.*, 2013). However, the majority of constructed skin models are insufficient to meet the relative complexity of human skin because they include only one or two cell types and lack skin appendages (Guo *et al.*, 2013b). In dermatology, many attempts were made in the early 1990s to establish skin equivalents *in vitro,* starting with cultured epidermal sheets, an organotypic culture for cytotoxicity assays and then, an advanced living skin equivalent consisting of collagen lattice of fibroblasts covered with an epidermal layer (Parenteau *et al.*, 1991). In 1993, companies started to develop skin models such as Advanced Tissue Sciences / USA, which launched two successful versions of the 3D skin equivalent, branded as 'Skin²TM ZK1300 and ZK1350, used worldwide for many tasks such as toxicological tests, skin irritation and dermal absorption. In 1995, these models were replaced by a developed clinical skin equivalent (Dermagraft-TC), which was mainly used for wound therapy in patients with cutaneous burns (Stoppie *et al.*, 1993). Later, other models were developed such as The EpiSkin™ and SkinEthic RHE™ skin models in France, which contained a collagen lattice and collagen IV (Tinois, 1991) and The EpiDerm™ skin models in the USA (Cannon *et al.*, 1994), The Vitrolife-SKIN™ skin model, Japan (Noriyuki Morikawa, 2007), The Phenion® Full-Thickness Skin

Model and the OS-REp model, Germany (Mewes *et al.*, 2007) and The LabCyte™ skin model, Japan (Niwa (Niwa *et al.*, 2009) et al., 2009). More recently, attempts have been made to establish a 3D skin model that mimics real skin for many purposes such as skin disorders, cytotoxicity assessment and wound healing. All these models have utilised different substances and materials of non-human origin. For instance (Vörsmann *et al.*, 2013; Klimkiewicz *et al.*, 2017) developed a 3D model which contained collagen I isolated from rat-tails for studying melanoma metastasis. In addition, 3D models have been developed using a scaffold and collagen gels generated from bovine collagen I to study melanoma metastasis (Li *et al.*, 2011a) and wound healing (Marquardt *et al.*, 2015). Laterally, a 3D skin equivalent for melanoma studies, that does not require collagen has been developed that relies on the production of its own extracellular matrix, improving its overall longevity (Hill *et al.*, 2015).

1.17 AIMS OF THE STUDY

1.17.1 *THE PROBLEM*

In many cases, skin wounds fail to heal normally due to two main causes; the first one is alteration of the characteristics of the keratinocytes at the injury site which in turn are unable to cross talk with other cell types and participate in the healing process. The second factor is deficiency in growth factors and cytokines required for the initiation and termination the different phases of the healing process such as homeostasis, inflammation, cell migration and proliferation, and re-epithelialization. These problems lead to the development of chronic wounds (Pastar *et al.*, 2008).

1.17.2 *HYPOTHESES*

In this study, three hypotheses were proposed and addressed. Firstly, the hypothesis that MSC secretions contain growth factors and cytokines which could be collected from *in vitro* culture to promote proliferation and migration of skin cells into the wounded area in both 2D and 3D cultures. Secondly, the hypothesis that bone marrow derived stem cells (BM-MSCs) migrate and differentiate into skin cells *in vivo.* Herein, this hypothesis was tested *in vitro* using both 2D and 3D cultures. The third hypothesis is that small non-coding

RNAs could participate in regulating the healing process. This hypothesis was tested via microRNA profiling during wound healing using a developed 3D skin model.

1.17.3 *AIMS OF THE STUDY*

This project aims to address how MSCs and their secretions promote migration, proliferation and / or differentiation of skin cells into the injury site. To this aim, the specific objectives are:

1. Isolate MSCs from bone marrow, establish their maintenance in cell culture *in vitro* and define their secretory profile of growth factors and cytokines.
2. Determine the effect of growth factors and cytokines secreted by MSCs on wound healing in 2D culture using an established *in vitro* scratch assay using human keratinocyte cell lines (HaCat), human primary keratinocytes and human dermal fibroblasts.
3. Reproduce a 3D human skin equivalent model and validate epidermal and dermal biomarker expression.
4. Develop a prototype of the 3D skin model for wound healing studies and study the effect of MSC or MSC derived secretions, containing specific growth factors or cytokines on this wound healing model.
5. Use the developed 3D skin model to study the molecular mechanisms of wound healing using microRNA profiling.

CHAPTER 2 MATERIALS AND METHODS

CHAPTER TWO: MATERIALS AND METHODS

2.1 ETHICS AND CONSENT

All human MSC samples used in this study were obtained with donor informed consent. The research was approved with full Local Research Ethics approval (NRES Newcastle and North Tyneside 1 REC reference 14/NE/1212) which was obtained on 5th December 2014. For more information about the approvals (See Ethics Approval Page 315).

2.2 MATERIALS AND EQUIPMENT

A variety of reagents, substances, tools, equipment and systems were used in this study. All information about these materials and their providers are listed in the Tables depending on their type and use during the experiments, to avoid repetition in the text.

2.2.1 *CULTURE MEDIA*

Item	Catalogue #	Company	Origin
Dulbecco's Modified Eagle's Medium - high glucose	D6546-500ML	Sigma-Aldrich	UK
Keratinocyte-SFM (1X), without calcium chloride	37010022	ThermoFisher Scientific	UK
EpiLife® Medium, with 60 µM calcium	MEPI500CA	EpiLife	UK
MCDB153 with L-Glutamine, 28 mM HEPES	M7403-10L	Sigma-Aldrich	UK
Nutrient Mixture F-12 Ham	N6658-500ML	Sigma-Aldrich	UK
Roswell Park Memorial Institute-1640 (RPMI-1640)	R0883-500ML	Sigma-Aldrich	UK
StemMACS MSC Expansion Media, human	130-091-680	Miltenyi Biotec	Germany
StemMACS™ AdipoDiff Media, human	130-091-677	Miltenyi Biotec	Germany
StemMACS™ ChondroDiff Media, human	130-091-679	Miltenyi Biotec	Germany
StemMACS™ OsteoDiff Media, human	130-091-678	Miltenyi Biotec	Germany
X-VIVO™ 10 Chemically Defined, Serum-free Haematopoietic Cell Medium	04-380Q	Lonza (SLS)	UK

Table 2.1 Types of media used for culturing different cell types.

2.2.2 *MSC PHENOTYPIC CHARACTERISATION KIT*

Item	Catalogue #	Company	Origin
PE Mouse Anti-Human CD73 Clone AD2 (RUO)	550257	BD Bioscience	UK
PerCP-Cy™5.5 Mouse Anti-Human CD90 Clone 5E10 (RUO)	561557	BD Bioscience	UK
APC Mouse Anti-Human CD105 Clone 266 (RUO)	562408	BD Bioscience	UK
FITC Mouse Anti-Human CD14 Clone M5E2 (RUO)	555397	BD Bioscience	UK
FITC Mouse Anti-Human CD19 Clone HIB19 (RUO)	555412	BD Bioscience	UK
FITC Mouse Anti-Human CD34 Clone 581 (RUO)	555821	BD Bioscience	UK
FITC Mouse Anti-Human CD45 Clone HI30 (RUO)	555482	BD Bioscience	UK
APC-H7 Mouse Anti-Human HLA-DR Clone G46-6 (RUO)	561358	BD Bioscience	UK
CD14 FITC Clone MφP9 (CE/IVD) Isotype	345784	BD Bioscience	UK
CD19 FITC Clone 4G7 (CE/IVD) Isotype	345776	BD Bioscience	UK

Anti-HLA-DR APC-H7 Clone L243 (CE/IVD) Isotype	641411	BD Bioscience	UK
DAPI [4,6-Diamidino-2-phenylindole, dihydrochloride]	564907	BD Bioscience	UK

Table 2.2 Antibodies and isotypes used for phenotypic assay of MSCs.

2.2.3 *ELISA KITS*

Kit	Catalogue #	Company	Origin
HGF ELISA Kit, Human	KAC2211	Lifetechnologies	USA
PDGF-AB ELISA Kit, Human	EHPDGFAB	Lifetechnologies	USA
TGF beta 1 ELISA Kit, Multispecies	KAC1688	Lifetechnologies	USA
SDF-1a (CXCL12A) ELISA Kit, Human	EHCXCL12A	Lifetechnologies	USA
MSP (MST1) ELISA Kit, Human	EHMST1	Lifetechnologies	USA
FGF-7 (KGF) ELISA Kit, Human	EHFGF7	Lifetechnologies	USA

Table 2.3 ELISA kits used to measure the concentrations of growth factors and cytokines in MSC-CM.

2.2.4 *IMMUNOFLUORESCENCE ANTIBODIES AND STAINS*

Antibody	Catalogue #	Company	Origin
Alexa flour 568 goat anti-rabbit IgG (H+L) secondary antibody	A-11036	Life Technologies	UK
Alexa fluor 488 goat anti-mouse IgG (H+L) secondary antibody	A11001	Life Technologies	UK
Anti-BrdU antibody	ab152095	Abcam	UK
Anti-collagen IV antibody [COL-94]	ab6311	Abcam	UK
Anti-Cytokeratin 10 antibody	ab111447	Abcam	UK
Anti-Cytokeratin 14 antibody [LL002]	ab7800	Abcam	UK
Anti-involucrin antibody [SY5]	ab68	Abcam	UK
Anti-Loricrin antibody	ab85679	Abcam	UK
BrdU (5-bromo-2'-deoxyuridine)	ab142567	Abcam	UK
Donkey Anti-Rabbit IgG H&L (Alexa Fluor® 488)	ab150073	Abcam	UK
Dibutylphthalate Polystyrene Xylene (DPX) mounting medium	1.00579.0500	VWR International	UK
Fluoroshield Mounting Medium (20 ml)	ab104135	Abcam	UK
Goat Anti-Mouse IgG H&L (Alexa Fluor® 488) preadsorbed	ab150117	Abcam	UK
Mouse mAb to collagen III [1E7-D7/col3]	ab23445	Abcam	UK
Loricrin Polyclonal Antibody, Purified (Formerly Covance PRB-145P-100)	905101	Cambridge Bioscience	UK

Table 2.4 Primary and secondary antibodies and other reagents used for immunofluorescence staining.

2.2.5 *MATERIALS AND REAGENTS OF GENE EXPRESSION*

Item	Catalogue #	Company	Origin
High-Capacity cDNA Reverse Transcription Kit with RNase Inhibitor	4374967	ThermoFisher Scientific	USA
High-Capacity cDNA Reverse Transcription Kit with RNase Inhibitor	4374966	ThermoFisher Scientific	USA

MicroAmp® Optical Adhesive Film	4360954	ThermoFisher Scientific	USA
Nuclease-Free Water (not DEPC-Treated)	AM9938	ThermoFisher Scientific	USA
RNeasy Micro Kit (50)	74004	QIAGEN	USA
RNeasy Mini Kit (50)	74104	QIAGEN	USA
TaqMan® Gene Expression Assay / CXCL12, hCG25667	4331182	ThermoFisher Scientific	USA
TaqMan® Gene Expression Assay / FGF2, Hcg37365	4331182	ThermoFisher Scientific	USA
TaqMan® Gene Expression Assay / GAPDH Hs02758991_g1	4331182	ThermoFisher Scientific	USA
TaqMan® Gene Expression Assay / MET, Hcg38705	4331182	ThermoFisher Scientific	USA
TaqMan® Gene Expression Assay / MST1R, hCG95986	4331182	ThermoFisher Scientific	USA
TaqMan® Gene Expression Assay / PDGFRA, Hcg22159 (20X)	4331182	ThermoFisher Scientific	USA
TaqMan® Gene Expression Assay / TGFBR1, hCG30154	4331182	ThermoFisher Scientific	USA
TaqMan® Gene Expression Master Mix	4369016	ThermoFisher Scientific	USA
TaqMan® Gene Expression Master Mix	4369514	ThermoFisher Scientific	USA

Table 2.5 Reagent and substances used for gene expression assay.

2.2.6 *MICRORNA PROFILING KITS*

Item	Catalogue #	Company	Origin
Agilent Small RNA Kit	5067-1548	Agilent Technologies	Germany
mirVana™ microRNA Isolation Kit, with phenol	AM1560	ThermoFisher Scientific	Lithuania
nCounter Human v3 microRNA Expression Assay Kit	GXA-MIR3-12	NanoString Technologies	USA
RNAlater® Stabilization Solution	AM7020	ThermoFisher Scientific	USA

Table 2.6 Kits and reagents used for microRNA analysis.

2.2.7 *STAINS AND STAINING REAGENTS*

Different stains and reagents were used to stain the cells and the 3D skin model during this study and are listed in (Table 2.7).

Item	Catalogue #	Company	Origin
Alcian Blue 8GX	A5268-10G	Sigma-Aldrich	UK
N,N-Dimethylformamide	227056-100ML	Sigma-Aldrich	UK
Eosin Stain	6766007	Thermo	UK
Fast Blue RR	201545-5G	Sigma-Aldrich	UK
Haematoxylin satin	HS315-1L	Cell Path	UK
Methylene Blue Dye	556416-1G	Sigma-Aldrich	UK
Naphthol AS-MX phosphate disodium salt (phosphatase substrate)	N5000-100MG	Sigma-Aldrich	UK
Oil Red O	O0625	Sigma-Aldrich	UK
Tris base	TRIS-RO	Sigma-Aldrich	UK
Trypan Blue Dye	302643-25G	Sigma-Aldrich	UK

Table 2.7 Stains and reagents used during the different staining protocols.

2.2.8 *GENERAL REAGENTS*

Item	Catalogue #	Company	Origin
3,3',5-Triiodo-L-thyronine sodium salt (T3)	T6397-100MG	Sigma-Aldrich	USA
4% Paraformaldehyde 1 * 500 ml	BSBTAR1068	VWR	UK
Amphotericin B solution	A2942-50ML	Sigma-Aldrich	USA
Calcium chloride solution volumetric, 1.0 M CaCl2	21114-1L	Sigma-Aldrich	USA
CellTiter 96® AQueous One Solution Cell Proliferation Assay	G3580	Promega	UK
200 mM L-Glutamine Solution	G7513-100ML	Sigma-Aldrich	UK
Bovine Serum Albumin	A2153-50G	Sigma-Aldrich	UK
Chelex® 100 Chelating Resin, biotechnology grade, 100–200 mesh, sodium form, 100 g	1432832	BioRad	UK
Cholecalciferol (Vitamin D3)	PHR1237-500MG	Sigma-Aldrich	UK
Coomassie Plus protein assay reagent	10495315	Thermo Scientific Pierce	UK
CXCL12 (SDF-1) Recombinant Human Protein, N-His Tag	13511-H07E-50	Thermofisher Scientific	UK
Dispase	07923	Stem Cell Technologies	UK
Donkey Serum	D9663-10ML	Sigma-Aldrich	UK
Dulbecco's Phosphate Buffered Saline (PBS)	D8537-500ML	Sigma-Aldrich	UK
Foetal Bovine Serum	10270106	Gibco	UK
Human Keratinocyte Growth Supplement (HKGS)	S-001-5	Thermofisher Scientific	UK
Human/Mouse CXCL12/SDF1 Antibody	MAB310-500	R & D Systems	USA
Hydrocortisone	H0888-1G	Sigma-Aldrich	UK
Insulin, Recombinant Human	91077C-100MG	Sigma-Aldrich	UK
Insulin-Transferrin-Selenium (ITS -G) (100X)	41400045	Thermofisher Scientific	UK
L-Ascorbic acid	A5960-100G	Sigma-Aldrich	UK
Lymphoprep	1114547	Axis-Shield	UK
Mitomycin C (MMC)	ab120797	Abcam	UK
Penicillin – Streptomycin	P4333-100ML	Sigma-Aldrich	UK
Rabbit serum	R9133-10ML	Sigma	UK
Tris (Hydroxymethyl)-methylamine	77-86-1	Fisher Scientific	UK
Triton™ X-100	X100-100ML	Sigma-Aldrich	UK
Trypsin inhibitor from Glycine max (soybean)	T6522-250MG	Sigma-Aldrich	UK
Trypsin-EDTA Solution	T3924-100ML	Sigma-Aldrich	UK

Table 2.8 General reagents and materials used during the study.

2.2.9 *EQUIPMENT AND MACHINES*

Item	Company	Origin
2720 Thermal Cycler	Applied Biosystems	USA
7900HT Fast Real-Time PCR System	Applied Biosystems	USA
Agilent 2100 Bioanalyzer	Agilent	Germany
Galaxy B CO2 Incubator (Model 150-400)	Scientific Supplies Ltd	UK
Cooled Centrifuge accuSpin™ 3R	Fisher Scientific	USA
CytoMAT Pharmaceutical Safety Cabinet	CytoMAT Medical Air Technology Ltd.	USA
DRI-BLOCK DB.2A Heater	Techne	UK
ELISA Reader (Multiskan Ascent)	Thermo Lab systems	USA

Floating–out Bath	Gallenkamp	UK
FACS Canto II FlowCytometry	BD Biosciences	USA
Freezer (-80)	Cool Repair UK Ltd	UK
Heraeus Megafuge 8 Centrifuge	Thermo Scientific	UK
NU-5841 Hypoxic and Humidity Controlled CO2 Incubator	TripleRed	USA
IKA MS 3 basic S36 Agilent	Agilent	Germany
Labnet MPS 1000 Mini plate spinner	Labnet	UK
MicroCL 17 Centrifuge	Thermo Electron Corporation	USA
Mini see-saw rocker SSM4	Stuart	UK
NanoDrop Spectrometry NanoDrop 1000	ThermoFisher Scientific	USA
Oven MIDIS/1/SS/G/F	GENLAB	UK
pH Meter	Mettler Toledo	UK
Sartorius analytic Balance	Sartorius	Germany
Shandon Finesse 325 Microtome	ThermoFisher Scientific	USA
Vortex-Genie 2	Scientific Industries	USA
Water Bath JB Aqua 5	Grant	UK

Table 2.9 Systems and machines used to carry out experiments during the study.

2.2.10 *PLASTIC AND GLASS WARES*

Item	Catalogue #	Company
0.2 ml PCR Tube, Flat Cap (mixed)	I1402-8108	Start Lab
8-well on glass detachable	94.6170.802	Sarstedt
Alvetex 12 Well Insert Format	AVP005-12	Reprocell / Reinnervate
Cover Glasses for Slides 18 mm × 18 mm (200)	12343138	Fisher Scientific
Cryotube 1.8 ml SI INT. ROUND	363401	Thermo Scientific
Flasks (25 cm2, 75 cm2, 175 cm2)	660175-TRI	Greiner
MicroAmp® Optical 96-Well Reaction Plate	N8010560	Thermofisher Scientific
Serological Pipettes Different Sizes (5 ml, 10 ml and 25 ml)	760107	Greiner
Superfrost™ Ultra Plus Adhesion Slides, size 25 mm × 75 mm (50)	1014356145	Fisher Scientific
Tissue Culture plates (6-wells, 12 wells, 24 wells, 48 well and 96 wells)	657160	Greiner
Tissue Culture Test Plate 6	92006	TPP / Switzerland
Well Insert Holder in Deep Petri Dish for Alvetex Well Insert	AVP015-2	Reprocell / Reinnervate

Table 2.10 Consumables used for general techniques throughout the study.

2.2.11 *OTHER TOOLS*

Item	Catalogue #	Company
Acrodisc 32 Syring Filter with 0.2 µm Supor Membrane	4652	Pall Corporation
Disposable Scalpels Sterile R	0525	Swan Morton
Falcon® 100µm Cell Strainer, Yellow, Sterile	352360	Falcon A Corning Brand
Premier Disposable Microtome Blade, 34° cutting angle	MB35	Thermofisher Scientific
Stiefel Biopsy Punch 3mm (pack of 10)	BC-BI-1000	SCHUCO

Table 2.11 Other tools used for different lab purposes.

2.2.12 *BIOIMAGING MACHINES*

Different microscopes listed in (Table 2.12) below were used to investigate cells including MSCs, HaCat cell lines, primary keratinocytes and primary fibroblasts and their behaviour such as migration, proliferation and differentiation under different conditions and at different time points. All bioimaging machines used in this study were available at the Medical School / Newcastle University.

Machine	Purpose	Location
Olympus CK2 Microscope	Regular Monitoring of Cell Culture	Academic Haematology
Carlzeiss Jena Jenamed 2 Microscope	Regular Cell count	Academic Haematology
Leica DM IRB	Imaging MSC Morphology	BioBank
	MSC Differentiation into Tri-lineages	
Nikon BioStation	Cell Migration (Scratch assay)	BioImaging Unit
Nikon TiE Multi-Modality (WF, BF, TIRF, SD Confocal (invert))	Cell Migration (Scratch assay)	BioImaging Unit
Zeiss AxioImager with Apotome (wide field fluorescence, upright)	Keratinocyte Differentiation Markers Immunofluorescence (IF)	BioImaging Unit
	MSC Differentiation into Skin-like Cells Immunofluorescence (IF)	
	3D Skin Model Immunofluorescence (IF)	
	3D Skin Model Bright Field (BF)	

Table 2.12 Microscopes used to image the live cells, dead stained cells and 3D skin equivalent models (3D-SEM).

2.2.13 *PREPARATION OF CULTURE MEDIA*

Culture media and reagents required addition of supplements at specific concentrations and volumes before use. Therefore, two main equations (Equation 2.1 and Equation 2.2) were used to prepare the correct amount of these additives.

$$\boldsymbol{Molarity\ (M)} = \frac{\boldsymbol{Weight\ (W)}}{\boldsymbol{Molecular\ Weight\ (Mwt)}} \times \boldsymbol{Volume\ (V)} \quad \ldots\ldots\ldots \quad \text{Equation 2.1}$$

$$\boldsymbol{C1 \times V1 = C2 \times V2} \quad \ldots\ldots\ldots \quad \text{Equation 2.2}$$

When:
C1 V1= Start concentration and start volume.
C2 V2= Final concentration and final volume.

2.2.13.1 *STEM CELL CULTURE MEDIA*

This media was used as complete media already supplemented with foetal calf serum and L-Glutamine. Before use, it was supplemented with 5 ml of 100IU/ml penicillin - 100 µg/ml streptomycin and used to grow and expand MSCs.

2.2.13.2 *STANDARD CULTURE MEDIA*

This media was used to grow HaCat cell lines and primary fibroblasts. It was also used to suspend and seed fibroblasts onto the Alvetex® in the 3D skin equivalent model (3D-SEM) and referred to as media A. The ingredients of this media are detailed in (Table 2.13).

Item	Volume (ml)	Concentration
Dulbecco's Modified Eagles Media (DMEM)	500	---
FCS or FBS	50	10 %
200 mM L-Glutamine	20	4 %
100 IU/ml penicillin, 100 µg/ml streptomycin (PS)	5	1%

Table 2.13 Components of standard culture media.

2.2.13.3 *MCDB MEDIA*

This media was used to grow primary keratinocytes. It is composed of the following ingredients listed in (Table 2.14).

Ingredients	Volume / Concentration	Final Concentration
MCDB153 with L-glutamine, 28 mmol/L HEPES	500 ml	------
Histidine	18.65 mg	240 µmol/L
Isoleucine	49.2 mg	750 µmol/L
Methioninen	6.7 mg	90 µmol/L
Phenylalanine	7.45 mg	90 µmol/L
Tryptophan	4.6 mg	45 µmol/L
Tyrosine	9.775 mg	100 µmol/L
Ethanolamine (98% w/v)	3.05 µL	100 µmol/L
Phosphorylethanolamine	7.05 mg	100 µmol/L
Calcium chloride (1 mol/L)	20 µL	40 µmol/L
Sodium bicarbonate	588 mg	15 mmol/L
Human keratinocyte growth supplement	5 mL	≈1%
Penicillin/streptomycin/amphotericin (PSA)	5 mL	≈1%

Table 2.14 Constituents of MCDB media.

2.2.13.4 *CONDITIONED MEDIA*

This media was used to collect MSC secretions. Two types of conditioned media were used; high calcium level (which is a DMEM based formula and used to collect MSC secretions for experiments involving HaCat cells and fibroblasts) and low calcium level

(which is MCDB based formula and used to collect MSC secretions for primary keratinocyte experiments). For both media, 1% of insulin-transferrin-selenium (ITS) was added to support MSC growth. The ingredients of these media are listed in (Table 2.15).

Media Type	Formula based	Purpose	Ingredients	Volume
High-Calcium Conditioned Media (HC-CM)	DMEM	experiments involving HaCat cells and fibroblast	DMEM	500 ml
			PS	5 ml
			L-Glutamine	20 ml
			ITS	5 ml
Low-Calcium Conditioned Media (LC-CM)	MCDB	keratinocyte experiments	MCDB	500 ml
			PSA	5 ml
			L-Glutamine	20 ml
			ITS	3ml

Table 2.15 Types of media used to collect MSC secretions.

2.2.13.5 *EPIDERMAL DIFFERENTIATION MEDIA (EDM)*

This media was used to grow MSCs and test their ability to differentiate into skin-like cells. It is composed of the following ingredients listed in (Table 2.16) below:

Item	Volume (ml)	Concentration
Dulbecco's Modified Eagles Media (DMEM)	375 ml	---
Ham's F12 Nutrient Mixture	125 ml	---
Chelex-treated Foetal Calf Serum	25 ml	5 %
200 mM L-Glutamine	20 ml	4 %
100 IU/ml Penicillin, 100 µg/ml Streptomycin (PS)	5 ml	1 %
250 µg/ml Amphotericin B	5 ml	2.5 %
Recombinant Human Epidermal Growth Ffactor (0.2 mg/ml)	50 µl	10 ng/ml
Adenine (6 mg/ml)	2 ml	24 µg/ml
Cholecalciferol (Vitamin D3)	10 µl	1 µM
Cholera toxin (0.85 mg/ml)	5 µl	8.5 ng/ml
3,3',5-Triiodo-L-thyronine sodium salt (T3)	200 µl	1 nM
Hydrocortisone (0.5 mg/ml)	400 µl	0.5 µg/ml
Insulin, Recombinant Human (10 mg/ml)	250 µl	5 µg/ml
Transferrin (10 mg/ml)	250 µl	10 ng/ml
L-Ascorbic acid (10 mg/ml) added fresh	100 µl per 10 ml media	100 µg/ml

Table 2.16 Ingredients of epidermal differentiation media.

2.2.13.6 *MEDIA OF 3D SKIN EQUIVALENT MODEL (3D-SEM)*

According to the methods of Hill and colleagues (Hill *et al.*, 2015), four types of media were used to feed the 3D-SEM during the different phases of the model construction as shown below.

2.2.13.6.1 STANDARD CULTURE MEDIA (MEDIA A)

This is the same standard culture media listed in 2.2.13.2. It was used to suspend the fibroblasts and seed them on to the Alvetex®.

2.2.13.6.2 DERMAL LAYER FEEDING MEDIA (MEDIA B)

This is a DMEM based formula with the additives listed in (Table 2.17) below. It was used to feed first and second fibroblast layers of the 3D-SEM for three weeks.

Item	Volume (ml)	Concentration
Dulbecco's Modified Eagles Media (DMEM)	500	---
FCS or FBS	50	10 %
200 mM L-Glutamine	20	4 %
100 IU/ml Penicillin, 100 µg/ml Streptomycin (PS)	5	1 %
100 IU/ml Amphotericin B	5	1 %
L-ascorbic acid (10 mg/mL) added fresh	100 µl per 10 mL media	100 µg/ml

Table 2.17 Components of dermal layer feeding media (media B).

2.2.13.6.3KERATINOCYTE CHELATING MEDIA (MEDIA C)

The serum of this media was treated with chelex by dissolving 1 g of chelex in 25 ml FCS, centrifuged for 12 hours at 2500 rpm, filtered via 0.22-µm filter and added to the remainder of the media component. This media was used for co-culture of keratinocytes over the dermal fibroblast layer of the 3D skin model. These co-cultures were fed with this media for three days with a daily change. The ingredients of this media are listed in (Table 2.18).

Item	Volume (ml)	Concentration
Dulbecco's Modified Eagles Media (DMEM)	375 ml	---
Ham's F12 Nutrient Mixture	125 ml	---
Chelex-treated Foetal Calf Serum	25 ml	5 %
200 mM L-Glutamine	20 ml	4 %
100 IU/ml Penicillin, 100 µg/ml Streptomycin (PS)	5 ml	1 %
100 IU/ml Amphotericin B	5 ml	1 %
Recombinant Human Epidermal Growth Factor (0.2 mg/ml)	50 µl	10 ng/ml
Insulin, Recombinant Human (10 mg/ml)	250 µl	5 µg/ml
Adenine (6 mg/ml)	2 ml	24 µg/ml
Cholera toxin (0.85 mg/ml)	5 µl	8.5 ng/ml
Hydrocortisone (0.5 mg/ml)	400 µl	0.5 µg/ml
L-ascorbic acid (10 mg/mL) added fresh	100 µl per 10 mL media	100µg/ml

Table 2.18 Constituents of keratinocyte chelating media (Media C).

2.2.13.6.4 AIR-LIQUID INTERPHASE MEDIA (MEDIA D)

This media was used to feed the dermal fibroblast layer of the 3D-SEM after exposure of the model to the air-liquid interface with 6 changes for two weeks. The ingredients of this media are listed in (Table 2.19).

Item	Volume (ml)	Concentration
Dulbecco's Modified Eagles Media (DMEM)	375 ml	---
Ham's F12 nutrient mixture	125 ml	---
FCS or FBS	50 ml	10 %
200 mM L-Glutamine	20 ml	4 %
100 IU/ml Amphotericin B	5 ml	1 %
100 IU/ml penicillin, 100 µg/ml streptomycin (PS)	5 ml	1 %
Recombinant Human Epidermal Growth Factor (0.2 mg/ml)	50 µl	10 ng/ml
Transferrin (10 mg/mL)	250 µl	250 µg/ml
Cholera toxin	5 µl	0.85 mg/ml
Hydrocortisone (0.5 mg/ml)	400 µl	0.5 µg/ml
L-ascorbic acid (10 mg/mL) added fresh	100 µl per 10 mL media	100 µg/ml

Table 2.19 Ingredients of air-liquid interphase media (Media D).

2.2.13.7 *FREEZING SOLUTIONS*

Different solutions were used to freeze the different cell types as shown in (Table 2.20).

Freezing Solution	Ingredients	Cell Type
Freezing Solution A	70% RPMI + 20% FCS + 10% DMSO	HaCat cell line
Freezing solution N	90% FCS or FBS + 10% DMSO	MSCs and Fibroblast
Kers Freezing Solution	90% MCDB + 10% DMSO	Primary keratinocytes

Table 2.20 Freezing solutions of different cell types.

2.3 METHODS

2.3.1 *GENERAL PROTOCOLS OF CELL CULTURE*

All cell culture was performed in class II cabinets to reduce the risk of infection and contamination. Then, all the cells and skin models were incubated at standard culture conditions (SCC) which were provided by humidified incubator adjusted to 37ºC, ≈20%O_2 and 5% CO_2. Unless otherwise stated, all culture conditions set out in in this study for cell culture and cell experiments were SCC.

2.3.1.1 *SPLITTING PROTOCOL FOR MONOLAYER CELLS*

Old media was aspirated and cells were rinsed with PBS, trypsinised with trypsin 1X and incubated for 10 minutes. A quantity of 10 ml of DMEM with 10 % FCS was added to prepare the cell suspension and centrifuged at 1500 rpm for 5 minutes. The supernatant was discarded and cells were counted and a cell number of 5×10^5 to 1×10^6 was seeded into a T75 flask. A quantity of 15-20 ml of fresh growth medium (4mM L-glutamine, 4500 mg glucose / L, 1500 mg/L sodium bicarbonate, FCS (110 ml), 10,000 I.U./ml penicillin, 10,000 (ug/ml) streptomycin) were added to the flask and incubated under SCC (Sandell and Sakai, 2008).

2.3.1.2 *CELL COUNT*

Methylene blue stain was used to stain mononuclear cells to assess their total count during MSC isolation. Trypan blue stain was used to assess viability of all cells including MSCs, HaCat cells, fibroblasts and primary keratinocytes. In both stains, a volume of each was mixed with an equal volume of cell suspension. A quantity of 10 µl of this mixture was transferred to a Neubauer chamber and covered with a cover slip prior to counting under the microscope (Sandell and Sakai, 2008). (Equation 2.3) and (Equation 2.4) were used to calculate cell count and cell viability.

$$\boldsymbol{Total\ Cell\ Count = No\ of\ cells\ in\ 25\ small\ square \times Dilution\ Fcator \times 10^4} \quad \text{....} \quad \text{Equation 2.3}$$

$$\boldsymbol{Cell\ Viability = \frac{No\ of\ viable\ cells\ in\ 25\ small\ square}{Total\ cell\ count\ (Live + dead\ cells)} \times 100\ \%} \quad \text{.....} \quad \text{Equation 2.4}$$

2.3.1.3 *CRYOPRESERVATION*

HaCat cells, fibroblasts and primary keratinocytes were frozen when they reached 80 % confluency at each passage (P1, P2 and P3). After trypsinisation with trypsin-EDTA 1X, cells were washed twice with PBS, suspended in 1 ml of growth medium and counted after staining with trypan blue. The cell suspension was centrifuged for 5 min at 2500 rpm and the supernatant was discarded. HaCat cells were re-suspended in the freezing solution A (70% RPMI, 20% FCS, and 10% DMSO), fibroblasts were re-suspended in the freezing solution N and primary keratinocytes were re-suspended in the Kers-freezing solution. A cell number of 0.5 $\times 10^6$ to 3×10^6 cells was seeded per 1.8 ml cryotube and stored in -80 freezer until use (Sandell and Sakai, 2008).

2.3.2 *ISOLATION OF MSCS FROM BONE MARROW (PRIMARY CULTURE)*

All the hip joints were obtained from Musculoskeletal Research Lab (Newcastle University, Institute of Cellular Medicine). The marrow from the femoral head of the hip joint was dislodged into a sterile tissue culture dish using sterilised pliers. After harvesting the marrow, it was mixed with 10 ml sterile PBS and filtered using a BD sieve to release cells. The bone marrow suspension was layered onto Lymphoprep into a 50 ml falcon tube with a dilution ratio of 15 ml lymphprep: 35 ml diluted BM then the mononuclear cells (MNC) were separated by density gradient centrifugation at 800 g at 20^{o}C for 15 minutes followed by collecting Lymphoprep-plasma interface which was washed twice in PBS at 500 g for 5 minutes each. The cell pellet was re-suspended in 1 ml non-haematopoietic medium (NH) and counted with methylene blue dye. A total count of $3 \times 10^7 – 8 \times 10^7$ MNCs was seeded per T25 flask and incubated lying horizontally under SCC. The medium was changed every three days and cells were split when they reached 80 % confleunce (Quiroz et al., 2013).

2.3.3 *EXPANSION OF MSCS IN VITRO*

The old medium was discarded and the cells were rinsed with PBS, followed by addition of 4 ml Trypsin-EDTA for a T25 flask or 7 ml for a T75 flask and incubated at 37°C for 5 minutes. When cells were completely detached from the flask surface, a quantity of FCS (0.5 ml to T25 and 1.0 ml to T75) was added to deactivate Trypsin–EDTA activity, followed

by washing the cells twice with PBS. The cell pellet was re-suspended in 1 ml NH medium and counted using trypan blue dye. A total count of $1x10^5$ to $2x10^5$ cells was seeded into a T25 flask in 10 mls of medium or $3x10^5$ to $5x10^5$ cells into T75 flasks in 20 mls of medium depending how quickly the cells were needed for the assays (Jung *et al.*, 2012). Both population doubling (PD) and doubling time (DT) were measured according to (Mareschi *et al.*, 2012) by applying (Equation 2.5) and (Equation 2.6) respectively.

$$PD = \frac{lOG\ (H) - Log\ (s)}{Log\ (2)} \quad \text{. . . . .} \quad \text{Equation 2.5}$$

$$DT = \frac{\Delta T\ Log\ (2)}{lOG\ (H) - Log\ (s)} \quad \text{. . . . .} \quad \text{Equation 2.6}$$

When:
S= Number of Seeded cells.
H= Number of Harvested cells.
ΔT= Time from seeding to harvesting (time required to reach 80% confluence at a given passage).

2.3.4 *CRYOPRESERVATION OF MSCS*

All MSC samples were frozen when they reached 80% confluence at each passage (P1, P2 and P3). MSCs were detached and counted as mentioned above in expansion protocol, but, instead of seeding cells into a culture flask, a cell number of 10^5 cell / ml was transferred into cryogenic vials (2 ml Nalgene)and centrifuged for 5 min (1000 rpm at room temperature) to obtain a cell pellet. The medium was discarded and 1 ml of freezing solution (90% FCS, 10% DMSO) was slowly added. All vials were stored at –80°C freezers until needed (Naaldijk *et al.*, 2012).

2.3.5 *CHARACTERISATION OF MSCS*

Isolated MSCs were tested for the minimal criteria defining h-MSCs stipulated by the ISCT in 2006 (Jung *et al.*, 2012). These tests were the following:-

2.3.5.1 *MORPHOLOGICAL CHARACTERISATION TEST*

The isolated cells were tested for their morphology by monitoring their shape and the ability to attach to the plastic surface of the culture flask (Jung *et al.*, 2012).

2.3.5.2 *PHENOTYPIC CHARACTERISATION TEST*

All isolated MSCs were analysed for their phenotypic characteristics at passage 3 (P3). AMSC suspension consisting of 2×10^6 cell / ml was prepared by suspending MSCs in FACS buffer (10 ml of FBS or FCS + 1 ml of 1 mM EDTA in 500 ml Dulbecco's PBS) (Pravdyuk, Petrenko et al. 2013). As demonstrated in (Table 2.21), the suspension was equally divided (300 µl/tube) into five different tubes, isotype stained tube-1, Ab stained tube-2, HLA-DR isotype tube-3, HLA-DR ab-4 and negative control tube-5. The following isotypes were added to tube-1 (7µl FITC mIgG1, 2µl FITC mIgG2b, 1 µl PE mIgG1, 0.5 µl perCPCymIgG1 and 1 µl APC mIgG1). Tube-2 contained the following antibodies (4µl CD73-PE, 2µl CD105-APC, 2µl CD90-PerCPCy5.5, 4µl CD14-FITC, 4µl CD19 FITC, 4µl CD34 FITC and 4µl CD45 FITC). In addition, 0.25µl APC-H7mIgG2a was added to tube-3, and 1µl HLA-DR APC H7 to tube-4. While neither isotype nor antibody were added to the negative control (Jung *et al.*, 2012). All tubes were incubated at 4ºC for 20 minutes. After the incubation period, 2 ml of FACS buffer was added to each tube and centrifuged for 5 min at 500 g to remove unbound antibodies. The washing buffer was removed and the cells were re-suspended in 400 µl FACS buffer prior to analysis on the Fluorescent Activated Cell Sorter (FACS Canto II). Immediately prior to running the tube on the FACS Canto II, 50 ul DAPI were added to assess viability (Akiyama *et al.*, 2012; Pravdyuk *et al.*, 2013).

Tube No & Conditions →	Tube 1 Isotype Stained	Tube 2 Ab Stained	Tube 3 HLA-DR Iso	Tube 4 HLA-DR Ab	Tube 5 Unstained
Steps ↓					
MSCs	300 µl 0.15 × 10^6 cell	300 µl 0.15 × 10^6 cell	300 µl 0.15 × 10^6 cell	300 µl 0.15 × 10^6 cell	300 µl 0.15 × 10^6 cell
Ab ------- Isotype	7µl FITC mIgG1 2µl FITC mIgG2b 1 µl PE mIgG1 0.5 µl perCPCy mIgG1 1 µl APC mIgG1	4µl CD73-PE 2µl CD105-APC 2µl CD90-PerCPCy5.5 4µl CD14-FITC 4µl CD19-FITC 4µl CD34-FITC 4µl CD45-FITC	0.25µl APC-H7mIgG2a	1µl HLA-DR APC H7	None
Incubation	All tubes were incubated at 4° C for 20 minutes				
FB	2000 µl	2000 µl	2000 µl	2000 µl	2000 µl
Spinning	centrifuged for 5 min at 500 g				
FB	400 µl	400 µl	400 µl	400 µl	400 µl
DAPI	50 µl	50 µl	50 µl	50 µl	50 µl

Table 2.21 Summary of MSC phenotyping assay.

The MSC phenotypic assay consists of 7 steps as detailed before starting the assay, five tubes were labeled; Tube 1 Isotype stained, Tube 2-Antibody stained, Tube 3-HLA-DR Isotype, Tube 4-HLA-DR Antibody and Tube 5 Unstained cells. 300 µl of MSCs were added at a cell count 0.15×10^6 cell in each tube as shown in step 1. Conjugated antibodies and isotypes were added at the stated volumes in step 2 then, cells were incubated at 4°C for 20 minutes in step 3. Followed by addition of 400 µl of FB and cells were centrifuged for 5 minutes at 500g as in step 5. Then at step 6, cells were suspended in 400 µl of FB and mixed with 50 µl of DAPI immediately before assessment by the FACS Canto II. FITC= fluorescein isothiocyanate, PE= phycoerythrin, perCPC= peridinin chlorophyll protein, APC= Allophycocyanin, FB= FACS Buffer= (10 ml of FBS or FCS + 1 ml of 1 mM EDTA in 500 ml Dulbecco's PBS)

2.3.5.3 *ASSESSMENT OF MSC DIFFERENTIATION POTENTIAL*

When MSCs reached 80 % confluence at P3, they were trypsinised with trypsin-EDTA and counted prior to testing for their differentiation potential. (Table 2.22) summarises the steps of MSC differentiation into tri-linages; adipocyte, osteoblast and chondroblast.

2.3.5.3.1 ADIPOGENESIS ASSAY

2 x10^5 MSCs per well were seeded into 6-well plates followed by addition of 2 ml NH medium. The plate was incubated under SCC until confluent. When a confluent monolayer was formed, the NH medium was replaced with fresh Lonza adipogenic differentiation medium (ADM) with a sequential medium change of ADM every three days for 15-18 days. Cells were then fed with ADM for 3 days at SCC to reach confluence (roughly 18-21 days)

and stained with oil red stain to assess the accumulation of cytoplasmic lipid droplets under light microscopy (Vishnubalaji *et al.*, 2013). The control wells contained the same cell number and the NH medium was changed every three days.

To stain the cells, the media was removed and the cells were rinsed with PBS and fixed with 2 ml 10% formalin and left for 30-60 minutes. The formalin was then removed and cells rinsed with distilled water (DW), followed by addition of 2 ml 60% isopropanol to the well and left for 5 minutes. The isopropanol was then completely removed and 2 ml of 0.3% Oil Red O working solution was added and left for 5 minutes. Cells were rinsed with distilled water until the water ran clear and assessed using an inverted microscope.

2.3.5.3.2 OSTEOGENESIS ASSAY

Cell count of 3×10^4 MSCs per well were seeded in duplicate into a 6 well plate followed by addition of 2 ml of osteogenic differentiation medium (ODM). The negative control well contained the same cell number but was supplemented with NH medium. The plate was incubated under SCC and after 24 h, both the test and the negative control wells were enriched with fresh ODM and NH media respectively every three days. Twenty-one days later, cells were stained with alkaline phosphatase (ALP) and Von Kossa stain for further assessment by light microscopy (Akiyama *et al.*, 2012)..

The staining protocol required preparation of alkaline phosphate substrate solution (ALSS) which was prepared by diluting 6 mg of Napthol AS phosphate in 0.1 ml of dimethylformamide, then mixed with 20 ml of Tris HCl buffer (0.2M), followed by addition of 2 mg of fast blue dye and filtered before use.

For staining cells, the media was removed and the cells rinsed with 2 ml of PBS to remove any residual media. Cells were then fixed with 10% formalin for at least 10 minutes at 37^{o}C. The formalin was removed and cells washed twice with 0.2M Tris HCl buffer and then with DW,followed by staining with filtered ALSS overnight in a 37^{o}C. ALSS was then discarded and the cells washed with double DW three times and covered with 2 ml of Von Kossa stain (3% silver nitrate “AgNO3”) and left for at least one hour under a white light lamp. Silver nitrate was then discarded and cells washed with double DW three times, covered with water and assessed under light microscopy.

2.3.5.3.3 CHONDROGENESIS ASSAY

$0.25x10^6$ MSCs were suspended in 1 ml NH medium in a 15 ml polypropylene conical tube and centrifuged for 5 minutes at 150 g at room temperature. The supernatant was completely aspirated and a fresh pre warmed chondrogenic differentiation medium (CDM) was added and centrifuged for 5 minutes at 150g, at room temperature. The tube was incubated upright under SCC keeping the cap loose without disturbing the cell pellet. CDM was replaced every three days for 21 days. At day 21, the supernatant was removed and the pellet was fixed with 10% formalin for three hours at room temperature. The formalin was then discarded and the pellet was embedded in paraffin before taking thin sections for slide preparation and staining for further microscopic examination (Akiyama *et al.*, 2012).

After 21 days, the culture supernatant was discarded and chondrogenic pellets washed with PBS and fixed in 10% formalin for a minimum of 3 hours at room temperature. Formalin was then discarded and cells were stored in 70% ethanol at room temperature (RT) and embedded in paraffin wax (Biobank Service) and sectioned (5 µm) on slides. The slides were deparaffinised by soaking in xylene for 10 minutes, 100% ethanol for 5 minutes, 95% ethanol for 5 minutes, 70% ethanol for 5 minutes, washed in 0.1N HCl for 1 hour and stained with 0.1% alcian blue solution overnight. On the next day, the slides were washed in 0.1N HCl and assessed for proteoglycan staining using a bright field Leica microscope.

Step	Period (Days)	Lineage Manipulation			
		Adipogenesis	Osteogenesis	Control	Chondrogenesis
1	0	0.2×10^6 cells Plate (*NH)	0.03×10^6 cells Plate (ODM*)	0.2×10^6 cells Plate (NH)	0.25×10^6 cells in 15 ml Vial (1 ml CDM*)
2	1	-----	ODM after 24h	------	------
3	3	Change *ADM	Change ODM	Change NH	Change CDM
4	6	Change ADM	Change ODM	Change NH	Change CDM
5	9	Change ADM	Change ODM	Change NH	Change CDM
6	12	Change ADM	Change ODM	Change NH	Change CDM
7	15	Change ADM	Change ODM	Change NH	Change CDM
8	18	Staining with Oil Red	Change ODM	Change NH	Change CDM
9	21		*ALP / Von Kossa	----------	Formalin fixation Paraffin embedding Alcian Staining

Table 2.22 Summary of MSC differentiation assays.

This table explains the steps of manipulating MSCs during the differentiation assay into tri-lineages. At day zero, a cell count of 0.2×10^6 cells/well of MSCs were seeded into six-well plates, labelled as adipocytes and fed with NH media for three days followed by feeding with ADM until day 18 and then stained with oil red. For osteoblasts, 0.03×10^6 MSC cells/well were seeded into six-well plates in ODM for 24 hours followed by changing the media every three days for 21 days and then stained with ALP / Von Kossa satin. For chondrogenesis, MSCs were seeded at a density of 2.5×10^6 cells/wells in 1 ml CDM in a 15 ml tube and fed with CDM for three weeks followed by fixation of the pellet with 10% formalin, paraffin embedding, sectioning, slide fixation and staining with Alcian satin. The control cells for each lineage were treated the same as the test cells but fed with only NH media. NH= Non-haematopoietic Medium, ADM*= Adipogenic Differentiation Media, ODM*= Osteogenic Differentiation Medium, CDM*= Chondrogenic Differentiation Medium, ALP*= Alkaline Phosphatase*

2.3.6 *PREPARATION OF MSC CONDITIONED MEDIA (MSC-CM)*

MSC conditioned medium (MSC-CM) was collected when the cells reached 80 % confluence by discarding the NH medium, washing the cells with PBS twice and adding 20 ml of either fresh serum free medium with standard calcium levels (1.8 mM/L) (DMEM based formula for HaCat and fibroblasts) or low calcium levels (0.07 mM/L) (MCDB based formula for primary keratinocytes). Both media were supplemented with 1 % insulin-transferrin-selenium (ITS) to support MSC growth (Walter et al., 2010), 20 ml L-glutamine and streptomycin-penicillin. MSC-CM was collected after 24, 48 and 72 hours and referred to as (CM24, CM48 and CM72) and centrifuged at 3,000 rpm for 5 minutes to remove cell debris, filtered through a 0.2 µm filter and stored at -80ºC until needed (Walter *et al.*, 2010; Hsiao *et al.*, 2012; Tamama and Kerpedjieva, 2012; Moghadasali *et al.*, 2013).

2.3.6.1 *PROTEOMIC ANALYSIS OF MSC-CM*

ELISA kits from Lifetechnologies Company were used to detect the protein content of 5 MSC-CM samples. The most important growth factors and cytokines which were well

documented to possess a positive effect on wound healing were studied and were; KGF, HGF, EDGF, PDGF-α, TGF-1β, SDF-1α, and MSP-1. An example of an ELISA kit is shown in (Table 2.23).

Item	Quantity	Preparation
Anti-Human GF Precoated 96-well Strip Plate	1	Ready to use
Assay Diluent, 5X concentrated buffer	15 mL	Diluted 5 times in DDW to get 1X assay diluent (1X AD)
Lyophilized Recombinant Human GF Standard	2 vials	Diluted in 400 µl 1X AD. See 2.3.11.1 for more details
20X Wash Buffer	25 mL	Dilute 20 times in DDW to get 1X wash buffer (WB)
Biotinylated Antibody Reagent	2 vials	Dilute in 100 µl 1X AD then, diluted 80 times in 1X AD
Streptavidin-HRP Reagent	200 µL	Dilute 200 times in 1X AD
TMB Substrate	12 mL	Ready to use
Stop Solution, contains 0.2M sulfuric acid	8 mL	Ready to use
Adhesive Plate Sealer	2	Ready to use

Table 2.23 An example of an ELISA kit and reagent preparation.

2.3.6.2 *PREPARATION OF STANDARDS AND SAMPLES*

All kit reagents and samples (MSC-CM and controls) were brought to room temperature (18-25ºC) before use. 1X assay diluent was used to dilute the MSC-CM and controls up to 2 fold. For preparation of standards, 400µL 1X assay diluent was added into the lyophilized standard of a given growth factor and used as the starter standard (SS) which was then used to prepare serial dilutions of the lower concentrations as shown in (Figure 2.1).

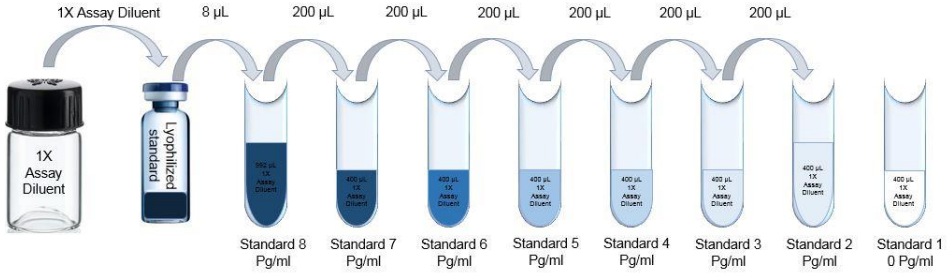

Figure 2.1 Preparation of ELISA standards.

Preparing standards of the ELISA kit. The lyophilised standard was diluted with 1X assay diluent to give the standard solution (SS) which differed depending on the growth factor (see Table 2.24 below). After dissolving the lyophilised standard, a specific volume was taken from the SS and added to a vial containing a specific volume of 1X assay diluent to make standard no 8. Other standards (7-2) were prepared by serial dilution of the standards in the same volume of 1X assay diluent. Standard number 1 represents 1X assay diluent only at 0 pg/ml.

The concentrations of standards were different depending on the growth factor; therefore, the required volumes to prepare each standard concentration were different as showed in (Table 2.24).

GFs	Assay Diluent Volume (µl)	Concentration of Starter Standard (ng/ml)	Stand 8 Pg/ml	Stand 7 Pg/ml	Stand 6 Pg/ml	Stand 5 Pg/ml	Stand 4 Pg/ml	Stand 3 Pg/ml	Stand 2 Pg/ml	Stand 1 Pg/ml
HGF	1000	20	8000	4000	2000	1000	500	250	125	0
KGF	400	50	400	133.3	44.44	14.81	4.94	1.65	0.55	0
TGF-β1	1000	10	2000	1000	500	250	125	62.5	31.2	0
SDF-1	400	17	6000	3000	1500	750	375	187.5	93.75	0
PDGF-AB	400	50	2500	1000	400	160	64	25.6	10.24	0
MSP-1	400	50	-------	2000	666.7	222.2	74.07	24.69	8.23	0

Table 2.24 Concentrations of standards differ depending on growth factors.

ELISA kits designed for estimating the concentration of growth factor are provided with standards specific for each growth factor. The concentrations of these standards vary depending on the concentration of the growth factor found in human serum and other body fluids. The standard range was above and below the standard level of the growth factor.

To prepare the biotinylated antibody working reagent, 100 µl of 1X assay diluent was added to the biotinylated antibody stock reagent, and diluted 80 fold with 1X assay diluent. The streptavidin-HRP working reagent was prepared by diluting 200-fold with 1X assay diluent as shown in (Table 2.23).

2.3.6.3 *GENERAL ELISA PROTOCOL*

The summary steps of an ELISA protocol are shown in (Figure 2.2). Briefly, 100 µl of the standards and MSC-CM were added into appropriate wells, covered and incubated for 2:30 hours at room temperature with gentle shaking. After the incubation time, the content of each well was discarded and washed four times with 1X washing buffer, which was then discarded and the wells inverted over clean absorbance tissue to remove any remaining wash buffer. 100 µl of 1X prepared biotinylated antibody working reagent was then added to each well and incubated for 1 hour at room temperature with gentle shaking. Well contents were discarded and the well was washed with wash buffer before addition of 100 µl of prepared streptavidin-HRP working reagent and a further incubation of 45 minutes at room temperature with gentle shaking. The wells were washed before addition of 100 µl of tetramethylbenzidine (TMB) substrate and a further incubation of 30 minutes at room temperature in the dark with gentle shaking. The final step was stopping the

reaction by adding 50 µl of stop solution (sulphuric acid) to each well and the absorbance was read at 450 nm using an ELISA reader within 30 minutes of stopping the reaction. Data were analysed by plotting the optical densities (ODs) of each standard to generate a standard curve for the standard concentrations. Then, the ODs of each MSC-CM were compared to the ODs of the standards and the concentrations of growth factors in MSC-CM were determined by comparing and plotting against the concentrations of each standard.

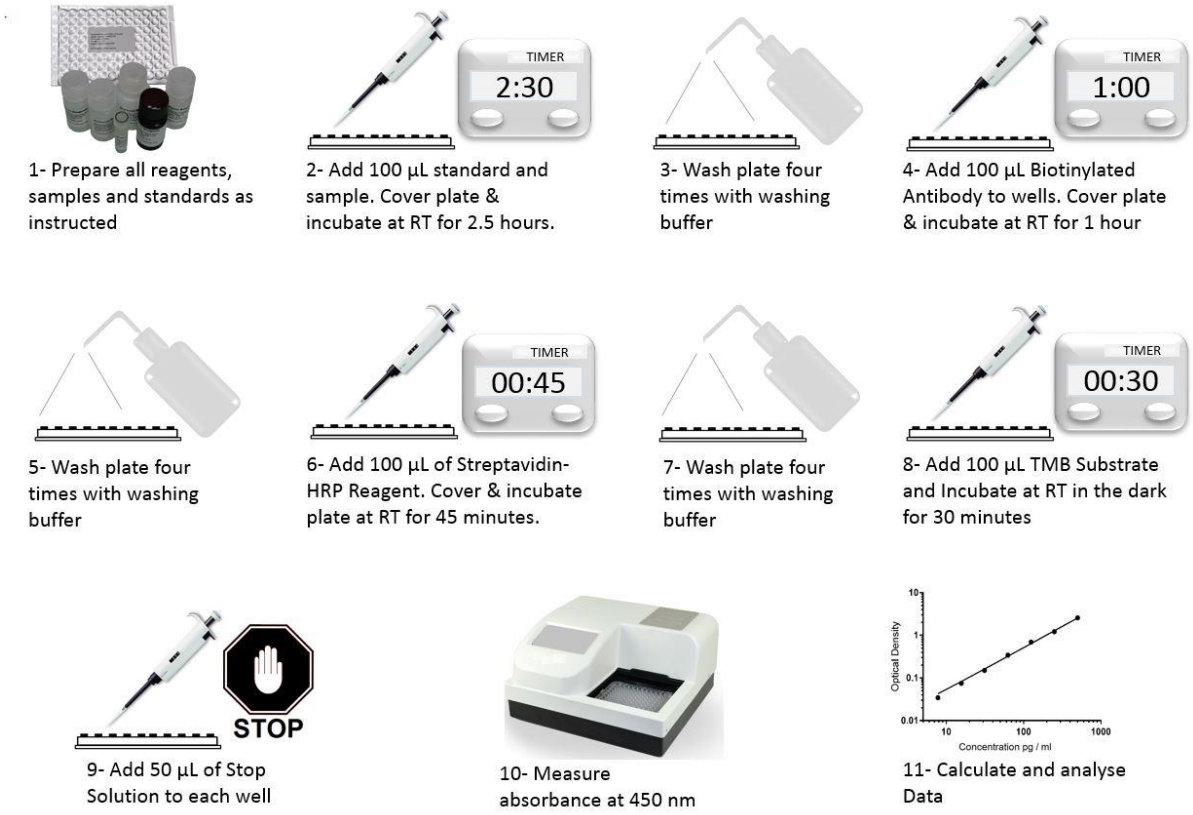

Figure 2.2 Explanatory scheme of ELISA protocol.

This flow chart summaries a general ELISA protocol. Standards and MSC-CM are added and incubated for 2:30 hours followed by washing with washing buffer (WB) four times. Then biotinylated antibody are added and incubated for one hour at room temperature followed by discarding and washing. The third addition is streptavidin reagent and incubation for 45 minutes at room temperature followed by discarding and washing. The next step is the addition of TMB and incubation for 30 minutes in dark at room temperature. The final step is stopping the reaction by addition of stop solution. The optical density (OD) of both standards and MSC-CM are measured at 450 nm and compared to each other to determine the relative concentration.

ELISA readings showed consistent optical densities proportional to the corresponding concentrations of standards of a given growth factor as explained in (Figure 2.3).

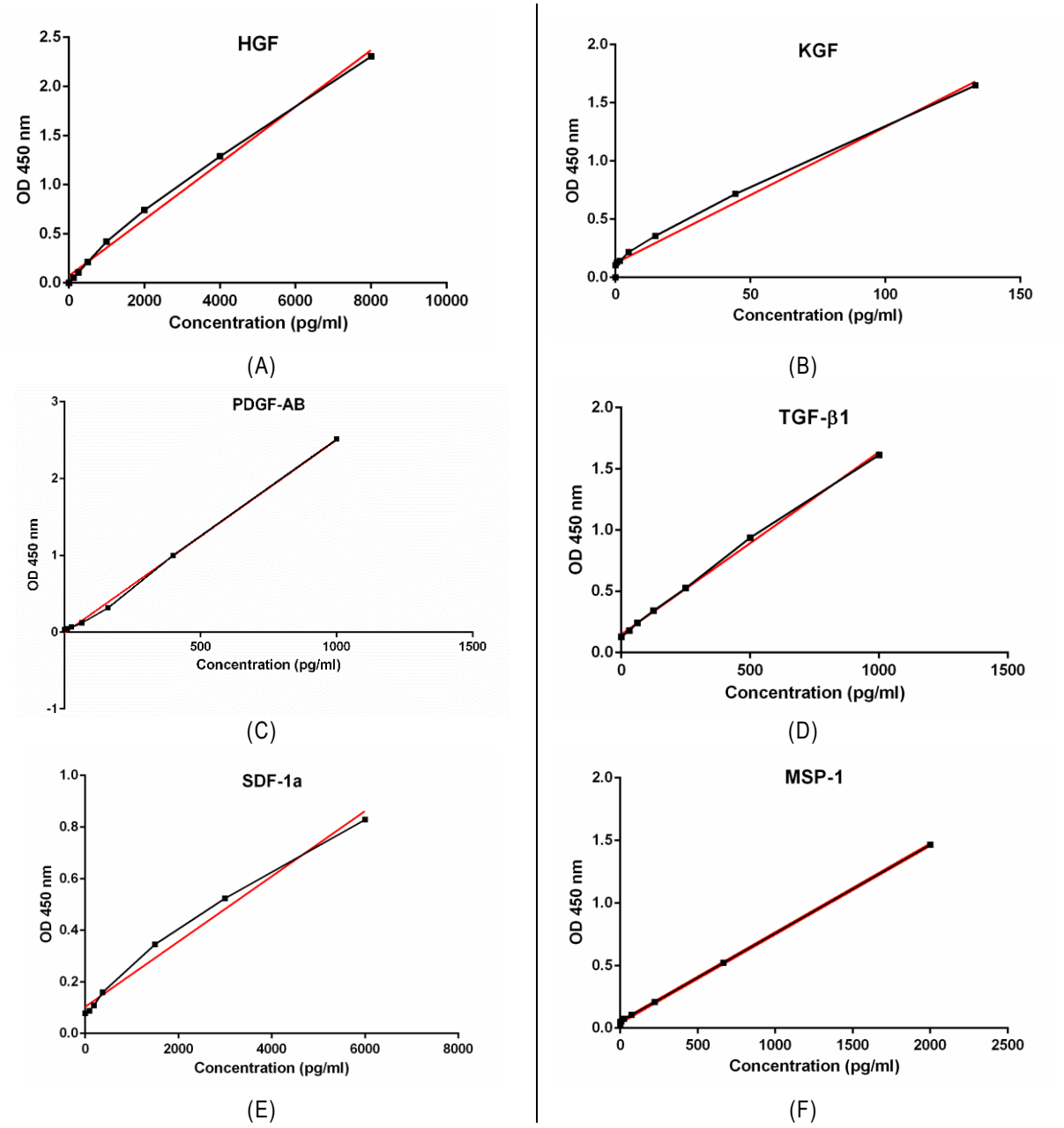

Figure 2.3 Standards curves of growth factors and cytokines.

Each growth factor has specific serial concentrations that differ from the others. All standards were read at 450 nm and their absorbance were plotted against the corresponding standard concentration which are presented in picogram / ml unit. (A) Standard curve of hepatocyte growth factor (HGF) which has serial standards (8000, 4000, 2000, 1000, 500, 250, 125 and 0.0) pg/ml. (B) Standard curve of keratinocyte growth factor (KGF) with serial standards (400, 133.3, 44.44, 14.81, 4.94, 1.65, 0.55 and 0.0) pg/ml. (C) Standard curve of platelet derived growth factor α and ß (PDGF-AB) with serial standards (1000, 400. 160, 64, 25, 10.0 and 0.0) pg/ml. (D) Standard curve of transforming growth factor ß1 (TGF- ß1) with serial standards (1000, 500, 250, 125, 62.5, 31.2, 15.6 and 0.0) pg/ml. (E) Standard curve of stromal derived factor-1 (SDF-1) with serial standards (6000, 3000, 1500, 750, 375, 187, 93.75 and 0.0) pg/ml. (F) Standard curve of macrophage stimulating protein-1 (MSP-1) with serial standards (2000, 666.7, 222.2, 74.07, 24.69, 8.23 and 0.0) pg/ml.

2.3.7 *HUMAN SKIN PRIMARY CELLS AND CELL LINES*

2.3.7.1 *CONSENT AND ETHICS*

Human skin cells including (keratinocyte and fibroblast) used in this study were obtained with agreement and consent of each donor. Approval for the study was given by the Local Research Ethics Committee (NRES Newcastle and North Tyneside 1 REC 08/H0906/95+5) which was obtained on the 10th March 2014.

2.3.7.2 *ISOLATION OF SKIN CELLS*

A volume of 1 ml of dispase was mixed with 1 ml Penicillin-Streptomycin-Amphotericin (PSA) then the mixture was added to 8 ml of PBS in a universal tube labelled with name or the code of the corresponding skin. The skin bioposy was transferred to a petri dish containing PBS. Scratches along and across the epidermal side of the skin were made in the skin biopsy to allow dispase to penetrate and embed the cocktail of Dispase-PSA-PBS solution. The biopsy was incubated under SCC for at least 4 hours to allow separation of the dermal layer from the epidermal layer. After the incubation period, skin cells were isolated as detailed below.

2.3.7.2.1 KERATINOCYTE ISOLATION

The scratched skin was removed from the universal and placed in a petri dish containing PBS and the epidermis peeled off using forceps and soaked in 5 ml trypsin-EDTA and incubated for 5 minutes under SCC. The Trypsin-EDTA was then neutralized by 15 ml of 10% FCS-DMEM and centrifuged at 3000 rpm for 5 minutes. The supernatant was discarded and the pellet was mixed with 20 ml MCDB, and transferred to a 175 cm^2 culture flask and incubated at SCC overnight to allow keratinocytes to adhere. On the next day, the MCDB media was discarded and 20 ml of fresh MCDB medium were added. MCDB media was changed until splitting at passage 1.

2.3.7.2.2 FIBROBLAST ISOLATION

The remaining dermis was cut into small sections using a scalpel and placed over a tissue wet with 70% ethanol for 2 minutes and each section was transferred into a well of a 6 well plate, covered with FBS incubated at SCC for overnight. On the next day, a volume

of 5 ml of DMEM was added to each well. The dermal sections were kept in the wells with a regular change of media until splitting at passage1.

2.3.7.3 *HaCaT Cell Line*

HaCat cell line is an immortalised human keratinocyte cell line isolated from adult human skin. It is characterised for its ability to proliferate and differentiate *in vitro* therefore and it is widely used in scientific research.

2.3.7.4 *HeLa Cells*

HeLa cells showed in (Figure 2.4) are an immortalised cervical adenocarcinoma cancer cell line. The name HeLa was derived from the patients' name **He**nrietta **La**cks (Scherer *et al.*, 1953). Dr Amy Anderson / Musculoskeletal Research Group, the Faculty of Medical Sciences, Newcastle University kindly provided these cells at passage 38 and they were used as a positive control in the experiments assessing proliferation markers.

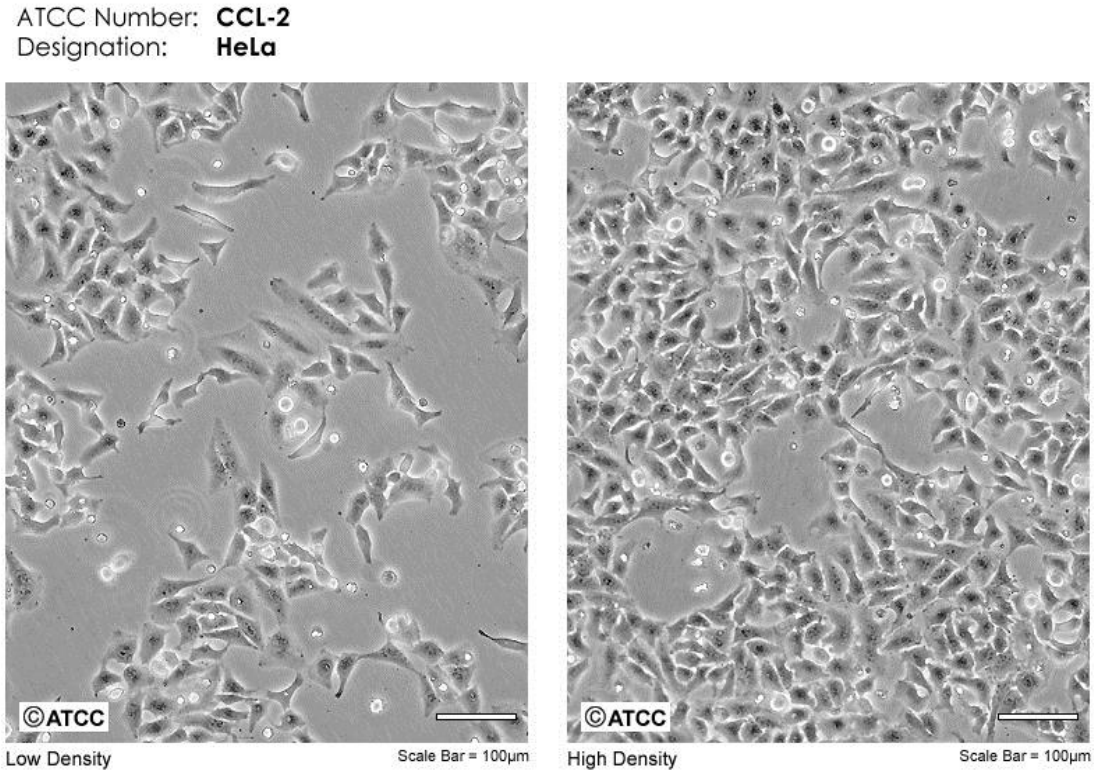

Figure 2.4 HeLa cell line in culture at different densities (Adopted from ATCC).

2.3.8 *ASSESSMENT OF CELL MIGRATION*

The scratch assay was applied to assess cell migration by measuring the area of the scratch during different periods utilising the protocol described by (Walter et al., 2010) with some modifications. Briefly, three cell types were assessed in this test for their ability to migrate under the effect of MSC-CM, namely, the human keratinocyte cell line (HaCat), human primary keratinocytes and human primary fibroblasts. Each cell type was seeded in 48 well plates at a density of 0.05×106 cells per well and incubated at SCC overnight to allow cell adherence (Figure 2.5). On the second day, each confluent monolayer was scratched with a sterile yellow tip making a scratch of ≈ 0.4–0.5 mm in width along the diameter of each well. The medium was removed and replaced with test substances; MSC-CM and controls (cells treated with DMEM in case of HaCat cells and fibroblasts, or with MCDB media in the case of primary keratinocytes) as shown in (Figure 2.5) below. The plate was re-incubated under an inverted microscope (Nikon ECLIPSE Ti) under SCC to monitor wound closure by taking images every two hours. The scratch assay was also performed for primary keratinocytes under hypoxic conditions (1% O2, 5% CO2, 37°C). To investigate whether MSC-CM enhance migration or proliferation, experiments also included inhibition of keratinocyte proliferation using 10 µg/ml mitomycin c (MMC) for 3 hours before making the scratch. The area of each single scratch was measured at different time points using image J software.

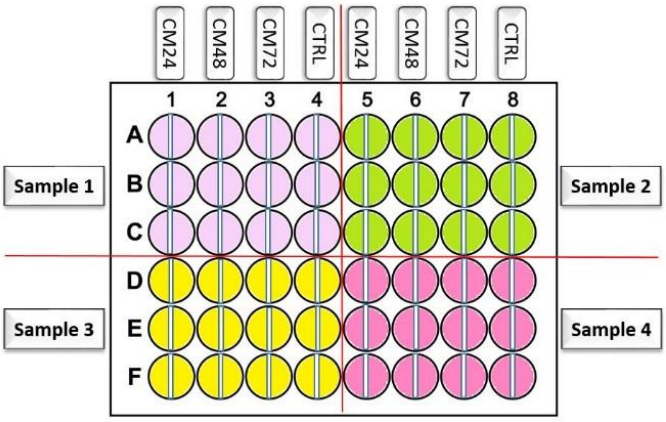

Figure 2.5 Design of scratch assay.

In the scratch assay of each cell type (HaCat cells, fibroblast and keratinocytes) 48 well plates was used separately. Each cell type was assessed in quadruplicate and the plate was divided into four quarters; each quarter contained 12 wells which were specified to fulfil four conditions which were (CM24, CM48, CM72 and Control) for the same donor. 4 different donors were assessed per one assay. When the cells formed a confluent monolayer, a scratch was made in each cell layer using a sterile yellow tip. The cells then treated with MSC-CM and the plate was incubated at the SCC for three days under an inverted NIKON microscope to monitor cell migration by capturing images every two hours.

In addition, a scratch assay was performed by adding 0.02 µg/ml of SDF-1 antibody (MAB310-500) (Guo *et al.*, 2015) to the confluent monolayer for 30 minutes to block SDF-1α receptor (CXCR4) prior to inducing the scratch. The positive controls consisted of addition of 0.2 µg/ml SDF-1α human recombinant protein to the monolayer (Wang et al., 2014), whereas keratinocyte growth media (KGM) alone represented the negative control. The plate was incubated under SCC for three days and time-lapse images were taken every two hours.

2.3.9 *Detection of Proliferation Markers*

To test whether keratinocytes migrate or proliferate during the wound closure process, a proliferation marker was incorporated by labelling the cells with BrdU synthetic nucleoside (see the following sections).

2.3.9.1 *Seeding Cells*

Primary keratinocytes were seeded at a density 0.05×10^6 cells per well in 8-glass well chambers in keratinocyte growth media (KGM) (N=3). The chamber was then incubated under SCC overnight to allow cell adhesion. Next day, a scratch was induced onto the monolayer followed by treatment with MSC-CM. Other wells of keratinocytes were scratched on the day of imaging and used as a time zero scratch control. HeLa cells were

used as a control and seeded at a density 0.1×10^6 cells per well in DMEM-10%-FCS and incubated for 4 hours under SCC to allow cell attachment.

2.3.9.2 *LABELLING WITH BRDU*

A stock solution of BrdU (10 mM) was prepared by dissolving 3 mg of BrdU powder in 1 ml water and filtered through 0.22-µm filter under sterile conditions. The working solution (3 µg/ml BrdU) was prepared by mixing 10 µl of BrdU stock solution with 1 ml MSC-CM and used to treat primary keratinocytes and HeLa cells overnight. The next day, BrdU labeling solution was discarded and cells washed 3 times with PBS for 5 minutes for each wash.

2.3.9.3 *FIXATION AND PERMEABILISATION*

The cells were then fixed with 4% ice-cold paraformaldehyde (PFA) for 15 minutes at room temperature, washed 3 times with PBS and permeabilised with 0.2% Triton X for 10 minutes at room temperature and again washed 3 times with PBS.

2.3.9.4 *DNA HYDROLYSIS (DNA DENATURATION)*

A volume of 83.3 ml of 1% PBS-T (3 ml Tween-20 + 97 ml PBS) was mixed with 16.7 ml concentrated HCL to prepare the DNA hydrolysis buffer (2 M HCL). The cells were incubated with this buffer for 15 minutes at 37°C and washed 3 times with PBS.

2.3.9.5 *BLOCKING AND STAINING WITH ANTI-BRDU-ANTIBODY*

Nonspecific binding was blocked with blocking buffer (1% BSA) (1 g bovine serum albumin + 100 ml PBST) for 60 minutes at room temperature followed by incubation with 120 µl anti-BrdU-antibody (1:60) diluted in 1% BSA and left in the dark for 1 hour at room temperature. Cells were then washed three times in PBS followed by incubation with the secondary antibody (Donkey Anti-Rabbit IgG H&L (Alexa Fluor® 488) (1:250) in (1% BSA) for a further 2 hours in the dark. The cells were then washed 3 times in PBS and stained with (DAPI 1:1000) in 1% BSA in the dark for 30 minutes at room temperature and washed 3 times in PBS. The cells were then covered with 50 µl mounting medium on a coverslip and visualised by fluorescence field microscopy.

2.3.10 *VIABILITY AND PROLIFERATION ASSAY*

MSC-CM were tested for their effect on survival and proliferation activity of skin cells including HaCat cells, primary fibroblasts and primary keratinocytes. Figure 2.6 shows the design of the proliferation assay in 96 well plates. Briefly, a cell count of 0.01×10^6 cell / well of each cell type were seeded into the 96 well plates in 1 ml suitable culture media (DMEM for HaCats and fibroblasts, MCDB for primary keratinocytes) and incubated for 4 hours under SCC to allow cell adherence. After the incubation time, cells were washed twice in serum free medium followed by addition of 1 ml of MSC-CM and suitable control (LC-CTRL in case of primary keratinocytes and HC-CTRL in case of HaCat cells and fibroblasts) as shown in (Figure 2.6. A) and incubated at SCC. A volume of 20 µl of (3-(4,5-dimethylthiazol-2-yl)-5-(3-carboxymethoxyphenyl)-2-(4-sulfophenyl)-2H-tetrazolium (MTS) was added to the wells after 24, 48 and 72 hours. The plate was then incubated for 3 hours to allow the viable cells to reduce the tetrazolium and release the coloured formazan compound into the culture media giving a colour depending on cell viability, which was then read at a wavelength of 490 nm using an ELISA reader. Both HaCat cells and fibroblasts were treated with HC-CM, while primary keratinocytes were treated with HC-CM as well as LC-CM. Controls included DMEM-SF media and MCDB media. Each condition was tested on four different donors for both fibroblasts and keratinocytes.

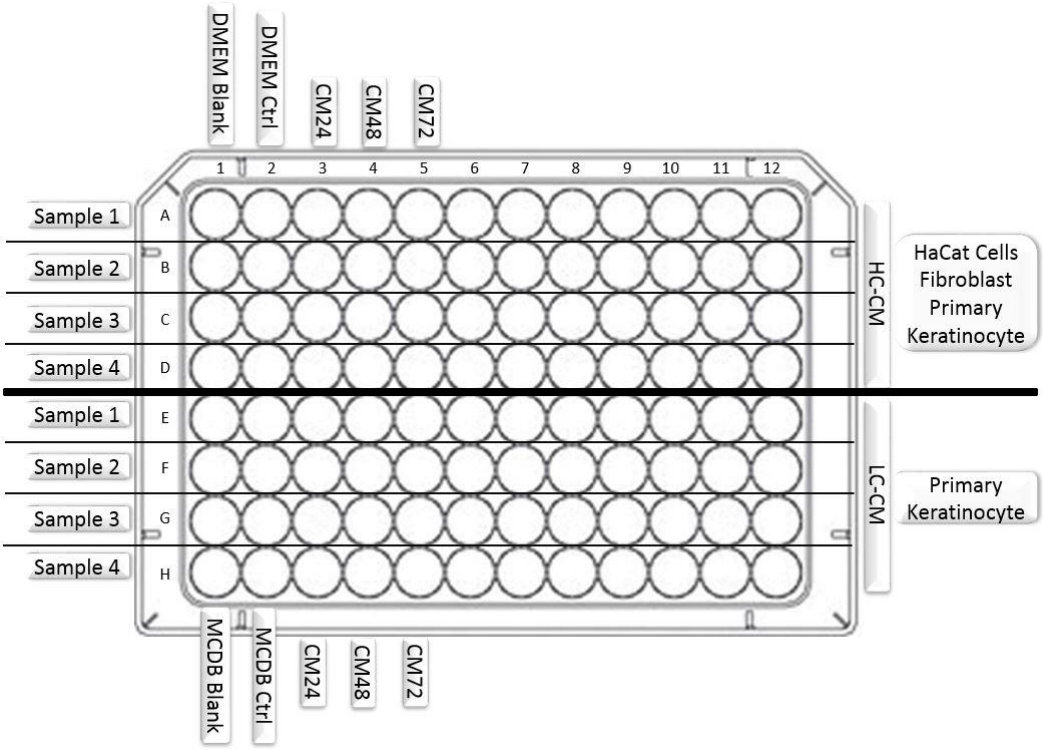

Figure 2.6 Design of proliferation assay.

In the proliferation assay, skin cells including HaCat cell lines, primary fibroblasts and primary keratinocytes were seeded at a density of 0.01×10^6 cell / well in 96 well plates and incubated for 4 hours under SCC to allow cell attachment as shown above. Then they were treated with absolute and 50 % diluted MSC-CM. HaCat cells and fibroblasts were treated with HC-CM only, whereas primary keratinocytes were treated with both HC-CM and LC-CM. then, the plates were incubated under SCC and their viability measured after 24, 48 and 72 hours using MTS solution. The optical density was measured at 490 nm using an ELISA reader.

2.3.11 *DIFFERENTIATION OF MSCS INTO EPIDERMAL-LIKE CELLS*

MSCs were seeded on sterile cover slips in NH media in 6-well plates at a density of 0.01×10^6 cells / well. The plates were incubated at SCC of for 24 hours to allow cell adherence. Then cells were then fed with epidermal differentiation media (EDM) for different time points to investigate their ability to express skin markers. For instance, after 7 days of treatment with EDM, MSCs were tested for their ability to express cytokeratin K14 (K14), after 10 days for K14 and cytokeratin 10 (K10) and after 17 days for K10 and loricrin.

2.3.12 *Immunofluorescence of Slide Fixed Cells*

After the treatment period, MSCs were washed with PBS 3 times for 5 minutes each, fixed with 4% iced cold paraformaldehyde for 15 minutes at room temperature. The fixative was aspirated and cells washed as before. For permeabilisation, cells were treated with 0.2% Triton-X (200 µl Triton-X +99.800 ml PBS) for 10 minutes at room temperature, then washed 3 times with PBS for 5 minutes each. To block non-specific binding, MSCs were incubated with blocking buffer (10% FBS in PBS) for 60 minutes. Cells were separately stained with 100 µl of 1:200 diluted primary antibodies such as keratin 14, keratin 10 and loricrin and incubated overnight at 4°C. On the next day, cells were rinsed 3 times with PBS for 5 min each. The cells were then stained with 100 µl diluted 1:200 Alexa Fluor-488 secondary antibody and incubated for 1 hour in the dark at room temperature, followed by rinsing 3 times with PBS for 5 minutes each. DAPI (1/2000) was then added and the cells incubated in the dark for 30 minutes at room temperature and rinsed again as before. The cells were then covered with 50 µl mounting medium and visualized using a confocal microscope.

2.3.13 *Detection of Growth Factor Receptors in Primary Keratinocytes*

2.3.13.1 *Conditions*

As shown in (Figure 2.7) four samples of primary keratinocytes were seeded in MCDB media in 15 ml petri dishes and incubated under SCC until reaching confluent. All samples were subjected to the same conditions; no scratch (NS), scratched non-treated with MSC-CM (SNT) and scratched treated with MSC-CM (ST-CM). Then, cells of each condition were harvested after different time points; 24, 48 and 72 hours for RNA extraction. Detection of the receptors,FGF-R2, c-Met, TGFR-β1, PDGR-A, CXCL12 and MST-R1 which are receptors for KGF, HGF, TGF-1β, PDGF-α, SDF-1α and MSP-1 respectively was carried out using gene expression profiling .

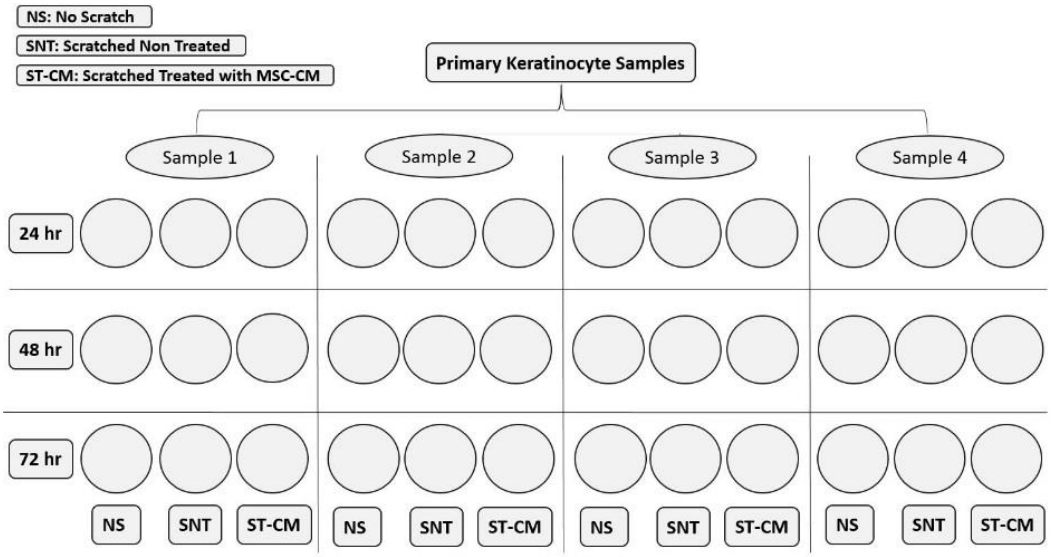

Figure 2.7 Conditions applied to primary keratinocytes for further gene expression of growth factor receptors.

Four samples of human primary keratinocytes were seeded into 15 ml petri dishes and incubated under SCC to reach confluence. Each sample was subjected to three conditions; non-scratched cells (NS), scratched cells without any treatment (SNT) and scratched cells treated with MSC-CM (ST-CM). Cells were harvested after different time points (24, 48 and 72 hours) for further RNA extraction.

To detect gene expression, three sequential protocols were followed; total RNA isolation, synthesis of complementary DNA (c-DNA) and quantification of gene expression using TaqMan assay by real time-polymerase chain reaction (RT-qPCR). These steps are summarised in (Figure 2.8).

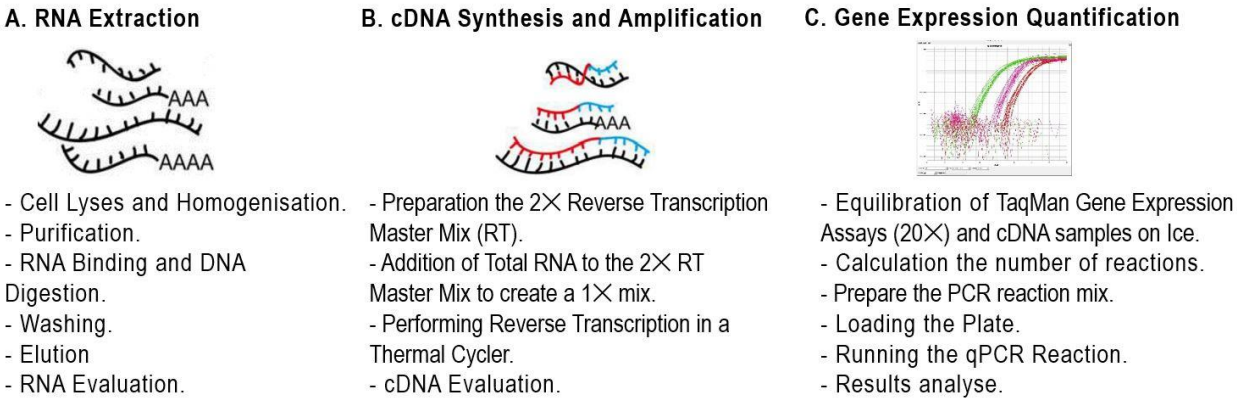

Figure 2.8 Steps of gene expression assay.

Gene expression could be detected by using the real time reverse transcriptase polymerase chain reaction (RT-PCR) technique which involved three main steps; A. total RNA extraction from cell lysate, B. cDNA synthesis using reverse transcription and D. Quantification of gene expression by real time PCR.

2.3.13.2 *TOTAL RNA ISOLATION*

RNeasy Micro Kit from QIAGEN was used to extract RNA from primary keratinocytes. The content of the kit and reagent preparation are explained in (Table 2.25).

Item	Quantity	Preparation
RNeasy MinElute® Spin Columns (each in a 2 ml Collection Tube)	50	Ready to use
Collection Tubes (1.5 ml)	50	Ready to use
Collection Tubes (2 ml)	100	Ready to use
Buffer RLT	45 ml	10 ml RLT mixed with 100 µl β-mercaptoethanol (β-ME)
Buffer RW1	45 ml	Ready to use
Buffer RPE (concentrate)	11 ml	Mixed with 44 ml (Absolute Ethanol 96-100 %)
RNase-Free Water	3 x 10 ml	Ready to use
Carrier RNA, poly-A	310 µg	Ready to use
RNase-Free DNase Set		
RNase-Free DNase I (lyophilized)	1500 units	The lyophilized DNase I dissolved in 550 µl RNase-free water mixed gently and stored as single-use aliquots at –80°C for up to 9 months.
Buffer RDD	2 x 2 ml	70 µl Buffer RDD mixed with 10 µl DNase I stock solution to prepare DNase I incubation mix (80 µl).
RNase-Free Water	1.5 ml	Ready to use

Table 2.25 Content of RNeasy micro kit and their preparation.

All steps of RNA isolation were completed according to the manufacturer's protocol (QIAGEN) in the presence of RNase inhibiting reagents to avoid unwanted changes in the gene expression profile. In addition, samples were either processed immediately after harvesting or kept in RNA stabilising solution (RNA later) in – 80°C until use. Briefly, a maximum of 5×10^5 cells were harvested and directly treated with 350 µl tissue and cell lysis buffer for RNA extraction (RLT) working solution to lyse the cell plasma membrane. Cell lysate was then homogenised using a 2G sterile needle to shear high molecular weight (HMW) genomic DNA and other HMW cellular components to reduce the viscosity of the lysate and create a homogenous lysate. RNA purification was done by addition of one volume of 70% ethanol (350 µl) to the lysate, transferred to RNeasy MinElute columns in 2 ml collection tubes and centrifuged for 15 seconds at ≥ 8000g with closed lid and the flow-through was discarded. The next addition was 350 µl buffer RW1 to the RNeasy MinElute spin column, which was centrifuged for 15 seconds at ≥8000g and the flow-through discarded. Then, DNase I incubation mix (80 µl) was directly added to the RNeasy MinElute column membrane and placed on the benchtop for 15 minutes at room temperature (20–30°C) to allow full digestion of the DNA. The next addition was 350 µl

buffer RW1 to the RNeasy MinElute spin column and centrifuged as before. The RNeasy MinElute spin columns were placed in a new 2 ml collection tube and 500 µl buffer RPE were added to the spin column and centrifuged as above. A volume of 500 µl of 80% ethanol were added to the RNeasy MinElute spin column and centrifuged for 2 minutes at ≥8000g. The collection tubes were discarded and the RNeasy MinElute spin columns were placed in a new 2 ml collection tube, centrifuged at 15000g for 5 minutes with an open lid to dry the membrane and remove any ethanol residue which may interfere with downstream reactions. The flow-through and collection tube were discarded and the RNeasy MinElute spin columns were placed in new 1.5 ml collection tubes. The final addition was 14 µl RNase-free water added directly to the centre of the spin column membrane and centrifuged for 1 minute at 15000 g to elute the RNA. Then, RNA concentrations were quantified and analysed for purity using Nanodrop spectrometry and stored at – 80 until use.

2.3.13.3 *cDNA Synthesis by Reverse Transcriptase PCR (RT-PCR)*

High capacity cDNA Reverse Transcription Kit from Applied Biosystems was used to synthesise complementary DNA. The materials of the kit and their volumes for specific number of reactions are shown in (Table 2.26). The first step was preparation of 2X reverse transcriptase master mix (2X-RT-MM). Briefly, all kit components were allowed to thaw on ice followed by mixing the volumes as listed in (Table 2.26).

Item	Quantity	Preparation of 2X-RT-MM		
		Volume (µl) / Reaction(s)		Volume / 6 tubes (10 µl / tubes)
10× RT Buffer 1.0 ml	2 tubes	2.0	60	14
10× RT Random Primers, 1.0 ml	2 tubes	0.8	24	5.6
25× dNTP Mix (100 mM) 1.0 ml	1 tube	2.0	60	14.0
MultiScribe™ Reverse Transcriptase, 50 U/µL, 1.0 ml	1 tube	1.0	30	7.0
RNase Inhibitor‡, 100 µL	10 tubes	1.0	30	7.0
Nuclease-free H2O 100 ml	1 bottle	3.2	96	22.4
Total per Reaction	---	10.0	300	70.0

Table 2.26 Content of high capacity cDNA reverse transcription kit and their preparations.

To prepare the cDNA reverse transcription reaction, 10 µl of 2X-RT-MM were pipetted into single tubes followed by addition of 10 µl of RNA, mixed well and kept on ice until loaded into the thermal cycler which was adjusted to the conditions shown in (Table 2.27).

Reaction volume 20 µl				
Conditions	Step I	Step II	Step III	Step IV
Temperature (°C)	25	37	85	4
Time (Minutes)	10	120	5	∞

Table 2.27 Conditions of the thermal cycler for reverse transcriptase PCR.

After finishing the run, cDNA purity was assessed using NanoDrop spectrometry and stored at -80°C or immediately used for gene expression evaluation using the TaqMan® technique.

2.3.13.4 *ASSESSMENT OF NUCLEIC ACID PURITY*

Extracted RNAs and synthesised cDNA were analysed for any contamination that could interfere the purity of RNA and DNA such as phenol or other contaminants. NanoDrop spectrometry (NanoDrop 1000, Thermo Scientific) was used to measure A260/A280 which should generally be 2.0 for RNA and 1.8 for DNA to be accepted as “pure” according to the ThermoFisher guidelines. In addition, the A260/230 ratios, which should range from 2.0 – 2.2 for pure nucleic acids were measured to detect any impurities that could be absorbed at 230 nm as shown in the explanatory figure (Figure 2.9). Briefly, 1 µl of a nucleic acid sample was placed on the sensor and the lid was placed on the NanoDrop and then the software was used to analyse the sample for any interfering contaminants.

(A)

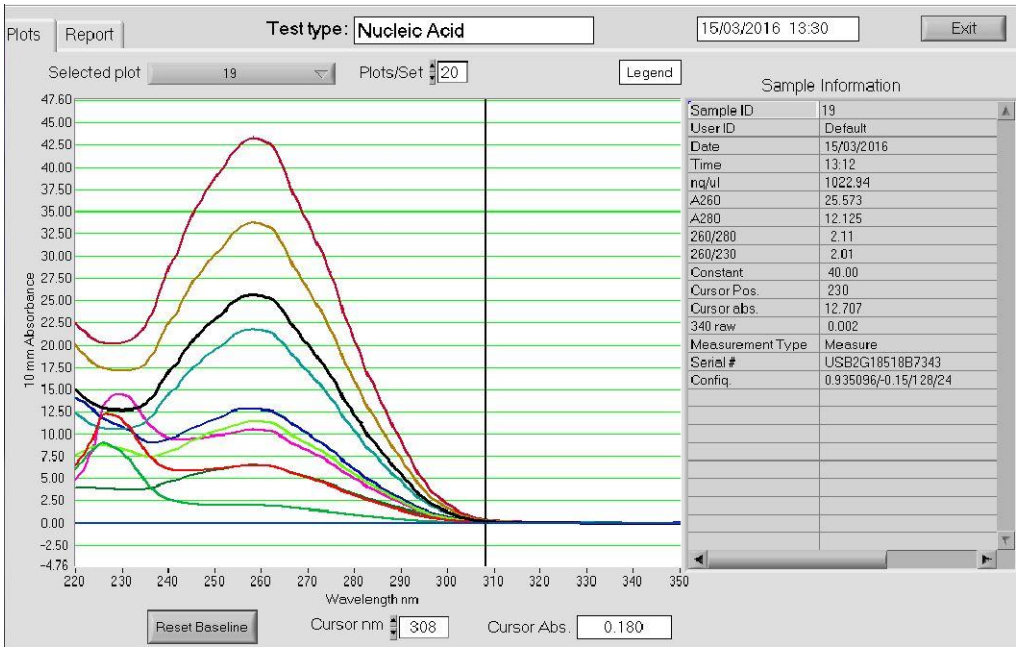

(B)

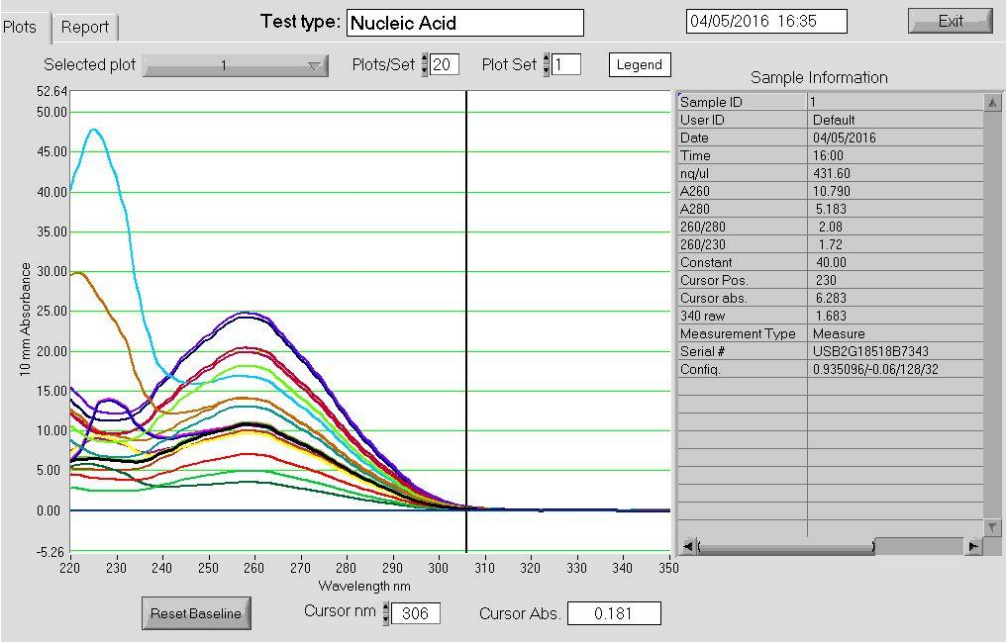

Figure 2.9 Explanatory images of assessing nucleic acid purity.

Samples of nucleic acids analysed for purity and measured for concentration by NanoDrop 1000. Each line in the plot of each image represents a single sample. Data in the right hand side of each image represents one sample which could be selected manually by the software. A- An RNA sample shows that the concentration of total RNA in the sample is 1022.94 ng/µl with a ratio of 260/280=2.11 and 260/230=2.01. B- A DNA sample shows that it contains a concentration of DNA = 431.60 ng/µl with a ratio 260/280=2.08 and 260/230=1.72. Thermofisher Scientific guidelines state that a ratio of ~1.8 is generally accepted as "pure" for DNA and a ratio of ~2.0 is generally accepted as "pure" for RNA. So, these samples could be classified as pure.

2.3.13.5 *TaqMan Gene Expression by RT-PCR*

The first step in RT-qPCR is preparation of the PCR reaction mix (PCR-RM). Each condition was run in quadruplicate and the volumes for preparing the PCR-MM are shown in (Table 2.28).

Component of PCR Master Mix	Volume per 20 (µl) Reaction (µl)		
	1 Reaction	Quadruplicate	10 Reactions
2× TaqMan® Gene Expression Master Mix	10.0	50.0	100.0
cDNA template (1 to 100 ng)	4.0	20.0	40.0
RNase-free water	5.0	25.0	50.0
20× TaqMan® Gene Expression Assay	1.0	5.0	10.0 (Added as 1.0 µl to the Plate later)

Table 2.28 The components of PCR master mix and their preparations.

This table shows the components required for the RT-PCR reaction. These volumes vary depending on the number of samples processed per single run and the number of replicates. For example, in the experiments two genes and one housekeeping gene (GAPDH) were analysed in triplicate; in total 9 wells. Volumes for 10 reactions were prepared to avoid lost volumes during pipetting.

Then, 19 µl of PCR-RM were added to the corresponding wells of a MicroAmp Optical 96-Well Reaction Plate, followed by addition of 1.0 µl of 20× TaqMan® Gene Expression Assay of the gene of interest. GAPDH was used as a housekeeping gene control and used at the same volume prepared for the test genes for quantitative evaluation. Additionally, non-treated controls (NTC) were included which were Nuclease Free H_2O+ PCR-RM to detect any contamination that may interfere with the results as shown in (Figure 2.10).

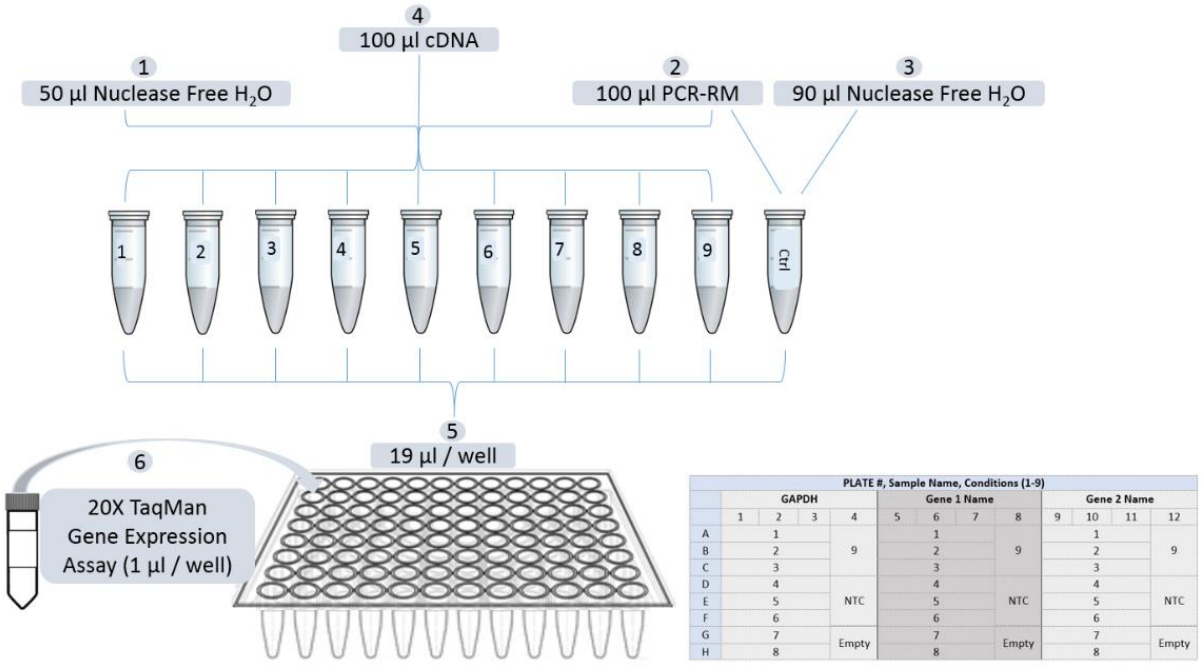

Figure 2.10 Flowchart of preparing RT-PCR reaction and PCR plate.

As mentioned in Table above, the PCR reaction required preparation of specific volume of PCR-MM depending on the number of samples and duplicates. These volumes were added to the corresponding wells. MicroAmp Optical 96-Well Reaction Plate was used to process 9 conditions in triplicate for two genes and one houskeeping gene (GAPDH).In addition, the plate included triplicates of non-treated controls (NTC) for each single gene and GAPDH.

The plate was centrifuged briefly using Labnet MPS 1000 Mini plate spinner and loaded onto the RT-PCR machine (Applied Biosystems 7900HT Real-Time PCR System) with the settings as shown in (Table 2.29).

System	Run	Reaction Plate	Experiment Parameters	Thermal Cycler Conditions		
				Step	Temperature (°C)	Time (mm:ss)
Applied Biosystems 7900HT Real-Time PCR System	Fast	96-well plate	Rxn. Volume: 20 µl	Hold	50	2:00
			Ramp Rate: Fast	Hold	95	0:22

Table 2.29 Conditions of RT-PCR system required for TaqMan gene expression

Information obtained from the PCR machine were generated as numeric data in SDS software (2.4) then exported into an excel sheet for further calculation and quantification of gene expression using (Equation 2.7) and (Equation 2.7).

$$\Delta \boldsymbol{Ct} = \boldsymbol{Ct}\,(\boldsymbol{gene}) - \boldsymbol{Ct}\,(\boldsymbol{control}) \quad \text{. . . . .} \quad \text{Equation 2.7}$$

$$\boldsymbol{Relative\ Quantification}\ (\boldsymbol{RQ}) = \mathbf{2}^{-\Delta \boldsymbol{Ct}} \quad \text{. . . . .} \quad \text{Equation 2.8}$$

When:
Ct= cycle threshold: number of cycles required by fluorescence signal of the target gene and reference gene to exceed the background signal in PCR.

2.3.14 *CONSTRUCTION OF 3D SKIN EQUIVALENT MODEL (3D-SEM)*

Hill and colleagues developed a 3D skin model for melanoma invasion studies (Hill et al., 2015). Based on this model, we developed the same model in our lab for further developing a prototype 3D model for wound healing studies. The basis of this model is the Alvetex®scaffold explained in Figure 2.11 A. Before seeding cells, Alvetex® was activated with 70 % ethanol for 30 seconds, treated with media A (Section 2.2.13.6.1) for 30 seconds, fixed in 6 well plates and incubated under SCC until required. To form the dermal equivalent of the model, 2×10^6 fibroblasts were suspended in 100 µl media A and seeded onto the Alvetex® and incubated at SCC for 90 minutes. 9 ml of media B (Section 2.2.13.6.2) was added to each Alvetex® well and incubated under SCC with a change of media B every two days for 18 days (Figure 2.11 B). The epidermal layer was prepared by seeding 100 µl of media C containing 2×10^6 keratinocytes over the dermal fibroblast layer and incubated under SCC for 3 hours to allow cell adherence. Concurrently, the dermal layer was fed from the bottom with 4 ml media C (2.2.13.6.3). After the incubation time, the whole model was covered with media C for three days with a daily change of media C as demonstrated in Figure 2.11 C. Stratification of the model was enhanced by subjecting the epidermal layer to the air liquid interface for 14 days while feeding the

dermal layer with air-liquid interface media (media D) (Section 2.2.13.6.4) with two day changes of media D (Figure 2.11 D).

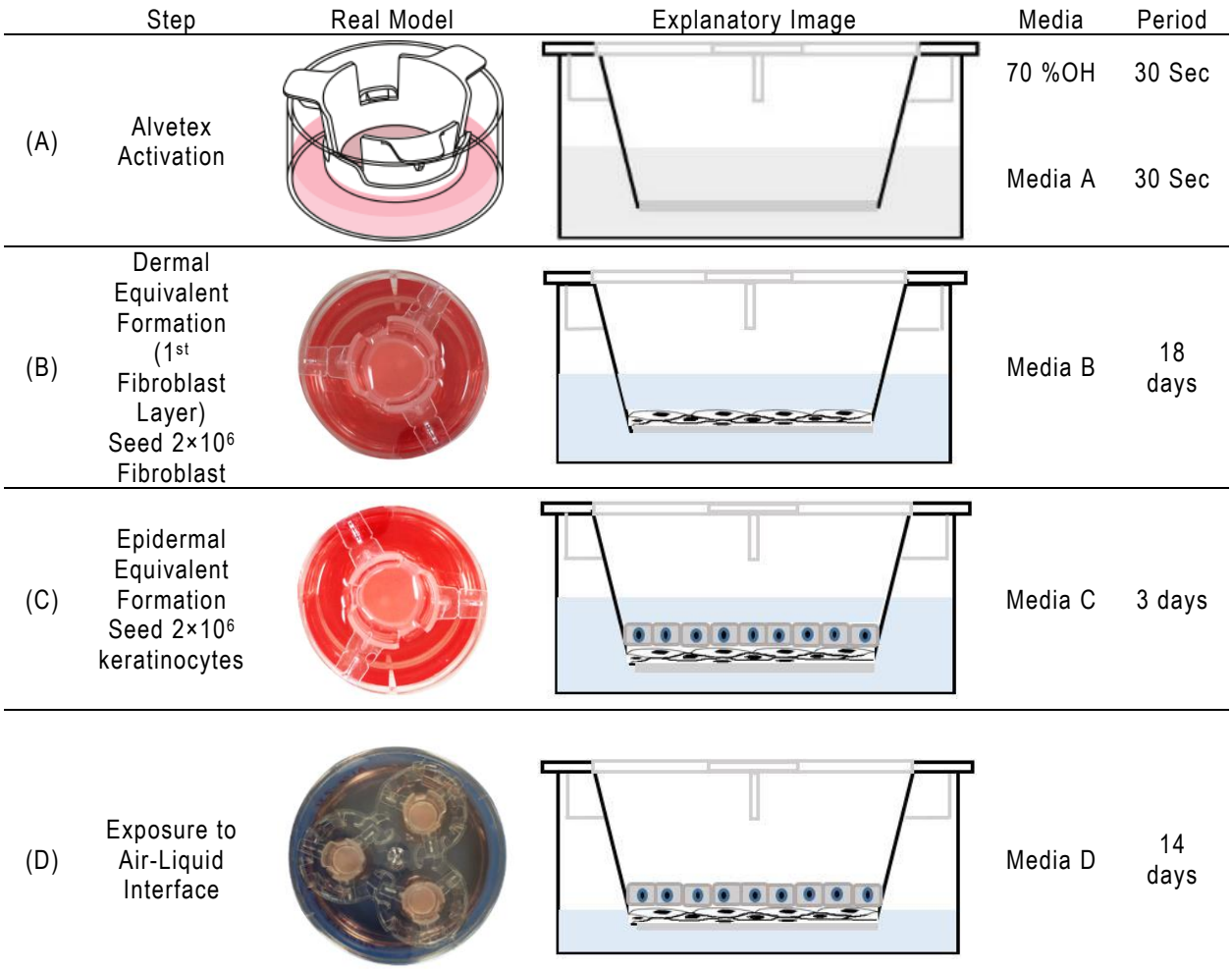

Figure 2.11 Generation of a 3D skin equivalent model (3D-SEM) using the Alvetex®.

(A) Alvetex® activated by rinsing in 70 % ethanol for 30 seconds and soaked in media A for 30 seconds again, then every single Alvetex® was fixed in a single well of 6 well plates until fibroblasts are ready for seeding. (B) Formation of dermal layer in media B on the Alvetex® under SCC for 18 days with 3 changes of media B per week. (C) Generation of the epidermal layer over the dermal fibroblast layer incubated under SCC with 9 ml of media C for three days. (D) Exposure to the air-liquid Interface for 14 days and feeding the dermal layer with media D while leaving the epidermal layer exposed to the air without media.

2.3.15 *Differentiation of MSCs into Epidermal-like Structure in 3D Culture*

After testing their ability to differentiate into skin like cells in a 2D culture, MSCs were tested for their ability to differentiate into epidermal-like structures. The same protocol used to construct a 3D-SEM using fibroblasts and keratinocytes (Section 2.3.14) was used

to examine the ability of MSCs to differentiate into epidermal-like layers with some modification in terms of the media used. Briefly, the dermal layer was generated as described in the protocol above (Section 2.3.14). When the dermal layer was obtained, 2×10^6 MSCs were suspended in 100 µl of epidermal differentiation media (EDM) (Section 2.2.13.5) and seeded over the dermal fibroblast layer and incubated for 3 hours under SCC to allow cell attachment. The skin equivalent was then fed with EDM supplemented with vitamin C for three weeks. The model was subjected to the air liquid interface in EDM to enhance epidermal stratification and with a regular change of media every 3 days.
The constructed models from keratinocytes in (Section 2.3.14) and from MSCs in this section were validated structurally by haematoxylin-eosin (H-E) staining (this service was carried out in the Department of Pathology/ RVI) and by detection of dermal and epidermal differentiation markers as described in the following protocol.

2.3.16 *Developing a Prototype 3D Skin Equivalent Model (3D-SEM) for Wound Healing Studies*

In this study, a robust method was developed to evaluate wound healing using a fully humanised skin model which was generated in (section 2.3.14). The aim of this protocol was to establish a model to mimic the environment of a cutaneous wound in which the skin cells at the injury site such as fibroblasts and keratinocytes could migrate over another cellular layer such as dermal fibroblast layer. The idea of the protocol was to allow the cells at the wound site of the model to migrate over another intact cellular layer of fibroblasts. Therefore, a second fibroblast layer was prepared on a new Alvetex® (Figure 2.12 A) by following the same steps of preparing the first dermal fibroblast layer. When the full skin model was constructed it was washed twice with PBS, taken out of the Alvetex® using a circular cutter, and transferred to a sterile Petri dish (Figure 2.12 B). A 3 mm punch was made in the model using a sterile 3 mm punch (Figure 2.12 C). The punched model was then transferred over the second fibroblast layer and fed with media B and left for 3 hours to allow attachment of the first fibroblast layer to the second one. (Figure 2.12 D). Then all punched models were treated with MSC-CM for different time points; 1 week, 2 weeks and 4 weeks with three changes of MSC-CM per week (Figure 2.12 E). Control models were treated with media B with a regular change of media every two days. Allogenic models (unmatched dermal and epidermal layer) were used for wound

healing visualisation by (H-E), while autologous models (matched dermal and epidermal layers) were used for microRNA profiling.

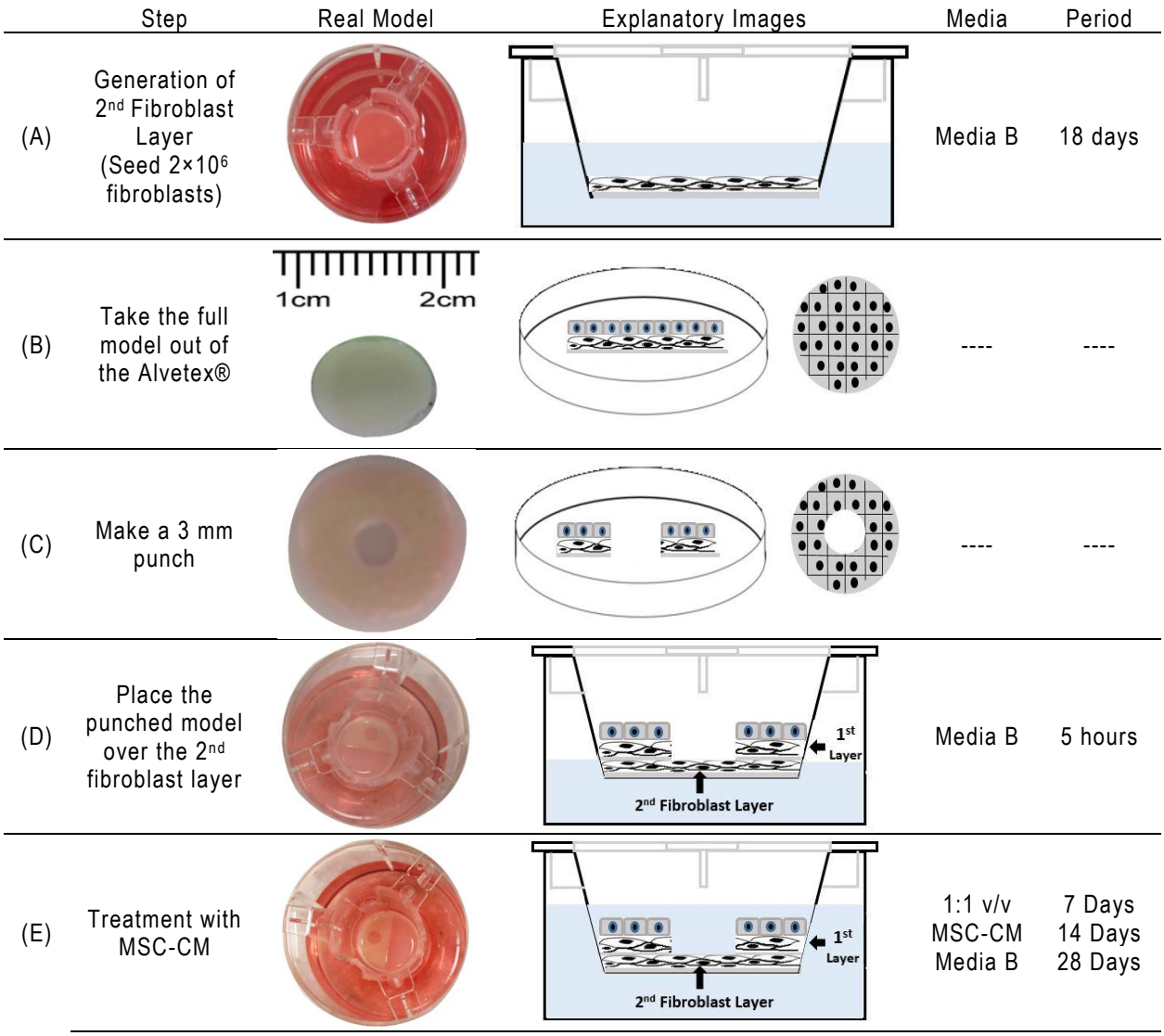

Figure 2.12 The developed protocol for wound healing using a fully humanised 3D kin equivalent model (3D-SEM).

Explanatory figure showing the developed protocol for wound healing using a 3D-SEM. (A) Formation of the second dermal layer to act as a bed to support migration of the epidermis of the wounded model. (B) The previously constructed model was taken out the Alvetex® and placed in sterile petri dish. (C) The model was punched using a 3 mm punch biopsy. (D) Placing the punched model over the second fibroblast layer and left for 5 hours at SCC to allow adherence and feeding only the second layer with 4 ml media B. (E) Treating the punched model with MSC-CM and media B (1:1 v/v) for different time points (1,2 and 4 weeks).

2.3.17 *Evaluation of Wound Healing*

The evaluation of wound healing was carried out by using two main techniques; the first one was monitoring migration of dermal and epidermal layers at the wound edges towards the wound centre which was detected by Haematoxylin-eosin (H-E) staining. The other technique was detecting the epidermal and dermal differentiation markers at the wounded site using immunofluorescence primary and secondary antibodies.

2.3.18 *Immunofluorescence Staining of the 3D Skin Equivalent Model (3D-SEM)*

2.3.18.1 *Sectioning Using Microtome and Slide Preparation*

Paraffin embedded skin model tissues were always kept on ice during sectioning to ensure effective sectioning. The microtome was adjusted to 4 µm and sections were kept in a water bath adjusted at 40^{o}C for 2-3 minutes before transferring to slides. The slides were then heated in an oven at 60^{o}C overnight and the next day, dehydrated by washing for 5 minutes in each xylene, 100% ethanol, 95% ethanol, 70% ethanol and distilled water.

2.3.18.2 *Antigen Retrieval*

For antigen retrieval, slides were placed in previously heated 10 mM citrate buffer, pH 6.0, in a microwave for 1 minute and then left to cool at room temperature for 30 minutes, and washed in 5 mM Tris buffered saline (TBS) pH 7.6 for 5 minutes. Permeabilisation of the slides was performed in 0.2% Triton-X for 10 minutes at room temperature.

2.3.18.3 *Single Immunostaining*

All sections were blocked by 10% goat serum in PBS for 10 minutes at room temperature and washed with Tris base solution (TBS) four times to remove the goat serum. The sections were stained with 100 µ of the following primary antibodies which were diluted before use; (K14 1:250, K10 1:200, Loricrin 1:200, Involucrin 1:250, collagen III 1:50) and incubated in a moist chamber at 4^{o}C overnight. Control slides were not stained but were incubated with blocking solution instead. The following day the sections were washed four times in TBS for 2 minutes each and incubated with100 µl of secondary antibody-DAPI mix at a dilution of 1:250 and 1:1000 respectively for 2 hours at 37^{o}C in a moist chamber in the dark. Sections were then washed four times in TBS for 2 minutes, covered with

DPX, left in the dark at room temperature overnight, and analysed the next day using confocal microscopy.

2.3.18.4 *MULTIPLE IMMUNOSTAINING (SEQUENTIAL FLUORESCENCE STAINING)*

In order to detect more than one biomarker in one slide at the same time and to clarify the spatial-temporal order of the epidermal layers, a sequential labelling protocol was used. Briefly, firstly the blocking was carried out by incubation with serum compatible with the first secondary antibody. Sections were then incubated with K14 antibody (1:250) for one hour at room temperature (RT) and then washed three times with TBS followed by incubation with a secondary antibody specific for K14 for one hour at RT. Sections were then washed three times with TBS and re blocked with a second serum corresponding to the second secondary antibody. Sections were then re-incubated with K10 antibody (1:200) for 1 hour at RT and washed 3 times with TBS followed by incubation with a secondary antibody specific for K10 for 1 hour at RT. The same steps (blocking and washes) under the same conditions (RT and incubation times) were followed to for staining with involucrin (1:250) antibodies and their corresponding secondary antibodies.

2.3.19 *MICRORNA PROFILING DURING WOUND HEALING USING 3D-SEM*

*mir*Vana™ microRNA Isolation Kit was used to extract microRNAs from the skin models and the kit contents are listed in (Table 2.30).

Item	Quantity
microRNA Wash Solution I	30 ml (To prepare working reagent, mixed with 21 mL 100% ethanol before use)
Wash Solution 2/3	50 ml (To prepare working reagent, mixed with 40 mL 100% ethanol before use)
Collection Tubes	80
Filter Cartridges	40
Lysis/Binding Buffer	100 ml
microRNA Homogenate Additive	10 ml
Acid–Phenol: Chloroform (APC)	100 ml
Gel Loading Buffer II	1.4 ml
Elution Solution	5 ml

Table 2.30 Contents of microRNA isolation kit (mirVana™)

2.3.19.1 *ISOLATION OF SMALL RNAS INCLUDING MICRORNAS*

The first step in microRNA extraction is lysis of the sample (punched and intact 3D-SEM) in 300 µl of a denaturing lysis buffer (LB) with continuous chopping and teasing with a scalpel blade for 3-5 minutes until the tissue is broken down. Cells were lysed immediately with 300 µl of lysis buffer. The organic extraction step was completed by addition of 30 µl of RNA homogenate to the samples, which were then vortexed and incubated on ice for 10 minutes. For a robust initial purification and DNA removal, 300 µl of acid–phenol-chloroform (APC) were added to the model in a fume hood, mixed by vortex for 30-60 seconds and centrifugation for 5 min at 10,000g. Again, in the fume hood, 100 µl (in 5 times; 20 µl each) of the upper (aqueous phase) was carefully extracted without disturbing the phenol phase and transferred to a new Eppendorf vial. For the final purification, the lysate/ethanol was mixed with 375 µl of absolute ethanol making a colourless mixture and passed through a filter cartridge containing a glass-fiber filter to immobilise the RNA, then, centrifuged for 15 seconds at 10,000g followed by discarding the flow through. The washing step was performed three times; the first one with 700 µl of microRNA wash solution I was added and centrifuged for 10 seconds at 10,000g followed by discarding the flow through again. The second and the third washes were with volumes of 500 µl of microRNA wash solution and centrifuged. After discarding the flow through from the final wash, the assembly was spin for 1 minute at 10,000 g to remove any residual fluid and to dry the filter. The filter cartridge was then transferred to a new labelled collection tube and the final step was elution with a low ionic-strength solution such as 100 µl of pre heated (95°C) nuclease free water added to the centre of the filter and spun at maximum speed for 20 to 30 seconds to recover the RNA which was stored at – 80 until use.

2.3.19.2 *DETERMINATION OF MICRORNA INTEGRITY NUMBER*

Agilent RNA 6000 Nano Kit was used to analyse the microRNA integrity number, which is composed of the following reagents and tools as listed in (Table 2.31).

Content	Quantity	Preparation / Explanation

RNA 6000 Nano Ladder	1 vial	The ladder vial was spin down, denatured by heating for 2 min at 70ºC and Immediately cooled on ice. It then dispensed in aliquots and stored at -70ºC until use. Before use, the ladder aliquots were thawed on ice avoiding extensive warming
RNA 6000 Nano Gel Matrix	2 vials	A volume of 550 µl of the gel matrix was pipetted into a spin filter showed in red in Figure 2.13 B, centrifuged at 10000g for 15 minutes at room temperature and aliquoted in 0.5 ml RNAse free micro centrifuge tubes and stored at 4ºC until use within one month.
RNA 6000 Nano Chips	25	As shown in Figure 2.13 A
Electrode Cleaners	2	
Syringe Kit	1	
Eppendorf Tubes	30	Safe-Lock Eppendorf Tubes PCR clean (DNase/RNase free) for gel-dye mix
RNA 6000 Nano Dye Concentrate	1 vial	Before use, RNA 6000 Nano Dye Concentrate was allowed to equilibrate at room temperature for 30 minutes, then vortexed and for 10 seconds at 10000 g.
RNA 6000 Nano Marker	2 vials	
Spin Filters	4	

Table 2.31 Content and reagents of Agilent RNA 6000 Nano kit.

All reagents were brought to equilibrate to room temperature for 30 minutes before starting the experiment.

2.3.19.2.1 PREPARING THE GEL-DYE MIX (GDM)

Dye concentrate was vortexed for 10 seconds and spin down at 10000 g followed by pipetting 1 µl of dye into 0.5 mL RNase free micro tubes containing 65 µL of filtered gel and mixed by vortex for 10 seconds until the dye was distributed equally and the mixture became homogeneous, and then spun at 13000 g for 10 min at room temperature.

2.3.19.2.2 LOADING THE GEL-DYE MIX (GDM)

A volume of 9 µL of GDM was loaded in the chip well- labelled pink in (Figure 2.13 C). The plunger was pressed until it was held by the clip and released after 30 seconds. Then, 9 µL of GDM were added in the wells- labelled pink in (Figure 2.13 D)**.**

2.3.19.2.3 LOADING THE MARKER

A volume of 5 µL of RNA marker was added into all 12 sample wells as well as the ladder well - labelled green in (Figure 2.13 E).

2.3.19.2.4 LOADING THE LADDER AND SAMPLES

A volume of 1 µL of prepared ladder was pipetted into the yellow well in (Figure 2.13 F), and 1 µL of each sample was pipetted in each of the 12 sample wells labelled as blue in (Figure 2.13 G). For unused sample wells, 1 µl of RNA Marker was pipetted in each well. The chip then was then placed horizontally in the IKA vortexer and vortexed for 1 minute at 2400 rpm followed by running the chip in the Agilent 2100 Bioanalyzer instrument within 5 minutes.

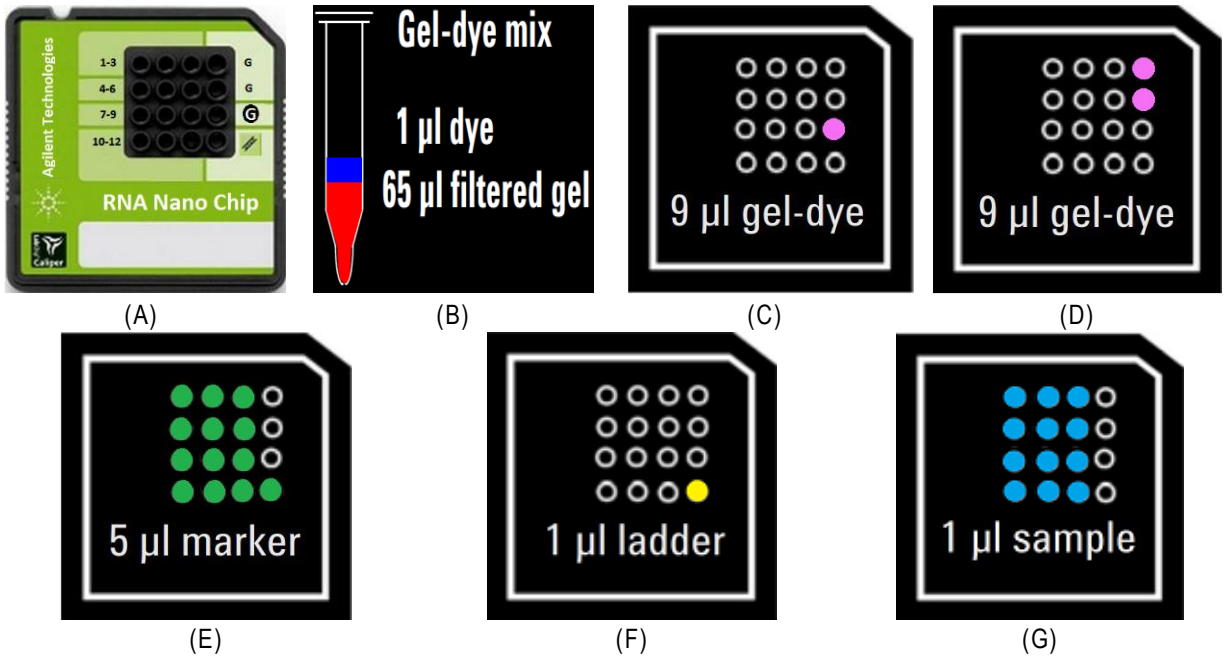

Figure 2.13 Summary of protocol for determining microRNA integrity number.

The Figure was adapted from Agilent RNA 6000 Nano Kit Guide with modification. Agilent RNA 6000 Nano Kit Guide and Agilent RNA chips were used to determine RNA integrity number. (A) A 6000 RNA Nano chip with labelled wells. (B) Preparing the GDM by mixing 1 µl of dye concentrate with 65 µl filtered gel. (C) Addition of 9 µl GDM to the well G labelled pink and pressing the plunger until being held by the clip for 30 seconds. (D) Releasing the plunger and addition of 9 µl GDM to the wells G labelled pink colour. (E) Addition of 9 µl of RNA marker to the wells 1-12 (green colour) in addition to the well labelled as ladder (green colour). (F) Addition of 1 µl of the ladder to the ladder well (yellow colour). (G) Addition of 1 µl of each sample to the wells 1-12 (blue colour).

The bioanalyzer is a very productive machine utilised to analyse nucleic acids and protein utilising a chip-based technique. It provides information with high sensitivity about the sample of interest. The bioanalyzer cab utilise different sizes of chips; 11 samples or 12 samples depending on the kit type, which in turn is determined by the molecule to be analysed such as small RNAs, DNA, exosomes or protein. As explained in (Figure 2.14),

the analysis provided information about the RNA Integrity Number (RIN), electrophoresis, time required to detect and analyse the sample, microRNA concentration and microRNA size or length (in nucleotide) of the detected molecule.

(A)

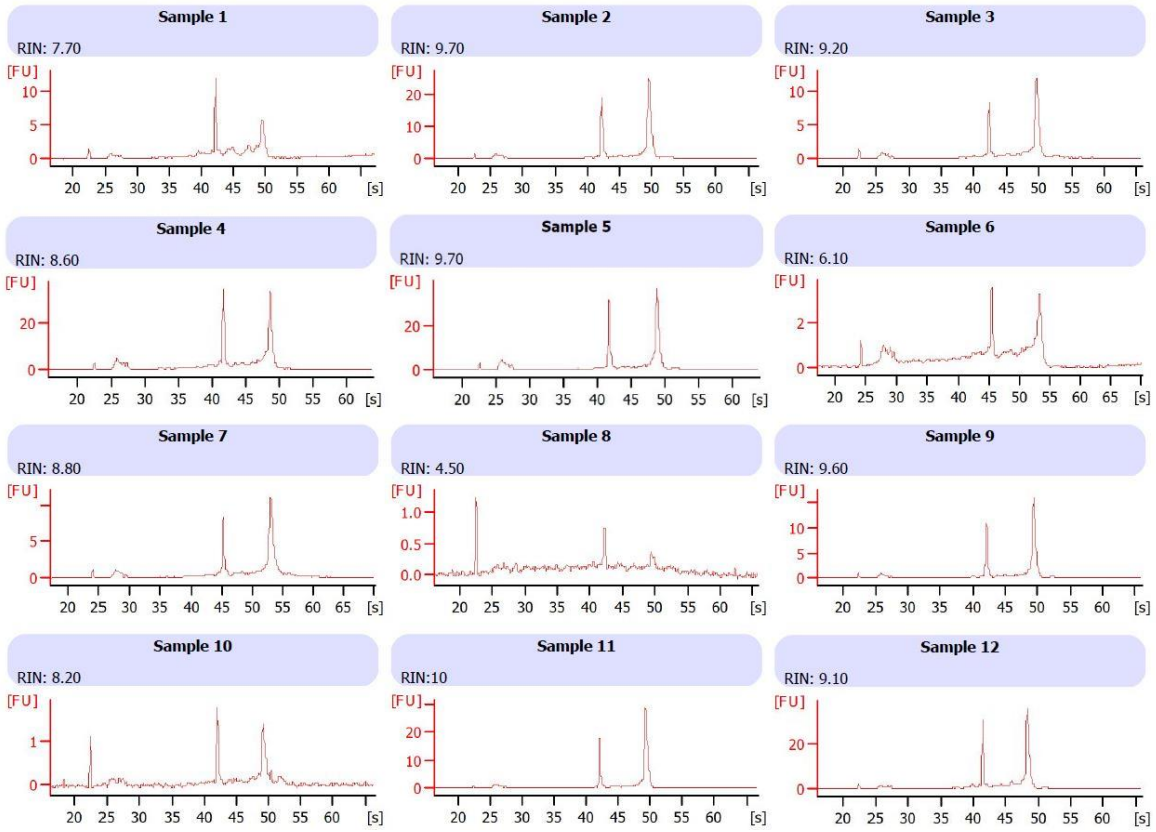

(B)

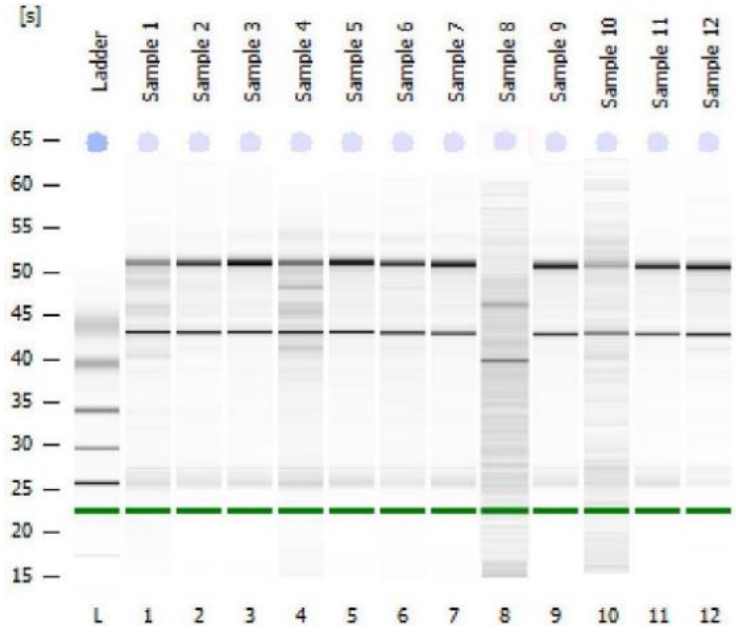

(C)

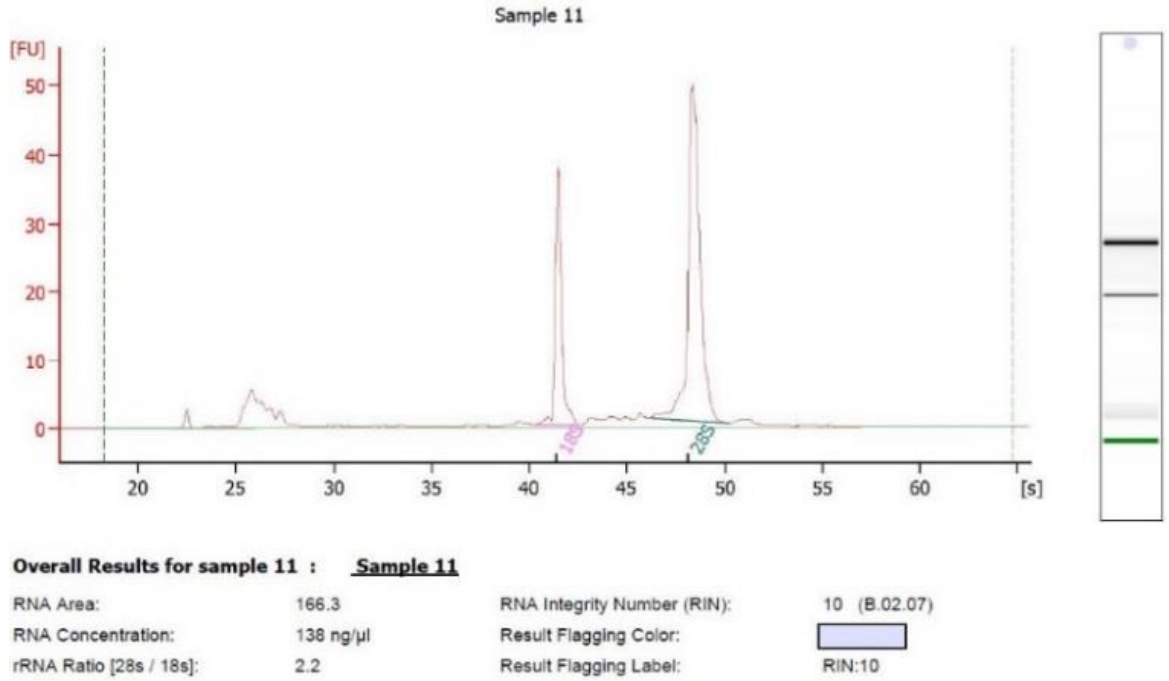

Figure 2.14 Evaluation of microRNAs using bioanalyzer.

Twelve samples could be run per chip. (A) Output of the analysis showed that all samples have high RNA integrity number (RIN) indicating that these samples contained intact and not degraded RNAs suitable for further analysis by NanoString technology. (B) Explains electrophoresis and bands of microRNAs depending on the concentrations of microRNA in each sample in comparison to the ladder bands. (C) Provides more information about each sample such as the time required to detect microRNAs peaks; mainly between 40 and 50 seconds to detect small RNAs between 18 and 28 nucleotides and the concentration of microRNAs in each sample.

2.3.19.3 *MicroRNA Profiling Using NanoString Technology*

Two main steps were utilised in this technology; preparation and microRNA hybridisation protocol. The preparation step includes setting the thermocycler temperature and sample preparation for annealing, ligation and purification.

2.3.19.3.1 Thermocycler Setting

Before starting the microRNA profiling using NanoString technology, the thermocycler was programmed to warm up for each protocol as shown in (Table 2.32).

Annealing protocol		Ligation Protocol		Purification Protocol	
Temperature	Time	Temperature	Time	Temperature	Time
94 ºC	1 minute	48 ºC	3 minutes	37 ºC	2 hours
65 ºC	2 minutes	47 ºC	3 minutes	70 ºC	10minutes
45 ºC	10 minutes	46 ºC	3 minutes	4 ºC	Hold
48 ºC	Hold	45 ºC	5 minutes	Total Time	2 hours+10 min
Total Time	13 minutes	65 ºC	10 minutes		
		4 ºC	Hold		
		Total Time	24 minutes		

Table 2.32 Temperature setting of the thermocycler for annealing, ligation and purification protocols during microRNA profiling technique using NanoString technology.

2.3.19.3.2 ANNEALING PROTOCOL

All RNA samples were normalised to 33 ng/µl using RNAse-free water. MicroRNA Assay controls were used at a dilution of 1:500 by mixing of 499 µl DEPC H20 with 1 µl of the microRNA Assay Controls were placed in a sterile micro-centrifuge tube, mixed by vortexing and spun down and kept on ice during the procedure. Annealing master mix (AMM) was prepared by combining 13 µl of Annealing Buffer, 26 µl of nCounter microRNA Tag Reagent and 6.5 µl of the 1:500 dilution microRNA Assay Control. All the contents were mixed by pipetting up and down. A volume of 3.5 µl of the AMM was aliquoted into each tube of a 12×0.2 ml strip tube. Then, a volume of 3 µl (100 ng) of RNA sample was added to each tube and mixed by gentle flicking and spinning down followed by initiating the annealing protocol with temperature and time setting as shown in (Table 2.32).

2.3.19.3.3 LIGATION PROTOCOL

Ligation Master Mix (LMM) was prepared by combining 19.5 µl PEG and 13 µl ligation buffer and mixing by pipetting up and down to ensure accurate transfer of the total volume of the viscous PEG. When the thermocycler reached 48ºC, after completion of the annealing process, 2.5 µl of LMM was added to each tube and mixed well by gentle flicking and spinning down followed by returning the tubes to the thermocycler and incubation at 48ºC for 5 minutes. After 5 minutes, the cap of each tube was removed carefully and the strips were left on the heat block followed by addition of 1 µl of ligase directly to each tube while they were still incubated on the heat block at 48ºC. After addition of ligase to the final tube, all tubes were re capped while they still on the heat block, the lid was closed and the ligation protocol initiated with the setting as shown in (Table 2.32).

2.3.19.3.4 PURIFICATION PROTOCOL

The purification protocol was initiated by addition of 1 µl of Ligation Clean-Up Enzyme to each reaction with gentle mixing by flicking and spinning down and the tubes were returned to the thermocycler and the purification initiated with the settings shown in (Table 2.32). After completion of the purification protocol, 40 µl DEPC (or RNAse-free), water was added to each sample, mixed well and spun down. A denaturation step was performed before adding the prepared sample to the hybridisation protocol as explained in the sections below.

2.3.19.3.5 CODESET HYBRIDISATION PROTOCOL

Reporter CodeSet and Capture ProbeSet reagents were thawed and kept on ice, inverted several times to mix well and briefly spin down at <1000 rpm for 30 seconds. The final hybridization reaction (FHR) composed of 10 µl Reporter CodeSet, 10 µl hybridisation buffer, a 5 µl aliquot from the microRNA Sample Preparation Protocol, and 5 µl Capture ProbeSet. To prepare the master mix (MM), 130 µl of hybridisation buffer was added to a tube containing 130 µl of the Reporter CodeSet, mixed well by inverting and spinning down. Twelve tube strips were cut in half to fit in the picofuge and labelled with the corresponding samples numbers, followed by addition of 20 µl of master mix (MM) to each of the 12 tubes. Samples from the microRNA sample prep protocol were denatured at 85ºC for 5 minutes, and quickly-cooled on ice, followed by addition of 5 µl aliquots from the microRNA Sample Preparation Protocol into each tube. At this time, the thermocycler was pre-heated to 65ºC using a 30 µl volume, calculated temperature, heated lid and “forever” time setting. Before placing samples at 65ºC, 5 µl of Capture ProbeSet were added to each tube and immediately capped and mixed by inverting the strip tubes several times and flicking to ensure complete mixing. They were then spun down at <1000 rpm and the strip tube was immediately placed in the 65ºC thermocycler. The hybridisation assays were left at 65ºC until ready for processing, and then incubated for at least 12 hours. Once removed from the thermocycler, post-hybridisation processing with the nCounter Prep Station was performed.

2.4 Data Collection and Statistical Analysis

Several types of software were used to collect, export and analyse data throughout the study. FlowJo (7.5) was used for fluorescence-activated cell sorting (FACS) of the phenotypic markers of MSCs. Both NIS-Elements Viewer (4.2) and Image J (1.49t) were used to export images obtained from the NIKON microscope for measuring the scratch area. Ascent software for multiskan ascent (2.6) was used to export data from the microplate reader, which was used for the estimation of protein concentration and evaluating cell viability in the MTS assay. ND-1000 software was used to export data generated by NanoDrop, for the nucleic acid purity and concentration. While, SDS (2.4) was used to export data generated from the PCR machine during gene expression analysis. 2100 Expert (2.3) was a software used to export data obtained from the bioanalyzer, for analysis of microRNA concentration and integrity. Other software was used for microRNA analyses such nSolver (3.0) to export and normalise data obtained from NanoString machine and R studio which was used to create images and figures of microRNA analyses as well as to assess significant variations between groups. Finally, Prism software (6.0) from Graphpad was the most commonly used software for statistical analyses.

2.4.1 *Data Types and choosing of Statistical Test*

Data of this study were variable depending on the type of experiment. In order to choose the most suitable statistical test, data were divided into related and unrelated data.

2.4.1.1 *Related Data*

These data were produced from repetitive measurements and matched pairs. Examples of these data include percentages of MSCs that express specific markers (CD+MSCs %), protein concentration (pg/ml), scratch area (μm^2), cell viability (%), migrating cells (%), proliferating cells (%) and gene expression which are all types of quantitative continuous data. This type of data (quantitative continuous data) was analysed by using means ± standard error of the mean (SEM) and a Two-way RM ANOVA test to determine significant differences between samples (when P values were less than 0.05). Multiple comparisons were required to find differences between pairs of means with appropriate

adjustment for multiple testing in every single condition during different time points in each separate experiment. Tukey's multiple comparisons test was used to detect variations, which were considered as significant when the P value was less than 0.05.

2.4.1.2 *UNRELATED DATA*

These data were produced from different independent groups of non-related variables. To find significant variations between the variables in this type of data, Sidak's multiple comparison test was used. For instance, comparing two groups of unrelated variables at different time points. For example, comparing cell doubling which was measured by fold change and doubling time which was measured in days for the same population at different time points. Another example was comparing the ratio of proliferating cells to the ratio of migrating cells in the same population at different time points.

For both types, Prism software version 6 from Graphpad was used in this study.

2.4.2 *STATISTICAL ANALYSIS OF MICRORNA PROFILING*

Data of microRNA profiling were generated as comma-separated values (CSVs) from nCounter digital analyser to nSolver (3.0) for normalisation. Data analysis was set to compare the correlation between microRNA signatures in the 3D model in relation to microRNA signatures of real skin. In addition, microRNA signatures at different time points in the punched models were compared in relation to microRNA signatures of intact models for further analysis of differentially expressed microRNAs during the healing process. Normalised data along with the fold change data were imported into R software (3.3.3) from The R Project for Statistical Computing. A two-tailed t-test was used to find significant variations of differentially expressed microRNAs between groups ($P<0.05$). While ggplot2 (2.1.0) was used to generate functions and create volcano plots. Additionally, based on an unsupervised clustering of the normalised expression counts, gplots" (2.17.0) and "RColorBrewer" (v1.1-2) with a Euclidean 2 from (www.ingenuity.com) were utilised to construct heatmaps (L2 norm) space measure and complete as the agglomeration method. All scripts and analysis pipelines were developed by Dr Rachel Crossland, Haematological Sciences, Institute of Cellular Medicine, Faculty of Medical Silences, Newcastle University, UK.

CHAPTER 3 CHARACTERISTICS OF MESENCHYMAL STEM CELLS AND DEFINING THEIR SECRETIONS

CHAPTER THREE: CHARACTERISTICS OF MESENCHYMAL STEM CELLS AND DEFINING THEIR SECRETIONS

3.1 INTRODUCTION

Despite the numerous sources for isolating MSCs, bone marrow represents the most suitable cell source to generate MSCs (BM-MSCs) for tissue engineering and potential therapeutic application (Liu *et al.*, 2009; Mafi *et al.*, 2011). BM-MSCs have the potential to differentiate into mesodermal lineages such as adipocytes, osteoblasts (Pittenger *et al.*, 1999), chondrocytes (Johnstone *et al.*, 1998), tenocytes, skeletal myocytes, and visceral mesodermal cells (Jiang *et al.*, 2002) astrocyte (Kopen *et al.*, 1999). They can also differentiate into endodermal and ectodermal cell types and tissues such as cardiomcyocytes (Fukuda, 2002), hepatocytes (Qu-Petersen *et al.*, 2002), mesangial cells (Ito *et al.*, 2001), muscle (Ferrari *et al.*, 1998) (Tamama *et al.*, 2008), neurons (Azizi *et al.*, 1998), stromal cells (Majumdar *et al.*, 2000), embryonic tissue (Stott *et al.*, 1999) and multiple skin cell types (Sasaki *et al.*, 2008). MSCs therefore have the potential to become the basis of tissue repair (Phinney and Prockop, 2007). This therapeutic potential to repair damaged tissues could be attributed not only to their transdifferentiation ability but also to the biomolecules secreted by these cells which alter the microenvironment of the injured tissue and are involved in a wide range of biological processes such as inflammation, angiogenesis, migration, proliferation and cell differentiation (Mafi *et al.*, 2011). Since the main secretions of MSCs are proteins such as growth factors and cytokines, the best technique to detect these biomolecules is by the use of an enzyme linked immunosorbent assay (ELISA) or enzyme immunoassay (EIA). With regard to wound healing and skin repair, MSCs have several roles. They can differentiate into skin like cells to compensate for cell loss during tissue damage and they can secrete a broad range of growth factors and cytokines which can initiate cellular functions such as migration, proliferation and differentiation of skin cells as well as an inflammatory response. (Sasaki *et al.*, 2008). The International Society for Cell Therapy (ISCT) has stipulated the main characterstics of MSCs. They should be fibroblast like cells with the ability to expand *in vitro* in non haematopoietic media and should possess the ability to differentiate into three lineages; adipocyte, chondroblasts and osteoblasts when grow in appropriate differentiation media. They should also be positive for the expression of the stem cell markers, CD73, CD90

and CD105 while negative for the expression of the haematopoietic stem cell markers, CD14, CD19, CD34, CD45 and HLA-DR (Dominici *et al.*, 2006). Their ability to express these markers can be detected using the fluorescence activated cell sorting (FACs) technology. FACs is used to analyse the phenotype of cells at the single cell level and particle size of 0.2-150 μm. FACs analysis includes cell counting, cell sorting, detection of phenotypic biomarkers to reveal heterogeneity in a population and protein engineering depending on the chemical and physical characteristics of the cells. It is composed of three systems; fluidic, optic and electronic. Each system performs a specific function; the fluidic part passes the cells or particles through a fluidic stream and transports them to the optical part where the laser beams illuminate the stained cells depending on the type of flourochome used during the cell staining. Any fluorescent molecules in the stream scatter the light in proportion to the signals and emit fluorescence which is then detected by specific lenses and directed by optical filters to detectors where the electronic system changes these light signals to electronic pulses and then computer analysis.

One of the most important ingredients required for MSC growth and expansion *in vitro* is that the calcium level is equal to 1.8 mM/L. Lower calcium concentrations significantly reduce the ability of MSCs to proliferate and expand *in vitro* (Liu *et al.*, 2009). The media used to grow MSCs and expand them successfully is complete non haematopoietic media with standard (high) calcium level (HC-Media) and is the optimal media for the cells to secrete their biomolecules for wound healing purposes (Hwang *et al.*, 2009; Walter *et al.*, 2010; Tamama and Kerpedjieva, 2012). However, collection of MSC secretions from their *in vitro* culture in complete media is unsatisfactory due to the serum content, which interferes with effect of MSC secreted molecules when tested on skin cells during migration and proliferation assays. The conventional method to collect MSCs secretions is using serum free media (DMEM based formula) enriched with some suppliments that support MSC growth and propagation (Walter *et al.*, 2010). However, collection of MSC secretions from their *in vitro* culture using this method is again unsatisfactory when the used cells are primary keratinocytes due to the HCL which would enhance their differentiation and therefore arrest their migration and proliferation. Therefore, a new method is required to collect MSC secretions for use in wound healing studies.

3.2 SPECIFIC AIMS OF CHAPTER THREE

1. To characterise isolated human MSCs from the femoral heads of human hip joints in terms of morphology, phenotypic markers and differentiation potential.
2. To test the ability of MSCs to grow in serum free media in both standard (high) and low calcium concentrations and to compare MSC characteristics under these conditions.
3. To collect MSC secretions under serum free media with low and standard (high) calcium level) conditions and analyse their protein content by ELISA. Use and compare these secretions in wound healing experiments including testing their effects on migration proliferation and differentiation of human skin cells such as primary keratinocytes and primary dermal fibroblasts.
4. To test the potential of MSCs to differentiate into epidermal-like cells in 2D culture.

3.3 RESULTS

3.3.1 *DONORS AND SAMPLE COLLECTION*

As mentioned in the methods chapter (Chapter 2), MSCs were isolated from hip joints from 12 osteoarthritis patients after informed consent. The patients consisted of 5 males aged 64 and 94 years and 7 females aged between 55 and 82 years. Isolated MSCs were referred to as BB92, BB93, BB95 and BB95a, BB100, BB103, BB104, BB105, BB106, BB107, BB108 and BB109). One sample failed to generate MSCs (BB104). Two samples; BB103 and BB106 were unable to grow and expand under standard growth conditions during *in vitro* expansion as shown in (Table 3.1) and (Figure 3.1).

Collection and Processing Date	DTOS #	MRG N#	Haem BB#	G	Age (Yr)	Hip	Condition	Notes
30.04.14	5189	N3476	BB92	F	56	L	OA*	Characterised and utilised
08.05.14	5212	N3485	BB93	F	74	R	OA	Characterised and utilised
03.06.14	5256	N3515	BB95	M	82	L	OA	Characterised and utilised
03.06.14	5256	N3515	BB95a	M	82	L	OA	Characterised and utilised
07.08.14	5385	N3599	BB100	F	65	R	OA	Characterised and utilised
29.10.14	5514	N3669	BB103	F	75	L	OA	Failed to expand at P1
06.11.14	5527	N3672	BB104	F	75	R	OA	No cells obtained
19.11.14	5555	N3687	BB105	F	63	L	OA	Characterised and utilised
20.11.14	5553	N3688	BB106	M	64	R	OA	Failed to expand at P2
20.11.14	5554	N3689	BB107	M	94	R	OA	Characterised and utilised
20.11.14	5556	N3690	BB108	F	55	L	OA	Characterised and utilised
26.11.14	5567	N37	BB109	M	67	R	OA	Characterised and utilised

Table 3.1 Information about MSCs used in the study.

This table shows MSC samples isolated from the femoral head of human hip joints. Twelve samples were isolated at different times from male and female donors aged between 55 and 94 years. The isolated cells were given different numbers and anonymised codes depending on the department storing the samples. In Academic Haematology, they are given a BB number, which was the code and ID for MSCs in this study. Two samples; BB103 and BB106 were lost during processing at P1 and P2 respectively, while no cells were obtained from BB104. Other samples were processed and yielded MSCs successfully and further used in the study. MRG= Musculoskeletal Research Group, Haem= Haematological Sciences Unit, G= Gender, Yr=Year, L= Left, R= Right, OA=Osteoarthritis.

3.3.2 *Characteristics of Human MSCs*

3.3.2.1 *Morphological Characteristics and Expansion Ability*

Under standard growth conditions, MSCs have a small cell body with a nucleus located in the middle of the cell body and long and thin processes. They are mainly spindle-shaped elongated cells i.e. fibroblast like cells. However, they can appear in two more shapes; e.g. star-shaped cells (cuboidal and stellate) and triangular-shaped cells with the ability to propagate and expand *in vitro* when grown in non-haematopoietic (NH) media (Banik et al., 2016) (Figure 3.1 A, B, C and D). They have the ability to attach to plastic surface after 24 hours of isolation from bone marrow. (Figure 3.1 A). Interestingly, MSCs have the ability to grow under other culture conditions such as serum free media and low calcium media (LC-Media) for three days retaining their spindle shape morphology but losing their expansion ability (Figure 3.1 E and F).

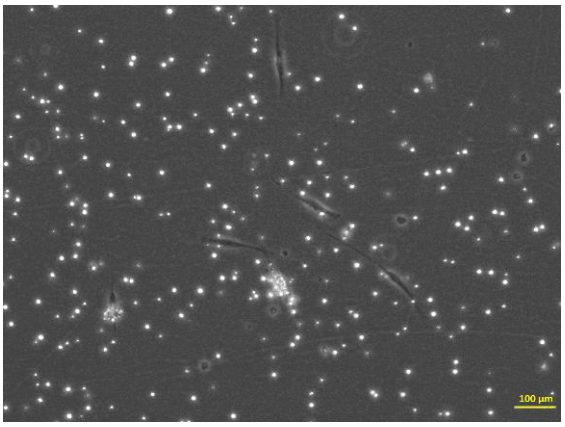

(A)

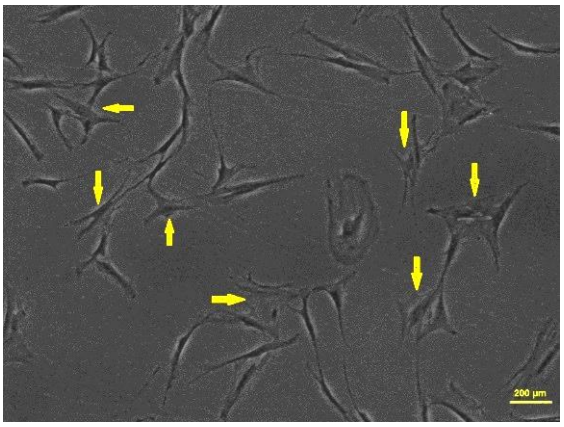

(D)

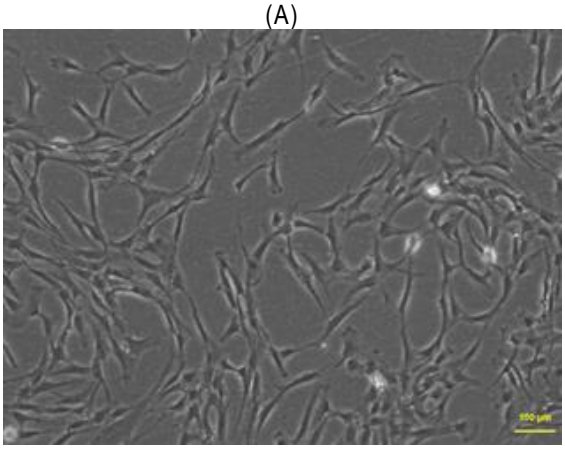

(B)

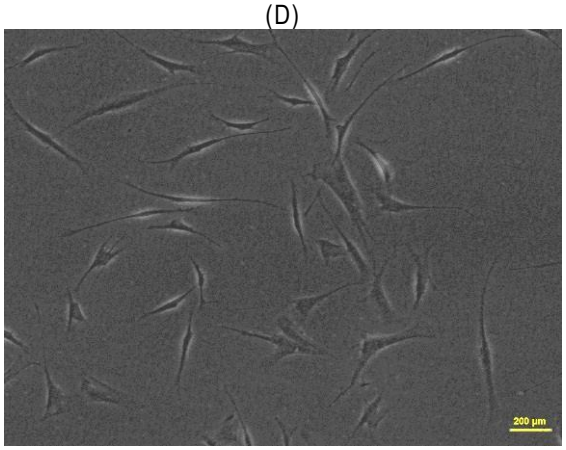

(E)

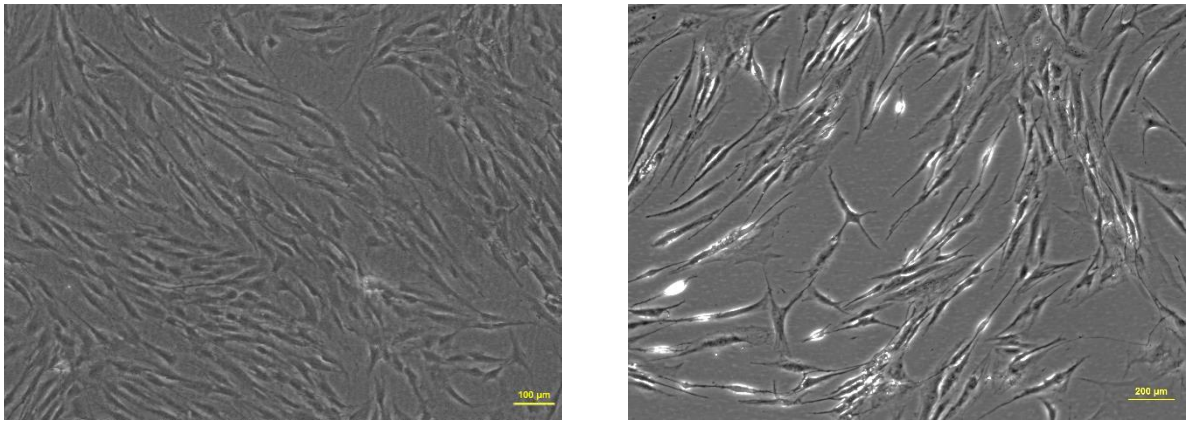

(C) (F)

Figure 3.1 Morphology and shapes of MSCs at different time points and different growth conditions.

Representative images of isolated MSCs mentioned in (Table 3.1). (A) MSC sample (BB100) are generally spindle-shaped cells with the ability to adhere to plastic after 24 hours of isolation from the bone marrow. (B) MSCs (BB100) at 50 % confluence, they are mainly spindle-shaped. (C) MSCs (BB100) at 80 % confluence. (D) MSCs (BB100) appear as star shapes and triangular shapes (Yellow arrows). (E) MSCs (BB100) grown in serum free media with a calcium level of 1.8 mM/L can retain their morphology but lose their expansion ability. (F) MSCs (BB105) grown in serum free media containing low calcium levels (0.04 mM/L) for three days lost their expansion ability but retained their spindle shaped morphology. Scale Bar: A-C: 100 µm, D-E; 200 µm.

In term of expansion ability, MSCs are able to expand *in vitro* under standard culture conditions (SCC) in NH medium (supplemented with 10% FBS, 1.8 mM/L calcium level, 200 mM L-glutamine and 1% penicillin-streptomycin). *In vitro* expansion ability was measured by calculating proliferation indices; the cell count of harvested cells, doubling time (DT) and population doubling (PD) for each passage. The cell count significantly increased from $0.96\times10^6 \pm 0.17\times10^6$ at passage 1 to $1.565\times10^6 \pm 0.285\times10^6$ at passage 2 and $3.505\times10^6 \pm 0.105\times10^6$ at passage 3 ($P>0.01$ and $P>0.001$) respectively (Figure 3.2 A). On the other hand, DT was reduced from 4 days at passages one and two to 1 day and half days at passage three (Figure 3.2 B).

(A)

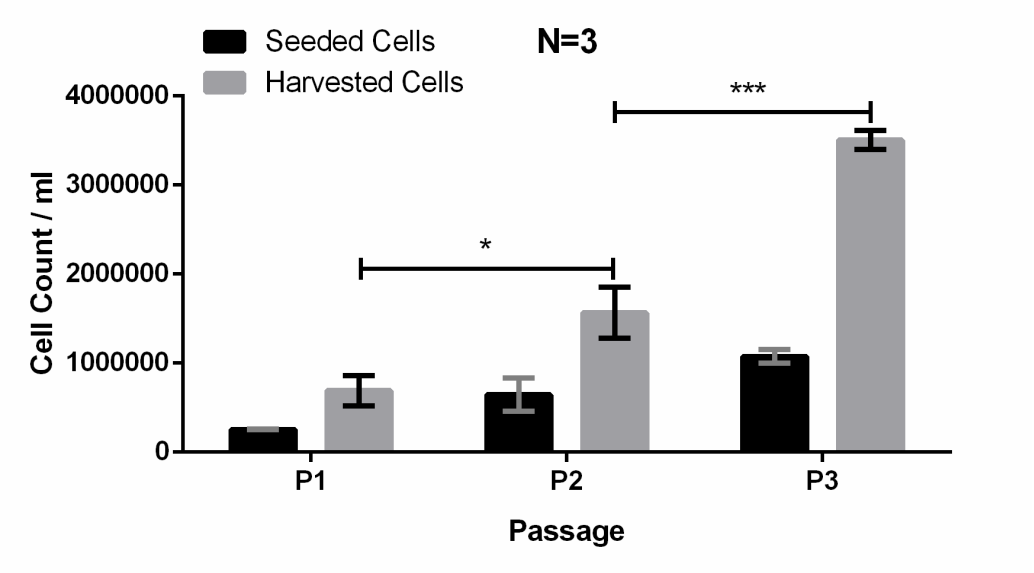

(B)

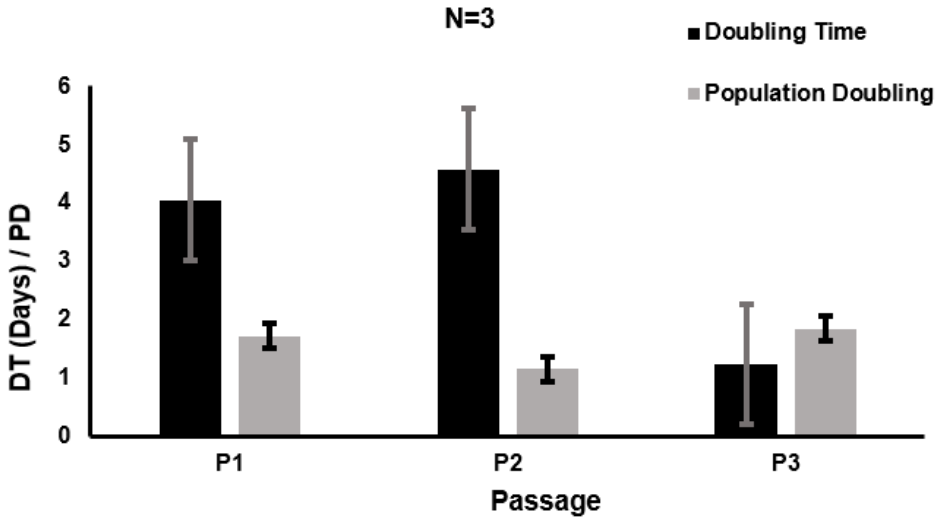

Figure 3.2 Expansion indices of MSCs.

(A) Numbers of harvested MSCs significantly increased when passage number increased. (B) MSC doubling time reduced at later passages i.e. MSCs took 4 days to double their number at passage 1 while they duplicated their count within one and half days at passage 3. Columns in (A) represent means of the cell count at the assigned passage (N=3), Columns in (B) Black columns in (B) represent means of the doubling time (DT) (N=3), Gray columns in (B) represent means of the population doubling (PD) (N=3), Error bar= standard error of the mean (SEM).

3.3.2.2 *PHENOTYPIC CHARACTERISTICS OF MSCS*

After staining cells with specific CD markers and analysing using the FACScan analyser (Canto II) (Chapter 2, Section 2.3.5.2), Flow Jo software was used to gate cells depending on their stain. Briefly, cell debris were excluded from the total analysed cells. Live cells

(DAPI negative) were used to segregate other cells that express specific CD marker depending on the dye wave length.

Under standard conditions for MSCs (N=9), 97±0.55 % and over of the isolated MSCs expressed the stem cell markers CD73 (97.0±0.55 %), CD90 (97.8±0.55 %) and CD105 (97.5±0.54 %). These samples minimally expressed CD14, CD19, CD34, CD45 (0.90±0.15 %) and human leucocyte antigen (HLA-DR) (2.3±0.96 %). In another words, more than 98% of MSCs were negative for the expression of CD14 (which is expressed by monocytes, macrophages and endothelial progenitor cells), CD19 (a B-lymphocyte antigen), CD34 (a marker expressed by primitive haematopoietic stem cells), CD45 (a marker of all haematopoietic cells) and HLA-DR (Figure 3.3).

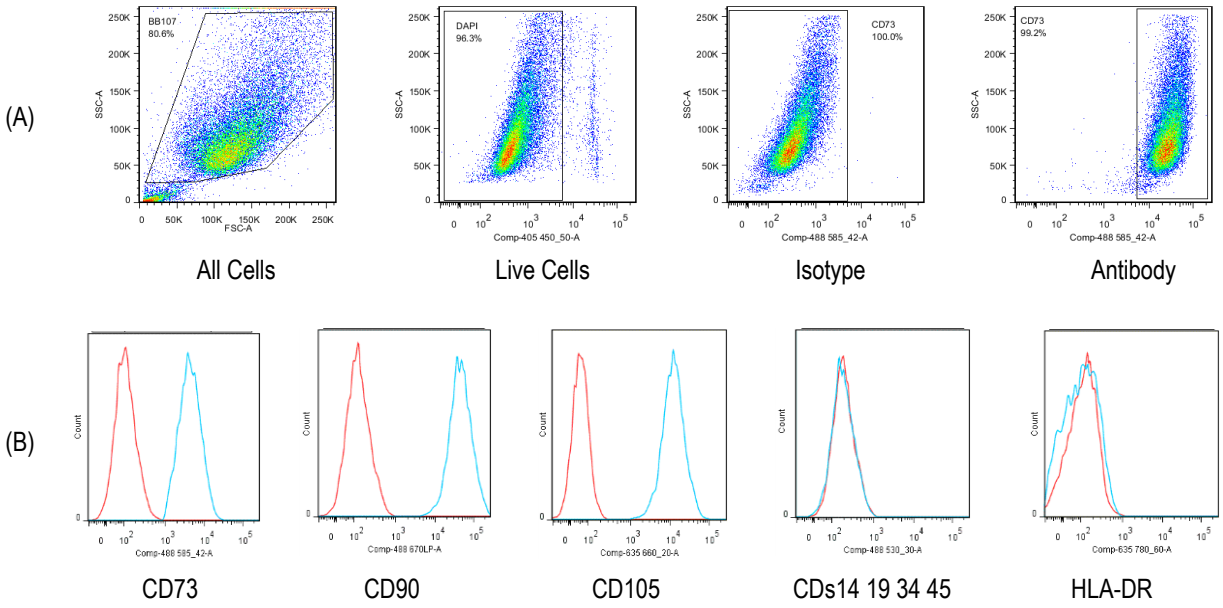

(C)

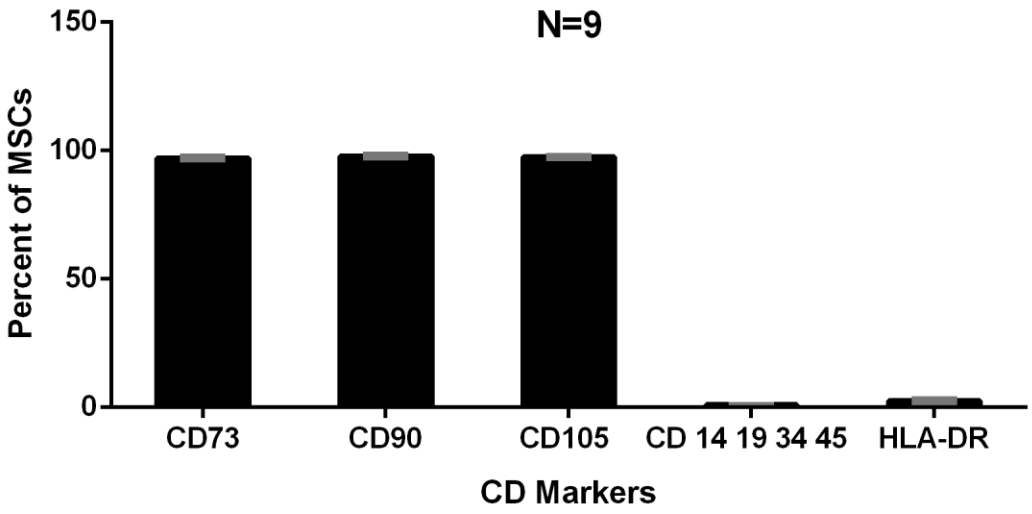

Figure 3.3 Phenotypic characteristics of MSCs at standard (high) calcium media (HC-Media).

All isolated MSCs (N=9) were stained with specific antibodies for each marker such as PE Mouse Anti-Human CD73 Clone AD2 (RUO), PerCP-Cy™5.5 Mouse Anti-Human CD90 Clone 5E10 (RUO), APC Mouse Anti-Human CD105 Clone 266 (RUO), FITC Mouse Anti-Human CD14 Clone M5E2 (RUO), FITC Mouse Anti-Human CD19 Clone HIB19 (RUO), FITC Mouse Anti-Human CD34 Clone 581 (RUO), FITC Mouse Anti-Human CD45 Clone HI30 (RUO) and APC-H7 Mouse Anti-Human HLA-DR Clone G46-6 (RUO) for 20 minutes at 4ºC then stained with DAPI and sorted in FACs. (A) Gating strategy showing that all stained cells were analysed and then gated on live cells versus specific antibody. (B) Gating strategy of representative overlapping antibody stained cells (blue line) and isotype stained cells (red line) for the given marker. (C) Statistical analysis showing the ratio of MSCs expressing CD markers presented as the mean on cell percentages. Error bars= standard error of the mean (SEM), (N=9).

MSCs where grown in low calcium media (LC-Media), 0.04 mM/L, for 3 days. LC-Media medium is a new potentially stressful environment for MSCs; with the possibility that it may cause a change their biological behaviour in particular their stemness, phenotypic features and differentiation potential. The phenotypic characterisation was therefore repeated under LC-Media. Again, MSCs showed the ability to grow in LC-Media for 3 days keeping their morphology as fibroblast like cells as shown in (Figure 3.1 F) but they lost their expansion ability. In addition, over 96% of the cells expressed CD73 (96.9±0.65 %), CD90 (99.3±0.18 %) and CD105 (96.9±0.97 %) and minimal number of cells were positive for the expression of the haematopoietic stem cell markers CD14, CD19 CD34, CD45 (1.65±0.87 %) and HLA-DR (1.00±0.10 %) i.e. over 98 % were negative for these markers (Figure 3.4). Therefore, MSCs can retain the criteria stipulated by the International Society for Cell Therapy (ISCT) when grown in LC-Media for three days.

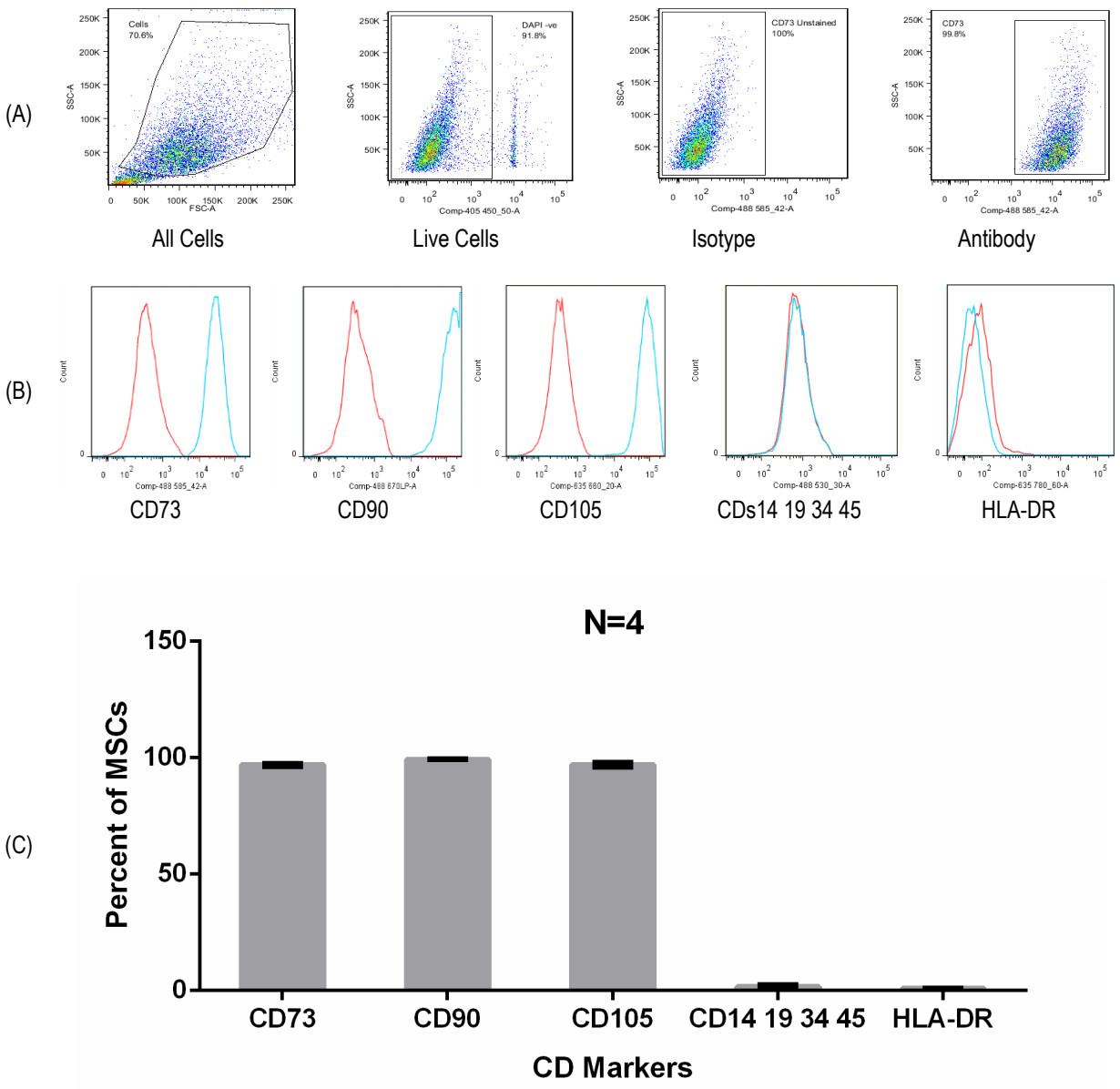

Figure 3.4 Phenotypic characteristics of human MSCs at low calcium media (LC-Media).

Four samples of isolated MSCs were analysed for their ability to express the CD marker panel after growth in LC-Media (0.04 mM/L) for 72 hours. Cells then stained with the same antibodies as explained in the legend of (Figure 3.3). (A) Gating strategy showing that all stained cells were analysed and used to generate positive cells for specific antibody. (B) Gating strategy of representative overlapping antibody stained cells (blue line) and isotype stained cells (red line) for the given marker. (C) Statistical analysis showing the ratio of MSCs expressing CD markers presented as the mean on cell percentages. Error bars= standard error of the mean (SEM) (N=4).

When the ratio of CD markers expressed by MSCs at both high and low calcium concentrations were compared, there was no significant difference (P>0.05) and the MSCs kept their phenotypic characteristics as shown in (Figure 3.5). Over 98% of the cells

expressed CD73, CD90 and CD105 and were negative for the expression of the haematopoietic stem cell markers CD14, CD19 CD34, CD45 and HLA-DR. Therefore, MSCs can retain the criteria stipulated by the ISCT when grown in LC-Media for three days.

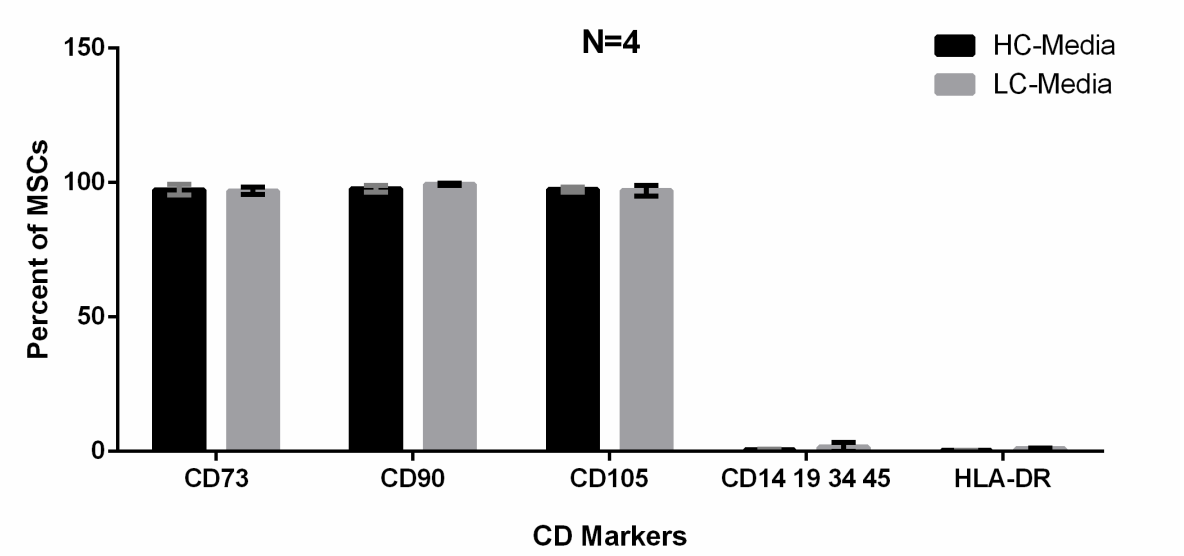

Figure 3.5 Comparison between MSC phenotypic markers expressed at standard high calcium media (HC-Media) and low calcium media (LC-Media).

MSCs grown in HC-Media and LC-Media expressed the phenotypic markers stipulated by the ISCT. MSCs at both HC-Media (Black columns) and LC-Media (Gray columns) expressed CD72, CD90 and CD105 with a ratio more than 97% with no significant variation (P>0.05). Also, more than 98% of MSCs at HC-Media and LC-Media were negative for the expression of CD14, CD19, CD34, CD45 and HLA-DR with no significant differences between samples (P>0.05). Data presented in columns as mean of percentages of MSCs that express specific marker. Error bars= standard error of the mean (SEM), (N=4).

3.3.2.3 *DIFFERENTIATION POTENTIAL OF MSCS*

Four MSC samples were analysed for their differentiation potential. All the samples have showed the ability to differentiate *in vitro* into three lineages; adipocytes, osteoblasts and chondrocytes as shown in (Figure 3.6). At high and low calcium concentrations, MSCs showed the ability to differentiate into lipid droplets (Figure 3.6 A), which represent the early stages of adipogenesis. These lipid vacuoles when stained with oil red dye give a red to orange colour. In addition, when MSCs were grown in osteogenic differentiation media for three weeks, they were able to differentiate into osteoblasts and developed calcium crystals, which turned to black when stained with Von Kossa stain. The observed purple colour resulted from the binding of ALP stain to other minerals present in the bone

such as iron (Figure 3.6 B). They were also able to differentiate into chondroblasts by growing as pellet *in vitro* and formed proteoglycan when grown in chondrogenic differentiation media for three weeks as demonstrated in (Figure 3.6 C).

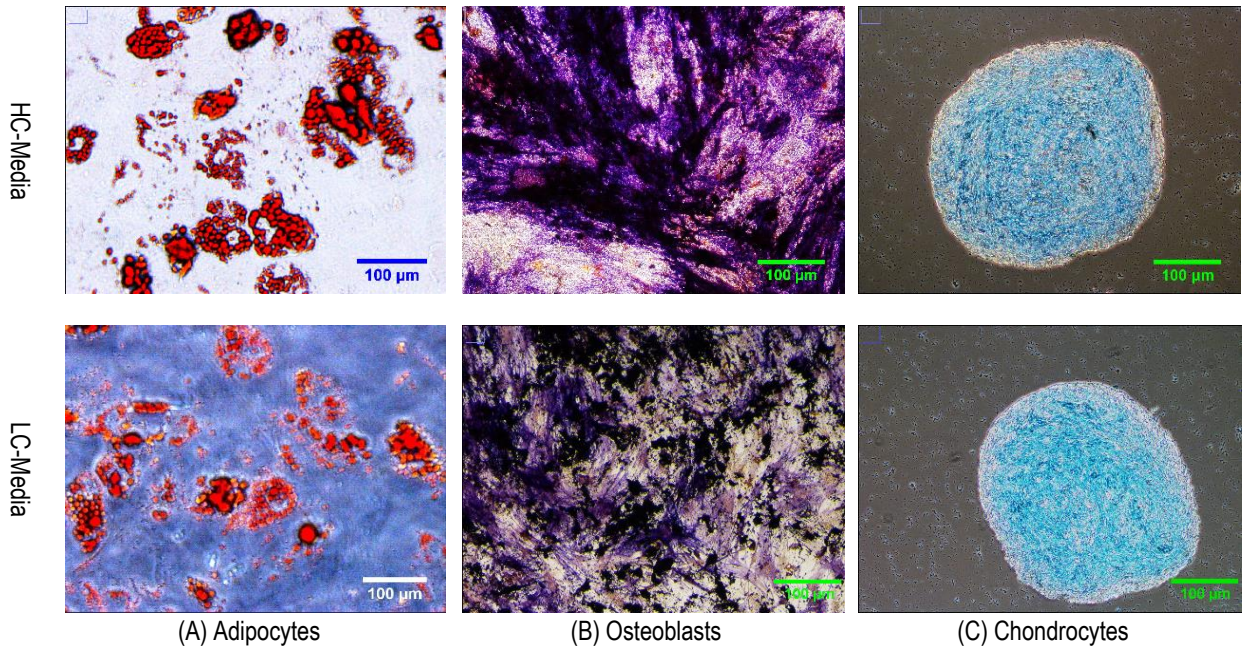

Figure 3.6 Differentiation potential of MSCs into tri-lineages.

Representative images showing the ability of MSCs to differentiate into tri-lineages; adipocytes, osteoblasts and chondrocytes. (A) MSCs grown in adipogenic differentiation media for 18 days developed into lipid vacuoles which upon staining with oil red dye gave a red to orange colour. (B) MSCs grown in osteogenic differentiation media for 21 days developed into osteoblasts which contained osteogenic minerals such calcium which upon staining with gave the dark blue and purple colour. (C) MSCs grown in chondrogenic differentiation media for 21 days developed to a pellet when stained with Alcian blue, shown as a bright blue colour indicating the formation of proteoglycan demonstrating the early stage of chondrogenesis. Scale bar 100 µm.

3.3.2.4 *DIFFERENTIATION OF MSCS INTO EPIDERMAL-LIKE CELLS*

In these experiments, the potential of MSCs to differentiate into epidermal-like cells in 2D cell culture was investigated. MSCs were grown in epidermal differentiation medium (EDM) for 17 days and both their morphology and ability to express epidermal differentiation markers at different time points was investigated. Morphologically, after 14 and 17 days of growth in EDM, MSCs changed their shape and no longer became spindle-shaped cells and lost their long body becoming rounded cells with reduction in their processes (Figure 3.7 A and B).compared to the control cells C and D respectively.

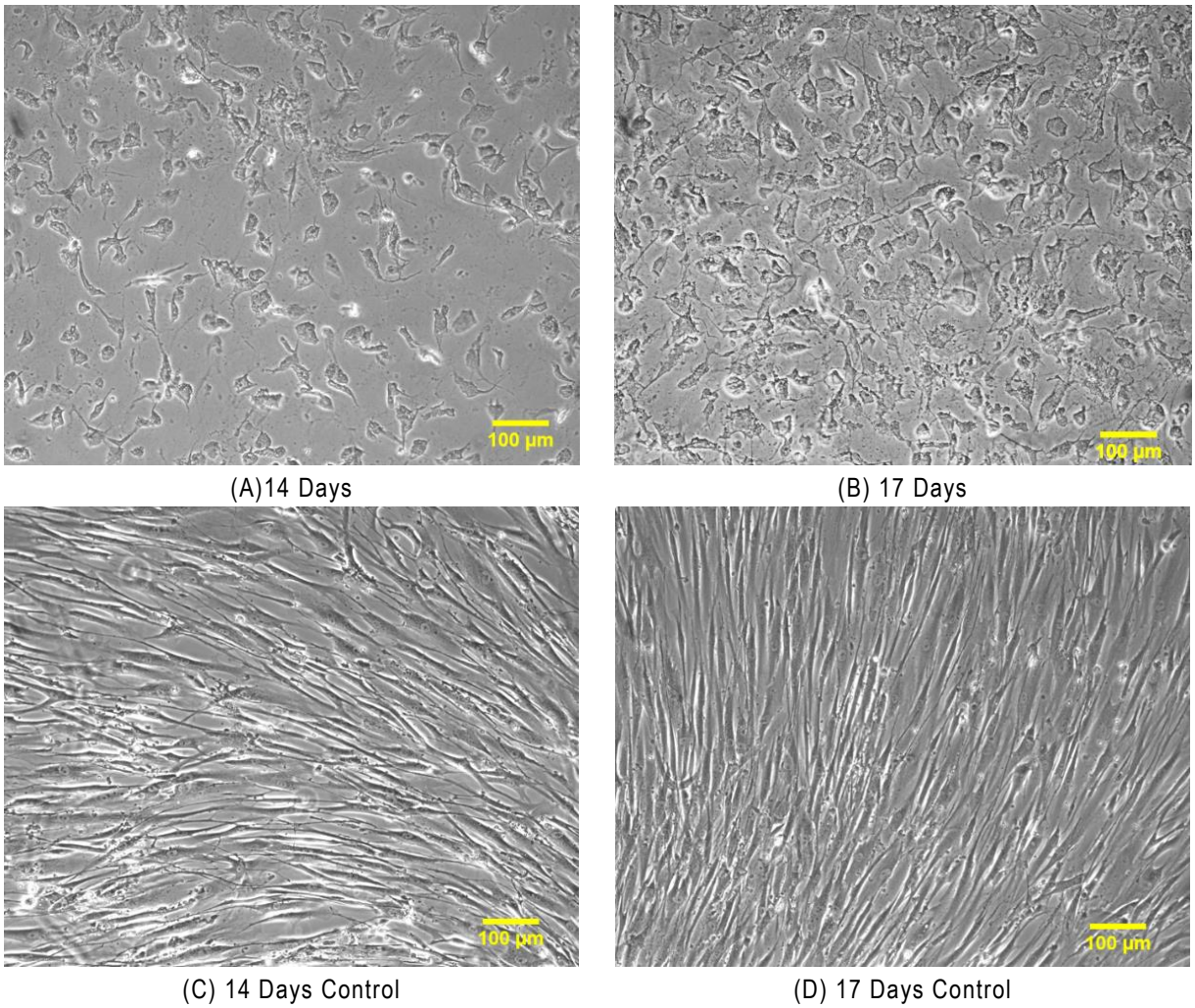

Figure 3.7 Morphology of MSCs in EDM at different time points.

Representative images showing MSC ability to change their morphology with time when grown in EDM. (A) and (B) MSCs grown in EDM for 14 and 17 days respectively; they changed their shape from spindle shaped cell to rounded cells with reduced protrusions from their body. (C) and (D) MSCs grown in standard MSC media (NH media) for 14 and 17 days respectively kept their morphology as fibroblast like cells with an elongated cell body. EDM= Epidermal differentiation media, Scale bar= 100 µm.

MSCs were shown to express epidermal markers. For example, after 10 days cytokeratin 14 (K14) was investigated and there was no expression as shown in (Figure 3.8 A). However, after 14 days, some cells started to express K14 as shown in (Figure 3.8 B) indicating that MSCs started to differentiate into keratinocyte-like cells. Moreover, after 17 days more MSCs started to express both cytokeratin 10 (K10) and loricrin as shown in (Figure 3.8 C and D) respectively.

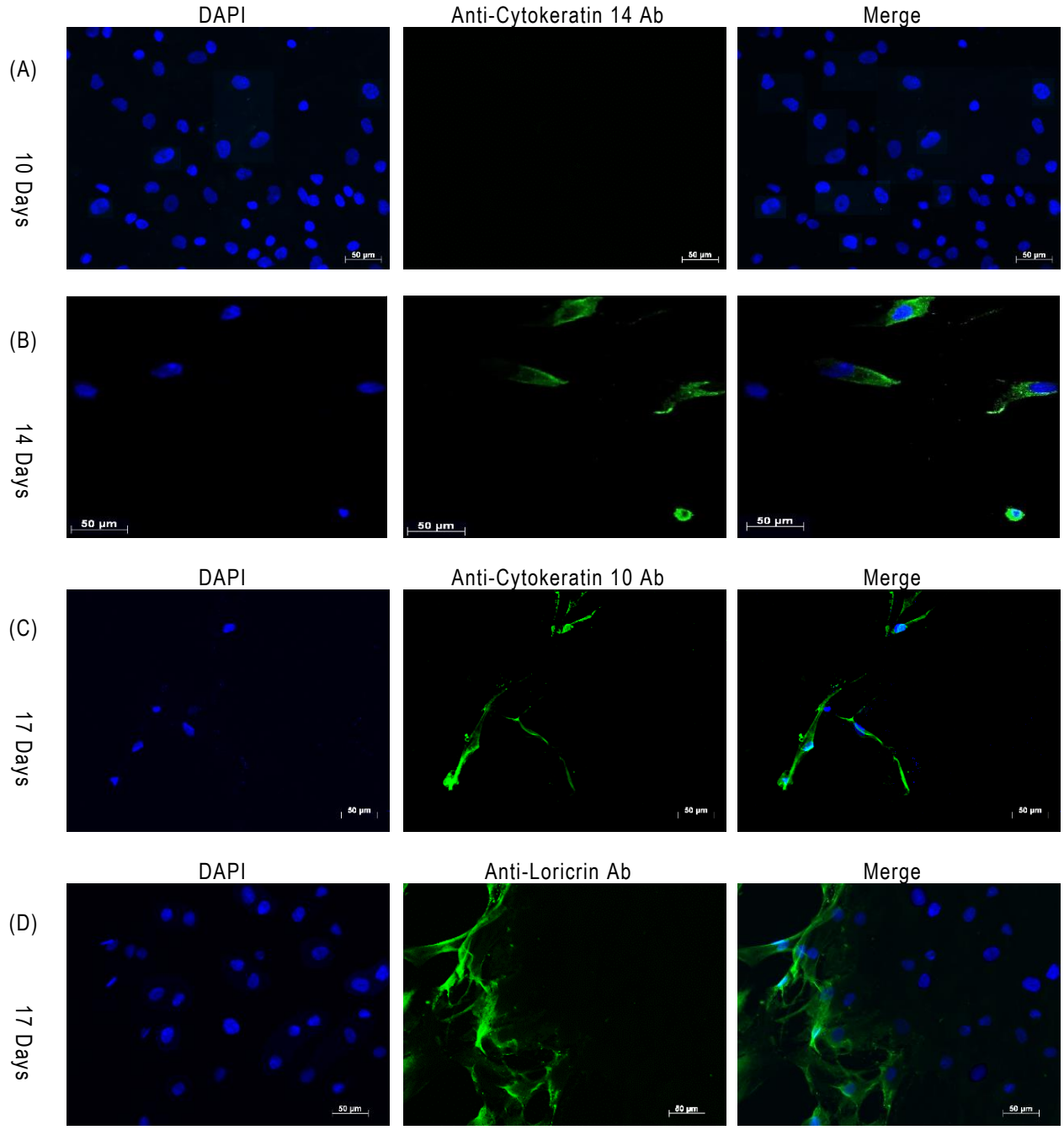

Figure 3.8 Differentiation potential of MSCs into epidermal like cells (ELCs).

Representative immunofluorescence images showing that MSCs have the ability to differentiate into epidermal like cells when grown in EDM. (A) MSCs grown in EDM for 10 days and failed to express K14. (B) MSCs grown in DMEM for 14 days expressed K14. MSCs in (A) and (B) are stained with Anti-Cytokeratin 14 antibody giving green signal with *Alexa fluor 488 goat anti-mouse IgG (H+L) secondary antibody. (C) MSCs grown in DMEM for 17 days expressed K10 when stained with Anti-Cytokeratin 10 antibody (ab111447)* gives green signal with *Donkey Anti-Rabbit IgG H&L (Alexa Fluor® 488). (D) MSCs grown in DMEM for 17 days expressed the late differentiation marker (loricrin) when stained with Anti-Loricrin antibody (ab85679)* and gives green signal with *Donkey Anti-Rabbit IgG H&L (Alexa Fluor® 488). Blue stain DAPI stain. Scale bar=50 µm.*

3.3.2.5 *PROTEOMIC CONTENT OF MSC-CM*

MSC-CM was analysed by ELISA kits as listed in (Table 2.3) to detect the protein content of growth factors, cytokines and chemokines that may influence migration, proliferation and differentiation of skin cells (keratinocytes and fibroblasts). As mentioned in Chapter 2, MSC-CM was collected at different time points (24, 48 and 72) hours in different media; stem cell non-haematopoietic media (NHM), low calcium media (LC-Media) and standard high calcium media (HC-Media). To avoid the confusion in the nomenclature of media types, serum levels, calcium levels and types of MSC-CM collected at different time points are shown in (Table 3.2).

Media Name	Serum	Calcium Level	MSC Secretion	Experimental Use	Collection Time (hours)		
					24	48	72
NH	Complete	1.8 mM	NH-CM	Comparison	NH-CM24	NH-CM48	NH-CM72
DMEM	10% FCS	1.8 mM	HC-CM	HaCat cells Primary Fibroblasts	HC-CM24	HC-CM48	HC-CM72
MCDB	NIL	0.04 mM	LC-CM	Primary keratinocytes	LC-CM24	LC-CM48	LC-CM72

Table 3.2 Information about MSC secretions in different media.

MSC secretions were collected in different types of media with varying levels of calcium and serum for different experiments. For example, NH media is the standard growth media of MSCs used to collect MSC-CM and was used as a control. DMEM was used to collect MSC-CM (high calcium HC-CM) for fibroblast and HaCat experiments. MCDB was used to collect MSC-CM (low calcium LC-CM) for primary keratinocyte experiments.

LC-CM was collected for use in keratinocyte experiments and the standard calcium media was termed high calcium media (HC-CM) for fibroblast and HaCat experiments. MSCs secreted detectable levels of some growth factors, cytokines and chemokines at different concentrations in the three types of media (Figure 3.9 A, B and C) such as keratinocyte growth factor (KGF), hepatocyte growth factor (HGF), platelet derived growth factor-AB (PDGF-AB), stromal derived factor-1 alpha (SDF-1α) and macrophage stimulating protein-1 (MSP-1).

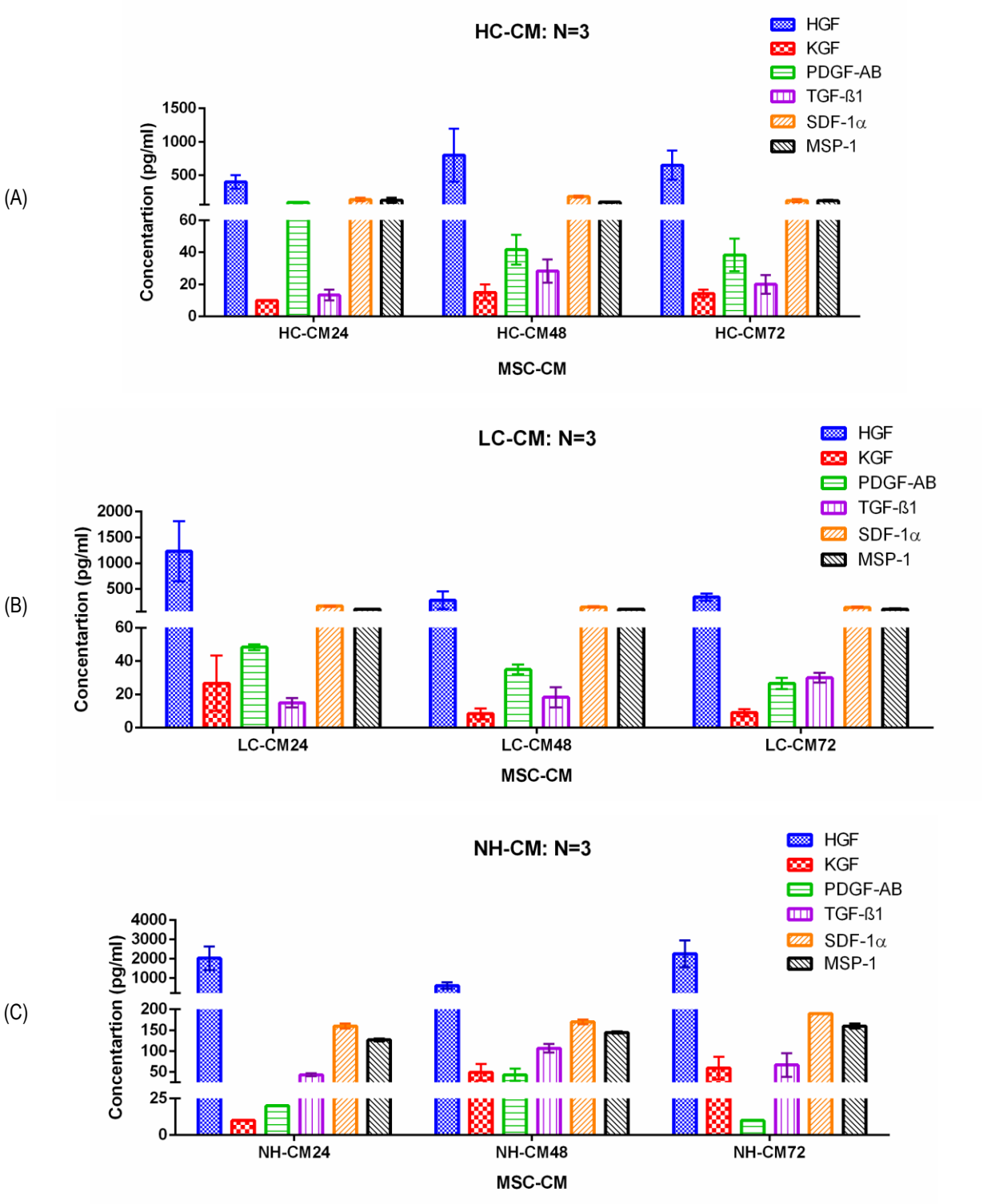

Figure 3.9 Growth factors present in MSC-CM.

MSC secretions in media different types and their concentrations in (A) HC-CM (1.8 mM/L) serum free media. (B) LC-CM (0.04 mM/L). (D) Standard MSC growth media with HC-CM (1.8 mM/L). X-axis represents mean of concentrations of growth factors in pg/ml. Data presented as mean of the concentration for a given growth factor. Error bars= standard error of the mean (SEM), (N=3).

As shown in (Figure 3.9 A), HC-CM collected at different time points contained different concentrations of the six growth factors; HGF, KGF, PDGF-AB, TGF-β1, SDF-1α and MSP-1. HGF was the only growth factor that increased during time; i.e. the concentration was significantly increased after 48 hours and 72 hours ($P<0.001$) and ($P<0.01$) respectively, when compared to the concentration at 24 hours. There was no significant variation between the concentrations of other growth factors collected at the same time points ($P>0.05$). For example, there was no significant increase in concentrations of KGF, PDGF-AB, TGF-β1, SDF-1α and MSP-1 neither after 48 hours nor after 72 hours ($P>0.05$) when compared to their concentrations at 24 hours.

In LC-CM, the concentrations of HGF had significantly reduced after 24 hours; e.g., it was reduced after 48 hours with continuous reduction after 72 hours ($P<0.001$) and ($P<0.01$) respectively when compared to its concentration at 24 hours. While other growth factors and cytokines showed similar concentrations during all collection times (24, 48 and 72 hours) ($P>0.05$) (Figure 3.9 B).

In case of NH media, the concentration of HGF remained the same during the different time points since there was no significant increase in the concentration after 72 hours ($P>0.05$) when compared to 24 hours. Again, other growth factors showed similar concentrations during the different time points; 24, 48 and 72 hours ($P>0.05$) (Figure 3.9 C).

The amounts of growth factors collected at the different time points, in the three types of media were then compared. For example, NH-CM72 contained higher concentrations of HGF when compared with HC-CM72 and LC-CM72 ($P<0.0001$) (Figure 3.10 A). At high calcium media (HC-Media) and serum free conditions, MSCs secreted higher concentrations of PDGF-AB when compared to LCL-serum free media. While other growth factors; KGF, TGF-β1, SDF-1α and MSP-1 were secreted equal amounts in the different types of media ($P>0.999$) (Figure 3.10 B, C, D, E and F).

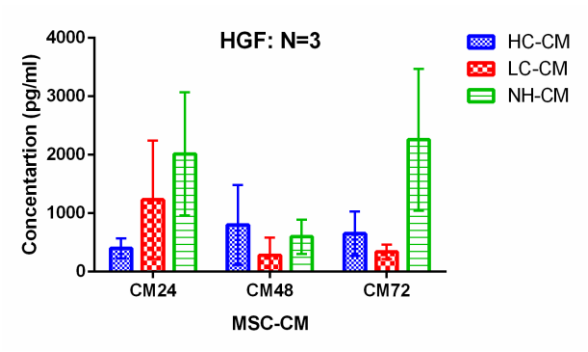

(A)

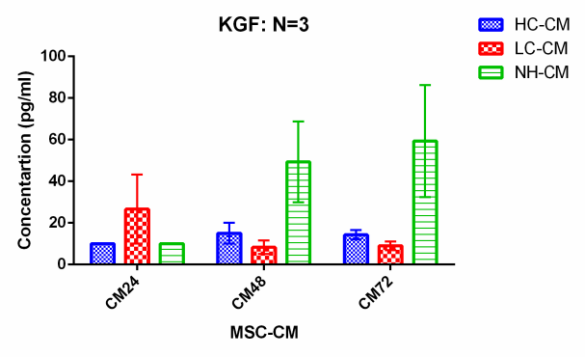

(B)

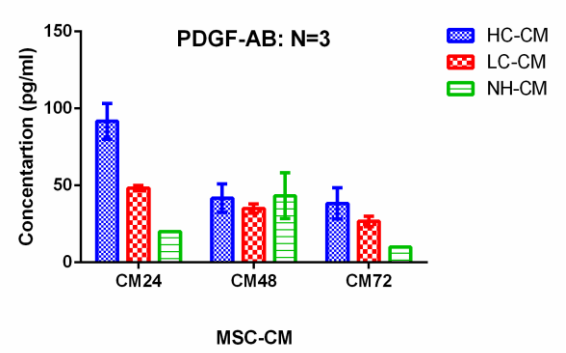

(C)

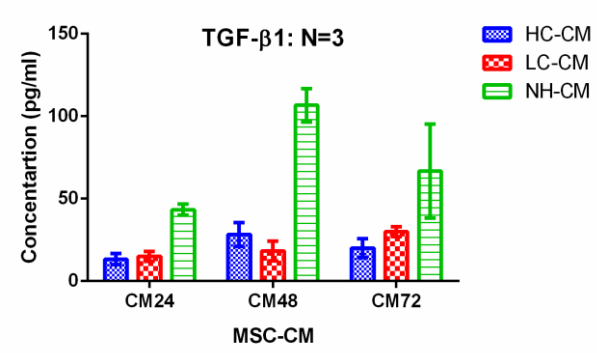

(D)

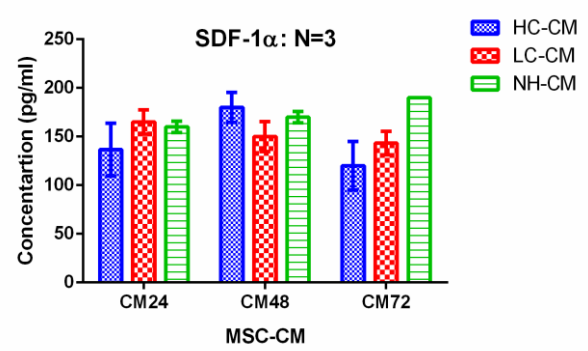

(E)

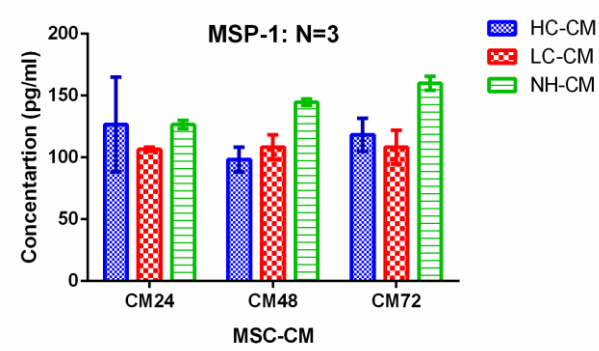

(F)

Figure 3.10 Concentrations of growth factors and cytokines present in MSC-CM collected at different conditions.

Concentrations of growth factors and cytokines secreted by MSCs at different calcium levels. (A) HGF concentration in NH media was higher than the concentration in LC-CM and HC-CM at the 72 hour collection time point (P<0.0001). (B) Concentrations of KGF collected in the three types of media were closer to each at 72 hours (P>0.999). (C) PDGR-AB was secreted in equal quantities at different calcium levels. (D) Concentrations of TGF-ß1 (E) Concentrations of SDF-1α. (F) Concentrations of MSP-1. Data represented as mean of the concentration of a given growth factor. Error bars= standard error of the mean (SEM), N=3.

3.4 DISCUSSION

Mesenchymal stem cells (MSCs) represent a promising tool for use in regenerative medicine with potential therapeutic applications in many diseases including repairing injured tissues and healing chronic wounds. This is due to their differentiation potential and their secretory contents which harbour a variety of growth factors and cytokines (Mafi *et al.*, 2011). Although they could be isolated from different sources such as adipose tissue, umbilical cord and Wharton's jelly, bone marrow (BM) represents the most frequently used source (Secunda *et al.*, 2015). The preference of BM over other sources is due to the high yield of cells, more homogeneity of the MSCs, and lack of differentiated or committed cells (Mareschi *et al.*, 2012) as well as their higher proliferation rate (Secunda *et al.*, 2015). In this Chapter, MSCs were isolated from the femoral head of human hip joints and characterised according to the criteria stipulated by The International Society for Cell Therapy (ISCT) (Dominici *et al.*, 2006). The MSC spindle-like shape facilitates cell distribution and homing and makes the cell ready to initiate proliferation. The faster the cells become spindle shaped after adherence to the flask surface the more proliferative and duplicative the cells become (Secunda *et al.*, 2015). MSCs also undergo self-renewal, which is a criterion of stem cells, and could be defined as the ability of cells to generate numerous clones from a single cell with the ability to retain their stemness characteristics. Therefore, isolated MSCs should be able to renew themselves and produce clones of cells similar in shape and characteristics to their parent cells (Roccaro *et al.*, 2013). The ISCT stated that MSCs should have the ability to differentiate into to tri-linages; adipocytes, chondrocytes and osteoblasts, which are mesodermal cell types (Dominici *et al.*, 2006). The mesoderm is one of the three germ layers that is formed at early stages of embryonic development (Sadler, 2010). Mesodermal adipocytes are lineages of the lateral plate mesoderm and represent the majority of adipocytes in adult body (Sheng, 2015). They perform specific functions such as energy storage including development of the brown fat heat insulator assisting the skin to control the temperature of the human body, in addition to protecting and supporting some organs such as the kidneys (Cristancho and Lazar, 2011). Therefore, adipose tissues are very important for the human body. Hence, the mesodermal adipocytes and the majority of the human body adipose tissue could be originated from MSCs. Consequently, the differentiation potential of MSCs into adipocytes is an important feature which could be used for mesodermal

tissue morphogenesis and regeneration. On the other hand, the ability of MSCs to differentiate into skeletogenic lineages such as chondrocytes, and osteoblasts suggest that the biological characteristics of MSCs is similar to those of mesodermal precursors when they still part of the epiblast (Alev *et al.*, 2013) which, in turn generates all the skeletal elements (except the cranial bones) (Sheng, 2015). Hence, MSCs act as functional pluripotent progenitors and share several common molecular and cellular similarities to embryonic stem cells (ESC) and could be involved in the application of bone and cartilage repair and regeneration (Klontzas *et al.*, 2015; Goldberg *et al.*, 2017). Collectively, both self-renewal and differentiation ability to mesodermal lineages are hallmarks of stem cells; therefore, by possessing these features, MSCs are important for sustaining tissue regeneration, development, maintenance and serial transplantation ability of MSCs (Nombela-Arrieta *et al.*, 2011).

Besides the ability to adhere to plastic, a panel of phenotypic positive and negative phenotypic markers has been proposed by the ISCT in an attempt to reduce experimental variability and confirm the purity of and homogeneity of isolated MSCs. For example, antibodies against CD73, CD90 and CD105 represent the positive selection panel for MSCs while antibodies against the haematopoietic stem cell markers CD14, CD19, CD34, CD45 and HLA-DR represent the negative selection panel (Dominici *et al.*, 2006; Jung *et al.*, 2012). MSCs were able to express the panel of markers proposed by the ISCT. Over 95 % of the isolated cells were positive for cluster differentiation (CD) antigens CD73, CD90 and CD105. CD73 is also called ecto-5'-nucleotidase and is a general marker for variant stem cells and is expressed by the cell membrane on many cell types e.g. dendritic cells (DCs), endothelial cells, epithelial cells, lymphocytes and macrophages. It is a multifunctional cell surface protein and performs many physiological roles such as organises epithelial ion and fluid transport, controls tissue barrier functions, enhances adaptive response of the cell to hypoxic conditions, preconditions the cell for the ischemic stresses, and attenuates an inflammatory response (Antonioli *et al.*, 2013). CD73 is a coenzyme which catalyses the conversion of monophosphate (AMP) to adenosine, which in turn binds to one of four adenosine receptors (A1, A2A, A2B or A3) and initiates cell activation to perform one of the functions mentioned above (St. Hilaire *et al.*, 2009) et al., 2011). Although, the expression of this marker is not restricted to MSCs, the ability to express it is very important for facilitating cell adhesion, migration and proliferation (Wang

et al., 2008). CD90 is also referred to as Thy-1, because it was first antigen detected on mouse thymocytes by (Reif and Allen, 1964). It is a cell surface glycoprotein with 111 amino acids expressed by variant stem cells in addition to activated endothelial cells, brain cells, fibroblasts, neurons and ovarian follicular cells (Kisselbach *et al.*, 2009). It binds mainly to integrins β2, β3 and β5 and activates several cellular activities including adhesion, extravasation and migration of cells, activation of T-cells, regulation of axon growth and suppression of tumours (Wetzel *et al.*, 2004). CD105 is also known as endoglin, is cell membrane glycoprotein and acts as TGF-β receptor with a high affinity to TGF-β1 TGF-β3 and a low affinity to TGF-β2 (Guerrero-Esteo *et al.*, 2002). It is activated upon ligand binding and involved in many cellular functions such as the development of the cardiovascular system, differentiation of smooth muscle, morphology and migration of the cell, remodelling of the vascular system and neovascularisation and angiogenesis (Guerrero-Esteo *et al.*, 2002). Although CD73, CD90 and CD105 are expressed on many other cell types separately, their expression in one cell type the MSC, will verify them as stem cell-like cells with stemness traits enabling them to perform a wide range of functions and increased differentiation potential.

On the other hand, 98% of the isolated MSCs were negative for the haematopoietic stem cell markers. For example, CD14, is a marker, expressed by macrophages, monocytes, neutrophils, dendritic cells and endothelial progenitor cells and is involved in their differentiation (Deans and Moseley, 2000). CD19, is a B-lymphocyte antigen, involved in their proliferation and differentiation (Tedder and Isaacs, 1989). CD34 is a haematopoietic progenitor cell antigen (Griffiths *et al.*, 2005; Hass *et al.*, 2011; Jin *et al.*, 2013a), It is expressed on haematopoietic and vascular tissue (Nielsen and McNagny, 2008). It acts as adhesion molecule, supports T-cells to penetration into the lymph nodes (Suzawa *et al.*, 2007) and plays a role in migration of eosinophils and precursors of dendritic cells (Blanchet *et al.*, 2011). CD45 is a marker of all mature haematopoietic cells and involved in their activation with the exclusion of erythrocytes and plasma cells (Zuk *et al.*, 2002; Jin *et al.*, 2013a). It is also involved in the regulation of haematopoiesis and used to distinguish between haematopoietic stem cells (HSCs) and MSCs derived from the bone marrow (Saint-Paul *et al.*, 2016). Finally, MSCs are negative for human leukocyte antigen (HLA-DR) which is typically found on immune cells such as antigen presenting cells i.e.

macrophages, B-cells and dendritic cells and evoke T_{Helper} cells to help B cells produce antibodies upon binding to foreign antigen (Hass *et al.*, 2011; Jin *et al.*, 2013a).

The phenotypic positive and negative panels proposed ISCT are collectively strong evidence that MSCs derived from bone marrow are non-haematopoietic stem cells (Lin *et al.*, 2012). However, there may be some variations in the percentages of the cells in expressing some markers such as HLA class II under cytokine stimulation (Lin *et al.*, 2012; Mabuchi *et al.*, 2013). Moreover, CD34 has shown to be a controversial marker since some studies reported that adipose tissue derived MSCs could express CD34 at the time of isolation but that it is lost later during *in vitro* expansion (Quirici *et al.*, 2010; Bourin *et al.*, 2013). Therefore positive or negative selection using CD34 may vary depending on the MSC source.

Growth factors, cytokines and chemokines are involved in the main signalling pathways and play a pivotal role in signal transduction during the daily cellular activities including cell division, homeostasis, proliferation, migration, differentiation, survival, tissue repair and regeneration and apoptosis (Vlahopoulos *et al.*, 2015). Some growth factors are multifunctional molecules and promote cellular activities in a variety of cells; however, others are monofunctional and are restricted to one cell type. The main receptors of growth factors are tyrosine kinases, small G-protein coupled receptors (GPCRs) and serine/threonine kinases (Alfaro *et al.*, 2013; van de Kamp *et al.*, 2013).

These biomolecules (growth factors and cytokines) may work synergistically and form an intricate network, which controls and amplifies cellular responses upon stimulation conferring flexibility and stability of the cell. Dysregulation therefore, of the secretion of this panel of biomolecules by progressive disease will affect the biological function of the cell (Park *et al.*, 2009). Therefore, the presence of this wide spectrum of growth factors and cytokines in MSC secretions boosts the application, contribution and utilisation of MSCs and their secretions in cellular therapies including tissue regeneration and regenerative medicine. In this study, the presence of some growth factors and cytokines were detected in MSC secretions that could promote wound healing. These included keratinocyte growth factor (KGF), hepatocyte growth factor (HGF), platelet derived growth factor-AB (PDGF-AB), stromal derived factor-1α (SDF-1α) and macrophage stimulating protein-1 (MSP-1). The secretions of this panel of biomolecules was shown to be conserved amongst three different samples of MSCs.

Previous studies have described using of serum free medium to collect MSC conditioned medium (MSC-CM) for cellular therapy applications to avoid xenogeneic interactions. For wound healing experiments, using primary cells, in particular, trials on primary keratinocytes have given more realistic results than those obtained from cell lines and hence giving a better understanding about cell behaviour at the injury site. The main formula of serum free media is DMEM which contains HC-Media ranging from 1.0 mM/L - 1.8 mM/L which is sufficient to enhance primary keratinocyte differentiation; thereby, affecting their migration and proliferation which could give inaccurate results about keratinocyte behaviour at the injury site. This therefore limits the value of *in vitro* studies of MSC-CM collected in HC-Media when the target cells are primary keratinocytes. Therefore, there is an urgent demand to find an alternative solution. In this study a new method was developed to isolate and grow MSCs in LCL (0.04 mM/L) cell culture medium and to develop the optimal conditions to collect MSC secretions for their effect on human skin cell (including primary cells) viability, differentiation and would healing. The ability of MSCs to grow in a low calcium environment has rarely been studied. Only two studies described the effect of different calcium levels on growth, proliferation and differentiation of MSCs. The first study conducted by (Yu Kan *et al.*, 2009) described the effect of different combinations of calcium and inorganic phosphatase (Pi) (0, 0.45, 0.9, 1.8, 3.6 and 7.2 mM/L) on bone marrow derived MSCs (BM-MSCs). They reported that the optimum concentration of calcium and Pi for MSC growth and osteogenic differentiation was1.8 mM/L and 0.09 mM/L, respectively. Any decrease or increase in these concentrations for five days inhibited the growth of BM-MSC. In addition, treating BM-MSCs with lower or higher concentrations of calcium and Pi for 15 days retarded the ability of BM-MSCs to differentiate into osteogenic linages. Another team (Dry *et al.*, 2013) tested the effect of different HC-Media (1.9, 3.4, 5.0 and 6.9 mM/L) on porcine synovium derived MSCs (S-MSCs) and reported that elevated calcium levels promoted S-MSCs proliferation A concentration of 5.0 mM/L calcium resulted in the greatest increase in growth after 5 days when compared with higher and lower concentrations. Additionally, they found that S-MSCs were positive for expression of CD29, CD90 and CD105 and negative for CD14 and CD45 and were able to tri-differentiate towards the adipogenic, osteogenic and chondrogenic lineages.

Comparing the two studies, there is a clear discrepancy between the findings because (Yu Kan *et al.*, 2009) reported that any calcium concentration higher or lower than1.8 mM/L would inhibit MSCs proliferation and differentiation. On the other hand, Dry and colleagues (Dry *et al.*, 2013) showed that MSCs could proliferate and differentiate successfully with an optimised calcium concentration of 5.0 mM/L. Therefore, the ability of MSCs to grow in LCL remains controversial and more studies are required about this topic.

The results presented in Chapter 3 were in agreement with (Yu Kan *et al.*, 2009) in that MSC proliferation was arrested in reduced calcium conditions (0.04 mM/L); however, they were able to survive for three days, which is the period required to collect MSC-CM and remained in keeping with the criteria stipulated by the ISCT. Moreover, secretions of MSCs grown at LCL were similar to that of MSCs grown at high calcium conditions since they were able to secret different concentrations of the same growth factors and cytokines such as KGF, HGF, PDGF-AB, SDF-1α and MSP-1.

In both conditions (high and low calcium), HGF was produced in the highest concentrations indicating that HGF might be a growth factor released predominantly by MSCs and involved in several biological processes such as proliferation, migration, angiogenesis and production of matrix metalloproteinase (Maxson *et al.*, 2012). Separately or collectively, this panel of growth factors and cytokines may play a core functional role in tissue repair and regeneration by evoking diverse cellular functions including cell division, proliferation, migration, differentiation, survival and apoptosis.

Inhibition of MSC proliferation noticed by (Yu Kan *et al.*, 2009) and this present study could be attributed not only to the low calcium level but also due to the medium was serum free, since it is well reported that MSCs require complete medium for expansion and proliferation. On the other hand, MSCs showed the ability to differentiate into keratinocyte-like cells and expressed K14, K10 and loricrin. This differentiation ability has a potential application of MSCs in wound healing by fulfilling the need of the damaged tissue by compensating for the cells lost during tissue damage and participating in tissue regeneration by replenishing cells and other cellular components (Sasaki *et al.*, 2008). However, more investigations are required to confirm the potential participation of MSCs in wound healing via transdifferentiation into skin-like cells. More information about this issue will be discussed in Chapter 6 when MSCs were used to generate a 3D-SEM to test

their ability to form an epidermal like structure and to investigate their role in skin regeneration.

In summary, regardless of the trophic environment, MSCs showed the ability to grow normally at LCL for three days keeping their identity, stemness characteristics and secretory molecules. These criteria collectively raising the valuable insight of MSC applications in various conditions and disorders and facilitate the future research on primary cells instead of cell lines underlying their pivotal role in cell therapy and regenerative medicine. The study demonstrated a novel method to isolate and grow MSCs in low calcium medium and the optimal conditions to collect MSC secretions for the analysis of their effect on human skin cell (in particular, primary cells) viability, differentiation and wound healing *in vitro*. Previous studies have described culture medium in which to grow MSCs and collect growth factor rich supernatants but have not addressed issues of high calcium level contained in such media, which is sufficient to induce keratinocyte differentiation and restricts the potential beneficial effects of MSC secretions on wound healing in primary keratinocytes. Therefore, the protocol reported in this study addresses the issue of HC-Media in MSC-CM. Hence, in the next chapter (Chapter 4) the effect of high and low calcium levels in MSC- CM on the migration of skin cells will be addressed.

CHAPTER 4 EFFECT OF MSC-CM ON MIGRATION OF SKIN CELLS

CHAPTER FOUR: EFFECT OF MSC-CM ON MIGRATION OF SKIN CELLS

4.1 INTRODUCTION

Migration is a generic term used in biology to describe any controlled and directed cell motility inside the body when cells change their place and position between tissues or other organs (Kramer *et al.*, 2013). Cell migration is a highly organised cellular response and a substantial process for live cells and a key role for not only normal embryonic development and regeneration but also, disease restriction such as cancer metastasis, wound healing and the immune response (Mak *et al.*, 2016). Cell motility could be singular cell movement i.e., migration of embryonic cells and leukocytes through the extracellular matrix (ECM) (Fackler and Grosse, 2008), or multicellular movement or so called collective cellular streaming i.e., motility of epithelial sheets through the base membrane during wound healing (Gerharz *et al.*, 2007; Kramer *et al.*, 2013). Cell migration, in particular, collective cellular streaming is one of the main steps required for tissue regeneration and wound healing since epithelial cells migrate as cohesive sheets of cells (Friedl and Gilmour, 2009; Vitorino *et al.*, 2011). Additionally, collective cell migration maintains intercellular connection, relative velocity and conserved position of cells during wound healing for several types of epithelial wounds e.g., cornea, skin, epithelia and endothelia of respiratory and digestive tissue (Fong *et al.*, 2010; Vitorino *et al.*, 2011). Therefore, studying the migratory behaviour of the cell is a very useful tool for many biomedical disciplines and related fields e.g., biology and bioengineering (Yoshida *et al.*, 2003; Justus *et al.*, 2014). Migrating cells undergo some basic changes such as changing body shape via actomyosin-cytoskeleton (Keren *et al.*, 2008), displaying directional polarity and possessing leading and lagging edges in the cell body (Ridley *et al.*, 2003). In culture, cell motility can be detected and investigated using different migratory assays; for example, the trans-well migration assay (Boyden chamber assay) (Boyden, 1962), the scratch assay (wound closure assay) (Todaro *et al.*, 1965), the microfluidic chamber assay (capillary chamber migration assays) (Zigmond, 1988; Zicha *et al.*, 1991), the fence assay (ring assay) (Fischer *et al.*, 1990), the micro-carrier beads assay (Rosen *et al.*, 1990), the spheroid migration assay (Konduri *et al.*, 2001) and the cell exclusion zone assay (Poujade *et al.*, 2007). Additionally, there are specific assays to evaluate single cell

migration e.g., the leukocyte migration agarose technique assay (LMAT assay) (Carpenter *et al.*, 1968), the colloidal particle assay (colloidal gold single cell migration assay) (Albrecht-Buehler, 1977) and the time-lapse/cell tracking assay (Jaqaman *et al.*, 2008).

The scratch assay is a popular, inexpensive technique to measure cell migration in 2D culture (Liang *et al.*, 2007). In a scratch assay, a scratch is induced in a confluent cellular layer of any cell type grown on a plastic or glass surface, using a pipette tip. Cells migrate from the edges of the gap towards the scratch centre and cell migration microscopically monitored between time zero until the time of full closure or assay termination at a specific time point (Liang *et al.*, 2007; Kramer *et al.*, 2013). Wound healing is evaluated by measuring the scratch areas at different time points between time zero and full treatment time (Todaro *et al.*, 1965; Justus *et al.*, 2014). To mimic *in vivo* cell migration, cells are grown on a plastic surface pre-coated with different substrates i.e., collagen type I or type IV, fibronectin or matrigel (basal membrane extract “BME”) (Friedl *et al.*, 2004; Kramer *et al.*, 2013; Justus *et al.*, 2014). Migration of various cell types have been analysed using a 2D scratch assay e.g., keratinocytes (Chigurupati *et al.*, 2007), a human keratinocyte cell line (HaCat) and fibroblasts (Walter *et al.*, 2010), endothelial cells (Zhang *et al.*, 2011c), epithelial and mesenchymal cancer cells (Inoue *et al.*, 2007) and normal epithelial cells (Doehn *et al.*, 2009). Aside from low cost, ease and simplicity of data analysis, 2D scratch assay mimics, to some extent, migration of endothelial cells (ECs) into the wounded area upon induction of an *in vivo* wound in the endothelium of blood vessels. It is also suitable for studying the regulation of cell migration upon interaction with the extracellular matrix and cell-to-cell interaction (Liang *et al.*, 2007; Kramer *et al.*, 2013). Additionally, it is compatible with live cell imaging thereby enabling evaluation and analysis of intracellular signalling events and activities such as detecting subcellular localisation by visualisation of green fluorescent protein (GFP)-tagged proteins or detection of energy transfer during protein–protein interactions (Liang *et al.*, 2007). Moreover, it can be combined with other techniques e.g., gene transfection and microinjection, to analyse the impact of gene expression on cell migration (Abbi *et al.*, 2002). One of the drawbacks of the scratch assay is that it takes a long time to perform in comparison to other methods, it also consumes relatively large number of cells and large volumes of test substances for one assay, since it is performed in a tissue culture plate. Therefore, it is not a choice when the availability

of the cells is limited and the testing compound is expensive. Despite these technical drawbacks, the 2D scratch assay remains the most applicable assay for monitoring cell migration (Liang *et al.*, 2007). Collectively, migration of skin cells is a critical and the most important repair mechanism in the healing process (Qing, 2017). Therefore, studying the effect of MSC-CM on the migration of skin cells and monitoring cell behaviour through these events are very important and critical for a better understanding of the cellular mechanisms during the skin healing process.

4.2 SPECIFIC AIMS OF CHAPTER FOUR

1. **To study the effect of MSC-CM on the migration of skin cells (keratinocytes and fibroblasts).**
2. To study the effect MSC-CM on the migration of primary keratinocytes at hypoxic conditions.
3. To study the effect of MSC-CM on the migration of primary keratinocytes while blocking SDF-1α.
4. To compare the effect of high calcium conditioned media (HC-CM) and low calcium conditioned media (LC-CM) on the migration of primary keratinocytes.
5. To determine the best time for collecting MSC secretions in order to enhance the wound healing process.

4.3 RESULTS

4.3.1 SKIN CELLS

All human skin cells used in this study; HaCat cell line, human primary keratinocytes, human primary dermal fibroblasts (Figure 4.1 A, B, C and D) respectively, were provided by the Dermatology Department and Tissue Solutions Ltd / Glasgow, UK.

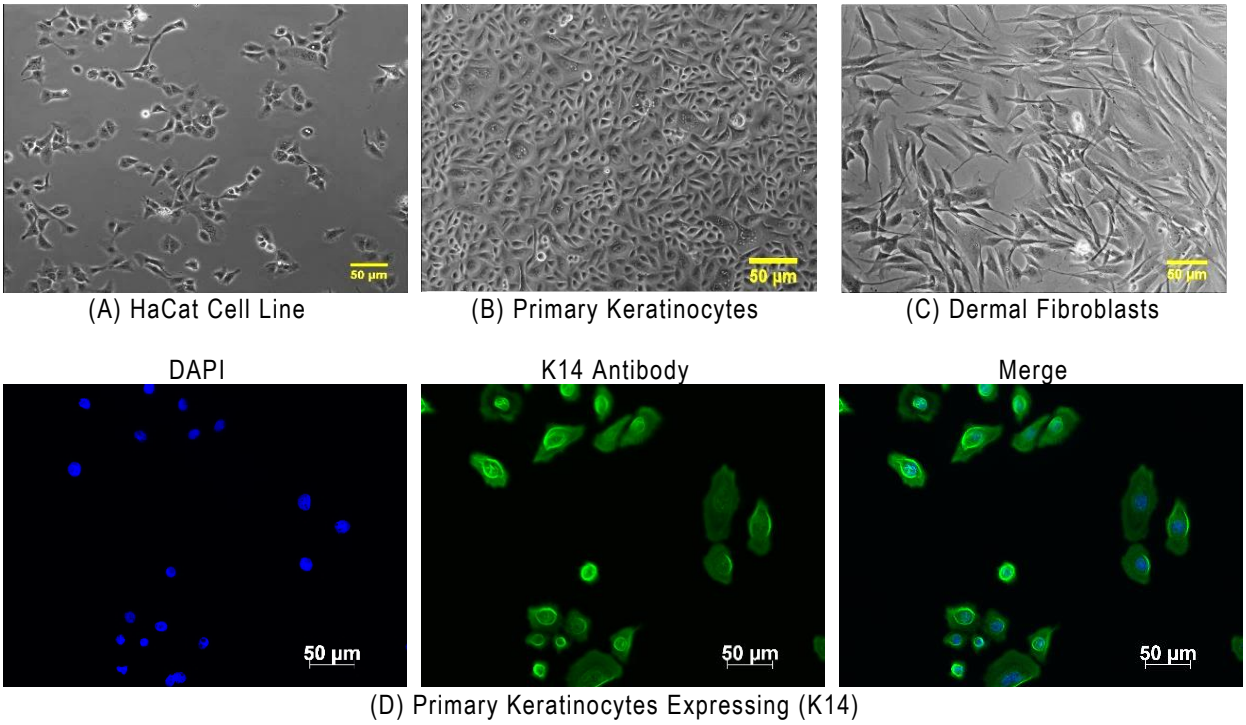

Figure 4.1 Human skin cells used in the study.

This figure shows human skin cells used during the study. (A) Monolayer of HaCat cell line (50% confluence). (B) Confluent monolayer of primary keratinocytes. (C) Confluent monolayer of dermal fibroblasts. (D) Primary keratinocytes stained with Anti-Cytokeratin 14 antibody [LL002] (ab7800) at (1:200) diluted in (10% foetal bovine serum (FBS) in PBS) and Goat Anti-Mouse IgG H&L (Alexa Fluor® 488) preadsorbed (ab150117) at (1:200) diluted in (10% FBS in PBS). Scale bar= 50 µm.

All cells, including the HaCat cell line and primary keratinocytes were obtained as frozen cells from the Dermatology Department, Newcastle University, other samples were obtained from Alcyomics Ltd. as shown in (Table 4.1).

	Cell Code	Provider	Passage	Age (Year)	Collection Date	Experimental Use
1	HaCat	DER	1	N/A	25.03.14	SA+MTS
2	S859FK	DER	1	41	26.06.14	SA+MTS
3	S912FK	DER	1	50	27.10.14	SA+MTS
4	S916FK	DER	2	22	03.11.14	SA+MTS+3D Model
5	S920FK	DER	2	54	10.11.14	SA+MTS+3D Model
6	S955FK	DER	2	61	16.02.15	SA+MTS
7	S962FK	DER	2	58	23.03.15	SA+MTS
8	S936FK	DER	3	53	05.01.15	3D Model
9	AL-O4	Alcyomics	0	NONE	21.12.15	3D Model+SA+Gene Expression
10	S946FK	DER	2	79	27.01.15	3D Model+SA+Gene Expression
11	S937FK	DER	2	24	15.01.15	3D Model+SA+Gene Expression
12	AL-O3	Alcyomics	1	NONE	15.01.16	3D Model+SA+Gene Expression
13	K935FK	DER	2	NONE	06.01.15	SA Block SDF-1α
14	S936FK	DER	2	53	05.01.15	SA Block SDF-1α
15	S1212FK	Alcyomics	2	NONE	NONE	BrdU labelling SA
16	S1214FK	Alcyomics	2	NONE	NONE	BrdU labelling SA
17	S1216FK	Alcyomics	2	NONE	NONE	BrdU labelling SA

Table 4.1 Human epidermal keratinocytes and HaCat cell line obtained as frozen cells.

Information about skin cells which were collected as frozen cells including sample code, provider, passage, age and gender of donors, collection date and experimental use. DER= Dermatology Department, S#FK=Sample # Foreskin Keratinocyte, SA= Scratch Assay, MTS= (3-(4,5-dimethylthiazol-2-yl)-5-(3-carboxymethoxyphenyl)-2-(4-sulfophenyl)-2H-tetrazolium.

Human dermal fibroblasts listed in (Table 4.2) were also obtained as frozen cells from the Dermatology Department, Newcastle University.

	Cell Code	Provider	Passage	Age (Year)	Collection Date	Experimental Use
1	S920FF	DER	1	54	10.11.14	SA+MTS
2	S916FF	DER	3	22	03.11.14	SA+3D Model
3	S945FF	DER	5	33	22.01.15	SA+MTS
4	S990FF	DER	5	67	26.5.15	SA+MTS
5	S1053FF	DER	2	34	29.10.15	SA+3D Model
6	S1054FF	DER	2	27	28.10.15	SA+3D Model
7	S1055FF	DER	2	47	28.10.15	SA+3D Model
8	S1056FF	DER	2	43	29.10.15	SA+3D Model

Table 4.2 Human dermal fibroblasts obtained as frozen cells.

Information about skin dermal fibroblasts which were collected as frozen cells including sample code, provider, passage, age and gender of donors, collection date and experimental use. DER= Dermatology Department, S#FF=Sample # Foreskin Fibroblast, SA= Scratch Assay, MTS= (3-(4,5-dimethylthiazol-2-yl)-5-(3-carboxymethoxyphenyl)-2-(4-sulfophenyl)-2H-tetrazolium.

While other samples, which listed in (Table 4.3) below were received as either plastic surgery skin sample or skin biopsies provided by Tissue Solutions Ltd. Glasgow / UK, Dermatology Department or Alcyomics Ltd. These samples were processed in Academic Haematology for the isolation of human skin cells; primary keratinocytes and primary dermal fibroblasts.

	Sample Code	Provider	Age (Year)	Region	Surgery Date	Experimental Use
1	PSS1	Alcyomics	56	Abdominal	07.04.15	Wound healing/miRNA Profiling
2	PSS2	Alcyomics	26	Abdominal	09.04.15	Wound healing/miRNA Profiling
3	AL-10	Alcyomics	58	Abdominal	25.02.16	SA Block SDF-1α + 3D Model
4	AL-11	Alcyomics	33	Breast	25.02.16	SA Block SDF-1α + 3D Model
5	DO62	Tissue Solutions	40	Abdominal	23.06.16	SA Block SDF-1α + 3D Model
6	DO63	Tissue Solutions	33	Abdominal	23.06.16	SA Block SDF-1α + 3D Model
7	D064	Tissue Solutions	46	Abdominal	23.06.16	SA Block SDF-1α + 3D Model
8	ALCO-733	Alcyomics	30	Abdominal	02.08.16	SA Block SDF-1α + 3D Model
9	ALCO-734	Alcyomics	31	Abdominal	02.08.16	SA Block SDF-1α + 3D Model
10	S1135F	DER	83	Abdominal	23.08.16	SA Block SDF-1α + 3D Model
11	S1136F	DER	45	Abdominal	23.08.16	SA Block SDF-1α + 3D Model
12	S1156F	DER	51	Abdominal	07.12.16	3D-SEM / miRNA Profiling
13	S1157F	DER	51	Abdominal	07.12.16	3D-SEM / miRNA Profiling
14	S1158F	DER	17	Abdominal	07.12.16	3D-SEM / miRNA Profiling

Table 4.3 Skin samples and biopsies used to isolate human primary skin cells.

Information about skin samples which were collected as skin biopsies or plastic surgery skin (PSS) including sample code, provider, passage, age and gender of donors, collection date and experimental use. DER= Dermatology Department, S#F= S#Foreskin, SA= Scratch Assay.

4.3.2 EFFECT OF MSC-CM ON MIGRATION OF SKIN CELLS

The 2D scratch assay was used to detect the effect of MSC-CM on migration of primary skin cells (primary keratinocytes and primary fibroblasts), whereas the HaCat cell line was used to optimise the assay. Since, the calcium level is a critical factor for differentiation of primary keratinocytes, two types of MSC-CM; high calcium conditioned media (HC-CM) and low calcium conditioned media (LC-CM) were tested on the migration of primary keratinocytes. Additionally, LC-CM was also tested on migration of primary keratinocytes at, hypoxia and after blocking SDF-1α. Primary fibroblasts were treated with HC-CM only.

4.3.2.1 OPTIMISATION OF 2D SCRATCH ASSAY USING HACAT CELL LINE

HaCat cells were seeded at a density of 1×10^5 cells per well in 24 well plates and incubated at standard culture conditions (SCC in humidified incubator, 37°C and 5 % CO_2) for 24 hours to allow cell adhesion. A scratch was then made in the monolayer using a sterile yellow tip. The dislodged cells were discarded and the wells were washed with PBS, followed by adding MSC-CM (HC-CM24, HC-CM48 and HC-CM72) to the corresponding wells. Celle treated with DMEM supplemented with 10% foetal calf serum (DMEM-FCS) were used as a control (HC-CTRL). Results showed that MSC-CM (HC-CM) collected at different time points enhanced the migration of HaCat cells leading to close of the scratch area with increased effect during time. After 28 hours of treatment the gap was closed when compared to both controls (Figure 4.2).

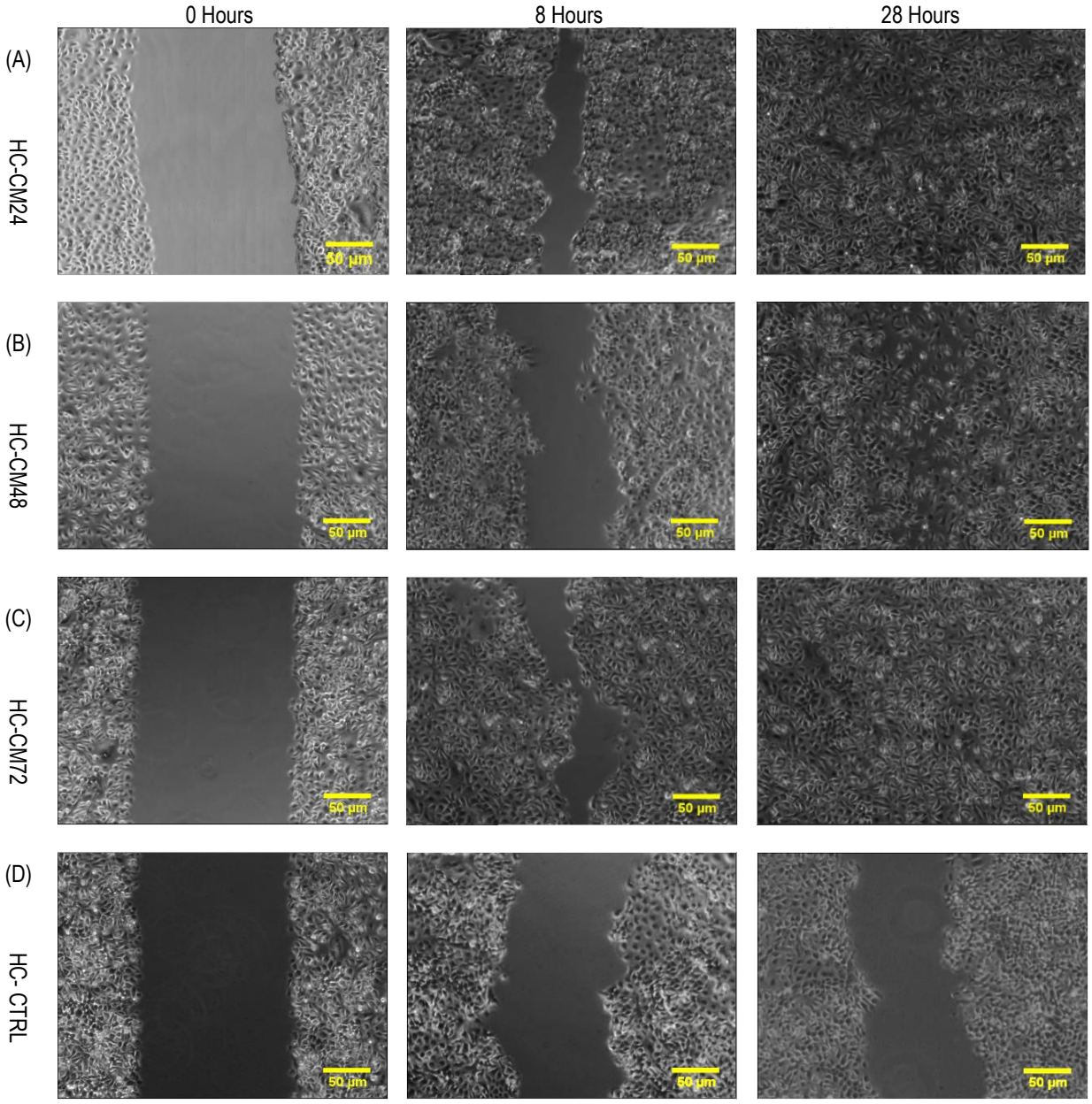

Figure 4.2 Scratch assay of HaCat cell line.

Representative images of migration of HaCat cells during scratch closure assay. A monolayer of HaCat cells were scratched and treated with MSC-CM for 28 hours. (A) HC-CM24. (B) HC-CM48. (C) HC-CM72. (D) HC-CTRL (DMEM-FCS) as a control. HaCat cells treated with all types of HC-CM (A, B and C) migrated from the wound edged towards the scratch centre with time and closed the scratch area completely at 28 hours. HaCat cells in the control (D) failed to close the scratch area at 28 hours. HaCat cells used at passage 6, Scale bar=50 µm.

Two way ANOVA showed that all MSC-CM (HC-CM24, HC-CM48 and HCCM72) accelerated the migration of HaCat cells and enhanced cell migration after 8 hours of treatment compared to HC-CTRL ($P<0.01$, $P<0.001$). The effect of the three MSC-CM

increased with time to completely close the scratch area after 28 hours of treatment whereas the cells treated with control failed to close the whole scratch area leaving a gap after the same treatment period (28 hours) (P<0.001. P<0.01 and P<0.001) respectively (Figure 4.3).

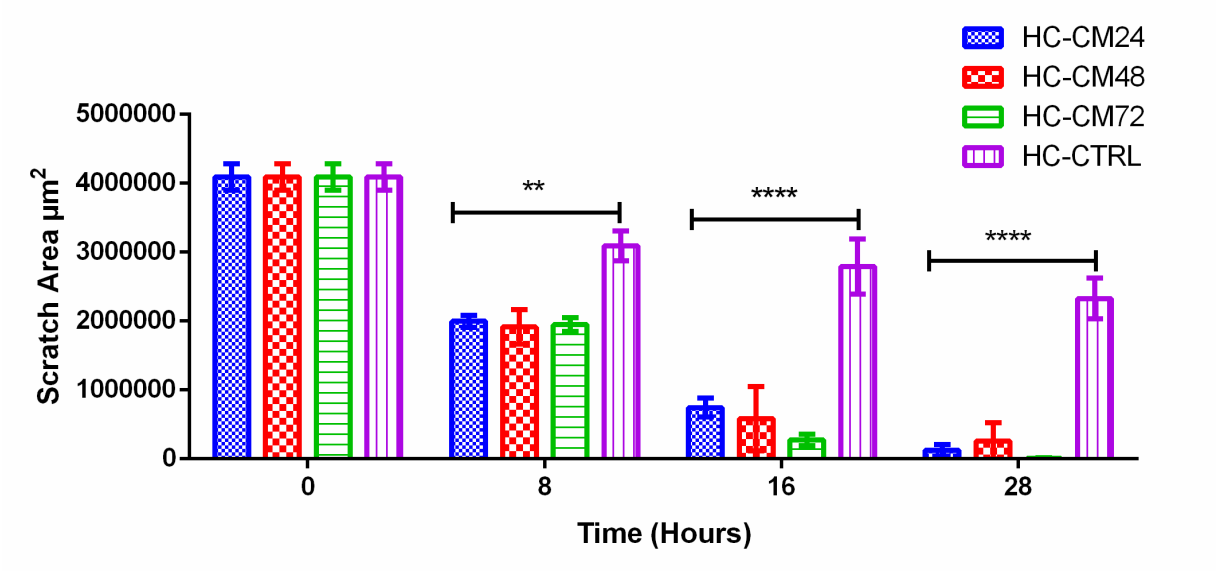

Figure 4.3 Kinetics of scratch closure of HaCat cells.

*Statistical analysis revealed that the three MSC-CM (HC-CM24: Blue columns, HC-CM48: Red columns and HC-CM72: Green columns) significantly reduced the scratch areas with times compared to the control (HC-CTRL) (Purple columns). Significant variations between HC-CM and HC-CTRL started at 8 hours (P<0.01) and increased at other time points (at 16 and 28 hours P<0.0001). Columns = mean of scratch areas (N=3 technical replicates), Error bars= standard error of the mean (SEM). (**=P<0.01), (****=P<0.0001).*

4.3.2.2 *Effect of High Calcium-CM (HC-CM) on Migration of Primary Keratinocytes*

When the effect of HC-CM was tested on the migration of primary keratinocyte, HC-CM failed to promote the migration of primary keratinocyte towards the wound centre (Figure 4.4). After 8 hours of treatment with HC-CM, cells became more flattened, enlarged and contacted via cell-to-cell narrow junctions. In addition, after 72 hours cells formed a tissue like structure compared to the control, which still showed cells as a confluent monolayer in low calcium conditions. These signs are indicators for keratinocyte differentiation. HC-CM was collected in DMEM based formula containing high calcium levels (ranging from 1.2 to 1.8 mM/L) which was sufficient to enhance differentiation of primary keratinocytes.

To overcome this obstacle, MSC secretions were collected in low calcium conditions (LC-CM) then scratch assay repeated.

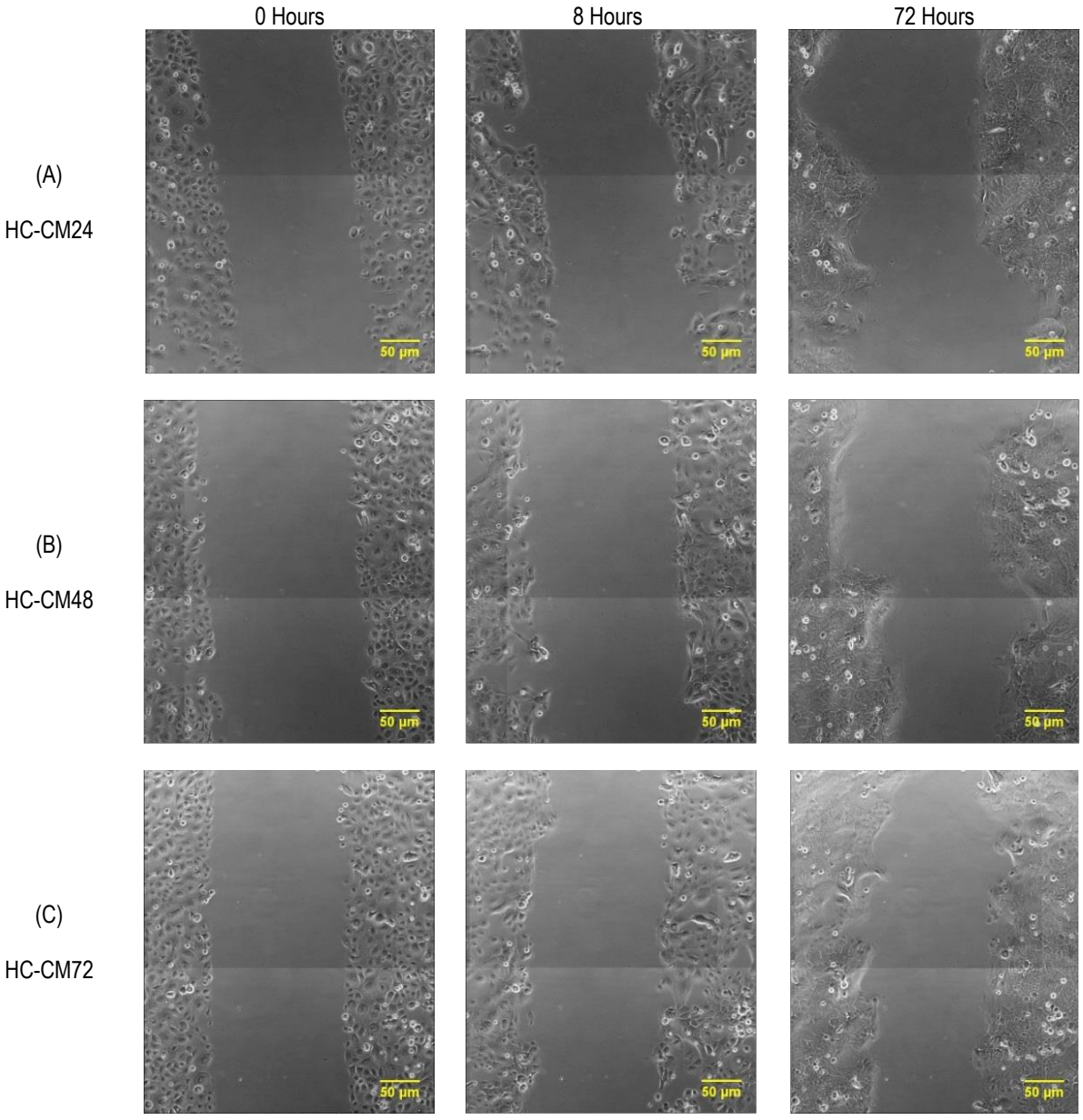

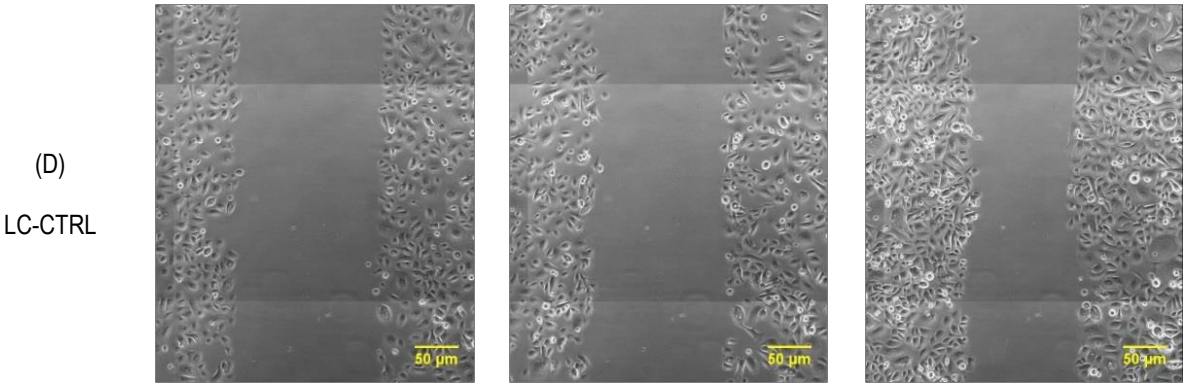

Figure 4.4 The effect of HC-CM on migration of primary keratinocytes.

Representative images of the scratch assay of primary keratinocytes treated with HC-CM for 72 hours. (A) HC-CM24. (B) HC-CM48. (C) HC-CM72. (D) Keratinocytes treated with LC-CTRL (MCDB). Migration of keratinocytes treated with HC-CM was arrested and the cells failed to close the scratch gap after 72 hours. Cells used at passage 3, Scale bar=50 µm.

Two way ANOVA showed that there was no obvious migration of the cells treated with the different types of MSC-CM without any progress in wound closure (P=0.77, P=0.85 and P= 0.86) respectively compared to the control cells grown in low calcium conditions across the whole treatment period (Figure 4.5). These results demonstrated that it is necessary to optimise the culture media formula when testing the effect of MSC-CM on migration of different cell types.

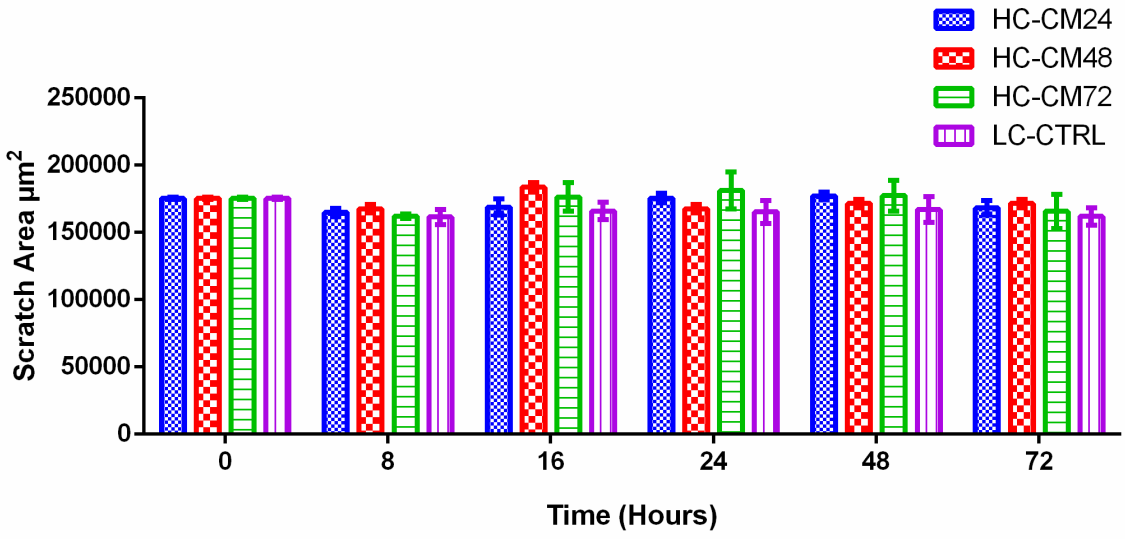

Figure 4.5 Kinetics of scratch closure of primary keratinocytes treated with HC-CM.

Statistical analysis revealed that HC-CM24 (Blue columns), HC-CM48 (Red columns) and HC-CM72 (Green columns) failed to reduce the scratch area with time compared to the control (Purple columns). Data presented as mean of scratch areas (N=4), Error bars= standard error of the mean (SEM).

4.3.2.3 *Effect of Low Calcium-CM (LC-CM) on Migration of Primary Keratinocytes*

The effect of MSC-CM collected at low calcium levels (LC-CM) on the migration of primary keratinocyte was tested. LC-CM collected at different time points enhanced the migration of primary keratinocytes and accelerated wound closure compared to the control (LC=CTRL) and closed the scratch area completely at 72 hours using LC-CM24 and partially at 72 hours using LC-CM48 and LC-CM72 (Figure 4.6).

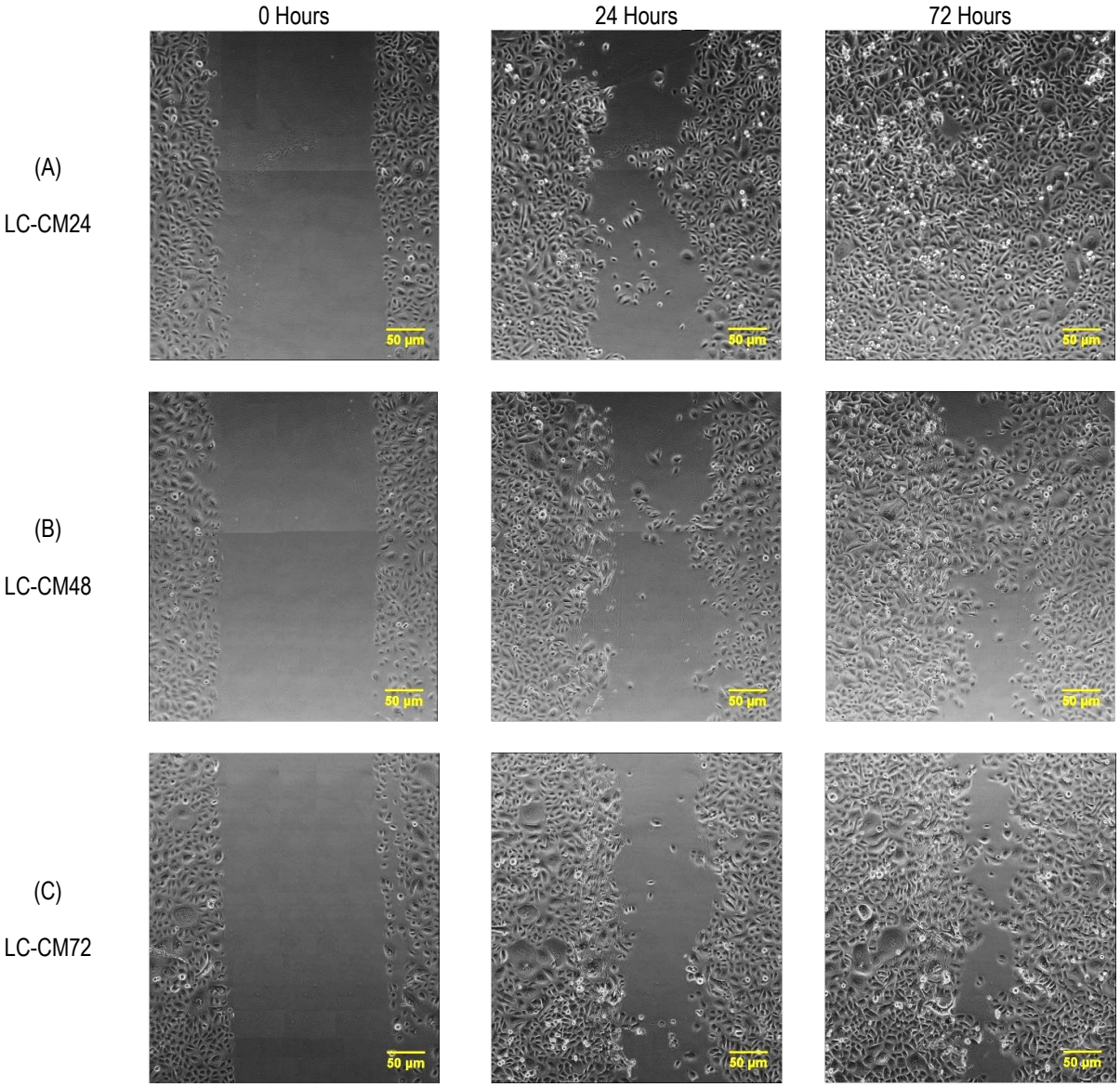

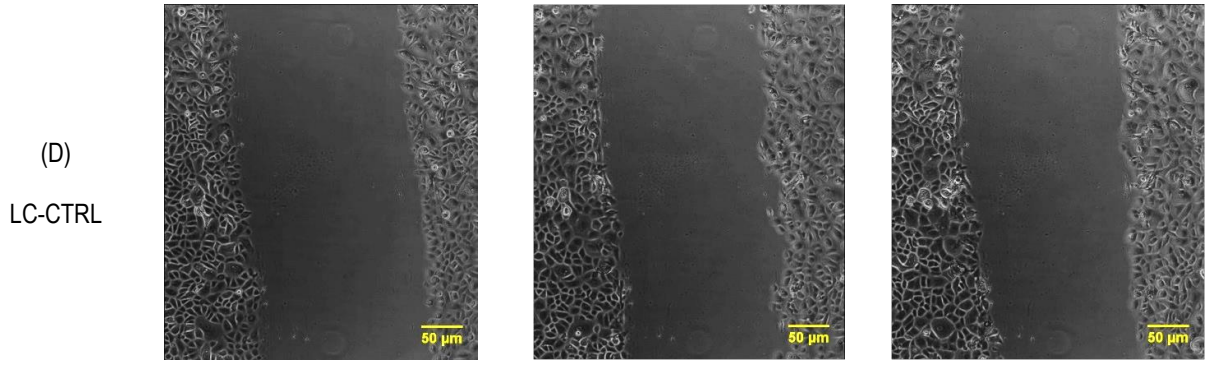

Figure 4.6 Effect of LC-CM on migration of primary keratinocytes using scratch assay.

Representative images of migration of primary keratinocytes during the scratch closure assay. Monolayers of primary keratinocytes (N=4) were scratched and treated with MSC-CM (LC-CM) for 72 hours. (A) LC-CM24. (B) LC-CM48. (C) LC-CM72. (D) LC-CTRL (MCDB) and used as a control. Primary keratinocytes treated with all types of HC-CM (A, B and C) started migration at 24 hours from the wound edge towards the scratch centre. LC-CM24 revealed the best effect and closed the gap within 72 hours compared to the control (D). Cells used at passage 3, Scale bar=50 µm.

Significant enhancement in scratch closure was observed for all LC-CM at 16 hours of treatment (P<0.01) compared to the control with increasing effects over time (P<0.0001) at 72 hours (Figure 4.7).

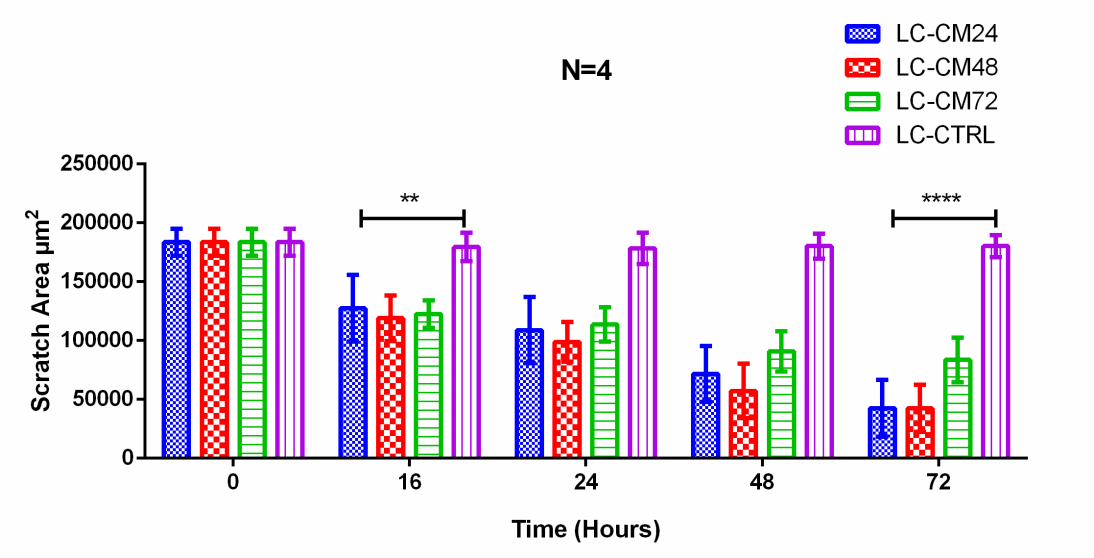

Figure 4.7 Kinetics of migration of primary keratinocytes treated with LC-CM.

*Statistical analysis revealed that LC-CM24 (Blue columns), LC-CM48 (Red columns) and LC-CM72 (Green columns) significantly reduced the scratch areas with time compared to the control (LC-CTRL) (Purple columns). Significant variations between LC-CM and LC-CTRL started at 16 hours (P<0.01). The reduction in scratch area was reduced within time with maximum reduction at 72 hours (P<0.0001). Data presented as mean of scratch areas (N=4), Error bars= standard error of the mean (SEM). (**=P<0.01), (****=P<0.0001).*

LC-CM and HC-CM were compared at different time points in pairs (LC-CM24 vs HC-CM24, LC-CM48 vs HC-CM48 and LC-CM72 vs HC-CM72). Results revealed that LC-CM were the most effective in enhancing cell migration than their counterparts (HC-CM24, HC-CM48 and HC-CM72). The effect of LC-CM24 could be observed after 16 hours of treatment with significant effects ($P<0.05$) which increased over time until full closure of the scratched areas after 72 hours ($P<0.0001$) (Figure 4.8 A, B and C).

(A)

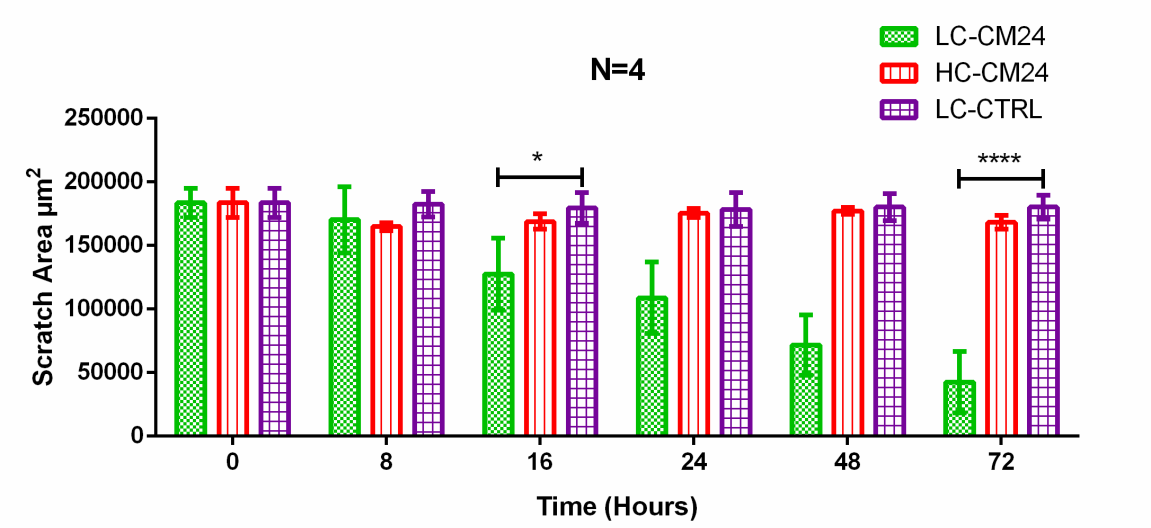

(B)

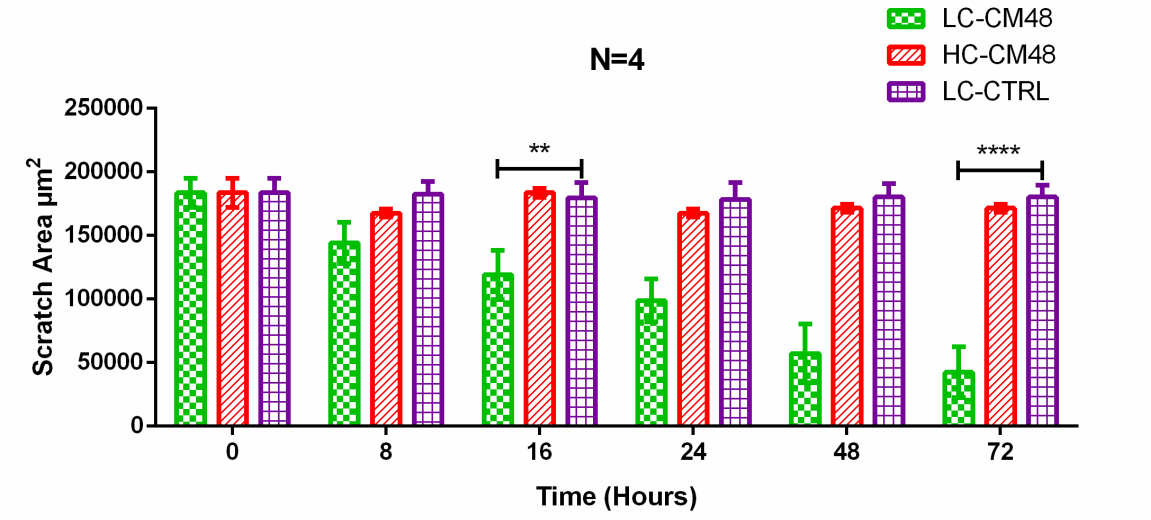

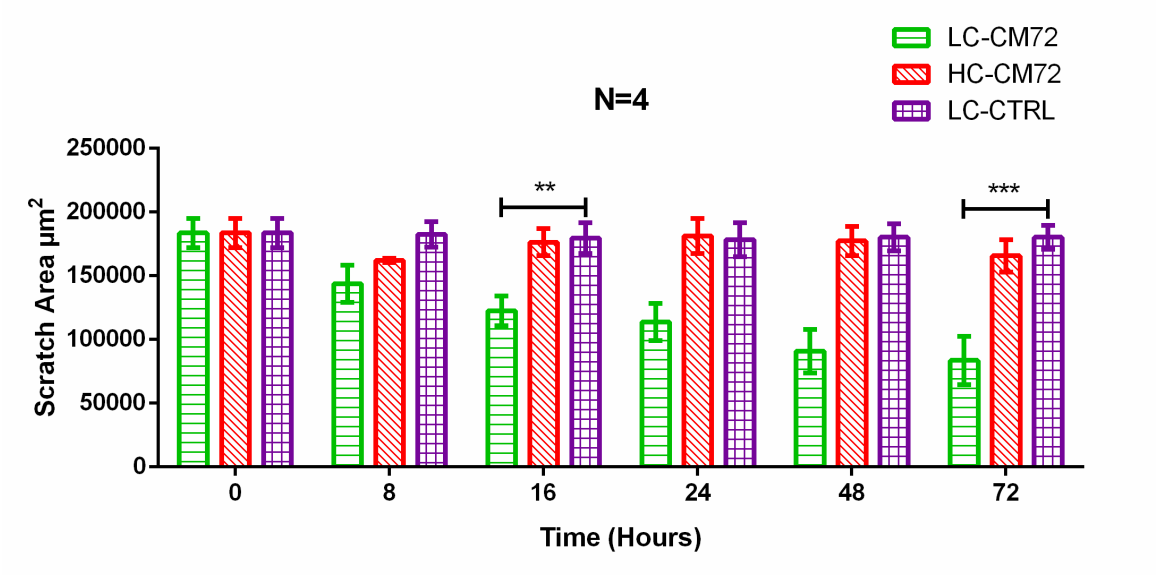

Figure 4.8 Comparison between the effect of LC-CM and HC-CM on migration of primary keratinocytes.

(A) Statistical comparison between (LC-CM24 and HC-CM24) showed that LC-CM24 had a stronger effect on wound closure than HC-CM24. (B) Statistical comparison between (LC-CM48 and HC-CM48) showed that LC-CM48 had a stronger effect on wound closure than HC-CM48. (C) Statistical comparison between (LC-CM72 and HC-CM72) showed that LC-CM72 had a stronger effect on wound closure than HC-CM72. Data presented as mean of scratch areas (N=4), Error bars= standard error of the mean (SEM). (=P<0.05), (**=P<0.01), (****=P<0.0001).*

4.3.2.4 *Effect of LC-CM on Migration of Primary Keratinocytes in Hypoxic Conditions*

Since the environment of chronic wounds is usually hypoxic (Bosco *et al.*, 2008; Sen, 2009), the effect of MSC-CM on the migration of primary keratinocytes was performed under hypoxic conditions to examine whether MSC secretions were able to enhance migration of epidermal cells at low levels of oxygen. All LC-CM enhanced primary keratinocyte migration at 24 hours and proceeded to promote migration until 72 hours, although, complete closure was only observed in LC-CM24 treated cells (Figure 4.9).

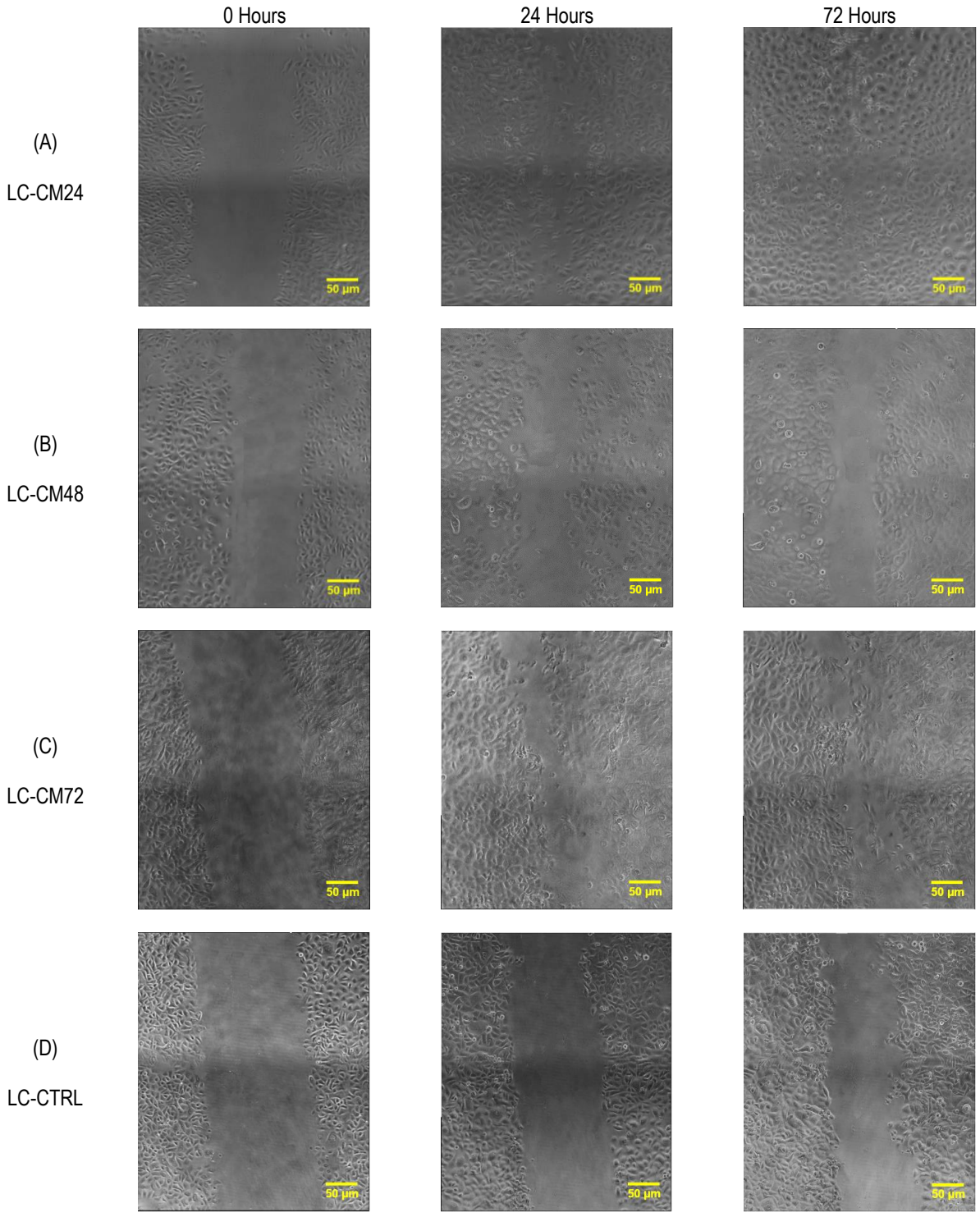

Figure 4.9 Migration of primary keratinocytes treated with LC-CM in hypoxic conditions.

Representative images of scratched monolayers of primary keratinocytes treated with LC-CM for 72 hours in hypoxic conditions (37°C, 5%CO_2, ≈1% O_2). (A) LC-CM24. (B) LC-CM48. (C) LC-CM72. (D) LC-CTRL (control). All LC-CM enhanced cell migration compared to the control and only LC-CM24 caused full closure at the end of the assay. Cells used at passage (3). Scale bar= 50µm.

LC-CM24 showed a significant effect on cell migration at 24 hours (P<0.05) which increased with time (P<0.001) till 72 hours compared to the control. Both LC-CM48 and LC-CM72 had no significant effect on cell migration during the entire treatment time (P>0.05) compared to the control. At the end of the assay (72 hours) LC-CM24 showed a significant effect compared to LC-CM48 and LC-CM72 (P<0.01) (Figure 4.10).

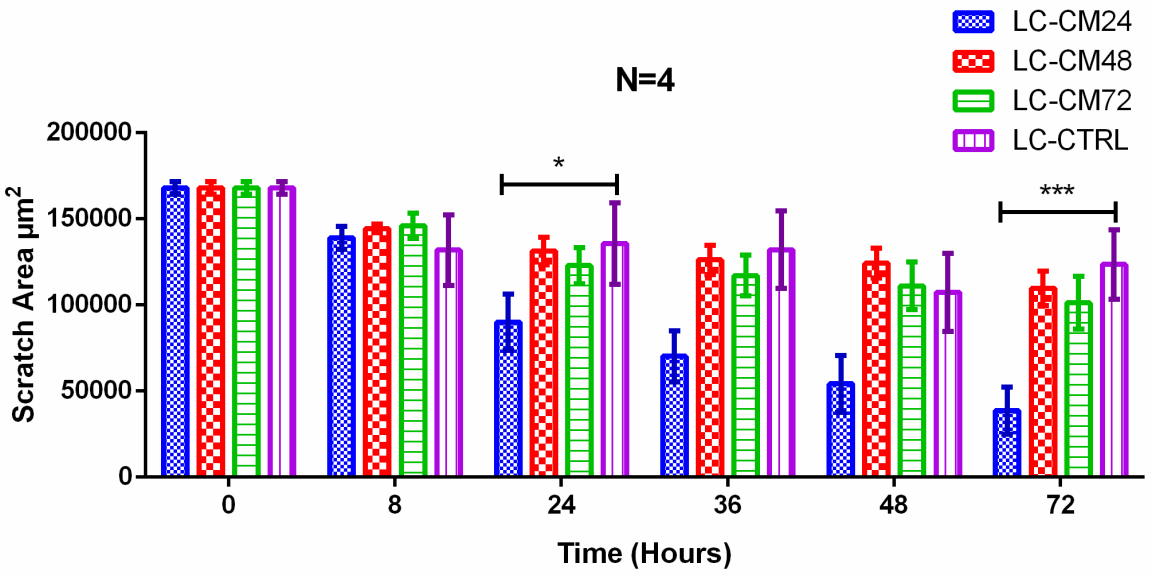

Figure 4.10 Kinetics of the effect of LC-CM on migration of primary keratinocytes in hypoxic conditions.

Effect of MSC-CM (LC-CM24: Blue columns, LC-CM48: Red columns and LC-CM72: Green columns) Only LC-CM24 reduced scratch area with time and the effect started at 24 hours (P<0.01) which increased with time (P<0.001) compared to the LC-CTRL (Purple columns). Scratch areas treated with both LC-CM48 and LC-CM72 showed no progress in wound closure by the end of the assay (P>0.05) compared to the LC-CTRL. Cells used at passage 3, Data presented as the mean of scratch areas (N=4), Error bars= standard error of the mean (SEM). (=P<0.05), (**=P<0.01), (****=P<0.0001).*

4.3.2.5 *Effect of MSC-CM on Migration of Primary Keratinocytes During Blocking SDF-1α Receptor (CXCR4)*

SDF-1α is a well-known chemokine that enhances cell mobility during many physiological processes (Cherla and Ganju, 2001; Arenzana-Seisdedos, 2015). The effect of MSC-CM on migration of primary keratinocytes was examined during SDF-1α blocking. A concentration of 0.02 µg/ml of SDF-1α antibody (MAB310-500) was added to the cell monolayer 30 minutes prior to the initiation of the scratch assay to block SDF-1α receptor (CXCR4). Cells were then scratched and treated with the following substances; LC-CM24,

LC-CM72, SDF-1α recombinant human protein (rSDF-1α) and a mixture of rSDF-1α with MSC-CM (rSDF-1α-CM) (1:1 v/v) and LC-CTRL (MCDB media). Concurrently, the same experiment was set up without blocking SDF-1α i.e. without addition of antibody (MAB310-500 to the cell monolayer to compare results of blocking (BC) and non-blocking conditions (NBC).

Under NBC, results revealed that LC-CM24 closed the scratched area after 16 hours (Figure 4.11 A). LC-CM72 accelerated the migration of primary keratinocytes closing the scratch area completely by 48 hours (Figure 4.11 B) while rSDF-1α-CM closed the gap at 72 hours compared to the control (Figure 4.11 C). Cells treated with rSDF-1α alone migrated at 24 hours with increasing migration with time compared to the control, however, cells failed to close the scratch area completely at 72 hours (Figure 4.11 D).

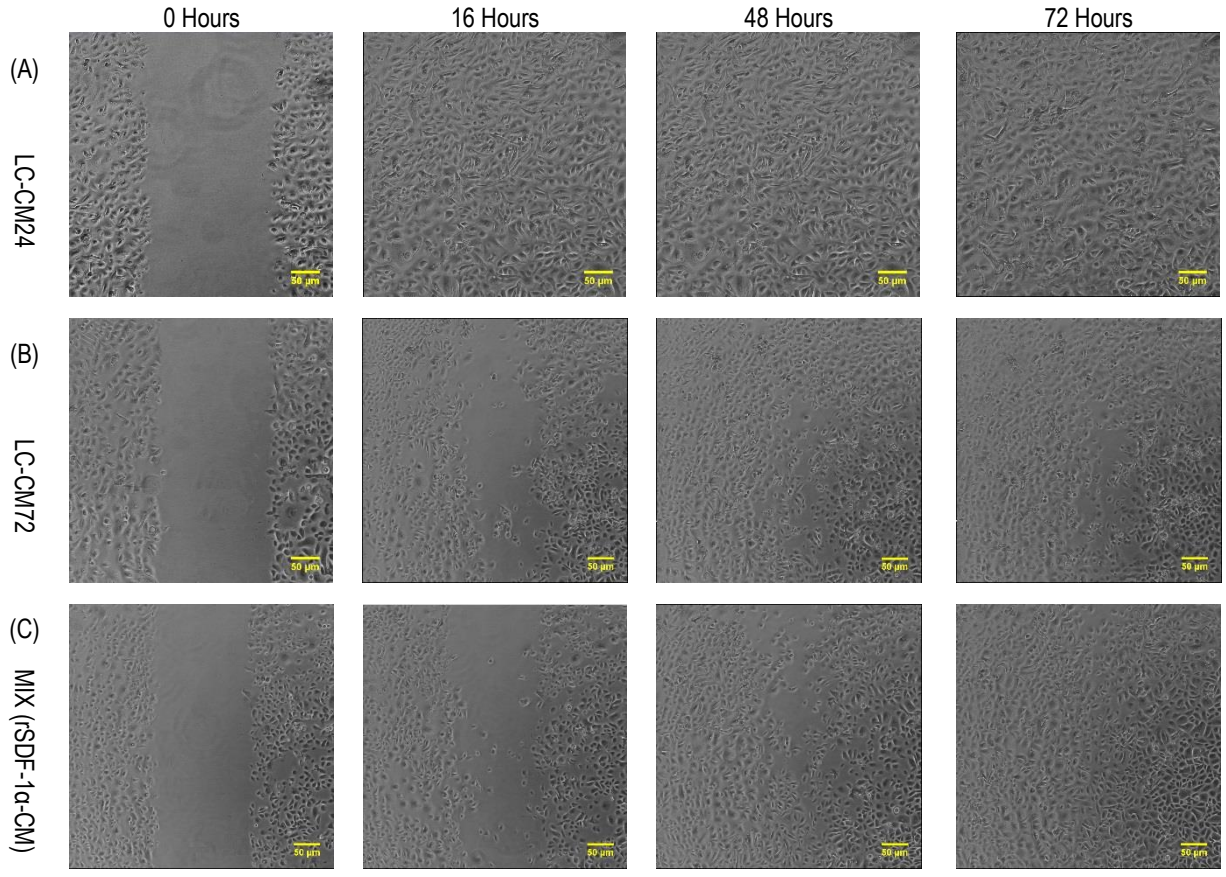

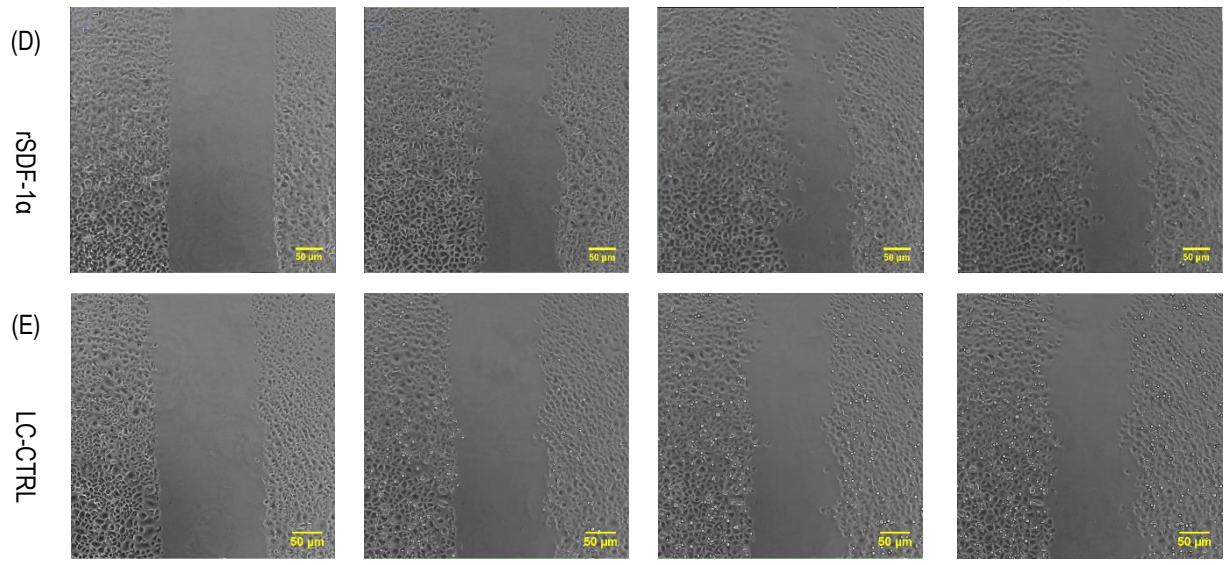

Figure 4.11 Migration of primary keratinocytes treated with LC-CM during SDF-1α non-blocking conditions.

Representative images of primary keratinocytes treated with different substances during wound healing assay to set SDF-1α blocking experiment. (A) LC-CM24 closed the scratch area completely at 16 hours. (B) LC-CM72 closed the scratch area completely at 48 hours. (C) rSDF-1α-CM closed the scratch area completely at 48 hours. (D) rSDF-1α started migration at 26 hours; however, failed to close the scratch area completely at 72 hours. (E) LC-CTRL showed no observed migration. Cells used at passage 3. Error bar=50 µm.

Two way ANOVA demonstrated that all tested substances showed significant effect on wound closure at 72 hours ($P<0.0001$). However, LC-CM24 was the most effective since it caused an effect at 16 hours ($P<0.0001$), followed by rSDF-1α ($P<0.01$), rSDF-1α-CM ($p<0.05$) and then LC-CM72 ($P<0.001$) at 20 hours compared to the control (Figure 4.12).

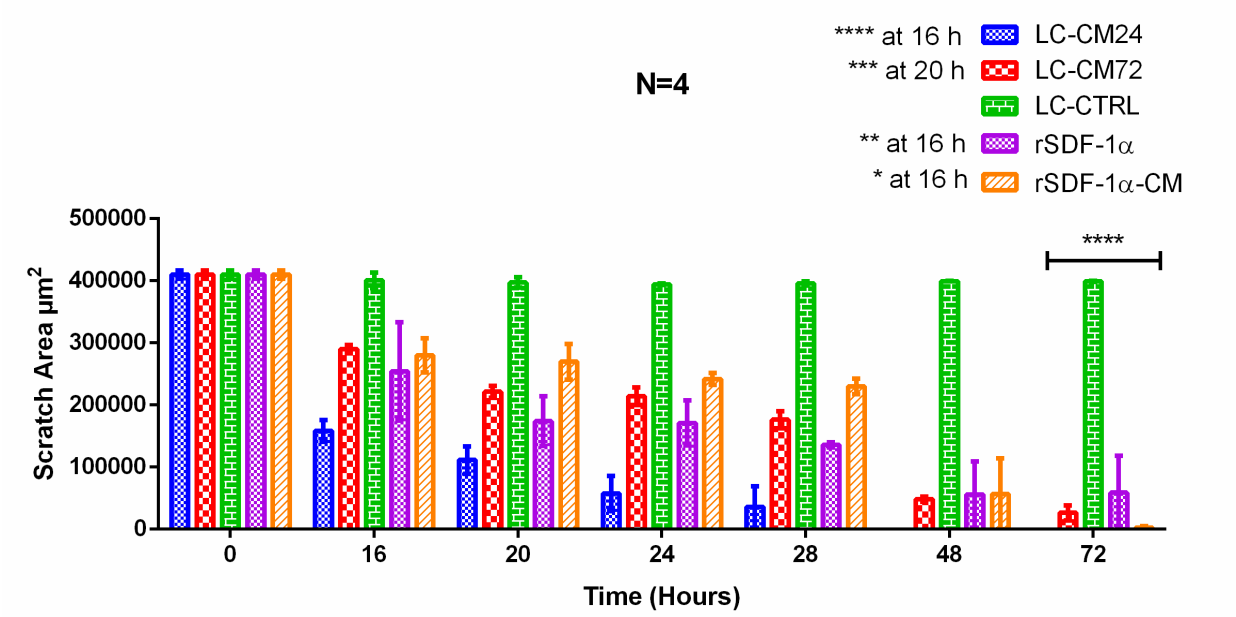

Figure 4.12 Kinetics of the effect of LC-CM on migration of primary keratinocytes during non-blocking of SDF-1α.

Scratched keratinocytes treated with different substances; LC-CM24: blue columns started the effect at 16 hours (P<0.0001). LC-CM72: red columns started the effect at 20 hours (P<0.001). rSDF-1α: purple columns started the effect at 16 hours (P<0.01) A mixture of rSDF-1α-CM: orange columns started the effect at 16 hours (P<0.05) compared to the LC-CTRL: green columns. Cells used at passage 3, Data presented as mean of scratch areas (N=4), Error bars= standard error of the mean (SEM), (=P<0.05), (**=P<0.01), (***=P<0.0001), (****=P<0.0001).*

Under blocking conditions (BC), LC-CM and rSDF-1α-CM accelerated migration of primary keratinocyte and closed the scratch gap at 48 hours compared to controls. While rSDF-1α failed to enhance cell migration with time and cell mobility was arrested leaving a scratch gap during the whole treatment time compared to the control (Figure 4.13).

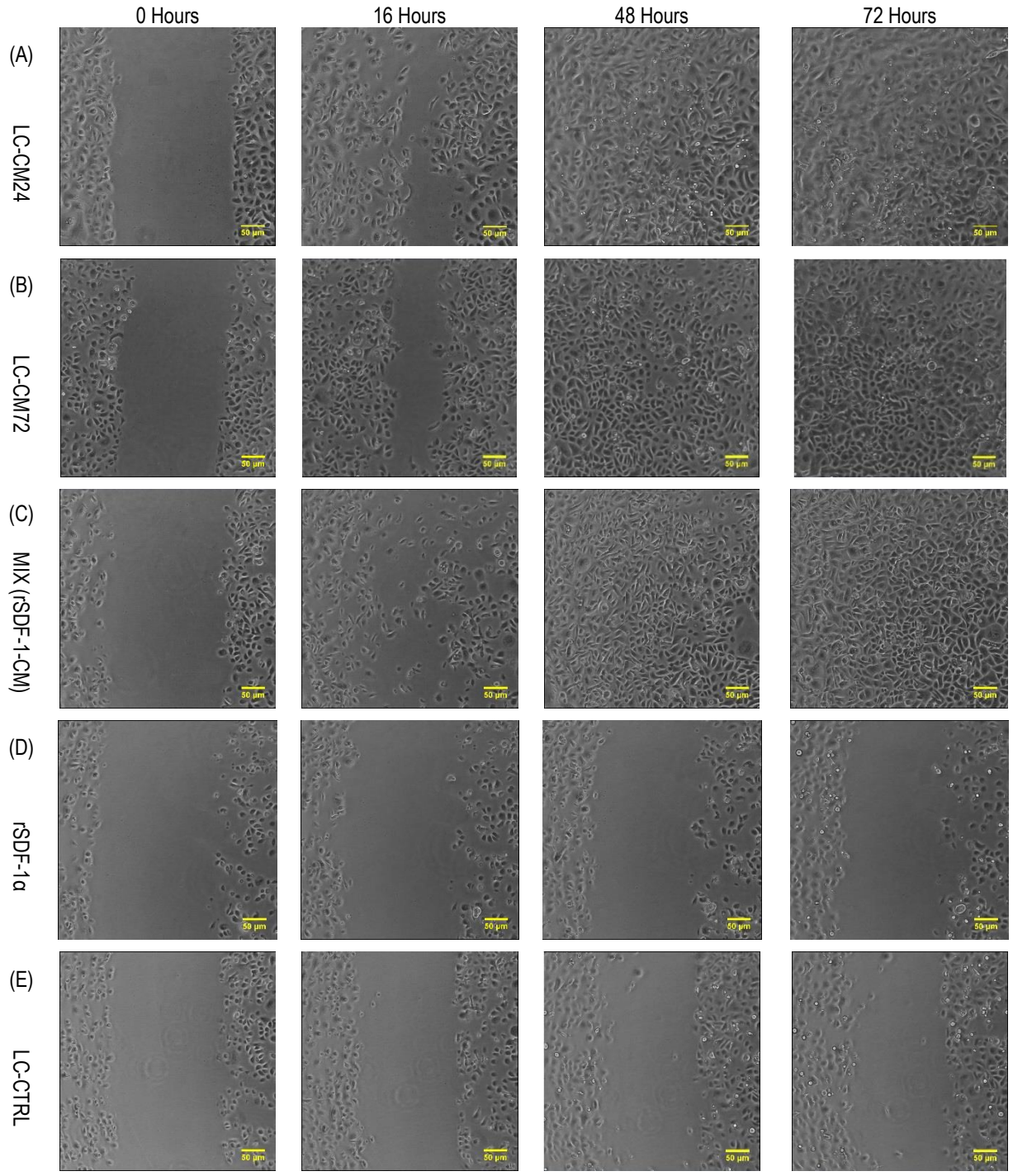

Figure 4.13 Migration of primary keratinocytes treated with LC-CM during SDF-1α blocking.

Representative images of primary keratinocytes treated with SDF-1α antibody to block CXCR4 then scratched and treated with different substances. (A) LC-CM24 closed the scratch area completely at 48 hours. (B) LC-CM72 closed the scratch area completely at 48 hours. (C) rSDF-1α-CM closed the scratch area completely at 48 hours. (D) rSDF-1α failed to close the scratch area completely at 72 hours. (E) LC-CTRL showed no observed migration. Cells used at passage 3, Scale bar=50 µm.

Two way ANOVA showed that LC-CM24 caused an effect after 16 hours of treatment compared to the control (P<0.5) with increased effect with time until complete closure at 48 hours (P<0.0001). Again LC-CM72 started the effect at 20 hours (P<0.5) with complete closure at 48 hours (P<0.0001) compared to the control. The rSDF-1α-CM combination caused an effect after 24 hours of treatment (P<0.5) with complete closure at 48 hours (P<0.0001) in comparison to the control. Interestingly, rSDF-1α failed to enhance migration of primary keratinocytes during the entire treatment time and cells failed to migrate and close the scratch gap at the end of treatment (P>0.05) as explained in (Figure 4.14).

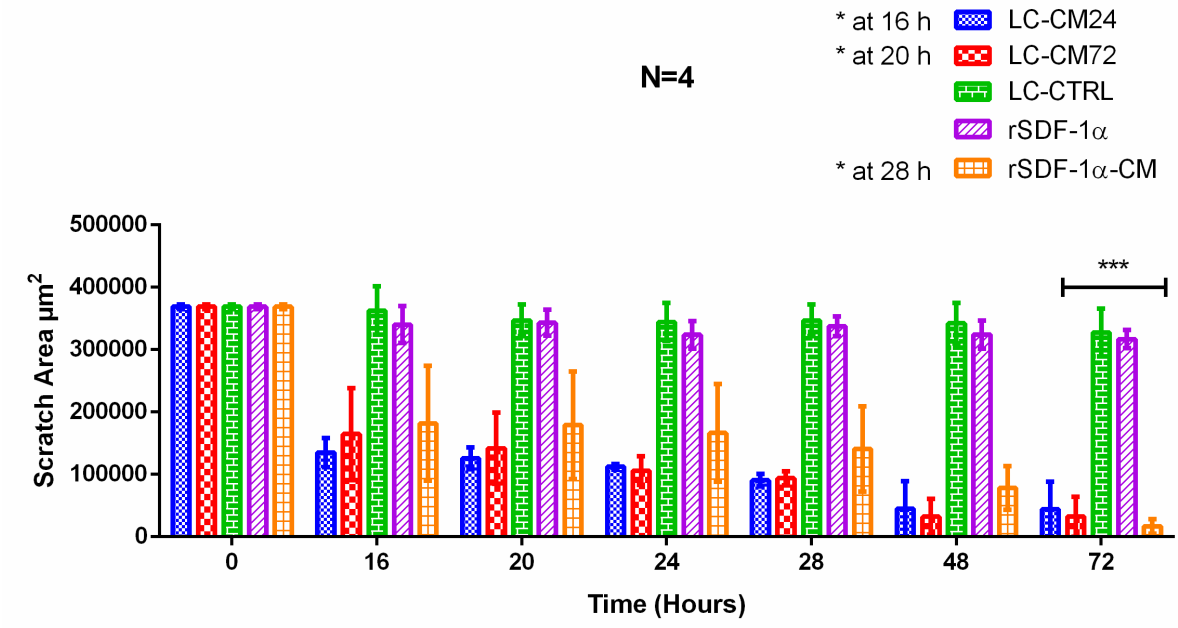

Figure 4.14 Kinetics of the effect of LC-CM on migration of primary keratinocytes during blocking SDF-1α.

Scratched keratinocytes treated with SDF-1α antibody to block CXCR4 then treated with different substances; LC-CM24: blue columns, LC-CM72: red columns, rSDF-1α: purple columns, A mixture of rSDF-1α-CM: orange columns and LC-CTRL: green columns. Cells used at passage 3, Data presented as mean of scratch areas (N=4), Error bars= standard error of the mean (SEM). (=P<0.05), (**=P<0.01), (***=P<0.0001), (****=P<0.0001).*

The effect of each tested substance was compared under blocking and non-blocking conditions (BC and NBC). No significant variations were observed between the effects of LC-CM24, LC-CM72 and rSDF-1α-CM under BC and NBC (P>0.05) at the end of the assay (72 hours) (Figure 4.15 A, B and C) respectively. The effect of rSDF-1α was

significantly stronger under NBC than under BC ($P<0.05$) at 16 hours and ($P<0.0001$) 72 hours (Figure 4.15 D).

(A)

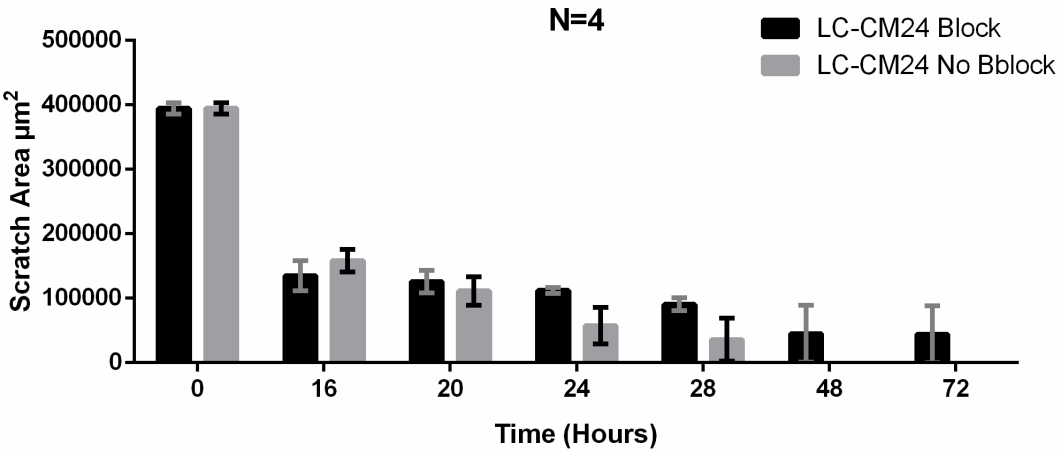

(B)

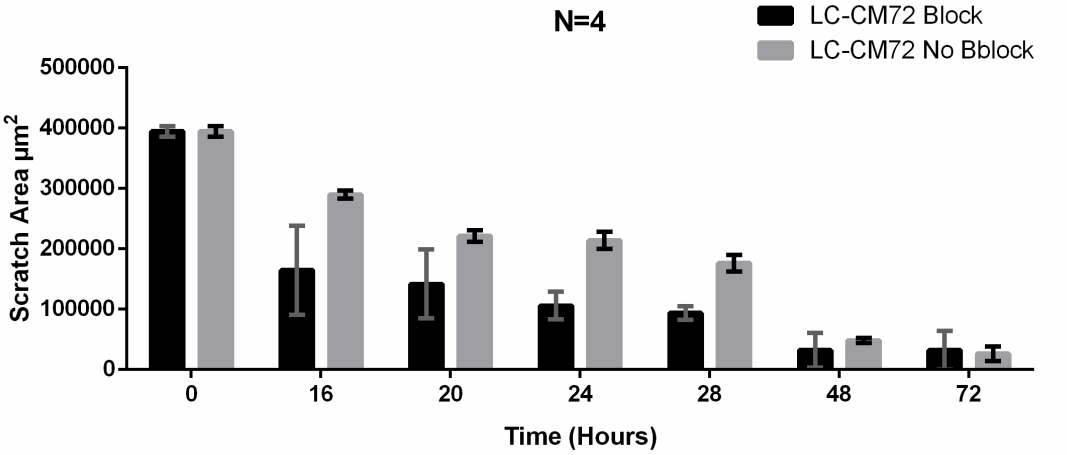

(C)

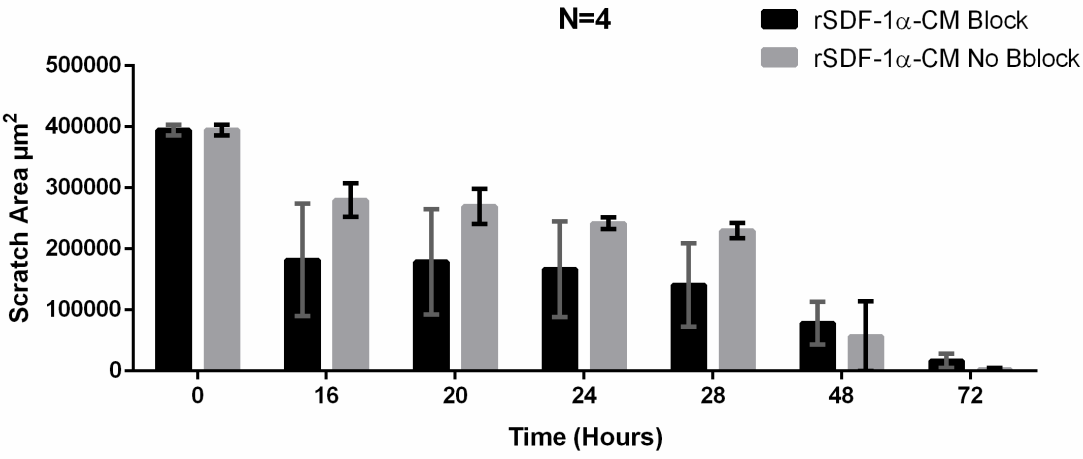

(D)

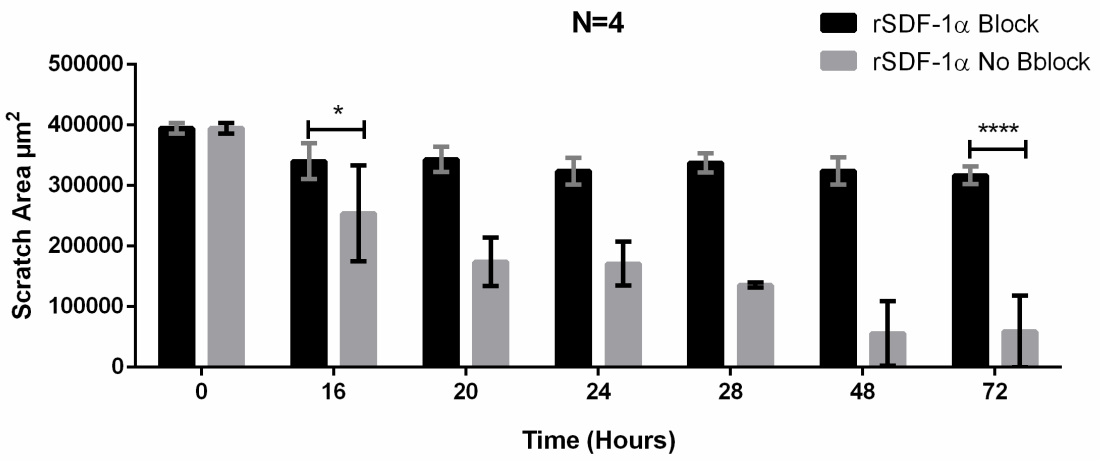

Figure 4.15 Kinetics the effects of different substances on migration of primary keratinocytes during blocking and non-blocking of SDF-1α.

A statistical comparison revealed that LC-CM24 (A), LC-CM72 (B) and rSDF1α-CM (C) equally reduced the scratch area under both BC (Black columns) and NBC (Gray columns) with time (P>0.05). (D) rSDF-1α reduced the scratch area under NBC only (P<0.05) at 16 hours and (P<0.0001) at 72 hours and failed to reduce scratch area under BC. Cells used at passage 3, Data presented as mean of scratch areas (N=4), Error bars= standard error of the mean (SEM). (=P<0.05), (**=P<0.01), (***=P<0.0001), (****=P<0.0001).*

4.3.2.6 *EFFECT OF MSC-CM ON MIGRATION OF PRIMARY FIBROBLASTS*

MSC-CM (HC-CM24, HC-CM48 and HC-CM72) accelerated migration of primary fibroblasts with time. As explained in (Figure 4.16), all HC-CM enhanced migration of the fibroblasts by 16 hours and closed the scratch area completely at the end of the experiment (72 hours) compared to the control cells treated with HC-CTRL (DMEM-FCS media).

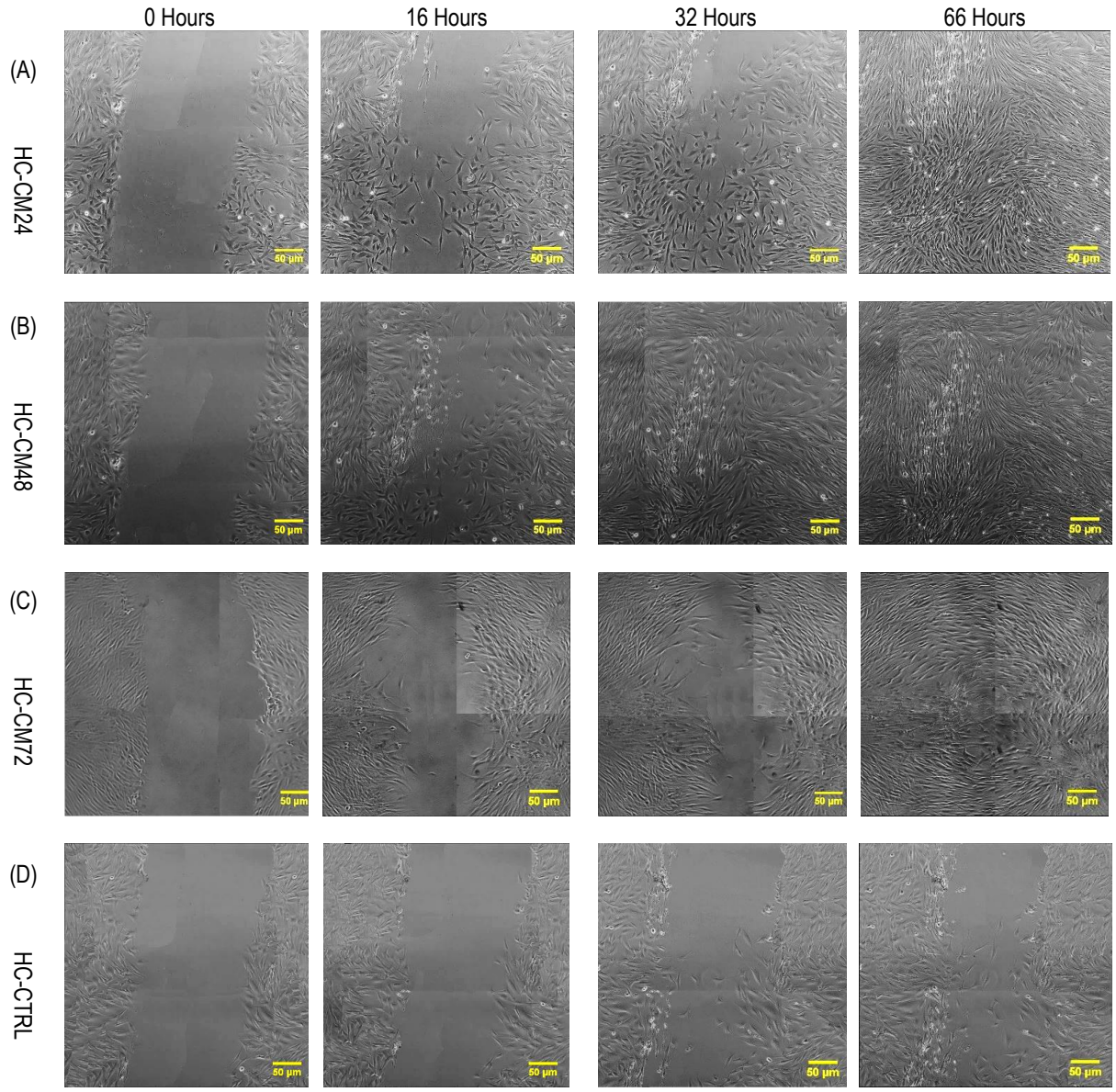

Figure 4.16 Migration of primary dermal fibroblasts after treatment with HC-CM.

Representative images of fibroblast migration during scratch closure after treatment with HC-CM for 66 hours. (A) HC-CM24 caused cell migration at 16 hours and the scratch area completely closed at 66 hours. (B) HC-CM48 caused cell migration at 16 hours and the scratch area completely closed at 32 hours. (C) HC-CM72 caused cell migration at 16 hours and the scratch area completely closed at 72 hours. (D) HC-CTRL caused cell migration at 32 and 66 hours without complete closure. Cells used at passages 4 and 5. Scale bar=50 µm.

Two way NOVA showed that HC-CM24 enhanced migration by 32 hours ($P<0.05$) with increasing effect with time until complete closure of the scratch gap at 48 hours ($P<0.01$). HC-CM48 enhanced migration earlier than other HC-CM and significantly enhanced cell migration at 16 hours ($P<0.01$) with increasing effect until full closure of the gap after 32 hours ($P<0.001$). HC-CM72 enhanced migration at 24 hours ($P<0.05$) with increasing

effect with time until complete closure at 48 hours (P<0.001) compared to the control (Figure 4.17).

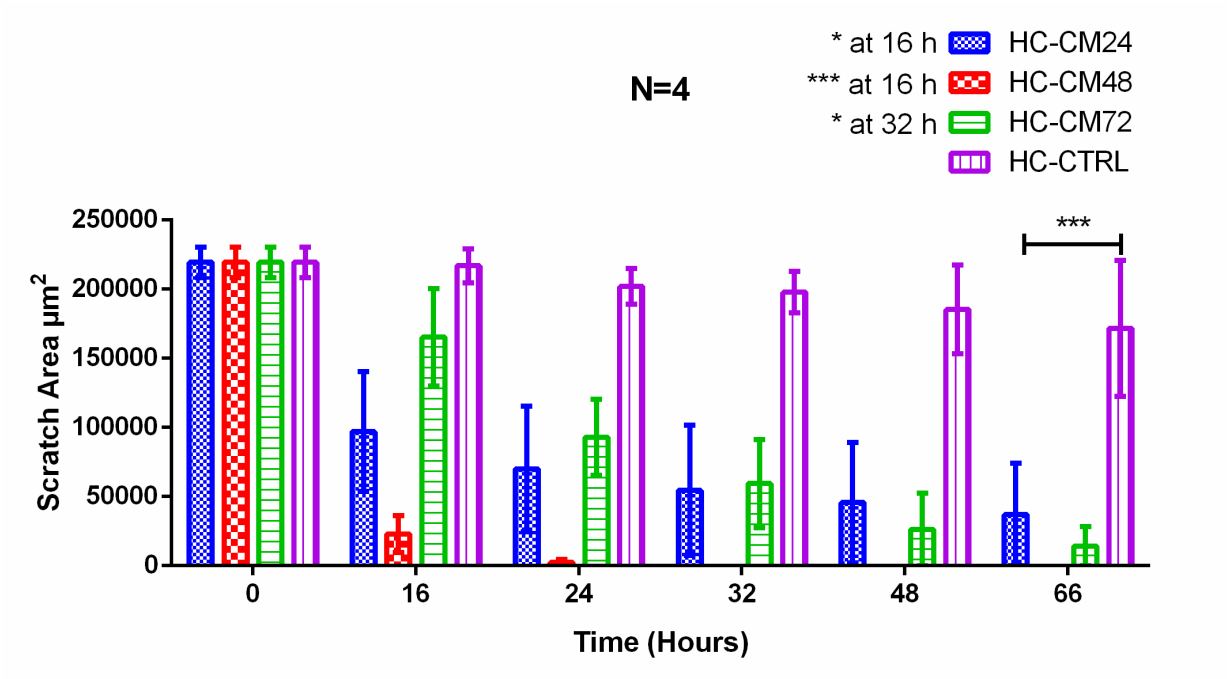

Figure 4.17 Kinetics of the effect of HC-CM on migration of primary fibroblasts.

Scratched fibroblasts treated with HC-CM24: blue column, HC-CM48: red columns HC-CM72: green column and DMEM as a control (HC-CTRL): purple columns. Cells used at passage 4 and 5, Data presented as mean of scratch areas (N=4), Error bars= standard error of the mean (SEM), (=P<0.05), (***=P<0.001).*

4.4 DISCUSSION

Migration, of keratinocytes and fibroblasts are important mechanisms for cutaneous wound healing. It is well known that MSCs and their secretions could be used as therapeutic options in the healing process. Some studies have previously shown that MSC-CM possess positive effect on migration of keratinocyte cell line (HaCat) during wound closure (Walter *et al.*, 2010). The same results were obtained in the current study during the optimisation of the scratch assay. The use of cell lines in research has disadvantages since immortalised cells are highly proliferative with differences in their morphology and genetics compared to primary tissue. In contrast, primary cells maintain original phenotypic markers and functions as well as possess normal morphology (Alge *et al.*, 2006; Pan *et al.*, 2009). Scientists are therefore cautious when interpreting results obtained from experiments carried out on cell lines (Alston-Roberts *et al.*, 2010; Lorsch *et al.*, 2014). The use of primary epidermal keratinocytes are a more realistic approach to study the healing process and are more representative for use in skin wound healing studies than the use of cell lines. The highly proliferative of HaCat cell line could significantly affect the results of assays that depend on the proliferation rate such as the migration assay and proliferation assays. In addition, to date, there is no satisfactory study, which has investigated the effect of MSC-CM on primary keratinocytes. All previous studies have collected MSC secretions in serum free media (DMEM-based formula) to avoid any interference due to serum constituents. The use of MSC secretions collected in serum free DMEM is still unsatisfactory and inapplicable for primary keratinocyte wound healing studies due to the high calcium levels (1.8 mM/L) present in this type of media. It is well established that calcium is a key regulator for keratinocyte differentiation both *in vitro and in vivo*. It is involved in many internal and external signalling pathways that enhance successive differentiation in the epidermal keratinocyte to form the different layers of the epidermis including the permeable barrier of the stratum corneum (Bikle *et al.*, 1996; Bikle *et al.*, 2012). On the other hand, keratinocytes can grow rapidly as monolayers and proliferate without differentiation in low calcium concentrations (0.05 – 0.1 mM/L), whereas calcium concentration higher than 0.1 mM enhances keratinocyte differentiation (Hennings *et al.*, 1980). Therefore, DMEM contains calcium levels which enhance cell differentiation and thereby arrest their migration and proliferation. Arrested

migration of primary keratinocytes treated with HC-CM could be therefore interpreted by the effect of high calcium levels in the media. The high calcium concentrations could interfere with the effect of growth factors present in MSC-CM, due to its high permeability through the cell membrane and its involvement in the vast majority of intrinsic and extrinsic signalling pathways. This explanation due to the high calcium permeability through cell membrane could be supported by the results of (Bikle *et al.*, 2012). They reported that keratinocytes responded to calcium acutely due to the presence of the GTP-binding protein receptor, a group of seven transmembrane proteins which spread on cell membrane of different tissues including keratinocytes (Bikle *et al.*, 1996; Oda *et al.*, 1998; Tu *et al.*, 2001). Therefore, high calcium levels direct the primary cells to enter a differentiation state, where the cells start to change their morphological characteristics and became flattened, engage via cell-to-cell tight channels and form tissue-like structures which in turn immobilise the cells and inhibit their migration.

The ability of MSC to grow successfully in low calcium-serum free media for three days opened the possibility to collect their secretions in low calcium conditions for further applications in wound healing studies using primary keratinocytes. In this research, the scratch assay was used to show that primary keratinocyte treated with LC-CM migrated to promote void closure more rapidly than primary keratinocytes grown in keratinocyte growth medium. In addition, a comparison was made between LC-CM and HC-CM for their effect on cell migration. Under the same conditions in the absence of serum, LC-CM enhanced primary cells to migrate and completely fill the scratch area compared to HC-CM. This novel method using low calcium media (LC-Media) to collect MSC secretions may provide a useful protocol for collecting growth factors and cytokines that affect cutaneous wound healing. Variations in responses of primary keratinocytes to both HC-CM and LC-CM during the healing process using a 2D scratch assay could be due to the high calcium concentrations (1.8 mM/L) contained in HC-CM which is sufficient to enhance differentiation of primary keratinocytes. Segrelles and colleagues stated that differentiation of primary keratinocytes could be induced by elevating the calcium level to (1.2 mM/L) which after 24 hours cause the keratinocytes to become more flattened and make contact with each other thereby arresting their migration. Hence, LC-CM and HC-

CM differed in their effect on cell migration depending on the calcium level (Segrelles *et al.*, 2011)

The response of primary keratinocytes to close wounds under low calcium levels could also include alterations in gene expression involved in cell matrix interaction (Walter *et al.*, 2010). Results obtained in the current study showed that MSC secretions (MSC-CM) collected in serum free and low calcium conditions significantly promoted primary keratinocyte migration to close the scratched area under normal oxygen levels compared to the control. This is therefore a strong evidence in support of the use of MSCs as a therapeutic strategy for cutaneous wound healing.

Oxygen levels play a vital role during the healing process and are essential for oxidation, phosphorylation, signalling pathways and enzymatic reactions (Yan *et al.*, 2017). Oxygen is also a key regulator and pivotal requirement for several physiological events during the repair process such as angiogenesis, re-epithelisation, collagen deposition, fibroplasia and even infection resistance (Castilla *et al.*, 2012). During cell migration under hypoxic conditions, positive effect was observed with LC-CM24 whereas neither LC-CM48 nor LC-MC72 showed a positive effect during the entire treatment time. It has been reported that hypoxic conditions promote keratinocyte migration during wound closure (Benizri *et al.*, 2008). However, hypoxic conditions enhance the production of hypoxia inducible factor (HIF) which arrests cell proliferation at G1-phase of cell cycle (Cho *et al.*, 2008; Straseski *et al.*, 2009). Therefore, the positive effect of hypoxia on cell migration could be simply illustrated by the fact that tissue deprivation of oxygen stop many cellular actions such as proliferation and differentiation (Benizri *et al.*, 2008; Yan *et al.*, 2017). On the other hand, hypoxic conditions suppress keratinocyte proliferation via miR-210 and impair wound closure (Biswas *et al.*, 2010). Failure of LC-CM48 and LC-CM72 to enhance cell migration could be simply interpreted by the fact that hypoxia enhanced cell migration to some extent in the control cells; subsequently, the effect of LC-CM48 and LC-CM72 was non-significant (Darby *et al.*, 2014). In another words, the closure rate of the migrating cells by the effect of LC-CM48 and LC-CM72 equalled to the closure rate of the migrating cells by the effect of hypoxia. While the significant positive effect of LC-CM24 could be attributed to the fact that the biomolecules present in this media contained secretions collected earlier than LCCM48 and LCCM72 when MSCs were still active and before prolonged

stress conditions, such as low calcium and serum free conditions at 48 and 72 hours prevailed. It has been well documented that deprivation of tissue from adequate oxygen will hinder the healing outcomes (Castilla *et al.*, 2012). In addition, only tissue under mild or moderate hypoxia could survive while those experiencing severe or chronic hypoxia are unable to survive (Sen, 2009). Yan and colleagues (Yan *et al.*, 2017) showed that hypoxia enhances motility and migration of keratinocytes but not proliferation and differentiation within 24 hours but did not explain the overall outcome of the healing process after prolonged hypoxic conditions i.e. 72 hours. Modarressi and others reported that mild hypoxia enhances the healing process while the chronic hypoxia delay it. They reported that hypoxia is initiated due to the disruption of vascular perfusion by injury and induces growth factors that promote the healing process such as vascular endothelial growth factor (VEGF) (Modarressi *et al.*, 2010). Therefore, within the first 24 hours of the healing process, hypoxia plays a key role in the healing process. However, in chronic wounds, hypoxia reduces the synthesis of collagen and impairs differentiation and function of the myofibroblasts (Darby *et al.*, 2014). Migrating keratinocytes present in the wound site therefore represent hypoxia-induced migrating cells when the hypoxic condition is still mild or moderate enable the cells to adapt and produce HIF and promote their migration. In another words, in a hypoxic microenvironment cell migration within the first 24 hours or early phases could be mainly attributed to moderate levels of hypoxia when the level of hypoxia still moderate. Later during a prolonged healing process, the hypoxic conditions become more detrimental to the cells and stop all cellular activities including cell motility rather than inducing migration inducer. Hence, the continuous consistent positive effect of LC-CM24 on keratinocyte migration in hypoxic conditions after 24 hours of treatment could be mainly attributed to the active biomolecules of LC-CM24. Additionally, when cells continue migrate after 24 hours, these cells had survived the hypoxic conditions and retained their physiological activity.

When SDF-1α was blocked, LC-CM24, LC-CM72 and rSDF-1α-CM retained their ability to enhance cell migration and resulted in full scratch closure at 72 hours while rSDF-1α treated cells failed to migrate within the time and a gap still remained at the end of the assay at 72 hours. These data suggest that LC-CM enhance cell migration with and without the action of SDF-1α. This could be clarified by the hypothesis that LC-CM contain

a wide spectrum of growth factors and cytokines in addition to SDF-1α. These biomolecules work separately of collectively to enhance cell migration during the healing process (Tamama and Kerpedjieva, 2012).

Fibroblast migration is a key requirement for formation of granulation tissue and further dermal wound healing. Since fibroblasts grow in high calcium levels, HC-CM was used to enhance their migration. Schreier and colleagues reported that participation of fibroblasts in wound repair could be attributed to the action of growth factors such as PDGF and TGF-β that attract fibroblasts and accumulate them at the wound edges within the first 24 hours post wounding. They produce the first set of matrix proteins which fill the gap with granulation tissue (Schreier *et al.*, 1993). Therefore, in the case of a deficiency in growth factors at the injury site, MSC secretions would play an important role in attracting fibroblasts towards the wound.

The effect of different MSC-CMs (LC-CM24, LC-48 and LC-CM72) on cell migration were compared under different conditions such as normoxia, hypoxia and SDF-1α blocking. Notably, LC-CM24, LC-CM48 and LC-CM72 promoted keratinocyte migration with time under normal oxygen levels (≈ 20% O_2) and the effects were all initiated at 16 hours ($P<0.01$) and resulted in almost full closure. Under hypoxic conditions (≈1% O_2), only LC-CM24 showed positive effect starting at 24 hours ($P<0.05$) and resulted in full closure at the termination of the experiment, whereas LC-CM48 and LC-CM72 failed to enhance cell migration and resulted in non-closed closure at the end of the assay. Under BC, LC-CM24 initiated the effect at 16 hours ($P<0.05$) while LC-CM72 initiated the effect after 20 hours. Overall, LC-CM24 always initiated cell migration earlier than LC-CM48 and LC-CM72. Therefore, CM24 appeared the most effective and consistent type of conditioned media to enhance migration of different cell types under different conditions. Collectively, migration of skin cells (keratinocyte and fibroblast) were enhanced by the action of MSC-CM. As explained in Chapter 3, a number of growth factors and cytokines were secreted in MSC-CM under serum free conditions containing both low and high calcium levels. Many factors collected from the MSC cultures are known to enhance the healing process. In particular, KGF promotes wound closure (Barrientos *et al.*, 2008a; Chen *et al.*, 2008) by being a transporter for alveolar epithelial fluid (Wang *et al.*, 2012c) and by being involved in tissue remodelling (Maxson *et al.*, 2012). Also, HGF which is referred to as

plasminogen-related growth factor-1 (PRGF-1) and scatter factor (SF) as a powerful mitogen for hepatocytes and a stimulator for epithelial cell dissociation (Werner and Grose, 2003). Additionally, it enhances keratinocytes to migrate, proliferate and produce matrix metalloproteinases; as well as, stimulating new blood vessel formation. It has therefore been suggested to play a role in cutaneous wound repair (van de Kamp *et al.*, 2013). Moreover, it has widely been suggested that PDGF is the major player in treating non healing wound and wound disorders especially human ulcers (Werner and Grose, 2003). This view has been attributed to the main roles played by this growth factor. According to Maxson and colleagues, PDGF was first chemotactic growth factor described to be involved in the migration of fibroblasts, monocytes, and neutrophils into the skin wound. In addition, it stimulates these cells to produce the extracellular matrix and induces the myofibroblast phenotype in these cells. Additionally, it enhances fibroblasts to proliferate and contract collagen matrices. Finally, it promotes proliferation (Maxson *et al.*, 2012). As per Werner and Grose, SDF-1α is suggested to play a role in regulating skin homeostasis and tissue remodelling (Werner and Grose, 2003). It also promotes wound closure (Barrientos *et al.*, 2008a; Chen *et al.*, 2008) by inducing cell migration especially MSC migration (Patel *et al.*, 2013). Like HGF, MSP also known by other names such as scatter factor-2 (SF-2) and hepatocyte growth factor like protein (HGFL) since it is derived from liver serum. It regulates the proliferation and differentiation of different cells including keratinocytes and macrophages (Werner and Grose, 2003). Finally, secretions of MSCs collected at low calcium conditions (LC-CM) enhanced migration of primary keratinocyte while HC-CM failed to enhance cell migration. The results showed that LC-CM is better for wound healing studies than HC-CM since the later activates cell differentiation, which in turn arrests cell proliferation and migration. Consequently, HC-CM gives false negative results when the target cells are primary keratinocytes. Results here showed that the use of LC-CM overcomes the false negative problem caused by using inappropriate HC-CM and generates results which are a true reflection of the *in vivo* healing process. However, more investigations are required to verify whether cell migration is the only the mechanism enhanced by MSC-CM during the healing process or whether other cellular responses can be evoked as well by MSC-CM such as cell proliferation and differentiation.

In summary, a new method was developed for skin wound healing studies based on MSC secretions collected under low calcium conditions (LC-CM) which was more suitable for studying skin wound healing using a 2D scratch assay under serum free conditions. Findings from this study indicate that biomolecules collected during early MSC expansion could be more effective than those collected at later time points. Moreover, a number of growth factors and cytokines secreted by MSCs were shown to participate in the wound healing process. These findings provide a new way to develop *in vitro* studies in order to analyse the effect of MSC secretions on the migration of primary keratinocyte skin wound healing studies. In the next chapter (Chapter 5), the effect of MSC-CM on the proliferation of skin cells during the scratch assay will studied.

CHAPTER 5 EFFECT OF MSC-CM ON PROLIFERATION OF SKIN CELLS

CHAPTER FIVE: EFFECT OF MSC-CM ON PROLIFERATION OF SKIN CELLS

5.1 INTRODUCTION

Cell proliferation is another key step in wound healing which is defined as a duplication of cell number balancing the number of dividing cells and the number of lost cells by death or differentiation (Reinke and Sorg, 2012). In intact skin, keratinocytes of the basal layer represent the infrastructure of epidermis since they proliferate and migrate towards the skin surface crossing the spinous, granular and stratum corneum (Pastar *et al.*, 2014). During the healing process, keratinocytes migrate to cover the wounded site, proliferate, move upwards and differentiate to form spinous, granular and stratum corneum epidermal layers (Werner and Grose, 2003; Morasso and Tomic-Canic, 2005). They therefore reconstitute full thickness skin and retain tissue integrity (Santoro and Gaudino, 2005). Cell proliferation can be measured by one of four main methods; DNA synthesis cell proliferation assays (Bick and Davidson, 1974; Gratzner, 1982), metabolic cell proliferation assays (colorimetric methods) (Mosmann, 1983; Berridge *et al.*, 2005; Quent *et al.*, 2010), detection of proliferation markers (Mokry and Nemecek, 1995) and measurement of adenosine triphosphate (ATP) (Lundin *et al.*, 1986; Stanley, 1986; Crouch *et al.*, 1993). Determination of metabolic activity for a population of cells is one of the most popular methods to measure cell viability. MTS (3-(4,5-dimethylthiazol-2-yl)-5-(3-carboxymethoxyphenyl)-2-(4-sulfophenyl)-2H-tetrazolium is one of the most common substances used in this method which, upon reduction by metabolically active cells, produce a coloured compound called formazan, which subsequently changes the media colour depending on the density of active cells (Mosmann, 1983; Berridge *et al.*, 2005). Compared to other substances, MTS requires no additional steps or additives such as DMSO or isopropanol, and is completely reduced by metabolically active cells and for these reasons it was chosen to detect cell viability in this study. Mitomycin C MMC is an anti-proliferative substance, which cross-links to DNA and inhibits cell proliferation via many mechanisms. MMC reacts with cytosine and guanine when one phosphate group separates them (5'—C—phosphate—G—3') (CpG) site in a DNA sequence. It exerts its mode of action in a concentration dependant manner resulting in varying effects between proliferation inhibition and arrest of the cell cycle at S and G2/M phase to cell death via induction of apoptosis (Tomasz, 1995; Kang *et al.*, 2001; Kersey and Vivian, 2008) and is

used in cancer chemotherapy (Tomasz, 1995). Collectively, proliferation of skin cells during wound healing is a critical and important repair mechanism in the healing process (Qing, 2017). Therefore, studying the effect of MSC-CM on proliferation of skin cells and monitoring cell behaviour through these events is very important and critical to the understanding of the cellular mechanisms occurring during the healing process.

5.2 Specific Aims of Chapter Five

1. To assess the effect of stock and diluted MSC-CM on proliferation of skin cells (keratinocytes and fibroblasts).
2. To compare the effect of high calcium conditioned media (HC-CM) and low calcium conditioned media (LC-CM) on proliferation of primary keratinocytes.
3. To determine the effect of MSC-CM on the migration of primary keratinocytes during inhibition of proliferation.
4. To determine whether migration or proliferation is the first initiation event in the MSC-CM on the healing process.

5.3 RESULTS

5.3.1 *EFFECT OF MSC-CM ON PROLIFERATION OF SKIN CELLS*

MTS proliferation assay was used to detect the effect of MSC-CM on proliferation of skin cells (primary keratinocytes and primary fibroblasts). The HaCat cell line was used to optimise the assay. Both HC-CM and LC-CM were tested for their effect on proliferation of primary keratinocytes. Primary fibroblasts were treated with HC-CM only.

5.3.1.1 *OPTIMISATION OF MTS PROLIFERATION ASSAY USING THE HACAT CELL LINE*

HaCat cells were seeded at a density of 0.01×10^6 cells per well in 96 well plates and incubated under standard culture conditions (SCC) (humidified incubator, 37°C and 5 % CO_2) for 4 hours to allow cell adhesion. The culture media was then discarded and the cells were washed twice in PBS followed by addition of MSC-CM (HC-CM24, HC-CM48 and HC-CM72) to the corresponding wells. DMEM supplemented with 10% foetal calf serum (DMEM-FCS) was used as a control (HC-CTRL). Cell viability was estimated after different time points (0, 24, 48 72 and 96 hours) by treating cells with 20 µl MTS salt for 3 hours followed by reading the absorbance of the developed colour at 492 nm using a micro-plate reader. Results showed that HaCat cells could proliferate normally in MSC-CM collected at different time points when compared to the control.

Statistically, viability of HaCat cells treated with MSC-CM significantly increased during time. For example, after 24 hours cell viability increased in comparison to cell viability at time zero ($P<0.0001$) for the three MSC-CM and there was no significant differences in comparison to the control tested at the same time points. Again at the end of the experiment (72) hours, viability of the cells treated with MSC-CM was higher than the cell viability at 24 hours ($P<0.05$, $P<0.001$ and $P<0.05$) for CM24, CM48 and CM72 respectively indicating that the cells were continuing to proliferate during this time. On the other hand, there was no significant variation between cell viability of cells treated with MSC-CM and the control at the end of the treatment time (72 hours) ($P>0.05$) as shown in (Figure 5.1).

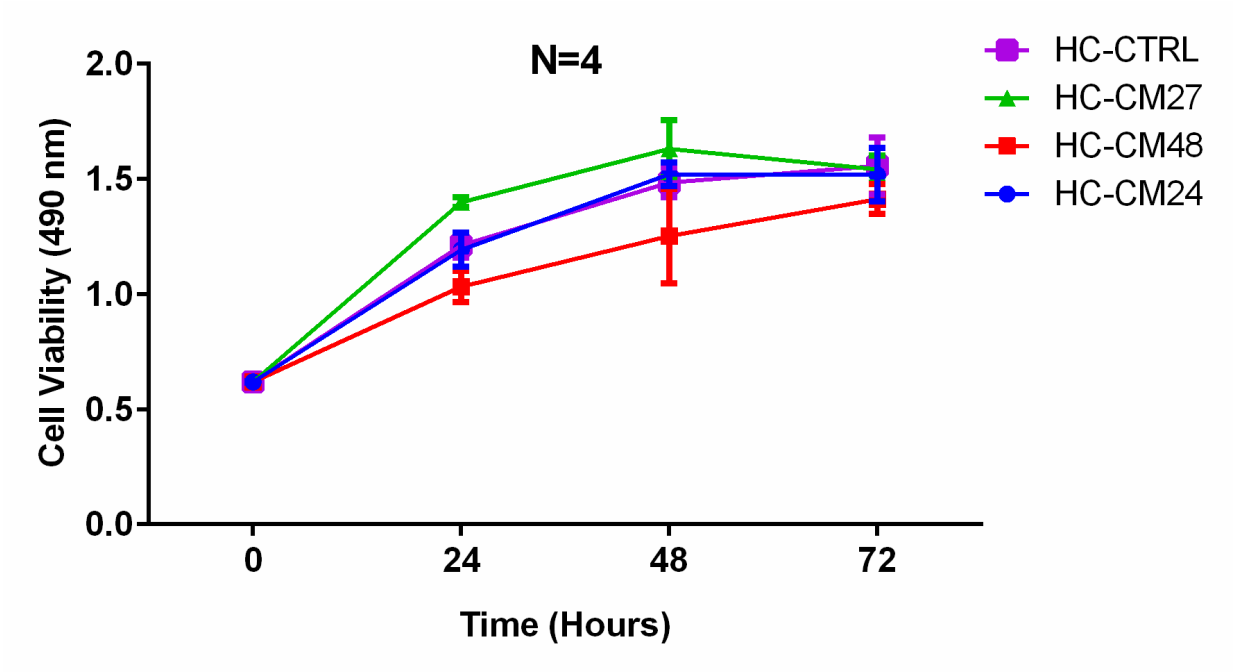

Figure 5.1 Statistical analysis of the effect of MSC-CM on proliferation of HaCat cells using MTS assay.

Different line colours represent cell viability of HaCat cell line treated with the different types of MSC-CM in addition to the control at different time points (0, 24, 48 and 72 hours). The blue line represents the mean of optical density of viable HaCat cells treated with HC-CM24. The red line represents the mean of optical density of viable HaCat cells treated with HC-CM48. The green line represents the mean of optical density of viable HaCat cells treated with HC-CM72. The purple line represents the mean of optical density of viable HaCat cell control treated with DMEM-FCS (HC-CTRL). Data presented as mean of optical density (N=4 technical replicates). Error bars= Standard error of the mean (SEM), (=P<0.05). Cell viability was measured at 450 nm.*

5.3.1.2 *Effect of MSC-CM on Proliferation of Primary Keratinocytes*

Primary keratinocytes were treated with high calcium conditioned media (HC-CM) and incubated for 96 hours. As demonstrated in (Figure 5.2) all HC-CM (HC-CM24, HC-CM48 and HC-CM72) arrested the proliferation of primary keratinocytes. There was no significant variation in cell viability at time zero compared with cell viability at 96 hours (P>0.5). Interestingly, the viability of control cells, which were treated with DMEM-FCS was arrested as well due to the high calcium level (1.8 mM/L) present in the DMEM media. For example, there was no significant variation in cell viability at 48 hours compared with the cell viability at time zero (P>0.05). However, after 72 hours and 96 hours, cell viability of the control slightly increased in comparison to the viability at time zero (P<0.05).

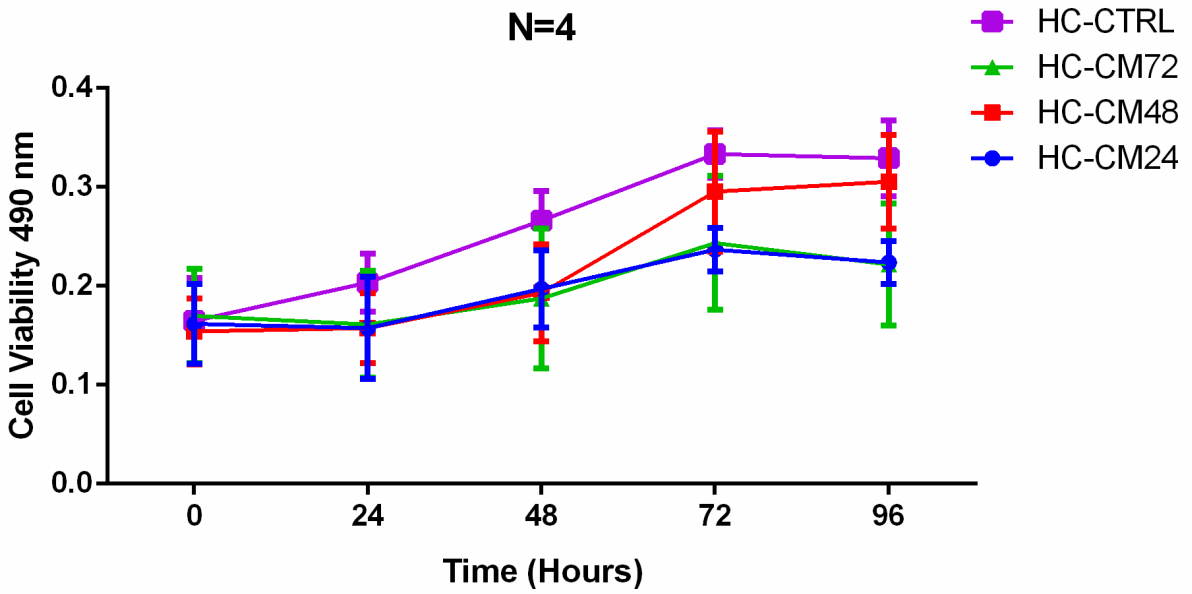

Figure 5.2 Statistical analysis of the effect of high calcium-conditioned media (HC-CM) on proliferation of primary keratinocytes using MTS assay.

Different line colours represent cell viability of primary keratinocytes treated with the different types of HC-CM in addition to the control (HC-CTRL) at different time points (0, 24, 48, 72 and 96 hours). The blue line represents the mean of the optical density of viable primary keratinocytes treated with HC-CM24. The red line represents the mean of the optical density of viable primary keratinocytes treated with HC-CM48. The green line represents the mean of the optical density of viable primary keratinocytes treated with HC-CM72. The purple line represents the mean of the optical density of viable primary keratinocytes control treated with high calcium media (DMEM-FCS) (HC-CTRL). Data presented as mean of optical density (N=4). Error bars= Standard error of the mean (SEM). Cell viability was measured at 450 nm.

On the other hand, the same experiment repeated using low calcium conditioned media (LC-CM) showed that all LC-CM (LC-CM24, LC-CM48 and LC-CM72) had a negative effect on proliferation of primary keratinocytes (Figure 5.3). For example, after 48 hours there was no significant increase in cell viability compared to the viability at time zero ($P>0.05$). However, after 72 hours cells treated with MSC-CM started to proliferate significantly ($P<0.0001$, $P<0.01$ and $P<0.05$) for (LC-CM24, LC-CM48 and LC-CM72) respectively compared to the viability at time zero. Cells also retained their ability to proliferate until the end of the assay (96 hours) when cell viability significantly increased compared to cell viability at 48 hours ($P<0.0001$). The control cells (low calcium concentration treated= 0.04 mM/L) significantly proliferated ($P<0.0001$) during the entire treatment time (96 hours) compared to cell viability at 48 hours.

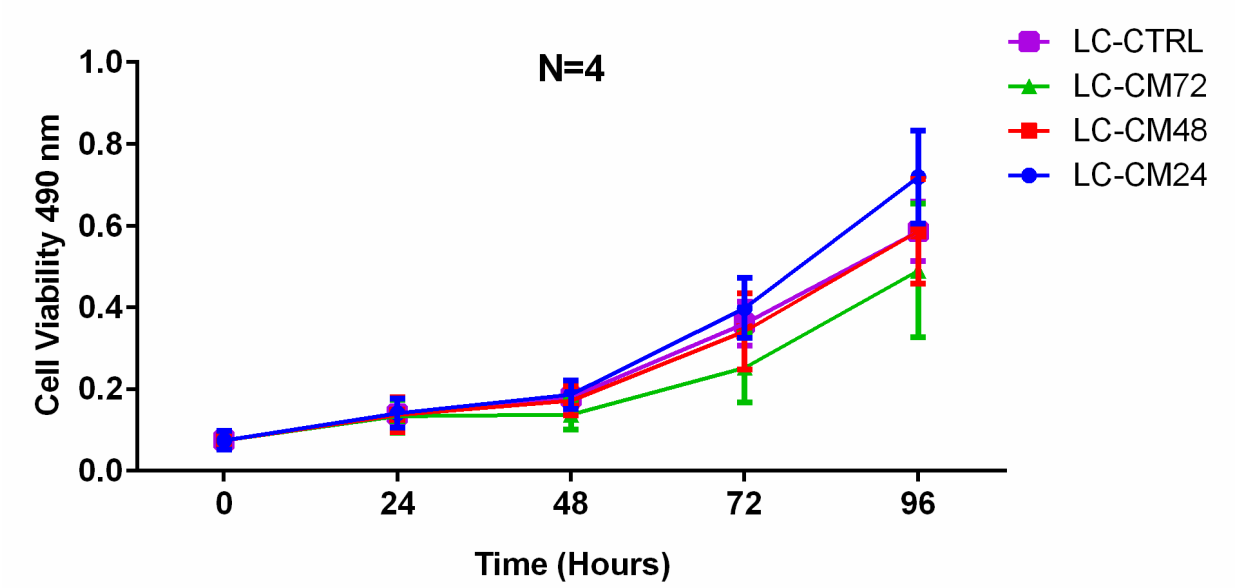

Figure 5.3 Statistical analysis of the effect of low calcium-conditioned media (LC-CM) on proliferation of primary keratinocytes using MTS assay.

Different line colours represent cell viability of primary keratinocytes treated with the different types of LC-CM in addition to the control (LC-CTRL) at different time points (0, 24, 48, 72 and 96 hours). The blue line represents the optical density of viable primary keratinocytes treated with LC-CM24. The red line represents the optical density of viable primary keratinocytes treated with LC-CM48. The green line represents the optical density of viable primary keratinocytes treated with LC-CM72. The purple line represents the optical density of viable primary keratinocytes control (LC-CTRL). Data presented as mean of optical density of viable cells (N=4). Error bars= standard error of the mean (SEM). Cell viability was measured at 450 nm.

LC-CM and HC-CM were compared at different paired time points (LC-CM24 vs HC-CM24, LC-CM48 vs HC-CM48 and LC-CM72 vs HC-CM72). Results showed that LC-CM was more effective at inducing cell proliferation. As shown in (Figure 5.4 A), after 72 hours, cells treated with LC-CM24 proliferated to a greater extent than those treated with HC-CM24 ($P<0.05$) with increased significant viability at 96 hours ($P<0.001$). The increase in cell proliferation between cells treated with LC-CM48 and HC-CM48 was also observed at 96 hours ($P<0.01$) (Figure 5.4 B). The same was observed for LC-CM72 versus HC-CM72 with no significant difference in cell viability at 72 hours ($P>0.5$) until 96 hours ($P<0.01$) (Figure 5.4 C).

These data collectively suggest that primary keratinocytes proliferate normally during treatment with LC-CM. In contrast, cell proliferation was arrested with HC-CM compared to the controls.

(A)

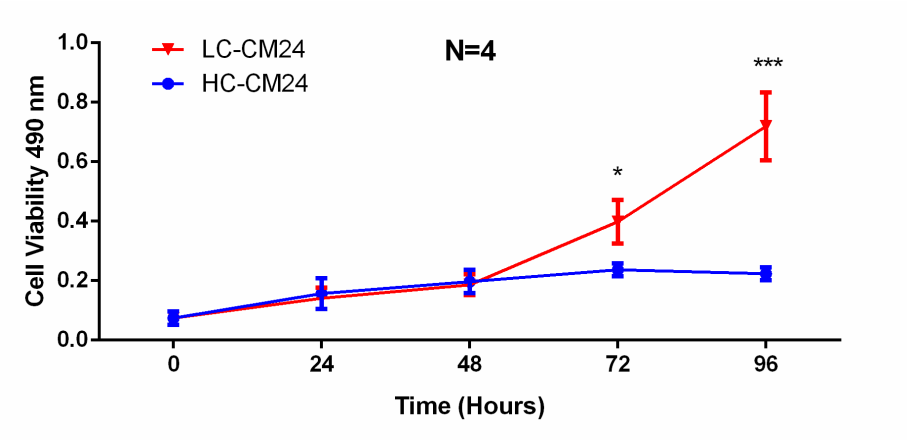

(B)

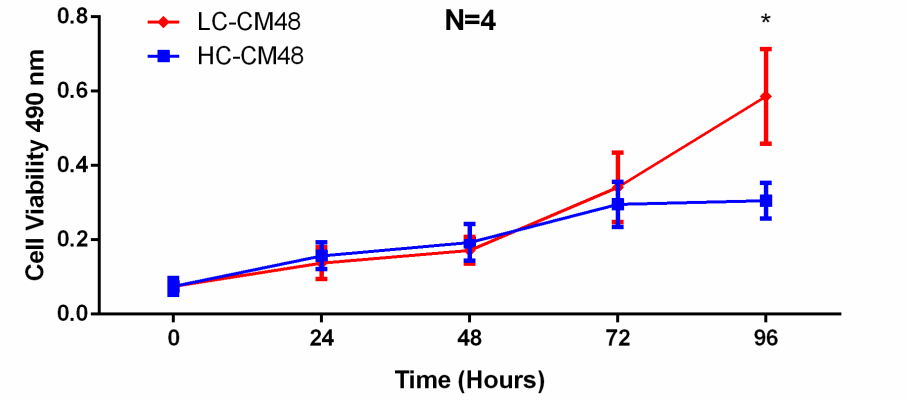

(C)

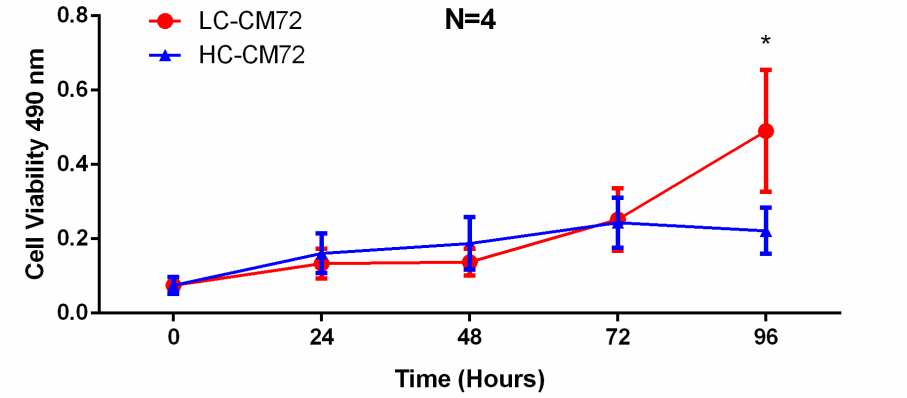

Figure 5.4 Comparison between the effect of LC-CM and HC-CM on proliferation of primary keratinocytes using MTS assay.

Cell viability of primary keratinocytes treated with LC-CM and HC-CM at different time points (0, 24, 48, 72 and 96 hours). (A) The blue line is the optical density of viable primary keratinocytes treated with HC-CM24, while the red line is the optical density of viable primary keratinocytes treated with LC-CM24. (B) The blue line is the optical density of viable primary keratinocytes treated with HC-CM48 and the red line is the optical density of viable primary keratinocytes treated with LC-CM48. (C) The blue line is the optical density of viable primary keratinocytes treated with HC-CM72 and the red line is the optical density of viable primary keratinocytes treated with LC-CM72. Data presented as mean of optical density of viable cells (N=4), Error bar= standard error of the mean (SEM), (=P<0.05), (***=P<0.001), Cell viability was measured at 450 nm.*

Both HC-CM and LC-CM arrested proliferation of keratinocytes until 48 hours. The negative effect of HC-CM continued until the termination of the assay at 96 hours. However, LC-CM enhanced cell proliferation post 48 hours and the positive effect increased until the end of the assay. The reason for the lack of proliferation with HC-CM could be attributed to the high calcium level, which enhances cell differentiation rather than cell proliferation. More investigations were required to decipher the main role of MSC-CM on the behaviour of the primary keratinocytes at the injury site. One of these investigations is the detection of proliferation markers during cell migration in the presence and absence of MMC.

5.3.1.3 *Effect of MSC-CM (MSC-CM) on Proliferation of Primary Fibroblasts*

Primary fibroblasts were treated with HC-CM because they were grown in DMEM containing calcium at a high concentration (1.8 Mm/L). Results in (Figure 5.5) showed that primary fibroblasts proliferated in MSC-CM. HC-CM24, HC-CM48 and HC-CM72 and demonstrated a positive effect on fibroblast proliferation at 24 hours ($P<0.05$) which increased at 48 and 72 hours ($P<0.01$) compared to time zero. The viability of the control cells significantly increased with time (24, 48 and 72 hours ($P<0.0001$) in comparison to the viability at time zero. Comparing the MSC-CM to the control showed that there was no significant variation ($P>0.05$) at 48 hours and the proliferation of the control was significantly higher than MSC-CM-treated cells at 72 hours ($P<0.01$).

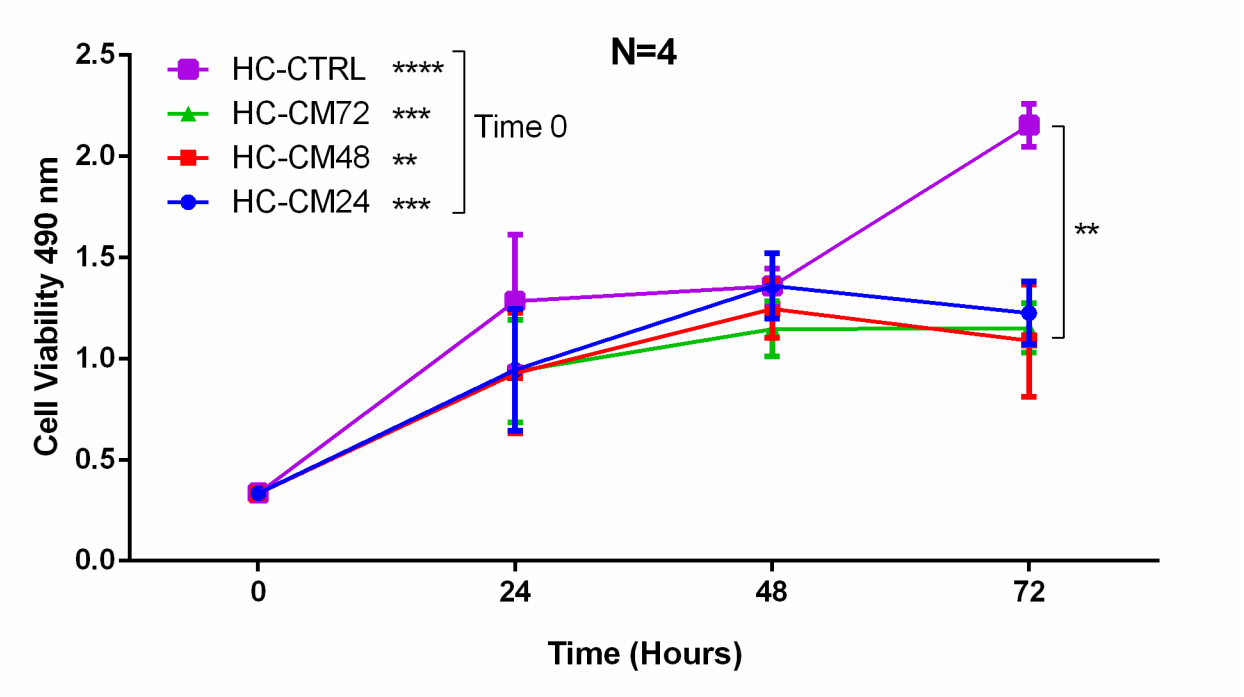

Figure 5.5 Statistical analysis of the effect of MSC-CM (HC-CM) on proliferation of primary fibroblasts using MTS assay.

Different line colours represent cell viability of primary fibroblasts treated with HC-CM in addition to the control (HC-CTRL) at different time points (0, 24, 48 and 72 hours). The blue line represents the optical density of viable primary fibroblasts treated with HC-CM24. The red line represents the optical density of viable primary fibroblasts treated with HC-CM48. The green line represents the optical density of viable primary fibroblasts treated with HC-CM72. The purple line represents the optical density of viable primary fibroblast control treated with high calcium media (HC-CTRL). Fibroblasts treated with HC-CM24, HC-CM48 and HC-CM72 significantly proliferated at 72 hours (P<0.001, P<0.01 and P<0.001) respectively. Proliferation of control cells was significantly higher than proliferation of MSC-CM treated cells (P<0.01) at 72 hours. Data presented as mean of the optical density of viable cells (N=4), Error bars= standard error of the mean (SEM), (=P<0.05), (**=P=0.01), (***=P=0.001), (****P=0.0001), Cell viability was measured at 450 nm.*

5.3.2 *Determining Migrating and Proliferating Cells During Wound Closure*

The scratch assay was used to assess if MSC-CM could enhance cell migration rather than proliferation during wound closure. Proliferating cells were detected in the scratch area post wound closure. Proliferating cells were detected by using the specific proliferation marker 5-bromo-2'-deoxyuridine (BrdU). Original nucleosides of the DNA of proliferating cells are replaced by these synthetic nucleoside analogues. BrdU is a synthetic nucleoside analogue to thymidine and used to detect proliferating cells (Lehner et al., 2011). During the S-phase of the cell cycle of replicating cells, BrdU is translocated into the newly synthesised DNA and replaces thymidine during DNA replication (Konishi

et al., 2011). Interestingly, BrdU passes to the daughter cells upon replication (Kee et al., 2002) and can be detected two years post incorporation (Eriksson et al., 1998). Upon staining with specific anti-BrdU antibodies, BrdU positive cells can be easily detected indicating that these cells are actively replicating their DNA and proliferating normally (Konishi et al., 2011).

5.3.2.1 *Optimisation: using HeLa Cell Line and Primary Keratinocytes*

HeLa cells were used as a positive control to optimise the proliferation assay. Briefly, 0.005×10^6 cells / well were seeded in DMEM-FCS in an 8-well glass chamber and incubated under SCC (37°C in a humidified incubator supplemented with 5% CO_2) for 4 hours to allow cell attachment. Two conditions were used to investigate proliferation. The first one was HeLa cells grown in their normal growth media (DMEM supplemented with 10% FCS, 5% penicillin-streptomycin and 200 mM L-glutamine). The second condition was HeLa cells treated with 30 µg/ml mitomycin C (MMC) for three hours to inhibit their proliferation. Cells were then incubated with 3 µg/ml of synthetic BrdU nucleoside overnight under SCC to allow sufficient time for replacing BrdU with thymidine in the replicating cells. Following day, cells were stained with anti-BrdU antibody and then a secondary antibody (Donkey Anti-Rabbit IgG H&L (Alexa Fluor® 488) following a standard immunofluorescence (IF) staining protocol (See Methods Chapter 2, Section 2.3.9) using anti-BrdU antibody to investigate BrdU incorporation. Bioimaging analysis (Figure 5.6 A) showed that cells treated with MMC had no increase in cell number after 24 hours with no staining with the anti-BrdU antibodies. In contrast, untreated cells (Figure 5.6 B) demonstrated an increased cell count after 24 hours with positive staining for BrdU antibodies. Continuous DNA replication led to continuous BrdU-thymidine replacement, which resulted in an increased number of BrdU positive cells after 24 hours suggesting that MMC inhibited the proliferation of HeLa cells.

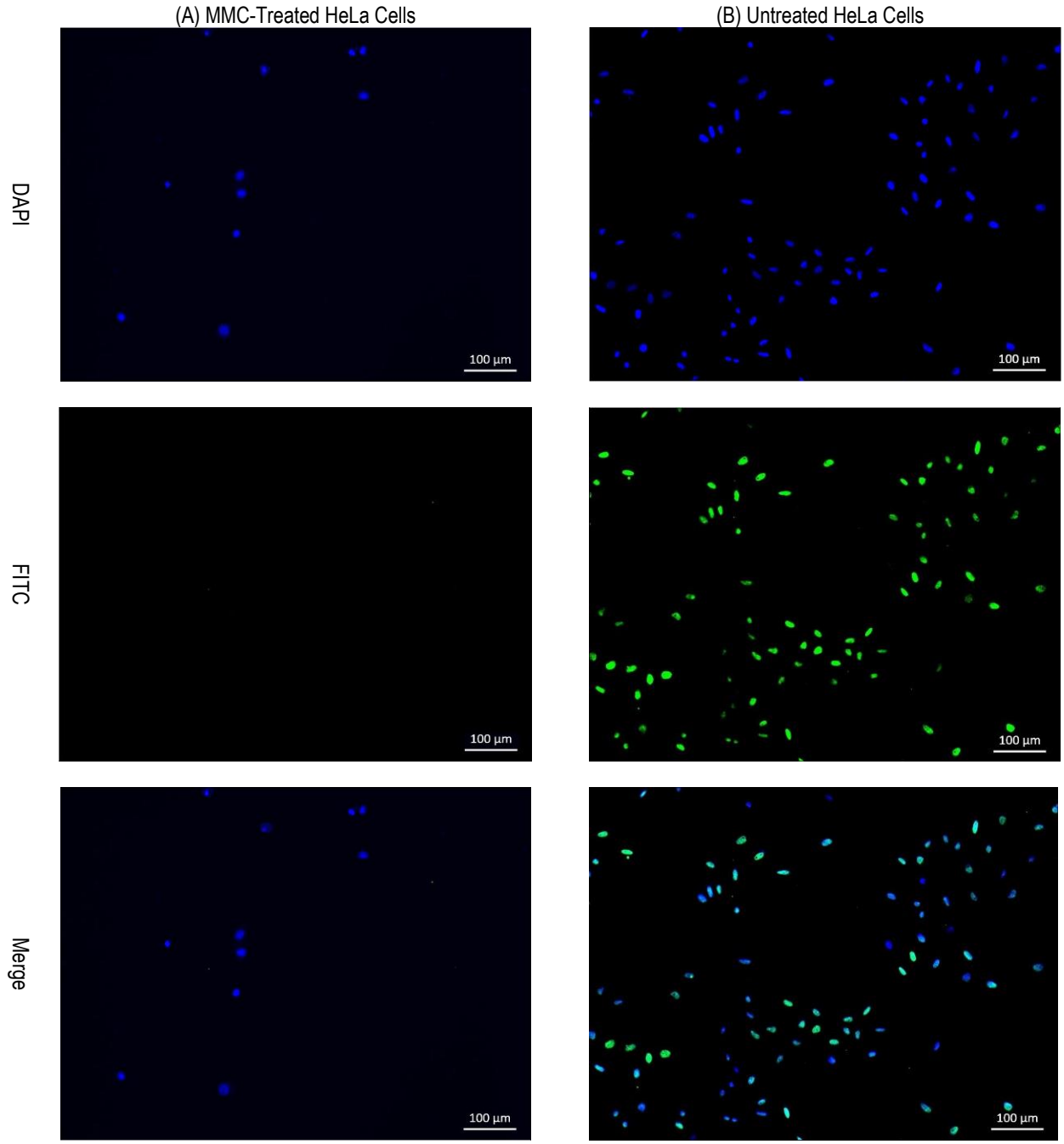

Figure 5.6 Proliferating HeLa cells express the proliferation marker (BrdU).

Representative immunofluorescence image revealing proliferating and non-proliferating HeLa cells. (A) HeLa cells treated with 20 µg/ml MMC for 3 hours at SCC. (B) HeLa cells grown in standard culture media for 3 hours at SCC. HeLa cells in (A) and (B) are labelled with BrdU overnight at SCC then stained with anti-BrdU antibody (ab152095) at (1:60) in (1% bovine serum albumin (BSA). Green signal in (B) revealed binding of anti-BrdU antibody with BrdU of replicating cells and when stained with Donkey Anti-Rabbit IgG H&L (Alexa Fluor® 488) (ab150073) at (1:250) in (1% bovine serum albumin) gave green signal (FITC). MMC treated HeLa cells (A) revealed negative staining for anti-BrdU antibody. Blue= DAPI stain (1:1000) in (1% BSA). Scale bar= 100 µm.

Upon successful optimisation of the protocol with HeLa cells, the same conditions were used to detect proliferation in primary keratinocytes. Since the doubling time of primary keratinocytes is longer than that of HeLa cells, keratinocytes were seeded at a density of 0.03×10^6 cells/well in an 8-well glass chamber and incubated overnight at SCC to allow cell adhesion. On the next day, cell proliferation was inhibited by treating the cells with 20 µg/ml MMC for 3 hours at SCC. Cells were then treated with 3 µg/ml BrdU. The cells were then stained with anti-BrdU antibody and secondary antibody using the standard IF staining protocol. Figure 5.7 A and Figure 5.7 B show cells treated with MMC and normal untreated keratinocytes respectively. When stained with DAPI after 24 hours of treatment with MMC, cells were less dense after staining with anti-BrdU antibody and secondary antibody and showed fewer positive signals compared to normal cells.

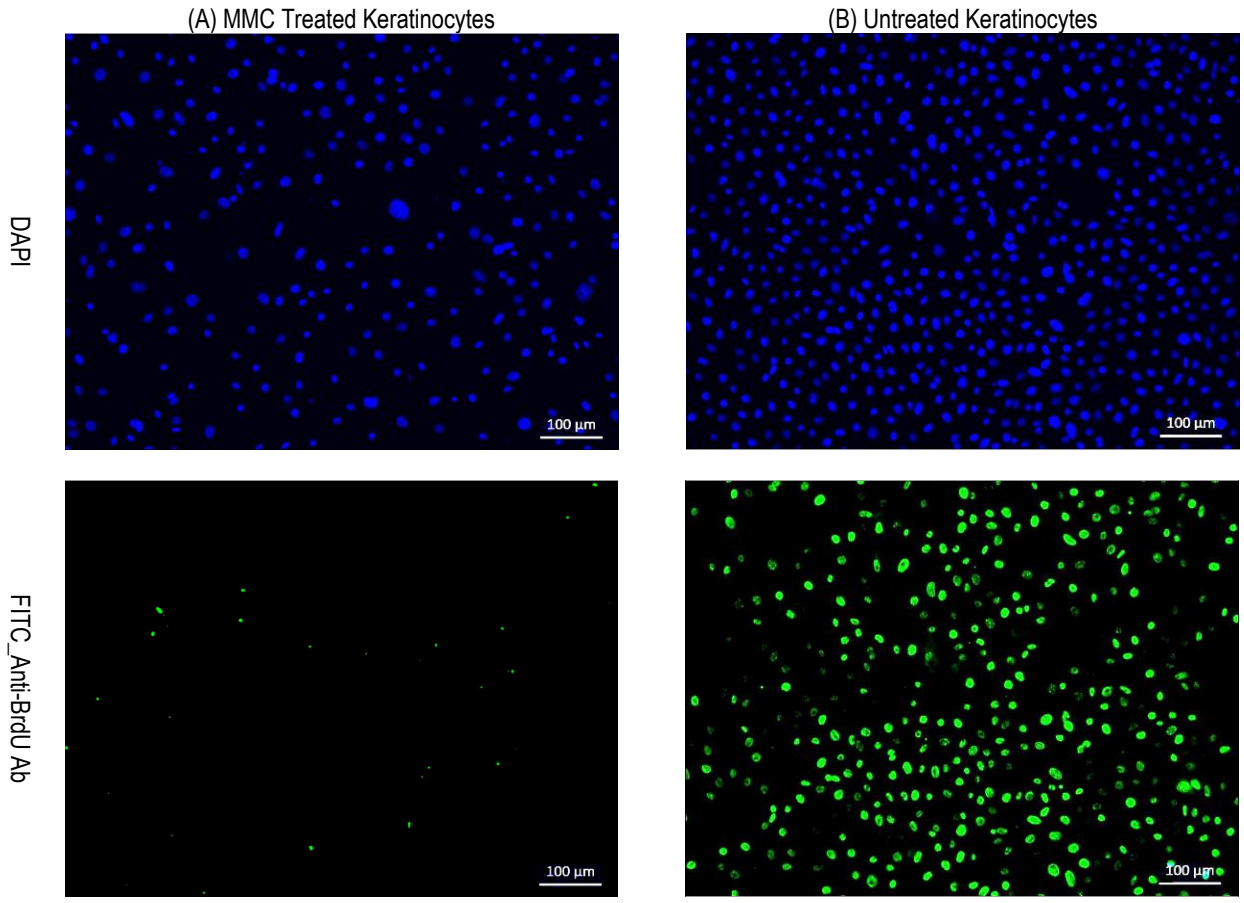

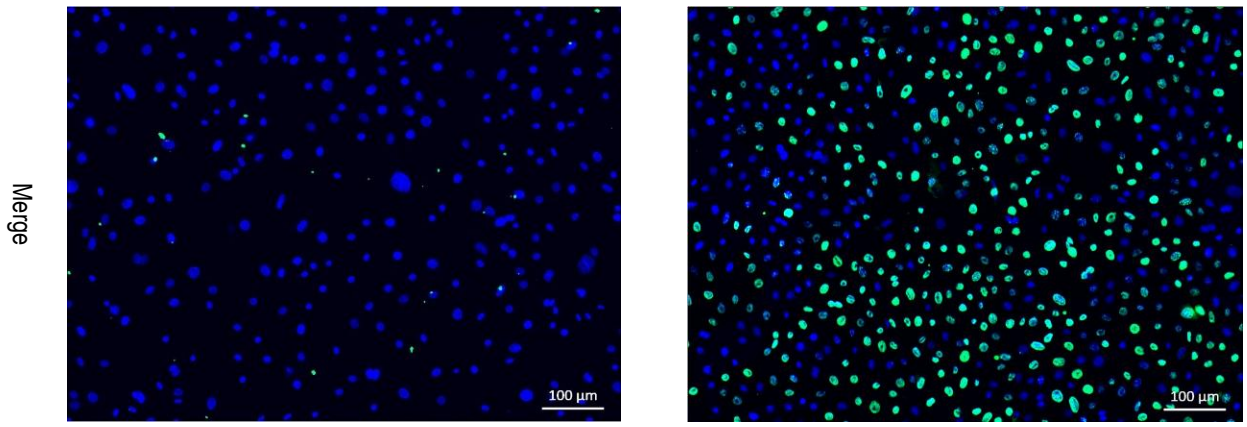

Figure 5.7 Proliferating primary keratinocytes express the proliferation marker (BrdU).

Representative immunofluorescence image revealing proliferating and non-proliferating primary keratinocytes. (A) Primary keratinocytes treated with 20 µg/ml MMC for 3 hours at SCC. (B) Primary keratinocytes grown in keratinocyte growth media (KGM) for 3 hours at SCC. Primary keratinocytes in (A) and (B) are labelled with BrdU overnight at SCC then stained with anti-BrdU antibody (ab152095) at (1:60) in (1% bovine serum albumin (BSA). Green signal in (B) revealed binding of anti-BrdU antibody with BrdU of replicating cells and when stained with Donkey Anti-Rabbit IgG H&L (Alexa Fluor® 488) (ab150073) at (1:250) in (1% bovine serum albumin) gave a green signal (FITC). MMC treated HeLa cells (A) Showed negative staining for anti-BrdU antibody. Blue= DAPI stain (1:1000) in (1% BSA). Scale bar= 100 µm.

5.3.2.2 *Detection of Migrating and Proliferating Cells During Wound Closure at Normal Conditions (Non Inhibited Proliferation "NIP")*

Proliferating cells were detected in the scratch area at different time points (24, 48 and 72 hours) during wound closure after treatment with MSC-CM. Briefly; primary keratinocytes (N=3; S1212K, S1214K and S1216K) were seeded at a density of 0.04×10^6 cells/well in an 8-well glass chamber for 24 hours at SCC to allow cell adhesion. On the next day, a scratch was made in the confluent monolayer and cells were treated with MSC-CM for different time points (24, 48 and 72 hours). 24 hours before the staining, cells were treated with 3 µg/ml BrdU followed by standard IF staining with BrdU antibody and secondary Donkey Anti-Rabbit IgG H&L (Alexa Fluor® 488) (ab150073). Results are shown in (Figure 5.8), (Figure 5.9) and (Figure 5.10) for samples S1212K, S1214K and S1216K respectively. Part A of each figure represents cell migration after 24 hours showing cells which have moved from the edges of the scratch towards the centre compared to the control at time zero. The number of proliferating cells (BrdU positive cells) were less than non-proliferating cells (BrdU negative cells) or migrating cells. Part B of each figure represents cell migration after 48 hours showing an increase in the cell density in the scratch area in comparison to time zero and 24 hours. Migrating cells (BrdU negative

cells) were proportionally higher than proliferating cells (BrdU +ve cells). In part C of each figure, cell densities of migrating cells (BrdU negative cells) at 72 hours in the scratch area were higher than the cell densities of BrdU +ve cells (proliferating cells) at 0, 24 and 48 hours. These data suggest that MSC-CM mainly enhance cell migration rather than cell proliferation in the scratch area during the wound healing process.

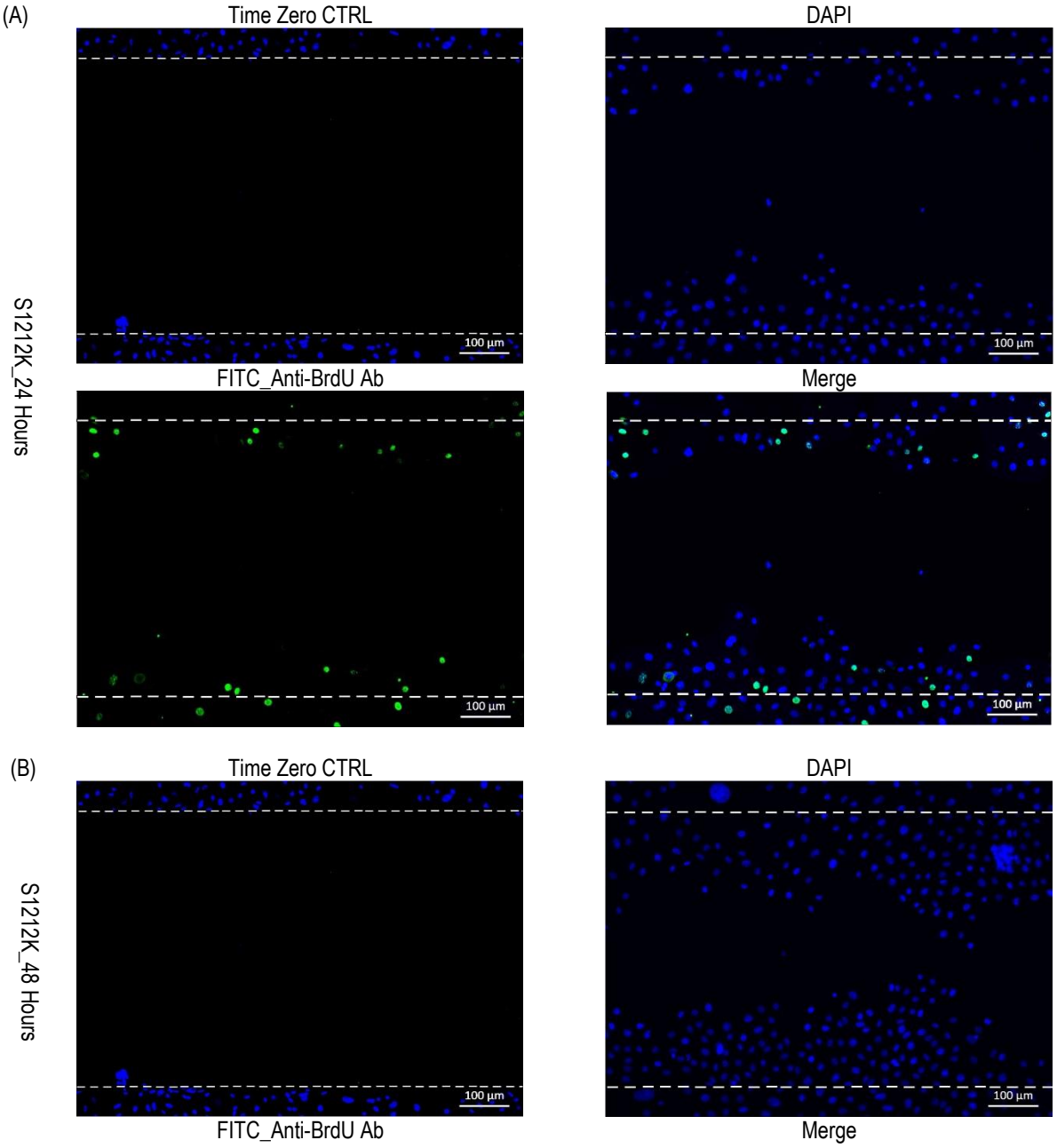

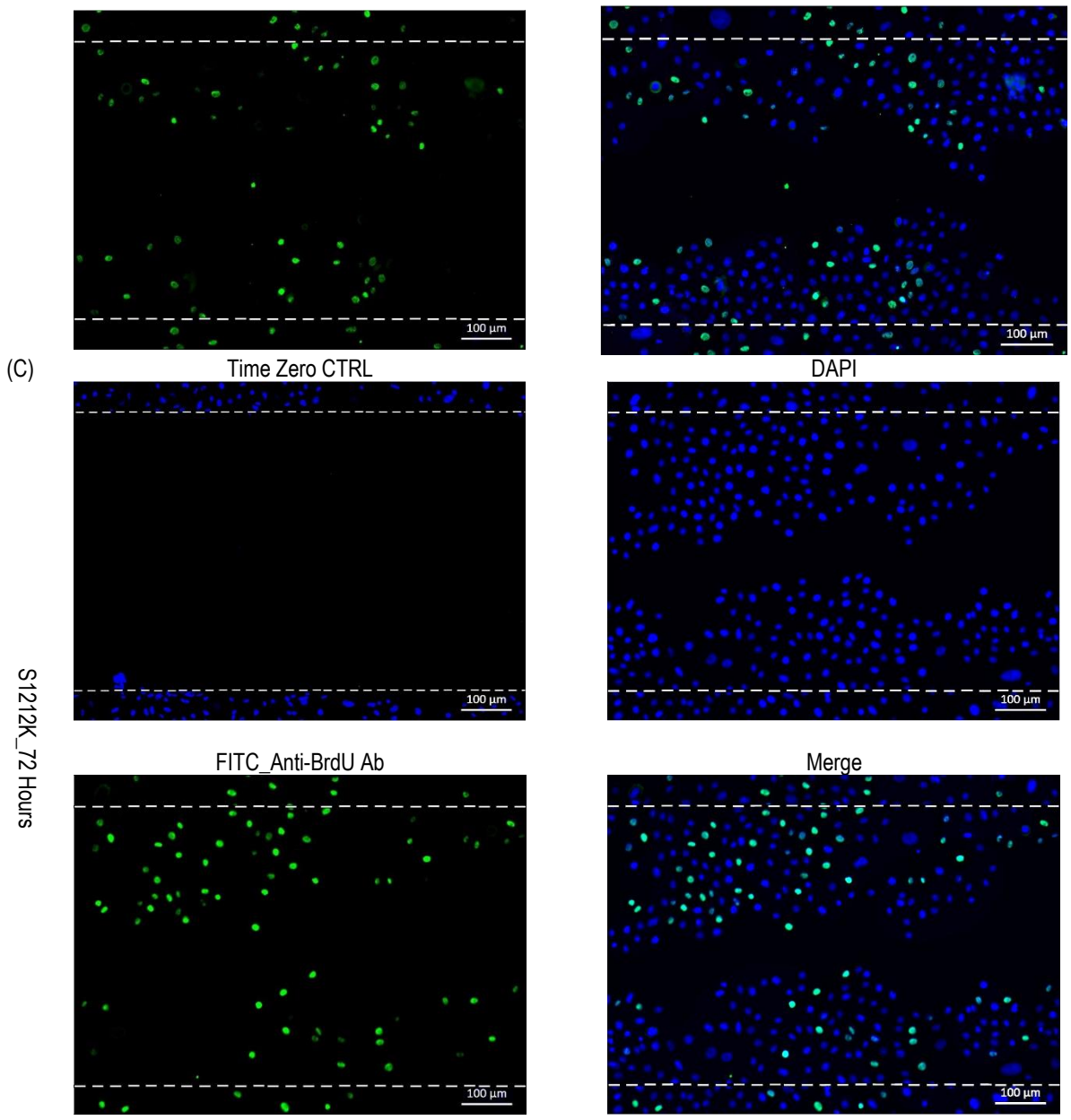

Figure 5.8 Migrating and proliferating cells during wound closure in sample S1212K.

Representative immunofluorescence images revealing proliferating and migrating primary keratinocytes during wound closure assay for different time points (A) 24 hours, (B) 48 hours and (C) 72 hours. Confluent monolayer of primary keratinocytes labelled with BrdU overnight at SCC then scratched and treated with MSC-CM. Green signal represent Proliferating cells (BrdU positive cells) stained with anti-BrdU antibody (ab152095) at (1:60) in (1% bovine serum albumin (BSA). Green signal revealed binding of anti-BrdU antibody with BrdU of replicating cells and when stained with Donkey Anti-Rabbit IgG H&L (Alexa Fluor® 488) (ab150073) at (1:250) in (1% bovine serum albumin) gave green signal (FITC). BrdU negative cells represent migrating cells which mainly stained with DAPI. Time zero control cells are DAPI stained. Blue= DAPI stain (1:1000) in (1% BSA). Scale bar=100 µm.

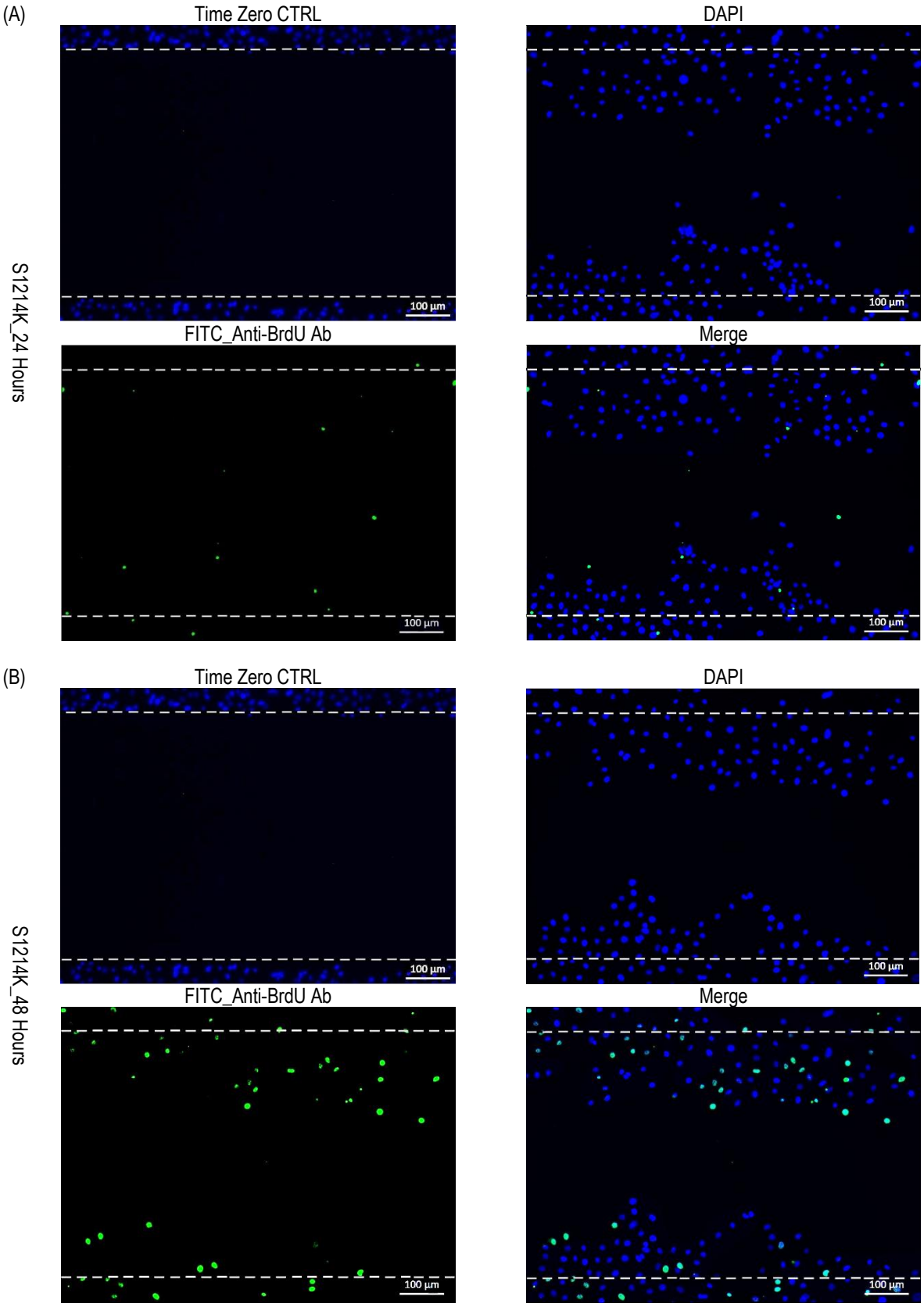
(A)
Time Zero CTRL
DAPI
S1214K_24 Hours
FITC_Anti-BrdU Ab
Merge
100 µm
(B)
Time Zero CTRL
DAPI
S1214K_48 Hours
FITC_Anti-BrdU Ab
Merge
100 µm

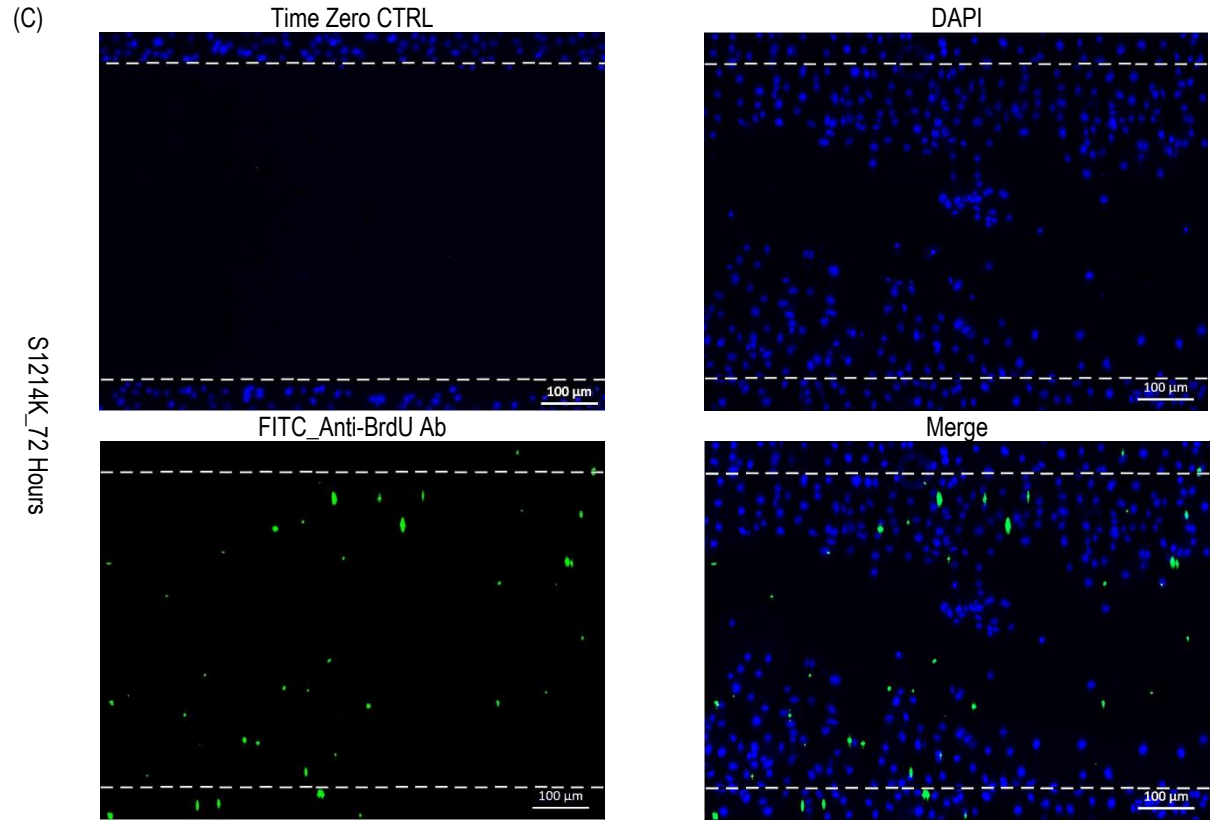

Figure 5.9 Migrating and proliferating cells during wound closure in sample S1214K.

Representative immunofluorescence images revealing proliferating and migrating primary keratinocytes during wound closure assay for different time points (A) 24 hours, (B) 48 hours and (C) 72 hours. Confluent monolayer of primary keratinocytes labelled with BrdU overnight at SCC then scratched and treated with MSC-CM. Green signal represent Proliferating cells (BrdU positive cells) stained with anti-BrdU antibody (ab152095) at (1:60) in (1% bovine serum albumin (BSA). Green signal revealed binding of anti-BrdU antibody with BrdU of replicating cells and when stained with Donkey Anti-Rabbit IgG H&L (Alexa Fluor® 488) (ab150073) at (1:250) in (1% bovine serum albumin) gave green signal (FITC). BrdU negative cells represent migrating cells which mainly stained with DAPI. Time zero control cells are DAPI stained. Blue= DAPI stain (1:1000) in (1% BSA). Scale bar=100 µm.

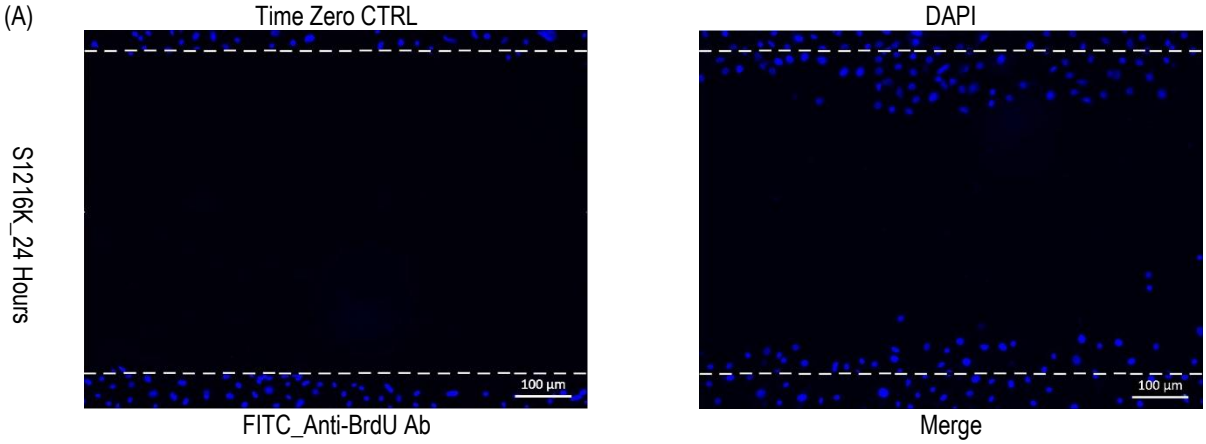

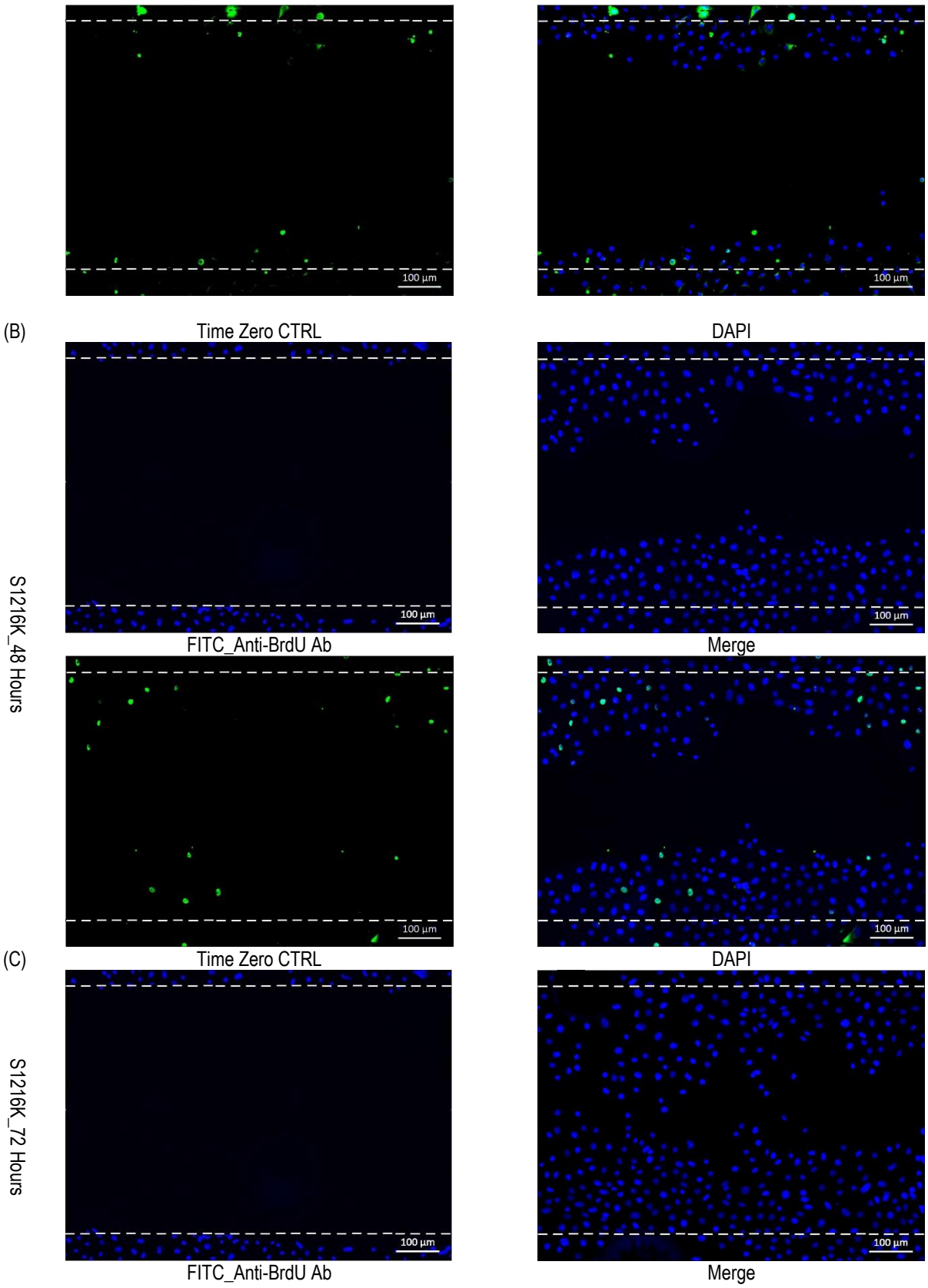
(B)
Time Zero CTRL
DAPI
S1216K_48 Hours
FITC_Anti-BrdU Ab
Merge
(C)
Time Zero CTRL
DAPI
S1216K_72 Hours
FITC_Anti-BrdU Ab
Merge
100 µm

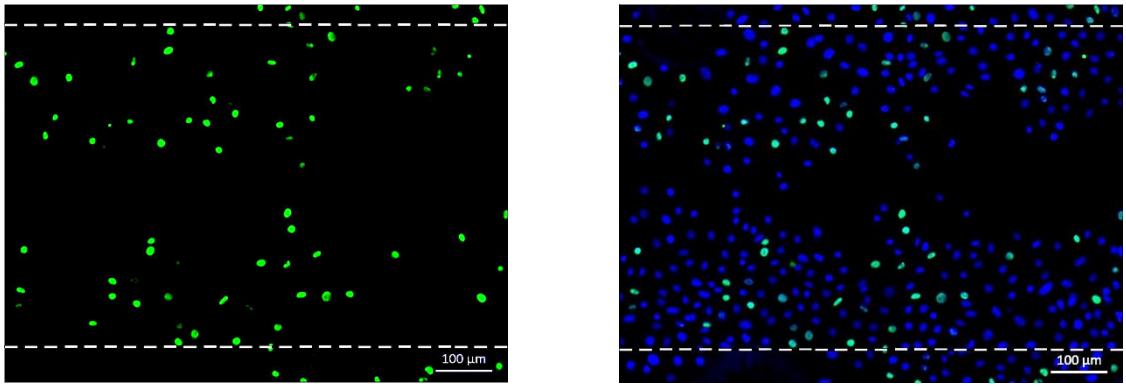

Figure 5.10 Migrating and proliferating cells during wound closure in sample S1216K.

Representative immunofluorescence images revealing proliferating and migrating primary keratinocytes during wound closure assay for different time points (A) 24 hours, (B) 48 hours and (C) 72 hours. Confluent monolayer of primary keratinocytes labelled with BrdU overnight at SCC then scratched and treated with MSC-CM. Green signal represent Proliferating cells (BrdU positive cells) stained with anti-BrdU antibody (ab152095) at (1:60) in (1% bovine serum albumin (BSA). Green signal revealed binding of anti-BrdU antibody with BrdU of replicating cells and when stained with Donkey Anti-Rabbit IgG H&L (Alexa Fluor® 488) (ab150073) at (1:250) in (1% bovine serum albumin) gave green signal (FITC). BrdU negative cells represent migrating cells which mainly stained with DAPI. Time zero control cells are DAPI stained. Blue= DAPI stain (1:1000) in (1% BSA). Scale bar=100 µm.

For statistical analysis, numbers and ratios of cells in the scratch area were calculated at different time points (24, 48 and 72 hours) and presented in (Table 5.1 A and B).

	Time	Migrating Cells				Proliferating Cells			
		S1212K	S1214K	S1216K	Total	S1212K	S1214K	S1216K	Total
(A)	24 Hours	80	80	96	256	21	18	23	62
	48 Hours	216	212	244	672	27	21	49	97
	72 Hours	272	266	248	786	60	28	68	156
	Time	Migrating Cells				Proliferating Cells			
		S1212K	S1214K	S1216K	Average	S1212K	S1214K	S1216K	Average
(B)	24 Hours	79	82	81	80.66	21	18	19	19.33
	48 Hours	89	91	83	87.66	11	9	17	12.33
	72 Hours	82	90	78	83.33	18	10	22	16.66

Table 5.1 Numbers and percentages of migrating and proliferating cells in the scratch area during wound healing.

Counts and ratios of migrating and proliferating keratinocytes (N=3) during wound closure at different time points (24, 48 and 72 hours). (A) Numbers presented as cell number seen in a field of 10X magnification. (B) Percentages of cells in the scratch area at different time points.

Two way ANOVA showed that there was a significant increase in cell number of migrating cells at the different time points during wound closure. The number of migrating cells in the scratch area after 72 hours (262±7) was significantly higher than cell number at 48 hours (1912±40) ($P<0.05$) which in turn was significantly higher than cell number after 24 hours (85±5) ($P<0.01$). The cell number at 72 ($P<0.001$) was significantly higher than the cell number at 24 hours (Table 5.1 A) and (Figure 5.11 A). In another words, at every time point (24, 58 and 72 hours) more than 80±2.28% of the cells in the scratch area were migrating cells while the proliferating cells represented 20±2.28% only (Table 5.1 B) (Figure 5.11 B). The results also show that there was no significant increase in numbers of proliferating cells after 48 hours of treatment compared to 24 hours ($P>0.05$) with a slight increase in number of proliferating cells after 72 hours compared to 48 hours ($P<0.05$) (Figure 5.11 B). Again, when migrating and proliferating cells were compared at each time point, migrating cells were always significantly higher than proliferating cells. For instance, after 24, 48 and 72 hours the numbers of migrating cells were higher than numbers of proliferating cells ($P<0.0001$). These data suggest that MSC-CM enhanced primary keratinocyte migration during wound closure until the wound was healed overtime. Keratinocyte proliferation was arrested between time zero and 48 hours of treatment with MSC-CM and when migrating cells reached an optimum number in the scratch area (after 48 hours) some of the early migrating cells appeared to stop their migration and switch to proliferation and / or differentiation.

(A)

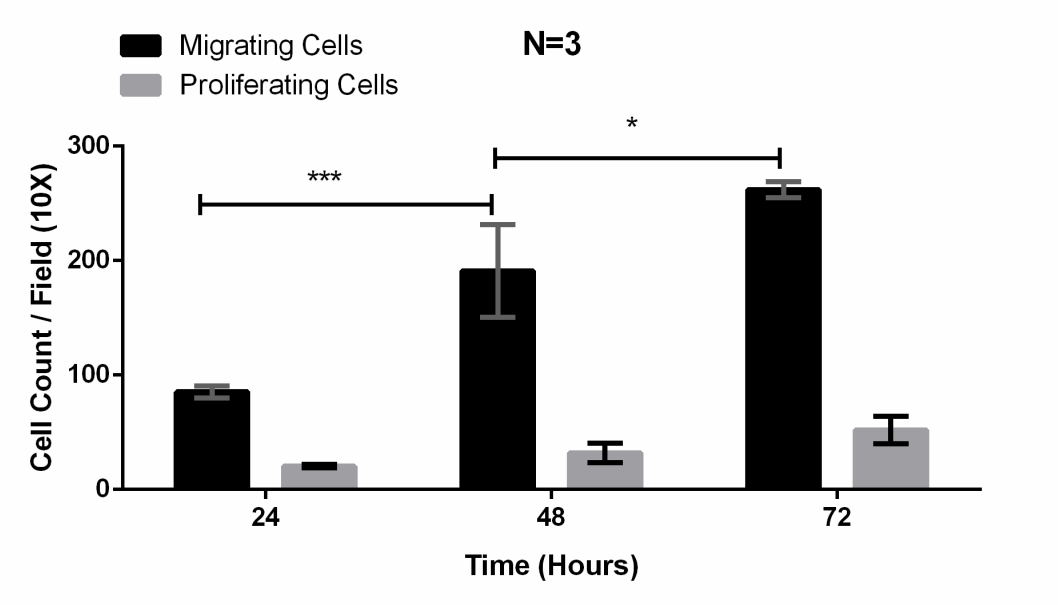

(B)

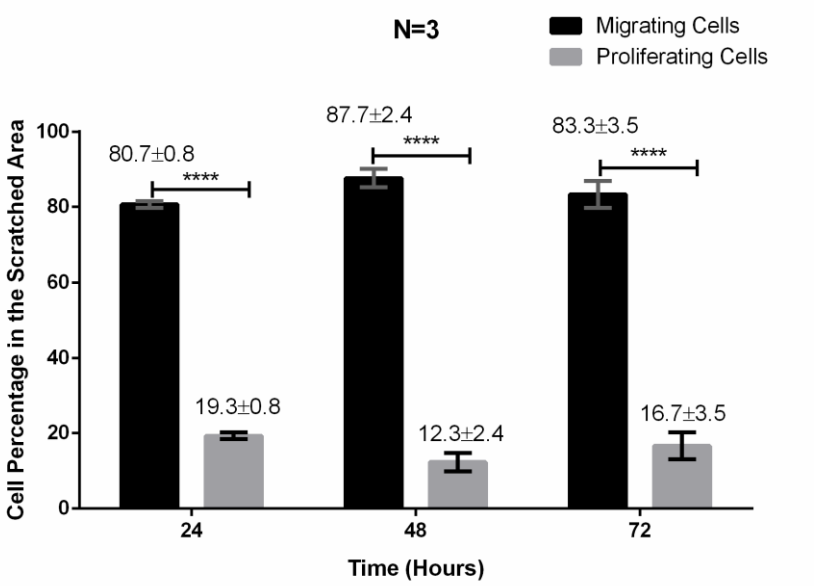

Figure 5.11 Numbers and ratios of migrating and proliferating cells during wound closure.

Numbers and ratios of migrating and proliferating cells in the scratched area at different time points (24, 48 and 72 hours). (A) Numbers of cells seen in a field of 10X magnification and revealed that numbers of migrating cells were larger than numbers than proliferating cells at the different time points. (B) Percentages of migrating and proliferating cells in the field of 10X magnification and presented as percentage ± standard error (SE) and showed that percentage of migrating cells were higher than numbers of proliferating cells. Bars and error bar= mean and standard error of mean (SEM), (=P<0.05), (**=P<0.01), (***=P<0.001) and (****=P<0.0001).*

5.3.2.3 *Effect of MSC-CM on Migration of Primary Keratinocytes treated with Mitomycin C (MMC)*

Since the ratio of proliferating keratinocytes during the healing process were non-significant compared to migrating cells within the first 48 hours, more experiments were undertaken to confirm whether wound closure was mainly attributed to migration, proliferation, or both. Therefore, the scratch assay using primary keratinocytes was repeated again in the presence of the proliferation inhibitor Mitomycin C (MMC). In the scratch assay, 20 µg / ml of MMC was added to the cells 3 hours before scratching the monolayer and prior to treatment with MSC-CM (LC-CM).

As shown in (Figure 4.10) LC-CM enhanced migration of the cells towards the scratch centre after 24 hours of treatment compared to the control. However, at the end of the treatment time (72 hours), cells treated with LC-CM failed to close the scratch area completely. Interestingly, after 40 hours of treatment, there were some changes observed in the migrating cells. For instance, the cells started to change their morphology, became more flattened and stacked up against each other resulting in a tissue-like structure and no single cells could be observed. In addition, migration was restricted resulting in partial and incomplete closure. These features were signs of keratinocyte differentiation suggesting that after 40 hours, when cells stopped migrating and did not proliferate anymore because of the action of MMC, they switched from migration to differentiation leading to the formation of an epidermal-like layer instead of a single cell monolayer. Subsequently, cells pulled outwards from the wound from centre resulting in non-complete or partial wound closure.

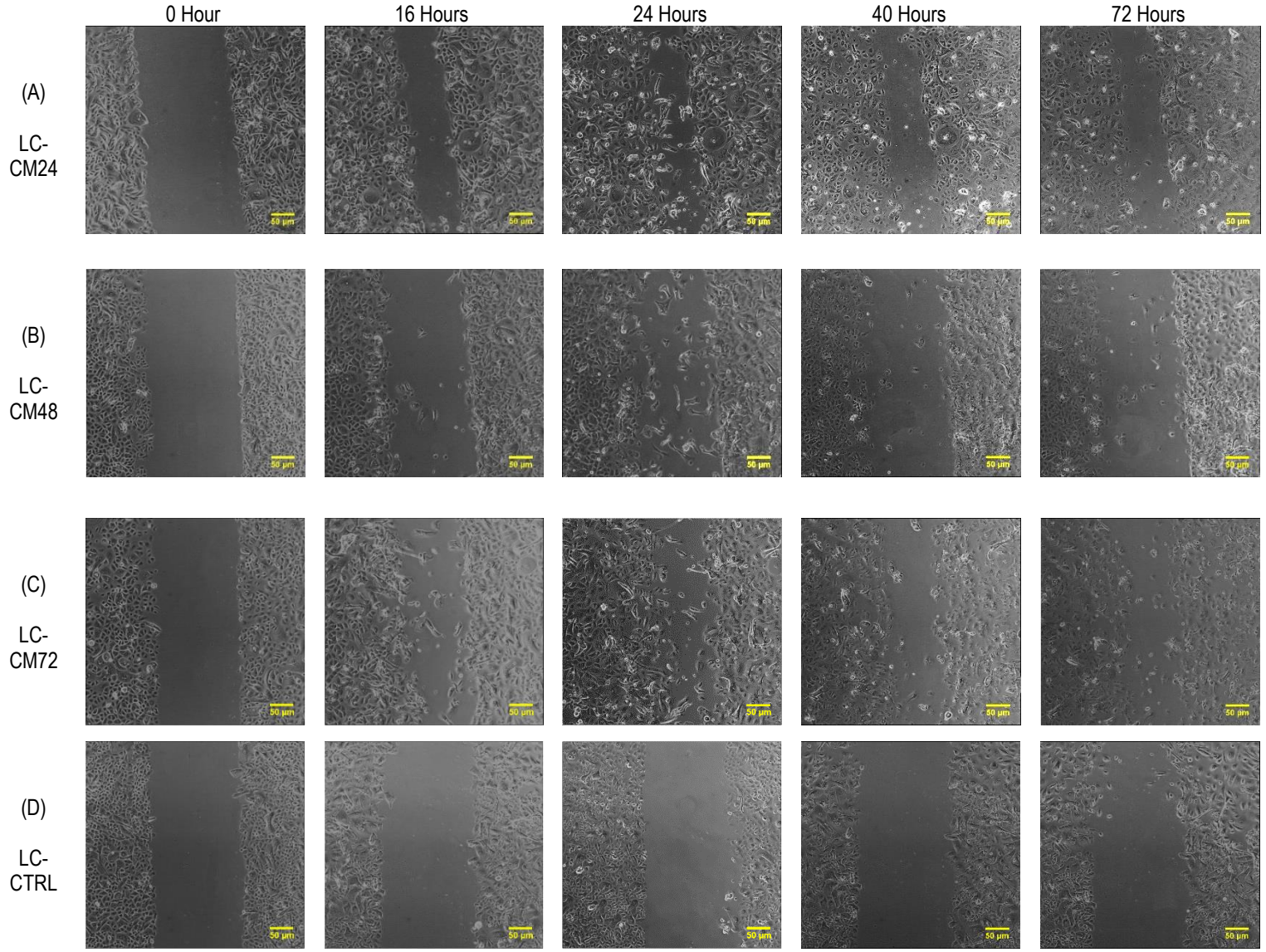

Representative images of the scratch assay using primary keratinocytes treated with 20 µg/ml MMC for 3 hours then treated with (A) LC-CM24, (B) LC-CM48, (C) LC-CM72, (D) control (LC-CTRL) for 72 hours. LC-CM enhanced migration of keratinocytes after 16 hours compared to the control. At 40 hours cells stopped migrating, changed their morphology and gained differentiation characteristics with partial closure at 72 hours. Scale bar=50 µm.

Figure 5.12 Migration of primary keratinocytes treated with MMC using a 2D scratch assay.

Two way ANOVA (Figure 5.13) showed that both LC-CM24 and LC-CM72 caused enhanced cell migration after 16 hours of treatment (P<0.01) while LC-CM48 enhanced migration at 48 hours (P<0.0001) compared to the control. Migration was arrested between 24 and 40 hours, since cells treated with MSC-CM stopped migrating and the wound size at 48 hours was the same in size as the gap at 24 hours (P>0.05). However, the three LC-CM caused enhanced cell migration again at 48 hours until the end of the assay (72 hours) (P<0.0001) compared to the control.

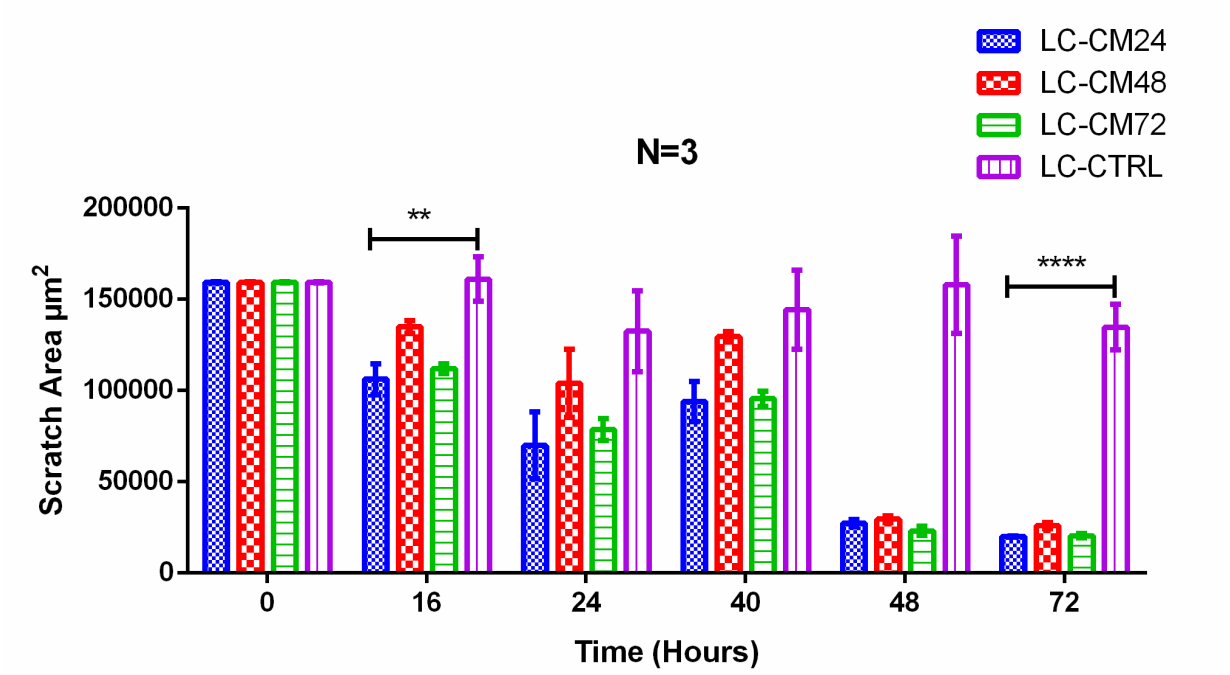

Figure 5.13 Statistical analysis of the effect of LC-CM on migration of primary keratinocytes treated with MMC.

MSC-CM (LC-CM) significantly enhanced migration of keratinocytes inhibited to proliferate (IP) by MMC compared to the control. LC-CM24 and LC-CM72 enhanced migration after 16 hours (P<0.01) while LC-CM48 started the effect after 48 hours (P<0.01). Migration of cells treated with the three CM was arrested between 24 and 48 hours (P>0.0001). However, the cells retained their ability to migrate again after 40 hours resulting in reduction of the scratch area after 72 hours compared to the control (P<0.0001). Bar and error bars= Mean and standard error of mean (SEM). (=P<0.05), (**=P<0.01), (***=P<0.001) and (****=P<0.0001).*

These data suggest that primary keratinocytes can migrate, proliferate and differentiate during the healing process. The order of these activities may vary depending on demand at the injury site.

5.3.2.4 *Detection of Migrating and Proliferating Cells During Wound Closure of MMC-treated Keratinocytes (Inhibited Proliferation "IP")*

The same samples (S112K, S1214K and S1216K) (N=3) were treated with 20 µg/ml MMC for 3 hours at SCC followed by incubation with 3 µg/ml BrdU overnight. The following day, cells were scratched and treated with MSC-CM and stained with anti-BrdU antibody and secondary antibody at different time points (24, 48 and 72 hours). As shown in (Figure 5.14), (Figure 5.15), and (Figure 5.16) part A of each figure showed no BrdU positive cells were observed in the scratch area at 24 hours. Meanwhile, there was mobility of non-proliferating cells (BrdU negative cells) which represented migrating cells (DAPI stained). Parts B and C represent wound closure at 48 and 72 hours respectively and showed that more proliferating cells were observed in the scratch area compared to 24 hours. These data suggest that when cells were treated with MMC they lost their ability to proliferate, hence they either migrated or differentiated. Since the biological demand requires cell migration to fill the wound gap, cells migrated rather than differentiated until the end of the assay.

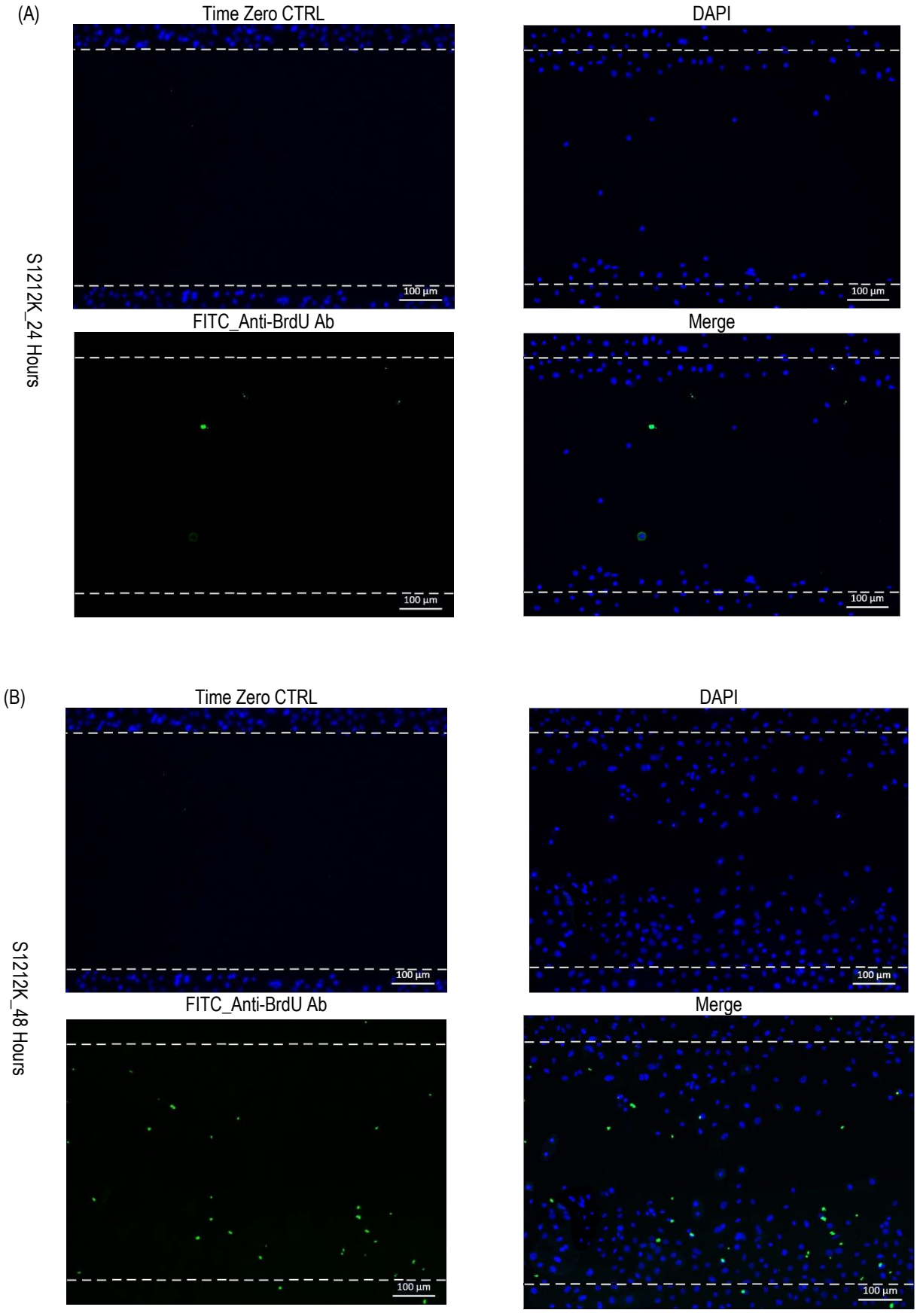
(A)
Time Zero CTRL
DAPI
S1212K_24 Hours
FITC_Anti-BrdU Ab
Merge
100 µm
(B)
Time Zero CTRL
DAPI
S1212K_48 Hours
FITC_Anti-BrdU Ab
Merge
100 µm

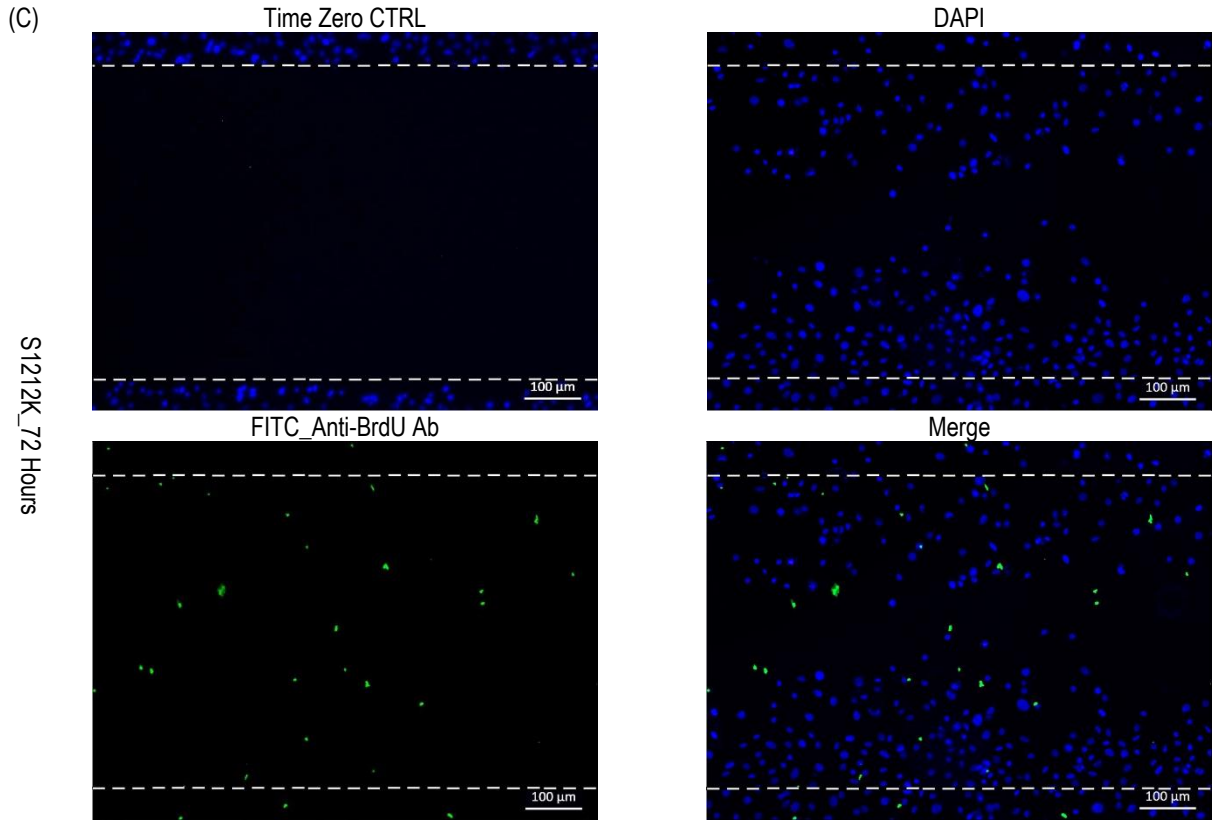

Figure 5.14 Migrating and proliferating MMC-treated cells during wound closure using sample S1212K.

Representative immunofluorescence images revealing proliferating and migrating primary keratinocytes during the wound closure assay for different time points (A) 24 hours, (B) 48 hours and (C) 72 hours. Confluent monolayer of primary keratinocytes treated with 20 µg/ml MMC for 3 hours at SCC then labelled with BrdU overnight at SCC then scratched and treated with MSC-CM. Green signal represent proliferating cells (BrdU positive cells) stained with anti-BrdU antibody (ab152095) at (1:60) in (1% bovine serum albumin (BSA). Green signal revealed binding of anti-BrdU antibody with BrdU of replicating cells and when stained with Donkey Anti-Rabbit IgG H&L (Alexa Fluor® 488) (ab150073) at (1:250) in (1% bovine serum albumin) gave a green signal (FITC). BrdU negative cells represent migrating cells which mainly stained with DAPI. Time zero control cells are DAPI stained. Blue= DAPI stain (1:1000) in (1% BSA). Magnifier 10X, Scale bar= 100 µm.

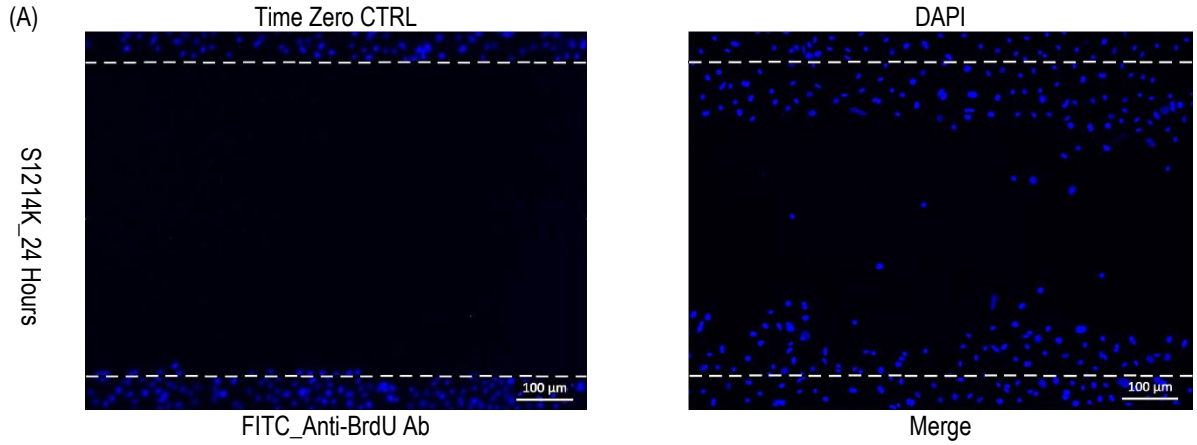

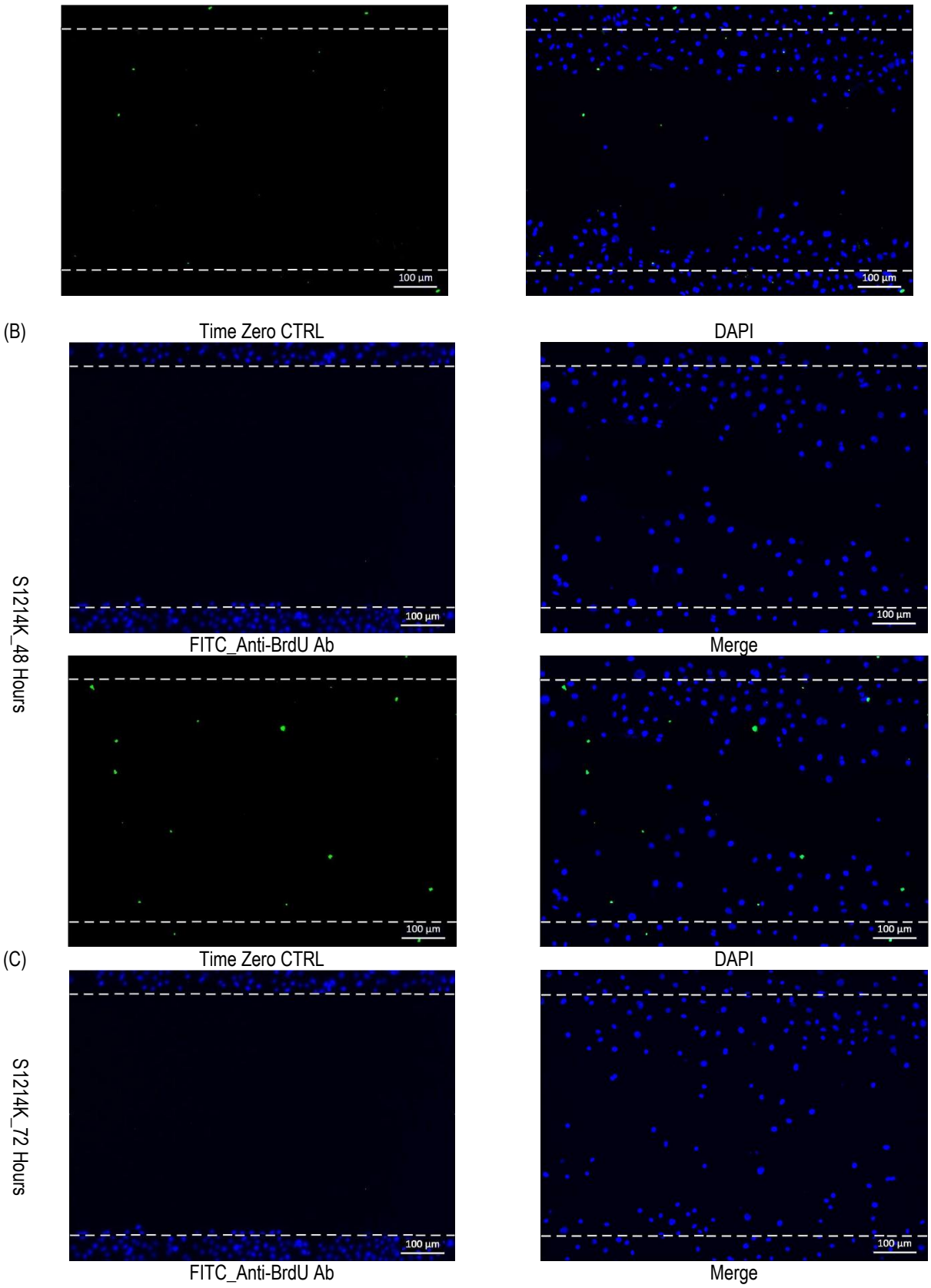
100 µm
(B)
Time Zero CTRL
DAPI
S1214K_48 Hours
FITC_Anti-BrdU Ab
Merge
(C)
Time Zero CTRL
DAPI
S1214K_72 Hours
FITC_Anti-BrdU Ab
Merge

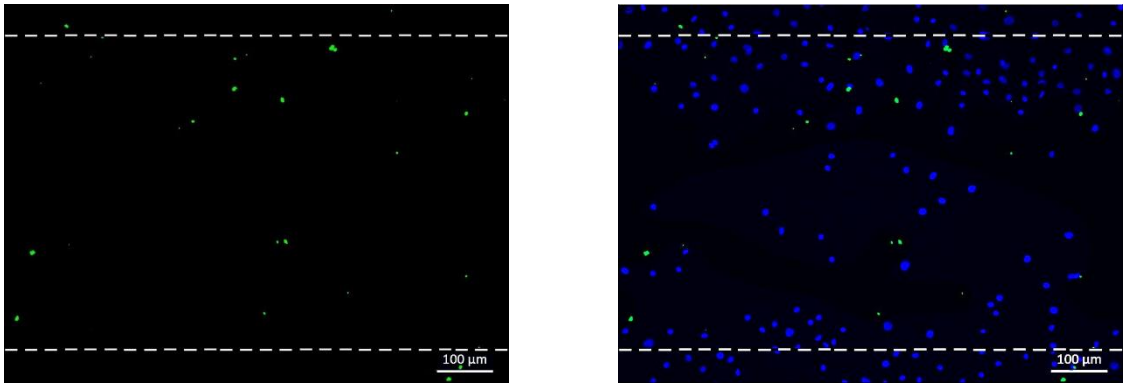

Figure 5.15 Migrating and proliferating MMC-treated cells during wound closure using sample S1214K.

Representative immunofluorescence images revealing proliferating and migrating primary keratinocytes during the wound closure assay for different time points (A) 24 hours, (B) 48 hours and (C) 72 hours. Confluent monolayer of primary keratinocytes treated with 20 µg/ml MMC for 3 hours at SCC then labelled with BrdU overnight at SCC then scratched and treated with MSC-CM. Green signal represent proliferating cells (BrdU positive cells) stained with anti-BrdU antibody (ab152095) at (1:60) in (1% bovine serum albumin (BSA). Green signal revealed binding of anti-BrdU antibody with BrdU of replicating cells and when stained with Donkey Anti-Rabbit IgG H&L (Alexa Fluor® 488) (ab150073) at (1:250) in (1% bovine serum albumin) gave a green signal (FITC). BrdU negative cells represent migrating cells which mainly stained with DAPI. Time zero control cells are DAPI stained. Blue= DAPI stain (1:1000) in (1% BSA). Magnifier 10X, Scale bar= 100 µm.

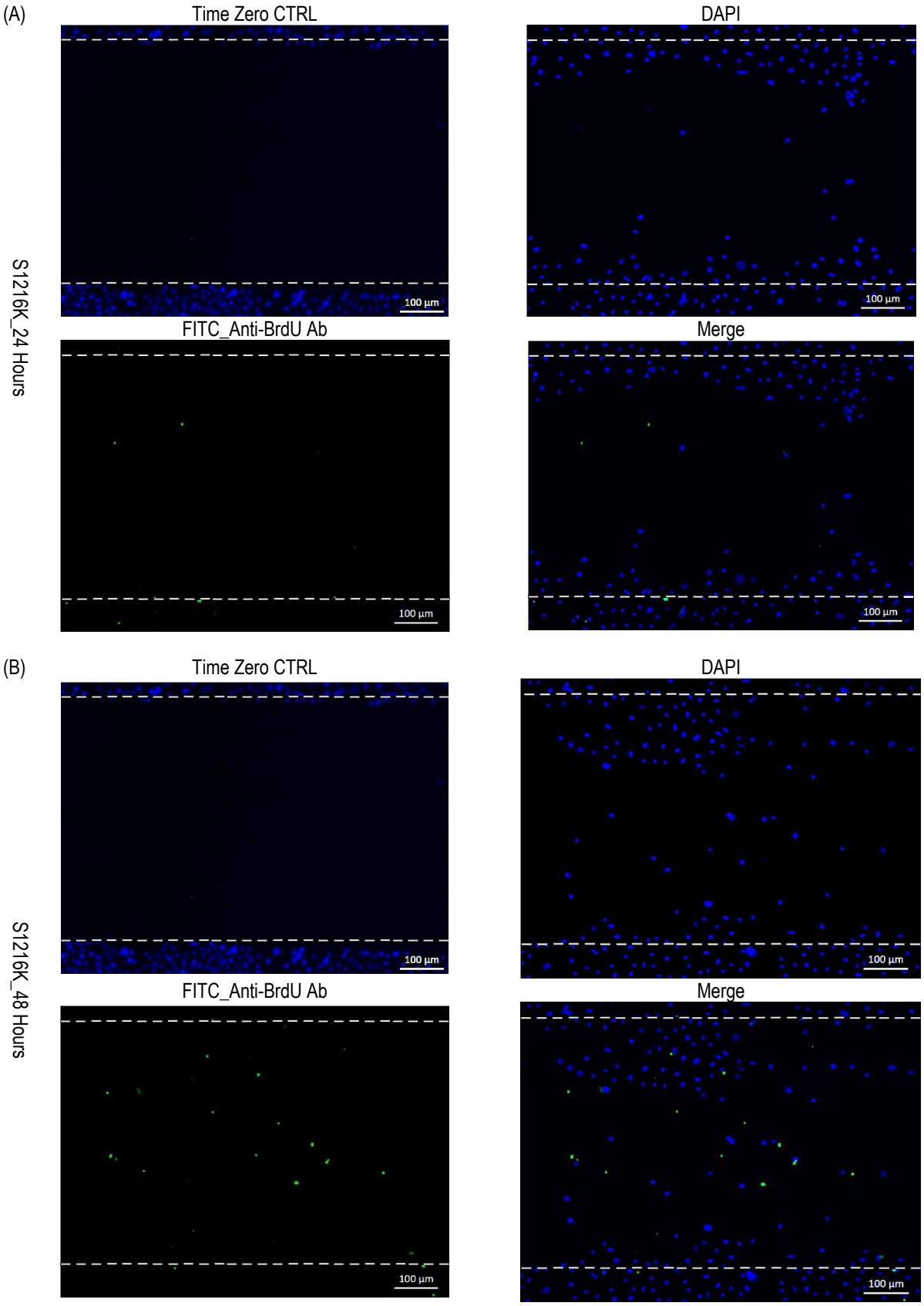
(A)
Time Zero CTRL
DAPI
S1216K_24 Hours
FITC_Anti-BrdU Ab
Merge
100 µm
(B)
Time Zero CTRL
DAPI
S1216K_48 Hours
FITC_Anti-BrdU Ab
Merge
100 µm

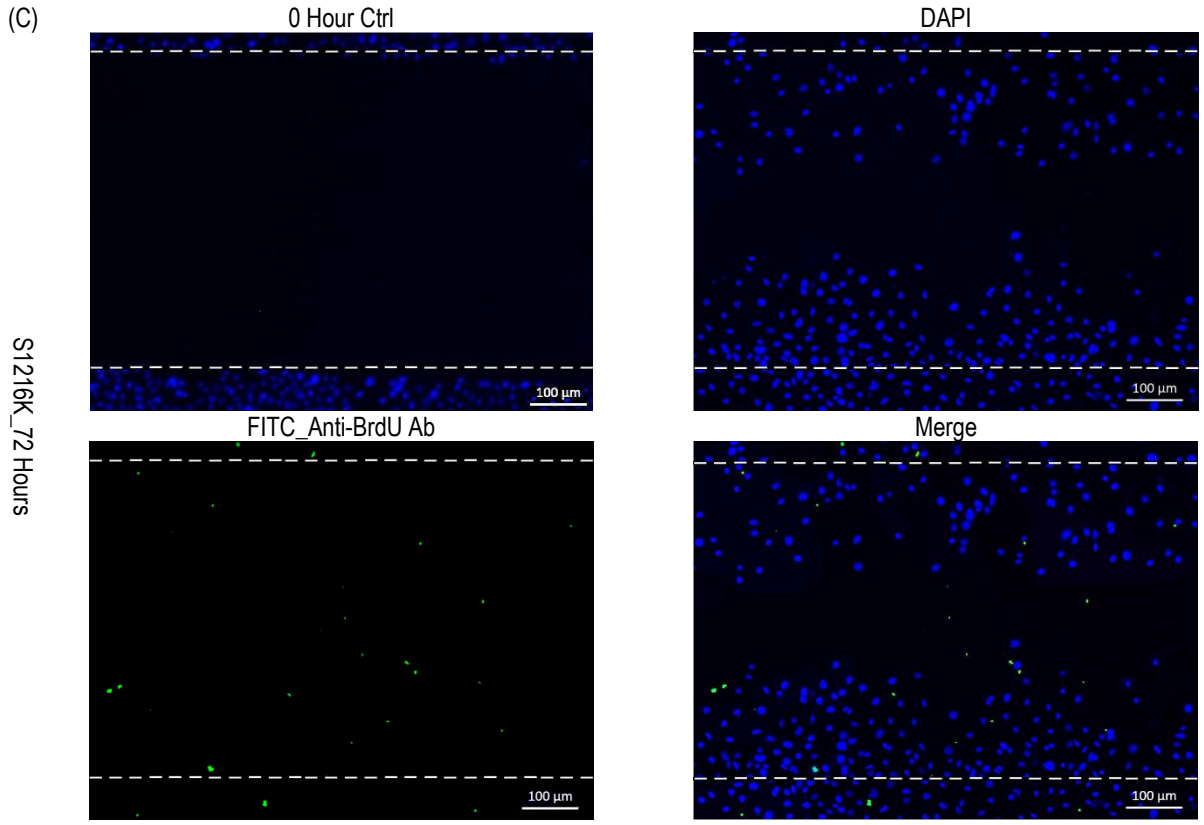

Figure 5.16 Migrating and proliferating MMC-treated cells of inhibited proliferation during wound closure using sample S1216K.

Representative immunofluorescence images revealing proliferating and migrating primary keratinocytes during the wound closure assay for different time points (A) 24 hours, (B) 48 hours and (C) 72 hours. Confluent monolayer of primary keratinocytes treated with 20 µg/ml MMC for 3 hours at SCC then labelled with BrdU overnight at SCC then scratched and treated with MSC-CM. Green signal represent proliferating cells (BrdU positive cells) stained with anti-BrdU antibody (ab152095) at (1:60) in (1% bovine serum albumin (BSA). Green signal revealed binding of anti-BrdU antibody with BrdU of replicating cells and when stained with Donkey Anti-Rabbit IgG H&L (Alexa Fluor® 488) (ab150073) at (1:250) in (1% bovine serum albumin) gave a green signal (FITC). BrdU negative cells represent migrating cells which mainly stained with DAPI. Time zero control cells are DAPI stained. Blue= DAPI stain (1:1000) in (1% BSA). Magnifier 10X, Scale bar= 100 µm.

For statistical analysis, counts and percentages of cells in the scratch area were calculated at different time points (24, 48 and 72 hours) and presented in (Table 5.2 A and B).

	Time	Migrating Cells				Proliferating Cells			
		S1212K	S1214K	S1216K	Total	S1212K	S1214K	S1216K	Total
(A)	24 Hours	72	97	122	291	4	9	3	16
	48 Hours	254	131	114	499	25	12	15	52
	72 Hours	278	119	240	637	25	16	17	58
	Time	Migrating Cells				Proliferating Cells			
		S1212K	S1214K	S1216K	Average	S1212K	S1214K	S1216K	Average
(B)	24 Hours	95	92	97	94.66	5	8	3	5.33
	48 Hours	91	92	88	90.33	9	8	12	9.66
	72 Hours	92	88	93	91	8	12	7	9

Table 5.2 Numbers and ratios of migrating and proliferating MMC-treated cells in the scratch area during wound healing.

Counts and ratios of migrating and proliferating keratinocytes treated with MMC to inhibit their proliferation during wound closure at different time points (24, 48 and 72 hours). (A) Numbers presented as cell number seen in a field of 10X magnification. (B) Percentages of cells in the scratch area at different time points.

Two way ANOVA showed that there was a significant increase in the number of migrating cells with time. As explained in (Table 5.2 A) and (Figure 5.17 A), the cell count after 72 hours (212±47) was significantly higher than the cell count at 24 hours (97±14) ($P<0.05$) and ($P<0.01$). However, there was no significant difference in cell count between 48 hours (166±44) and 24 hours ($P>0.05$). The numbers of migrating cells at 24, 48 and 72 hours were significantly increased compared to the numbers of proliferating cells (5±2, 17±4 and 19±3) at the same time points ($P<0.05$, $P<0.01$ and $P<0.0001$) respectively. In other words, the percentage of migrating cells (95±1%, 90±1% and 91±2%) was significantly higher than the percentage of proliferating cells (5±1%, 10±2% and 9±2%) ($P<0.0001$) at the three time points (24, 48 and 72 hours) respectively as illustrated in (Table 5.2 B) and (Figure 5.17 B). On the other hand, there was no significant increase in the percentage of proliferating cells at 24, 48 and 72 hours ($P>0.05$).

(A)

(B)

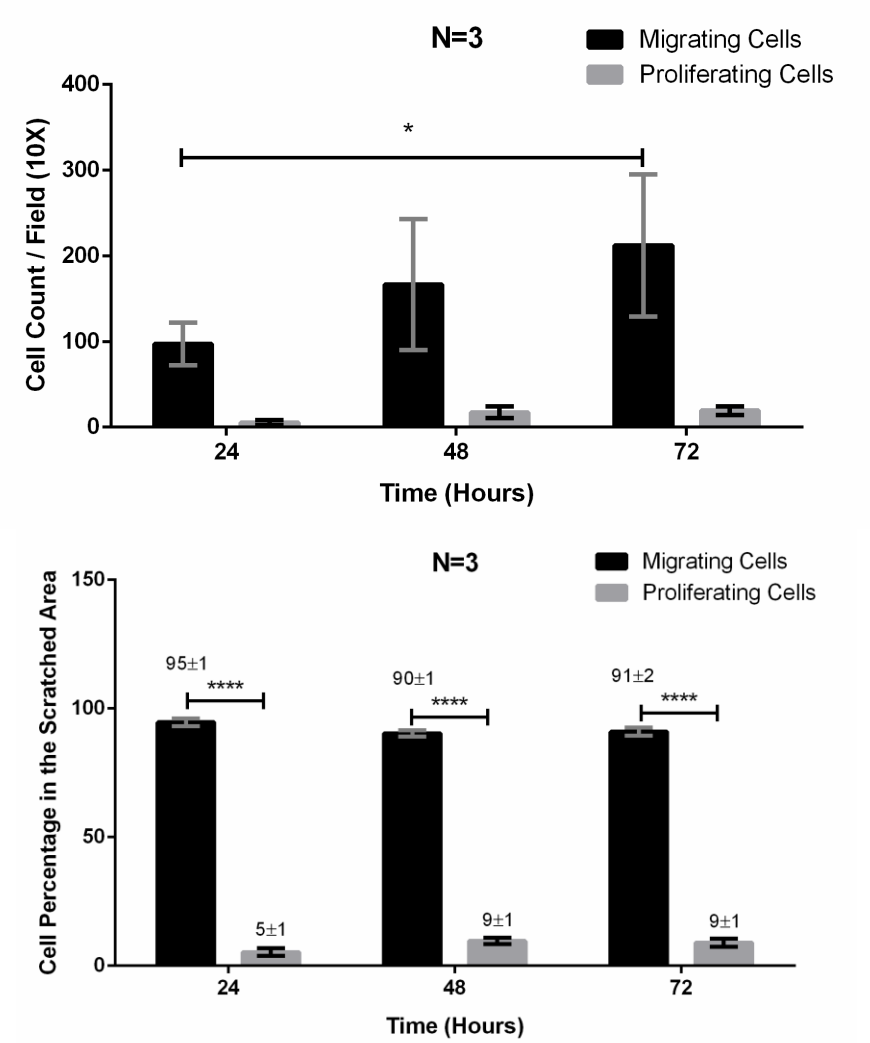

Figure 5.17 Numbers and ratios of migrating and proliferating keratinocytes treated with MMC inhibited proliferation (IP) during wound closure.

Numbers and ratios of migrating and proliferating cells (MMC treated keratinocytes) in the scratched area at different time points (24, 48 and 72 hours). (A) Numbers of cells seen in a field of 10X magnification and revealed that numbers of migrating cells were larger than numbers of proliferating cells at the different time points. (B) Percentages of migrating and proliferating cells in the field of 10X magnifier presented as percentage ± standard error (SE) and revealed that percentage of migrating cells were higher than that of proliferating cells. Bars and error bar= mean and standard error of mean (SEM), (=P<0.05), (**=P<0.01), (***=P<0.001) and (****=P<0.0001).*

Migration of MMC treated and untreated keratinocytes (inhibition of proliferation (IP) and non-inhibition of proliferation (NIP)) were statistically compared using two-way ANOVA. There was no significant differences (P>0.05) between the numbers of migrating cells in the scratch area in both conditions (IP and NIP) at the different time points (24, 48 and 72 hours) (Figure 5.18 A). In addition, there was no significant variations (P>0.05) between the percentage of migrating cells in both conditions (IP and NIP) at 48 and 72 hours.

However, at 24 hours the ratio of migrating IP cells in the scratch area was significantly higher than the ratio of migrating NIP cells (P<0.01) (Figure 5.18 B). Interestingly, the percentage of IP cells was higher than that of NIP cells at 24 hours (P<0.01). However, there was no significant variation between proliferating IP and NIP cells at time 48 and 72 hours (P>0.05). These data suggest that MSC-CM mainly enhanced migration of primary keratinocytes during wound healing rather than proliferation and differentiation.

(A)

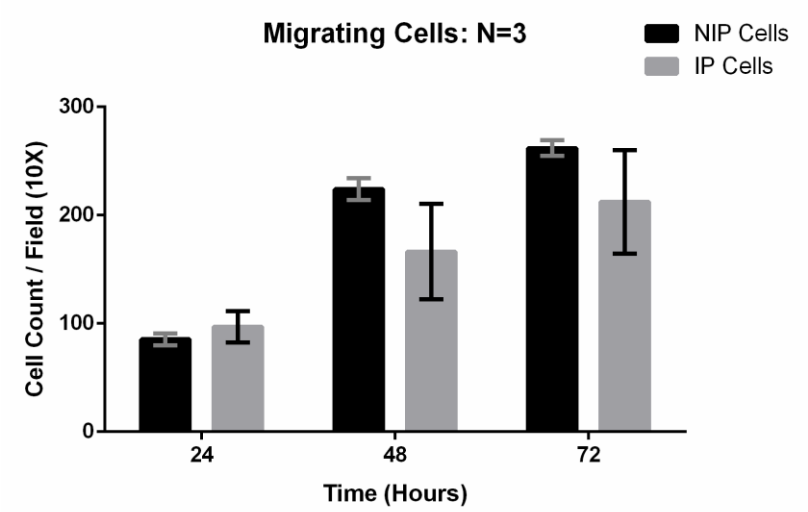

(B)

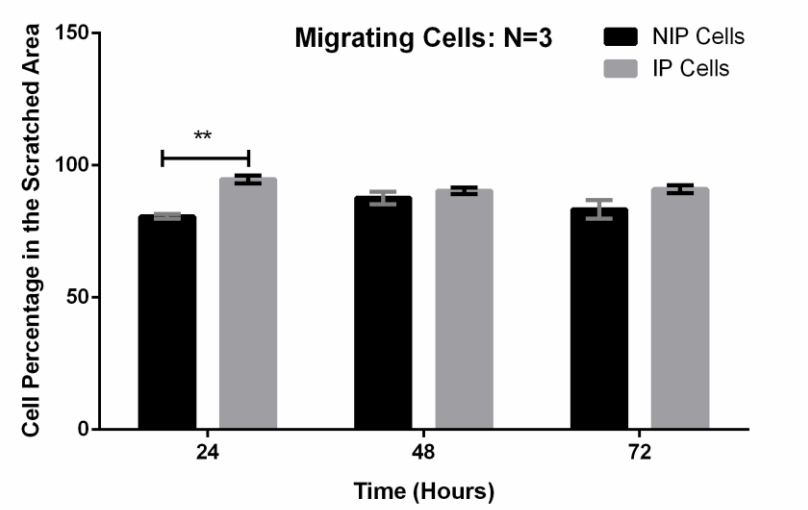

Figure 5.18 Statistical comparison between numbers of migrating keratinocytes treated with MMC (inhibition of proliferation (IP) and untreated keratinocytes (non-inhibition of proliferation (NIP) during wound closure.

*Migrating keratinocytes in both conditions (IP and NIP) showed consistent ability to migrate during wound closure. (A) Cell numbers at the two conditions were similar with no significant variation (P>0.05) at the different time points (24, 48 and 72 hours). (B) Percentages of migrating IP cells was significantly higher (P<0.01) than the percentage of NIP cells at 24 hours. Bar and error bars= mean and standard error of mean (SEM), (**=P<0.01).*

The statistical comparison of proliferating cells in IP cells and NIP cells revealed that numbers of proliferating NIP cells and IP cells were similar at 24 and 48 hours (P>0.05) while the number of NIP cells was greater than IP cells at 72 hours (P<0.01) as shown in (Figure 5.19 A). On the other hand, percentages of proliferating NIP cells were significantly higher than that of proliferating IP cells only at 24 hours (P<0.01) while they were similar at 48 and 72 hours (P>0.05) (Figure 5.19 B).

(A)

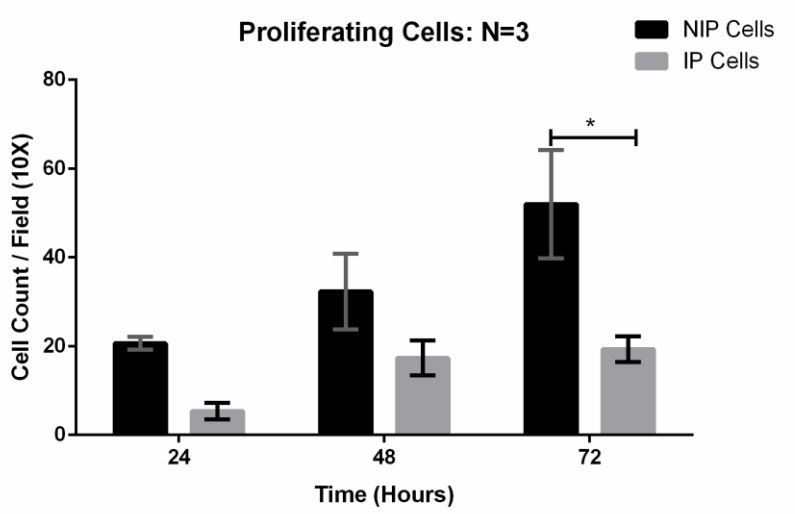

(B)

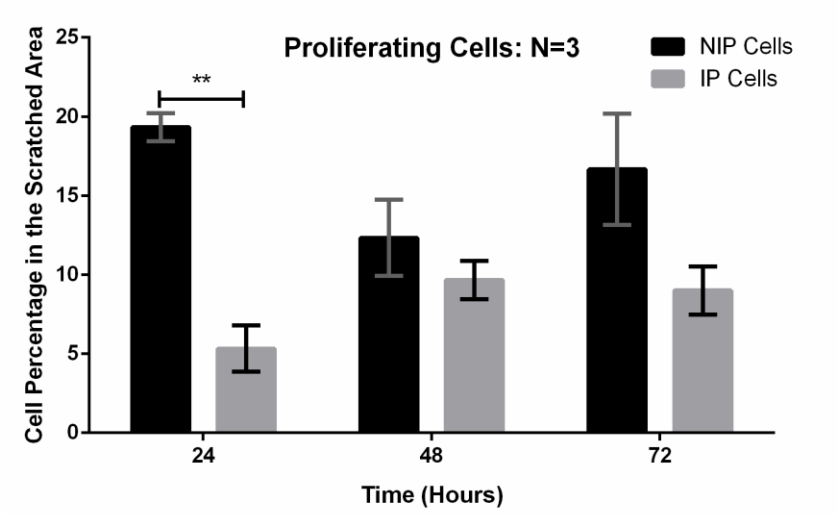

Figure 5.19 Comparison between proliferating cells with inhibited (IP) and non-inhibited proliferation (NIP) during wound closure.

*Primary keratinocytes in both conditions (IP and NIP) showed only a slight ability to proliferate during wound closure. (A) Cell numbers at the two conditions were similar with only significantly higher numbers of NIP cells (P<0.01) at 72 hours. (B) Percentages of proliferating cells at the two conditions were similar with only significantly higher numbers of NIP cells (P<0.01) at 24 hours. Bar and error bars= mean and standard error of mean (SEM), (**=P<0.01).*

5.4 DISCUSSION

During normal conditions and homeostasis, proliferation and differentiation of keratinocytes are equally balanced. In contrast, during skin disease and pathological conditions such as epidermal wounds these two cellular activities will be imbalanced and dysregulated. Cross talk of growth factors and cytokines derived from MSCs can affect these events (Taniguchi *et al.*, 2014). Therefore, the effect of MSC-CM was tested on proliferation of keratinocytes and fibroblasts. Keratinocyte proliferation was tested at different conditions including intact primary cells at normal conditions and scratched keratinocytes with and without MMC (proliferation inhibitor) to determine whether MSC-CM enhanced migration or proliferation or both during the healing process. Beyond covering the wound with the epidermal layer by migrating keratinocytes, the early migrating cells start to proliferate and act as a supply for cells to enclose the wound area. Results of HaCat cells treated with MSC-CM showed that they retained their ability to grow and proliferate normally without significant variation compared to the control. As mentioned before, studies from cell lines are inaccurate due to the highly proliferative ability of the cells, which may interfere with the actual effect that could be caused by MSC-CM, subsequently, giving rise to false positive results.

Treating primary keratinocytes with HC-CM showed no significant changes in cell proliferation between time zero and 96 hours indicating that MSC-CM arrested cell proliferation. However, results using LC-CM showed that cell proliferation was arrested between time zero and 48 hours and that there was significant increase in cells viability after 96 hours indicating that MSC-CM enhanced cell proliferation. These results suggest that the high calcium level present in HC-CM enhances cell differentiation rather than proliferation. Proliferation and differentiation are remarkably inverse relationships since precursor cells retain their dividing ability until acquisition of full differentiation, whereas terminally differentiated cells trigger the cell to exit cell division and thereby, arrest cell proliferation (Ruijtenberg and van den Heuvel, 2016). Therefore, during normal conditions (where there is no damage), upon stimulation by the external stimulators cells respond and evoke one main cellular activity. In the case of monolayer culture, cells are directed to either proliferate or differentiate. Upon treatment with MSC-CM (HC-CM), the high calcium level promoted cell differentiation rather than proliferation in contrast to LC-CM, which enhanced cell proliferation at 48 hours, which in turn blocked differentiation.

Consequently, using of LC-CM was preferred for the wound healing studies. However, HC-CM could be used when fibroblast were tested since primary fibroblasts retained their proliferative ability when treated with HC-CM and showed significant increase in cell viability within time.

The increase in viability of primary keratinocytes treated with LC-CM was not significantly different compared to the serum free control within 48 hours, suggesting that migration of these cells, instead of proliferation, was the major mechanism for accelerated wound closure, irrespective of LC-CM. In contrast, HC-CM arrested both proliferation and migration of primary keratinocytes during the entire treatment period (72 hours) and resulted in non-closed scratches compared with the control. This could be attributed to the early differentiation of these cells which was enhanced at 24 hours by the high calcium level (Segrelles *et al.*, 2011). Since primary keratinocyte retained their ability to proliferate in LC-CM, more investigations were carried out to identify which cellular response could be the first to enhance wound closure; migration or proliferation. The 2D scratch assay was repeated again to detect migrating and proliferating cells in the scratch area in the presence of MMC to inhibit proliferation. In the absence of MMC, cells at the wound area were increased during time resulting in wound closure. Upon analysis of BrdU positive proliferating cells, less than 20±2.28% of the cells in the scratch area were positive indicating that the rest of cells (80±2.28%) were migrating cells. To explore the hypothesis that MSC-CM enhanced both migration and proliferation in the early stages of the healing process, the ability of cells to migrate in response to MSC-CM in the presence of MMC was further tested. Results were in agreement of Wickert and colleagues and revealed that inhibition of proliferation did not have a negative effect on wound repair (Wickert *et al.*, 2016). On the other hand, cells treated with MMC retained their ability to migrate under the effect of LC-CM, moving towards the scratch centre and significantly reducing the gap with time. The presence of 20±2.28% proliferating cells in the scratch area could be interpreted by the fact that keratinocytes at the wound edges are highly proliferative rather than being migrating or differentiating (Usui *et al.*, 2008b; Wickert *et al.*, 2016). In another words, the proliferating cells at the wound edges could not be attributed to the action of MSC-CM. Usui and colleagues have suggested that although keratinocyte proliferation is needed to fill the wound gap, the absence of the appropriate signalling molecules that downregulate proliferation and upregulate migration would delay the healing process

(Usui *et al.*, 2008b). The activity of MSC-CM appear to perform two functions; the first one is preventing the proliferation of the cells and the second is enhancing them to migrate. The consistency of migrating cells during the entire healing process (80±2.28%) at 24, 48 and 72 hours indicating that MSC-CM enhanced primary keratinocyte migratory behaviour during the healing process resulting in a so-called collective cell migration, an important step for re-epithelialisation. Treatment with MSC-CM therefore overcomes discontinuous migration leading to successful repair (Ng *et al.*, 2012).

In the MMC treated cell scratch assay, termination of cell migration at 40 hours was observed and the primary cells started to change their morphology, became flatten cells, contacted neighbouring cells, and started to form tissue-like structures indicating their differentiation. This could be interpreted by the fact that upon termination of migration, cells started to either proliferate or differentiate. Since their proliferation was inhibited by MMC in this experiment, the only activity they can respond to is cell differentiation. Another explanation of termination of migration and starting differentiation is the fact that upon filling the gap, cells started to contact each other and became under physical stress due to the formation of cell adhesion structures. These structures in turn activate membrane kinases, leading to increasing membranous permeability for calcium, thereby, enhancing differentiation and terminating migration (Jacinto *et al.*, 2001).

The activity of MSC-CM on wound healing could be caused by HGF which enhances keratinocytes to migrate, proliferate and produce matrix metalloproteinase (van de Kamp *et al.*, 2013) and MSP-1 which regulates proliferation and differentiation of different cells including keratinocytes (Werner and Grose, 2003). As discussed above, several factors secreted by MSCs create an optimal environment for the healing process including controlling cell migration, cell division, survival and / or proliferation and differentiation. Therefore, the role of MSC-CM in the wound healing process suggests increasing stimulating cell mobility, proliferation and differentiation.

Comparing the ratio of proliferating cells in the scratch area after 72 hours in both MMC treated and MMC-untreated assays showed that there was no variation between cell counts suggesting that during damage, the primary cell behaviour is enhancing cell migration rather than cell proliferation. MSC secretions could significantly affect this on/off switching of cellular activities.

Collective data from this study suggest a combination of cell responses during the healing process. Healing of cutaneous wounds represent a paradigm for the spatiotemporal interactions of growth factors and cytokines to regulate cell mobility and cell division and proliferation (Werner and Grose, 2003). It is well documented that keratinocytes at the wound borders are highly proliferative (Werner and Grose, 2003; Usui *et al.*, 2008b; Wickert *et al.*, 2016). Since proliferation and motility are mutually exclusive (De Donatis *et al.*, 2008), the challenge will be to terminate cell proliferation and enhance cell migration in order to promote the healing process (Werner and Grose, 2003). This mechanism could be achieved by growth factors such as KGF, HGF (Florin *et al.*, 2004; Schnickmann *et al.*, 2009) and PDGF (De Donatis *et al.*, 2008). A possible interpretation of how these growth factors coordinate two cellular activities concurrently is demonstrated by Donatis and colleagues who reported that cell migration could be evoked by low concentrations of platelet derived growth factor (PDGF) and terminated with high concentrations and vice versa for cell proliferation. In another words, low concentrations of PDGF evokes signalling pathways related to cytoskeletal cascades required for cell mobility while high concentrations of PDGF trigger signalling pathways related to mitogenesis induction (De Donatis *et al.*, 2008). Alternatively, cell growth factor requirements for migration may be lower than that required for proliferation. This explanation could be one interpretation of the scratch assays, when keratinocyte migration was always evoked at early stages of the healing process (after 8 hours of inducing the scratch). In contrast, cell proliferation was evoked after 72 hours of the scratch when cell migration terminated and the concentration of growth factors had increased with time.

In summary, secretions of mesenchymal stem cells (MSC-CM) collected at low calcium conditions (LC-CM) exerted a positive effect on primary keratinocyte proliferation while HC-CM failed to enhance cell proliferation. These data suggest four main findings. First, there was an inverse relationship between migrating and proliferating cells after 24 hours; when proliferating cells were inhibited, their migration increased. Second, migrating cells were observed in greater numbers than proliferating cells in the scratch area regardless of whether their proliferation was inhibited or not. Third, migrating cells at both conditions (IP and NIP) were similar after 24 hours. Fourth, the ratio of proliferating cells of both IP and NIP were relatively the same after 24 hours. Collectively, these data suggest that MSC-CM enhanced cell migration during wound healing rather than proliferation and

differentiation. When the cells filled the scratch area, they appeared to switch their biological function from migration to proliferation and/or differentiation. However, results obtained from 2D culture are still inadequate and more investigations using 3D model are required to verify the vital role of MSC-CM on cell migration and proliferation during the healing process using a realistic wound healing 3D skin model involving whole tissue layers or tissue-like structures. In the next chapter (Chapter 6), a 3D skin model equivalent is developed for use in wound healing studies.

CHAPTER 6 DEVELOPING A PROTOTYPE 3D SKIN EQUIVALENT MODEL (3D-SEM) AND ROBUST PROTOCOL FOR WOUND HEALING STUDIES

CHAPTER SIX: ADAPTING A PROTOTYPE 3D SKIN EQUIVALENT MODEL (3D-SEM) FOR WOUND HEALING STUDIES

6.1 INTRODUCTION

The standard screening procedure in drug discovery involves assessing the compound of interest through three main serial assessment steps; (1) testing *in vitro* in 2D cell culture, (2) testing *in vivo* in animal models and (3) clinical trials (DiMasi and Grabowski, 2007; Breslin and O'Driscoll, 2013). About 90% of the compounds and drugs tested following this procedure lacked clinical efficacy and showed unaccepted toxicity during clinical development indicating failure of the compound of interest (Hopkins, 2008; Breslin and O'Driscoll, 2013). Many of these failures may be attributed to the misleading results obtained from 2D cell culture assays, which represent an unnatural microenvironment with inappropriate cellular response to drugs (Edmondson *et al.*, 2014). To overcome the limitations such as high cost of clinical development and ineffective toxicity during *in vivo* trials, there is an urgent need to establish a new screening step before the *in vivo* screening phase in animal models. The 3D *in vitro* screening represents the most realistic step and mimics the cellular behaviour of cells living in the *in vivo* niche thereby, providing more predictable data and more accurate results (Breslin and O'Driscoll, 2013; Edmondson *et al.*, 2014).

All cutaneous models constructed for wound healing studies demand a standard method for wound induction. The main protocols for wound creation include needle puncture (Xu and Chisholm, 2014), laser exposure (Xu and Chisholm, 2014; Marquardt *et al.*, 2015), electric cauterisation, ultrasound irradiation, punch biopsy (Marquardt *et al.*, 2015) and the suction blister method, used only for wound induction *in vivo* and not applicable for 3D models (Ferraq *et al.*, 2012) . The first and second methods require extra professional manipulation; and frequently result in a wound of inconsistent depth, size and shape making the comparison between the test and the control inaccurate (Ferraq *et al.*, 2012; Marquardt *et al.*, 2015). To date, there is an urgent need to adapt and establish more robust 3D-SEM suitable for the application of wound healing that mimics the conditions of a cutaneous wound *in vivo* (Marquardt *et al.*, 2015). Invention of the Alvetex®Scaffold has provided new means through which to establish a 3D-SEM for wound healing studies. The Alvetex®Scaffold is a highly porous cross-linked polystyrene membrane (200 µm in

thickness) with approximate pore sizes 36-40 microns, allowing cells and specifically fibroblasts to grow in a microenvironment similar to *in vivo* conditions while enabling them to retain their morphological and physiological characteristics and achieve cellular responses and communication to neighboring cells, similar to that of the *in vivo* environment (ReproCell Europe Ltd,) (former name: Reinnervate). Furthermore, the Alvetex®Scaffold has extended the application to different research areas. For example, Hill and colleagues developed a reliable robust 3D model for melanoma invasion studies using the Alvetex®Scaffold that does not contain collagen and relies on the production of the extra cellular matrix by dermal fibroblasts and is therefore most like human skin (Hill *et al.*, 2015). The Alvetex®Scaffold could be used not only for constructing a 3D skin model, but also for characterising other cell types and their behaviour in 3D cell culture rather than 2D culture. For example, in this study the Alvetex®Scaffold was used for testing the ability of MSCs to penetrate the Alvetex®Scaffold and testing their differentiation potential into skin or epidermal-like structures *in vitro.* Although, the ability of MSCs to differentiate into multi-lineages has been well studied and documented using scaffolds, the differentiation potential of these cells into skin or epidermal like cells remains largely undefined. A few papers have reported the ability of MSCs to differentiate into K14-expressing cells in 2D culture (Sasaki *et al.*, 2008). Ma and colleagues developed an organotypic co-culture of MSCs and fibroblasts enriched with collagen type I to test the ability of MSC to form an epidermal-like structure (Ma *et al.*, 2009). The disadvantages of this method however, are that it is constructed from animal materials and the generated model is very contractible, despite the use of a metal ring to prevent the contraction making the procedure more complicated. In this model, MSCs showed the ability to express keratin 10 and filaggrin but failed to express involucrin. In addition, haematoxylin-eosin (H-E) staining showed MSC's failed to form an epidermal like structure with clear stratification similar to that of real skin. Given the limitations of current 3D skin equivalents, which mainly contain animal materials and the lack of a consistent protocol for wound healing studies using fully humanised 3D skin models, the aims of the present chapter described below, were to further investigate the use 3D-SEM for wound healing studies.

6.2 SPECIFIC AIMS OF CHAPTER SIX

1. To reproduce a 3D skin equivalent model (3D-SEM) developed by Hill et al (Hill et al., 2015).
2. To validate the constructed 3D-SEM histopathologically by haematoxylin-eosin (H-E) staining and by the detection of dermal and epidermal differentiation markers using immunofluorescence (IF) and compare with normal skin.
3. To adapt the above *in vitro* 3D-SEM for wound healing studies.
4. To develop a donor-matched 3D-SEM protocol to induce either a superficial or a full thickness wound in the 3D-SEM with consistent depth, size and shape and fully characterised by IF.
5. To test the effect of MSC-CM on wound healing in the developed 3D-SEM.
6. To evaluate the differentiation potential of MSCs into epidermal-like cells in 3D culture using the Alvetex®Scaffold.

6.3 RESULTS

6.3.1 VALIDATION OF THE REPRODUCED 3D SKIN EQUIVALENT MODEL

All models generated in this study (N=3) were prepared as an organotypic culture composed of dermal and epidermal layers. The dermal layer was built from seeding fibroblasts which was then encased with the epidermal layer by seeding primary keratinocytes to form a multi-layered skin-like structure as

Haematoxylin-eosin (H-E) staining (Figure 6.1) revealed two distinct layers of dermis and epidermis separated by an obvious undulating junction with some collagen filaments were evident in the dermal layer. Additionally, the epidermal layer showed apparent stratification indicating full differentiation of keratinocytes into different epidermal sublayers, i.e. spinosum, granulosum, lucidum and corneum.

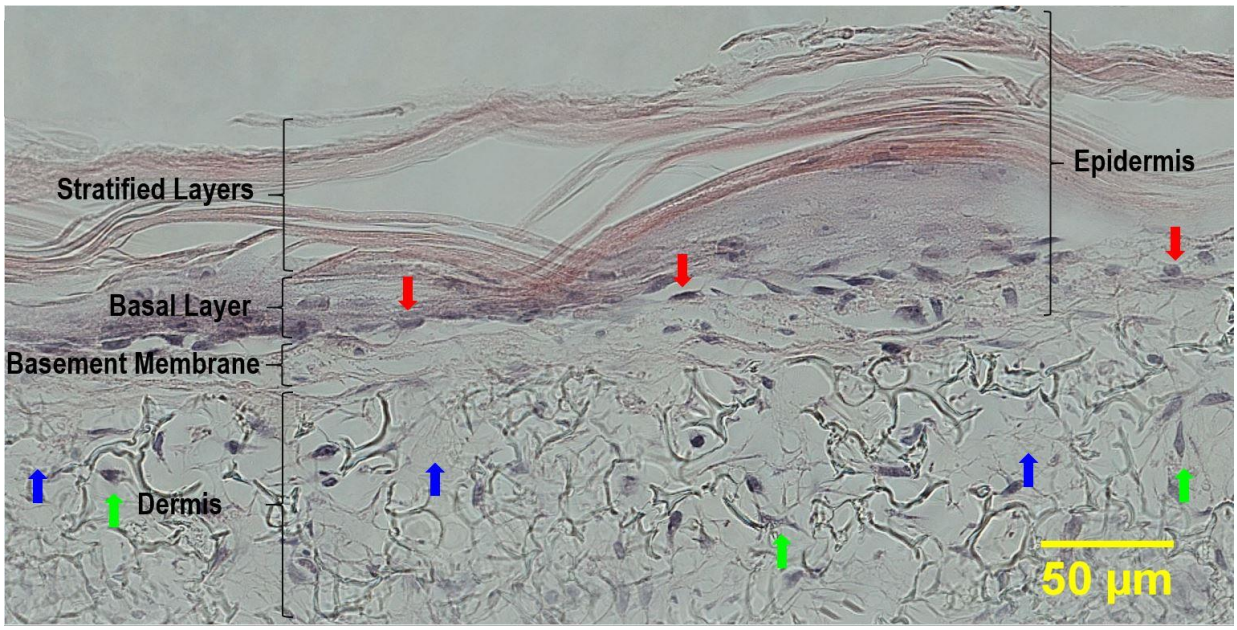

Figure 6.1 Haematoxylin-Eosin (H-E) image of constructed 3D skin equivalent model (3D-SEM).

Representative H and E image of a full thickness 3D-SEM depicting distinct dermal and epidermal layers separated by a distinct basal membrane. Red arrows= basal keratinocytes, Green arrows=dermal fibroblast, Blue arrows= collagen filaments, Scale bar: 50 µm.

The immunofluorescent expression of cutaneous differentiation markers (loricrin, K10 and K14) was optimised (Figure 6.2 A, B and C) in paraffin embedded human primary skin prior to confirmation of their expression in the 3D human skin equivalent.

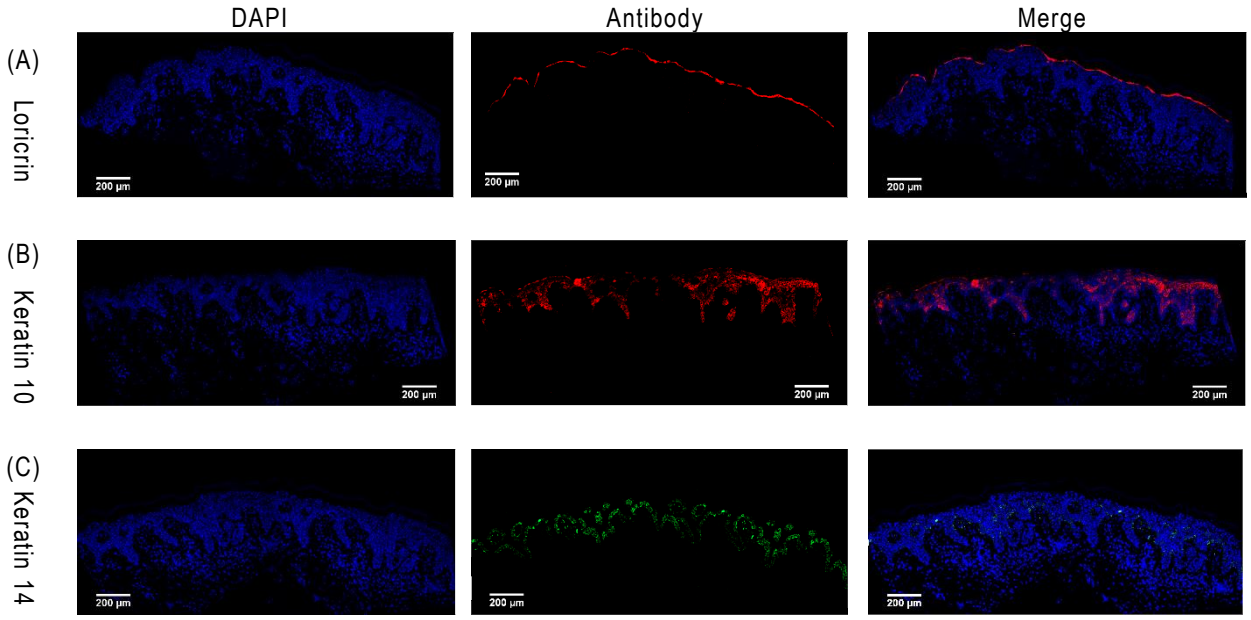

Figure 6.2 Epidermal differentiation markers expressed by human skin.

Representative Immunofluorescence images of normal human skin (Paraffin embedded) depicting the expression of loricrin, K10 and K14 in the epidermis. (A) Loricrin expressed in the stratum corneum layer of epidermis (Red=Rhodamine stain). (B) K10 expressed in the spinous and granular layer of epidermis (Red=Rhodamine stain). (C) Keratin 14 expressed in the basal layer of epidermis (Green=FITC stain). Blue=DAPI stain (depicting cell nuclei). Scale bar=200 µm.

Results clearly revealed the differentiation of keratinocytes within different epidermal layers as evidenced by the expression of K10, an early differentiation marker expressed by keratinocytes in the spinous and granular layers, as well as the expression of involucrin and loricirn, late differentiation markers expressed in the stratum corneum layer.

To verify the reconstructed 3D-SEM, the formation of the basal layer was assessed by evaluating the expression of K14, while the immunofluorescent expression of collagen III was assessed in the dermal layer. Results revealed a thick layer of cells expressing K14 indicating the formation of a basal layer (Figure 6.3 D). Consistent with basal keratinocytes entering a differentiation phase, results also revealed the expression of the early differentiation marker K10 (Figure 6.3 C). In addition, the expression of the late differentiation markers involucrin (Figure 6.3 B) and loricrin (Figure 6.3 A) were also observed, confirming the formation of an epidermal layer in the 3D-SEM closely resembling that of human skin. Finally, fibroblasts of the dermal layer expressed collagen type III (Figure 6.3 E) in addition to collagen IV (Figure 6.3 F) confirming the formation of a dermal layer and basement membrane respectively in the 3D-SEM closely resembling

human skin. These data thus confirmed the successful formation of 3D-SEM that mimics the cutaneous *in vivo* environment.

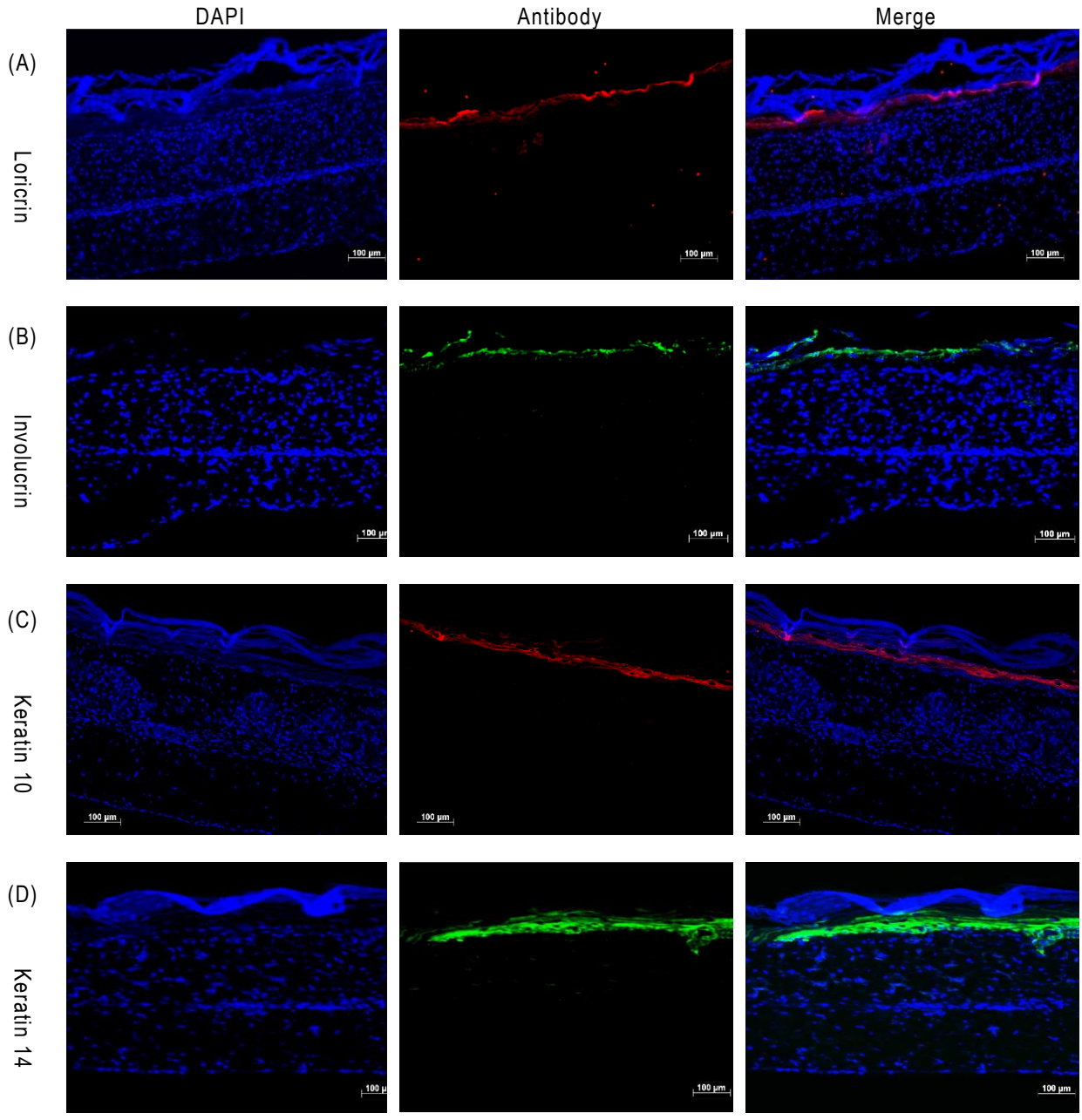

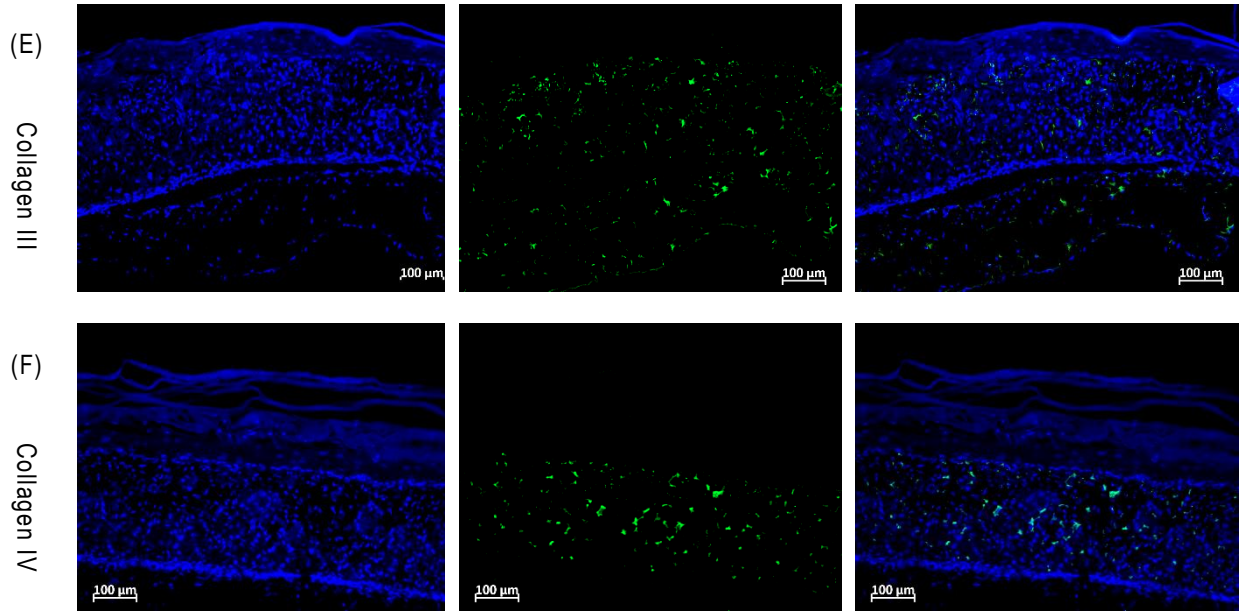

Figure 6.3 Epidermal Differentiation and Dermal markers expressed by a reconstructed 3D skin equivalent model (3D-SEM).

Representative Immunofluorescence images of a 3D-SEM revealing the expression of epidermal differentation markers. (A) Loricrin, (B) Involucrin, (C) Keratin 10, (D) Keratin 14, (D) Dermal markers collagen III (F) Collagen IV. Green=FITC stain, Red= Rhodamine stain, Blue=DAPI stained-cell nuclei. Scale Bar=100 µm.

Multiple immunofluorescence staining of reconstructed 3D-SEM also (Figure 6.4) revealed full stratification of the epidermal layer as evidenced by K14 expression just over the dermal layer followed by a layer of positive staining for K10 in the superficial layer.

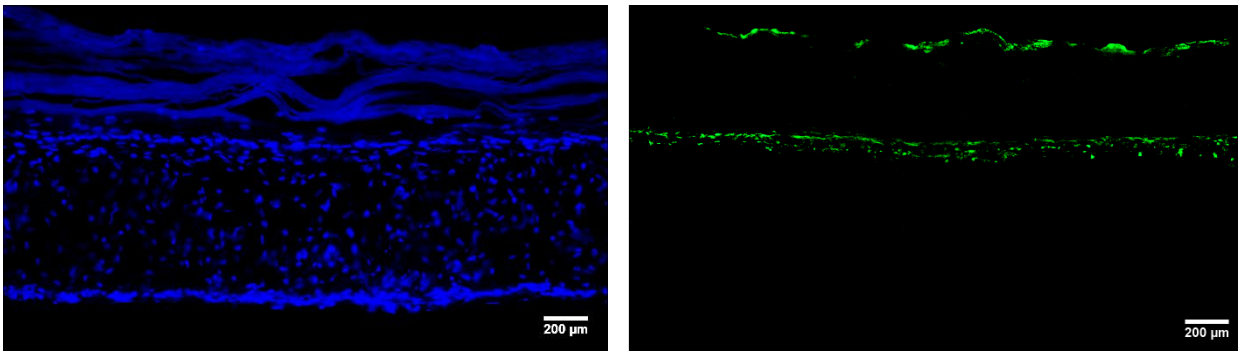

(A) DAPI (B) FITC

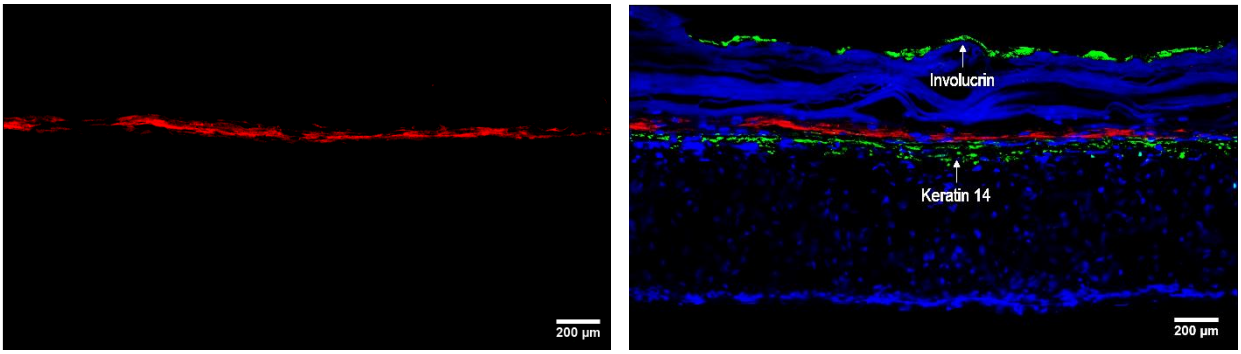

(C) Rhodamine (D) MERGE

Figure 6.4 Multiple immunofluorescence staining of 3D skin equivalent model (3D-SEM).

Representative sequential immunofluorescence images of a 3D-SEM revealing epidermal differentiation markers. (A) Cell nuclei in the epidermal and dermal compartments stained with DAPI (blue). (B) FITC green fluorescent expression of involucrin in the stratum lucidum layer of the epidermis and keratin 14 expression in the basal layers. (C) Red Rhodamine fluorescent staining of K10 in the spinosum, granulosum layer of the epidermis and (D) A merged image of involucrin, keratin 14 (green), K10 (red) expression. In addition to DAPI (blue). Scale Bar: 200 µm. The exposure time was raised to obtain stronger signal.

6.3.2 Developing a Prototype 3D Skin equivalent Model (3D-SEM) for Wound Healing Studies

To establish a reproducible means of wounding the established 3D-SEM described above, an additional step of seeding the fully stratified equivalent onto additional fibroblast monolayer was explored. A full thickness wound penetrating both the epidermis and the dermis was first created by means of a 3 mm punch biopsy before the wounded full thickness skin equivalent was then placed over a previously established fibroblast layer in 6-well plates and culture continued in the presence or absence of MSC-CM for1,2 or 4 weeks. At each time point (1,2 or 4 weeks), wounded 3D-SEM on a fibroblast layer in MSC-CM were then fixed and stained with haematoxylin-eosin (H-E) staining in order to visualise dermal and epidermal migration as a measure of wound healing. As demonstrated in (Figure 6.5 A), epidermal layers at the punch margins of models treated with MSC-CM migrated towards the punch centre after 1 week, forming an epidermal tongue covering the punch area. In contrast, there was no evidence for cell movement at the epidermal edges of wounded 3D skin equivalents exposed to control media (Figure 6.5 B). After 2 weeks, epidermal tongues of models treated with MSC-CM continued to migrate towards the punch centre (Figure 6.5 C) while the epidermal layers of control models just started to form an epidermal tongue from one side (figure 6.5 D). Interestingly, MSC-CM enhanced cell migration at all wound edges to move towards the centre, in

contrast to the wound margins of the control models, which showed inconsistent movement, although some control models showed migration from only one side, which resulted in delayed healing. Notably, after 4 weeks of culture with MSC-CM, punch areas were completely encased with the epidermal layer and fully stratified epidermal layers, (Figure 6.5 E). Meanwhile, epidermal layers of control models moved very slowly over time and failed to cover the whole wound area with a gap still remaining at assay termination (Figure 6.5 F).

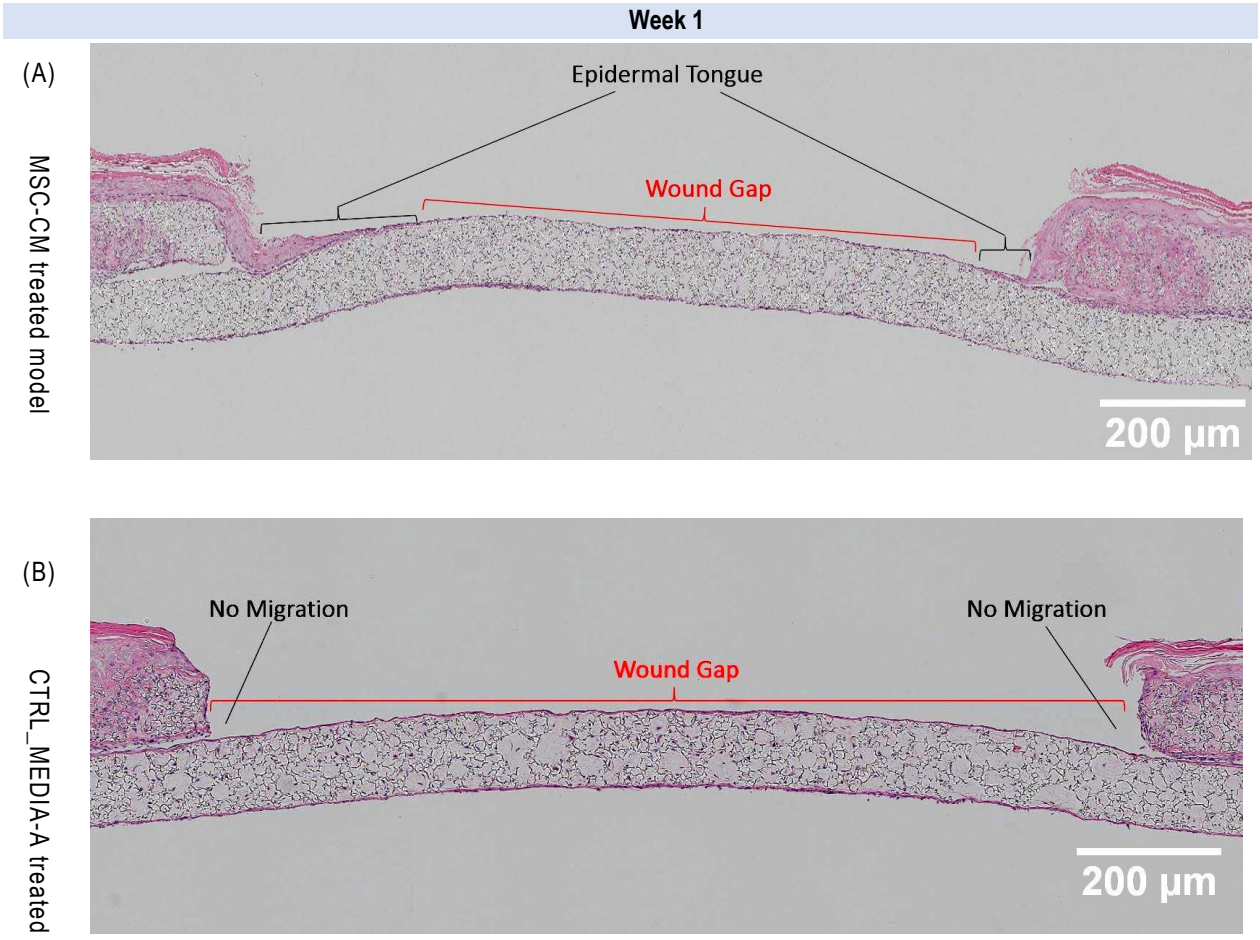

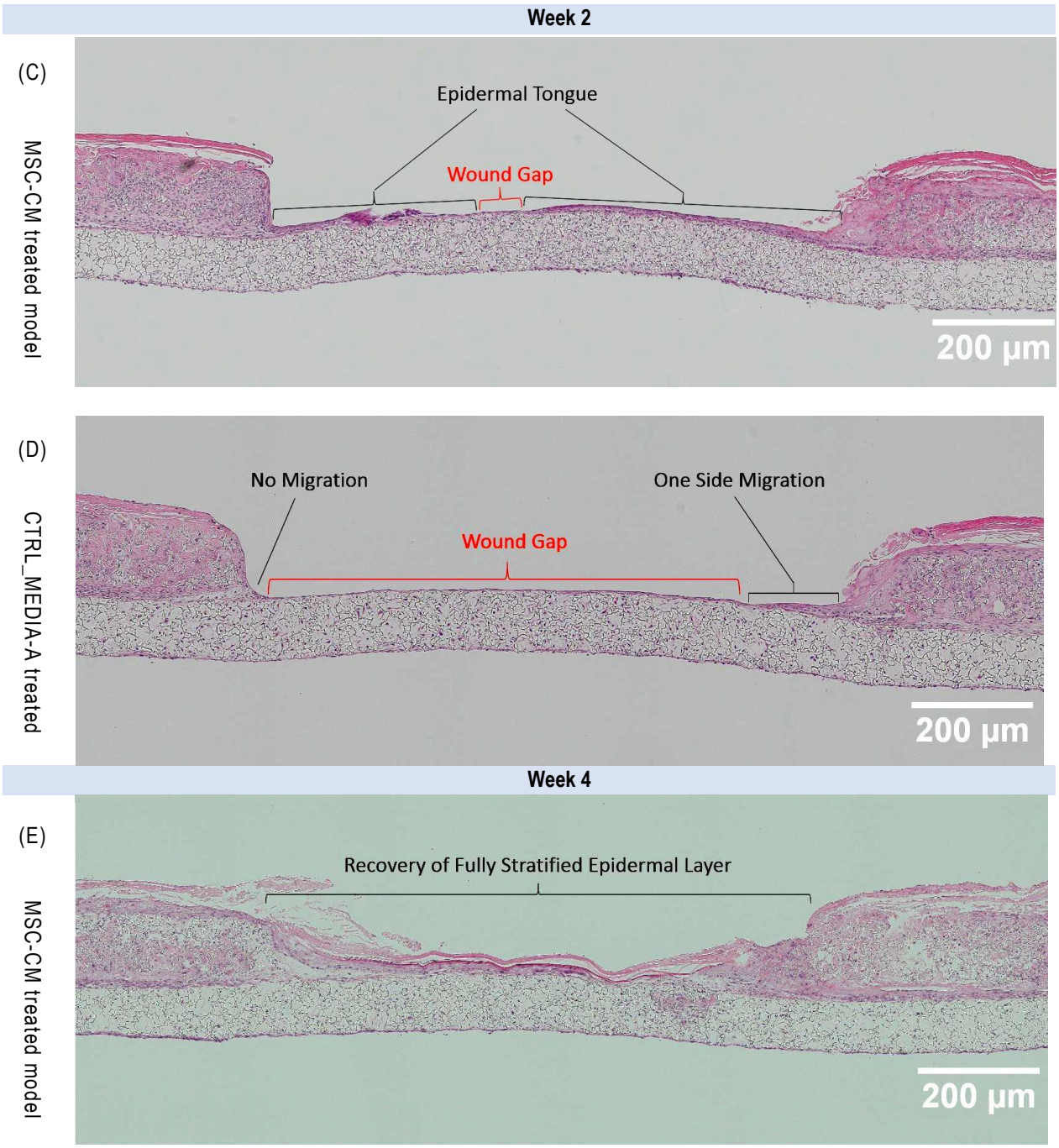
Week 2
(C)
MSC-CM treated model
Epidermal Tongue
Wound Gap
200 µm
(D)
CTRL_MEDIA-A treated
No Migration
One Side Migration
Wound Gap
200 µm
Week 4
(E)
MSC-CM treated model
Recovery of Fully Stratified Epidermal Layer
200 µm

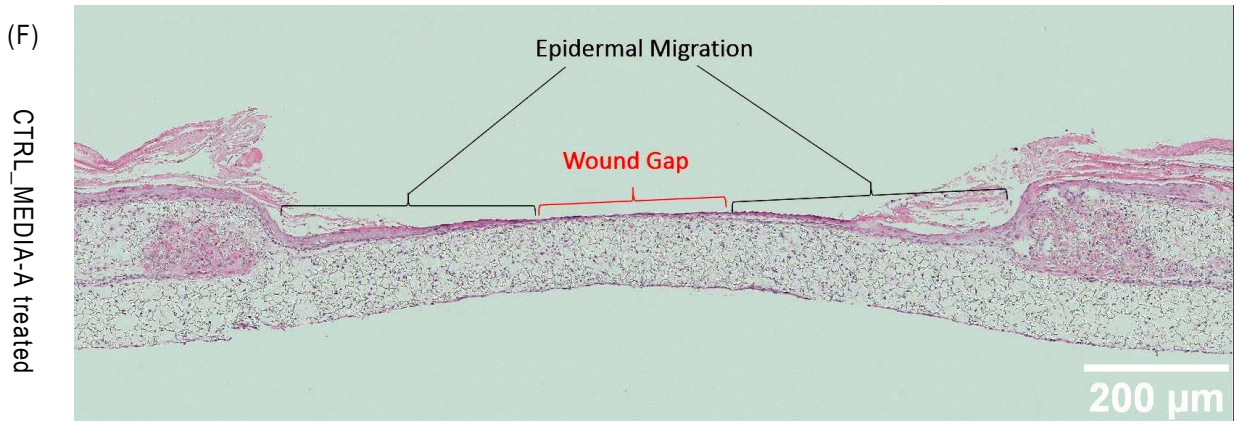

Figure 6.5 MSC-CM enhances wound healing in 3D skin equivalents model (3D-SEM).

Representative Photomicrographs of haematoxylin-eosin (H-E) staining revealing that 3D-SEM seeded onto fibroblast mono layers post induction of a 3 mm punch biopsy and cultured for 1 week (A & B), 2 weeks (C & D) or 4 weeks (E & F) in the presence of MSC-CM (A, C and E) or control (CTRL) media (B, D and F). (A) depicts the formation of an epidermal tongue at the two margins of the punch wound after 1 week in the presence of MSC-CM, not observed in wounded 3D-SEM's in CTRL media, while in (C), MSC-CM-increased epidermal migration is observed over the induced wound, with complete recovery and the presence of a fully stratified epidermis by week 4. Red brackets represent the wound gap. Black brackets indicate epidermal tongue/migration. Scale bar = 200 µm.

To best clarify the spatial-temporal events in the healing process in 3D-SEM, a 3D scheme was created (Figure 6.6), aligning the 3 dimensional measurements that may be used to evaluate the healing process i.e. the length of epidermal tongue (LET), the thickness of epidermal tongue (TET) epithelialisation (ER) and healing rates (HR).

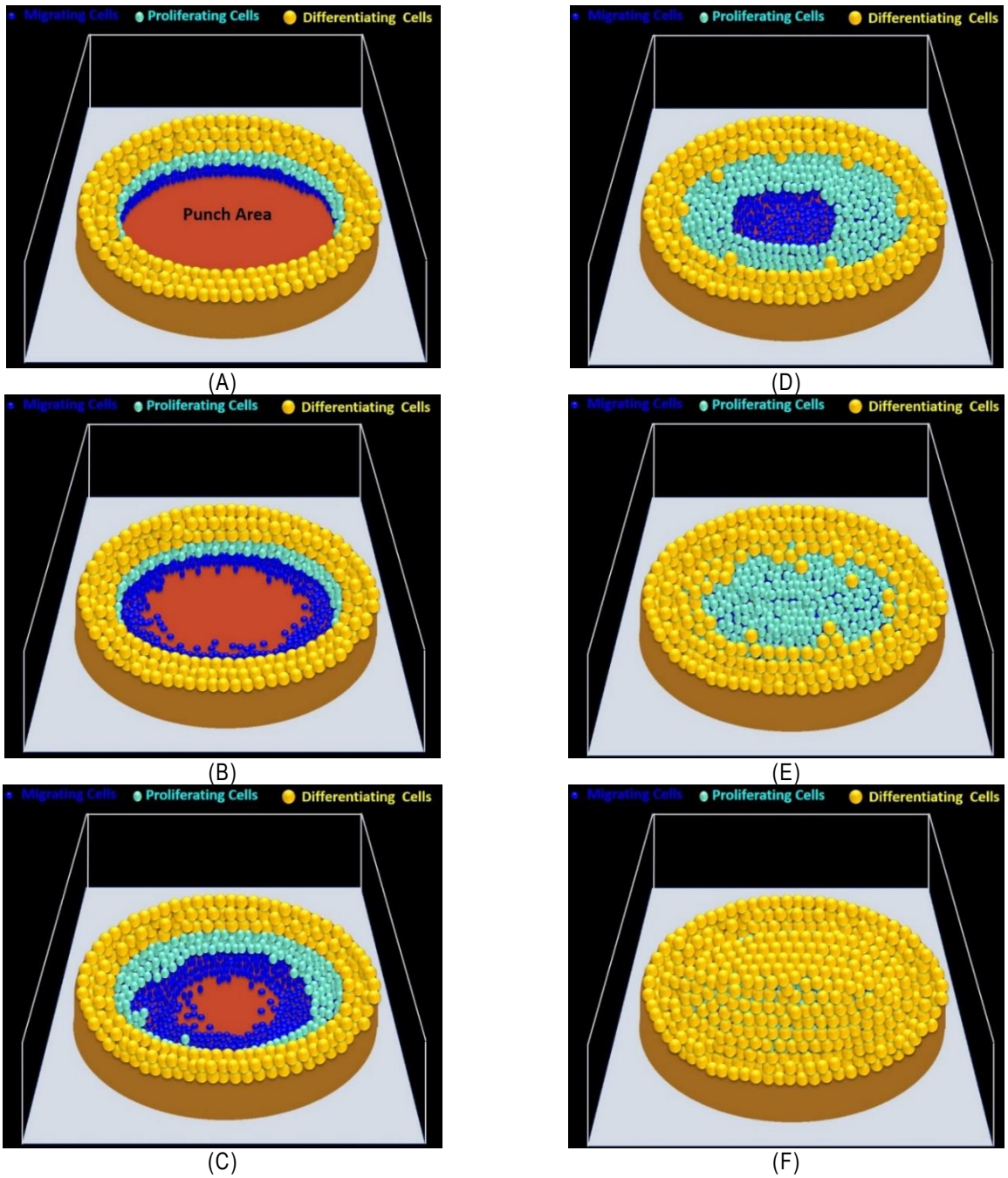

Figure 6.6 Schematic figure of the healing process in* in vitro *3D skin equivalent model (3D-SEM).

Schematic representing 3D migration of cellular epidermal sheets over wounded (punched) 3D-SEM over time. (A) New induced punch. (B) Initiation of cell migration. (C) Continuous cell migration with initiation of proliferation of cells that stopped their migration. (D) Complete epithelialisation of the punch area with migrating cells and increased proliferation. (E) Complete proliferation with initiation of differentiation resulting in an epidermis of partial thickness. (F) Recovery of full thickness epidermis with full differentiation. Blue Balls= Migrating Cells, Turquoise Balls= Proliferating Cells, Yellow Balls= Differentiating Cells.

To clarify mathematical calculations of the wound size to further evaluate the progress in the healing process, explanatory images are illustrated in (Figure 6.7) depicting the dimension of the wound and the newly growing epidermal sheet.

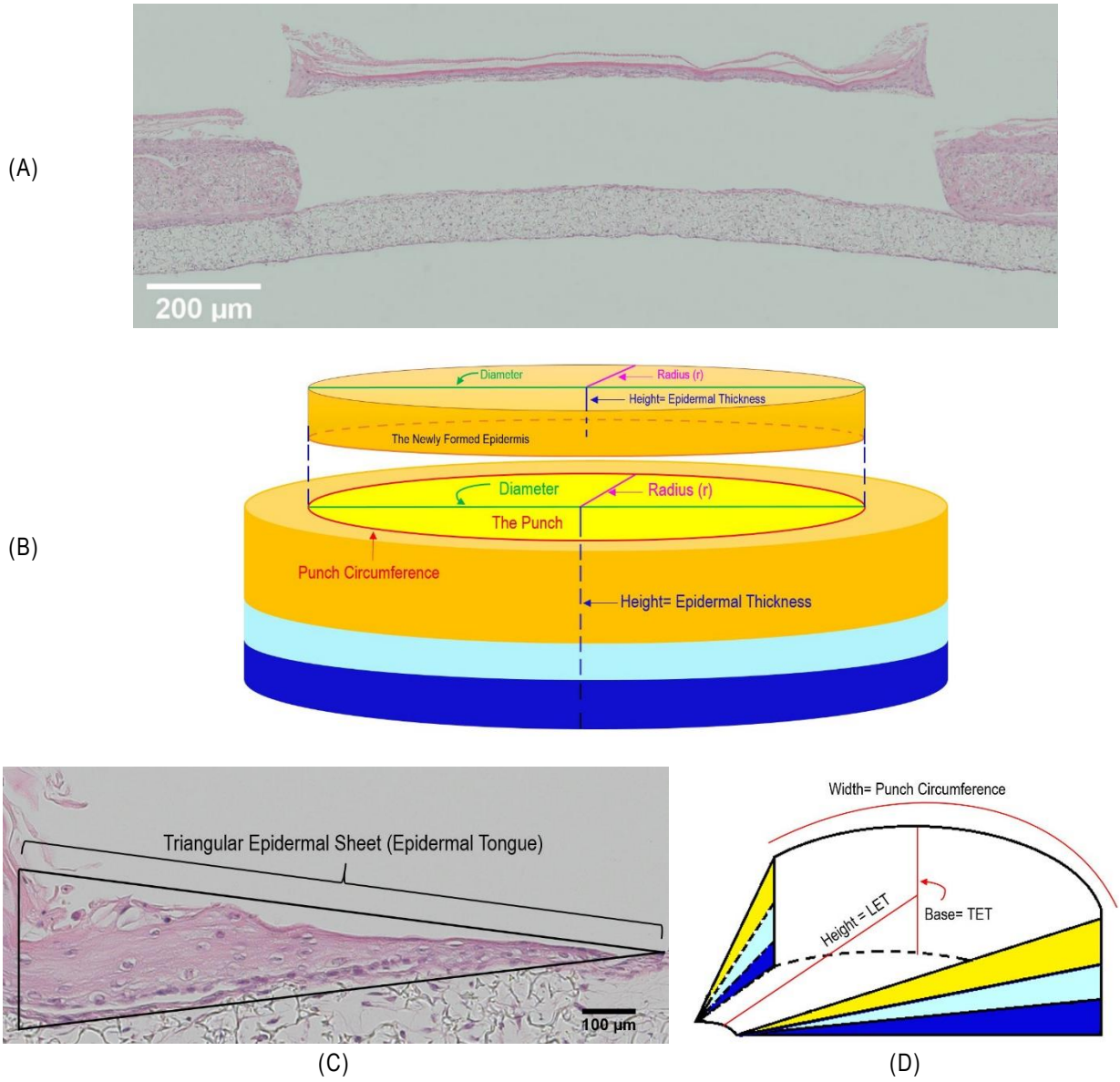

Figure 6.7 Schematic figure indicating the adopted process to quantify the healing progress and epithelialisation rate.

This figure explains the healing progress in an induced circular punch in 3D-SEM. (A) A 2D haematoxylin-eosin (H-E) image of a side view of a fully recovered epidermal sheet which covered the punch area. Scale bar=200 µm. (B) A 3D geometric figure explaining that the fully recovered epidermal sheet is actually cylindrical in shape which is recovered after 4 weeks of treatment with MSC-CM. (C) A 2D H-E image of a side view explaining that the newly formed epidermal sheet (the epidermal tongue) is a triangular shape which is formed after 1 week of treatment with MSC-CM. Scale bar=100 µm. (D) A 3D geometric figure explaining that the newly formed epidermal sheet (epidermal tongue) is actually a round triangular prism in shape.

As illustrated in (Figure 6.6) and (Figure 6.7 A), the wound healing process is presented by moving cells over a circular surface area. Hence, a formula of the circle area (Equation 6.1) was applied to measure the area of induced wound at day 0 for further comparison of reduction in wound area over time.

$$\boldsymbol{A = \pi r^2} \qquad \mu m^2 \qquad \text{. . . . .} \qquad \text{Equation 6.1}$$

When:
A= Area of Circular Punch.
π =3.14
r= radius of the punch area.

In addition, the circumference of the punch wound was calculated by applying the following equation (Equation 6.2):

$$\boldsymbol{Circumference\ (C) = \pi \times Diameter\ (D)} \qquad mm \qquad \text{. . . . .} \qquad \text{Equation 6.2}$$

Depending on the general formula of the circle area (Equation 6.1), a formula was then derived to evaluate the progress in the healing process (Epithelialisation) over time by calculating the healed area (HA). The HA could easily be calculated by measuring the length of the newly formed epidermis or so-called length of epidermal tongue (LET) to replace the radius in the main formula of circle area in (Equation 6.1). Therefore, the new derived formula to calculate the healed area (HA) so-called epithelialisation is presented as (Equation 6.3):

$$\boldsymbol{Epithelialization = HA = \pi\ (LET)^2} \qquad mm^2 \qquad \text{. . . . .} \qquad \text{Equation 6.3}$$

When:
HA= Healed Area.
π =3.14
LET= Length of Epidermal Tongue.

To evaluate the epithelialisation rate (ER), which represents an increase in the healed area at a given time point the following equation (Equation 6.4) was used.

$$\boldsymbol{ER = \frac{HAT2 - HAT1}{T2 - T1}} \qquad mm^2 \text{ / Week} \qquad \text{. . . . .} \qquad \text{Equation 6.4}$$

When:
ER= Epithelialisation Rate
HAT2= Healed Area at time point 2.
HAT1= Healed Area at time point 1.

On the other hand, the general formula of cylinder volume (Equation 6.5) was used to measure the void volume of the punch for further comparing the reduction in wound size (volume).

$$\boldsymbol{Cylinder\ Volume = \pi r^2 h} \qquad mm^3 \qquad \text{. . . . .} \qquad \text{Equation 6.5}$$

The healing rate (HR) was thus evaluated by measuring the thickness of the newly formed epidermis, calculated by measuring the length, width and the height of the newly formed epidermis.

Results demonstrated that the development of the new epidermis was irregular in shape; i.e. while initially a triangular shape at week one and two (Figure 6.7 B and C) this became more cylinder like once the formation of a full thickness epidermis (Figure 6.7 A) was complete. Therefore, the most appropriate formula to calculate the different thicknesses of the newly regenerated epidermis at weeks 1 and 2 was (Equation 6.6).

$$\boldsymbol{Volume\ of\ Trigonal\ Prism = \frac{1}{2} \times b \times h \times w} \qquad mm^3 \qquad \text{. . . . .} \qquad \text{Equation 6.6}$$

When:
b= base, h= height, w= width.

To calculate the volume of a newly formed epidermal tongue with triangular prism like shape, equation (Equation 6.6) was further adapted. Since the newly formed epidermis regenerates a round area, the circumference (C) was used instead of the width (W). Using of (W) in the standard formula of triangular prism volume will give the volume of a straight prism as explained in (Figure 6.8 C) while, using (C) instead, as explained in (Figure 6.8 A and B), enabled the calculation of the newly formed epidermal tongue in wounded skin equivalents at week one and two using (Equation 6.7).

$$\boldsymbol{ETV = \frac{1}{2} \times T \times LET \times C} \qquad mm^3 \qquad \text{. . . . .} \qquad \text{Equation 6.7}$$

ETV= Epidermal Tongue Volume or Size (Triangular prism shape).
T= Thickness of newly formed epidermis close to the wound edge.
LET= Length of Epidermal Tongue (the newly formed epidermis).
C= Circumference of the punch.

Theoretically, a round triangular prism could be cut at any point and spacing the ends of each other as explained in (Figure 6.8 B) to produce a standard triangular prism as

demonstrated in (Figure 6.8 C), hence, the newly developed formula is an accurate means of measuring the volume of a round triangular prism.

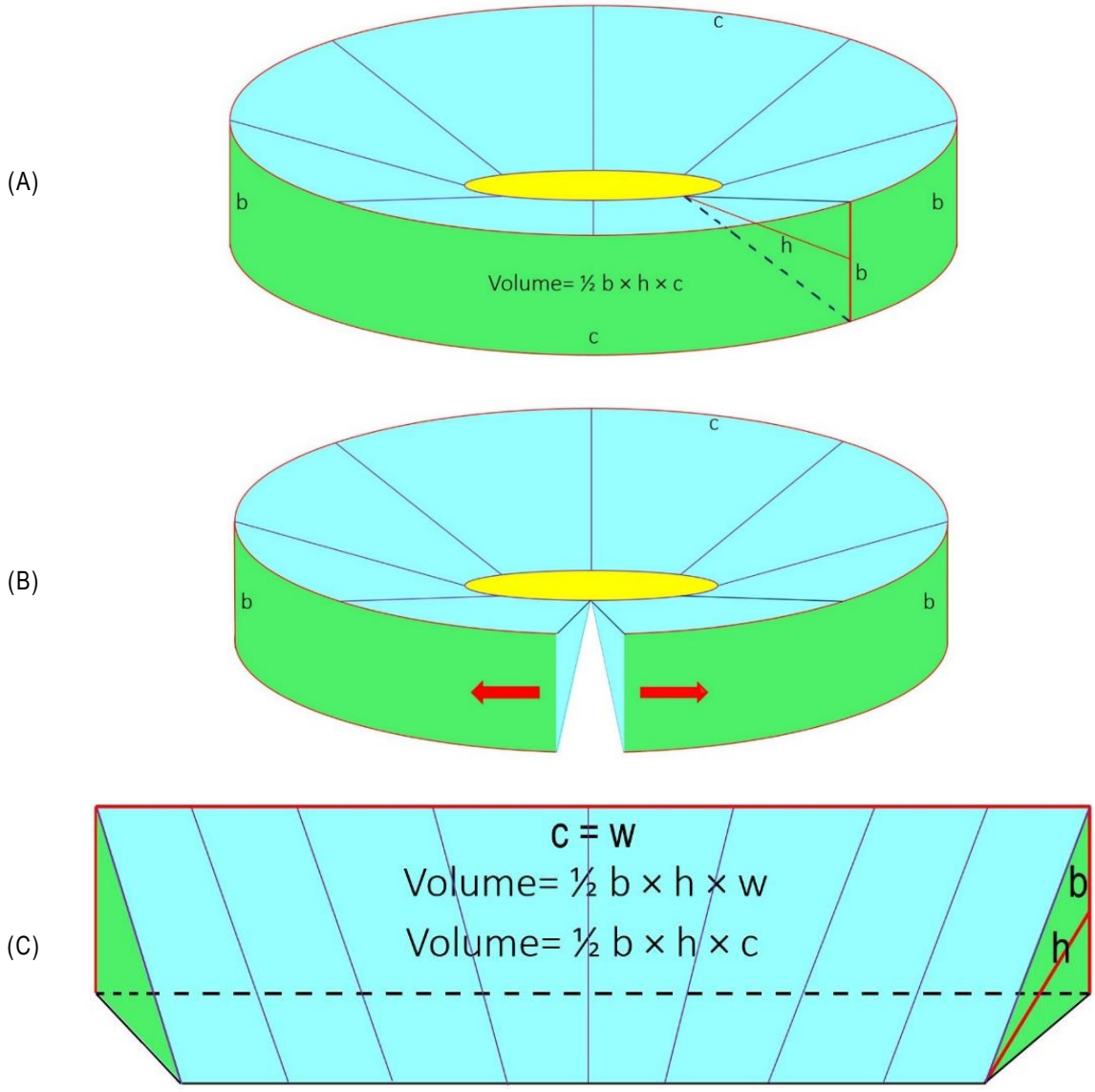

Figure 6.8 Explanatory geometric figure of the newly formed epidermal sheet.

Schematic image depicting the relationship between the shape of newly generated epidermal layer and a triangular prism during cutaneous wound healing of 3D-SEM. (A) Triangular prism with dimensions and the standard formula for calculating its volume. (B) Geometric figure resembles the newly formed epidermis according to the hypothesis that the regenerated epidermal tongue is a round triangular prism in shape. (C) An opened round triangular prism will give a straight triangular prism, hence the circumference of round triangular prism equals the width of straight triangular prism

In contrast the (Equation 6.8) derived from the general formula of cylinder volume was used to measure the wound size after 4 weeks (cylindrical shape).

$$ETV = \pi r^2 T \quad \text{mm}^3 \quad \text{. . . . .} \quad \text{Equation 6.8}$$

ETV= Epidermal Tongue Volume or Size (Cylindrical shape).
r= Radius of punch area.
T= Thickness of newly formed epidermis.

and allowing, the calculation of the HR by (Equation 6.9).

$$HR = \frac{ETST2 - ETSTT1}{T2 - T1} \quad \text{mm}^2 \text{ / Week} \quad \text{. . . . .} \quad \text{Equation 6.9}$$

When:
HR= Healing Rate
ETVT2= Epidermal Tongue Volume at time point 2.
ETVT1= Epidermal Tongue Volume at time point 1.

Finally, the fold change (FC) in epithelialisation rate (ER) and healing rate (HR) for MSC-CM treated models and control models was calculated at different time points using (Equation 6.10).

$$FC = \frac{RATE2}{RATE1} - 1 \quad \text{. . . . .} \quad \text{Equation 6.10}$$

Migration of epidermal cells was evaluated by measuring the area of a newly regenerated epidermal sheet at different time points during the healing process. Two way ANOVA in (Figure 6.9 A) revealed that the newly formed epidermal layer of MSC-CM treated models covered a wound area significantly larger than the area covered by epidermal layers of control models at different time points ($P<0.05$ after1 week, $P<0.01$ after 2 weeks and 4 weeks). Moreover, the epithelialisation rate (ER) was measured to evaluate the consistency in the healing process (Figure 6.9 B). Although there was a significant increase in the area of the newly formed epidermal sheet, the variation between the ER was non-significant between the different time points of models treated with MSC-CM ($P>0.05$) indicating the consistency of the formation of the new epidermis. In another words, the velocity of cell migration was consistent during the healing process suggesting that MSC-CM exerted a constant effect on cell migration during the entire healing process without any fluctuation.

The proliferation behaviour of epidermal cells was estimated by measuring the thickness of the newly generated epidermal sheet over different times of the healing process. As demonstrated in (Figure 6.9 C), two way ANOVA revealed that the thickness of the newly

formed epidermal layers was significantly increased over time in the presence of MSC-CM when compared to wounded equivalents cultured in control media ($P<0.001$ for 1 week and $P<0.0001$ for 2 and 4 weeks). Comparing models treated with MSC-CM at different time points, results demonstrated that the epidermal layer of models after four weeks was significantly thicker than the epidermal layer after two weeks ($P<0.001$). However, there was no significant variation between the thickness of the epidermis at week 1 or 2 ($P>0.05$). Furthermore, there was no significant increase in epidermal thickness of control models treated with media A ($P>0.05$) at any time point. On the other hand, the HR was consistent without collapsing during the entire healing process in the presence of MSC-CM. As demonstrated in (Figure 6.9), there was no significant difference between after 1 week or 2 weeks ($P>0.05$). However, the HR after 4 weeks was significantly higher than the HR at weeks 1 and 2 ($P<0.001$). Concurrently, control models showed no significant increase in the HR after completion of the healing process, with no significant difference at week, 1, 2 or 4 ($P>0.05$).

(A)

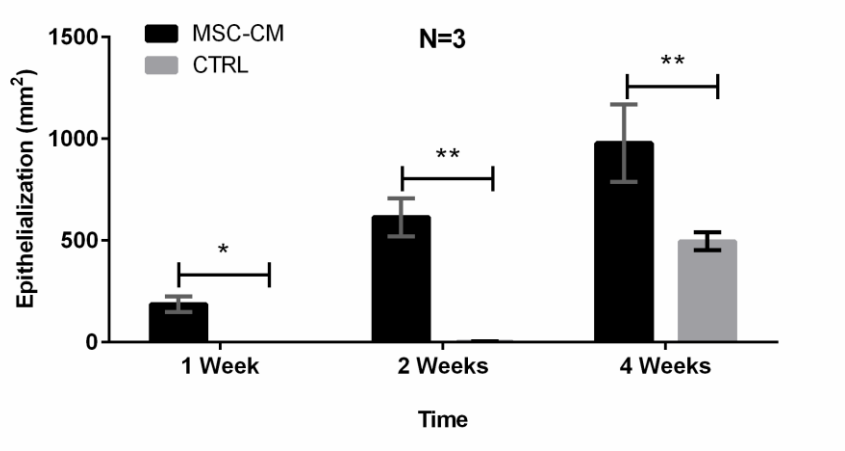

(B)

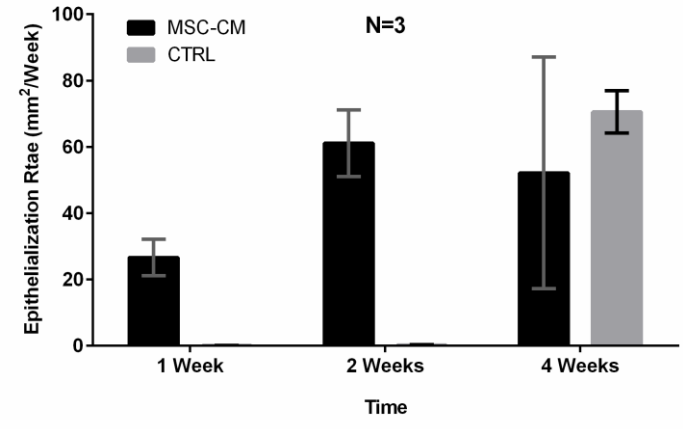

(C)

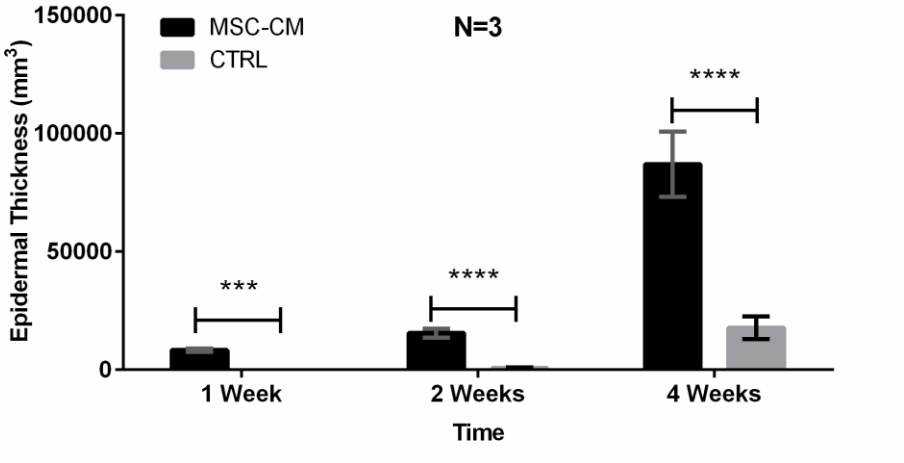

(D)

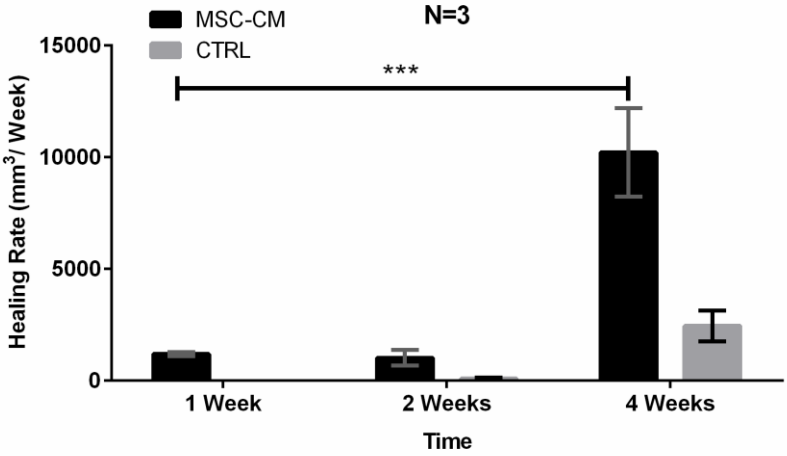

Figure 6.9 MSC-CM promotes epithelialisation and wound healing rates in 3D skin equivalent models (3D-SEM).

A graphical representation (A) Mean of epithelialisation (mm^2) in models treated with MSC-CM (Black boxes) and control (CTRL) models (Gray boxes) at 1, 2 or 4 weeks. (B) Mean of epithelialisation rate (mm^2/week) in models treated with MSC-CM (Black boxes) and control (CTRL) models (Gray boxes) at 1, 2 or 4 weeks. (C) Mean of epidermal thickness (mm^3) in models treated with MSC-CM (Black boxes) and control (CTRL) models (Gray boxes) at 1, 2 or 4 weeks. (D) Mean of healing rate (mm^3/week) in models treated with MSC-CM (Black boxes) and control (CTRL) models (Gray boxes) at 1, 2 or 4 weeks. In all graphs, N=3, Data presented as mean and the standard error of the mean (SEM), (P<0.05), (**P=0.01), (***=P=0.001), (****P=0.0001).*

Evaluation of the structure and morphology of the epidermal layer at the wound site of 3D-SEM revealed that culture in MSC-CM resulted in full recovery of fully stratified epidermal layers. As demonstrated in (Figure 6.10), the recovered epidermal sheet that encased the wound area after 4 weeks of treatment with MSC-CM was composed of the main components of an intact epidermis. Interestingly, a very distinct basement membrane

could be observed between the dermal and the basal layers of epidermis. The newly formed basal layer was also fully reconstituted as an intact layer, containing basal keratinocytes able to promote the recovery of other epidermal layers. Additionally, full stratification was observed after 4 weeks, with the observation of three to four distinct and intact stratum layers indicative of competent wound healing. Notably, the dermis and epidermis were also consistently attached to each other providing a firm skin structure.

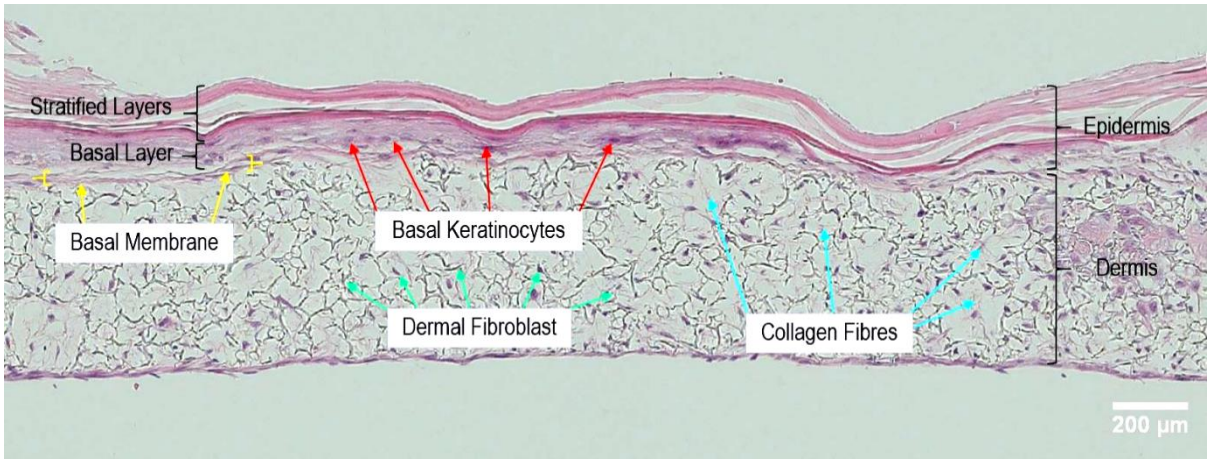

Figure 6.10 MSC-CM promotes re-epithelialisation in a punched 3D skin equivalent model (3D-SEM).

Representative photomicrograph of an H and E stained 3D skin equivalent previously subjected to a wound punch and cultured subsequently for 4 weeks in the presence of MSC-CM and depicting an epidermal layer containing all counterparts of an intact epidermis, a fully stratified corneum and showing the recovery of an intact basal layer containing basal keratinocytes. Additionally, a basement membrane could be observed between the dermal and epidermal layers. Scale bar = 200 µm.

Beyond evaluation of the structure and morphology of the recovered epidermis, the effect of MSC-CM on the expression of key epidermal and dermal biomarker expression on the wounded 3D skin models was also evaluated. Specifically, the expression K14, K10, involucrin, loricrin, collagen IV, and collagen III were evaluated.

As demonstrated in (Figure 6.11), culture of wounded 3D skin models in MSC-CM resulted in the induction of K14 after one week, indicating the presence and migration of basal keratinocyte from intact neighbouring margins surrounding the punch site. Beyond two weeks, the epidermal stretches retained expression of K14 suggesting continuous migration of basal keratinocytes from outside the wound. After four weeks, K14 positive cells were detected over the entire punched area indicating that the basal cells were

continuously moving during the healing process and forming a basal layer critical to the generation of upward epidermal layers.

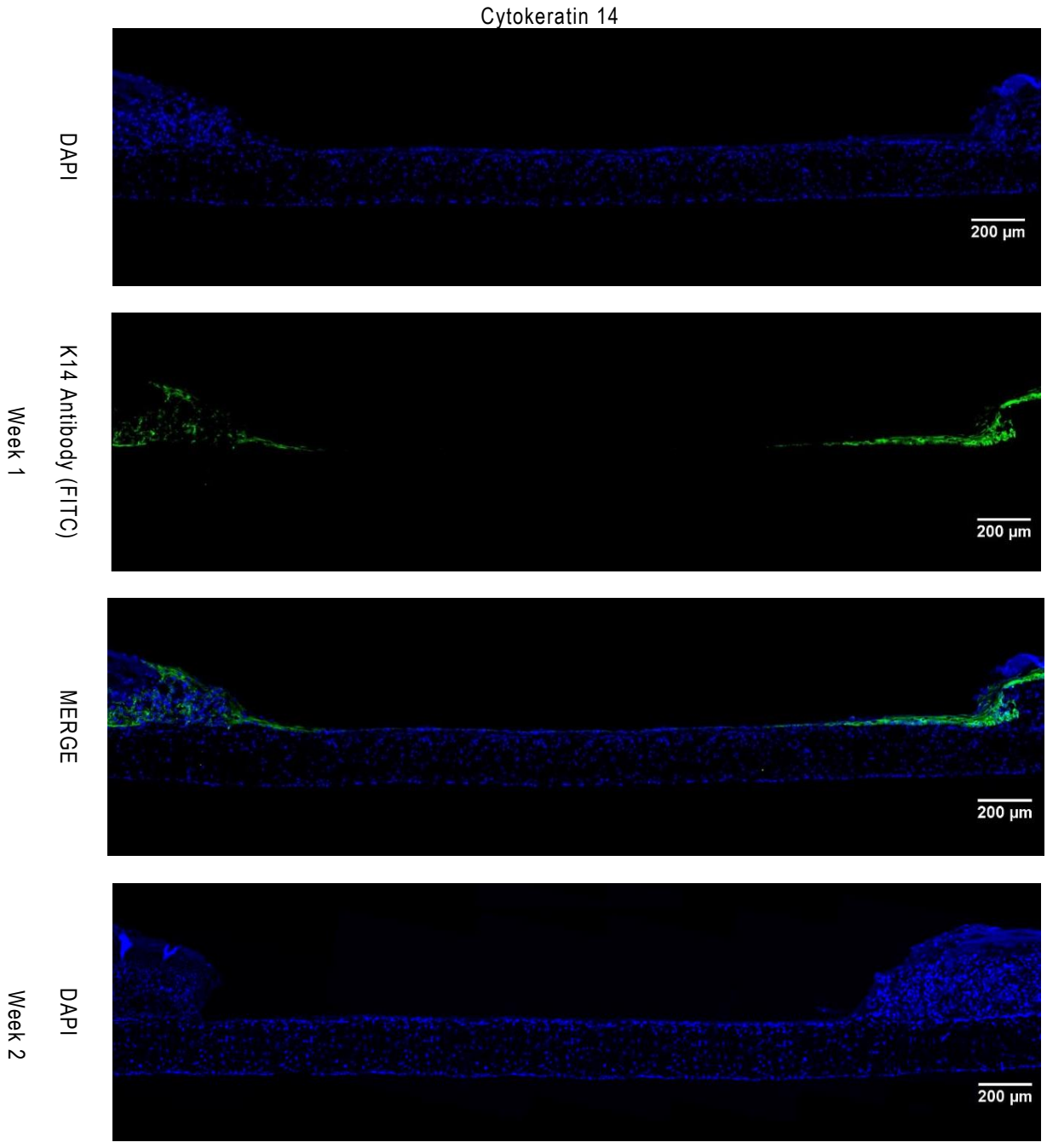

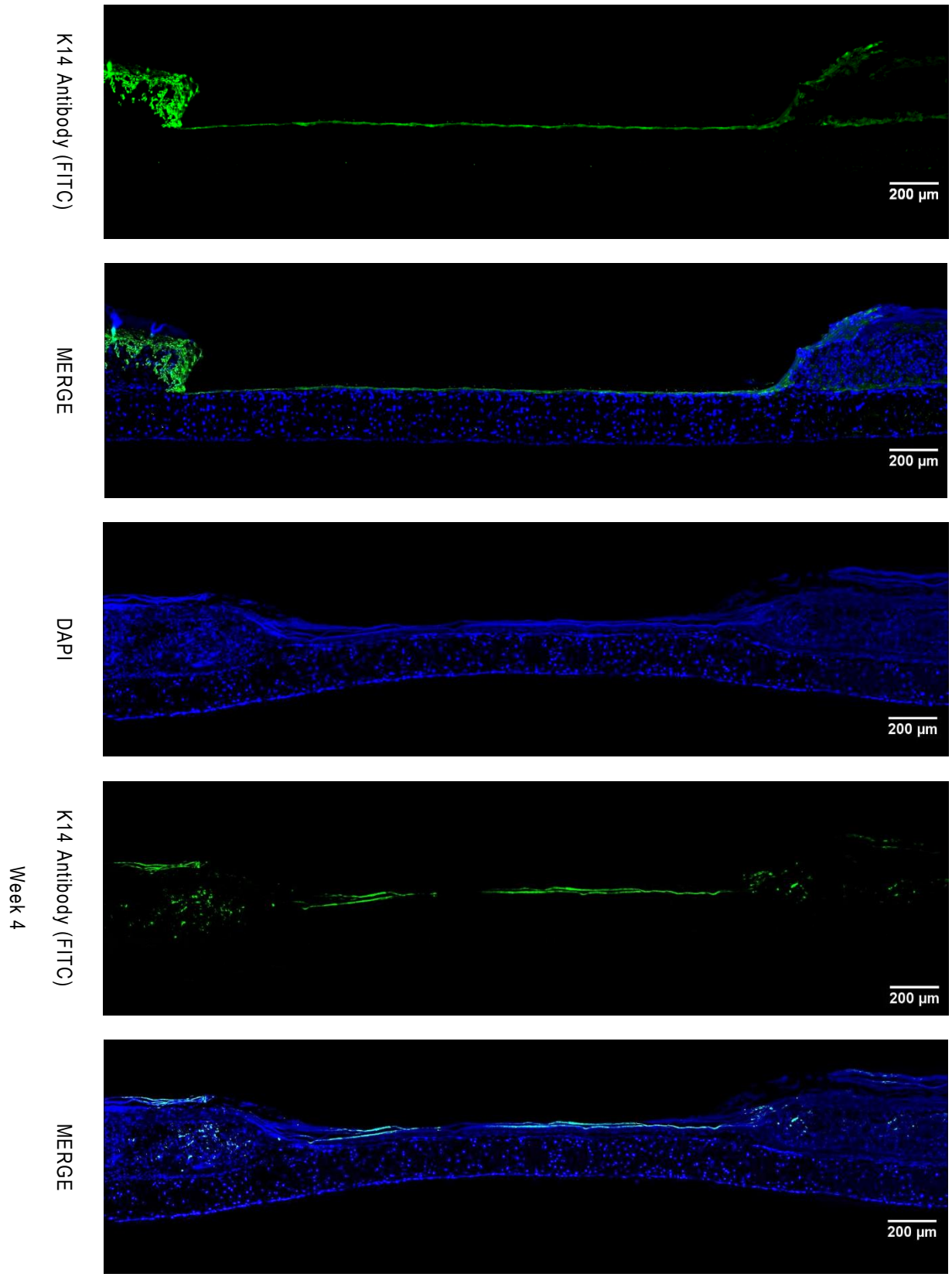
K14 Antibody (FITC)
MERGE
DAPI
K14 Antibody (FITC)
MERGE
Week 4
200 µm
200 µm
200 µm
200 µm
200 µm

Figure 6.11 MSC-CM promotes expression of K14 by the epidermal layer at different times during the healing process.

Representative immunofluorescence images of K14 expression in wounded 3D skin equivalent cultured in MSC-CM for 1, 2 or 4 weeks. Green fluorescence represents. Blue stain= cell nuclei stained with DAPI. Scale Bar: 200 µm.

Additionally, the newly formed epidermal tongue expressed K10 following one week of culture in MSC-CM which was continually expressed until formation of a full epidermal sheet at week 4 (Figure 6.12) and confirming the differentiation of basal keratinocytes into spinous and granular layers.

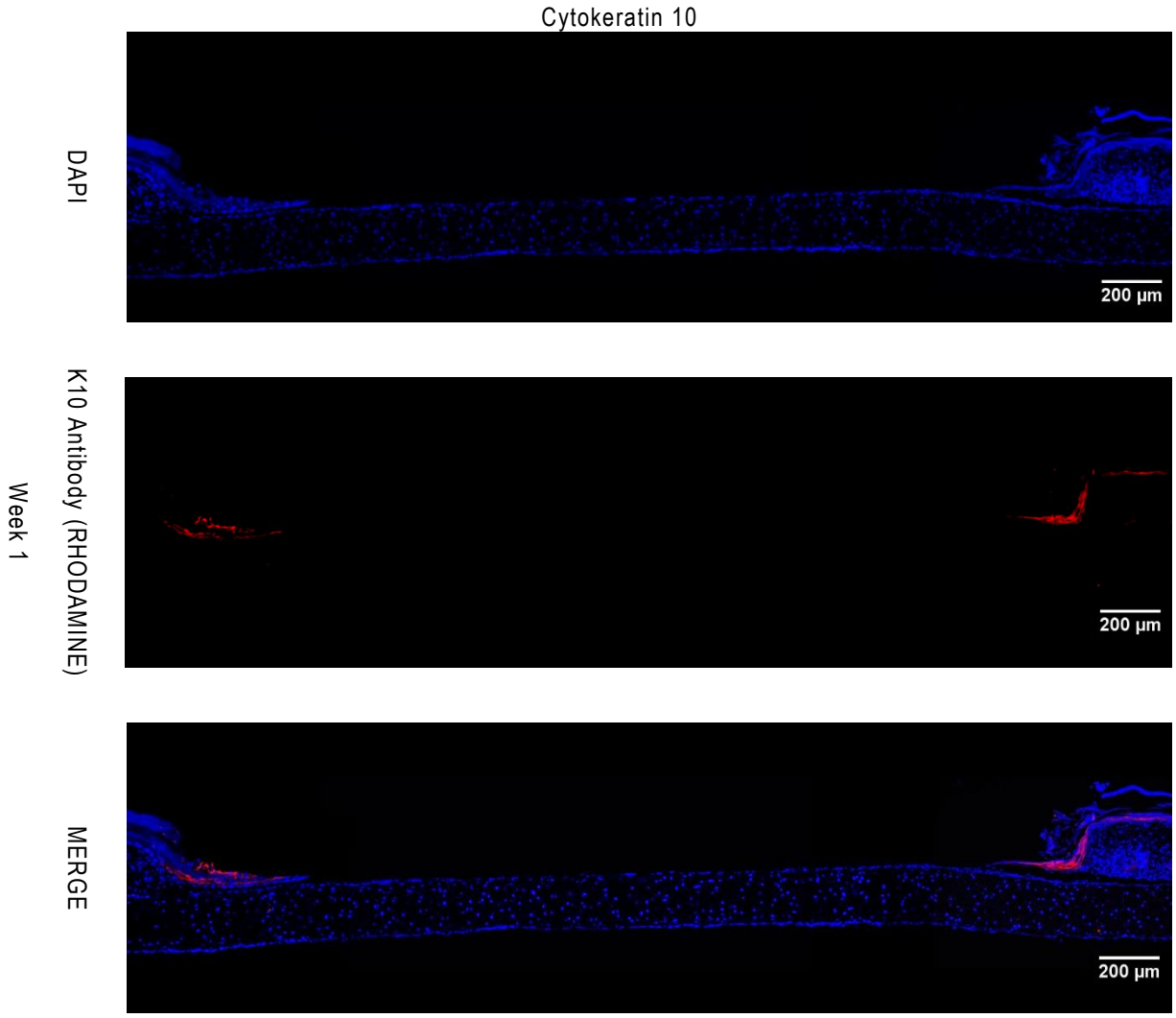

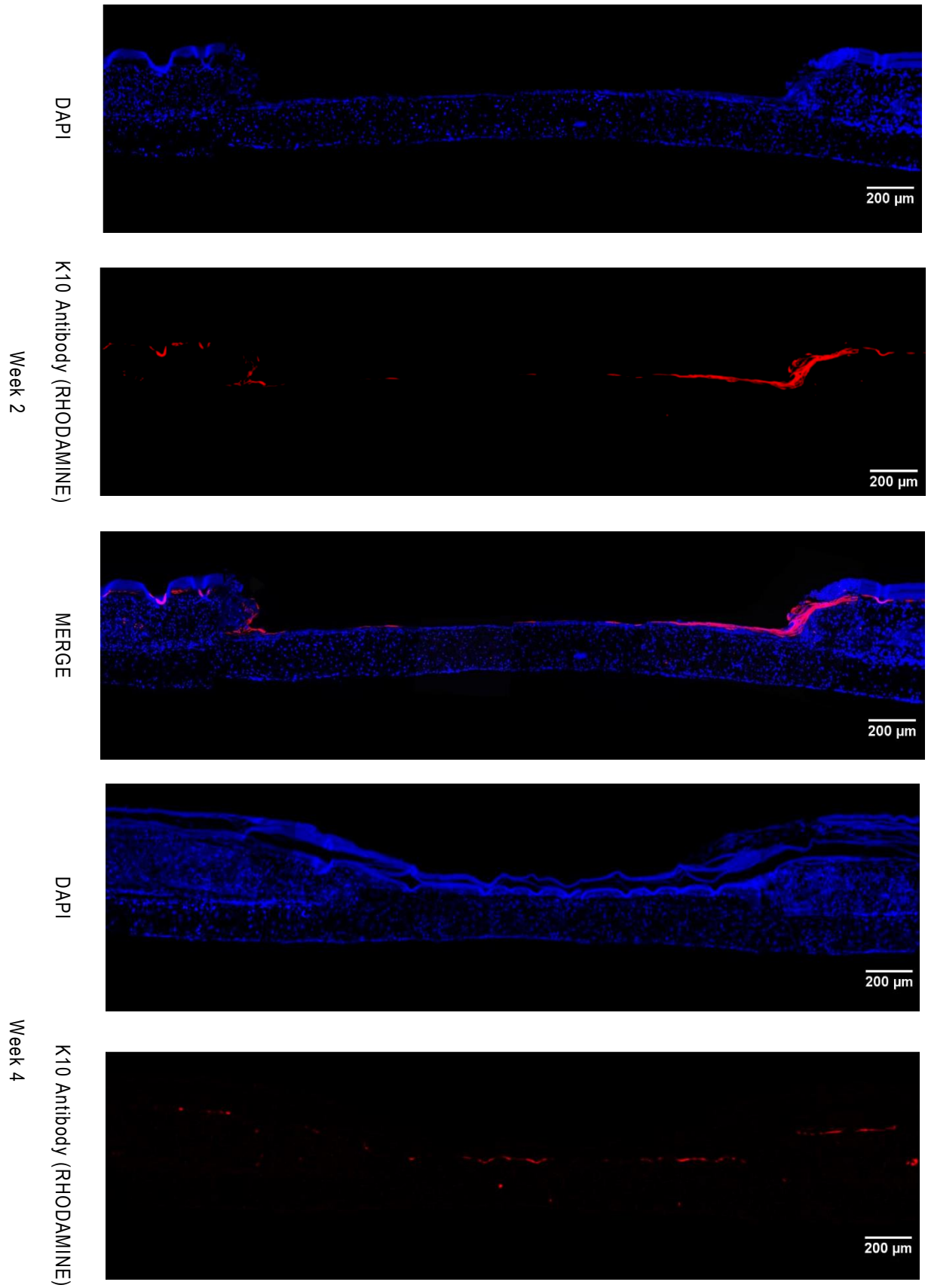
DAPI
200 µm
K10 Antibody (RHODAMINE)
Week 2
200 µm
MERGE
200 µm
DAPI
200 µm
Week 4
K10 Antibody (RHODAMINE)
200 µm

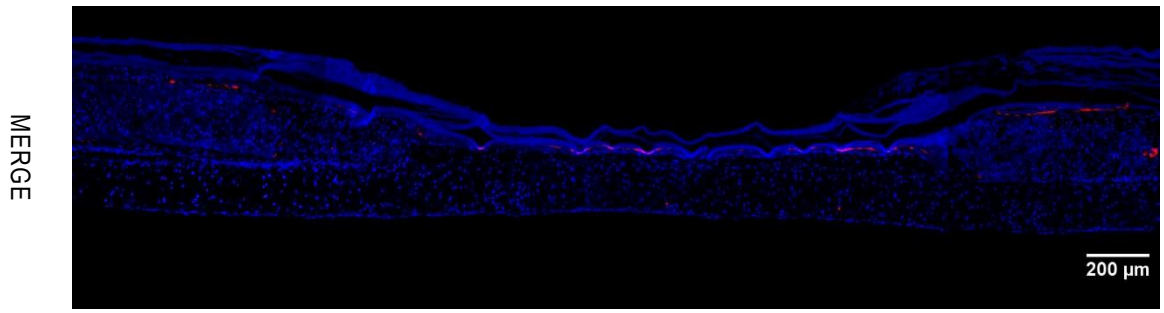

Figure 6.12 MSC-CM promotes expression of K10 by the epidermal layer at different time points during the healing process.

Representative immunofluorescence images of K10 expression in wounded 3D skin equivalents cultured in MSC-CM for 1, 2 or 4 weeks. Red Rhodamine fluorescence represents keratinocytes stained with Anti-Cytokeratin 10 antibody Blue= Cell nuclei stained with DAPI. Scale Bar=200 µm.

Analysis of involucrin expression (Figure 6.13) revealed expression in the newly generated epidermal sheet following culture in MSC-CM for one week, which was continually expressed until the wound site and was completely covered suggestive of the epidermal layer differentiating into the stratum lucidum layer.

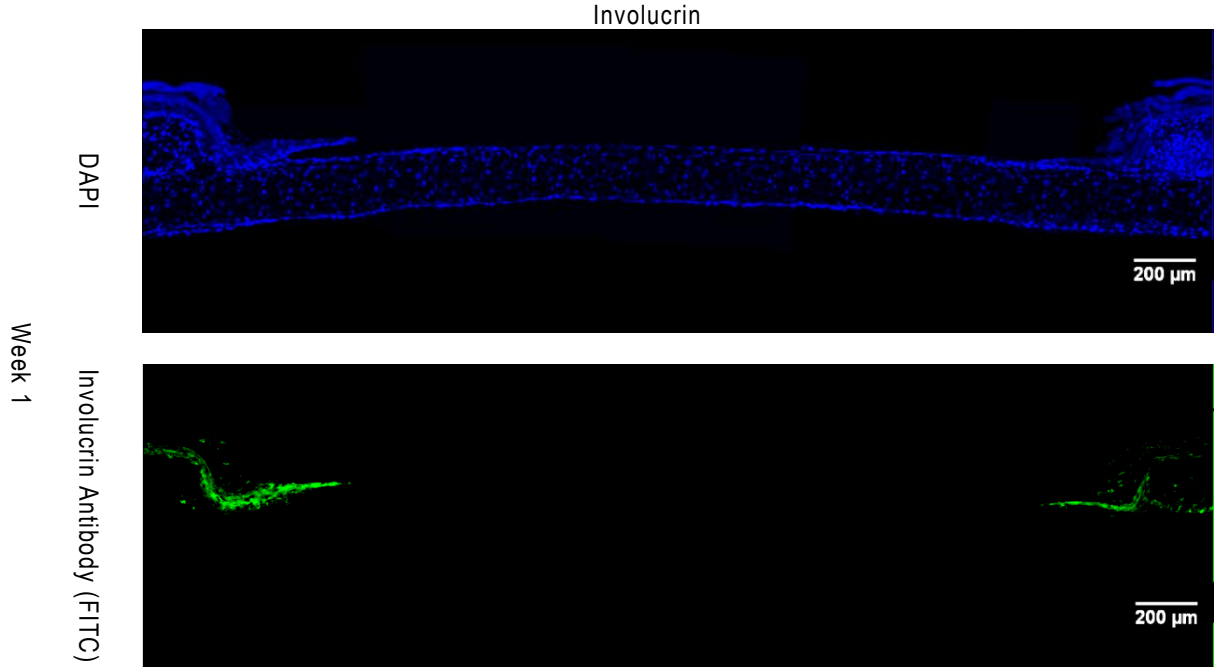

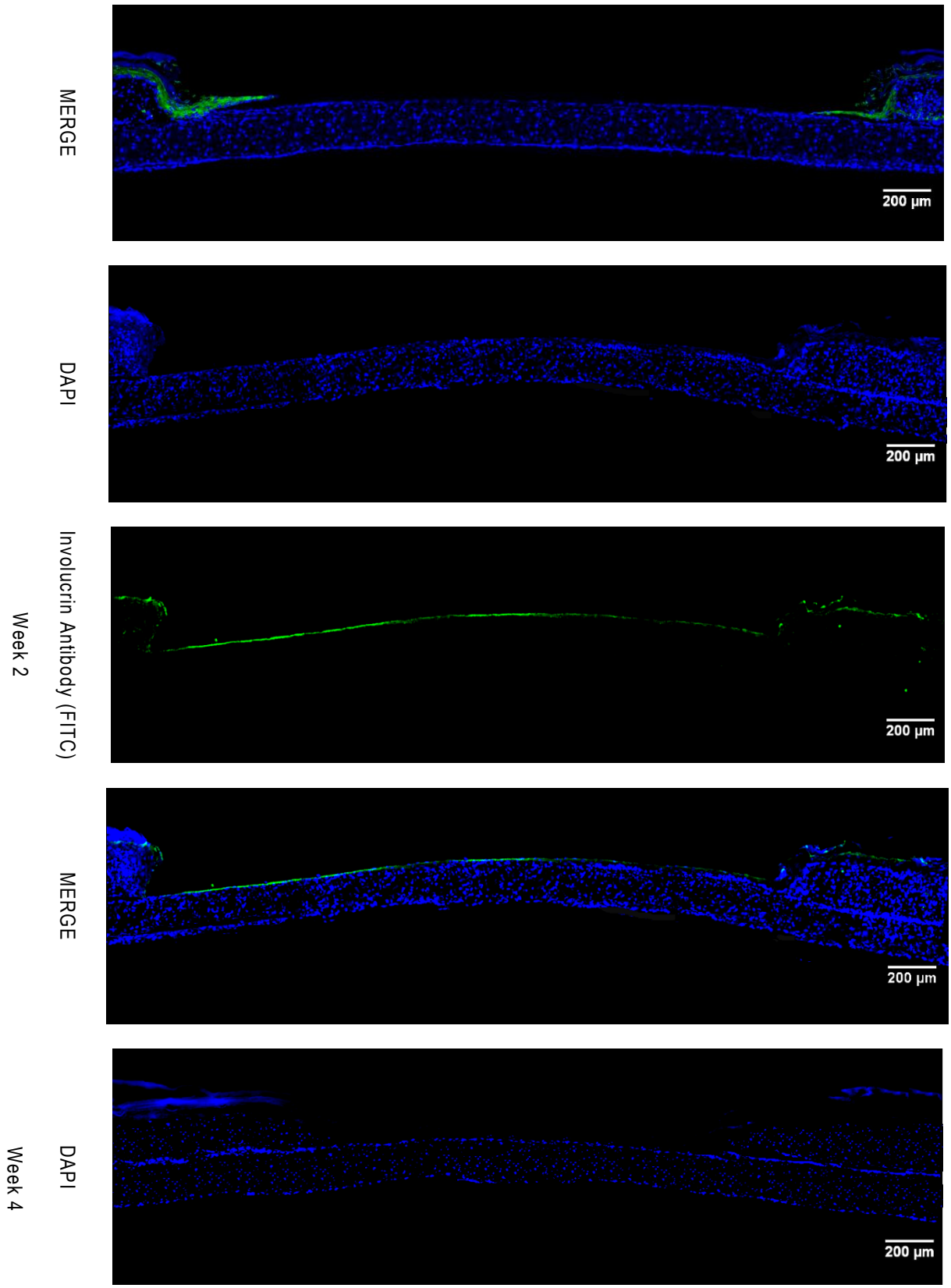
MERGE
200 µm
DAPI
200 µm
Involucrin Antibody (FITC)
Week 2
200 µm
MERGE
200 µm
DAPI
Week 4
200 µm

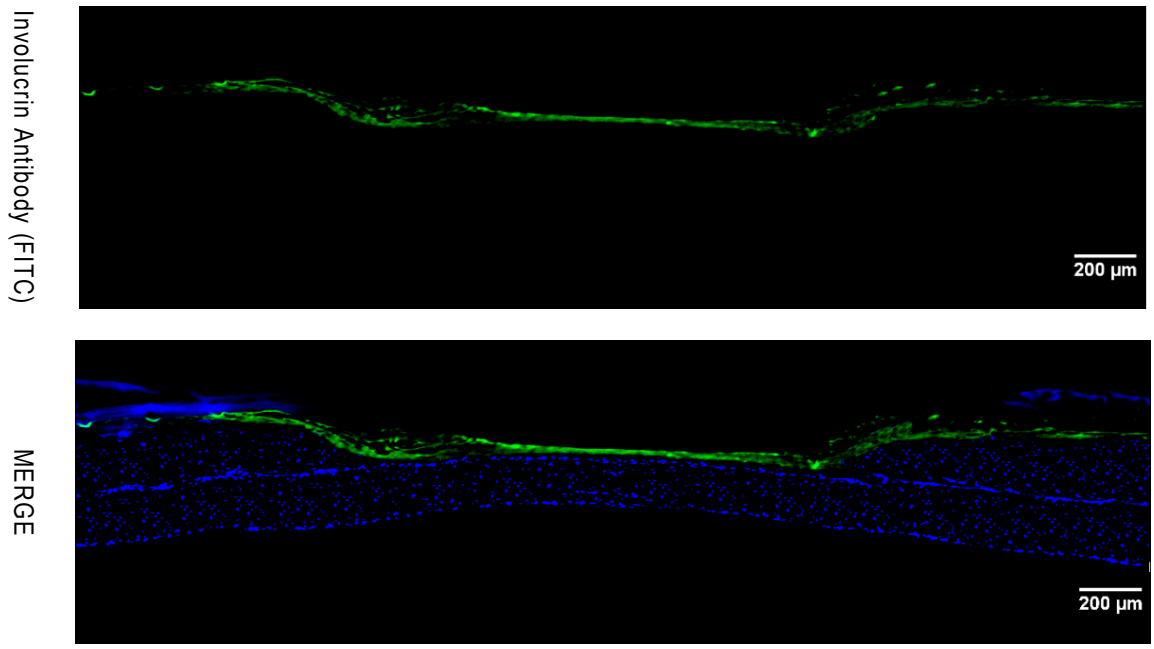

Figure 6.13 MSC-CM mediated expression of involucrin by the epidermal layer at different time points during the healing process.

Representative immunofluorescence images of involucrin expression in wounded 3D skin equivalents cultured in MSC-CM for different time points (1, 2 or 4 weeks). Green FITC fluorescence represents keratinocytes stained with anti-involucrin antibody. Blue= cell nuclei stained with DAPI. Scale Bar: 200 µm.

Furthermore, the re-epithelialised layer also expressed the differentiation marker, loricrin from the early stages of the healing process as illustrated in (Figure 6.14), further emphasising the ability of MSC-CM to promote terminal epidermal differentiation.

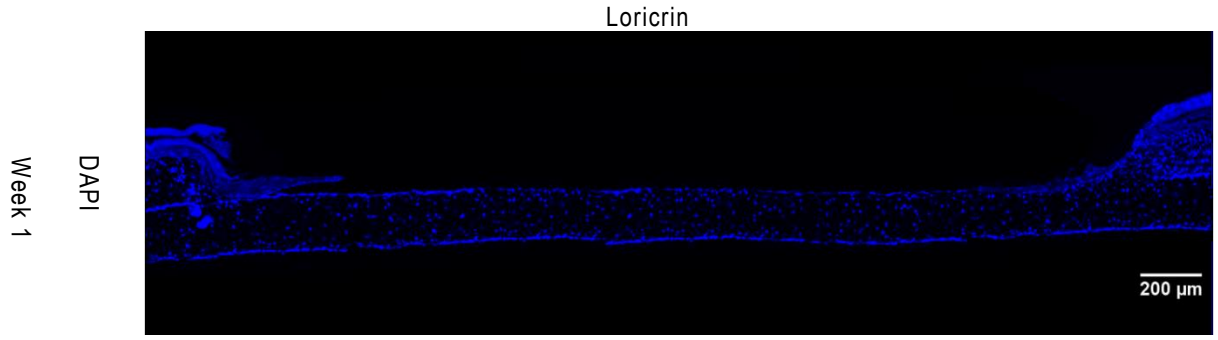

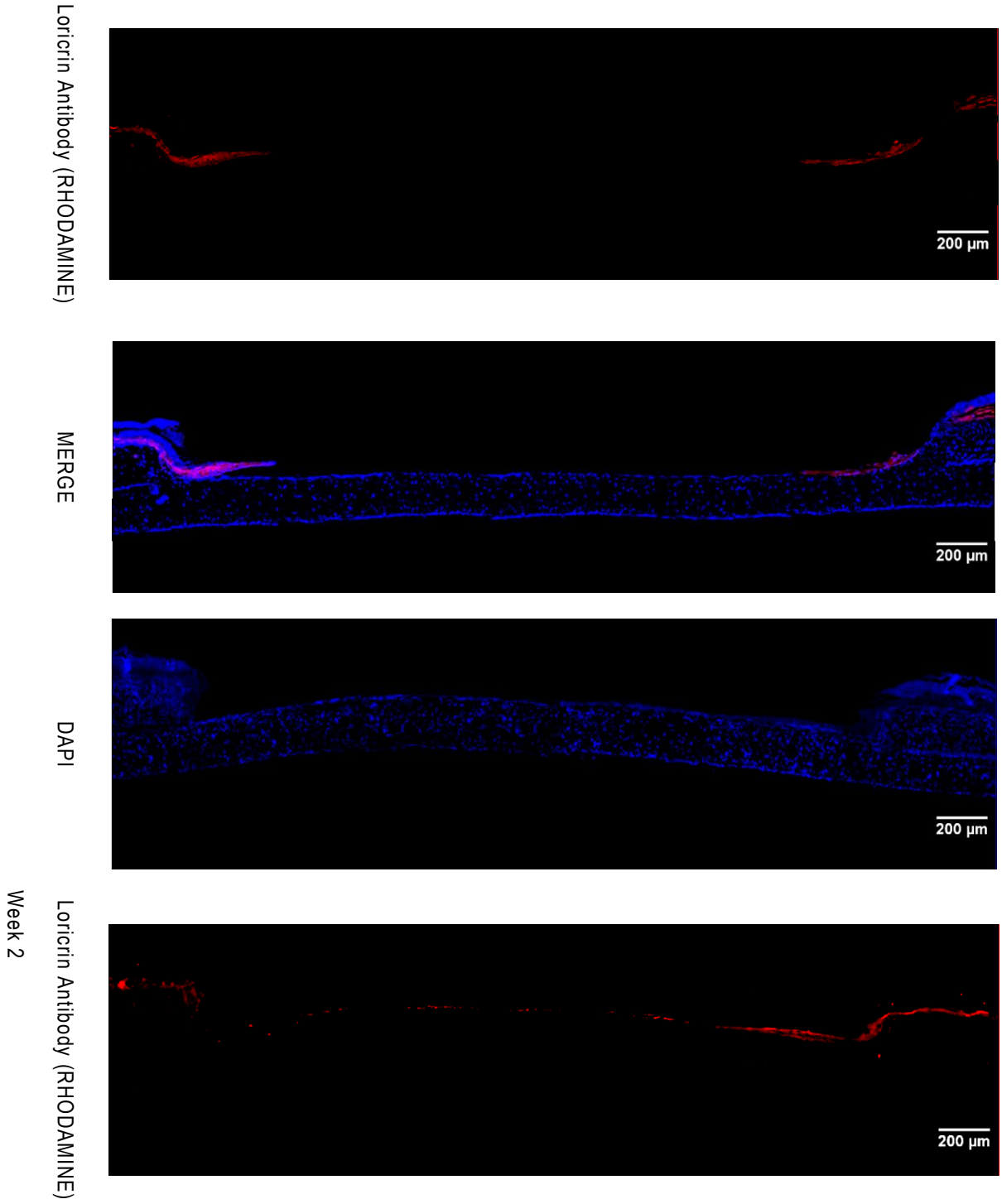
Loricrin Antibody (RHODAMINE)
MERGE
DAPI
Loricrin Antibody (RHODAMINE)
Week 2
200 µm
200 µm
200 µm
200 µm

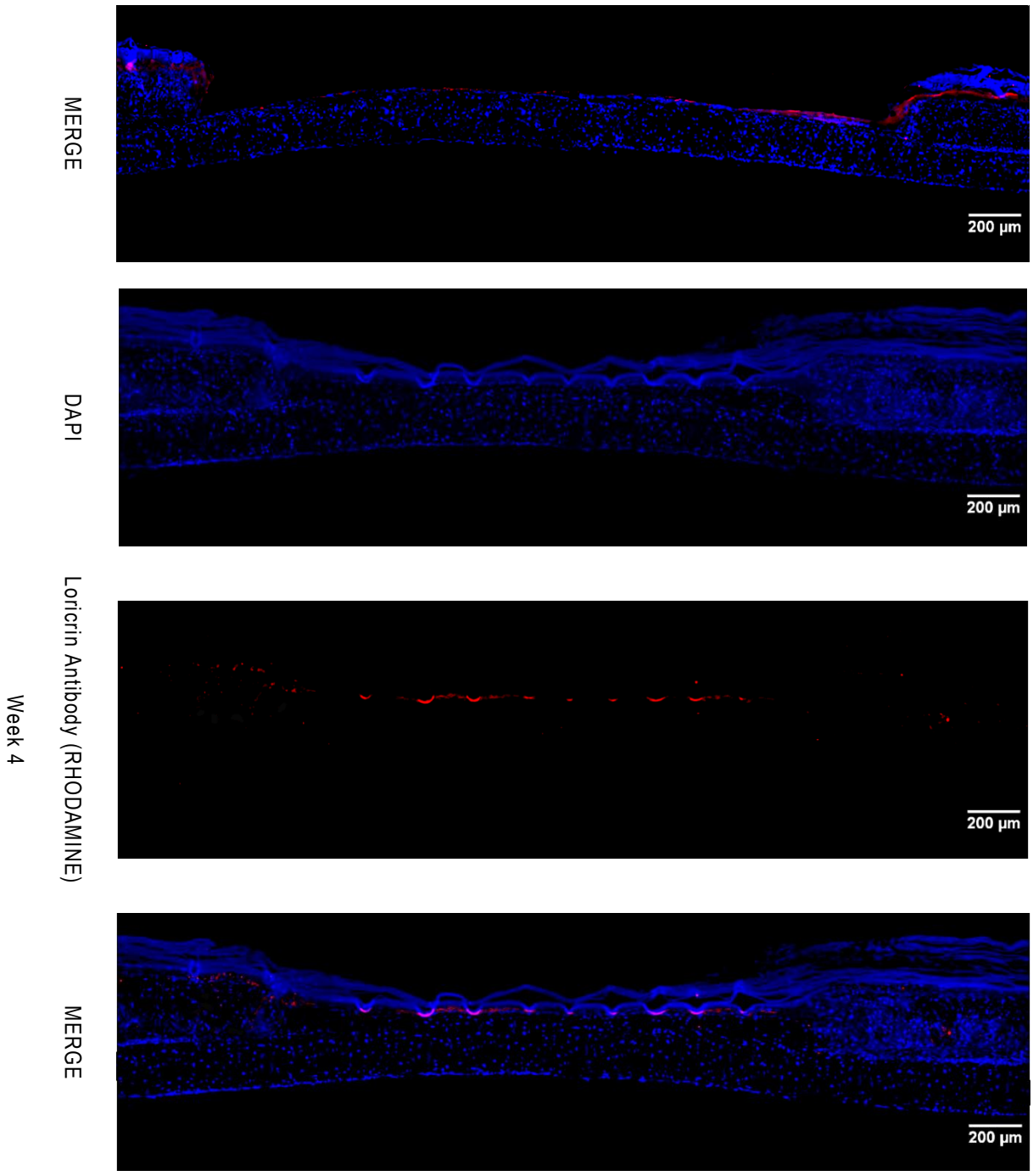

Figure 6.14 MSC-CM promotes Expression of loricrin by the epidermal layer at different time points during the wound healing process.

Representative immunofluorescence images of loricrin expression in wounded 3D skin equivalents cultured in MSC-CM for (1, 2 or 4 weeks). Red Rhodamine fluorescence represents keratinocytes stained with loricrin *Blue= cell nuclei stained with DAPI. Scale Bar=200 µm.*

In addition, MSC-CM also promoted the expression of collagen IV at the recovered wound site (Figure 6.15 A). Expression of this marker beneath the re-epithelialised sheet and over the dermal layer indicates that the recovered wound site was able to form dermal-

epidermal junction or the basement membrane. Additionally, the dermal layer beneath the damaged epidermis retained its ability to express collagen III fibres during the entire healing process (Figure 6.15 B).

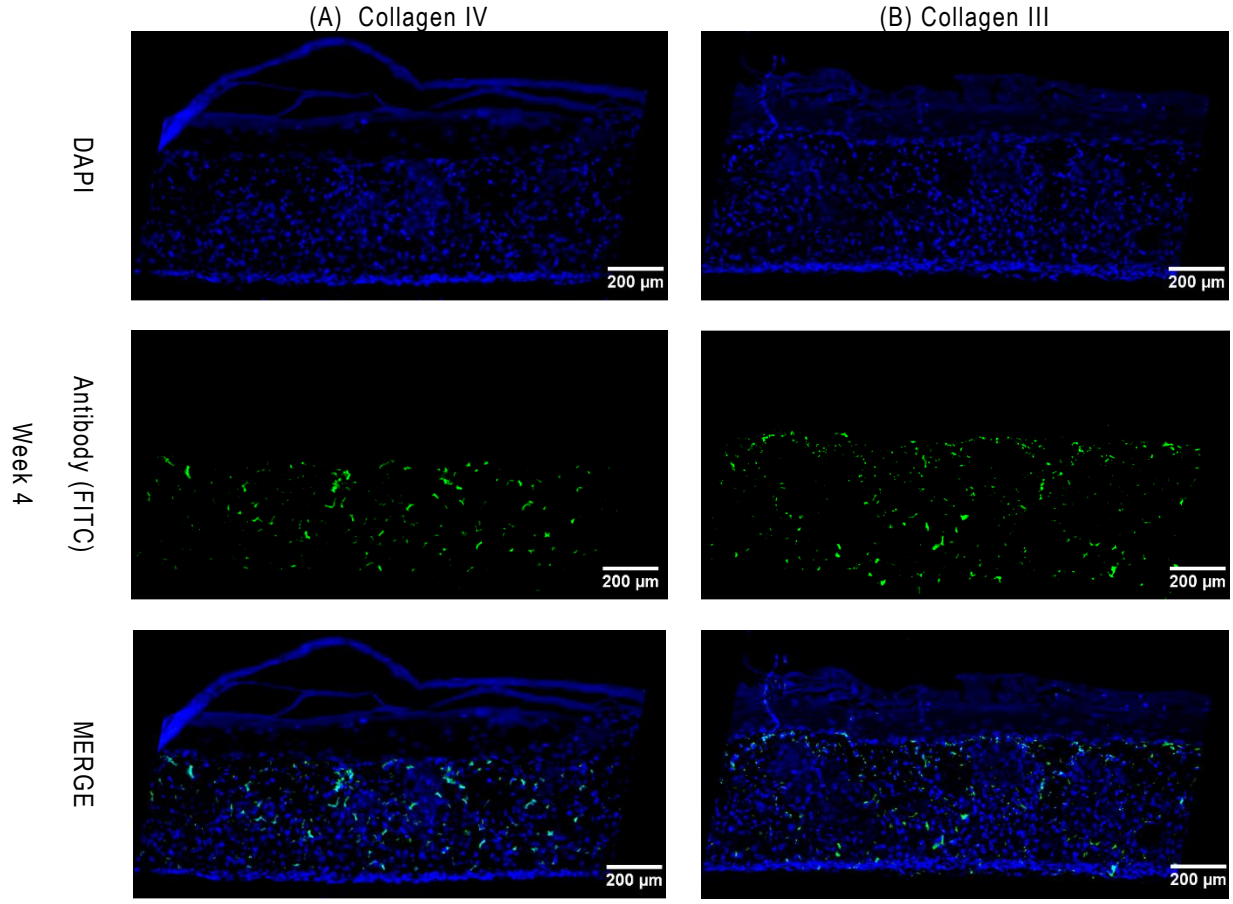

Figure 6.15 MSC-CM promotes expression of collagen IV (column A) and collagen III (column B) by the dermal layer during the healing process.

Representative immunofluorescence images of collagen III and collagen IV expression in wounded 3D skin equivalents cultured in MSC-CM at 4 weeks. (A) Green fluorescence represents collagen IV expression in the dermal layer. (B) Green FITC stain represents keratinocytes stained collagen III. Blue= cell nuclei stained with DAPI. Scale Bar=200 µm.

6.3.3 MSCs Differentiate into 3D Epidermal-like Structures When Incorporated Over Dermal Fibroblast Layers Using The alvetex® Scaffold

The potential for MSC's to differentiate into epidermal-like cells in 3D cell culture was evaluated by construction of a MSC derived epidermal like structure (MSC-ELS). MSCs were tested for their ability to form a full thickness epidermal layer using the same protocol for constructing the 3D skin model with some differences i.e., after obtaining the first fibroblast layer, MSCs were seeded over this fibroblast layer instead of primary

keratinocytes and maintained in epidermal differentiation media (EDM) for three weeks. While some models were harvested after 14 days, others were evaluated after 21 days. Evaluation of MSC differentiation into an epidermal like structure (ELS) was detected by two techniques; haematoxylin-eosin (H-E) staining (Figure 6.16) and immunofluorescence staining (Figure 6.17).

As demonstrated in (Figure 6.16), MSCs formed epidermal like layers similar to that of real skin following 3 weeks treatment with EDM, forming distinct layers stacked over each other, similar to stratified epidermis and indicating that MSCs were able to differentiate into different epidermal layers. On the other hand, the dermal layers were able to grow and retain their ability to produce collage fibres when covered with MSCs. Notably, the two layers (dermis and epidermis) were separated by an obvious junction which could serve as a basal zone between the two layers suggesting that both MSC and fibroblast co-culture could successfully produce a skin like structure.

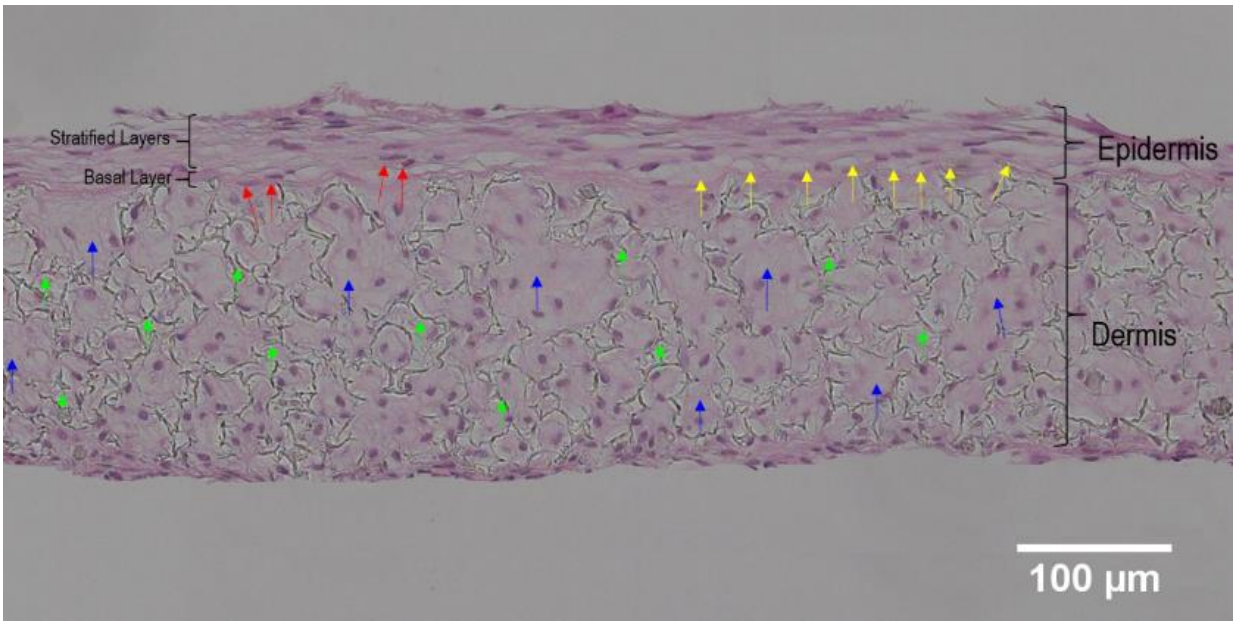

Figure 6.16 MSCs differentiate into epidermal like structure when incorporated onto dermal fibroblast layer on Alvetex® scaffold.

Representative photomicrograph of an H and E revealing that MSCs are able to differentiate into epidermal-like cells and form stratified epidermal like structures when seeded over a fibroblast layer in a 3D culture forming together a skin-like structure similar to real skin. The fibroblast in the dermal layer (green arrows) showed the ability to form collagen fibres (blue arrows). The dermal and epidermal layers are separated by a junction labelled with yellow arrows which could be a basal membrane.

Additionally the immunofluorescent expression of epidermal differentiation markers was analysed. As shown in figure (Figure 6.17) MSCs seeded over dermal fibroblasts

expressed almost the full panel of epidermal differentiation markers, including K14 in the basal layer (Figure 6.17 D), and K10, suggesting their ability to differentiate into spinoum and granum keratinocytes (Figure 6.17 C). MSCs also expressed involucrin (Figure 6.17 B) and loricrin (Figure 6.17 A). In addition, the dermal fibroblasts covered with MSCs retained their expression of collagen III (Figure 6.17 E) indicating the formation of collagen fibers. Furthermore, collagen IV expression was observed in the middle junction between the two layers (Figure 6.17F). Collectively the expression of this panel of biomarkers by MSC-fibroblast co-cultures suggested that MSCs could participate in skin regeneration and could perhaps thus be used as a cellular therapy for chronic wounds to compensate for the damaged epidermal cells in the wound site.

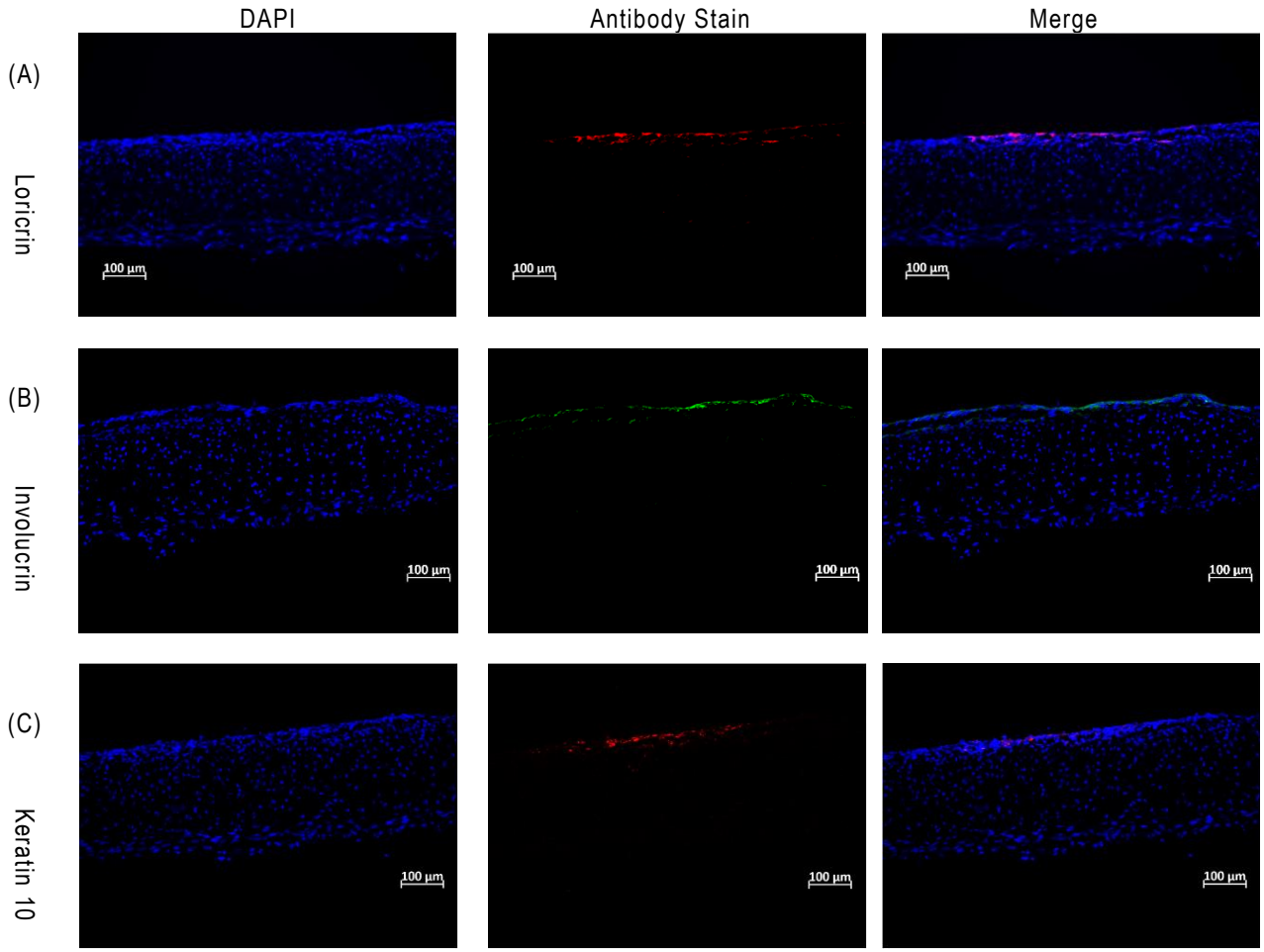

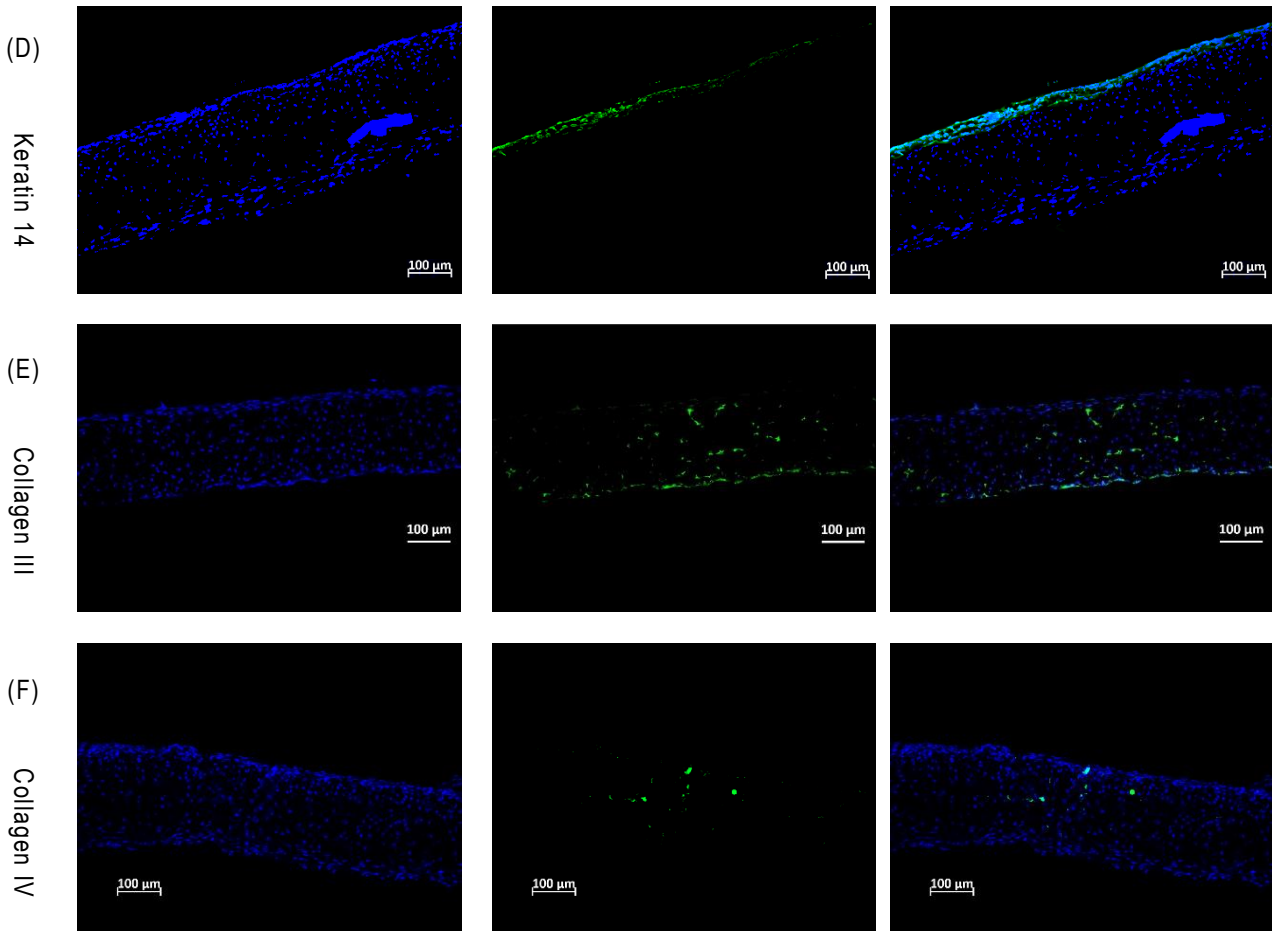

Figure 6.17 MSCs express full panel of epidermal differentiation markers and dermal markers when fed with epidermal differentiation media.

Immunofluorescence images of MSC-3D model revealing the expression of epidermal differentiation markers. (A) Loricrin (Rhodamine red), (B) Involucrin (FITC green), (C) Keratin 10 (Rhodamine red), (D) Keratin 14 (FITC green) and dermal markers (E) Collagen III (FITC green) and (F) Collagen IV (FITC green). Blue= cell nuclei stained with DAPI. Scale Bar=100 µm.

6.4 DISCUSSION

Not all events of the healing process are able to be evaluated in 2D culture. Instead, 3D models are required to investigate important events such as collective cell migration, epidermal layer formation, dermal substrate formation, re-epithelialisation and collagen production. In addition, to date there are no consistent protocols for screening the efficacy of wound healing drugs, and hence leaving an urgent demand to develop 3D skin models for wound healing studies and drug testing, including those suitable for evaluating the potential efficacy of MSC secretions on wound healing. The present study sought to develop a new model and robust protocol for wound healing studies to test MSC-CM as a candidate wound healing agent.

6.4.1 CREATING AND CHARACTERISING THE 3D-SEM FOR WOUND HEALING

The model developed in this study has been shown to be a reproducible tool for wound healing studies for many reasons. First, it is an autologous model as all cellular components are derived from the same donor. Secondly, it provides an easy means of inducing a consistent wound, in terms of size and depth without using complicated methods such as a laser, electricity or radiation. Thirdly, it allows for the migration of the epidermal layer at the wound edge over other cellular components (the second dermal layer) thereby mimicking cell migration in an *in vivo* wound. Furthermore, this adapted skin equivalent and novel model of wound healing also provides a healing index consistent with cutaneous wound repair, including collective cell migration, epidermal thickness and full stratification, constructed on a second fibroblast layer, promoting collagen production and increased longevity This model therefore is able to remain in culture for more than one month, which would allow investigation of cellular responses that require monitoring and which cannot be achieved via a 2D scratch assay.

Results also revealed that the seeding of a wounded 3D skin equivalent onto a second matched donor fibroblast monolayer served as an effective and stable bed, promoting the overall stability of the 3D equivalent and providing an optimal means through which to evaluate the wound healing process in 3D culture. Use of this system may therefore open up new trends for the possibility of constructing allogenic or autologous models for

immunological studies during the healing process. Collectively, this system thus closely mimics *in vivo* wounding and wound healing.

Compared to other studies, results obtained from experiments performed on this adapted 3D-SEM revealed that the epidermal cells exhibited collective migration similar to that of *in vivo* wound healing, as reported by Chavez and colleagues, who demonstrated the migration of K14 positive keratinocytes as a sheet from the intact edges around the wound towards the wound centre (Chavez *et al.*, 2012).

Results obtained here are consistent with previous studies and in the context of proliferation during wound healing, results from the present study also revealed the generation of an epidermal sheet (epidermal tongue) which grew as a triangle like shape with the thicker part close to the wound edge and the thinner element close to the wound centre (Evans *et al.*, 2013). Far from random regeneration, this represents a highly organised process comprising overlapping events of more than one cellular activity leading to ideal healing. Here it could be suggested that cells are firstly evoked to migrate to encase the wound area rather than proliferate at the early stages of the healing, with a later switch to a proliferative response. Upon termination of proliferation, results revealed that keratinocytes started to differentiate to retain a full thickness epidermis.

These findings are also supported by results derived from wound healing in 2D cultures (Chapter 5 Section 5.3.2.4) where keratinocyte proliferation was inhibited by MMC, and detection of the BrdU proliferation marker in migrated keratinocytes. The presence of 20% of proliferating cells in the scratch area of wounded keratinocytes in 2D and the presence of continuous migration during inhibition of proliferation indicated that the majority of keratinocytes undergo migration rather than proliferation or differentiation. It could therefore perhaps be suggested that migrating cells from the wound sides towards the wound centre move from the unwounded intact edges and not from the extending epidermal tongue. Later, migrating cells in the wound healing response may act as a bed to be further covered with proliferative cells generated from the intact wound edges. In another words, during the healing process, the first cellular layer that encases the wound area comprises migrating keratinocytes, while in other upper layers keratinocytes are proliferative; these findings are consistent with previous studies demonstrating that the healthy tissue surrounding the wound acts as a generator and supplier of migrating keratinocytes towards the punch centre while proliferative keratinocytes are supplied by

the intact wound margins (Safferling *et al.*, 2013). Another interpretation is that in addition to proliferative keratinocytes, cells coming from the intact wound margins, the migrating cells, stop migrating due to lack of space and switch their response from a migratory to a proliferative response. Hence, this newly formed epidermal layer acts as a basal keratinocyte layer that serves to supply the developing/differentiating upwards layers of epidermis. This suggestion could also explain the observed doubling in thickness of the newly generated epidermal tongue at the wound borders in comparison to the thickness of intact epidermis and supported by the fact that the upper epidermal layers close to the wound edges are supplied with keratinocytes from two sources i.e. from the intact wound margin and the to the newly formed epidermal sheet (Garlick, 2007). The thickness of the newly formed epidermal layer at the wound borders observed in the developed 3D model were in agreement with Odland and Ross, who reported that upon injury, epidermal keratinocytes are activated to participate in the healing process and enter a hypertrophic state when cells enlarge, resulting in an increase in tissue size (Odland and Ross, 1968). Observations from epithelialisation and epidermal thickness at different time points during the healing of the 3D skin model suggest that cell migration is the first response to be triggered during the healing process.

The healing rate (HR) of wounded 3D skin equivalents was evaluated by measuring the full epidermal thickness over time, calculated by combining the thickness of newly formed epidermis plus with the area covered by it or in another words, migration and proliferation rates collectively. Collectively, migration and proliferation of skin cells during wound healing are termed as regeneration (resulting in the formation of a tongue-like extension), which is a critical and the most important repair mechanism in the healing process (Qing, 2017). Since the early 1970s, many studies have investigated the mechanisms responsible for the regeneration of the new epidermis in the injury site. Three migration patterns have been reported through which the new epidermal layers are generated. The first pattern is a leapfrog mechanism in which, keratinocytes close to the wound edges crawl over each other implying that cells of the suprabasal layer move down into the basal layer and suggesting that migration of cells in the basal layer is slower than the migration of cells in the upper layers (Krawczyk, 1971; Paladini *et al.*, 1996; Danjo and Gipson, 2002; Safferling *et al.*, 2013). The second model is a continuous track-tread (cell sliding) through which cells of every layer migrate along their original extension without

overlapping and implying that cells of the suprabasal layer keep migrating over the basal layer retaining their position (Danjo and Gipson, 2002; Tanner *et al.*, 2009; Safferling *et al.*, 2013). However, this model suggests that that velocity of basal cells is 3 times higher than the velocity of the upper layers (Tanner *et al.*, 2009). The last mechanism proposed by Usui and colleagues (Usui *et al.*, 2005), suggests that only a few basal keratinocytes at the leading edges will migrate, while other post-wounding changes (proliferation and cascading movement of the cells of the suprabasal layer) will cover the wound bed and represent the primary players in recreation of the new epidermis. Formation of a triangular-like sheet could only be attributed to the track-tread mechanism by which basal cells migrate faster than suprabasal cells. However, IF studies in the present study revealed that cells from different layers are present in the newly extending tongue. Furthermore, observations from the present study and other studies suggest that both models (leapfrog and track-tread) could be involved in the wound healing process depending on circumstances such as epidermal thickness and the health and activity of cells close to the wound area. Although, it has been reported by (Tanner *et al.*, 2009) that cells at the wound edges are highly proliferative and act as a positive feedback to the wounding. Other studies have reported that in contrast to other terminally differentiated cells in the suprabasal layer, basal keratinocytes are the only cells with proliferative ability (Morasso and Tomic-Canic, 2005).

Immunofluorescence studies in the present Chapter showed that at week one, expression of K14 was not restricted to the basal layer, but rather expression was evident in the entire epidermal part at the wound margins, consistent with studies by Usui et al (Usui *et al.*, 2008b). This striking difference in K14 expression at the wound edge in comparison to intact skin has also been reported in other studies demonstrating that keratinocytes at the wound edges enter so-called keratinocyte activation (Wawersik *et al.*, 2001). During this stage, keratinocytes switch their response from terminal differentiation to participate in the healing process, undergoing morphological changes and genetic modifications. Additionally, they undergo alterations in keratin expression including the downregulation of differentiation markers (Tomic-Canic *et al.*, 1998). Interestingly, in the present study K14 was strictly expressed by the basal layer after 2 and 4 weeks. On the other hand, the newly formed epidermal sheet expressed the majority of the differentiation markers, from week 1 to full wound closure. These findings further suggest that cells in the regenerated

epidermis retain differential cellular responses such as migration, proliferation and differentiation.

Collectively, observations from the present 3D model for wound healing suggest that combined migration of both basal and suprabasal cells follow either a leapfrog or track-tread pattern. Concurrently, basal keratinocytes of terminated migration could switch their response to proliferate into upper layer cells giving rise to suprabasal cells instead of proliferation of the suprabasal cells themselves as suggested by (Usui *et al.*, 2005). Hence, the thickness of epidermal tongue at the thick side could be attributed not only to the highly proliferative rate of cells present in the wound margins but also to the newly generated cells from newly formed basal layer. Collectively, these post-wounding events may duplicate the cell count during the injury leading to increased thickness of the epidermal layer at the area close to the wound borders.

The shape of newly formed epidermis (thinner in the wound centre than wound edges) in 3D-SEM and presence of 80% migrating cells in the scratch area from the 2D scratch assay, are supported by published findings. For instance, Bellayr and colleagues attributed the priority of keratinocyte migration over cell proliferation at early stages of the healing process is probably mediated by the numerous amounts of chemoattractant growth factors in the niche of the wounded area (and in the current study of MSC-CM) overcoming the amount of proliferation-inducing factors, as evidenced by the rapid migratory response of keratinocytes within a few hours (between 6 and 24 hours) (Bellayr *et al.*, 2010). However, the proliferation phase represents another pivotal phase responsible for actual wound closure. Upon termination of migration, in the case of skin wounds, endothelial non-inflammatory cells such as keratinocytes and fibroblasts start to proliferate to develop new tissues (Santoro and Gaudino, 2005; Usui *et al.*, 2008b; Bellayr *et al.*, 2010). Additionally, fibroblasts are activated and start to differentiate into myofibroblasts which participate in reducing the wound size by contracting and secreting extracellular matrix (ECM) proteins giving rise to healing of the connective tissue (Li and Wang, 2011; Li *et al.*, 2011a).

Expression of collagen III in the dermal layer beneath the injured epidermis of wounded 3D skin equivalents treated with MSC-CM indicated the ability of the dermal layer to survive following injury. Availability of the intact dermal layer is another critical factor that aids the healing process via collagen production and the formation of the dermal-

epidermal zone (basal membrane). Collagen deposition is an important step in formation of granulation tissue during the remodelling phase of the healing process (Mora and Pessin, 2002). Additionally, the dermal fibroblasts in the wounded 3D equivalents in the presence of MSC-CM demonstrated consistent production of collagen III, a consistency that is important for successful remodelling (Zhou *et al.*, 2013). Moreover, continuous production of collagen is critical to compensate for lost collagen by the activity of collagenases and metalloproteinases, which aid in the removal of the excess collagen (Greenhalgh, 1998; Ruszczak, 2003). Additionally, intact dermal fibroblasts in association with the recovered epidermal keratinocytes contribute in the formation of a basement membrane (Varkey *et al.*, 2014). On the other hand, success of the punched model to express collagen IV, which is an essential collagenous glycoprotein produced by the basement membrane (Pöschl *et al.*, 2004) is another indicator for dermal-epidermal cross talk during the healing process since the production of this protein requires keratinocyte-fibroblast interaction (Marionnet *et al.*, 2006). Survival of dermal fibroblasts, their ability to produce collagen and collagen regulating enzymes, participation in formation of basement membrane and tissue remodelling could be mainly attributed to the activity of some growth factors secreted by MSCs such as PDGF and TGF-ß1 (Lynch *et al.*, 1987; Heldin and Westermark, 1999; Ruszczak, 2003).

6.4.2 Investigating the Role of MSC-CM on Wound Healing Using the Developed 3D-SEM

To determine the potential benefits of MSC-CM on cutaneous wound healing using wounded 3D skin equivalents, the punched models were seeded on a secondary fibroblast layer and treated with MSC-CM while the control models were cultured in media A. This healing pattern enhanced by MSC-CM compared to medium control, could be attributed to the role of growth factors present in MSC-CM such as KGF, HGF. PDGF-AB, TGF-1ß, SDF-1α and MSP-1, since these growth factors are well known to enhance cell migration with noted effects of HGF and SDF-1α on the promotion of both migration and proliferation (Alfaro *et al.*, 2008). Availability of this proteomic panel in MSC-CM is sufficient to enhance cutaneous healing with full thickness recovery. These biomolecules work separately or synergistically to heal the damaged tissue. For example, KGF promotes keratinocyte migration and proliferation (Pastar *et al.*, 2014), improving the

healing rate, the quality of epithelialisation, the density of blood vessels (Marti et al., 2008) as well as playing a role in tissue remodelling (Maxson *et al.*, 2012). PDGF stimulates DNA synthesis, attracting fibroblasts to wound sites, controlling collagen production by enhancing fibroblast to produce collagenase, collagen and glycosaminoglycan (Lynch *et al.*, 1987). PDGF is also the first chemotactic growth factor to participate in the migration of fibroblasts, monocytes, and neutrophils into the skin wound, subsequently stimulating the production of extracellular matrix and the induction of a myofibroblast phenotype (Heldin and Westermark, 1999). Additionally, PDGF participates in the inflammatory phase, and tissue remodelling (Barrientos *et al.*, 2008b) and promotes keratinocyte proliferation (Safari *et al.*, 2014). HGF also referred to as plasminogen-related growth factor-1 (PRGF-1) and scatter factor (SF), has been derived from its action as a powerful mitogen for hepatocytes and as a stimulator for epithelial cell dissociation (Werner and Grose, 2003). It also inhibits fibrosis and promotes re-epithelialisation (Chen *et al.*, 2012) as well as enhancing keratinocytes to migrate, proliferate and produce matrix metalloproteinase and stimulate new blood vessel formation. It has therefore been suggested to play a role in cutaneous wound repair (van de Kamp *et al.*, 2013). Like HGF, MSP is also known as scatter factor-2 (SF-2) or hepatocyte growth factor like protein (HGFL). The main actions of this molecule are acceleration of cell migration and proliferation with regulation of proliferation and differentiation of keratinocytes and macrophages. TGF-β1 regulates the inflammatory phase (Barrientos *et al.*, 2008b) by activating macrophages, and suppressing T-lymphocytes (Wang *et al.*, 2012c). TGF-β3 stimulates remodelling (Maxson *et al.*, 2012). Activins which are members of TGF-β family act as enhancers for granulation tissue formation and the induction of extracellular matrix deposition (Werner and Grose, 2003). Zhang and colleagues reported that activin B supports wound repair and regeneration of hair follicles (Zhang *et al.*, 2013); promoting wound closure (Barrientos *et al.*, 2008a; Chen *et al.*, 2008). It has been reported that SDF-1 plays a role in regulating skin homeostasis and tissue remodelling (Werner and Grose, 2003). It also promotes wound closure by inducing cell migration including MSCs migration (Patel *et al.*, 2013). Many of which play an integral role in inflammation, proliferation, migration, differentiation, collagen regulation, angiogenesis and the remodelling phases of the healing process (Cowin *et al.*, 2001)Werner and Grose, 2003). Collectively, these bioactive molecules as components of MSC secretion guide and judge

the healing process in acute and chronic wounds by coordinating numerous cellular responses of different cell types resulting in the re-establishment of the damaged barrier (Barrientos *et al.*, 2008b). In the present study MSC-CM treated models recovered full epithelialisation within two weeks, while control models took four weeks to recover full epithelialisation. On the other hand, epidermal thickness was significantly increased at week 4 indicating termination of migration when the entire punched area was completely encased with cells and the cellular response was switched from migration to proliferation. Hence, it could be suggested that MSC-CM enhances cellular responses including migration, proliferation and differentiation during the healing process and suggests that MSC secretions create an optimal environment for the wound healing process, underpinning their potential as a therapeutic strategy for chronic wounds. Under specific environments (stem cell niche), MSCs show ability to proliferate and differentiate into more specialised cell types to compensate and replace the damaged tissue and ameliorate the injury site (Sun *et al.*, 2007). Again, in the present study, MSCs showed the ability to differentiate into epidermal like cells in 2D culture; however, use of the derived 3D model was more convenient means through which to test the true ability of MSCs to form an epidermal like structure. MSCs in the 3D model in this study, were exposed to an air-liquid interface, they developed a fully stratified epidermis similar to the architecture of real skin and better than in 2D culture. These observations are supported by a hypothesis reported by (Tokuda *et al.*, 2000; Gangatirkar *et al.*, 2007; Ma *et al.*, 2009) that exposure of the culture surface to air will enhance the differentiation and stratification of keratinocytes due to the high oxygen level.

Structurally, MSCs formed a multilayered epidermal like structure in which MSCs possessed epidermal phenotypic traits. Additionally, they expressed the basal keratinocyte marker (K14) and other epidermal differentiation biomarkers such as K10, loricrin and involucrin. These data suggest that MSCs differentiate into the epidermal sublayers and that such differentiation is integral to skin regeneration raising the possibility that MSCs may compensate for lost cells in damaged tissue during the healing process. The ability of MSCs to produce fully differentiated and stratified epidermis is promising for wound healing therapies since differentiation and stratification are integral properties of intact skin when forming a cornified cell barrier that provides rigidity and water resistance (Segre, 2006).

In summary, the protocol developed in this thesis represents a novel, robust and reproducible means of studying wound healing that closely mimics wound healing *in vivo*. Critically, the second fibroblast layer based on seeding dermal fibroblast cells on an inert polystyrene membrane (Alvetex®scaffold) resulted in a dermal layer which served as a stable bed for the previously punched model to lie upon, allowing keratinocytes at the wound edges to migrate over the cellular components. Further modification however, such as the construction of a second dermal layer incorporating immune cells would be required to study the impact and contribution of the immune response to cutaneous healing. Importantly, the present study reveals that MSCs participate in wound healing in two ways; secretory-mediated repair via secretion of growth factors such as HGF, KGF, PDGF-AB, TGFß1, SDF-1α and MSP-1 and via cell-mediated repair. Specifically in this context MSCs might differentiate into basal keratinocytes and act as a reservoir for other epidermal multilayers, while their differentiation into any epidermal cell types might compensate for the required cell type resulting in full epidermal differentiation. The ability of MSC's to function in this capacity during wound healing suggests their potential as a cellular therapy to promote cutaneous wound healing due to their secretions and differentiation potential. However, more research is required to confirm this issue.

Due to the success of the constructed 3D-SEM to visualise the cellular response and behaviour during the healing process at the cellular level, more investigations were carried out to characterise and validate the model at the molecular level as will be discussed in Chapter 7.

CHAPTER 7 THE MOLECULAR BIOLOGY OF WOUND HEALING

CHAPTER SEVEN: THE MOLECULAR BIOLOGY OF WOUND HEALING

7.1 INTRODUCTION

Alongside the cellular mechanisms of wound healing, understanding the molecular events is also crucial in order to fully decipher the processes of chronic wound healing. Examples of these mechanisms include the molecular biology of growth factors and cytokines and their receptors (Qing, 2017), in addition to other molecules such as microRNAs (Banerjee and Sen, 2013).

MicroRNAs represent an essential player in cell fate, and have been identified as useful biomarkers to identify tissue differentiation and organism development (Alvarez (Alvarez-Garcia and Miska, 2005). Additionally, evaluation of microRNA expression is an important technique for understanding complex gene regulation during system-wide investigations, such as the interaction between microRNA expression, microRNA profiling and downstream protein regulation (Rosenfeld *et al.*, 2008). Moreover, microRNAs are advantageous to study over proteins as they are better conserved and preserved, with greater measurable sensitivity in a variety of specimen types such as urine, serum, plasma and even formalin-fixed tissue (Boeri *et al.*, 2011). Therefore, profiling of these small RNAs is an important molecular approach to study and understand the biogenesis, repair and progress in healing processes and diagnosis of many disorders at the molecular level (Rosenfeld *et al.*, 2008; Pritchard *et al.*, 2012). Importantly, microRNA expression profiling of the 3D skin model has not previously been performed, and investigation into the microRNA profile differences between the 3D skin model and real skin is lacking. Hence, developing a 3D-skin explant model (3D-SEM) retaining the same molecular signature of real human skin will open a new trend to use this model as an alternative tool for wound healing studies rather than animal models or *in vivo* clinical trials on patients. Therefore, in this study microRNA profiling was carried out on the 3D skin model and was compared to real skin at different time points during wound healing.

Advances in biotechnology and the development of new techniques has enabled scientists to investigate new mechanisms and strategies for studying and treating disorders including skin diseases. One of the most advanced technologies in this field is nCounter technology from Nanostring Technologies. The nCounter microRNA expression

assay is a novel technique that utilises molecular barcodes (nCounter Reporter Probes) to detect microRNAs in total RNA, during different biological levels of expression. The technique does not require reverse transcription or amplification, and thus provides an ultra-sensitive, reproducible and highly-multiplexed method. Utilising the assay, a large number of data points can be obtained after two principal steps; sample preparation and hybridisation. In the case of standard DNA and RNA analysis, the probe of oligonucleotide-based biosensors captures the sequences based on a 100bp region. However, since microRNAs are short sequences (19-24nucleotides), they need an extra step which involves a bridge sequence specifically binding to the target microRNA, to elongate the microRNA sequence and make it possible to be captured by the probe (Jolly *et al.*, 2016). Therefore, the initial preparation step involves multiplex annealing of the molecular tags to their target microRNAs, followed by the ligation reaction through which a complex (Tag-miRNA) is formed with high specificity and sensitivity at a specifically controlled temperature. A subsequent enzymatic purification removes unbound tags and the remaining barcode-bound microRNAs can be detected from total RNA in the sample (www.nanostring.com) as explained in (Figure.7.1).

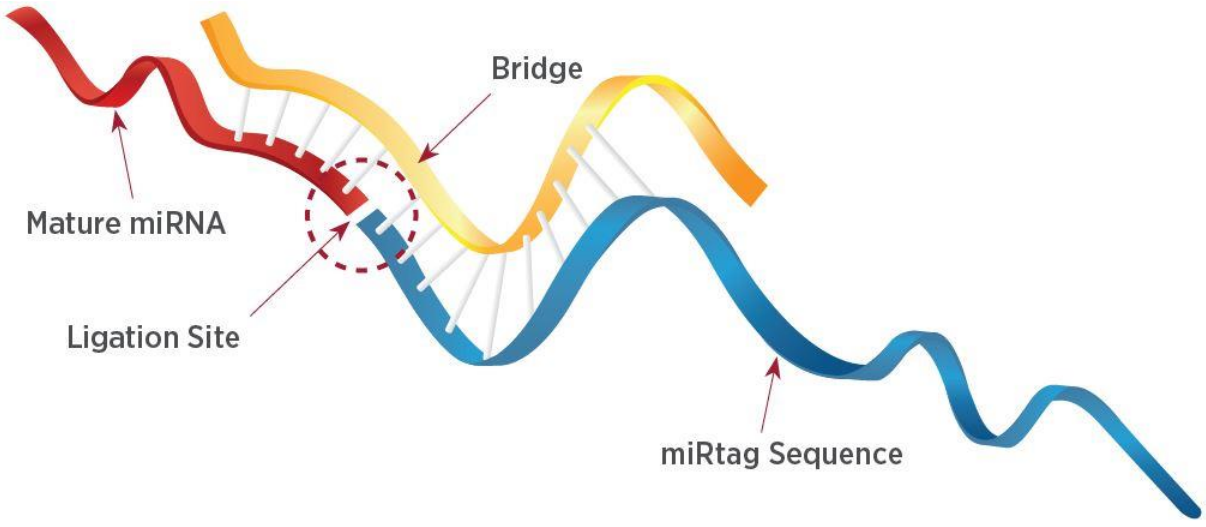

Figure.7.1 Ligation of specific tags to target microRNAs.

The Figure, adapted from (www.nanostring.com), explains the ligation process. The nCounter microRNA Expression Assay contains specific tags that recognise their target microRNA and anneal to these sequences, followed by a ligation step that forms a bridge through precise, stepwise control at specific annealing and ligation temperatures.

In the hybridisation process, a probe pair is introduced in order to achieve the molecular barcoding. It contains two sequences; the capture sequence (Capture Probe), which has a biotin molecule on its 3' end and the reporter sequence (Reporter Probe), which has a signal comprised of four colours in six positions on its 5' end (www.nanostring.com) (Figure 7.2 A).

(A)

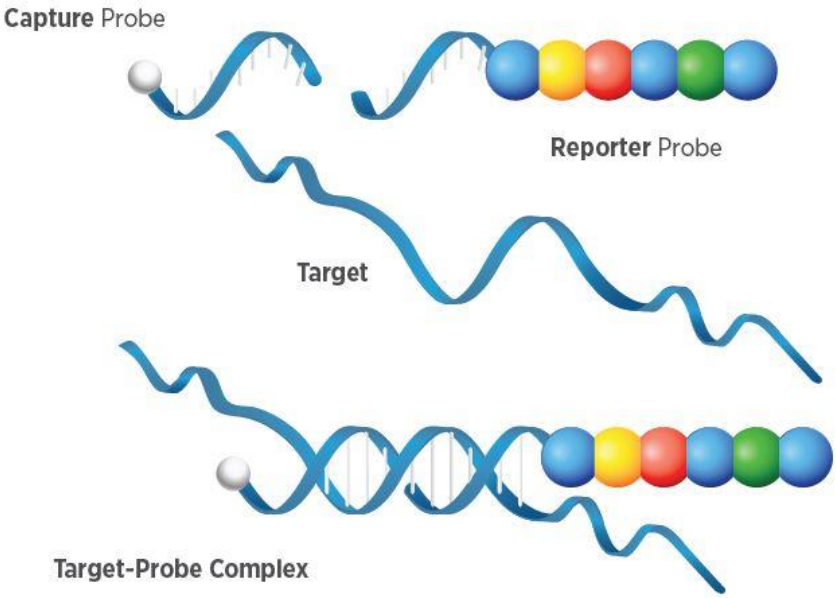

(B)

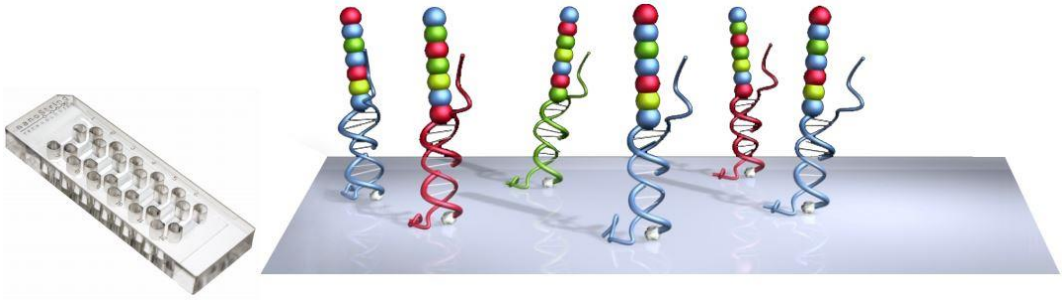

(C)

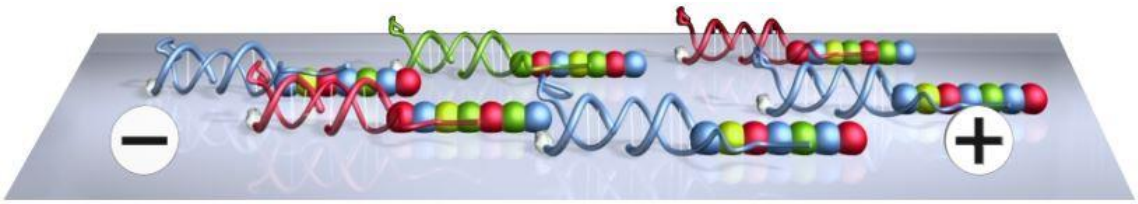

(D)

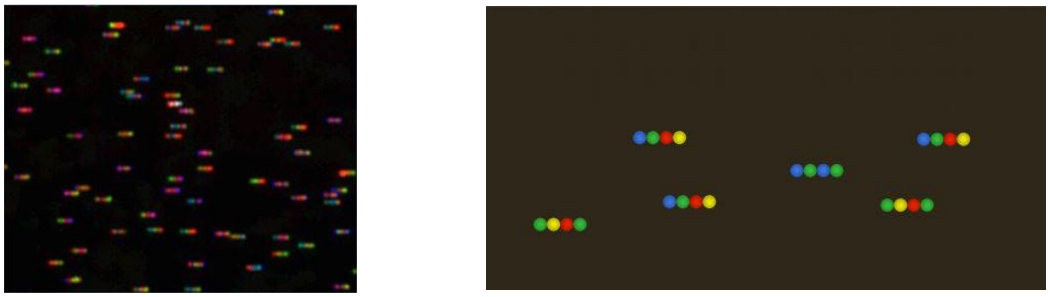

Figure 7.2 Hybridisation of specific tags to the target microRNAs.

The Figure, adapted from (www.nanostring.com). (A) Explains the hybridisation step. Hybridisation of target microRNAs is accomplished via specific binding of probe pairs (Capture probe and Reporter Probe), to form a target-probe complex containing a molecular barcode for digital detection. (B) Binding of the probe to cartridge surface. (C) Immobilisation of the reporters. (D) Image capturing.

During an overnight hybridisation step, incubation with a large excess of probe pairs ensures that every target will bind to a probe pair. The complexity of the coloured barcodes enables a large number of target microRNAs in the same sample for resolution and identification during data collection. After the hybridisation, unbound probes are removed by magnetic-bead purification through two steps; the first is binding of the target-probe complex on magnetic beads that are complementary to a sequence within the capture probe, followed by a washing step to remove unbound reporter probes and non-targeted molecular sequences. In the second step, the target-probe complex and capture probes are eluted from the beads, followed by a further hybridisation to magnetic beads complementary to sequences on the reporter probe. Another washing step is then applied in order to remove the excess capture probes. The final step involves eluting the purified target-probe complex from the beads and binding the hybridised probes to the NanoString cartridge surface which is coated with streptavidin to enable binding of the biotin present in the target-probe complex (Figure 7.2 B). Then, the reporter is immobilised and aligned for image collecting and barcode counting (Figure 7.2 C). Collected data is then analysed and processed by the nCounter digital analyser in order to translate the varying coloured barcodes into digital target counts for every individual microRNA (Figure 7.2 D).

Potential molecules that may be targeted by microRNAs during wound healing are growth factors and their receptors on keratinocytes. Growth factors are a group of proteins secreted by many cell types and serve as multifunctional molecules that promote cellular activities in a variety of cells; however, others are monofunctional and restricted to elicit a response in only one cell type. Hence, growth factors act as signalling molecules to initiate

signalling cascades and evoke cell responses via binding to transmembrane receptors to promote and regulate a variety of cell activities including cell proliferation, division, migration, differentiation, angiogenesis, morphogenesis and apoptosis (Alfaro *et al*., 2013; Barrientos *et al*., 2008b; Chen *et al.*, 2008; Maxson *et al*., 2012; Wang *et al*., 2012; Werner and Grose, 2003; van de Kamp *et al*., 2013). Since the main role of MSCs in promoting wound healing could be attributed to their secretion of growth factors, including those previously detected in MSC-CM such as HGF, KGF, PDGF-AB, TGF-β1, SDF-1α and MSP-1, it is also important to investigate the expression of receptors of these growth factors (c-MET, FGFR-2, PDGF-A, TGF-βR1, CXCR4 and MST-R1 "RON"). Therefore in addition to studying microRNA profiles, growth factor receptors were detected in primary keratinocytes at normal and damaged conditions of wound healing using RT-qPCR. Furthermore, the potential roles of microRNA on these receptors were analysed using various online prediction algorithm software.

Therefore, microRNA profiling was used to characterise the developed 3D SEM, in order to further understand the microRNA expression profiles of the model and to validate the model at the molecular level for future applications in wound healing studies. In addition, microRNA expression profiles were investigated at different time points during the wound healing process, in order to assign microRNA expression signatures. This data may be used to further investigate functional roles of the individual microRNAs and their impact during the wound healing process, which is an important field for developing future molecular therapies to treat non-healing wounds.

7.2 Specific Aims of Chapter Seven

1. **To characterise the developed 3D skin model (3D-SEM) in comparison to human skin at the molecular level using microRNA expression profiling.**
2. To detect differentially expressed microRNAs in the 3D-SEM during the wound healing process after treatment with MSC-CM.
3. To detect growth factor receptors in primary keratinocytes at different time points during wound healing.

7.3 RESULTS

Three samples of normal human skin (S1156K, S1157K and S1158K) were used to study the expression of microRNAs in cutaneous wound healing. Each sample was divided into 2 pieces. The first piece of skin was initially used directly for microRNA isolation, and later used as a reference and control. A second piece of skin was used for constructing an autologous 3D skin model for microRNA isolation after different time points of wound healing. Therefore, comparisons were made between microRNAs isolated from a 3D autologous skin model as well as microRNAs originating from the original autologous skin.

7.3.1 CHARACTERISATION OF THE 3D SKIN MODEL -MICRORNA EXPRESSION PROFILES

In addition to the previous characterisation of the 3D skin model (morphological, structural and epidermal differentiation markers, as mentioned in (Chapter 6), the models were also characterised at the molecular level by investigating their microRNA expression profiles using Nanostring technology which does not need any further amplification and enables the detection of up to 799 microRNAs per sample using bar code imaging. MicroRNA expression in intact 3D-SEM models were compared to expression of microRNAs isolated from the reference real skin in order to a) validate the 3D model as a replica of real skin and also to b) identify microRNAs that show similar expression profiles in the 3D model and real skin, which could be further evaluated to study wound healing. Results showed that the 3D skin model microRNA expression profiles significantly correlated with the original real skin at the molecular level; S1156K $R=0.64$, $p<0.001$, S1157K $R=0.5$, $p<0.001$ and S1158K $R=0.69$, $p<0.001$ (Figure 7.3 A, B and C).

(A)

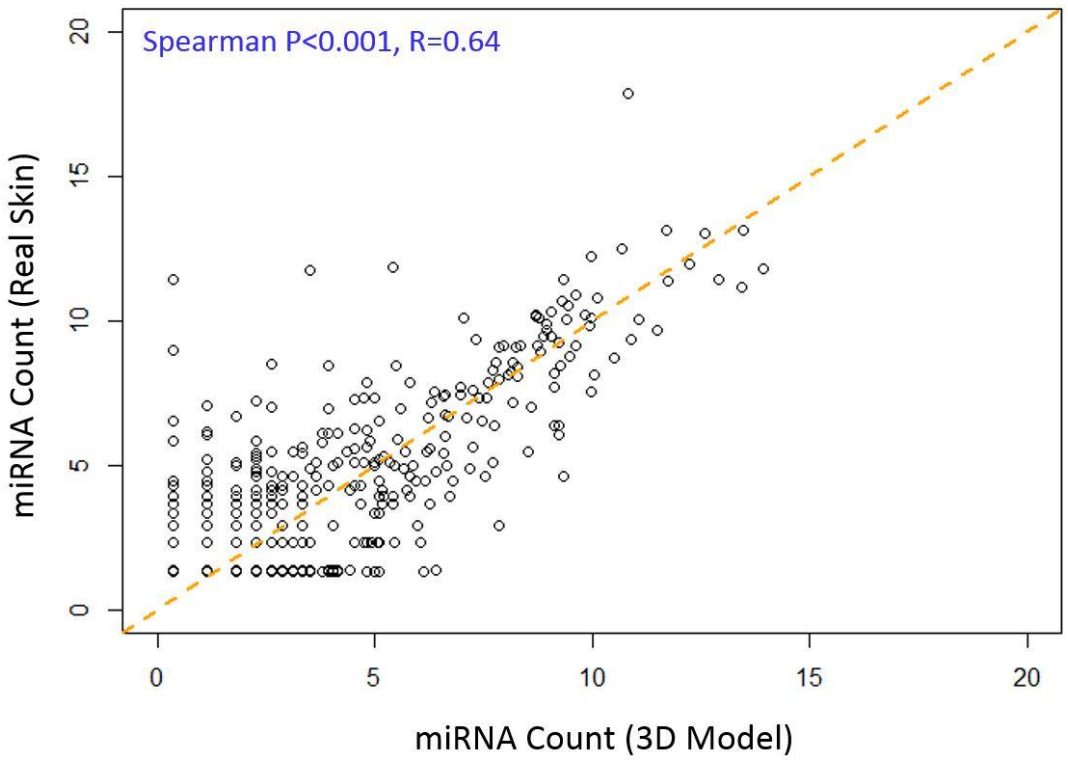
Spearman P<0.001, R=0.64
miRNA Count (Real Skin)
miRNA Count (3D Model)
0
5
10
15
20

(B)

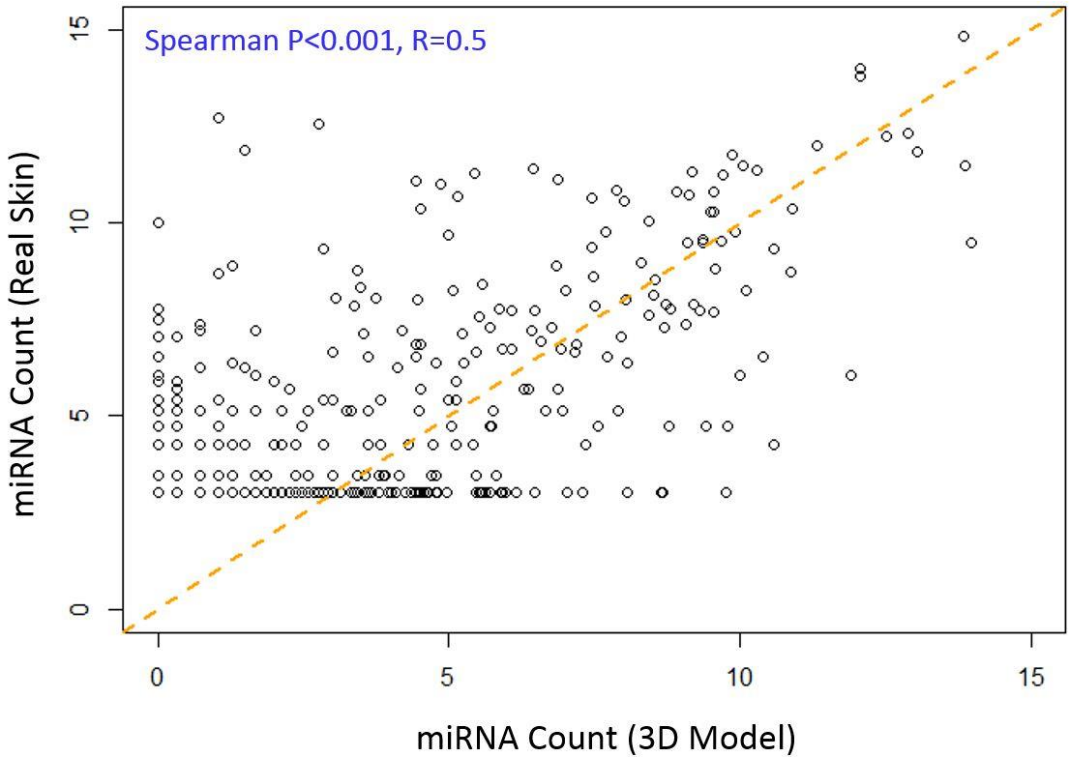
Spearman P<0.001, R=0.5
miRNA Count (Real Skin)
miRNA Count (3D Model)
0
5
10
15

(C)

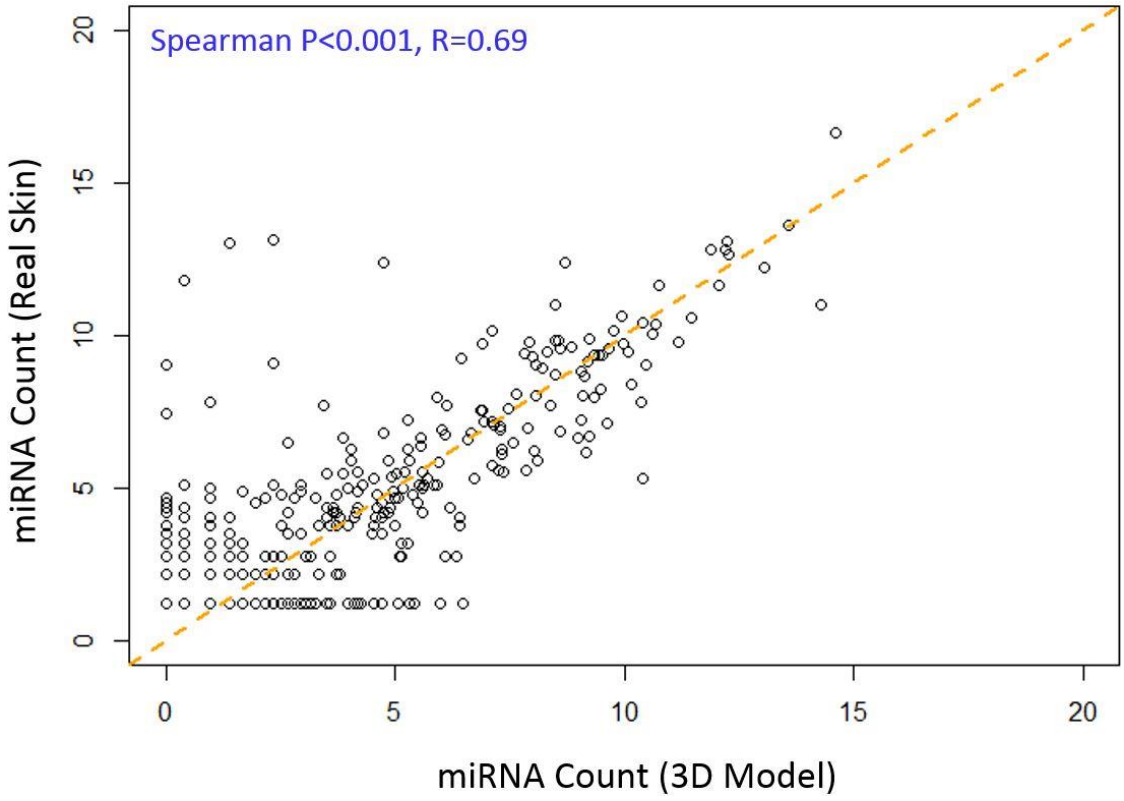

Figure 7.3 Correlation between microRNA expression in real skin and the derived 3D skin models.

Correlation plots represent similarities in the expression of microRNAs between real skin and their derived 3D skin equivalent model (3D-SEM). (A) The correlation between microRNA expressed by the skin sample (S1156K) (y-axis) and its derived 3D-SEM (x-axis) revealed significant correlation between the skin and the 3D-SEM (R=0.64, P=0.001 "Spearman"). (B) The correlation between microRNAs expressed by skin sample (S1157K) (y-axis) and its derived 3D-SEM (x-axis) revealed significant correlation between the skin and the 3D-SEM (R=0.5, P=0.001 "Spearman"). (C) The correlation between microRNAs expressed by the skin sample (S1158K) (y-axis) and its derived 3D-SEM (x-axis) revealed significant correlation between the skin and the 3D-SEM (R=0.69, P=0.001 "Spearman"). Counts of microRNA expression in this figure were generated by the nCounter platform and are represented as log2 of original values.

Despite a general correlation between the real skin and their derived 3D models, there was a significant difference in expression of 31 microRNAs out of the 787 tested microRNAs between the 3D models (N=3) and their original skin (N=3); P<0.05, as explained in (Figure 7.4 A and B).

(A)

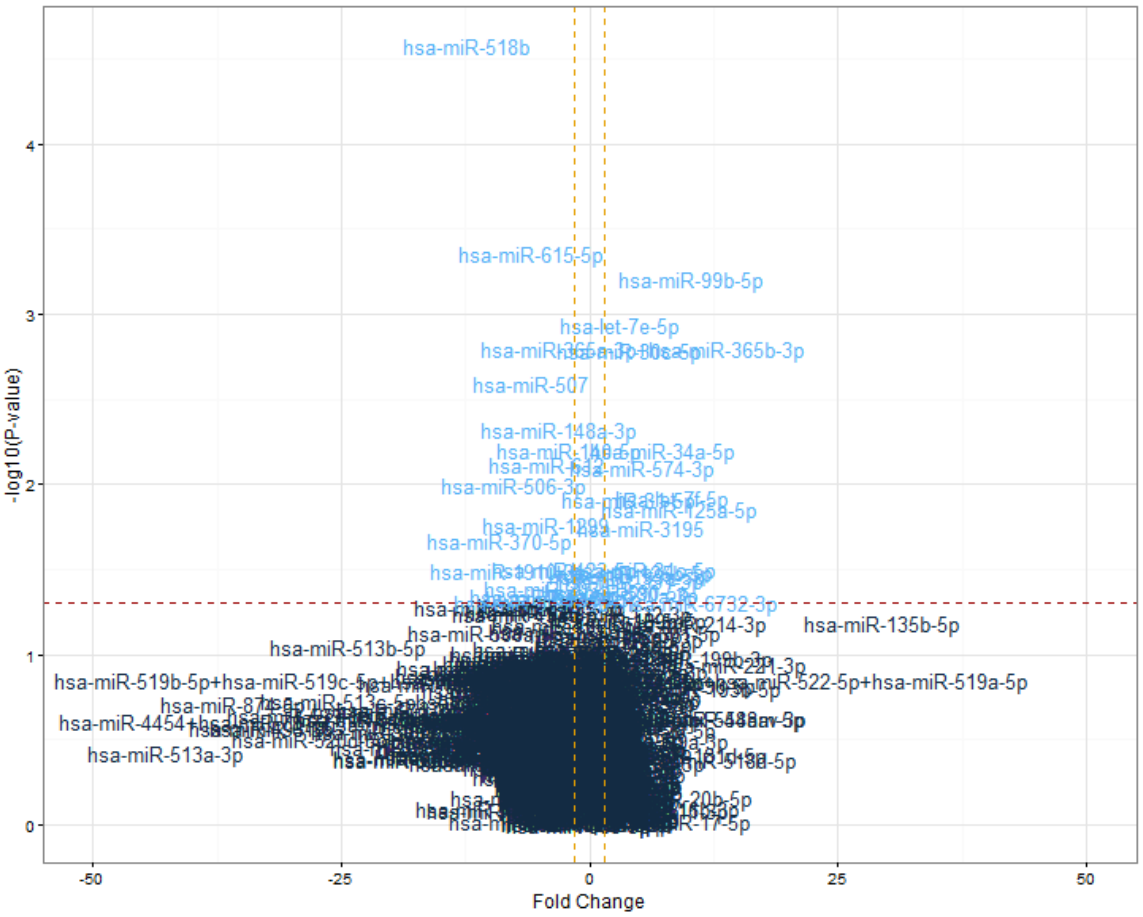

(B)

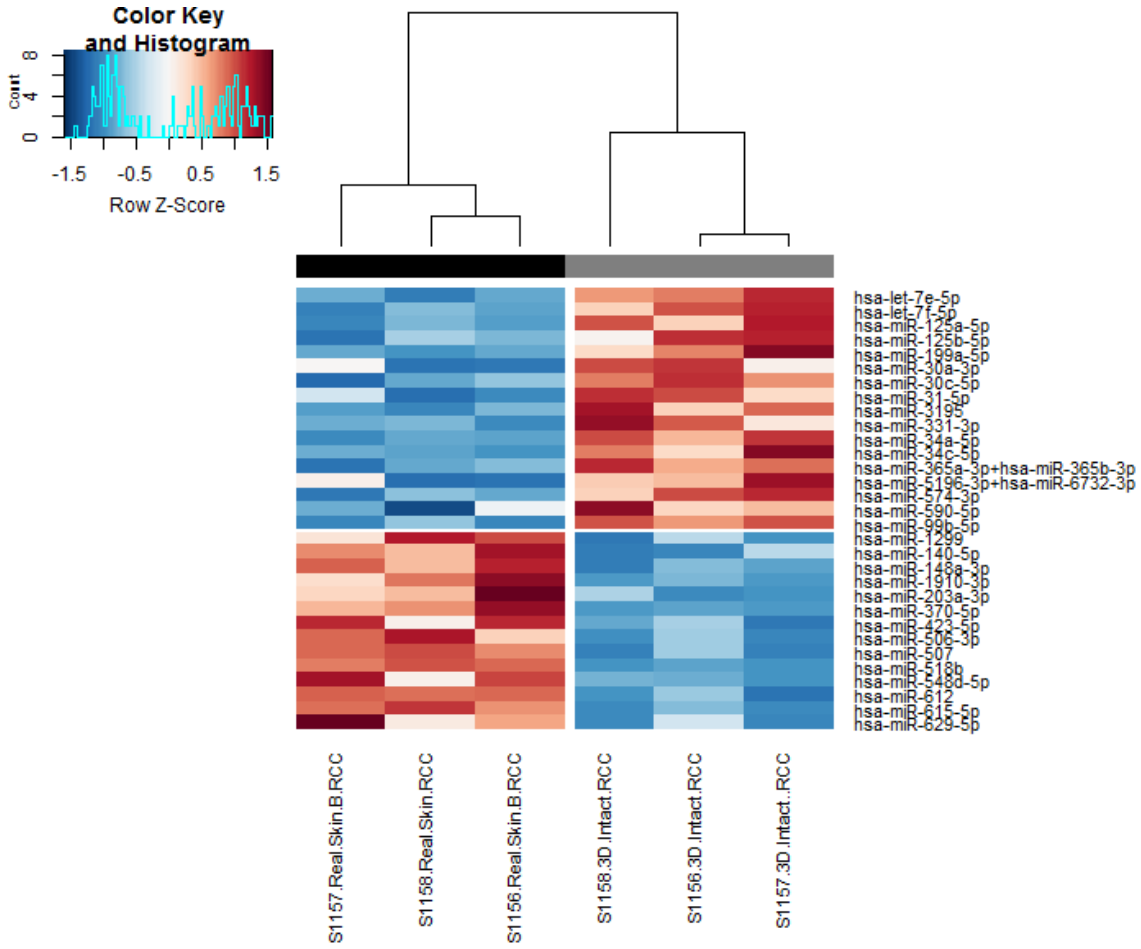

Figure 7.4 Differential microRNA expression between real skin and their derived 3D skin equivalent models (3D-SEM).

This figure shows that the microRNAs expressed by real skin (N=3) and their derived 3D-SEM (N=3). (A) Volcano plot representing a statistical analysis (fold change"x-axis" versus - log10 of P value "y-axis") of the whole panel of microRNAs assessed in 3D-SEM compared to their original skin sources. The analysis revealed that 31 microRNAs (pale blue colour) were significantly differentially expressed by the 3D models compared to the skin sample. A larger -log10 value represents a smaller P-value e.g. miR-518b has (-log 10 (4.5) ~ (P=0.00003)) which means it has the most significant variation in expression between the two groups. (B) Heat map plot representing the 31 significantly differentially expressed microRNAs between the 3D models compared to heir corresponding real skin. Colour Key; Red = Higher microRNA count, i.e. gradual change from orange to red means gradual increase in microRNA count. Blue = Lower microRNA count i.e. gradual change from light blue to dark blue means gradual decrease in microRNA count.

Details of the 31 differentially expressed microRNAs and more information about differences in their expression and their roles in skin morphogenesis and regeneration are listed in (Table 7.1). Fold change showed that some of these microRNAs (1-17) showed significantly higher expression in 3D-SEM than in real skin, while the opposite expression pattern was shown for other microRNAs (18-31), which demonstrated significantly lower expression in 3D-SEM compared to real skin.

	MicroRNAs	Expression (↑) or (↓)	Fold Change	P value	Role in Skin	References
1	has-let-7e-5p	↑	3.05	0.001	Keratinocyte differentiation	Hildebrand et al. 2011
2	has-let-7f-5p	↑	8.26	0.012	Keratinocyte differentiation	Hildebrand et al. 2011
3	miR-125a-5p	↑	8.90	0.013	Terminal keratinocyte differentiation	Hildebrand et al. 2011
4	miR-125b-5p	↑	4.47	0.032	Skin development and morphogenesis and epidermal differentiation	Yi et al., 2008
5	miR-199a-5p	↑	3.76	0.034	Skin development and morphogenesis	Zhang et al., 2011
6	miR-30a-3p	↑	3.69	0.044	Sclerosis and rheumatoid arthritis in dermal fibroblast	Alsaleh et al., 2014
7	miR-30c-5p	↑	4.09	0.001	Regulates coagulation	Marchand et al., 2012
8	miR-31-5p	↑	3.89	0.012	Enhances proliferation and migration of keratinocytes	Li et al., 2015
9	miR-3195	↑	5.10	0.017	Dermal papilla cell related molecule	Cha et al., 2014
10	miR-331-3p	↑	4.23	0.036	Normal melanocyte related molecule	Villaruz et al., 2015 and Sha et al., 2016
11	miR-34a-5p	↑	7.36	0.006	Scarless wound healing	Zhao et al., 2015
12	miR-34c-5p	↑	5.43	0.031	Scarless wound healing	Zhao et al., 2015
13	miR-365a-3p+miR-365b-3p	↑	5.27	0.001	No Data Found	
14	miR-5196-3p+miR-6732-3p	↑	2.85	0.049	No Data Found	
15	miR-574-3p	↑	5.29	0.007	Enhances keratinocyte differentiation and reduces cell proliferation	Chikh et al., 2011
16	miR-590-5p	↑	2.80	0.042	Atopic dermatitis	Rozalski, Rudnicka, Samochocki, 2011
17	miR-99b-5p	↑	10.23	0.0006	Promotes wound healing	Jin et al., 2013
18	miR-1299	↓	-4.36	0.016	Melasma pigmentation	Kim et al., 2017
19	miR-140-5p	↓	-2.03	0.006	Terminal keratinocyte differentiation	Hildebrand et al. 2011
20	miR-148a-3p	↓	-3.016	0.004	Terminal keratinocyte differentiation	Hildebrand et al. 2011
21	miR-1910-3p	↓	-8.18	0.031	No Data Found	

22	miR-203a-3p	↓	-2.85	0.040	Enhances migration and proliferation of keratinocytes. Re-epithelialisation and haemostasis.	Viticchiè et al., 2012
					Supports proliferation of basal keratinocytes. Maintains the stratification potential of epithelial cells.	Banerjee, Chan and Sen, 2011
23	miR-370-5p	↓	-8.99	0.021	Therapeutic target for Psoriasis	Anandaram and Anand, 2017
24	miR-423-5p	↓	-2.55	0.031	Involved in many skin diseases	Lawrence and Ceccoli, 2017
25	miR-506-3p	↓	-7.64	0.009	Melanoma related molecule	Carpi et al., 2016
26	miR-507	↓	-5.86	0.002	Melanoma related molecule	Wei et al., 2016
27	miR-518b	↓	-12.41	0.00002	Epithelial lineage differentiation	Kushwaha et al., 2014
28	miR-548d-5p	↓	-2.70	0.045	No Data Found	
29	miR-612	↓	-4.24	0.007	Migration and proliferation of RPE1 (Normal human epithelial cell line)	Bhajun et al., 2015
30	miR-615-5p	↓	-5.86	0.0004	No Data Found	
31	miR-629-5p	↓	-4.81	0.045	No Data Found	

Table 7.1 Further details of differentially expressed microRNAs by real skin and their derived 3D skin model equivalents (3D-SEM).

The table illustrates the 31 microRNAs that were differentially expressed between 3D models in comparison to their original source of real skin, including direction of expression fold change, fold change value, P-value and their roles in skin morphogenesis and regeneration according to recent literature. Expression of 17 microRNAs (1-17) in 3D-SEM were significantly higher than their counterparts in real skin. While expression of 14 microRNAs (18-31) were significantly lower than their counterparts in the real skin. (↑)= higher expression and (↓) = lower expression in 3D-SEM than real skin.

7.3.2 Differentially Expressed MicroRNAs by the 3D Skin Model During Wound Healing

To investigate the alterations in microRNA expression profiles during skin wound healing, the modified 3D model, validated and confirmed in Chapter 6, to mimic *in vivo* wound healing, was used monitor repair of the wound during real-time at different time points. For example, 2 and 4 hours (Madhyastha *et al.*, 2012; Li *et al.*, 2015b), 24 hours (Jin *et al.*, 2013b; Li *et al.*, 2014; Bhattacharya *et al.*, 2015; Li *et al.*, 2015b), 72 hours (Viticchie *et al.*, 2012) and 1 week (Wang *et al.*, 2012b; Bhattacharya *et al.*, 2015; Li *et al.*, 2015b).

These time points were selected to study microRNAs that were expected to participate in all phases of the healing process (haemostasis, inflammation, epithelialisation, contraction and remodelling) at different time points.

Data analysis revealed specific signatures using nCounter Human v3 microRNA Expression Assay Kit (GXA-MIR3-12) which allow detection of up to 799 microRNAs per sample. Briefly, a wound was induced to the 3D-SEM via 3 mm punch biopsy and models then treated with MSC-CM and harvested after different time points i.e. 2, 4, 24, 72 hours and 1 week for microRNA analysis. All Nanostring data was passed through quality control, normalisation and analysed according to statistical analysis of microRNA profiling (Chapter 2, Section 2.4.2) to detect microRNAs that were differentially expressed and modulated at the different time points during wound healing in comparison to the intact 3D models.

After 2 hours of initiating the healing process, microRNA expression analysis showed that 14 microRNAs were significantly differentially expressed in the wounded models compared to the intact models, as detailed in the (Figure 7.5 A and B) volcano plot and heat map.

(A)

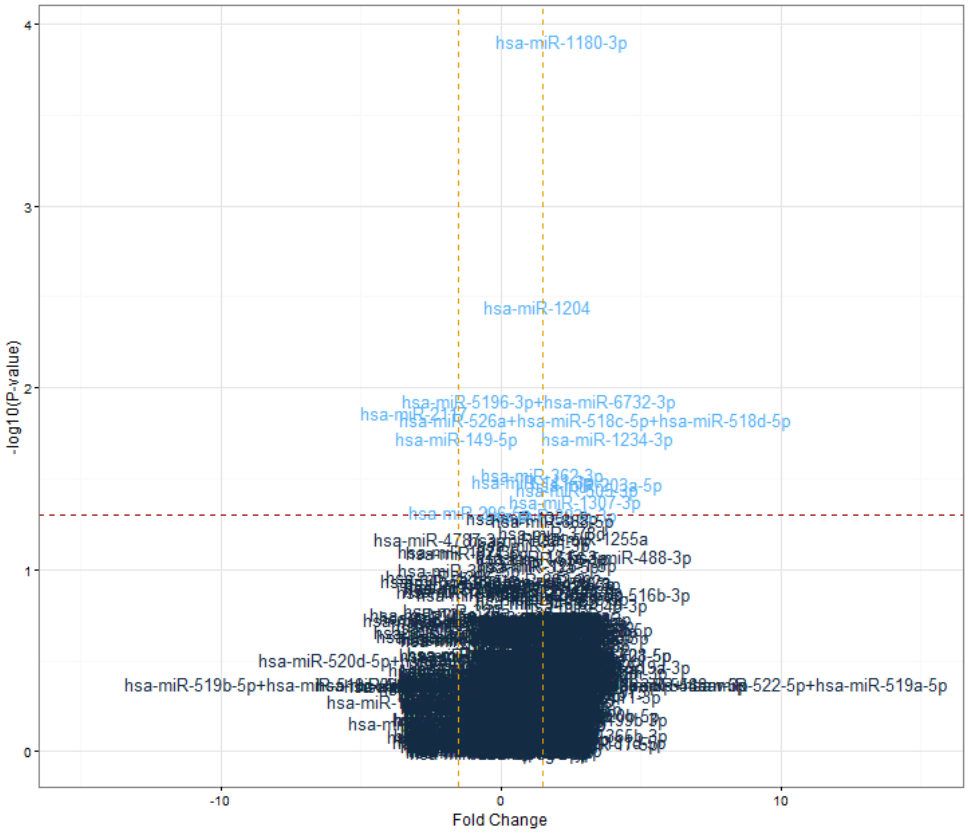
hsa-miR-1180-3p
hsa-miR-1204
hsa-miR-5196-3p+hsa-miR-6732-3p
hsa-miR-526a+hsa-miR-518c-5p+hsa-miR-518d-5p
hsa-miR-149-5p
hsa-miR-1234-3p
hsa-miR-1307-3p
hsa-miR-1255a
hsa-miR-488-3p
hsa-miR-516b-3p
hsa-miR-520d-5p
hsa-miR-519b-5p+hsa-miR-522-5p+hsa-miR-519a-5p
-log10(P-value)
Fold Change
4
3
2
1
0
-10
0
10

(B)

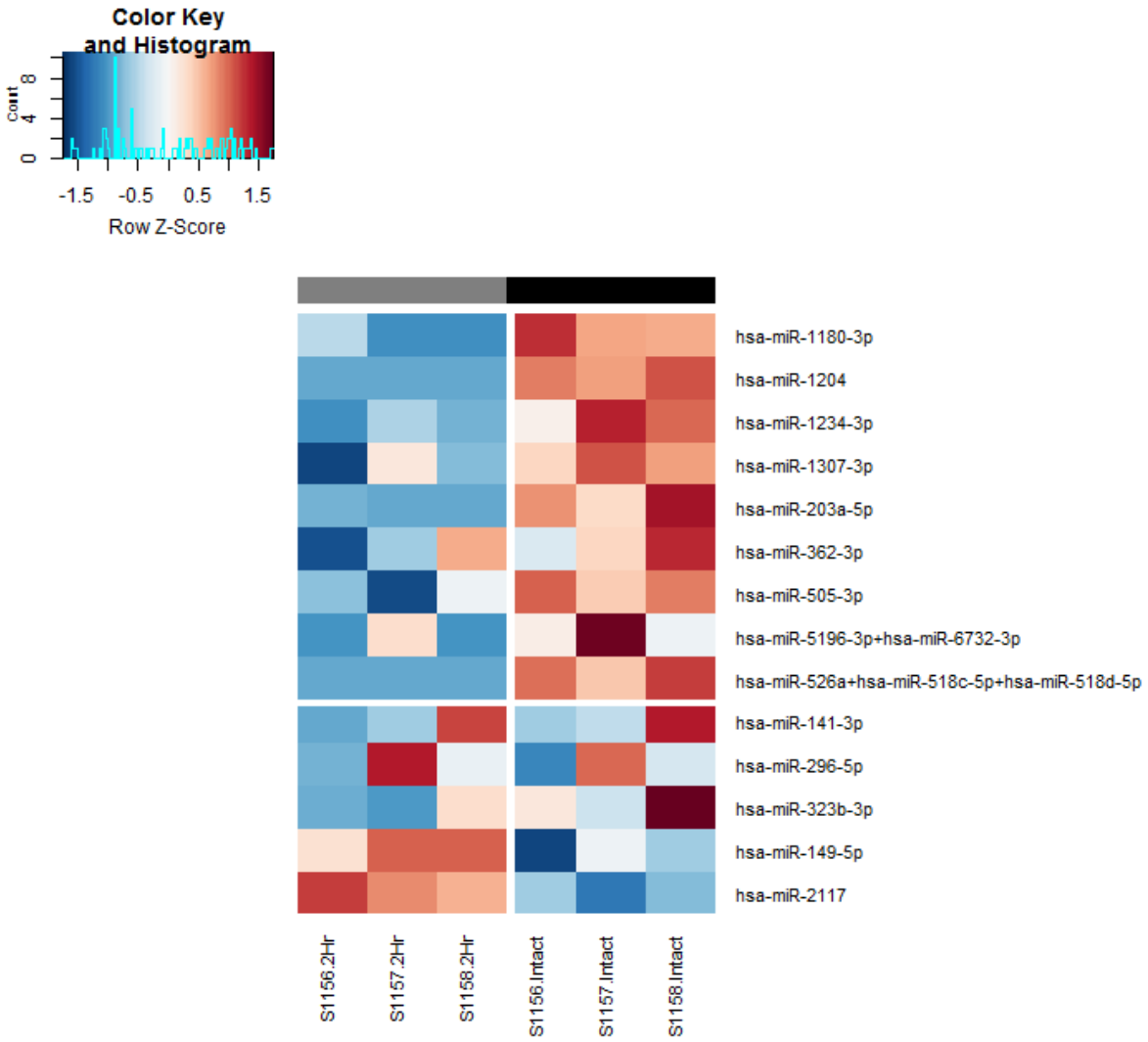

Figure 7.5 Differentially expressed microRNAs between intact 3D skin equivalent model (3D-SEM) and wounded 3D-SEM after 2 hours of initiating the healing process.

This figure demonstrates the microRNAs expressed by intact 3D-SEM (N=3) and wounded 3D-SEM (N=3) after two hours of initiating the healing process. (A) Volcano plot representing a statistical analysis (fold change "x-axis" versus - log10 of P value "y-axis") of the whole panel of microRNAs expressed in the wounded 3D-SEM compared to intact 3D-SEM. The analysis revealed that 14 microRNAs (pale blue colour) were significantly differentially expressed by the wounded 3D-SEM compared to intact 3D-SEM. A larger -log10 value represents a smaller P value e.g. miR-1180-3p has (-log 10 (3.9) ~ (P=0.00013)) which means it has the most significant variation in expression between the two groups. (B) Heat map plot representing the 14 significantly differentially expressed microRNAs between the wounded 3D-SEM compared to intact 3D-SEM. Colour Key; Red = Higher microRNA count, i.e. gradual change from orange to red means gradual increase in microRNA count. Blue = Lower microRNA count i.e. gradual change from light blue to dark blue means gradual decrease in microRNA count.

Fold changes in microRNA expression and corresponding p values showed that 12 out of the 14 differentially expressed microRNAs (1-12) were significantly downregulated in the punched wound models within 2 hours post initiation of the wound healing process, in comparison to intact models. In contrast, only two microRNAs (13 and 14) were significantly upregulated, as explained in (Table 7.2).

	MicroRNAs	Regulation (↑↓)	Fold Change	P value
1	hsa-miR-1180-3p	↓	-2.18	0.00012
2	hsa-miR-1204	↓	-1.29	0.00354
3	hsa-miR-1234-3p	↓	-3.79	0.01898
4	hsa-miR-1307-3p	↓	-2.66	0.04180
5	hsa-miR-203a-5p	↓	-3.41	0.03332
6	hsa-miR-362-3p	↓	-1.48	0.02965
7	hsa-miR-505-3p	↓	-2.72	0.03563
8	hsa-miR-5196-3p+hsa-miR-6732-3p	↓	-1.35	0.01173
9	hsa-miR-526a+hsa-miR-518c-5p+hsa-miR-518d-5p	↓	-3.36	0.01483
10	hsa-miR-141-3p	↓	-1.14	0.03250
11	hsa-miR-296-5p	↓	-11.53	0.04771
12	hsa-miR-323b-3p	↓	-1.76	0.04948
13	hsa-miR-149-5p	↑	1.55	0.01887
14	hsa-miR-2117	↑	3.08	0.01368

Table 7.2 Further details of differentially expressed microRNAs between intact 3D-SEM and wounded 3D-SEM after 2 hours of initiating the healing process.

Data presented in this table represents the 14 microRNAs that were significantly differentially expressed by the wounded 3D-SEM after two hours of the healing progress. 12 microRNAs (numbered 1-12) were significantly downregulated, while only 2 (numbered 13 & 14) were significantly upregulated in the wounded 3D-SEM compared to intact 3D-SEM. (↑)= Upregulation and (↓)= downregulation in wounded 3D-SEM compared to intact 3D-SEM.

At 4 hours into the healing progress, 30 microRNAs were significantly differentially expressed between the punched models in comparison to intact models as demonstrated in (Figure 7.6).

(A)

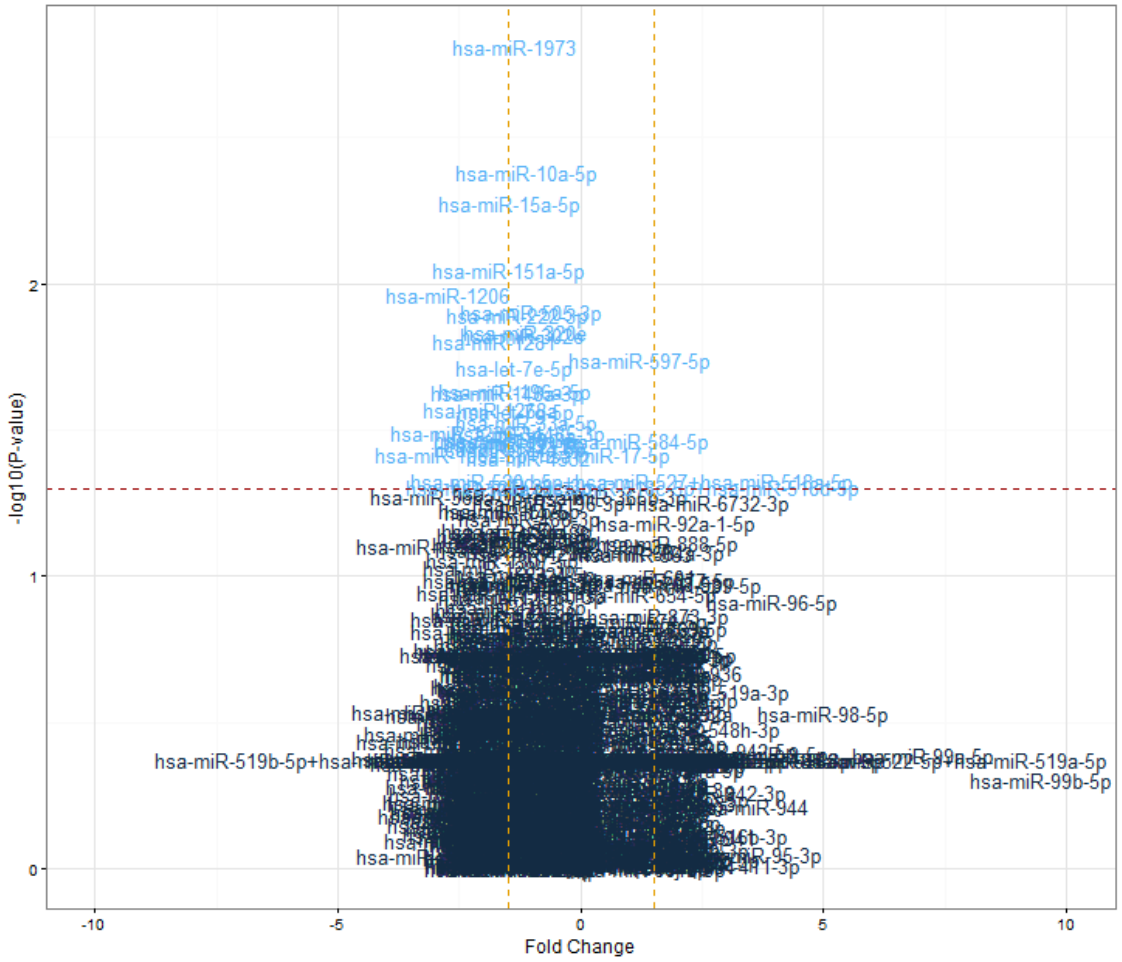

(B)

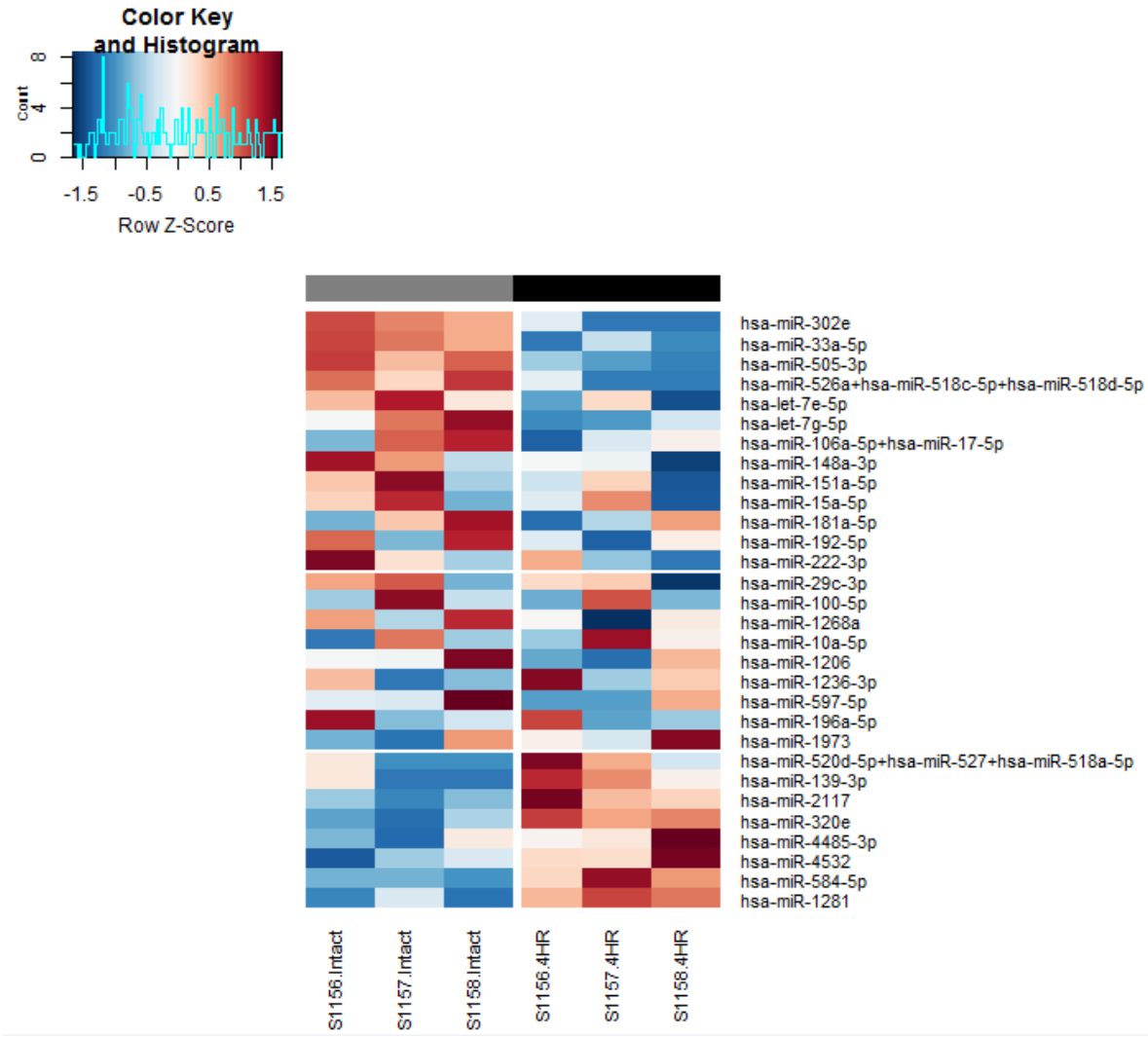

Figure 7.6 Differentially expressed microRNAs between intact 3D-SEM and wounded 3D-SEM after 4 hours of initiating the healing process.

This figure demonstrates the microRNAs expressed by intact 3D-SEM (N=3) and wounded 3D-SEM (N=3) after 4 hours of initiating the healing process. (A) Volcano plot representing a statistical analysis (fold change" x-axis" versus - log10 of P value "y-axis") of the whole panel of microRNAs expressed in the wounded 3D-SEM compared to intact 3D-SEM. The analysis revealed that 30 microRNAs (pale blue colour) were significantly differentially expressed by the wounded 3D-SEM compared to intact 3D-SEM. A larger (-log10 value) represents a smaller P value e.g. miR-1973 has -log 10 (2.8) ~ (P=0.0015) which means it has the most significant variation in expression between the two groups. (B) Heat map plot representing the 30 significantly differentially expressed microRNAs between the wounded 3D-SEM compared to intact 3D-SEM. Colour Key; Red = Higher microRNA count, i.e. gradual change from orange to red means gradual increase in microRNA count. Blue = Lower microRNA count i.e. gradual change from light blue to dark blue means gradual decrease in microRNA count.

Fold change analysis and p values of microRNAs revealed that 19 microRNAs (1-19) were significantly downregulated after 4 hours of the wound healing process in comparison to intact models, while 11 microRNAs (20-30) were significantly upregulated as explained in (Table 7.3).

	MicroRNAs	Regulation (↑↓)	Fold Change	P value
1	hsa-miR-302e	↓	-1.79	0.01495
2	hsa-miR-33a-5p	↓	-1.81	0.02960
3	hsa-miR-505-3p	↓	-2.74	0.01250
4	hsa-miR-526a+hsa-miR-518c-5p+hsa-miR-518d-5p	↓	-2.58	0.04936
5	hsa-let-7e-5p	↓	-1.31	0.01926
6	hsa-let-7g-5p	↓	-1.26	0.02725
7	hsa-miR-106a-5p+hsa-miR-17-5p	↓	-1.44	0.03815
8	hsa-miR-148a-3p	↓	-1.50	0.02345
9	hsa-miR-151a-5p	↓	-1.21	0.00898
10	hsa-miR-15a-5p	↓	-1.08	0.00530
11	hsa-miR-181a-5p	↓	-1.15	0.03656
12	hsa-miR-192-5p	↓	-1.57	0.03511
13	hsa-miR-222-3p	↓	-1.14	0.01279
14	hsa-miR-29c-3p	↓	-1.21	0.04902
15	hsa-miR-100-5p	↓	-1.25	0.03442
16	hsa-miR-1268a	↓	-1.80	0.02666
17	hsa-miR-1206	↓	-2.34	0.01087
18	hsa-miR-597-5p	↓	-1.88	0.01813
19	hsa-miR-196a-5p	↓	-1.20	0.02328
20	hsa-miR-10a-5p	↑	1.54	0.00413
21	hsa-miR-1236-3p	↑	1.45	0.03221
22	hsa-miR-1973	↑	1.32	0.00155
23	hsa-miR-520d-5p+hsa-miR-527+hsa-miR-518a-5p	↑	1.95	0.04683
24	hsa-miR-139-3p	↑	1.29	0.03377
25	hsa-miR-2117	↑	3.45	0.03556
26	hsa-miR-320e	↑	2.78	0.01458
27	hsa-miR-4485-3p	↑	2.05	0.03220
28	hsa-miR-4532	↑	2.18	0.03918
29	hsa-miR-584-5p	↑	3.03	0.03442
30	hsa-miR-1281	↑	2.47	0.01574

Table 7.3 Further details of differentially expressed microRNAs between intact 3D-SEM and wounded 3D-SEM after 4 hours of initiating the healing process.

Data presented in this table represents the 30 microRNAs that were significantly differentially expressed by the wounded 3D-SEM at 4 hours of the wound healing progress. 19 microRNAs (numbered 1-19) were significantly downregulated and 11 (numbered 20-30) were significantly upregulated in the wounded 3D-SEM compared to intact 3D-SEM. (↑) = upregulation and (↓) = downregulation in wounded 3D-SEM compared to intact 3D-SEM.

Moreover, after 24 hours of the wound healing progress, 23 microRNAs were differentially expressed by the punched wound models in comparison to the intact models as illustrated in (Figure 7.7).

(A)

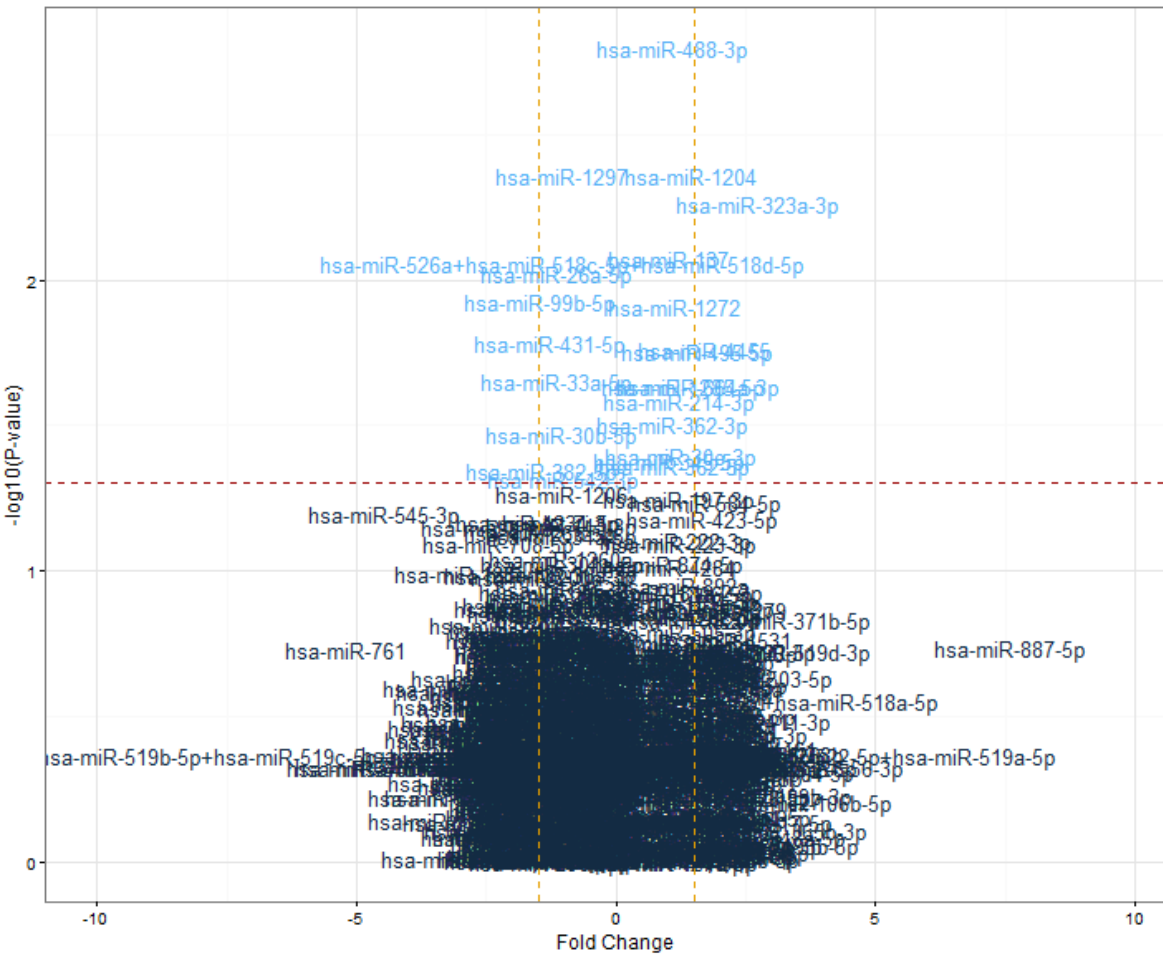

(B)

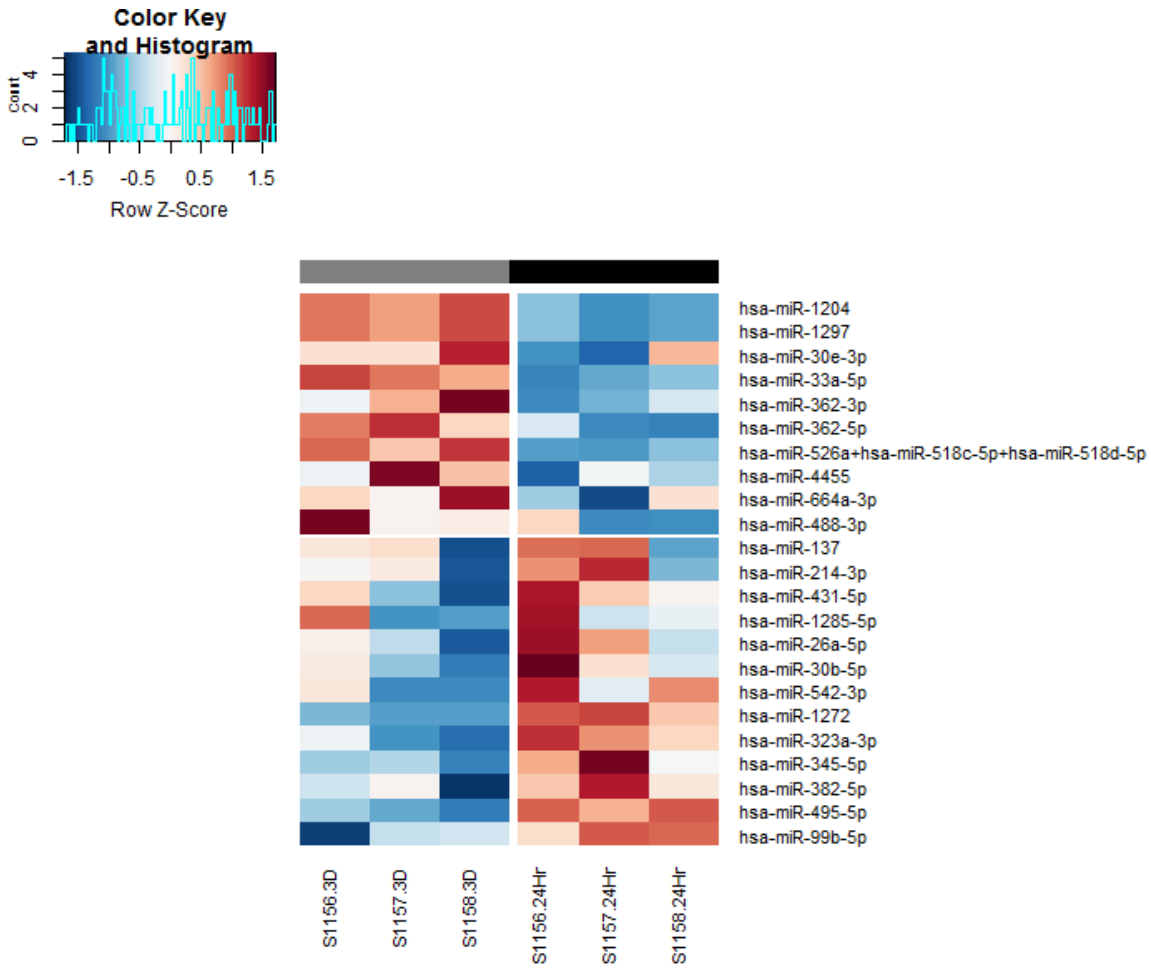

Figure 7.7 Differentially expressed microRNAs between intact 3D-SEM and wounded 3D-SEM after 24 hours of initiating the healing process.

This figure demonstrates the microRNAs that were significantly differentially expressed by intact 3D-SEM (N=3) and wounded 3D-SEM (N=3) after 24 hours of initiating the healing process. (A) Volcano plot representing a statistical analysis (fold change "x-axis" versus - log10 of P value "y-axis") of the whole panel of microRNAs expressed in wounded 3D-SEM compared to intact 3D-SEM. The analysis revealed that 23 microRNAs (pale blue colour) were significantly differentially expressed by the wounded 3D-SEM compared to intact 3D-SEM. A larger (-log10 value) = represents a smaller P value e.g. miR-488-3p has (-log 10 (2.8) ~ (P=0.0015)) which means it has the most significant variation in expression between the two groups. (B) Heat map plot representing the 23 significantly differentially expressed microRNAs between the wounded 3D-SEM compared to intact 3D-SEM. Colour Key; Red = Higher microRNA count, i.e. gradual change from orange to red means gradual increase in microRNA count. Blue = Lower microRNA count i.e. gradual change from light blue to dark blue means gradual decrease in microRNA count.

As demonstrated in (Table 7.4), statistical analysis, as reflected by fold change and p values, illustrated that 10 (1-10) microRNAs were significantly downregulated, while 13 microRNAs (11-23) were significantly upregulated in the 3D models in comparison to the intact models.

	MicroRNAs	Regulation (↑↓)	Fold Change	P value
1	hsa-miR-1204	↓	-1.26	0.00434
2	hsa-miR-1297	↓	-1.26	0.00434
3	hsa-miR-30e-3p	↓	-1.48	0.03988
4	hsa-miR-33a-5p	↓	-1.85	0.02231
5	hsa-miR-362-3p	↓	-1.64	0.03107
6	hsa-miR-362-5p	↓	-1.46	0.04347
7	hsa-miR-526a+hsa-miR-518c-5p+hsa-miR-518d-5p	↓	-2.99	0.00874
8	hsa-miR-4455	↓	-2.66	0.01720
9	hsa-miR-664a-3p	↓	-1.41	0.02317
10	hsa-miR-488-3p	↓	-2.84	0.00159
11	hsa-miR-137	↑	2.04	0.00838
12	hsa-miR-214-3p	↑	1.45	0.02587
13	hsa-miR-431-5p	↑	3.01	0.01635
14	hsa-miR-1285-5p	↑	1.39	0.02295
15	hsa-miR-26a-5p	↑	1.51	0.00942
16	hsa-miR-30b-5p	↑	1.46	0.03357
17	hsa-miR-542-3p	↑	4.07	0.04798
18	hsa-miR-1272	↑	3.72	0.01223
19	hsa-miR-323a-3p	↑	1.71	0.00548
20	hsa-miR-345-5p	↑	1.72	0.04188
21	hsa-miR-382-5p	↑	2.14	0.04509
22	hsa-miR-495-5p	↑	3.32	0.01759
23	hsa-miR-99b-5p	↑	1.20	0.01180

Table 7.4 Further details of differentially expressed microRNAs between intact 3D-SEM and wounded 3D-SEM after 24 hours of initiating the healing process.

Data presented in this table represents the 23 microRNAs that were significantly differentially expressed by the wounded 3D-SEM at 24 hours of the healing process. Ten microRNAs (numbered 1-10) were significantly downregulated and 13 (numbered 11-23) were significantly upregulated in the wounded 3D-SEM compared to intact 3D-SEM. (↑)= upregulation and (↓)= downregulation in wounded 3D-SEM compared to intact 3D-SEM.

After 72 hours of wound healing, punched models differentially and significantly expressed 15 microRNAs in comparison to the intact models, as shown in (Figure 7.8).

(A)

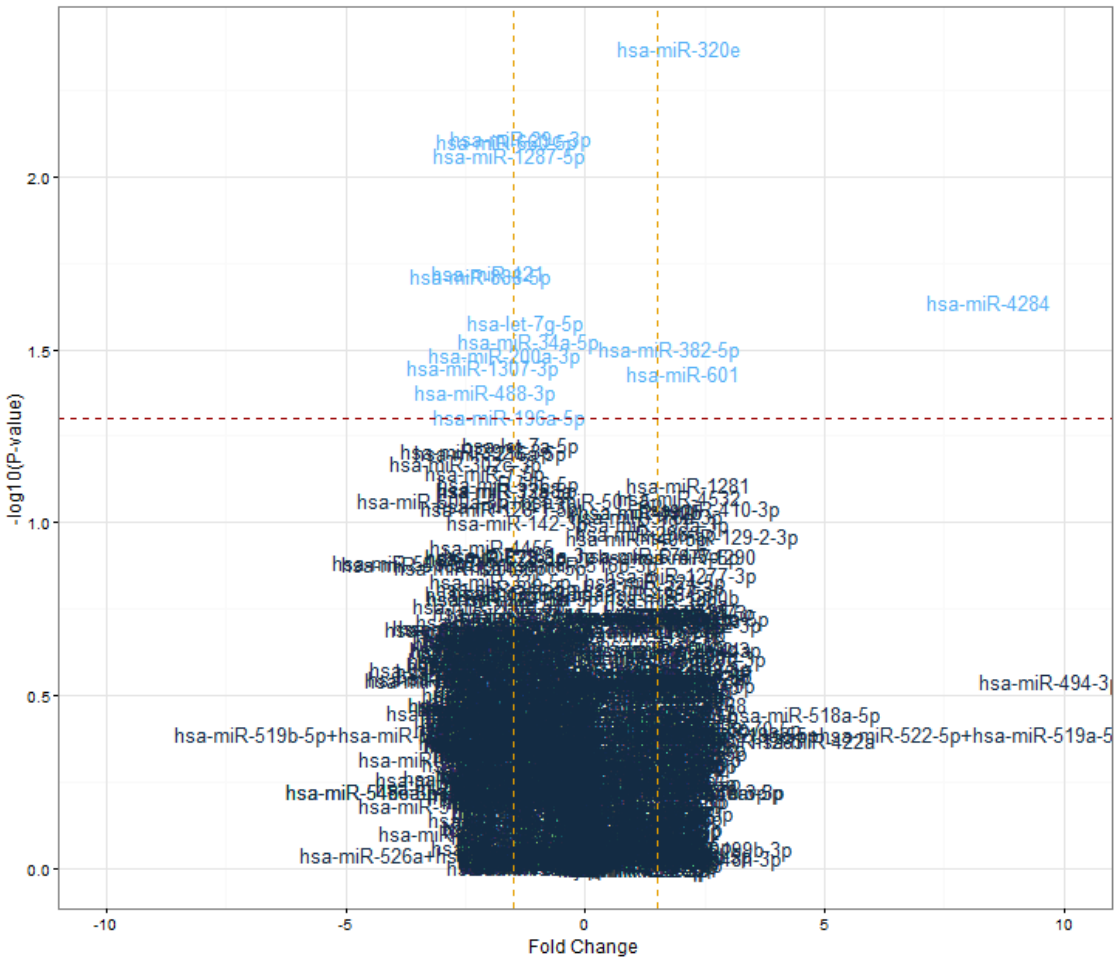

(B)

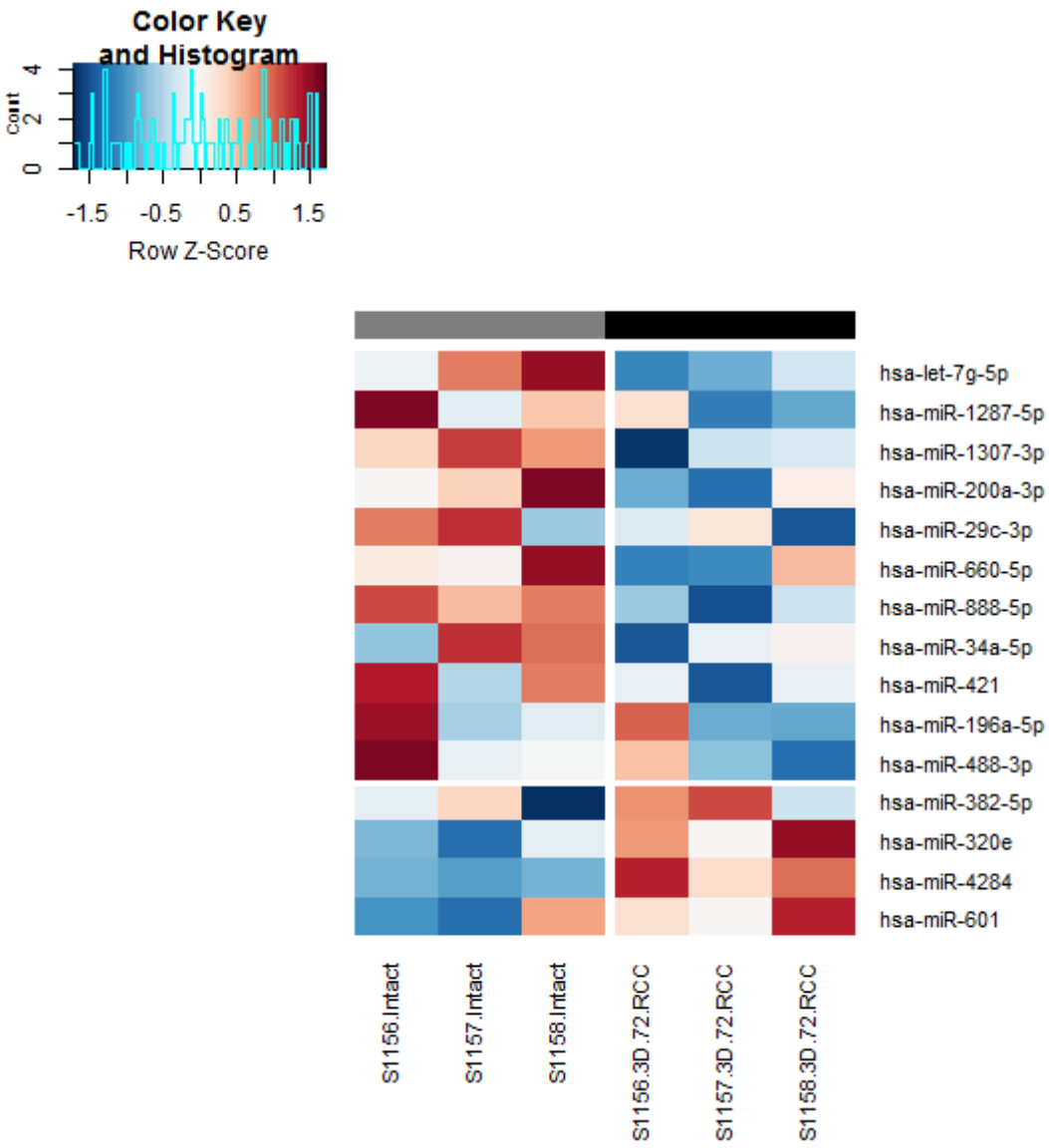

Figure 7.8 Differentially expressed microRNAs between intact 3D-SEM and wounded 3D-SEM after 72 hours of initiating the healing process.

This figure demonstrates the microRNAs expressed by intact 3D-SEM (N=3) and wounded 3D-SEM (N=3) after 72 hours of initiating the healing process. (A) Volcano plot representing a statistical analysis (fold change "x-axis" versus - log10 of P value "y-axis") of the whole panel of microRNAs expressed in wounded 3D-SEM compared to intact 3D-SEM. The analysis revealed that 15 microRNAs (pale blue colour) were significantly differentially expressed by the wounded 3D-SEM compared to intact 3D-SEM. A larger -log10 value represents a smaller P value i.e. miR-320e has -log 10 (2.398) ~ (P=0.004) which means it has the most significant variation in expression between the two groups. (B) Heat map plot representing the 15 significantly differentially expressed microRNAs between the wounded 3D-SEM compared to intact 3D-SEM. Colour Key; Red = Higher microRNA count, i.e. gradual change from orange to red means gradual increase in microRNA count. Blue = Lower microRNA count i.e. gradual change from light blue to dark blue means gradual decrease in microRNA count.

Among the fifteen significantly differentially expressed microRNAs, fold change and p values revealed that 11 were significantly downregulated and only 4 microRNAs were upregulated in wounded models compared to intact models after 72 hours following initiation of the healing process, as explained in (Table 7.5).

	MicroRNAs	Regulation (↑↓)	Fold Change	P value
1	hsa-let-7g-5p	↓	-1.24	0.02628
2	hsa-miR-1287-5p	↓	-1.6	0.00858
3	hsa-miR-1307-3p	↓	-2.16	0.03529
4	hsa-miR-200a-3p	↓	-1.7	0.03244
5	hsa-miR-29c-3p	↓	-1.33	0.00771
6	hsa-miR-660-5p	↓	-1.64	0.00789
7	hsa-miR-888-5p	↓	-2.17	0.01922
8	hsa-miR-34a-5p	↓	-1.19	0.02963
9	hsa-miR-421	↓	-2.03	0.01881
10	hsa-miR-196a-5p	↓	-1.58	0.04921
11	hsa-miR-488-3p	↓	-2.07	0.04183
12	hsa-miR-382-5p	↑	1.77	0.03141
13	hsa-miR-320e	↑	1.96	0.00425
14	hsa-miR-4284	↑	8.42	0.02297
15	hsa-miR-601	↑	2.05	0.03693

Table 7.5 Further details of differentially expressed microRNAs between intact 3D-SEM and wounded 3D-SEM after 72 hours of initiating the healing process.

Data presented in this table represents the 15 microRNAs that were significantly differentially expressed by the wounded 3D-SEM at 72 hours of the wound healing progress. 11 microRNAs (numbered 1-11) were significantly downregulated and only 4 microRNAs (numbered 12-15) were significantly upregulated in the wounded 3D-SEM compared to intact 3D-SEM. (↑)= upregulation and (↓)= downregulation in wounded 3D-SEM compared to intact 3D-SEM.

The healing process continued to demonstrate differential expression of microRNAs after 1 week in comparison to the intact models, as shown in (Figure 7.9).

(A)

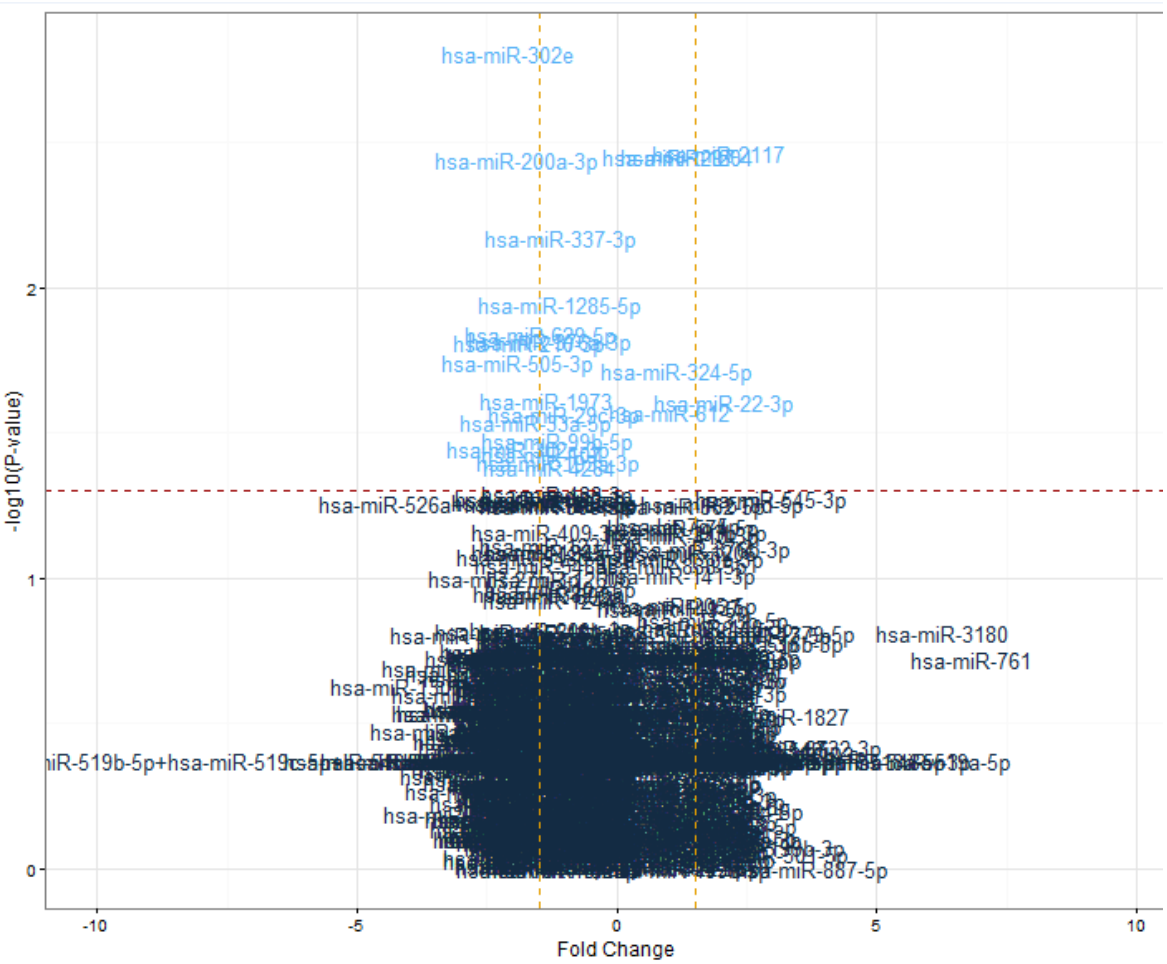

(B)

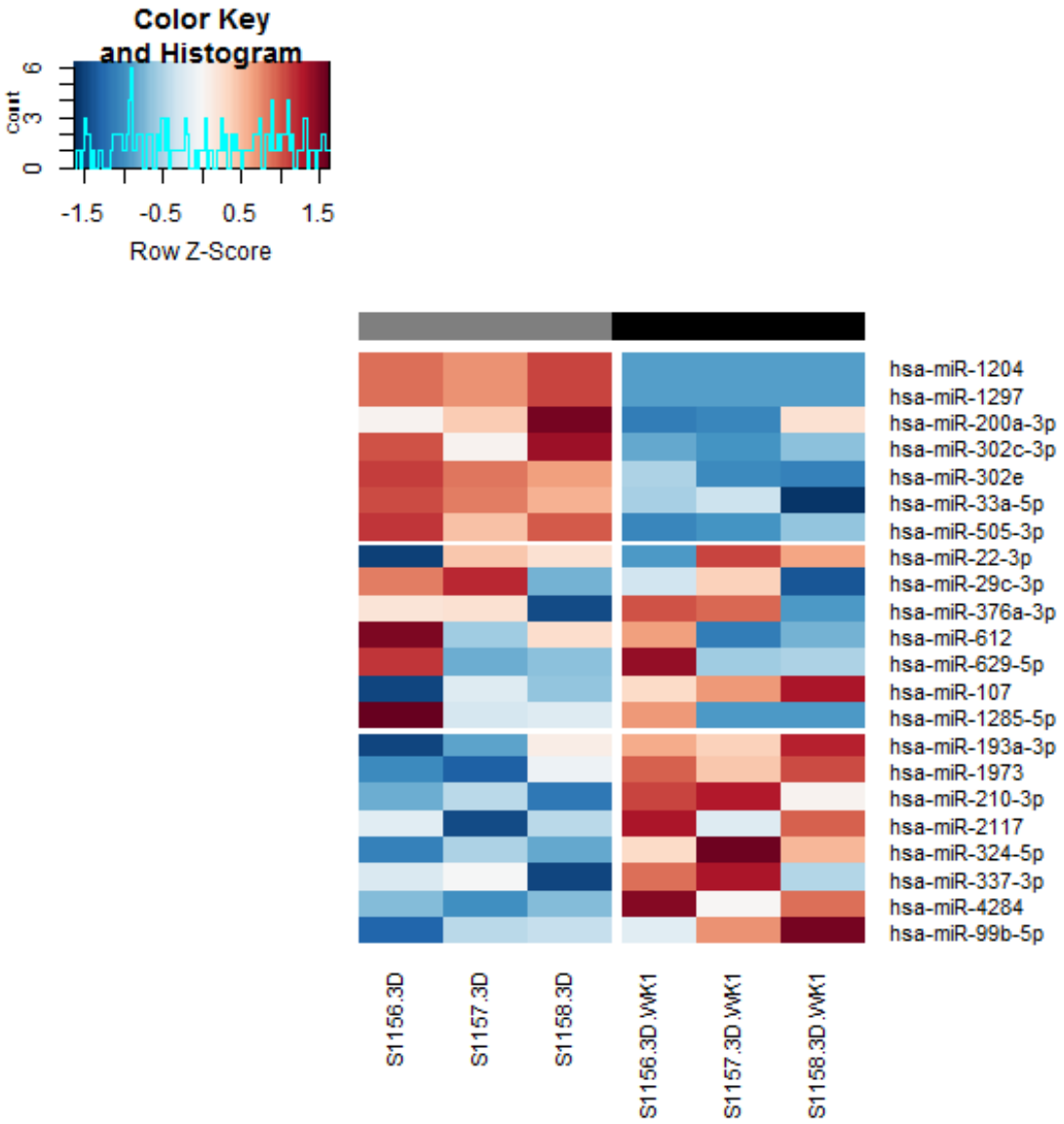

Figure 7.9 Differentially expressed microRNAs between intact 3D-SEM and wounded 3D-SEM after 1 week of initiating the healing process.

This figure demonstrates the microRNAs that were significantly differentially expressed by intact 3D-SEM (N=3) and wounded 3D-SEM (N=3) after 1 week of initiating the healing process. (A) Volcano plot representing a statistical analysis (fold change "x-axis" versus - log10 of P value "y-axis") of the whole panel of microRNAs expressed in wounded 3D-SEM compared to intact 3D-SEM. The analysis revealed that 22 microRNAs (pale blue colour) were significantly differentially expressed by the wounded 3D-SEM compared to intact 3D-SEM. A larger -log10 value represents a smaller P value e.g. miR-320e has -log 10 (2.8) ~ (P=0.0015) which means it has the most significant variation in expression between the two groups. (B) Heat map plot representing the 22 significantly differentially expressed microRNAs between the wounded 3D-SEM compared to intact 3D-SEM. Colour Key; Red = Higher microRNA count, i.e. gradual change from orange to red means gradual increase in microRNA count. Blue = Lower microRNA count i.e. gradual change from light blue to dark blue means gradual decrease in microRNA count.

As illustrated in (Table 7.6), analysis showed that 10 of the differentially expressed microRNAs were significantly downregulated, while 12 microRNAs were significantly upregulated after 1 week's progress of the healing process in comparison to the intact models, as demonstrated by fold change and p values.

	MicroRNAs	Regulation (↑↓)	Fold Change	P value
1	hsa-miR-1204	↓	-1.29	0.00354
2	hsa-miR-1297	↓	-1.29	0.00354
3	hsa-miR-200a-3p	↓	-1.78	0.00369
4	hsa-miR-302c-3p	↓	-3.98	0.03556
5	hsa-miR-302e	↓	-1.86	0.00157
6	hsa-miR-33a-5p	↓	-1.83	0.02897
7	hsa-miR-505-3p	↓	-2.21	0.01792
8	hsa-miR-29c-3p	↓	-1.26	0.02724
9	hsa-miR-612	↓	-1.81	0.02687
10	hsa-miR-1285-5p	↓	-1.84	0.01143
11	hsa-miR-22-3p	↑	1.07	0.02472
12	hsa-miR-376a-3p	↑	1.35	0.01519
13	hsa-miR-629-5p	↑	1.34	0.01443
14	hsa-miR-107	↑	1.21	0.03740
15	hsa-miR-193a-3p	↑	1.77	0.03962
16	hsa-miR-1973	↑	1.94	0.02455
17	hsa-miR-210-3p	↑	1.95	0.01541
18	hsa-miR-2117	↑	1.83	0.00343
19	hsa-miR-324-5p	↑	1.32	0.01938
20	hsa-miR-337-3p	↑	2.00	0.00668
21	hsa-miR-4284	↑	3.77	0.04145
22	hsa-miR-99b-5p	↑	1.25	0.03328

Table 7.6 Further details of differentially expressed microRNAs between intact 3D-SEM and wounded 3D-SEM after 1 week of initiating the healing process.

Data presented in this table represents the 30 microRNAs that were significantly differentially expressed by the wounded 3D-SEM at 1 week of the wound healing progress. Ten microRNAs (numbered 1-10) were significantly downregulated and 12 molecules (numbered 11-22) were significantly upregulated in the wounded 3D-SEM compared to intact 3D-SEM. (↑)= upregulation and (↓)= downregulation in wounded 3D-SEM compared to intact 3D-SEM.

Interestingly, twenty microRNAs were differentially expressed at more than one time point analysed during the healing process (overlapping microRNAs), suggesting that these microRNAs may play a role in different phases of the healing process. Twelve of these microRNAs were always downregulated, while seven were always upregulated in wounded 3D-SEM compared to intact 3D-SEM (Table 7.7). Only miR-1285-5p demonstrated fluctuation in expression over time. This microRNA was upregulated at 24 hours and downregulated after 1 week of the healing process. More information about these microRNAs is listed in (Table 7.7) and (Figure 7.10).

	MicroRNAs	Regulation at Time points				
		2 Hours	4 Hours	24 Hours	72 Hours	1 Week
1	miR-1204	-1.29 ↓		-1.26 ↓		-1.29 ↓
2	miR-1307-3p	-2.66 ↓			2.16 ↓	
3	miR-362-3p	-1.48 ↓		1.64 ↓		
4	miR-505-3p	-2.72 ↓	-2.74 ↓			-2.72 ↓
5	miR-526a+miR-518c-5p+miR-518d-5p	-3.36 ↓	-2.58 ↓	-2.99 ↓		
6	miR-2117	3.08 ↑	3.45 ↑			1.83 ↑
7	miR-302e		-1.79 ↓			-1.86 ↓
8	miR-33a-5p		-1.81 ↓	-1.85 ↓		-1.83 ↓
9	miR-let-7g-5p		-1.26 ↓		-1.24 ↓	
10	miR-29c-3p		-1.21 ↓		-1.33 ↓	1.26 ↓
11	miR-196a-5p		-1.2 ↓		-1.58 ↓	
12	miR-1973		1.32 ↑			1.94 ↑
13	miR-320e		2.78 ↑		1.96 ↑	
14	miR-1297			-1.26 ↓		-1.29 ↓
15	miR-488-3p			-2.84 ↓	-2.07 ↓	
16	miR-1285-5p			1.39 ↑		-1.84 ↓
17	miR-382-5p			2.14 ↑	1.77 ↑	
18	miR-99b-5p			1.20 ↑		1.25 ↑
19	miR-200a-3p				-1.70 ↓	-1.78 ↓
20	miR-4284				-8.42 ↑	-3.77 ↑

Table 7.7 Common differentially expressed microRNAs at different time points during the wound healing process.

There were 20 microRNAs that were commonly differentially expressed by wounded 3D-SEM compared to intact 3D-SEM at a minimum of two different time points during the wound healing process. Some were upregulated while others were down regulated, all with a significant fold change in expression.

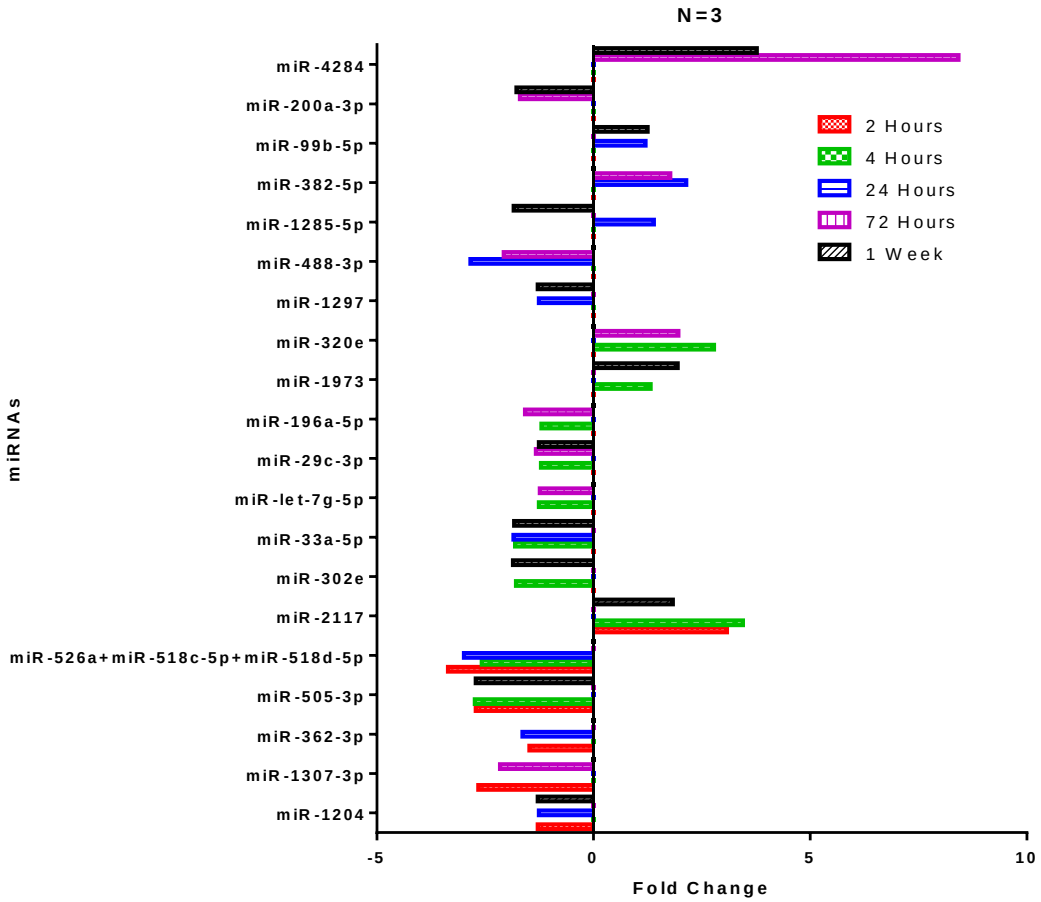

Figure 7.10 Fold change of overlapping microRNAs at different time points during the healing process.

The figure illustrates overlapping microRNAs that were significantly up or downregulated in wounded 3D-SEM compared to intact 3D-SEM at different time points during the healing process. Positive fold change (from 0 to 10) = upregulation. Negative fold change (from 0 to -5) = downregulation of microRNA expression in wounded 3D-SEM compared to intact 3D-SEM.

Ingenuity target explore from (targetexplorer.ingenuity.com) microT-CDS, TarBase v.8 and MirPath v.3 from DIANA tools (diana.imis.athena-innovation.gr) were used to investigate potential genes that might be targeted by the differentially expressed microRNAs. Only genes relating to signalling pathways that affect cellular responses during skin morphogenesis and wound healing were reported (Table 7.8). Some microRNAs such as miR-1307-3p, miR-302e, miR-33a-5p, miR-let-7g-5p, miR-196a-5p, miR-382-5p and miR-4284 were shown to influence more than one gene, and the gene targets may in turn participate in multiple cellular responses and signalling pathways.

	MicroRNAs	Regulation ↑↓	Target Gene(s)	Target Detector / Explorer (Software)
1	miR-1204	↓	TP53 (p53)	Ingenuity Target Explorer
2	miR-1307-3p	↓	EHMT1, NDRG2, FLII	MicroT-CDS / DIANA
3	miR-362-3p	↓	TRIM11	TarBase v.8 / DIANA
4	miR-505-3p	↓	TNC	MirPath v.3 / DIANA
5	miR-526a+miR-518c-5p+miR-518d-5p	↓	APC	Ingenuity Target Explorer
6	miR-2117	↑	VAV3	TarBase v.8 / DIANA
7	miR-302e	↓	TGFBR2, ENDRB	MicroT-CDS / DIANA
8	miR-33a-5p	↓	EDN1, MYC (c-MYC)	TarBase v.8 / DIANA
9	miR-let-7g-5p	↓	MYC (c-MYC), HMGA2	TarBase v.8 / DIANA
10	miR-29c-3p	↓	MPP	TarBase v.8 / DIANA
11	miR-196a-5p	↓	HOMEBOX Genes, KRT5, COL1A1	Ingenuity Target Explorer
12	miR-1973	↑	CRABP1	MicroT-CDS / DIANA
13	miR-320e	↑	JUN	MicroT-CDS / DIANA
14	miR-1297	↓	KLF5	TarBase v.8 / DIANA
15	miR-488-3p	↓	CRHR2	TarBase v.8 / DIANA
16	miR-1285-5p	↑ - ↓	HIPK 1	TarBase v.8 / DIANA
17	miR-382-5p	↑	CALPAIIN, TAGLN, VIM	Ingenuity Target Explorer
18	miR-99b-5p	↑	HOXA1	TarBase v.8 / DIANA
19	miR-200a-3p	↓	BAP1	TarBase v.8 / DIANA
20	miR-4284	↑	RUFY2, KMT2D	TarBase v.8 / DIANA

Table 7.8 Target genes of overlapping microRNAs during the healing process.

This table illustrates 20 microRNAs that consistently demonstrated differential expression during wound healing compared to intact skin models, and their predicted target genes. Predicted target genes were determined using online target explorer software such as Ingenuity target explore and DIANA tools (MicroT-CDS, TarBase v.8 and MirPath v.3). Some of the overlapping microRNAs were shown to target more than one gene. (↑)= Upregulated and (↓) = downregulated microRNAs expressed by wounded 3D-SEM compared to intact 3D-SEM. (↑ - ↓) = upregulated microRNA at specific time point and then downregulated at another time point, such as miR-1285-5p.

Conversely, there were 26 microRNAs that were upregulated at only one time point of the wound healing process, as explained in (Table 7.9).

	MicroRNAs	Time points				
		2 Hours	4 Hours	24 Hours	72 Hours	1 Week
1	hsa-miR-149-5p	1.55 ↑				
2	hsa-miR-10a-5p		1.54 ↑			
3	hsa-miR-1236-3p		1.45 ↑			
4	hsa-miR-520d-5p+hsa-miR-527+hsa-miR-518a-5p		1.95 ↑			
5	hsa-miR-139-3p		1.29 ↑			
6	hsa-miR-4485-3p		2.05 ↑			
7	hsa-miR-4532		2.18 ↑			
8	hsa-miR-584-5p		3.03 ↑			
9	hsa-miR-1281		2.47 ↑			
10	hsa-miR-214-3p			1.45 ↑		
11	hsa-miR-431-5p			3.01 ↑		
12	hsa-miR-26a-5p			1.51 ↑		
13	hsa-miR-30b-5p			1.46 ↑		
14	hsa-miR-542-3p			4.07 ↑		
15	hsa-miR-1272			3.72 ↑		
16	hsa-miR-323a-3p			1.71 ↑		
17	hsa-miR-345-5p			1.72 ↑		
18	hsa-miR-495-5p			3.32 ↑		
19	hsa-miR-601				2.05 ↑	
20	hsa-miR-376a-3p					1.35 ↑
21	hsa-miR-629-5p					1.34 ↑
22	hsa-miR-107					1.21 ↑
23	hsa-miR-193a-3p					1.77 ↑
24	hsa-miR-210-3p					1.95 ↑
25	hsa-miR-324-5p					1.32 ↑
26	hsa-miR-337-3p					2.00 ↑

Table 7.9 MicroRNAs upregulated in wounded 3D-SEM compared to intact 3D-SEM at only one time point during the entire healing process.

This table includes 26 microRNAs which were significantly upregulated at only one time point during the wound healing process and their corresponding fold change values. One microRNA was upregulated at 2 hours only, 8 microRNA were upregulated at 4 hours only, 9 microRNAs were upregulated at 24 hours only, one microRNA was upregulated at 72 hours only and 7 microRNAs were upregulated at 1 week only.

7.3.3 DETECTION OF GROWTH FACTOR RECEPTORS USING GENE EXPRESSION

Since six growth factors were detected in MSC-CM (HGF, KGF, PDGF-AB, TGF-β1, SDF-1α and MSP-1), receptors of these growth factors (c-MET, FGFR-2, PDGF-A, TGF-βR1, CXCR4 and MST-R1 "RON") respectively were investigated in primary keratinocytes under different conditions during wound (scratch) closure. Primary keratinocytes were incubated at different conditions i.e., non-scratched cells (NSC), scratched non-treated (SNT) and scratched treated with MSC-CM (ST-CM), then RT-qPCR was used to quantify gene expression in the cells. Target genes were quantified via relative quantification with the housekeeping gene (GAPDH). Although, under all conditions primary keratinocytes (N=4) expressed essential growth factor receptors, as explained in (Figure 7.11), there was no significant difference in expression of the growth factor receptors under any of the culture conditions assessed (P>0.05). These receptors which are tyrosine kinases are spread across the cell surface and could be activated immediately upon binding to their corresponding growth factors. Therefore the growth factors present in MSC-CM, work collectively to initiate several cell responses during the healing process.

(A)

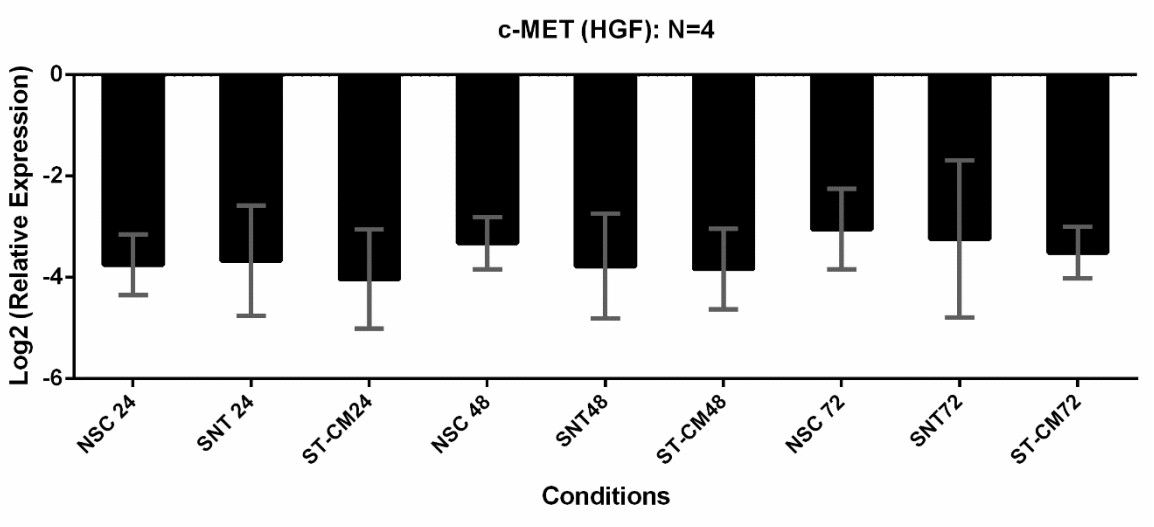

(B)

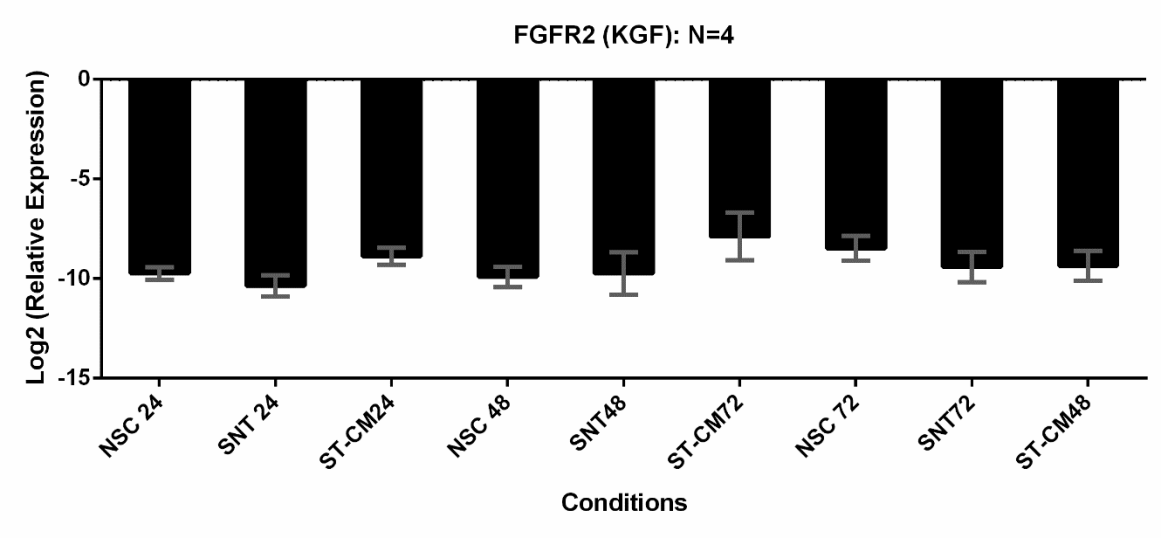
FGFR2 (KGF): N=4
Log2 (Relative Expression)
0
-5
-10
-15
NSC 24
SNT 24
ST-CM24
NSC 48
SNT48
ST-CM72
NSC 72
SNT72
ST-CM48
Conditions

(C)

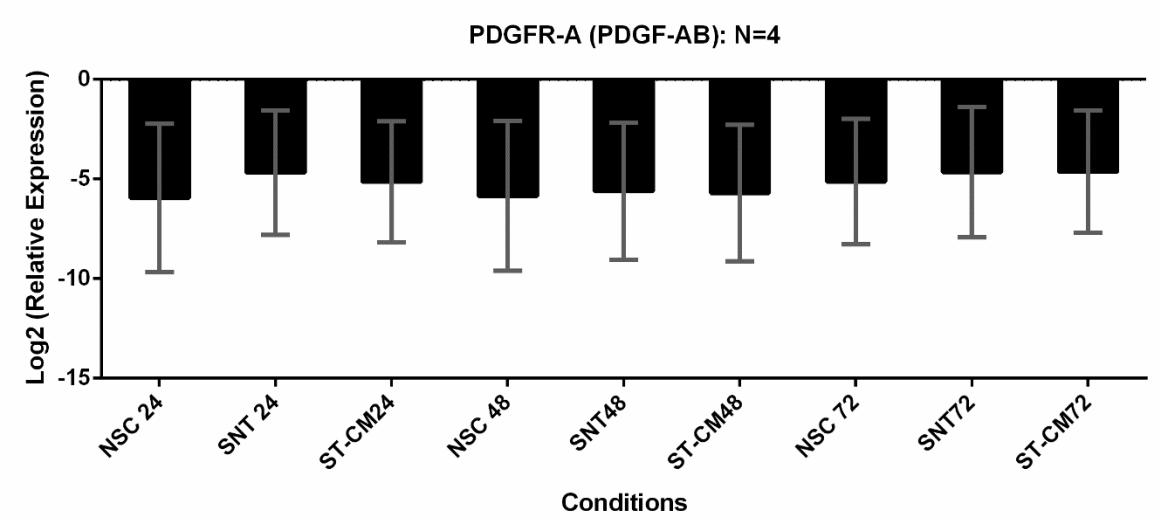
PDGFR-A (PDGF-AB): N=4
Log2 (Relative Expression)
0
-5
-10
-15
NSC 24
SNT 24
ST-CM24
NSC 48
SNT48
ST-CM48
NSC 72
SNT72
ST-CM72
Conditions

(D)

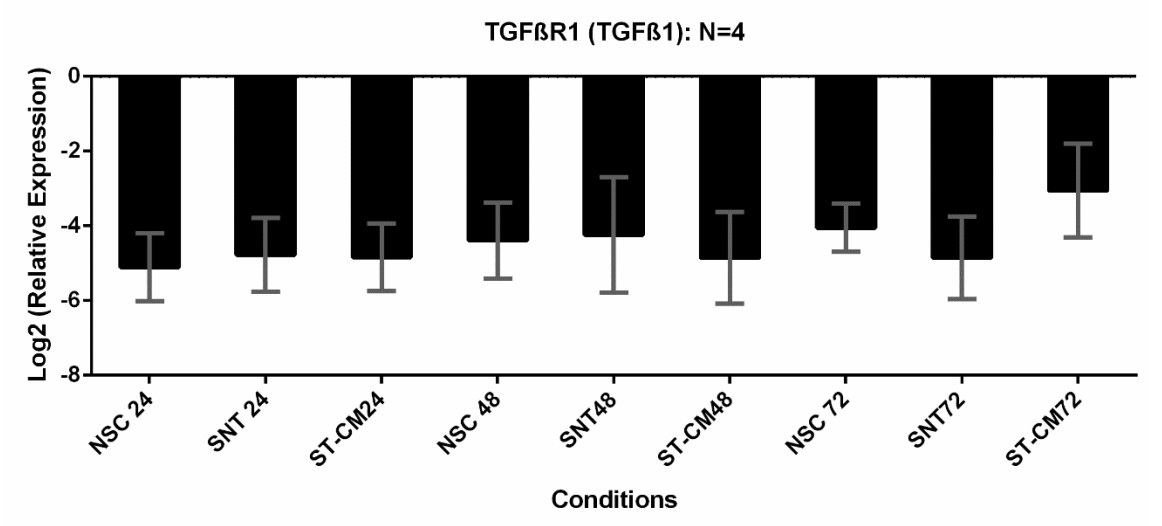
TGFßR1 (TGFß1): N=4
Log2 (Relative Expression)
0
-2
-4
-6
-8
NSC 24
SNT 24
ST-CM24
NSC 48
SNT48
ST-CM48
NSC 72
SNT72
ST-CM72
Conditions

(E)

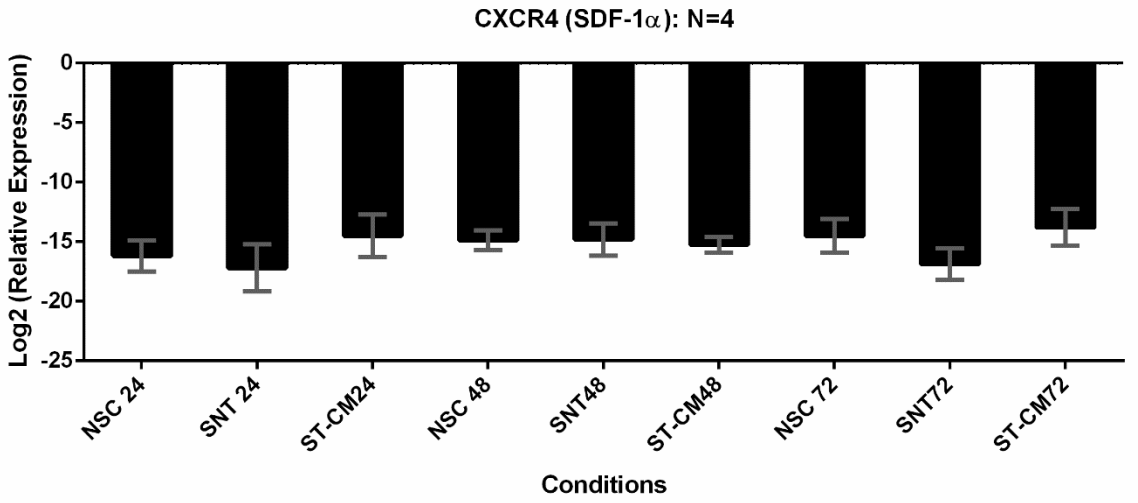

(F)

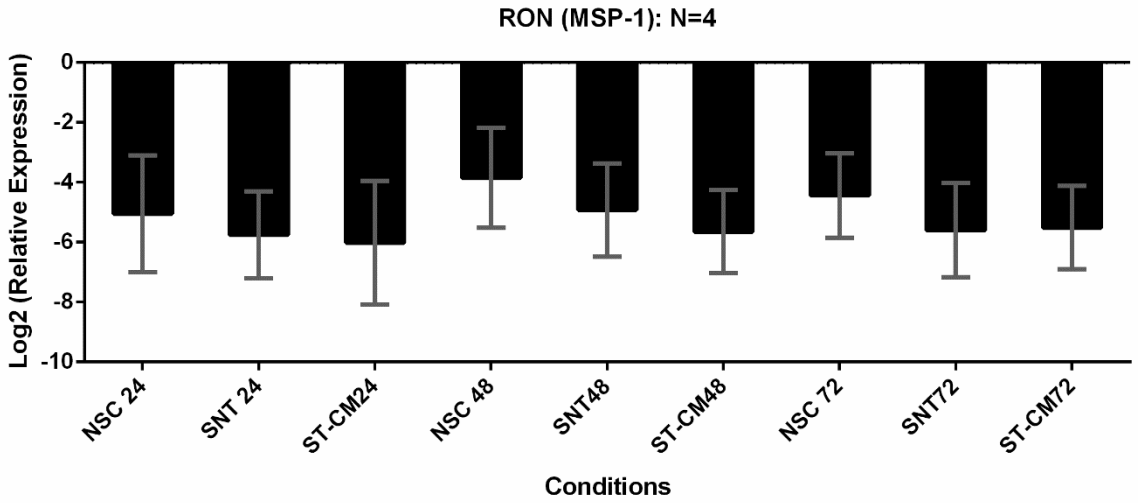

Figure 7.11 Receptors expressed by primary keratinocytes.

Primary keratinocytes at different conditions (normal non-scratched cells (NSC), scratched non-treated (SNT) and scratched treated with MSC-CM (ST-CM)) expressed the receptors of important growth factors and cytokines that participate in successful wound healing. (A) HGF receptor (c-MET). (B) KGF receptor (FGFR2). (C) PDGF-AB receptor (PDGFRA). (D) TGF-β1 receptor (TGFBR1). (E) SDF-1α receptor (CXCR4). (F) MSP-1 receptor (MST-1R or RON). Relative expression represents the expression of the target gene compared to the housekeeping gene (GAPDH). Comparative expression represents the expression of the target gene compared to the control cells (Non-scratched cells "NSC"). Data in this figure is presented as Log 2 of original values of normalised gene expression. Bars and error bars represent mean and standard error of the mean (SEM) (N=4).

To further understand the molecular mechanisms of wound healing, the relationship between microRNAs that were significantly differentially expressed at various time points and cellular receptors was investigated using TarBase v.8 software. As illustrated in (Table 7.10), some receptors were predicted to be regulated by one microRNA molecule

such as c-MET and FGFR2), while other receptors were shown to be targeted by more than on microRNA molecule such as PDGFRA, TGRBR1 and MST1R. Concerning CXCR4, information from TarBase v.8 software demonstrated that hsa-miR-106a-5p is the only molecule that regulates CXCR4. Data from this study revealed that hsa-miR-106a-5p+hsa-miR-17-5p which are different microRNAs, but with very similar base sequences (AAAAGUGCUUACAGUGCAGGUAG and CAAAGUGCUUACAGUGCAGGUAG) (www.mirbase.org), cannot be distinguished between by the NanoString platform due to the similarity of their sequences. Interestingly, the seed sequence of both of these microRNAs is the same. Therefore, despite target prediction software indicating that only miR-106a-5p may target CXCR4, it is possible that miR-17-5p may also regulate this gene.

Receptors	MicroRNAs	Expression Time
c-MET	miR-34a-5p	72 hours
FGFR2	miR-34a-5p	72 hours
PDGFRA	miR-15a-5p	4 hours
	miR-29c-3p	4 hours, 72 hours & 1 week
	miR-34a-5p	72 hours
TGFBR1	hsa-let-7g-5p	4 hours & 72 hours
	hsa-let-7e-5p	4 hours
	miR-196a-5p	4 hours & 72 hours
	miR-148a-3p	4 hours
	miR-30e-3p	24 hours
	miR-33a-5p	4 hours, 24 hours & 1 Week
	miR-362-3p	2 hours & 24 hours
MST1R	miR-34a-5p	72 hours
	miR-210-3p	1 Week
CXCR4	hsa-miR-106a-5p+hsa-miR-17-5p	4 hours

Table 7.10 MicroRNAs that are predicted to target cell surface receptors.

This table demonstrates receptors of growth factors and cytokines that could be regulated by microRNAs at different time points during the healing process, as predicted by TarBase v.8 software. Some of these receptors may be regulated by more than one microRNA such as PDGFRA, TGFBR1 and MST1R, while others, such c-MET and CXCR4, were only predicted to be targeted by one microRNA of the N=799 studied by the NanoString codeset. Expression time indicates the time point at which the microRNA was shown to be significantly differentially expressed.

7.4 DISCUSSION

In order to identify candidate microRNAs that might play a role in the wound healing and therefore, participate in the regeneration of damaged skin, an extended study was performed using a fully humanised 3D skin model. This study profiled microRNA expression of N=799 mature microRNAs in the 3D skin model (3D-SEM) compared to intact real skin, at varying time points of wound healing. This is a novel study and demonstrates for the first time the microRNA expression profiles of 3D-SEM compared to intact human skin, and is also the first study to assess the microRNA expression profiles of a 3D-SEM during the wound healing process. To better understand the potential roles of these microRNAs, their predicted effects on target genes were investigated using different *in silico* algorithms via online software packages. Previous studies investigated microRNA signatures in *in vivo* studies for different skin disorders and compared the results between normal and abnormal skin biopsies. For example, Mansuri and colleagues investigated skin microRNA profiling from non-segmental vitiligo patients using microarray customised kits for microRNA detection by RT PCR which investigate limited numbers of microRNAs (Mansuri *et al.*, 2014; Mansuri *et al.*, 2016). Other study investigated microRNAs profiling related to keratinocytes differentiation using stem loop primer-based real-time PCR methods which detect up to 380 microRNAs (Hildebrand *et al.*, 2012). Another study investigated microRNAs profiling in skin of wounded mouse and the study was restricted to investigate the role of miR-200 family member on wound healing (Aunin *et al.*, 2017). The only study investigated whole microRNA panel was carried out in surgical wounds of 5 healthy volunteers using TaqMan microRNA low-density array which allow to detect 754 microRNAs (Li *et al.*, 2015c). Hence, there is no previous studies used a constructed 3D-SEM for full profiling and comparing to real skin. Therefore, this study investigated for the first time the whole microRNA signature (799 microRNAs) in 3D model compared to real skin using NanoString technology, the most developed technology in the field of molecular investigations. Also, this study detected for the first time the whole panel of microRNA profiling at different time points during the healing process. Although, there were 31 microRNAs differentially expressed between the 3D-SEM and real skin (17 microRNAs were upregulated and 14 microRNAs were downregulated in 3D-SEM compared to real skin), the entire panel was similar.

Interestingly, the constructed 3D-SEM were able to express the same microRNA panel of real skin (799 microRNAs) indicating the ability of the constructed 3D-SEM to retain the molecular signature of real skin. Consequently confirming the validity of these models to be used as an experimental tool for future wound healing studies and testing drugs that might potentiate the healing process. Although, the massive compatibility between the models and real skin, microRNA profiling during wound healing was compared between wounded models and intact models not to real skin to avoid the variations in the 31 microRNAs differentially expressed between the models and real skin.

In context to comparing wounded 3D-SEM to intact models data showed that some microRNAs (26 microRNAs) were significantly differentially expressed at only one time point studied, while others (20 microRNAs) were differentially expressed at more than one of the time points under investigation (overlapping microRNAs). There was fluctuation in expression of these overlapping microRNAs, as although some microRNAs were downregulated at early stages, they then regulated back to the same level expression as intact models and then became downregulated in the 3D-SEM at later time points.

miR-1204 is shown to be downregulated at 2 hour, 24 hours and 1 week by 3D-SEM compared to the intact model, indicating its potential importance in the healing process. Among the predicted target genes of miR-1204 is tumour protein 53 (TP53), which plays an important role in arresting cell cycle at the G1/S phase (Rother *et al.*, 2007). Hence, downregulation of this microRNA may prevent suppression of TP53 and subsequently, cell cycle progression will activated resulting in continuous cell proliferation and/or migration. Additionally, Peng and colleagues reported that miR-1204 inhibits tumour growth and migration in nasopharyngeal carcinoma (Peng *et al.*, 2015). Hence, this microRNA may play a similar role in cutaneous wounds, by down-regulated expression resulting in increased cell growth and migration of skin cells. Therefore, its down regulation may be considered as advantageous in the 3D-SEM during the wound healing process.

Another microRNA, miR-1307-3p was downregulated at 2 and 72 hours of the wound healing process in the 3D-SEM compared to intact 3D-SEM. One of the potential target genes of this microRNA is euchromatic histone-lysine N-methyltransferase 1 (EHMT1), a gene encoding Metallothionein 1 h, which suppress migration and invasiveness of prostate cancerous cells (Han *et al.*, 2013). Additionally, miR-1307-3p targets proto-

oncogene protein (N-Myc) downstream regulated gene 2 (NDRG2), a gene which reduces cell viability and proliferation of epithelial cells involved in age-related cataracts in human (Zhang *et al.*, 2011c). Moreover, miR-1307-3p also targets protein flightless-1 homolog (FLII) gene, which produces cytoskeletal protein flightless I protein that inhibits fibroblast proliferation and reduces its function, resulting in impaired healing process (Ruzehaji *et al.*, 2012). It has been reported that attenuating FLII with neutralising antibodies improve the healing process in mice (Ruzehaji *et al.*, 2012) and in porcine (Turner *et al.*, 2017). Based on this information, upregulation of miR-1307-3p would be advantages during wound healing, as the effect would be to downregulate genes (EHMT1, NDRG2 and FLII) that are detrimental to the wound healing process. Hence, it is surprising that this microRNA is downregulated during time points of the healing process. The role of miR-1307-3p during wound healing warrants further investigation. It may also represent a potential target molecule to artificially upregulate, in order to improve wound healing and therefore be used as a potential molecular therapy for wound treatment.

miR-362-3p was downregulated at 2 and 24 hours in the 3D-SEM. This molecule is predicted to target tripartite motif-containing protein 11 (TRIM11), a gene that promotes proliferation and migration of glial tumour cells (Di *et al.*, 2013). Additionally, miR-362-3p inhibits growth, proliferation and migration of breast cancer cells (MCF7 cells) (Kang *et al.*, 2016). Therefore, miR-362-3p may possess similar functions in relation to wound healing, by suppressing skin cell proliferation and migration. Thus, downregulation of this microRNA at early stages of the healing process (2 hours and 24 hours) may be beneficial for the wound healing process. However, more studies are required to investigate the regulatory effect of miR-362-3p on TRIM11.

Another microRNA shown to be downregulated at more than one time point was miR-505-3p (downregulated at 2, 4 hours and at 1 week). This microRNA targets TNC gene which produces tenascin C (TN-C), a protein responsible for regulating cell migration and proliferation, particularly during developmental differentiation and wound healing (Erickson, 1993). Hence, if TN-C is upregulated, the effect may be enhanced migration, proliferation and differentiation of skin cells (mainly keratinocytes), consequently, enhanceing the healing process. It is therefore advantageous to wound healing that miR-505-3p is downregulated, resulting in increased TN-C expression. It would be interesting

to assess TN-C expression at the various time points of healing in the 3D-SEM, in order to assess whether expression is directly correlated with miiR-505-3p.

miR-526a+miR-518c-5p+miR-518d-5p was downregulated at 2, 4 and 72 hours. One of the target genes for this group of microRNA is adenomatous olyposis coli (APC) gene, which is involved in many cellular responses such as cell division, attachment and movement (Lesko *et al.*, 2015). Therefore, downregulation of this group of microRNAs between 2 and 24 hours during the healing process could result in upregulated, allowing this gene to play pivotal role in cell migration and proliferation. Interestingly, after 72 hours this molecule was regulated to the same level as the intact model, suggesting that the role of this microRNA molecule is mainly related to enhance cell migration during the early stages of healing.

miR-302e was also found to be downregulated at 4 hours and 1 week. One of the target genes of miR-302e is TGFRB2, which regulates the transforming growth factor beta-receptor (TGFRB) subfamily. This family are a group of transmembrane proteins that form a heterodimeric complex with another receptor, and binds TGF-beta to further regulate the transcription of genes related to cell proliferation (Yao *et al.*, 2002). Schultze-Mosgau and others reported that TGFRB2 is up regulated during the healing process (Schultze-Mosgau *et al.*, 2003). Hence, downregulation of miR-302e gives rise for the production of TGFRB2 to evoke numerous responses and signalling pathways regulated by the different members of TGF-ß family. Another target of miR-302e is EDNRB, which encodes endothelin receptor type B, a receptor involved in the Edn/EdnrB signalling pathway to promote proliferation and differentiation of epidermal melanocyte stem cell and hair regeneration in association with Wnt signalling pathway (Takeo *et al.*, 2016). However, the constructed models are free of melanocytes, miR-302e may target Edn/EdnrB cascade during *in vivo* injuries and participate in the healing process. On the other hand, downregulation of this microRNA could be attributed to the hypothesis that the role of this microRNA is mainly related and restricted to affect only melanocytes and since the constructed models are free of melanocytes, there was no participation was expected to be achieved by miR-302e resulted in its downregulation.

Expression of miR-33a-5p was downregulated at 4, 24 hours and 1 week in the wounded 3D-SEM. One of the target genes of this microRNA is MYC (c-MYC) which plays a pivotal

role in proliferation of epidermal stem cells, migration and differentiation of keratinocytes, and hair follicle regeneration via activation of the Wnt/β-catenin signalling pathway (Shi *et al.*, 2015). This data suggests a significant role for miR-33a-5p in wound repair, by which its lower expression at specific time points during the wound healing process may allow for MYC expression to promote mechanisms of wound healing. Interestingly, MYC is also targeted by miR-let-7g-5p (which was expressed at 4 and 72 hours), suggesting a synergistic role between miR-33a-5p and miR-let-7g-5p during the healing process. An additional target of miR-let-7g-5p is HMGA2, which encodes high-mobility group AT-hook 2. Kou and colleagues reported that HMGA2 facilitates migration and invasion of renal cell carcinoma cells by modulating the TGF-β/Smad2 signalling cascade (Kou *et al.*, 2018). Therefore, it could be suggested that a similar role (enhancing keratinocyte migration) could be achieved by miR-let-7g-5p via targeting HMGA2 for further activation of TGF-β/Smad2 during the healing process.

miR-29c-3p expression was downregulated at 4, 72 hours and 1 week in the 3D-SEM. It has been predicted that miR-29c-3p regulates matrix metalloproteinases (MMP) (Zhang *et al.*, 2017). These enzymes are necessary for repairing both acute and chronic wounds, by playing a vital role, with their inhibitory activity, in regulation of extracellular matrix deposition and degradation, which is an essential step for wound re-epithelialisation and tissue remodelling (Caley *et al.*, 2015). Additionally, miR-29c-3p has been reported to regulate secreted protein acidic and rich in cysteine (SPARC) which also called basement-membrane protein 40 (BM-40) (Zhang *et al.*, 2017) and shown to be beneficial to tumor invasion within bone by controlling many responses and events including cell-matrix interactions, and collagen binding angiogenesis, proliferation and migration (Guweidhi *et al.*, 2005). Hence, miR-29c-3p could be suggested to play a regulatory effect, by controlling collagen production and deposition, migration and proliferation during the healing process. However, more investigations are needed to ensure the regulatory manner of miR-29c-3p SPARC modulation.

Expression of miR-196a-5p was downregulated at 4 and 72 hours and this microRNA has been shown to influence Homeobox gene family including (HOXA7, HOXB8 HOXC8 and HOXD8). This gene family plays vital roles in morphogenesis of all multicellular organisms (Gehring, 1993). Subsequently, downregulation of miR-196a-5p between 24 and 72 hours

might be beneficial to enhance expression of one or all genes of the homeobox family, allowing these genes to participate in skin morphogenesis during the healing process. Additionally, keratin 5 gene (KRT5) is predicted as another target of miR-196a-5p. Keratin 5 enhances filament and cytoskeletal formation in the stratified epithelium of the skin (Atkinson *et al.*, 2011). These filaments are anchored to the desmosomes of basal cells and connect neighbouring basal cells to each other, and also to the basal lamina (Bouameur *et al.*, 2014). In addition, KRT5 modulates cell architecture, supporting the cells and increasing their hardness during mechanical and non-mechanical stresses (Coulombe and Omary, 2002; Atkinson *et al.*, 2011; Bouameur *et al.*, 2014). At the intermediate filament surface, keratin 5 has a non-helical tail, causing it to undergo extensive bundling with increased elasticity, thereby providing the epidermis with mechanical resilience (Coulombe and Omary, 2002). Furthermore, miR-196a-5p affects S100 calcium binding protein A9 (S100A9), which encodes S100A9 and is localised in the cytoplasm and/or nucleus of variety of cell types. This protein binds to calcium ions (Ca^{+2}) and regulates the amount of unbound calcium ions, thereby playing an axial role in calcium signalling pathways and cellular responses including cell cycle and cell differentiation. Taken together, this may suggest its role in keratinocyte differentiation during the healing process (Schnetkamp, 2016). Moreover, miR-196a-5p influences COL1A1 gene that encodes collagen type I alpha 1 chain, which is gives support and strength to many tissue types, including skin. Hence, the role of miR-196a-5p may be critical in skin development and regeneration and it's functional role in the 3D-SEM warrants further investigation.

miR-1297 expression was downregulated at 24 hours and 1 week in the 3D-SEM. It is predicted to controls Kruppel-like factor 5 (KLF5). This protein is a member of a transcription factor family that regulates numerous cellular responses including proliferation, differentiation and development. Additionally, it is expressed in proliferating epithelial cells (Li *et al.*, 2015d). Therefore, downregulation of miR-1297 after 24 hours of healing progress could be an indicator that cells have started to switch their response from migration to proliferation.

miR-488-3p expression was downregulated at 24 and 72 hours in the 3D-SEM. This microRNA has been predicted to modulate corticotropin releasing hormone receptor 2 (CRHR2) protein. This molecule has been shown to play a crucial role in promoting

proliferation, migration, and viability of epithelial cells and to initiate restoration of the epithelial barrier (Hoffman *et al.*, 2016). Thus, the results of this study suggest that downregulation of miR-488-3p between 24 and 72 hours may modulate CRHR2, subsequently enhancing cell proliferation.

Expression of miR-200a-3p was downregulated at 72 hours and 1 week. One of the predicted target genes regulated by miR-200a-3p is BAP1, a gene responsible for production of BRCA1 associated protein-1. This protein is a major player in promoting proliferation and migration of basal breast cells during tumour growth and metastasis (Qin *et al.*, 2015). Therefore, downregulation of miR-200a-3p during the healing process may function to upregulate BAP1 production for further enhancing proliferation and migration of skin cells.

While the majority of microRNAs that were differentially expressed were shown to be down-regulated in the 3D-SEM during wound healing compared to the control, there were some microRNAs that were upregulated at different time points during the healing process. For example, miR-2117 was upregulated at 2, 4 hours and 1 week. This microRNA has is predicted to modulate VAV3 gene, which plays a critical role in the healing process by promoting macrophage migration and phagocytosis activity of apoptotic neutrophils, via regulation of beta (2)-integrins. VAV3 deficient macrophages, but no other cells, demonstrate impaired wound healing in mice (Sindrilaru *et al.*, 2009). The 3D model used in this study lacks the presence of macrophage and other immune cells. Therefore, upregulation of miR-2117 could be of similar function to enhance skin cell migration.

miR-1973 expression was upregulated at 4 hours and 1 week in the 3D-SEM. It is predicted to target CRABP1 gene, which encodes cellular retinoic acid-binding protein 1. The latter is reported to slow proliferation of embryonic stem cells and neural stem cells in mice (Lin *et al.*, 2017). Therefore, upregulation of miR-1973 after 4 hours of initiating the healing process could suppress CRABP1, resulting in promoted cell proliferation.

Expression of miR-320e was upregulated 4 and 72 hours. One of the predicted genes regulated by miR-320e is JUN, a gene encoding c-jun protein. Giles and colleagues reported that inhibition of c-jun by a peptide inhibitor promotes wound healing via promoting proliferation of keratinocytes, but not fibroblasts. In addition, supressing

expression of c-jun using peptide inhibitors resulted in an increased rate of re-epithelialisation and reduced apoptosis in mouse suffering from full skin burns (Giles *et al.*, 2008). Therefore, upregulation of miR-320e after 4 hours of initiation of the healing process may have the effect of inhibiting c-jun expression and therefore, supporting improved and faster healing.

miR-382-5p expression was upregulated at 24 and 72 hours. It is predicted to influence calcium-dependent, non-lysosomal cysteine proteases (CALPAIN) gene. Nassar and colleagues reported that CALPAIN is a principal player in granulation tissue formation and TGF-β induced differentiation; however, it reduces collagen production and wound fibrosis resulting in scar formation (Nassar *et al.*, 2012). Therefore, normal levels of miR-382-5p during early time points of the healing process (within 24 hours) may allow CALPAIN to participate in the healing process through granulation tissue formation and differentiation. Later, (after 24 hours) miR-382-5p was upregulated which have the effect of suppressing CALPAIN and thus, reducing scar formation. Another target gene for miR-382-5p is TAGLN, a gene responsible for transgelin production. The latter is a protein reported to affect cell mobility and proliferation and its suppression results in impaired growth and migration (Zhou *et al.*, 2013). Therefore, upregulation of miR-382-5p may be advantageous by upregulating TAGLN; subsequently, promoting the production of transgelin leading to activated cell proliferation and migration. Another predicted target of miR-382-5p is VIM gene, which is responsible for production of vimentin, plays an important role in the healing process by enhancing fibroblast proliferation and keratinocyte differentiation (Cheng *et al.*, 2016). Upregulation of miR-382-5p between 24 and 72 hours may be explained by the fact that the priority of the cell response during this time is cell migration, rather than proliferation and differentiation. Therefore, after 72 hours regulation of miR-382-5p expression back down to levels similar to those seen in intact models may potentially give rise to upregulation of VIM, resulting in increased vimentin levels which functions to direct keratinocytes to switch their response to proliferation and/or differentiation instead of migration.

miR-99b-5p expression was upregulated at 24 hours and 1 week. It has been shown to regulate HOXA1 (Li *et al.*, 2015f), a gene responsible for production of homeobox protein Hox-A1. This protein along with other homebox proteins, is responsible for accelerating

wound healing via promoting cell migration and angiogenesis (Kachgal *et al.*, 2012). In another word, miR-99b-5p regulate HOXA1 to further promote the healing process.

miR-4284 was upregulated at 72 hours and 1 week. It is predicted to target RUFY2, a gene that produces the two RUN and FYVE domains of the RUFY family. Members of this family have been shown to enhance cell migration in gastric cancer cells (Wang *et al.*, 2015). Downregulation of miR-4284 could suppress the production of RUFY2 protein; subsequently delaying cell migration. Interestingly, levels of miR-4284 were upregulated at 72 hours of wound healing until the last time point measured (1 week). This data suggests that miR-4284 demonstrates normal levels during early wound healing (2-72 hours), similar to those seen in the intact model, resulting in normal levels of RUFY2 to enhance cell migration during this period. On the other hand, miR-4284 also predicted to downregulate histone-lysine N-methyltransferase 2D (KMT2D). Deficiency of this protein reduces proliferation of cancer cells in many colon and breast cancer cell lines (Guo *et al.*, 2013a; Kim *et al.*, 2014). These findings suggest that upregulation of miR-4284 after 72 hours might downregulate KMT2D, to suppress cell proliferation and retain cell migration. It would be of great interest to further study the role of miR-4284 in relation to cell migration and proliferation during wound healing.

Expression of miR-1285-5p was upregulated within the early stages (24 hours) of the healing process compared to intact 3D models, but downregulated at later time points (1 week). It has been shown that miR-1285-5p influences proliferation and migration of lung carcinoma cells (Zhou *et al.*, 2017). Hence, it could be suggested that miR-1285-5p may be upregulated within the first 24 hours to enhance cell mobility and propagation, and then downregulated after 1 week to terminate cell migration and proliferation in order to switch the cell response to differentiation. However, this hypothesis required further investigation.

Additionally, miR-1285-5p downregulates homeodomain-interacting protein kinase 1 (HIPK1). Downregulation of this protein has been shown to reduce cell migration, proliferation and tumorigenic potential of A549 cell line (Lee *et al.*, 2012). Therefore, down regulation of miR-1285-5p after 1 week may upregulate HIPK, resulting in enhancing cell migration and proliferation and switching the cell response to differentiation. Hence, these data suggest that miR-1285-5p play a bi-functional role in wound healing, by controlling cell migration and proliferation at different time points. It would be of great interest to

investigate markers of cell migration and proliferation in relation to miR-1285-5p expression in the 3D-SEM.

This study also focussed on microRNAs that were upregulated at only one time point during the healing process. Here in, representative microRNAs (the highly upregulated microRNAs) at different time points were selected for further investigation of their predicted target genes. For example, miR-149-5p which is upregulated after 2 hours of the healing process, is reported by Jin and co-workers to control many cellular activities. Its downregulation has been shown to suppress migration and proliferation of renal carcinoma cells, in addition to promoting cell apoptosis (Jin *et al.*, 2016). Hence, upregulation of this molecule may be beneficial to the healing process, because it might have the same effect on skin cells i.e. promoting their migration and proliferation.

Another microRNA that was upregulated at 4 hours is miR-584-5p. This molecule was shown to target rho-associated, coiled-coil-containing protein kinase 1 (ROCK-1), a protein that suppresses migration and proliferation of human renal carcinoma cells (Ueno *et al.*, 2011). Therefore, upregulation of miR-584-5p may have the effect of reducing ROCK-1 expression, therby resulting in increased migration and proliferation of skin cells. However, ROCK-1 has also been shown to regulate other processes such as activating VEGF-driven retinal neovascularisation and sprouting angiogenesis (Jens *et al.*, 2009). Therefore, upregulation of this molecule at 4 hours may downregulate ROCK-1 and support migration and proliferation of skin cells, and enhances neovascularisation and angiogenesis leading wound repair.

Another microRNA molecule that was upregulated after 24 hours is miR-542-3p. This microRNA targets bone morphogenesis protein-7 (BMP-7) signalling. BMP-7 has been shown to play a pivotal role in suppression of excessive scar formation (Guo *et al.*, 2017). Therefore, upregulation of miR-542-3p might downregulate BMP-7 and increase collagen production and resulting in scar formation. Yuan and colleagues reported that miR-542-3p inhibits proliferation and migration of colorectal cancer cells via targeting ubiquitin thioesterase also known as otubain-1 (OTUB1). Additionally, miR-542-3p inhibits epithelial-mesenchymal transition (EMT) during hepatocellular carcinoma, suppress cell motility and reduce cancer metastasis by targeting Ubiquitin-protein ligase E3C (UBE3C)

(Tao *et al.*, 2017). These data suggest that this microRNA is determinant of healing progress and its inhibition is supporting wound repair.

After 72 hours, miR-601 was upregulated, which has been shown to modulate epithelial–mesenchymal transition (EMT) progression and activate (PI3K)/AKT signalling (Cao *et al.*, 2017). Both EMT and the (PI3K)/AKT cascade are well documented to play a role in physiologic tissue repair and participate in the healing process by accelerating cutaneous wound healing (Chen *et al.*, 2014; Stone *et al.*, 2016). Therefore, upregulation of this microRNA is advantageous to the healing process, by activating these signalling cascades.

Expession of miR-337-3p was upregulated after 1 week in the 3D-SEM. This molecule is reported to target HOXB7 (Zhang *et al.*, 2014) a well-documented molecule that enhances growth, proliferation and migration of hepatocellular carcinoma by promoting stemness and epithelial-mesenchymal transition. Therefore, a similar activity of this microRNA may be achieved in chronic wounds i.e. by High level of miR-337-3p downregulates HOXB7 to terminate cell migration, proliferation and switch the cellular response to differentiation. Hence, upregulation of this microRNA is advantageous to the healing process.

Despite the investigation of predicted microRNA targets using *in silico* algorithms performed in this study, the function of these microRNAs in wound healing remains hypothetical. Additional investigations are required to confirm the direct targets of these microRNAs in the 3D-SEM and wound healing setting. In addition, functional studies may further elucidate the modulatory effect of these microRNAs and their targets, for better understanding of the molecular mechanism of wound healing.

The ability of keratinocytes to express receptors of target growth factors and cytokines at different time points during the healing process is another important factor in promoting tissue repair and wound healing. Expression of these receptors on the cell surface will activate soluble biomolecules (growth factors and cytokines) upon binding, to further activate relevant signalling cascades and evoke cellular response. Maintained expression of theses receptors during the different conditions and time points of the 3D-SEM wound healing model suggest their importance during the repair process. The role of microRNAs during the wound healing process may also be demonstrated by their ability to target key

grown factor and cytokine receptors, as demonstrated in (Table 7.10). Indeed, TGFBR1 has been predicted to be targeted by microRNAs that were differentially downregulated at several different time points (4 hours, 24 hours, 72 hours and 1 week), and PDGFRA is predicted to be targeted by 3 microRNAs that were differentially downregulated at 3 different time points (4 hours, 24 hours and 1 week) suggesting that these microRNAs are downregulated to give rise for upregulation the genes responsible for production of TGFBR1 and PDGFRA to participate in the healing process. MST1R was predicted to be targeted by two microRNAs tat demonstrated differential expression in the 3D-SEM, while other receptors such as c-MET, FFGFR2 and CXCR4 were predicted to be modulated by only one target microRNA.

In summary, we have shown that the wound healing model developed in this study is a good tool for a wide range of molecular investigations such as; gene expression, microRNA profiling, DNA analysis and proteomic studies. In addition to its advantages described in Chapter 6, using this model is preferable to using the 2D scratch assay at the molecular level analysis. For instance, in 2D culture, microRNAs are isolated from only one cell type such as keratinocytes, which is different from microRNA profiling of real skin, which contain keratinocyte and fibroblast. This drawback may be overcome by using the 3D model, which is comprised of both epidermal and dermal layers. Furthermore, in this Chapter we have shown that the 3D-SEM generally mimics microRNA profiling of real skin, with the exception of a signature of differentially expressed microRNAs, which have been discussed. Consequently, data obtained from this study could be used as a reference library for microRNA profiling studies during the wound healing process for future investigations in this field. MicroRNAs could also be used as molecular markers for characterising and validating 3D skin models constructed *in vitro* for further evaluating these 3D skin equivalents for their suitability for pre-clinical applications. Additionally, microRNAs are differentially expressed during the different phases of the healing process. Some of these molecules are upregulated while others are down regulated suggesting their essential participation in regulating the repair process. One of the mechanisms by which microRNAs may be involved in the repair mechanism is by targeting different genes with a role in wound repair. It would be of essential importance for further understanding of the wound healing process to further investigate these predicted target genes.

MicroRNAs may also be used as signals to evoke signalling pathways and trigger cellular responses during wound healing cascades. The most important genes regulated by these microRNAs are those related to cell migration, proliferation, differentiation, re-epithelialisation, cell cycle and receptors of growth factors. Giving these features, manipulation and control of microRNA expression during the healing process has the potential to be applied as a molecular therapy for non-healing wounds, and this would be an essential area of future investigation.

CHAPTER 8 GENERAL DISCUSSION AND CONCLUDING REMARKS

CHAPTER EIGHT: GENERAL DISCUSSION AND CONCLUDING REMARKS

8.1 INTRODUCTION

Cellular therapies for cutaneous wound healing have been given a large amount of research attention in order to try to address the problems associated with chronic wounds. Among the approaches has included applying keratinocytes to the wounded skin (Kopp *et al.*, 2004), using engineered skin equivalents for burns (Hocking, 2012) and specific extra cellular matrix (ECM) proteins to damaged skin (Maxson *et al.*, 2012). However, these approaches fail to successfully treat non-healing wounds due to complications such alteration of immune responses to avoid any further fibrotic reactions and incomplete integration of the implanted cells into normal uninjured skin (Metcalfe and Ferguson, 2007). Recently mesenchymal stem cells (MSCs) and their secretions have gained an attention as a potential cellular therapy for treating non healing wounds (Hocking, 2012; Tamama and Kerpedjieva, 2012). However, the cellular and molecular mechanisms of how MSCs and their secretions could be utilised for treating chronic wounds is still not fully understood and some issues need to be addressed before using MSCs as a treatment for wounds. This research was therefore conducted to investigate the main cellular and molecular mechanisms that could be involved in the healing process under the effect of MSC secretions.

8.2 GENERAL DISCUSSION

Wound healing is a complicated process consisting of overlapping phases and events. Cellular therapy is a promising strategy for treating chronic wounds. Migration, proliferation and differentiation of epidermal keratinocytes represent the most important steps in a successful healing process. Success of the healing process mainly depends on the time of initiation and termination of these overlapping phases. A substantial criteria for successful repair is recovery of an intact epidermal layer (Velnar *et al.*, 2009). Therefore, migration of epidermal cells is the first rate-determining step in the healing process (Yan *et al.*, 2017). Hence, the first aim of this study was investigating the effect of MSC-CM on migration of skin cells. To this aim, a new method was developed to enable the study of MSC-CM on primary keratinocytes, instead of using cell lines, by collecting MSC-CM in

low calcium level medium (LC-CM) and avoiding the interference caused by high calcium levels. Consequently, more realistic results were obtained using the developed protocol. To the best of our knowledge, this study has showed for the first time, the ability of MSCs to grow in low calcium level and serum free media conditions retaining their ability to secrete biologically active substances.

Migration and proliferation collectively comprise re-epithelialisation, which is the important key step in the healing process, restoring barrier function and initiating the healing process (Lau *et al.*, 2009). Therefore, the second aim of the study was to test the effect of MSC-CM on proliferation of skin cells during wound closure using the developed method by collecting MSC secretions in low calcium level containing media (LC-CM). The study showed that LC-CM enhanced cell proliferation by 48 hours after the initiation of the healing process. Observations from this study confirmed that the cellular responses, at the injury site were initiated in a step-wise manner. For example, cell migration is the most important response during the early stages of the healing process in order to successfully cover the wound. Covering the wounds with a newly formed cellular sheet protects from microbial contamination. Hence, it could be suggested that the treatment of non-healing wounds should be gradual i.e. in the early stages, growth factors that enhance cell migration could be given first until positive results are observed. Proliferation inducing factors could be given later followed by introducing differentiation inducing factors to finally obtain the best healing results (Wickert *et al.*, 2016). This study confirmed that cellular responses enhanced by LC-CM were ordered, depending on the cellular demand at the injury site i.e. LC-CM enhances cell migration during the first hours of injury (0 - 48 hours) when the cells then switch their response from migration to proliferation and differentiation. On the other hand, cells which were inhibited to proliferate due to mitomycin C (MMC) retained their ability to migrate under low calcium (LC-CM) conditions. LC-CM also enhanced cell migration at different conditions such as normoxia, hypoxia and after blocking SDF-1α. An interesting observation from this study was that MSC secretions collected at early times during their expansion (LC-CM24) demonstrated a stronger effect on cell migration compared to those collected at later time points (LC-CM48 and LC-CM72). In addition, there were no differences in the concentrations of growth factors present in either LC-CM 24, LC-CM 48 or LC-CM 72. This is a novel finding and since

previous studies collected MSCs secretions after 72 hours (Walter et al., 2010) could be useful for future research in terms of reducing the collection time, sparing media and other cell culture consumables. The stratum basal layer of the epidermis contains the epidermal stem cells, which proliferate and act as a source of cells that differentiate into upper epidermal layers (Bikle *et al.*, 2012). Upon injury, all the epidermal layers will be lost including the basal layer and epidermal stem cell precursor. The potential of MSCs to differentiate into epidermal like structures is a possible strategy which could be applied as a cellular therapeutic for chronic wounds, since they could be injected into the injury site in order to differentiate into epidermal layers and promote wound healing. This study also showed for the first time that MSCs were able to differentiate into epidermal like structures retaining the ability to express epidermal differentiation markers when seeded over human dermal fibroblast layers free of animal collagen. These results suggest cross-talk between MSCs and dermal fibroblasts in order to recover the damaged epidermis via differentiation into the different epidermal layers. Other studies have tested the ability of MSCs to differentiate into epidermal cells when seeded over dermal layers enriched with bovine collagen type I (Ma et al., 2009) which may interfere with the interpretation of results for use in human studies.

Growth factors such as PDGF-AB, TGF-ß1, HGF, KGF, SDF-1α and MSP-1 are secreted by MSC in *in vitro* culture and are reported to enhance cell migration and proliferation during wound repair. One of the critical parameters that impact the healing progress is the ability of skin cells, mainly keratinocytes, to express receptors that bind to the growth factors and cytokines and initiate signalling pathways to further evoke an appropriate cellular response. Failure of skin cells to express surface receptors hinder the healing process and introducing new therapeutics based on growth factors would be of no value unless the cells at and around the injury site expressed these receptors. A possible strategy therefore, could be to activate the cells surrounding the damaged tissue to express membrane receptors for the growth factor of interest. For example, PDGF interacts with its receptor on the cell surface of the target cell, induces and regulates several cellular pathological and physiological responses involved in tissue repair and wound healing (De Donatis *et al.*, 2008). Therefore, enhancing cells to express PDGFRA could be useful for ensuring the binding of the growth factor to the target cells and

enhancing tissue repair. A part from the 2D culture, in this study a 3D skin equivalent model for wound healing was developed and confirmed for its suitability at the cellular and molecular for use as a replica for skin for wound healing studies. Additionally, a robust reproducible protocol for wound healing studies was also developed with consistent and reproducible results. The developed 3D model was used, for the first time in this study, to investigate microRNA profiling compared to intact models at different time points during the healing process. Another strategy which could be considered for treating chronic wounds is using growth factors with high binding affinity to skin cells. For instance, the binding affinity could be determined by the parameters that enable the target cells to express receptors on the cell surface. MicroRNAs are molecules that can regulate receptor expression and these molecules may be up- or down-regulated to enhance the cells to express relevant receptors. Additionally, some receptors are predicted to be targeted by more than one microRNA and these are expressed on the cell surface at higher levels compare to receptors targeted by one only microRNA. Furthermore, expression of microRNAs at different time points during the wound healing process that target the same receptor may ensure controlled expression of their target receptor. An example of these receptors are TGFBR1 and PDGFRA, which are predicted to be targeted by more than 3 microRNAs that were differentially expressed at different time points of 3D-SEM wound healing. Therefore, treatment with growth factors TGF-1ß and PDGF may give rise to a better response than using other growth factors, such as HGF and KGF, which bind to c-MET and FGFR2 receptors respectively and are predicted to be regulated by microRNAs molecule that are only differentially expressed at one time point during wound healing (72 hours).

MicroRNAs have the potential to be used for treating non-healing wounds, by upregulating beneficial microRNAs and inhibiting detrimental microRNAs to the wound healing process. Inhibiting detrimental microRNAs at early stages of the healing process could be an effective therapeutic approach by arresting cell migration and proliferation. Our results showed that miR-542-3p retained its normal levels within the first 24 hours and was then down regulated after 24 hours in the 3D-SEM wound healing model. Therefore, it’s possible that this molecule was interacting with other microRNAs or target genes that enhance cell migration during the first 24 hours. A similar observation was made for miR-

584-5p, miR-601 and miR-337-3p. Hence, early inhibition of these molecules may allow for increased wound repair and support the healing process.

8.3 CONCLUSION

Mesenchymal stem cells (MSCs) and their secretions are promising therapeutics for chronic wounds. Availability, ease of isolation and expansion *in vitro* make MSCs an excellent candidate for treating wounds compared to other stem cells including embryonic stem cells (ESCs). Two main strategies could be applied for the use of MSCs in the treatment of chronic wounds. The first is cell mediated repair, when MSCs differentiate into epidermal like cells and the second, secretory mediated repair by the use of the biomolecules secreted by MSC *in vitro*. MSCs, therefore, are an improvement on therapies which involve implanting keratinocytes into the injury site, when keratinocytes can only differentiate but have no secretory role. At the molecular level, up or down regulation of certain genes should be carried out in an ordered manner, since cellular responses during the healing process are ordered events and switching on cell responses at particular times would lead to improved healing. Since the healing process is composed of overlapping phases and events, the function of microRNAs involved in the healing cascades may also be overlapping. Hence, microRNAs have the potential to control the healing process in a highly organised manner. For example, some microRNAs enhance cell migration mainly during the early stages (2-24 hours) of wound healing, while other microRNAs start to enhance cell proliferation (between 24 and 48 hours). However, some microRNAs that promote cell migration remain up regulated and retain cell migration until full coverage of the injury site. Other microRNAs that are related to differentiation are up regulated after 72 hours, when migration and proliferation are no longer required; therefore, these molecules start to switch the cellular responses to differentiation instead of mobility and propagation. In addition, some microRNAs play a major role in the healing process while others play a secondary role. MicroRNAs which play a major role are those involved at early stages (2-4 hours), to enhance the required response such as migration-inducing microRNAs which are upregulated first, followed by microRNAs required for proliferation which are upregulated later (24-72 hours). Finally, differentiation related microRNAs are up regulated during the final stages of wound healing, after 1 week.

Secondary microRNAs are those regulated at time points when there is more demand for specific cellular responses. For example, if the migration related major microRNAs are initiated but do not sufficiently enhance migration, secondary microRNAs are upregulated to aid the major microRNAs to induce an improved response.

8.4 Limitations of Using MSCs in Wound Treatment

MSCs can be considered as a promising tool for treating non-healing wounds; however, some aspects relating to MSC biology need to be studied intensively before using them for clinical application. One of these problems is finding a source of MSCs which does not involve an invasive procedure i.e. isolation of MSCs from peripheral blood instead of bone marrow. Other questions include the following: what is the ideal number and timing for MSC administration / implantation? How long can MSCs survive in the injury site after implantation? Are multiple implantations required for successful healing? When do the implanted MSCs start to secrete their effective soluble molecules after implantation? And finally, are MSC secretions controllable? Answers to these questions are important and essential for the therapeutic use of MSCs and for a safer and more effective treatment for non-healing wounds.

8.5 Future Work

Extracellular vesicles of MSCs, in particular, MSC-exosomes, may also play a significant role in the healing process; therefore, investigating the involvement of these molecules on wound healing in both 2D and 3D culture, may enable further strategies or micro therapy, to be developed for the treatment of chronic wounds

At the molecular level, there have been no previous studies or evidence that MSC-CM modulate (up or down regulate) the expression of specific microRNAs during the healing process. More investigations are therefore required to confirm the exact effect of MSC secretions (triggers or inhibitors) of microRNAs in both 2D and 3D culture.

More research into the involvement of microRNAs in signalling pathways, including functional studies, is required to investigate the interaction between microRNAs and supposed target genes or receptors to confirm the regulation type (up or down) and to clarify the role of these molecules in the healing process at the molecular level.

The modified 3D skin equivalent model, developed in this study, could be further developed to include immune cells for studying the immunological and inflammatory responses during the healing process. Finally, specific targeted genes could be further investigated for use as a genetic therapy for chronic wounds.

ETHICS APPROVAL

Health Research Authority
NRES Committee North East - Newcastle & North Tyneside 1
Jarrow Business Centre
Jarrow REC Centre
Room 002
Rolling Mill Road
Jarrow
NE32 3DT

Telephone: 0191 428 3565

5 December 2014

Professor A D Rowan
Musculoskeletal Research Group (ICM)
Newcastle University
Framlington Place
Newcastle upon Tyne
NE2 4HH

Dear Professor Rowan

Title of the Research Tissue Bank:	**Newcastle Bone and Joint Biobank**
REC reference:	**14/NE/1212**
Designated Individual:	**Professor A G Hall**
IRAS project ID:	**166522**

Thank you for your letter of 4 December 2014, responding to the Committee's request for further information on the above research tissue bank and submitting revised documentation.

The further information has been considered on behalf of the Committee by the Chair of the REC meeting.

We plan to publish your research summary wording for the above study on the NRES website, together with your contact details, unless you expressly withhold permission to do so. Publication will be no earlier than three months from the date of this favourable opinion letter. Should you wish to provide a substitute contact point, require further information, or wish to make a request to postpone publication, please contact the REC Manager Ms Gillian Mayer, nrescommittee.northeast-newcastleandnorthtyneside1@nhs.net.

Confirmation of ethical opinion

On behalf of the Committee, I am pleased to confirm a **Favourable** ethical opinion of the above research tissue bank on the basis described in the application form and supporting documentation as revised.

The Committee has also confirmed that the favourable ethical opinion applies to all research projects conducted in the UK using tissue or data supplied by the tissue bank, provided that the release of tissue or data complies with the attached conditions. It will not be necessary for these researchers to make project-based applications for ethical approval. They will be deemed to have ethical approval from this committee. You should provide the researcher with a copy of this letter as confirmation of this. The Committee should be notified of all projects receiving tissue and data from this tissue bank by means of an annual report.

Duration of ethical opinion

The favourable opinion is given for a period of five years from the date of this letter and

provided that you comply with the standard conditions of ethical approval for Research Tissue Banks set out in the attached document. You are advised to study the conditions carefully. The opinion may be renewed for a further period of up to five years on receipt of a fresh application. It is suggested that the fresh application is made 3-6 months before the five years expires, to ensure continuous approval for the research tissue bank.

Approved documents

The documents reviewed and approved at the meeting were:

Document	*Version*	*Date*
Covering letter on headed paper [cover letter]	1	31 October 2014
Covering letter on headed paper [cover letter]	1.1 (A D Rowan)	01 December 2014
Human Tissue Authority licence [Med School HTA Licence]		22 September 2014
Other [CV for scientific member of Governance Committee Professor John Loughlin]		
Other [CV for Tissue Bank Manager - A Rowan]	1	31 October 2014
Other [CV for Professor David Young]		
Other [CV for Dr Kenny Rankin]		
Other [CV for Dr Kenny Rankin]		
Other [Proforma for submitting request to use samples]		
Other [Flowchart]		
Other [Insurance Certificate - University of Newcastle]	Policy No. NHE-08CA03-0013	17 June 2014
Other [Protocol – changes highlighted]	1.1	01 December 2014
Other [Email Notification re named independent member of Governance Committee]	A D Rowan	04 December 2014
Participant consent form [Appendix 1b FRH and 1d RVI]	1.1	01 December 2014
Participant information sheet [Appendix 1a FRH and 1c RVI]	1.1	01 December 2014
Protocol for management of the tissue bank [Protocol]	1.1	01 December 2014
REC Application Form [RTB_Form_04112014]		04 November 2014
Summary of research programme(s) [Appendix 5a]	1.1	01 December 2014

Licence from the Human Tissue Authority

Thank you for providing a copy of the above licence.

Research governance

Under the Research Governance Framework (RGF), there is no requirement for NHS research permission for the establishment of research tissue banks in the NHS. Applications to NHS R&D offices through IRAS are not required as all NHS organisations are expected to have included management review in the process of establishing the research tissue bank.

Research permission is also not required by collaborators at tissue collection centres (TCCs) who provide tissue or data under the terms of a supply agreement between the organisation and the research tissue bank. TCCs are not research sites for the purposes of the RGF.

Research tissue bank managers are advised to provide R&D offices at all TCCs with a copy of the REC application for information, together with a copy of the favourable opinion letter when available. All TCCs should be listed in Part C of the REC application.

NHS researchers undertaking specific research projects using tissue or data supplied by a

research tissue bank must apply for permission to R&D offices at all organisations where the research is conducted, whether or not the research tissue bank has ethical approval.

Site-specific assessment (SSA) is not a requirement for ethical review of research tissue banks.

Statement of compliance

The Committee is constituted in accordance with the Governance Arrangements for Research Ethics Committees and complies fully with the Standard Operating Procedures for Research Ethics Committees in the UK.

After ethical review

Reporting requirements

The attached standard conditions give detailed guidance on reporting requirements for research tissue banks with a favourable opinion, including:

- Notifying substantial amendments
- Submitting Annual Progress reports

The HRA website also provides guidance on these topics, which is updated in the light of changes in reporting requirements or procedures.

User Feedback

The Health Research Authority is continually striving to provide a high quality service to all applicants and sponsors. You are invited to give your view of the service you have received and the application procedure. If you wish to make your views known please use the feedback form available on the HRA website: http://www.hra.nhs.uk/about-the-hra/governance/quality-assurance/

HRA Training

We are pleased to welcome researchers and R&D staff at our training days – see details at http://www.hra.nhs.uk/hra-training/

14/NE/1212	**Please quote this number on all correspondence**

Yours sincerely
pp

Mr Mike Wyatt
Chair of the REC Meeting

E-mail: nrescommittee.northeast-newcastleandnorthtyneside1@nhs.net

Enclosures: *Standard approval conditions SL-AC3*

Copy to: *Professor A G Hall – Medical School, Newcastle University*

A Research Ethics Committee established by the Health Research Authority

REFERENCES

Abbas, A.K. and Lichtman, A.H. (2010) *Basic Immunology: Functions and Disorders of the Immune System*. Saunders.

Abbi, S., Ueda, H., Zheng, C., Cooper, L.A., Zhao, J., Christopher, R. and Guan, J.-L. (2002) 'Regulation of Focal Adhesion Kinase by a Novel Protein Inhibitor FIP200', *Molecular Biology of the Cell*, 13(9), pp. 3178-3191.

Aberdam, D., Candi, E., Knight, R.A. and Melino, G. (2008) 'miRNAs, 'stemness' and skin', *Trends in Biochemical Sciences*, 33(12), pp. 583-591.

Abuharbeid, S., Czubayko, F. and Aigner, A. (2006) 'The fibroblast growth factor-binding protein FGF-BP', *The International Journal of Biochemistry & Cell Biology*, 38(9), pp. 1463-1468.

Aggarwal, S. and Pittenger, M.F. (2005) 'Human mesenchymal stem cells modulate allogeneic immune cell responses', *Blood*, 105(4), pp. 1815-22.

Akiyama, K., You, Y.-O., Yamaza, T., Chen, C., Tang, L., Jin, Y., Chen, X.-D., Gronthos, S. and Shi, S. (2012) 'Characterization of bone marrow derived mesenchymal stem cells in suspension', *Stem Cell Research & Therapy*, 3(5), p. 40.

Albrecht-Buehler, G. (1977) 'The phagokinetic tracks of 3T3 cells', *Cell*, 11(2), pp. 395-404.

Alev, C., Wu, Y., Nakaya, Y. and Sheng, G. (2013) 'Decoupling of amniote gastrulation and streak formation reveals a morphogenetic unity in vertebrate mesoderm induction', *Development*, 140(13), p. 2691.

Alfaro, M.P., Deskins, D.L., Wallus, M., DasGupta, J., Davidson, J.M., Nanney, L.B., M, A.G., Gannon, M. and Young, P.P. (2013) 'A physiological role for connective tissue growth factor in early wound healing', *Lab Invest*, 93(1), pp. 81-95.

Alfaro, M.P., Pagni, M., Vincent, A., Atkinson, J., Hill, M.F., Cates, J., Davidson, J.M., Rottman, J., Lee, E. and Young, P.P. (2008) 'The Wnt modulator sFRP2 enhances mesenchymal stem cell engraftment, granulation tissue formation and myocardial repair', *Proc Natl Acad Sci U S A*, 105(47), pp. 18366-71.

Alge, C.S., Hauck, S.M., Priglinger, S.G., Kampik, A. and Ueffing, M. (2006) 'Differential Protein Profiling of Primary versus Immortalized Human RPE Cells Identifies Expression

Patterns Associated with Cytoskeletal Remodeling and Cell Survival', *Journal of Proteome Research*, 5(4), pp. 862-878.

Alston-Roberts, Barallon, R., Bauer, S., Butler, Capes-Davis, A., Dirks, W., Elmore, E., Furtado, M., Kerrigan, Kline, M., Kohara, A., Los, G., MacLeod, Masters, J., Nardone, Nims, Price, Reid, Shewale and Thomson, J. (2010) *Cell line misidentification: the beginning of the end!*

Alvarez-Garcia, I. and Miska, E.A. (2005) 'MicroRNA functions in animal development and human disease', *Development*, 132(21), pp. 4653-4662.

Amoh, Y., Li, L., Campillo, R., Kawahara, K., Katsuoka, K., Penman, S. and Hoffman, R.M. (2005a) 'Implanted hair follicle stem cells form Schwann cells that support repair of severed peripheral nerves', *Proc Natl Acad Sci U S A*, 102(49), pp. 17734-8.

Amoh, Y., Li, L., Yang, M., Jiang, P., Moossa, A.R., Katsuoka, K. and Hoffman, R.M. (2005b) 'Hair follicle-derived blood vessels vascularize tumors in skin and are inhibited by Doxorubicin', *Cancer Res*, 65(6), pp. 2337-43.

Amoh, Y., Li, L., Yang, M., Moossa, A.R., Katsuoka, K., Penman, S. and Hoffman, R.M. (2004) 'Nascent blood vessels in the skin arise from nestin-expressing hair-follicle cells', *Proc Natl Acad Sci U S A*, 101(36), pp. 13291-5.

An, Y., wei, W., Jing, H., Ming, L., Liu, S. and Jin, Y. (2015) 'Bone marrow mesenchymal stem cell aggregate: an optimal cell therapy for full-layer cutaneous wound vascularization and regeneration', *Scientific Reports*, 5, p. 17036.

Andl, T., Murchison, E.P., Liu, F., Zhang, Y., Yunta-Gonzalez, M., Tobias, J.W., Andl, C.D., Seykora, J.T., Hannon, G.J. and Millar, S.E. (2006) 'The miRNA-Processing Enzyme Dicer Is Essential for the Morphogenesis and Maintenance of Hair Follicles', *Current Biology*, 16(10), pp. 1041-1049.

Antonini, D., Russo, M.T., De Rosa, L., Gorrese, M., Del Vecchio, L. and Missero, C. (2010) 'Transcriptional Repression of miR-34 Family Contributes to p63-Mediated Cell Cycle Progression in Epidermal Cells', *Journal of Investigative Dermatology*, 130(5), pp. 1249-1257.

Antonioli, L., Pacher, P., Vizi, E.S. and Haskó, G. (2013) 'CD39 and CD73 in immunity and inflammation', *Trends in molecular medicine*, 19(6), pp. 355-367.

Arenzana-Seisdedos, F. (2015) 'SDF-1/CXCL12: A Chemokine in the Life Cycle of HIV', *Frontiers in Immunology*, 6(256).

Ariel, A., Maridonneau-Parini, I., Rovere-Querini, P., Levine, J.S. and Mühl, H. (2012) 'Macrophages in inflammation and its resolution', *Frontiers in Immunology*, 3, p. 324.

Arufe, M.C., De la Fuente, A., Fuentes, I., Toro, F.J. and Blanco, F.J. (2011) 'Umbilical cord as a mesenchymal stem cell source for treating joint pathologies', *World J Orthop*, 2(6), pp. 43-50.

Astori, G., Vignati, F., Bardelli, S., Tubio, M., Gola, M., Albertini, V., Bambi, F., Scali, G., Castelli, D., Rasini, V., Soldati, G. and Moccetti, T. (2007) '"In vitro" and multicolor phenotypic characterization of cell subpopulations identified in fresh human adipose tissue stromal vascular fraction and in the derived mesenchymal stem cells', *J Transl Med*, 5, p. 55.

Atkinson, S.D., McGilligan, V.E., Liao, H., Szeverenyi, I., Smith, F.J.D., Tara Moore, C.B. and Irwin McLean, W.H. (2011) 'Development of Allele-Specific Therapeutic siRNA for Keratin 5 Mutations in Epidermolysis Bullosa Simplex', *Journal of Investigative Dermatology*, 131(10), pp. 2079-2086.

Aunin, E., Broadley, D., Ahmed, M.I., Mardaryev, A.N. and Botchkareva, N.V. (2017) 'Exploring a Role for Regulatory miRNAs In Wound Healing during Ageing:Involvement of miR-200c in wound repair', *Scientific Reports*, 7(1), p. 3257.

Avniel, S., Arik, Z., Maly, A., Sagie, A., Basst, H.B., Yahana, M.D., Weiss, I.D., Pal, B., Wald, O., Ad-El, D., Fujii, N., Arenzana-Seisdedos, F., Jung, S., Galun, E., Gur, E. and Peled, A. (2006) 'Involvement of the CXCL12/CXCR4 Pathway in the Recovery of Skin Following Burns', *Journal of Investigative Dermatology*, 126(2), pp. 468-476.

Azizi, S.A., Stokes, D., Augelli, B.J., DiGirolamo, C. and Prockop, D.J. (1998) 'Engraftment and migration of human bone marrow stromal cells implanted in the brains of albino rats—similarities to astrocyte grafts', *Proceedings of the National Academy of Sciences of the United States of America*, 95(7), pp. 3908-3913.

Badiavas, E.V., Abedi, M., Butmarc, J., Falanga, V. and Quesenberry, P. (2003) 'Participation of bone marrow derived cells in cutaneous wound healing', *Journal of Cellular Physiology*, 196(2), pp. 245-250.

Baer, P.C. and Geiger, H. (2012) 'Adipose-derived mesenchymal stromal/stem cells: tissue localization, characterization, and heterogeneity', *Stem Cells Int*, 2012, p. 812693.

Baharvand, H., Hashemi, S.M., Kazemi Ashtiani, S. and Farrokhi, A. (2006) 'Differentiation of human embryonic stem cells into hepatocytes in 2D and 3D culture systems in vitro', *Int J Dev Biol*, 50(7), pp. 645-52.

Bandyopadhyay, B., Han, A., Dai, J., Fan, J., Li, Y., Chen, M., Woodley, D.T. and Li, W. (2011) 'TβRI/Alk5-independent TβRII signaling to ERK1/2 in human skin cells according to distinct levels of TβRII expression', *Journal of Cell Science*, 124(1), pp. 19-24.

Banerjee, J., Chan, Y.C. and Sen, C.K. (2011) 'MicroRNAs in skin and wound healing', *Physiological Genomics*, 43(10), pp. 543-556.

Banerjee, J. and Sen, C.K. (2013) 'MicroRNAs in skin and wound healing', *Methods Mol Biol*, 936, pp. 343-56.

Baron, F. and Storb, R. (2012) 'Mesenchymal stromal cells: a new tool against graft-versus-host disease?', *Biol Blood Marrow Transplant*, 18(6), pp. 822-40.

Barrientos, S., Stojadinovic, O., Golinko, M.S., Brem, H. and Tomic-Canic, M. (2008a) 'Growth factors and cytokines in wound healing', *Wound Repair Regen*, 16(5), pp. 585-601.

Barrientos, S., Stojadinovic, O., Golinko, M.S., Brem, H. and Tomic-Canic, M. (2008b) 'PERSPECTIVE ARTICLE: Growth factors and cytokines in wound healing', *Wound Repair and Regeneration*, 16(5), pp. 585-601.

Barry, F.P. and Murphy, J.M. (2004) 'Mesenchymal stem cells: clinical applications and biological characterization', *Int J Biochem Cell Biol*, 36(4), pp. 568-84.

Bell, E., Ehrlich, H.P., Buttle, D.J. and Nakatsuji, T. (1981) 'Living tissue formed in vitro and accepted as skin-equivalent tissue of full thickness', *Science*, 211(4486), pp. 1052-4.

Bellayr, I.H., Walters, T.J. and Li, Y. (2010) 'Scarless Wound Healing', *The Journal of the American College of Certified Wound Specialists*, 2(2), pp. 40-43.

Benakanakere, M.R., Li, Q., Eskan, M.A., Singh, A.V., Zhao, J., Galicia, J.C., Stathopoulou, P., Knudsen, T.B. and Kinane, D.F. (2009) 'Modulation of TLR2 Protein Expression by miR-105 in Human Oral Keratinocytes', *The Journal of Biological Chemistry*, 284(34), pp. 23107-23115.

Benizri, E., Ginouvès, A. and Berra, E. (2008) 'The magic of the hypoxia-signaling cascade', *Cellular and Molecular Life Sciences*, 65(7), pp. 1133-1149.

Bergsten, E., Uutela, M., Li, X., Pietras, K., Ostman, A., Heldin, C.-H., Alitalo, K. and Eriksson, U. (2001) 'PDGF-D is a specific, protease-activated ligand for the PDGF [beta]-receptor', *Nat Cell Biol*, 3(5), pp. 512-516.

Berridge, M.V., Herst, P.M. and Tan, A.S. (2005) 'Tetrazolium dyes as tools in cell biology: New insights into their cellular reduction', *Biotechnology Annual Review*, 11, pp. 127-152.

Bhadriraju, K. and Chen, C.S. (2002) 'Engineering cellular microenvironments to improve cell-based drug testing', *Drug Discovery Today*, 7(11), pp. 612-620.

Bhattacharya, S., Aggarwal, R., Singh, V.P., Ramachandran, S. and Datta, M. (2015) 'Downregulation of miRNAs during Delayed Wound Healing in Diabetes: Role of Dicer', *Molecular Medicine*, 21(1), pp. 847-860.

Bianco, P., Robey, P.G. and Simmons, P.J. (2008) 'Mesenchymal stem cells: revisiting history, concepts, and assays', *Cell Stem Cell*, 2(4), pp. 313-9.

Bick, M.D. and Davidson, R.L. (1974) 'Total Substitution of Bromodeoxyuridine for Thymidine in the DNA of a Bromodeoxyuridine-Dependent Cell Line', *Proceedings of the National Academy of Sciences of the United States of America*, 71(5), pp. 2082-2086.

Bikle, D.D., Ratnam, A., Mauro, T., Harris, J. and Pillai, S. (1996) 'Changes in calcium responsiveness and handling during keratinocyte differentiation. Potential role of the calcium receptor', *Journal of Clinical Investigation*, 97(4), pp. 1085-1093.

Bikle, D.D., Xie, Z. and Tu, C.-L. (2012) 'Calcium regulation of keratinocyte differentiation', *Expert review of endocrinology & metabolism*, 7(4), pp. 461-472.

Birchmeier, C., Birchmeier, W., Gherardi, E. and Vande Woude, G.F. (2003) 'Met, metastasis, motility and more', *Nat Rev Mol Cell Biol*, 4(12), pp. 915-925.

Birgersdotter, A., Sandberg, R. and Ernberg, I. (2005) 'Gene expression perturbation in vitro—A growing case for three-dimensional (3D) culture systems', *Seminars in Cancer Biology*, 15(5), pp. 405-412.

Biswas, S., Roy, S., Banerjee, J., Hussain, S.-R.A., Khanna, S., Meenakshisundaram, G., Kuppusamy, P., Friedman, A. and Sen, C.K. (2010) 'Hypoxia inducible microRNA 210 attenuates keratinocyte proliferation and impairs closure in a murine model of ischemic wounds', *Proceedings of the National Academy of Sciences*, 107(15), pp. 6976-6981.

Blaber, S., Webster, R., Hill, C., Breen, E., Kuah, D., Vesey, G. and Herbert, B. (2012) 'Analysis of in vitro secretion profiles from adipose-derived cell populations', *Journal of Translational Medicine*, 10(1), p. 172.

Blanchet, M.-R., Bennett, J.L., Gold, M.J., Levantini, E., Tenen, D.G., Girard, M., Cormier, Y. and McNagny, K.M. (2011) 'CD34 Is Required for Dendritic Cell Trafficking and Pathology in Murine Hypersensitivity Pneumonitis', *American Journal of Respiratory and Critical Care Medicine*, 184(6), pp. 687-698.

Blanpain, C. and Fuchs, E. (2009) 'Epidermal homeostasis: a balancing act of stem cells in the skin', *Nature reviews. Molecular cell biology*, 10(3), pp. 207-217.

Boeri, M., Verri, C., Conte, D., Roz, L., Modena, P., Facchinetti, F., Calabrò, E., Croce, C.M., Pastorino, U. and Sozzi, G. (2011) 'MicroRNA signatures in tissues and plasma predict development and prognosis of computed tomography detected lung cancer', *Proceedings of the National Academy of Sciences*, 108(9), pp. 3713-3718.

Bollag, W.B. and Hill, W.D. (2013) 'CXCR4 in Epidermal Keratinocytes: Crosstalk within the Skin()', *The Journal of investigative dermatology*, 133(11), pp. 2505-2508.

Bonauer, A., Carmona, G., Iwasaki, M., Mione, M., Koyanagi, M., Fischer, A., Burchfield, J., Fox, H., Doebele, C., Ohtani, K., Chavakis, E., Potente, M., Tjwa, M., Urbich, C., Zeiher, A.M. and Dimmeler, S. (2009) 'MicroRNA-92a Controls Angiogenesis and Functional Recovery of Ischemic Tissues in Mice', *Science*, 324(5935), pp. 1710-1713.

Booth, A.M., Fang, Y., Fallon, J.K., Yang, J.-M., Hildreth, J.E.K. and Gould, S.J. (2006) 'Exosomes and HIV Gag bud from endosome-like domains of the T cell plasma membrane', *The Journal of Cell Biology*, 172(6), pp. 923-935.

Borowiak, M., Garratt, A.N., Wüstefeld, T., Strehle, M., Trautwein, C. and Birchmeier, C. (2004) 'Met provides essential signals for liver regeneration', *Proceedings of the National Academy of Sciences of the United States of America*, 101(29), pp. 10608-10613.

Bosco, M.C., Puppo, M., Blengio, F., Fraone, T., Cappello, P., Giovarelli, M. and Varesio, L. (2008) 'Monocytes and dendritic cells in a hypoxic environment: Spotlights on chemotaxis and migration', *Immunobiology*, 213(9), pp. 733-749.

Bottaro, D.P., Rubin, J.S., Faletto, D.L., Chan, A.M., Kmiecik, T.E., Vande Woude, G.F. and Aaronson, S.A. (1991) 'Identification of the hepatocyte growth factor receptor as the c-met proto-oncogene product', *Science*, 251(4995), pp. 802-804.

Bouameur, J.-E., Favre, B., Fontao, L., Lingasamy, P., Begré, N. and Borradori, L. (2014) 'Interaction of Plectin with Keratins 5 and 14: Dependence on Several Plectin Domains and Keratin Quaternary Structure', *Journal of Investigative Dermatology*, 134(11), pp. 2776-2783.

Bourin, P., Bunnell, B.A., Casteilla, L., Dominici, M., Katz, A.J., March, K.L., Redl, H., Rubin, J.P., Yoshimura, K. and Gimble, J.M. (2013) 'Stromal cells from the adipose tissue-derived stromal vascular fraction and culture expanded adipose tissue-derived stromal/stem cells: a joint statement of the International Federation for Adipose Therapeutics (IFATS) and Science and the International Society for Cellular Therapy (ISCT)', *Cytotherapy*, 15(6), pp. 641-648.

Boyden, S. (1962) 'THE CHEMOTACTIC EFFECT OF MIXTURES OF ANTIBODY AND ANTIGEN ON POLYMORPHONUCLEAR LEUCOCYTES', *The Journal of Experimental Medicine*, 115(3), pp. 453-466.

Breslin, S. and O'Driscoll, L. (2013) 'Three-dimensional cell culture: the missing link in drug discovery', *Drug Discovery Today*, 18(5), pp. 240-249.

Brighton, C.T. and Hunt, R.M. (1991) 'Early histological and ultrastructural changes in medullary fracture callus', *J Bone Joint Surg Am*, 73(6), pp. 832-47.

Bruder, S.P., Ricalton, N.S., Boynton, R.E., Connolly, T.J., Jaiswal, N., Zaia, J. and Barry, F.P. (1998) 'Mesenchymal stem cell surface antigen SB-10 corresponds to activated leukocyte cell adhesion molecule and is involved in osteogenic differentiation', *J Bone Miner Res*, 13(4), pp. 655-63.

Buchanan, E.P., Longaker, M.T. and Lorenz, H.P. (2009) 'Fetal skin wound healing', *Adv Clin Chem*, 48, pp. 137-61.

Bussolati, B., Bruno, S., Grange, C., Buttiglieri, S., Deregibus, M.C., Cantino, D. and Camussi, G. (2005) 'Isolation of renal progenitor cells from adult human kidney', *Am J Pathol*, 166(2), pp. 545-55.

Butcher, M. (2013) 'Assessment, management and prevention of infected wounds', *British Journal of Community Nursing*, 27(4), pp. 25-30.

Caley, M.P., Martins, V.L.C. and O'Toole, E.A. (2015) 'Metalloproteinases and Wound Healing', *Advances in Wound Care*, 4(4), pp. 225-234.

Campeau, L., Ding, J. and Tredget, E. (2015) 'A potential role of SDF-1/CXCR4 chemotactic pathway in wound healing and hypertrophic scar formation', *Receptors & Clinical Investigation*, 2(3).

Cannon, C.L., Neal, P.J., Southee, J.A., Kubilus, J. and Klausner, M. (1994) 'New epidermal model for dermal irritancy testing', *Toxicology in Vitro*, 8(4), pp. 889-891.

Cao, C. and Dong, Y. (2005) '[Study on culture and in vitro osteogenesis of blood-derived human mesenchymal stem cells]', *Zhongguo Xiu Fu Chong Jian Wai Ke Za Zhi*, 19(8), pp. 642-7.

Cao, W., Jin, H., Zhang, L., Chen, X. and Qian, H. (2017) 'Identification of miR-601 as a novel regulator in the development of pancreatic cancer', *Biochemical and Biophysical Research Communications*, 483(1), pp. 638-644.

Caplan, A.I. (1994) 'The mesengenic process', *Clin Plast Surg*, 21(3), pp. 429-35.

Caplan, A.I. (2009) 'Why are MSCs therapeutic? New data: new insight', *J Pathol*, 217(2), pp. 318-24.

Caplan, A.I. and Dennis, J.E. (2006) 'Mesenchymal stem cells as trophic mediators', *J Cell Biochem*, 98(5), pp. 1076-84.

Carlson, M.W., Alt-Holland, A., Egles, C. and Garlick, J.A. (2008) 'Three-Dimensional Tissue Models of Normal and Diseased Skin', *Current protocols in cell biology / editorial board, Juan S. Bonifacino ... [et al.]*, CHAPTER, pp. Unit-19.9.

Carpenter, R.R., Barsales, P.B. and Ganchan, R.P. (1968) 'Antigen-induced inhibition of cell migration in agar gel, plasma clot, and liquid media', *J Reticuloendothel Soc*, 5(5), pp. 472-83.

Carter, R.A. and Wicks, I.P. (2001) 'Vascular cell adhesion molecule 1 (CD106): a multifaceted regulator of joint inflammation', *Arthritis Rheum*, 44(5), pp. 985-94.

Cascio, S., D'Andrea, A., Ferla, R., Surmacz, E., Gulotta, E., Amodeo, V., Bazan, V., Gebbia, N. and Russo, A. (2010) 'miR-20b modulates VEGF expression by targeting HIF-1 alpha and STAT3 in MCF-7 breast cancer cells', *J Cell Physiol*, 224(1), pp. 242-9.

Castilla, D.M., Liu, Z.-J. and Velazquez, O.C. (2012) 'Oxygen: Implications for Wound Healing', *Advances in Wound Care*, 1(6), pp. 225-230.

Chamberlain, G., Fox, J., Ashton, B. and Middleton, J. (2007) 'Concise review: mesenchymal stem cells: their phenotype, differentiation capacity, immunological features, and potential for homing', *Stem Cells*, 25(11), pp. 2739-49.

Chan, Y.C., Khanna, S., Roy, S. and Sen, C.K. (2011) 'miR-200b Targets Ets-1 and Is Down-regulated by Hypoxia to Induce Angiogenic Response of Endothelial Cells', *The Journal of Biological Chemistry*, 286(3), pp. 2047-2056.

Chavez, M.G., Buhr, C.A., Petrie, W.K., Wandinger-Ness, A., Kusewitt, D.F. and Hudson, L.G. (2012) 'Differential Downregulation of E-Cadherin and Desmoglein by Epidermal Growth Factor', *Dermatology Research and Practice*, 2012, p. 309587.

Chen, D., Hao, H., Tong, C., Liu, J., Dong, L., Ti, D., Hou, Q., Liu, H., Han, W. and Fu, X. (2015) 'Transdifferentiation of Umbilical Cord–Derived Mesenchymal Stem Cells Into Epidermal-Like Cells by the Mimicking Skin Microenvironment', *The International Journal of Lower Extremity Wounds*.

Chen, F.H. and Tuan, R.S. (2008) 'Mesenchymal stem cells in arthritic diseases', *Arthritis Research & Therapy*, 10(5), pp. 223-223.

Chen, J.-C., Lin, B.-B., Hu, H.-W., Lin, C., Jin, W.-Y., Zhang, F.-B., Zhu, Y.-A., Lu, C.-J., Wei, X.-J. and Chen, R.-J. (2014) 'NGF Accelerates Cutaneous Wound Healing by Promoting the Migration of Dermal Fibroblasts via the PI3K/Akt-Rac1-JNK and ERK Pathways', *BioMed Research International*, 2014, p. 547187.

Chen, L., Tredget, E.E., Liu, C. and Wu, Y. (2009) 'Analysis of allogenicity of mesenchymal stem cells in engraftment and wound healing in mice', *Plos One*, 4(9), p. e7119.

Chen, L., Tredget, E.E., Wu, P.Y.G. and Wu, Y. (2008) 'Paracrine Factors of Mesenchymal Stem Cells Recruit Macrophages and Endothelial Lineage Cells and Enhance Wound Healing', *Plos One*, 3(4), p. e1886.

Chen, M., Guan, M., Li, J., Wang, H. and Yang, B. (2012) 'Effects of hepatocyte growth factor on wound healing of rabbit maxillary sinus mucosa', *J Otolaryngol Head Neck Surg*, 41(4), pp. 253-8.

Cheng, F., Shen, Y., Mohanasundaram, P., Lindström, M., Ivaska, J., Ny, T. and Eriksson, J.E. (2016) 'Vimentin coordinates fibroblast proliferation and keratinocyte differentiation in wound healing via TGF-β–Slug signaling', *Proceedings of the National Academy of Sciences of the United States of America*, 113(30), pp. E4320-E4327.

Cheng, J., Yu, H., Deng, S. and Shen, G. (2010) 'MicroRNA Profiling in Mid- and Late-Gestational Fetal Skin: Implication for Scarless Wound Healing', *The Tohoku Journal of Experimental Medicine*, 221(3), pp. 203-209.

Cherla, R.P. and Ganju, R.K. (2001) 'Stromal Cell-Derived Factor 1α-Induced Chemotaxis in T Cells Is Mediated by Nitric Oxide Signaling Pathways', *The Journal of Immunology*, 166(5), pp. 3067-3074.

Chigurupati, S., Arumugam, T.V., Son, T.G., Lathia, J.D., Jameel, S., Mughal, M.R., Tang, S.-C., Jo, D.-G., Camandola, S., Giunta, M., Rakova, I., McDonnell, N., Miele, L., Mattson, M.P. and Poosala, S. (2007) 'Involvement of Notch Signaling in Wound Healing', *PLoS ONE*, 2(11), p. e1167.

Chmielowiec, J., Borowiak, M., Morkel, M., Stradal, T., Munz, B., Werner, S., Wehland, J., Birchmeier, C. and Birchmeier, W. (2007) 'c-Met is essential for wound healing in the skin', *The Journal of Cell Biology*, 177(1), pp. 151-162.

Cho, Y.-S., Bae, J.-M., Chun, Y.-S., Chung, J.-H., Jeon, Y.-K., Kim, I.-S., Kim, M.-S. and Park, J.-W. (2008) 'HIF-1α controls keratinocyte proliferation by up-regulating p21(WAF1/Cip1)', *Biochimica et Biophysica Acta (BBA) - Molecular Cell Research*, 1783(2), pp. 323-333.

Chong, P.P., Selvaratnam, L., Abbas, A.A. and Kamarul, T. (2012) 'Human peripheral blood derived mesenchymal stem cells demonstrate similar characteristics and chondrogenic differentiation potential to bone marrow derived mesenchymal stem cells', *J Orthop Res*, 30(4), pp. 634-42.

Chu, D.H. (2008) 'Overview of biology, development, and structure of skin', *Fitzpatrick's dermatology in general medicine* In K. Wolff, L.A. Goldsmith, S.I. Katz, B.A. Gilchrest, A.S. Paller, & D.J. Leffell (Eds.)(New York: McGraw-Hill.), pp. 7th ed., pp. 57–73.

Chu, P.G. and Weiss, L.M. (2002) 'Keratin expression in human tissues and neoplasms', *Histopathology*, 40(5), pp. 403-439.

Clark, R.A.F. (1996) *The molecular and cellular biology of wound repair*. New York: Plenum Press.

Cook, L. and Ousey, K. (2011) 'Demystifying wound infection: identification and management', *Practice Nursing*, 22(8), pp. 424-428.

Corcione, A., Benvenuto, F., Ferretti, E., Giunti, D., Cappiello, V., Cazzanti, F., Risso, M., Gualandi, F., Mancardi, G.L., Pistoia, V. and Uccelli, A. (2006) 'Human mesenchymal stem cells modulate B-cell functions', *Blood*, 107(1), pp. 367-72.

Côté, M., Miller, A.D. and Liu, S.-L. (2007) 'Human RON receptor tyrosine kinase induces complete epithelial-to-mesenchymal transition but causes cellular senescence', *Biochemical and Biophysical Research Communications*, 360(1), pp. 219-225.

Coulombe, P.A. and Omary, M.B. (2002) ''Hard' and 'soft' principles defining the structure, function and regulation of keratin intermediate filaments', *Current Opinion in Cell Biology*, 14(1), pp. 110-122.

Cowin, A.J., Kallincos, N., Hatzirodos, N., Robertson, J.G., Pickering, K.J., Couper, J. and Belford, D.A. (2001) 'Hepatocyte growth factor and macrophage-stimulating protein are upregulated during excisional wound repair in rats', *Cell Tissue Res*, 306(2), pp. 239-50.

Cristancho, A.G. and Lazar, M.A. (2011) 'Forming functional fat: a growing understanding of adipocyte differentiation', *Nature Reviews Molecular Cell Biology*, 12, p. 722.

Crouch, S.P.M., Kozlowski, R., Slater, K.J. and Fletcher, J. (1993) 'The use of ATP bioluminescence as a measure of cell proliferation and cytotoxicity', *Journal of Immunological Methods*, 160(1), pp. 81-88.

da Silva, E.Z.M., Jamur, M.C. and Oliver, C. (2014) 'Mast Cell Function: A New Vision of an Old Cell', *Journal of Histochemistry and Cytochemistry*, 62(10), pp. 698-738.

da Silva Meirelles, L., Sand, T.T., Harman, R.J., Lennon, D.P. and Caplan, A.I. (2009) 'MSC frequency correlates with blood vessel density in equine adipose tissue', *Tissue Eng Part A*, 15(2), pp. 221-9.

Dan, Y.Y., Riehle, K.J., Lazaro, C., Teoh, N., Haque, J., Campbell, J.S. and Fausto, N. (2006) 'Isolation of multipotent progenitor cells from human fetal liver capable of differentiating into liver and mesenchymal lineages', *Proc Natl Acad Sci U S A*, 103(26), pp. 9912-7.

Danjo, Y. and Gipson, I.K. (2002) 'Specific Transduction of the Leading Edge Cells of Migrating Epithelia Demonstrates That They are Replaced During Healing', *Experimental Eye Research*, 74(2), pp. 199-204.

Darby, I.A., Laverdet, B., Bonté, F. and Desmoulière, A. (2014) 'Fibroblasts and myofibroblasts in wound healing', *Clinical, Cosmetic and Investigational Dermatology*, 7, pp. 301-311.

Dasu, M.R. and Rivkah Isseroff, R. (2012) 'Toll-Like Receptors in Wound Healing: Location, Accessibility, and Timing', *Journal of Investigative Dermatology*, 132(8), pp. 1955-1958.

De Donatis, A., Comito, G., Buricchi, F., Vinci, M.C., Parenti, A., Caselli, A., Camici, G., Manao, G., Ramponi, G. and Cirri, P. (2008) 'Proliferation Versus Migration in Platelet-derived Growth Factor Signaling: THE KEY ROLE OF ENDOCYTOSIS', *Journal of Biological Chemistry*, 283(29), pp. 19948-19956.

Deans, R.J. and Moseley, A.B. (2000) 'Mesenchymal stem cells: biology and potential clinical uses', *Exp Hematol*, 28(8), pp. 875-84.

Dews, M., Homayouni, A., Yu, D., Murphy, D., Sevignani, C., Wentzel, E., Furth, E.E., Lee, W.M., Enders, G.H., Mendell, J.T. and Thomas-Tikhonenko, A. (2006) 'Augmentation of tumor angiogenesis by a Myc-activated microRNA cluster', *Nature genetics*, 38(9), pp. 1060-1065.

Di, K., Linskey, M.E. and Bota, D.A. (2013) 'TRIM11 is over-expressed in high-grade gliomas and promotes proliferation, invasion, migration and glial tumor growth', *Oncogene*, 32(42), pp. 5038-5047.

Diaz-Prado, S., Muinos-Lopez, E., Hermida-Gomez, T., Rendal-Vazquez, M.E., Fuentes-Boquete, I., de Toro, F.J. and Blanco, F.J. (2010) 'Multilineage differentiation potential of cells isolated from the human amniotic membrane', *J Cell Biochem*, 111(4), pp. 846-57.

Diegelmann, R.F. and Evans, M.C. (2004) 'Wound healing: an overview of acute, fibrotic and delayed healing', *Front Biosci*, 9, pp. 283-9.

Dietrich, S., Abou-Rebyeh, F., Brohmann, H., Bladt, F., Sonnenberg-Riethmacher, E., Yamaai, T., Lumsden, A., Brand-Saberi, B. and Birchmeier, C. (1999) 'The role of SF/HGF and c-Met in the development of skeletal muscle', *Development*, 126(8), pp. 1621-1629.

Digirolamo, C.M., Stokes, D., Colter, D., Phinney, D.G., Class, R. and Prockop, D.J. (1999) 'Propagation and senescence of human marrow stromal cells in culture: a simple colony-forming assay identifies samples with the greatest potential to propagate and differentiate', *Br J Haematol*, 107(2), pp. 275-81.

DiMasi, J.A. and Grabowski, H.G. (2007) 'Economics of New Oncology Drug Development', *Journal of Clinical Oncology*, 25(2), pp. 209-216.

Ding, H., Wu, X., Bostrom, H., Kim, I., Wong, N., Tsoi, B., O'Rourke, M., Koh, G.Y., Soriano, P., Betsholtz, C., Hart, T.C., Marazita, M.L., Field, L.L., Tam, P.P.L. and Nagy, A. (2004) 'A specific requirement for PDGF-C in palate formation and PDGFR-[alpha] signaling', *Nat Genet*, 36(10), pp. 1111-1116.

Ding, J., Hori, K., Zhang, R., Marcoux, Y., Honardoust, D., Shankowsky, H.A. and Tredget, E.E. (2011) 'Stromal cell-derived factor 1 (SDF-1) and its receptor CXCR4 in the formation of postburn hypertrophic scar (HTS)', *Wound Repair and Regeneration*, 19(5), pp. 568-578.

Djouad, F., Charbonnier, L.M., Bouffi, C., Louis-Plence, P., Bony, C., Apparailly, F., Cantos, C., Jorgensen, C. and Noel, D. (2007) 'Mesenchymal stem cells inhibit the differentiation of dendritic cells through an interleukin-6-dependent mechanism', *Stem Cells*, 25(8), pp. 2025-32.

Doehn, U., Hauge, C., Frank, S.R., Jensen, C.J., Duda, K., Nielsen, J.V., Cohen, M.S., Johansen, J.V., Winther, B.R., Lund, L.R., Winther, O., Taunton, J., Hansen, S.H. and Frödin, M. (2009) 'RSK Is a Principal Effector of the RAS-ERK Pathway for Eliciting a Coordinate Promotile/Invasive Gene Program and Phenotype in Epithelial Cells', *Molecular Cell*, 35(4), pp. 511-522.

Dominici, M., Le Blanc, K., Mueller, I., Slaper-Cortenbach, I., Marini, F., Krause, D., Deans, R., Keating, A., Prockop, D. and Horwitz, E. (2006) 'Minimal criteria for defining multipotent mesenchymal stromal cells. The International Society for Cellular Therapy position statement', *Cytotherapy*, 8(4), pp. 315-7.

Drew, P., Posnett, J. and Rusling, L. (2007) 'The cost of wound care for a local population in England', *Int Wound J*, 4(2), pp. 149-55.

Dry, H., Jorgenson, K., Ando, W., Hart, D.A., Frank, C.B. and Sen, A. (2013) 'Effect of calcium on the proliferation kinetics of synovium-derived mesenchymal stromal cells', *Cytotherapy*, 15(7), pp. 805-819.

Dvorak, H.F. (2002) 'Vascular Permeability Factor/Vascular Endothelial Growth Factor: A Critical Cytokine in Tumor Angiogenesis and a Potential Target for Diagnosis and Therapy', *Journal of Clinical Oncology*, 20(21), pp. 4368-4380.

Edmondson, R., Broglie, J.J., Adcock, A.F. and Yang, L. (2014) 'Three-Dimensional Cell Culture Systems and Their Applications in Drug Discovery and Cell-Based Biosensors', *Assay and Drug Development Technologies*, 12(4), pp. 207-218.

Eichler, M.J. and Carlson, M.A. (2006) 'Modeling dermal granulation tissue with the linear fibroblast-populated collagen matrix: A comparison with the round matrix model', *Journal of Dermatological Science*, 41(2), pp. 97-108.

Eming, S.A., Krieg, T. and Davidson, J.M. (2007a) 'Inflammation in Wound Repair: Molecular and Cellular Mechanisms', *Journal of Investigative Dermatology*, 127(3), pp. 514-525.

Eming, S.A., Werner, S., Bugnon, P., Wickenhauser, C., Siewe, L., Utermöhlen, O., Davidson, J.M., Krieg, T. and Roers, A. (2007b) 'Accelerated Wound Closure in Mice Deficient for Interleukin-10', *The American Journal of Pathology*, 170(1), pp. 188-202.

Erickson, H.P. (1993) 'Tenascin-C, tenascin-R and tenascin-X: a family of talented proteins in search of functions', *Current Opinion in Cell Biology*, 5(5), pp. 869-876.

Estes, B.T., Wu, A.W. and Guilak, F. (2006) 'Potent induction of chondrocytic differentiation of human adipose-derived adult stem cells by bone morphogenetic protein 6', *Arthritis Rheum*, 54(4), pp. 1222-32.

Evans, N.D., Oreffo, R.O.C., Healy, E., Thurner, P.J. and Man, Y.H. (2013) 'Epithelial mechanobiology, skin wound healing, and the stem cell niche', *Journal of the Mechanical Behavior of Biomedical Materials*, 28, pp. 397-409.

Eyden, B. (2005) 'The myofibroblast: a study of normal, reactive and neoplastic tissues, with an emphasis on ultrastructure. part 2 - tumours and tumour-like lesions', *J Submicrosc Cytol Pathol*, 37(3-4), pp. 231-96.

Fackler, O.T. and Grosse, R. (2008) 'Cell motility through plasma membrane blebbing', *The Journal of Cell Biology*, 181(6), pp. 879-884.

Feoktistov, I., Biaggioni, I. and Cronstein, B.N. (2009) 'Adenosine Receptors in Wound Healing, Fibrosis and Angiogenesis', *Handbook of experimental pharmacology*, (193), pp. 383-397.

Feres, K.J., Ischenko, I. and Hayman, M.J. (2008) 'The RON receptor tyrosine kinase promotes MSP-independent cell spreading and survival in breast epithelial cells', *Oncogene*, 28(2), pp. 279-288.

Fernandes, S., Iyer, S. and Kerr, W.G. (2013) 'Role of SHIP1 in cancer and mucosal inflammation', *Annals of the New York Academy of Sciences*, 1280(1), pp. 6-10.

Ferraq, Y., Black, D.R., Theunis, J. and Mordon, S. (2012) 'Superficial wounding model for epidermal barrier repair studies: Comparison of erbium:YAG laser and the suction blister method', *Lasers in Surgery and Medicine*, 44(7), pp. 525-532.

Ferrari, G., Cusella–, G., Angelis, D., Coletta, M., Paolucci, E., Stornaiuolo, A., Cossu, G. and Mavilio, F. (1998) 'Muscle Regeneration by Bone Marrow-Derived Myogenic Progenitors', *Science*, 279(5356), pp. 1528-1530.

Ferrini, M.G., Vernet, D., Magee, T.R., Shahed, A., Qian, A., Rajfer, J. and Gonzalez-Cadavid, N.F. (2002) 'Antifibrotic role of inducible nitric oxide synthase', *Nitric Oxide*, 6(3), pp. 283-94.

Fischer, E.G., Stingl, A. and James Kirkpatrick, C. (1990) 'Migration assay for endothelial cells in multiwells', *Journal of Immunological Methods*, 128(2), pp. 235-239.

Fish, J.E., Santoro, M.M., Morton, S.U., Yu, S., Yeh, R.-F., Wythe, J.D., Bruneau, B.G., Stainier, D.Y.R. and Srivastava, D. (2008) 'miR-126 regulates angiogenic signaling and vascular integrity', *Developmental cell*, 15(2), pp. 272-284.

Fish, R.J. and Neerman-Arbez, M. (2012) 'Fibrinogen gene regulation', *Thrombosis and Haemostasis*, 108(9), pp. 419-426.

Florin, L., Hummerich, L., Dittrich, B.T., Kokocinski, F., Wrobel, G., Gack, S., Schorpp-Kistner, M., Werner, S., Hahn, M., Lichter, P., Szabowski, A. and Angel, P. (2004) 'Identification of novel AP-1 target genes in fibroblasts regulated during cutaneous wound healing', *Oncogene*, 23(42), pp. 7005-7017.

Fong, E., Tzlil, S. and Tirrell, D.A. (2010) 'Boundary crossing in epithelial wound healing', *Proceedings of the National Academy of Sciences of the United States of America*, 107(45), pp. 19302-19307.

Foraker, J.E., Oh, J.Y., Ylostalo, J.H., Lee, R.H., Watanabe, J. and Prockop, D.J. (2011) 'Cross-talk between human mesenchymal stem/progenitor cells (MSCs) and rat hippocampal slices in LPS-stimulated cocultures: the MSCs are activated to secrete prostaglandin E2', *J Neurochem*, 119(5), pp. 1052-63.

Franks, P.J. and Morgan, P.A. (2003) 'Health-related quality of life with chronic leg ulceration', *Expert Rev Pharmacoecon Outcomes Res*, 3(5), pp. 611-22.

Friedl, P. and Gilmour, D. (2009) 'Collective cell migration in morphogenesis, regeneration and cancer', *Nat Rev Mol Cell Biol*, 10(7), pp. 445-457.

Friedl, P., Hegerfeldt, Y. and Tusch, M. (2004) 'Collective cell migration in morphogenesis and cancer', *Int J Dev Biol*, 48(5-6), pp. 441-9.

Fu, X. and Li, H. (2009) 'Mesenchymal stem cells and skin wound repair and regeneration: possibilities and questions', *Cell Tissue Res*, 335(2), pp. 317-21.

Fuchs, E. (2008) 'Skin stem cells: rising to the surface', *The Journal of Cell Biology*, 180(2), pp. 273-284.

Fukuda, K. (2002) 'Molecular characterization of regenerated cardiomyocytes derived from adult mesenchymal stem cells', *Congenital Anomalies*, 42(1), pp. 1-9.

Gabbay, J.S., Heller, J.B., Mitchell, S.A., Zuk, P.A., Spoon, D.B., Wasson, K.L., Jarrahy, R., Benhaim, P. and Bradley, J.P. (2006) 'Osteogenic potentiation of human adipose-derived stem cells in a 3-dimensional matrix', *Ann Plast Surg*, 57(1), pp. 89-93.

Gang, E.J., Bosnakovski, D., Figueiredo, C.A., Visser, J.W. and Perlingeiro, R.C. (2007) 'SSEA-4 identifies mesenchymal stem cells from bone marrow', *Blood*, 109(4), pp. 1743-51.

Gangatirkar, P., Paquet-Fifield, S., Li, A., Rossi, R. and Kaur, P. (2007) 'Establishment of 3D organotypic cultures using human neonatal epidermal cells', *Nature Protocols*, 2, p. 178.

Garlick, J.A. (2007) 'Engineering Skin to Study Human Disease – Tissue Models for Cancer Biology and Wound Repair', in Lee, K. and Kaplan, D. (eds.) *Tissue Engineering II: Basics of Tissue Engineering and Tissue Applications*. Berlin, Heidelberg: Springer Berlin Heidelberg, pp. 207-239.

Gartside, M.G., Chen, H., Ibrahimi, O.A., Byron, S.A., Curtis, A.V. and Wellens, C.L. (2009) 'Loss-of-function fibroblast growth factor receptor-2 mutations in melanoma', *Mol Cancer Res.*, 7.

Gehring, W.J. (1993) 'Exploring the homeobox', *Gene*, 135(1), pp. 215-221.

Gerharz, M., Baranowsky, A., Siebolts, U., Eming, S., Nischt, R., Krieg, T. and Wickenhauser, C. (2007) 'Morphometric analysis of murine skin wound healing: Standardization of experimental procedures and impact of an advanced multitissue array technique', *Wound Repair and Regeneration*, 15(1), pp. 105-112.

Giles, N., Rea, S., Beer, T., Wood, F.M. and Fear, M.W. (2008) 'A peptide inhibitor of c-Jun promotes wound healing in a mouse full-thickness burn model', *Wound Repair and Regeneration*, 16(1), pp. 58-64.

Gillitzer, R. and Goebeler, M. (2001) 'Chemokines in cutaneous wound healing', *Journal of Leukocyte Biology*, 69(4), pp. 513-521.

Gimble, J.M., Guilak, F., Nuttall, M.E., Sathishkumar, S., Vidal, M. and Bunnell, B.A. (2008) 'In vitro Differentiation Potential of Mesenchymal Stem Cells', *Transfus Med Hemother*, 35(3), pp. 228-238.

Gnecchi, M., Zhang, Z., Ni, A. and Dzau, V.J. (2008) 'Paracrine mechanisms in adult stem cell signaling and therapy', *Circ Res*, 103(11), pp. 1204-19.

Goldberg, A., Mitchell, K., Soans, J., Kim, L. and Zaidi, R. (2017) 'The use of mesenchymal stem cells for cartilage repair and regeneration: a systematic review', *Journal of Orthopaedic Surgery and Research*, 12, p. 39.

Goumans, M.-J., Liu, Z. and ten Dijke, P. (2009) 'TGF-[beta] signaling in vascular biology and dysfunction', *Cell Res*, 19(1), pp. 116-127.

Gratzner, H.G. (1982) 'Monoclonal antibody to 5-bromo- and 5-iododeoxyuridine: A new reagent for detection of DNA replication', *Science*, 218(4571), p. 474.

Greco, S.J., Liu, K. and Rameshwar, P. (2007) 'Functional similarities among genes regulated by OCT4 in human mesenchymal and embryonic stem cells', *Stem Cells*, 25(12), pp. 3143-54.

Greenhalgh, D.G. (1998) 'The role of apoptosis in wound healing', *The International Journal of Biochemistry & Cell Biology*, 30(9), pp. 1019-1030.

Gregory, C.A., Prockop, D.J. and Spees, J.L. (2005) 'Non-hematopoietic bone marrow stem cells: molecular control of expansion and differentiation', *Exp Cell Res*, 306(2), pp. 330-5.

Grellner, W. (2002) 'Time-dependent immunohistochemical detection of proinflammatory cytokines (IL-1beta, IL-6, TNF-alpha) in human skin wounds', *Forensic Sci Int*, 130(2-3), pp. 90-6.

Griffiths, M.J., Bonnet, D. and Janes, S.M. (2005) 'Stem cells of the alveolar epithelium', *Lancet*, 366(9481), pp. 249-60.

Gronthos, S., Zannettino, A.C., Hay, S.J., Shi, S., Graves, S.E., Kortesidis, A. and Simmons, P.J. (2003) 'Molecular and cellular characterisation of highly purified stromal stem cells derived from human bone marrow', *J Cell Sci*, 116(Pt 9), pp. 1827-35.

Grote, K., Schütt, H. and Schieffer, B. (2011) 'Toll-Like Receptors in Angiogenesis', *TheScientificWorldJOURNAL*, 11.

Guerrero-Esteo, M., Sánchez-Elsner, T., Letamendia, A. and Bernabéu, C. (2002) 'Extracellular and Cytoplasmic Domains of Endoglin Interact with the Transforming Growth Factor-β Receptors I and II', *Journal of Biological Chemistry*, 277(32), pp. 29197-29209.

Guest, J.F., Ayoub, N., McIlwraith, T., Uchegbu, I., Gerrish, A., Weidlich, D., Vowden, K. and Vowden, P. (2015) 'Health economic burden that wounds impose on the National Health Service in the UK', *BMJ Open*, 5(12).

Guo, C., Chen, L.H., Huang, Y., Chang, C.-C., Wang, P., Pirozzi, C.J., Qin, X., Bao, X., Greer, P.K., McLendon, R.E., Yan, H., Keir, S.T., Bigner, D.D. and He, Y. (2013a) 'KMT2D maintains neoplastic cell proliferation and global histone H3 lysine 4 monomethylation', *Oncotarget*, 4(11), pp. 2144-2153.

Guo, J., Lin, Q., Shao, Y., Rong, L. and Zhang, D. (2017) 'BMP-7 suppresses excessive scar formation by activating the BMP-7/Smad1/5/8 signaling pathway', *Molecular Medicine Reports*, 16(2), pp. 1957-1963.

Guo, R., Chai, L., Chen, L., Chen, W., Ge, L., Li, X., Li, H., Li, S. and Cao, C. (2015) 'Stromal cell-derived factor 1 (SDF-1) accelerated skin wound healing by promoting the migration and proliferation of epidermal stem cells', *In Vitro Cellular & Developmental Biology - Animal*, 51(6), pp. 578-585.

Guo, S. and DiPietro, L.A. (2010) 'Critical Review in Oral Biology & Medicine: Factors Affecting Wound Healing', *Journal of Dental Research*, 89(3), pp. 219-229.

Guo, Z., Higgins, C.A., Gillette, B.M., Itoh, M., Umegaki, N., Gledhill, K., Sia, S.K. and Christiano, A.M. (2013b) 'Building a microphysiological skin model from induced pluripotent stem cells', *Stem Cell Res Ther*, 4 Suppl 1, p. S2.

Guweidhi, A., Kleeff, J., Adwan, H., Giese, N.A., Wente, M.N., Giese, T., Büchler, M.W., Berger, M.R. and Friess, H. (2005) 'Osteonectin Influences Growth and Invasion of Pancreatic Cancer Cells', *Annals of Surgery*, 242(2), pp. 224-234.

Ha, M. and Kim, V.N. (2014) 'Regulation of microRNA biogenesis', *Nat Rev Mol Cell Biol*, 15(8), pp. 509-524.

Han, Y.-C., Zheng, Z.-L., Zuo, Z.-H., Yu, Y.P., Chen, R., Tseng, G.C., Nelson, J.B. and Luo, J.-H. (2013) 'Metallothionein 1 h tumour suppressor activity in prostate cancer is mediated by euchromatin methyltransferase 1', *The Journal of pathology*, 230(2), pp. 184-193.

Hass, R., Kasper, C., Bohm, S. and Jacobs, R. (2011) 'Different populations and sources of human mesenchymal stem cells (MSC): A comparison of adult and neonatal tissue-derived MSC', *Cell Commun Signal*, 9, p. 12.

Hatziapostolou, M., Polytarchou, C., Aggelidou, E., Drakaki, A., Poultsides, G.A., Jaeger, S.A., Ogata, H., Karin, M., Struhl, K., Hadzopoulou-Cladaras, M. and Iliopoulos, D. (2011) 'An HNF4α-miRNA Inflammatory Feedback Circuit regulates Hepatocellular Oncogenesis', *Cell*, 147(6), pp. 1233-1247.

Haynesworth, S.E., Baber, M.A. and Caplan, A.I. (1992) 'Cell surface antigens on human marrow-derived mesenchymal cells are detected by monoclonal antibodies', *Bone*, 13(1), pp. 69-80.

Heldin, C.-H., Landström, M. and Moustakas, A. (2009) 'Mechanism of TGF-β signaling to growth arrest, apoptosis, and epithelial–mesenchymal transition', *Current Opinion in Cell Biology*, 21(2), pp. 166-176.

Heldin, C.-H. and Westermark, B. (1999) 'Mechanism of Action and In Vivo Role of Platelet-Derived Growth Factor', *Physiological Reviews*, 79(4), pp. 1283-1316.

Heldin, C.H., Bäckström, G., Ostman, A., Hammacher, A., Rönnstrand, L., Rubin, K., Nistér, M. and Westermark, B. (1988) 'Binding of different dimeric forms of PDGF to human fibroblasts: evidence for two separate receptor types', *The EMBO Journal*, 7(5), pp. 1387-1393.

Hennings, H., Michael, D., Cheng, C., Steinert, P., Holbrook, K. and Yuspa, S.H. (1980) 'Calcium regulation of growth and differentiation of mouse epidermal cells in culture', *Cell*, 19(1), pp. 245-254.

Hildebrand, J., Grundhoff, A., Gallinat, S., Wenck, H. and Knott, A. (2012) 'MicroRNA Profiling During Human Keratinocyte Differentiation Using a Quantitative Real-Time PCR Method #', in *T Molecular Dermatology*. pp. 193-200.

Hildebrand, J., Rutze, M., Walz, N., Gallinat, S., Wenck, H., Deppert, W., Grundhoff, A. and Knott, A. (2011) 'A Comprehensive Analysis of MicroRNA Expression During Human Keratinocyte Differentiation In Vitro and In Vivo', *J Invest Dermatol*, 131(1), pp. 20-29.

Hill, D.S., Robinson, N.D.P., Caley, M.P., Chen, M., O'Toole, E.A., Armstrong, J.L., Przyborski, S. and Lovat, P.E. (2015) 'A Novel Fully Humanized 3D Skin Equivalent to Model Early Melanoma Invasion', *Molecular Cancer Therapeutics*.

Hinz, B. (2006) 'Masters and servants of the force: The role of matrix adhesions in myofibroblast force perception and transmission', *European Journal of Cell Biology*, 85(3–4), pp. 175-181.

Hinz, B. and Gabbiani, G. (2003) 'Cell-matrix and cell-cell contacts of myofibroblasts: role in connective tissue remodeling', *Thrombosis and Haemostasis*, 90(12), pp. 993-1002.

Hocking, A.M. (2012) 'Mesenchymal Stem Cell Therapy for Cutaneous Wounds', *Adv Wound Care (New Rochelle)*, 1(4), pp. 166-171.

Hocking, A.M. and Gibran, N.S. (2010) 'Mesenchymal stem cells: paracrine signaling and differentiation during cutaneous wound repair', *Exp Cell Res*, 316(14), pp. 2213-9.

Hoffman, J.M., Baritaki, S., Ruiz, J.J., Sideri, A. and Pothoulakis, C. (2016) 'Corticotropin-Releasing Hormone Receptor 2 Signaling Promotes Mucosal Repair Responses after Colitis', *The American Journal of Pathology*, 186(1), pp. 134-144.

Honczarenko, M., Le, Y., Swierkowski, M., Ghiran, I., Glodek, A.M. and Silberstein, L.E. (2006) 'Human bone marrow stromal cells express a distinct set of biologically functional chemokine receptors', *Stem Cells*, 24(4), pp. 1030-41.

Hoogduijn, M.J. and Dor, F.J.M.F. (2013) 'Mesenchymal stem cells: are we ready for clinical application in Transplantation and Tissue Regeneration?', *Frontiers in Immunology*, 4.

Hopkins, A.L. (2008) 'Network pharmacology: the next paradigm in drug discovery', *Nat Chem Biol*, 4(11), pp. 682-690.

Hsiao, S.T., Asgari, A., Lokmic, Z., Sinclair, R., Dusting, G.J., Lim, S.Y. and Dilley, R.J. (2012) 'Comparative analysis of paracrine factor expression in human adult mesenchymal stem cells derived from bone marrow, adipose, and dermal tissue', *Stem Cells Dev*, 21(12), pp. 2189-203.

Hu, C., Yong, X., Li, C., Lü, M., Liu, D., Chen, L., Hu, J., Teng, M., Zhang, D., Fan, Y. and Liang, G. (2013) 'CXCL12/CXCR4 axis promotes mesenchymal stem cell mobilization to burn wounds and contributes to wound repair', *Journal of Surgical Research*, 183(1), pp. 427-434.

Hua, J., Yu, H., Dong, W., Yang, C., Gao, Z., Lei, A., Sun, Y., Pan, S., Wu, Y. and Dou, Z. (2009) 'Characterization of mesenchymal stem cells (MSCs) from human fetal lung: potential differentiation of germ cells', *Tissue Cell*, 41(6), pp. 448-55.

Hua, Z., Lv, Q., Ye, W., Wong, C.-K.A., Cai, G., Gu, D., Ji, Y., Zhao, C., Wang, J., Yang, B.B. and Zhang, Y. (2006) 'MiRNA-Directed Regulation of VEGF and Other Angiogenic Factors under Hypoxia', *PLoS ONE*, 1(1), p. e116.

Huang, L. and Burd, A. (2012) 'An update review of stem cell applications in burns and wound care', *Indian J Plast Surg*, 45(2), pp. 229-36.

Huminiecki, L., Goldovsky, L., Freilich, S., Moustakas, A., Ouzounis, C. and Heldin, C.-H. (2009) 'Emergence, development and diversification of the TGF-β signalling pathway within the animal kingdom', *BMC Evolutionary Biology*, 9, pp. 28-28.

Hwang, J.H., Shim, S.S., Seok, O.S., Lee, H.Y., Woo, S.K., Kim, B.H., Song, H.R., Lee, J.K. and Park, Y.K. (2009) 'Comparison of cytokine expression in mesenchymal stem cells from human placenta, cord blood, and bone marrow', *J Korean Med Sci*, 24(4), pp. 547-54.

Igarashi, A., Nashiro, K., Kikuchi, K., Sato, S., Ihn, H., Fujimoto, M., Grotendorst, G.R. and Takehara, K. (1996) 'Connective tissue growth factor gene expression in tissue sections from localized scleroderma, keloid, and other fibrotic skin disorders', *Journal of Investigative Dermatology*, 106(4), pp. 729-733.

Inoue, A., Sawata, S.Y., Taira, K. and Wadhwa, R. (2007) 'Loss-of-function screening by randomized intracellular antibodies: Identification of hnRNP-K as a potential target for metastasis', *Proceedings of the National Academy of Sciences of the United States of America*, 104(21), pp. 8983-8988.

Iozzo, R.V. (2005) 'Basement membrane proteoglycans: from cellar to ceiling', *Nat Rev Mol Cell Biol*, 6(8), pp. 646-656.

Ireton, J.E., Unger, J.G. and Rohrich, R.J. (2013) 'The Role of Wound Healing and Its Everyday Application in Plastic Surgery: A Practical Perspective and Systematic Review', *Plastic and Reconstructive Surgery Global Open*, 1(1), pp. e10-e19.

Ito, T., Suzuki, A., Okabe, M., Imai, E. and Hori, M. (2001) 'Application of bone marrow-derived stem cells in experimental nephrology', *Exp Nephrol*, 9(6), pp. 444-50.

Iwaki, T., Urano, T. and Umemura, K. (2012) 'PAI-1, progress in understanding the clinical problem and its aetiology', *British Journal of Haematology*, 157(3), pp. 291-298.

Jacinto, A., Martinez-Arias, A. and Martin, P. (2001) 'Mechanisms of epithelial fusion and repair', *Nat Cell Biol*, 3(5), pp. E117-E123.

Jackson, L., Jones, D.R., Scotting, P. and Sottile, V. (2007) 'Adult mesenchymal stem cells: differentiation potential and therapeutic applications', *J Postgrad Med*, 53(2), pp. 121-7.

Jackson, W., Nesti, L. and Tuan, R. (2012a) 'Mesenchymal stem cell therapy for attenuation of scar formation during wound healing', *Stem Cell Research & Therapy*, 3(3), p. 20.

Jackson, W.M., Nesti, L.J. and Tuan, R.S. (2012b) 'Mesenchymal stem cell therapy for attenuation of scar formation during wound healing', *Stem Cell Res Ther*, 3(3), p. 20.

Jaqaman, K., Loerke, D., Mettlen, M., Kuwata, H., Grinstein, S., Schmid, S.L. and Danuser, G. (2008) 'Robust single-particle tracking in live-cell time-lapse sequences', *Nat Meth*, 5(8), pp. 695-702.

Jens, K., Daniel, E., Katrin, K., Christian, T.D., Yuxi, F., Hans-Peter, H., Thomas, W. and Hellmut, G.A. (2009) 'Inhibition of Rho-dependent kinases ROCK I/II activates VEGF-driven retinal neovascularization and sprouting angiogenesis', *American Journal of Physiology-Heart and Circulatory Physiology*, 296(3), pp. H893-H899.

Jiang, Y., Jahagirdar, B.N., Reinhardt, R.L., Schwartz, R.E., Keene, C.D., Ortiz-Gonzalez, X.R., Reyes, M., Lenvik, T., Lund, T., Blackstad, M., Du, J., Aldrich, S., Lisberg, A., Low, W.C., Largaespada, D.A. and Verfaillie, C.M. (2002) 'Pluripotency of mesenchymal stem cells derived from adult marrow', *Nature*, 418(6893), pp. 41-49.

Jiang, Z., Georgel, P., Du, X., Shamel, L., Sovath, S., Mudd, S., Huber, M., Kalis, C., Keck, S., Galanos, C., Freudenberg, M. and Beutler, B. (2005) 'CD14 is required for MyD88-independent LPS signaling', *Nat Immunol*, 6(6), pp. 565-570.

Jin, H.J., Bae, Y.K., Kim, M., Kwon, S.J., Jeon, H.B., Choi, S.J., Kim, S.W., Yang, Y.S., Oh, W. and Chang, J.W. (2013a) 'Comparative analysis of human mesenchymal stem cells from bone marrow, adipose tissue, and umbilical cord blood as sources of cell therapy', *Int J Mol Sci*, 14(9), pp. 17986-8001.

Jin, L., Li, Y., Liu, J., Yang, S., Gui, Y., Mao, X., Nie, G. and Lai, Y. (2016) 'Tumor suppressor miR-149-5p is associated with cellular migration, proliferation and apoptosis in renal cell carcinoma', *Mol Med Rep*, 13(6), pp. 5386-92.

Jin, Y., Tymen, S.D., Chen, D., Fang, Z.J., Zhao, Y., Dragas, D., Dai, Y., Marucha, P.T. and Zhou, X. (2013b) 'MicroRNA-99 Family Targets AKT/mTOR Signaling Pathway in Dermal Wound Healing', *PLoS ONE*, 8(5), p. e64434.

Johnstone, B., Hering, T.M., Caplan, A.I., Goldberg, V.M. and Yoo, J.U. (1998) 'In VitroChondrogenesis of Bone Marrow-Derived Mesenchymal Progenitor Cells', *Experimental Cell Research*, 238(1), pp. 265-272.

Jolly, P., Estrela, P. and Ladomery, M. (2016) 'Oligonucleotide-based systems: DNA, microRNAs, DNA/RNA aptamers', *Essays in Biochemistry*, 60(1), pp. 27-35.

Jorgensen, L.N. (2003) 'Collagen deposition in the subcutaneous tissue during wound healing in humans: a model evaluation', *APMIS Suppl*, (115), pp. 1-56.

Jung, S., Panchalingam, K.M., Rosenberg, L. and Behie, L.A. (2012) 'Ex Vivo Expansion of Human Mesenchymal Stem Cells in Defined Serum-Free Media', *Stem Cells International*, 2012, p. 21.

Justus, C.R., Leffler, N., Ruiz-Echevarria, M. and Yang, L.V. (2014) 'In vitro Cell Migration and Invasion Assays', *Journal of Visualized Experiments : JoVE*, (88), p. 51046.

Kachgal, S., Mace, K.A. and Boudreau, N.J. (2012) 'The dual roles of homeobox genes in vascularization and wound healing', *Cell Adhesion & Migration*, 6(6), pp. 457-470.

Kadam, S., Muthyala, S., Nair, P. and Bhonde, R. (2010) 'Human placenta-derived mesenchymal stem cells and islet-like cell clusters generated from these cells as a novel source for stem cell therapy in diabetes', *Rev Diabet Stud*, 7(2), pp. 168-82.

Kadir, R.A., Ariffin, S.H.Z., Wahab, R.M.A. and Senafi, S. (2012) 'Molecular characterisation of human peripheral blood stem cells', *South African Journal of Science*, 108, pp. 67-73.

Kang, H., Kim, C., Lee, H., Rho, J.G., Seo, J.W., Nam, J.W., Song, W.K., Nam, S.W., Kim, W. and Lee, E.K. (2016) 'Downregulation of microRNA-362-3p and microRNA-329 promotes tumor progression in human breast cancer', *Cell Death and Differentiation*, 23(3), pp. 484-495.

Kang, S.G., Chung, H., Yoo, Y.D., Lee, J.G., Choi, Y.I. and Yu, Y.S. (2001) 'Mechanism of growth inhibitory effect of Mitomycin-C on cultured human retinal pigment epithelial cells: apoptosis and cell cycle arrest', *Curr Eye Res*, 22(3), pp. 174-81.

Kanitakis, J. (2002) 'Anatomy, histology and immunohistochemistry of normal human skin', *Eur J Dermatol*, 12(4), pp. 390-9; quiz 400-1.

Kassis, I., Zangi, L., Rivkin, R., Levdansky, L., Samuel, S., Marx, G. and Gorodetsky, R. (2006) 'Isolation of mesenchymal stem cells from G-CSF-mobilized human peripheral blood using fibrin microbeads', *Bone Marrow Transplant*, 37(10), pp. 967-76.

Kato, M., Zhang, J., Wang, M., Lanting, L., Yuan, H., Rossi, J.J. and Natarajan, R. (2007) 'MicroRNA-192 in diabetic kidney glomeruli and its function in TGF-β-induced collagen expression via inhibition of E-box repressors', *Proceedings of the National Academy of Sciences of the United States of America*, 104(9), pp. 3432-3437.

Keren, K., Pincus, Z., Allen, G.M., Barnhart, E.L., Marriott, G., Mogilner, A. and Theriot, J.A. (2008) 'Mechanism of shape determination in motile cells', *Nature*, 453(7194), pp. 475-480.

Kersey, J.P. and Vivian, A.J. (2008) 'Mitomycin and Amniotic Membrane: A New Method of Reducing Adhesions and Fibrosis in Strabismus Surgery', *Strabismus*, 16(3), pp. 116-118.

Kim, J.-H., Sharma, A., Dhar, S.S., Lee, S.-H., Gu, B., Chan, C.-H., Lin, H.-K. and Lee, M.G. (2014) 'UTX and MLL4 Coordinately Regulate Transcriptional Programs for Cell Proliferation and Invasiveness in Breast Cancer Cells', *Cancer Research*, 74(6), pp. 1705-1717.

Kim, J.H., Shin, J.H. and Kim, I.H. (2004) 'Susceptibility and radiosensitization of human glioblastoma cells to trichostatin A, a histone deacetylase inhibitor', *Int J Radiat Oncol Biol Phys*, 59.

Kim, W.S., Park, B.S., Sung, J.H., Yang, J.M., Park, S.B., Kwak, S.J. and Park, J.S. (2007) 'Wound healing effect of adipose-derived stem cells: a critical role of secretory factors on human dermal fibroblasts', *J Dermatol Sci*, 48(1), pp. 15-24.

Kisselbach, L., Merges, M., Bossie, A. and Boyd, A. (2009) 'CD90 Expression on human primary cells and elimination of contaminating fibroblasts from cell cultures', *Cytotechnology*, 59(1), pp. 31-44.

Klimkiewicz, K., Weglarczyk, K., Collet, G., Paprocka, M., Guichard, A., Sarna, M., Jozkowicz, A., Dulak, J., Sarna, T., Grillon, C. and Kieda, C. (2017) 'A 3D model of tumour angiogenic microenvironment to monitor hypoxia effects on cell interactions and cancer stem cell selection', *Cancer Letters*, 396, pp. 10-20.

Klontzas, M.E., Kenanidis, E.I., Heliotis, M., Tsiridis, E. and Mantalaris, A. (2015) 'Bone and cartilage regeneration with the use of umbilical cord mesenchymal stem cells', *Expert Opinion on Biological Therapy*, 15(11), pp. 1541-1552.

Kolf, C.M., Cho, E. and Tuan, R.S. (2007) 'Mesenchymal stromal cells. Biology of adult mesenchymal stem cells: regulation of niche, self-renewal and differentiation', *Arthritis Research & Therapy*, 9(1), pp. 204-204.

Konduri, S.D., Tasiou, A., Chandrasekar, N. and Rao, J.S. (2001) 'Overexpression of tissue factor pathway inhibitor-2 (TFPI-2), decreases the invasiveness of prostate cancer cells in vitro', *Int J Oncol*, 18(1), pp. 127-31.

Kopen, G.C., Prockop, D.J. and Phinney, D.G. (1999) 'Marrow stromal cells migrate throughout forebrain and cerebellum, and they differentiate into astrocytes after injection into neonatal mouse brains', *Proc Natl Acad Sci U S A*, 96(19), pp. 10711-6.

Kopp, J., Wang, G.Y., Kulmburg, P., Schultze-Mosgau, S., Huan, J.N., Ying, K., Seyhan, H., Jeschke, M.D., Kneser, U., Bach, A.D., Ge, S.D., Dooley, S. and Horch, R.E. (2004) 'Accelerated Wound Healing by In vivo Application of Keratinocytes Overexpressing KGF', *Molecular Therapy*, 10(1), pp. 86-96.

Kou, B., Liu, W., Tang, X. and Kou, Q. (2018) 'HMGA2 facilitates epithelial-mesenchymal transition in renal cell carcinoma by regulating the TGF-beta/Smad2 signaling pathway', *Oncol Rep*, 39(1), pp. 101-108.

Kramer, N., Walzl, A., Unger, C., Rosner, M., Krupitza, G., Hengstschläger, M. and Dolznig, H. (2013) 'In vitro cell migration and invasion assays', *Mutation Research/Reviews in Mutation Research*, 752(1), pp. 10-24.

Krasnodembskaya, A., Song, Y., Fang, X., Gupta, N., Serikov, V., Lee, J.W. and Matthay, M.A. (2010) 'Antibacterial effect of human mesenchymal stem cells is mediated in part from secretion of the antimicrobial peptide LL-37', *Stem Cells*, 28(12), pp. 2229-38.

Krawczyk, W.S. (1971) 'A PATTERN OF EPIDERMAL CELL MIGRATION DURING WOUND HEALING', *The Journal of Cell Biology*, 49(2), p. 247.

Kretschmann, K.L., Eyob, H., Buys, S.S. and Welm, A.L. (2010) 'The macrophage stimulating protein/Ron pathway as a potential therapeutic target to impede multiple mechanisms involved in breast cancer progression', *Curr Drug Targets*, 11(9), pp. 1157-68.

Kuhbier, J.W., Weyand, B., Radtke, C., Vogt, P.M., Kasper, C. and Reimers, K. (2010) 'Isolation, characterization, differentiation, and application of adipose-derived stem cells', *Adv Biochem Eng Biotechnol*, 123, pp. 55-105.

Laco, F., Kun, M., Weber, H.J., Ramakrishna, S. and Chan, C.K. (2009) 'The dose effect of human bone marrow-derived mesenchymal stem cells on epidermal development in organotypic co-culture', *J Dermatol Sci*, 55(3), pp. 150-60.

Lai, R.C., Yeo, R.W.Y. and Lim, S.K. (2015) 'Mesenchymal stem cell exosomes', *Seminars in Cell & Developmental Biology*, 40(Supplement C), pp. 82-88.

Lai, W.-F. and Siu, P. (2014) 'MicroRNAs as regulators of cutaneous wound healing', *Journal of Biosciences*, 39(3), pp. 519-524.

Landén, N.X., Li, D. and Ståhle, M. (2016) 'Transition from inflammation to proliferation: a critical step during wound healing', *Cellular and Molecular Life Sciences*, pp. 1-25.

Landry, P., Plante, I., Ouellet, D.L., Perron, M.P., Rousseau, G. and Provost, P. (2009) 'Existence of a microRNA pathway in anucleate platelets', *Nature structural & molecular biology*, 16(9), pp. 961-966.

Lau, K., Paus, R., Tiede, S., Day, P. and Bayat, A. (2009) 'Exploring the role of stem cells in cutaneous wound healing', *Experimental Dermatology*, 18(11), pp. 921-933.

Lee, D., Park, S.-J., Sung, K.S., Park, J., Lee, S.B., Park, S.-Y., Lee, H.J., Ahn, J.-W., Choi, S.J., Lee, S.-G., Kim, S.-H., Kim, D.-H., Kim, J., Kim, Y. and Choi, C.Y. (2012)

'Mdm2 associates with Ras effector NORE1 to induce the degradation of oncoprotein HIPK1', *EMBO Reports*, 13(2), pp. 163-169.

Lee, Y.S., Lee, J.E., Park, H.Y., Lim, Y.S., Lee, J.C., Wang, S.G. and Lee, B.J. (2013) 'Isolation of mesenchymal stromal cells (MSCs) from human adenoid tissue', *Cell Physiol Biochem*, 31(4-5), pp. 513-24.

Leierseder, S., Petzold, T., Zhang, L., Loyer, X., Massberg, S. and Engelhardt, S. (2013) 'MiR-223 is dispensable for platelet production and function in mice', *Thrombosis and Haemostasis*, 110(12), pp. 1207-1214.

Lesko, A.C., Goss, K.H., Yang, F.F., Schwertner, A., Hulur, I., Onel, K. and Prosperi, J.R. (2015) 'The APC tumor suppressor is required for epithelial cell polarization and three-dimensional morphogenesis', *Biochimica et biophysica acta*, 1854(3), pp. 711-723.

Li, B. and Wang, J.H.C. (2011) 'Fibroblasts and myofibroblasts in wound healing: Force generation and measurement', *Journal of Tissue Viability*, 20(4), pp. 108-120.

Li, C.-y., Wu, X.-y., Tong, J.-b., Yang, X.-x., Zhao, J.-l., Zheng, Q.-f., Zhao, G.-b. and Ma, Z.-j. (2015a) 'Comparative analysis of human mesenchymal stem cells from bone marrow and adipose tissue under xeno-free conditions for cell therapy', *Stem Cell Research & Therapy*, 6(1), p. 55.

Li, D., Li, X.I., Wang, A., Meisgen, F., Pivarcsi, A., Sonkoly, E., Ståhle, M. and Landén, N.X. (2015b) 'MicroRNA-31 Promotes Skin Wound Healing by Enhancing Keratinocyte Proliferation and Migration', *Journal of Investigative Dermatology*, 135(6), pp. 1676-1685.

Li, D., Wang, A., Liu, X., Meisgen, F., Grünler, J., Botusan, I.R., Narayanan, S., Erikci, E., Li, X., Blomqvist, L., Du, L., Pivarcsi, A., Sonkoly, E., Chowdhury, K., Catrina, S.-B., Ståhle, M. and Landén, N.X. (2015c) 'MicroRNA-132 enhances transition from inflammation to proliferation during wound healing', *The Journal of Clinical Investigation*, 125(8), pp. 3008-3026.

Li, H., Chang, L., Du, W.W., Gupta, S., Khorshidi, A., Sefton, M. and Yang, B.B. (2014) 'Anti-microRNA-378a Enhances Wound Healing Process by Upregulating Integrin Beta-3 and Vimentin', *Mol Ther*, 22(10), pp. 1839-1850.

Li, H., Fu, X., Ouyang, Y., Cai, C., Wang, J. and Sun, T. (2006) 'Adult bone-marrow-derived mesenchymal stem cells contribute to wound healing of skin appendages', *Cell Tissue Res*, 326(3), pp. 725-36.

Li, L., Fukunaga-Kalabis, M. and Herlyn, M. (2011a) 'The three-dimensional human skin reconstruct model: a tool to study normal skin and melanoma progression', *J Vis Exp*, (54).

Li, L., Fukunaga-Kalabis, M. and Herlyn, M. (2011b) 'The Three-Dimensional Human Skin Reconstruct Model: a Tool to Study Normal Skin and Melanoma Progression', (54), p. e2937.

Li, L., Zhang, S., Zhang, Y., Yu, B., Xu, Y. and Guan, Z. (2009) 'Paracrine action mediate the antifibrotic effect of transplanted mesenchymal stem cells in a rat model of global heart failure', *Mol Biol Rep*, 36(4), pp. 725-31.

Li, M., Gu, Y., Ma, Y.-C., Shang, Z.-F., Wang, C., Liu, F.-J., Cao, J.-P., Wan, H.-J. and Zhang, X.-G. (2015d) 'Krüppel-Like Factor 5 Promotes Epithelial Proliferation and DNA Damage Repair in the Intestine of Irradiated Mice', *International Journal of Biological Sciences*, 11(12), pp. 1458-1468.

Li, P., He, Q., Luo, C. and Qian, L. (2015e) 'Differentially Expressed miRNAs in Acute Wound Healing of the Skin: A Pilot Study', *Medicine*, 94(7), p. e458.

Li, T., Yan, Y., Wang, B., Qian, H., Zhang, X. and Shen, L. (2013) 'Exosomes derived from human umbilical cord mesenchymal stem cells alleviate liver fibrosis', *Stem Cells Dev*, 22.

Li, W., Chang, J., Wang, S., Liu, X., Peng, J., Huang, D., Sun, M., Chen, Z., Zhang, W., Guo, W. and Li, J. (2015f) 'miRNA-99b-5p suppresses liver metastasis of colorectal cancer by down-regulating mTOR', *Oncotarget*, 6(27), pp. 24448-24462.

Liang, C.C., Park, A.Y. and Guan, J.L. (2007) 'In vitro scratch assay: a convenient and inexpensive method for analysis of cell migration in vitro', *Nat Protoc*, 2(2), pp. 329-33.

Liechty, K.W., MacKenzie, T.C., Shaaban, A.F., Radu, A., Moseley, A.M., Deans, R., Marshak, D.R. and Flake, A.W. (2000) 'Human mesenchymal stem cells engraft and demonstrate site-specific differentiation after in utero transplantation in sheep', *Nat Med*, 6(11), pp. 1282-6.

Lin, C.-S., Ning, H., Lin, G. and Lue, T.F. (2012) 'Is CD34 Truly a Negative Marker for Mesenchymal Stem Cells?', *Cytotherapy*, 14(10), p. 10.3109/14653249.2012.729817.

Lin, Y.-L., Persaud, S.D., Nhieu, J. and Wei, L.-N. (2017) 'Cellular Retinoic Acid–Binding Protein 1 Modulates Stem Cell Proliferation to Affect Learning and Memory in Male Mice', *Endocrinology*, 158(9), pp. 3004-3014.

Liu, J.F., Wang, B.W., Hung, H.F., Chang, H. and Shyu, K.G. (2008) 'Human mesenchymal stem cells improve myocardial performance in a splenectomized rat model of chronic myocardial infarction', *J Formos Med Assoc*, 107(2), pp. 165-74.

Liu, Y., Petreaca, M., Yao, M. and Martins-Green, M. (2009) 'Cell and molecular mechanisms of keratinocyte function stimulated by insulin during wound healing', *BMC Cell Biology*, 10(1), p. 1.

Liu, Y., Yan, X., Sun, Z., Chen, B., Han, Q., Li, J. and Zhao, R.C. (2007) 'Flk-1+ adipose-derived mesenchymal stem cells differentiate into skeletal muscle satellite cells and ameliorate muscular dystrophy in mdx mice', *Stem Cells Dev*, 16(5), pp. 695-706.

Lorsch, J.R., Collins, F.S. and Lippincott-Schwartz, J. (2014) 'Fixing problems with cell lines', *Science*, 346(6216), pp. 1452-1453.

Lundin, A., Hasenson, M., Persson, J. and Pousette, A. (1986) 'Estimation of biomass in growing cell lines by adenosine triphosphate assay', *Methods Enzymol*, 133, pp. 27-42.

Lynch, S.E., Nixon, J.C., Colvin, R.B. and Antoniades, H.N. (1987) 'Role of platelet-derived growth factor in wound healing: synergistic effects with other growth factors', *Proceedings of the National Academy of Sciences of the United States of America*, 84(21), pp. 7696-7700.

Ma, K., Laco, F., Ramakrishna, S., Liao, S. and Chan, C.K. (2009) 'Differentiation of bone marrow-derived mesenchymal stem cells into multi-layered epidermis-like cells in 3D organotypic coculture', *Biomaterials*, 30(19), pp. 3251-3258.

Mabuchi, Y., Houlihan, D.D., Akazawa, C., Okano, H. and Matsuzaki, Y. (2013) 'Prospective isolation of murine and human bone marrow mesenchymal stem cells based on surface markers', *Stem Cells Int*, 2013, p. 507301.

Madhyastha, R., Madhyastha, H., Nakajima, Y., Omura, S. and Maruyama, M. (2012) 'MicroRNA signature in diabetic wound healing: promotive role of miR-21 in fibroblast migration', *Int Wound J*, 9(4), pp. 355-61.

Mafi, R., Hindocha, S., Mafi, P., Griffin, M. and Khan, W.S. (2011) 'Sources of adult mesenchymal stem cells applicable for musculoskeletal applications - a systematic review of the literature', *Open Orthop J*, 5 Suppl 2, pp. 242-8.

Majumdar, M.K., Thiede, M.A., Haynesworth, S.E., Bruder, S.P. and Gerson, S.L. (2000) 'Human marrow-derived mesenchymal stem cells (MSCs) express hematopoietic

cytokines and support long-term hematopoiesis when differentiated toward stromal and osteogenic lineages', *J Hematother Stem Cell Res*, 9(6), pp. 841-8.

Mak, M., Spill, F., Kamm, R.D. and Zaman, M.H. (2016) 'Single-Cell Migration in Complex Microenvironments: Mechanics and Signaling Dynamics', *Journal of Biomechanical Engineering*, 138(2), pp. 021004-021004-8.

Manavalan, B., Basith, S. and Choi, S. (2011) 'Similar Structures but Different Roles – An Updated Perspective on TLR Structures', *Frontiers in Physiology*, 2, p. 41.

Mansuri, M.S., Singh, M. and Begum, R. (2016) 'miRNA signatures and transcriptional regulation of their target genes in vitiligo', *Journal of Dermatological Science*, 84(1), pp. 50-58.

Mansuri, M.S., Singh, M., Laddha, N.C., Dwivedi, M., Marfatia, Y.S. and Begum, R. (2014) 'Skin miRNA profiling reveals differentially expressed miRNA signatures from non-segmental vitiligo patients', *Molecular Cytogenetics*, 7(Suppl 1), pp. P118-P118.

Mao, M., Alavi, M.V., Labelle-Dumais, C. and Gould, D.B. (2015) 'Type IV Collagens and Basement Membrane Diseases', *Current Topics in Membranes*, 76, pp. 61-116.

Marchand, A., Proust, C., Morange, P.-E., Lompré, A.-M. and Trégouët, D.-A. (2012) 'miR-421 and miR-30c Inhibit SERPINE 1 Gene Expression in Human Endothelial Cells', *PLoS ONE*, 7(8), p. e44532.

Mareschi, K., Rustichelli, D., Calabrese, R., Gunetti, M., Sanavio, F., Castiglia, S., Risso, A., Ferrero, I., Tarella, C. and Fagioli, F. (2012) 'Multipotent Mesenchymal Stromal Stem Cell Expansion by Plating Whole Bone Marrow at a Low Cellular Density: A More Advantageous Method for Clinical Use', *Stem Cells International*, 2012.

Marfia, G., Navone, S.E., Di Vito, C., Ughi, N., Tabano, S., Miozzo, M., Tremolada, C., Bolla, G., Crotti, C., Ingegnoli, F., Rampini, P., Riboni, L., Gualtierotti, R. and Campanella, R. (2015) 'Mesenchymal Stem Cells: Potential For Therapy And Treatment Of Chronic Non-Healing Skin Wounds', *Organogenesis*, p. 0.

Maring, J.A., Trojanowska, M. and Dijke, P.t. (2012) 'Endoglin in fibrosis and scleroderma', *International review of cell and molecular biology*, 297, pp. 10.1016/B978-0-12-394308-8.00008-X.

Marionnet, C., Pierrard, C., Vioux-Chagnoleau, C., Sok, J., Asselineau, D. and Bernerd, F. (2006) 'Interactions between Fibroblasts and Keratinocytes in Morphogenesis of

Dermal Epidermal Junction in a Model of Reconstructed Skin', *J Invest Dermatol*, 126(5), pp. 971-979.

Marquardt, Y., Amann, P.M., Heise, R., Czaja, K., Steiner, T., Merk, H.F., Skazik-Voogt, C. and Baron, J.M. (2015) 'Characterization of a novel standardized human three-dimensional skin wound healing model using non-sequential fractional ultrapulsed CO2 laser treatments', *Lasers in Surgery and Medicine*, 47(3), pp. 257-265.

Martin, P. (1997) 'Wound Healing--Aiming for Perfect Skin Regeneration', *Science*, 276(5309), pp. 75-81.

Martin, P. and Leibovich, S.J. (2005) 'Inflammatory cells during wound repair: the good, the bad and the ugly', *Trends in Cell Biology*, 15(11), pp. 599-607.

Mathieu, D., Linke, J.-C. and Wattel, F. (2006) 'Non-Healing Wounds', in Mathieu, D. (ed.) *Handbook on Hyperbaric Medicine*. Springer Netherlands, pp. 401-428.

Matikainen, T. and Laine, J. (2005) 'Placenta--an alternative source of stem cells', *Toxicol Appl Pharmacol*, 207(2 Suppl), pp. 544-9.

Maxson, S., Lopez, E.A., Yoo, D., Danilkovitch-Miagkova, A. and LeRoux, M.A. (2012) 'Concise Review: Role of Mesenchymal Stem Cells in Wound Repair', *Stem Cells Translational Medicine*, 1(2), pp. 142-149.

McAnulty, R.J. (2007) 'Fibroblasts and myofibroblasts: their source, function and role in disease', *Int J Biochem Cell Biol*, 39(4), pp. 666-71.

McDougall, S., Dallon, J., Sherratt, J. and Maini, P. (2006) 'Fibroblast migration and collagen deposition during dermal wound healing: mathematical modelling and clinical implications', *Philos Trans A Math Phys Eng Sci*, 364(1843), pp. 1385-405.

Mellado, M., Rodríguez-Frade, J.M., Mañes, S. and Martínez-A, C. (2001) 'CHEMOKINE SIGNALING AND FUNCTIONAL RESPONSES: The Role of Receptor Dimerization and TK Pathway Activation', *Annual Review of Immunology*, 19(1), pp. 397-421.

Melo, C.A. and Melo, S.A. (2014) 'Biogenesis and Physiology of MicroRNAs', in Fabbri, M. (ed.) *Non-coding RNAs and Cancer*. New York, NY: Springer New York, pp. 5-24.

Mendonça, R.J.d. and Coutinho-Netto, J. (2009) 'Aspectos celulares da cicatrização', *Anais Brasileiros de Dermatologia*, 84, pp. 257-262.

Metcalfe, A.D. and Ferguson, M.W.J. (2007) 'Tissue engineering of replacement skin: the crossroads of biomaterials, wound healing, embryonic development, stem cells and regeneration', *Journal of The Royal Society Interface*, 4(14), pp. 413-437.

Mewes, K.R., Raus, M., Bernd, A., Zöller, N.N., Sättler, A. and Graf, R. (2007) 'Elastin Expression in a Newly Developed Full-Thickness Skin Equivalent', *Skin Pharmacology and Physiology*, 20(2), pp. 85-95.

Miao, Z., Jin, J., Chen, L., Zhu, J., Huang, W., Zhao, J., Qian, H. and Zhang, X. (2006) 'Isolation of mesenchymal stem cells from human placenta: comparison with human bone marrow mesenchymal stem cells', *Cell Biol Int*, 30(9), pp. 681-7.

Micera, A., Vigneti, E., Pickholtz, D., Reich, R., Pappo, O., Bonini, S., Maquart, F.X., Aloe, L. and Levi-Schaffer, F. (2001) 'Nerve growth factor displays stimulatory effects on human skin and lung fibroblasts, demonstrating a direct role for this factor in tissue repair', *Proc Natl Acad Sci U S A*, 98(11), pp. 6162-7.

Michalopoulos, G.K. and DeFrances, M.C. (1997) 'Liver Regeneration', *Science*, 276(5309), pp. 60-66.

Midwood, K.S., Williams, L.V. and Schwarzbauer, J.E. (2004) 'Tissue repair and the dynamics of the extracellular matrix', *The International Journal of Biochemistry & Cell Biology*, 36(6), pp. 1031-1037.

Miller, R.J., Banisadr, G. and Bhattacharyya, B.J. (2008) 'CXCR4 signaling in the regulation of stem cell migration and development', *Journal of neuroimmunology*, 198(0), pp. 31-38.

Mills, S., Cowin, A. and Kaur, P. (2013) 'Pericytes, Mesenchymal Stem Cells and the Wound Healing Process', *Cells*, 2(3), pp. 621-634.

Mine, S., Fortunel, N.O., Pageon, H. and Asselineau, D. (2009) 'Aging Alters Functionally Human Dermal Papillary Fibroblasts but Not Reticular Fibroblasts: A New View of Skin Morphogenesis and Aging', *PLoS ONE*, 3(12), p. e4066.

Mishra, P.J. and Banerjee, D. (2012) 'Cell-free derivatives from mesenchymal stem cells are effective in wound therapy', *World J Stem Cells*, 4(5), pp. 35-43.

Modarressi, A., Pietramaggiori, G., Godbout, C., Vigato, E., Pittet, B. and Hinz, B. (2010) 'Hypoxia Impairs Skin Myofibroblast Differentiation and Function', *Journal of Investigative Dermatology*, 130(12), pp. 2818-2827.

Moghadasali, R., Mutsaers, H.A., Azarnia, M., Aghdami, N., Baharvand, H., Torensma, R., Wilmer, M.J. and Masereeuw, R. (2013) 'Mesenchymal stem cell-conditioned medium accelerates regeneration of human renal proximal tubule epithelial cells after gentamicin toxicity', *Exp Toxicol Pathol*, 65(5), pp. 595-600.

Mokry, J. and Nemecek, S. (1995) 'Immunohistochemical detection of proliferative cells', *Sb Ved Pr Lek Fak Karlovy Univerzity Hradci Kralove*, 38(3), pp. 107-13.

Monaco, J.L. and Lawrence, W.T. (2003) 'Acute wound healing an overview', *Clin Plast Surg*, 30(1), pp. 1-12.

Moore, K.W., de Waal Malefyt, R., Coffman, R.L. and O'Garra, A. (2001) 'Interleukin-10 and the interleukin-10 receptor', *Annu Rev Immunol*, 19, pp. 683-765.

Mora, S. and Pessin, J.E. (2002) 'An adipocentric view of signaling and intracellular trafficking', *Diabetes/Metabolism Research and Reviews*, 18(5), pp. 345-356.

Morasso, M.I. and Tomic-Canic, M. (2005) 'Epidermal stem cells: the cradle of epidermal determination, differentiation and wound healing', *Biology of the cell / under the auspices of the European Cell Biology Organization*, 97(3), pp. 173-183.

Morimoto, N., Kakudo, N., Matsui, M., Ogura, T., Hara, T., Suzuki, K., Yamamoto, M., Tabata, Y. and Kusumoto, K. (2015) 'Exploratory clinical trial of combination wound therapy with a gelatin sheet and platelet-rich plasma in patients with chronic skin ulcers: study protocol', *BMJ Open*, 5(5).

Mosmann, T. (1983) 'Rapid colorimetric assay for cellular growth and survival: Application to proliferation and cytotoxicity assays', *Journal of Immunological Methods*, 65(1), pp. 55-63.

Motaln, H., Schichor, C. and Lah, T.T. (2010) 'Human mesenchymal stem cells and their use in cell-based therapies', *Cancer*, 116(11), pp. 2519-30.

Mou, S., Wang, Q., Shi, B., Gu, L. and Ni, Z. (2009) 'Hepatocyte growth factor suppresses transforming growth factor-beta-1 and type III collagen in human primary renal fibroblasts', *Kaohsiung J Med Sci*, 25(11), pp. 577-87.

Moura, J., Borsheim, E. and Carvalho, E. (2014) 'The Role of MicroRNAs in Diabetic Complications-Special Emphasis on Wound Healing', *Genes (Basel)*, 5(4), pp. 926-56.

Moustakas, A. and Heldin, C.-H. (2009) 'The regulation of TGFβ signal transduction', *Development*, 136(22), pp. 3699-3714.

Muralidharan-Chari, V., Clancy, J.W., Sedgwick, A. and D'Souza-Schorey, C. (2010) 'Microvesicles: mediators of extracellular communication during cancer progression', *J Cell Sci*, 123.

Naaldijk, Y., Staude, M., Fedorova, V. and Stolzing, A. (2012) 'Effect of different freezing rates during cryopreservation of rat mesenchymal stem cells using combinations of hydroxyethyl starch and dimethylsulfoxide', *BMC Biotechnology*, 12(1), p. 49.

Nagalla, S., Shaw, C., Kong, X., Kondkar, A.A., Edelstein, L.C., Ma, L., Chen, J., McKnight, G.S., López, J.A., Yang, L., Jin, Y., Bray, M.S., Leal, S.M., Dong, J.-f. and Bray, P.F. (2011) 'Platelet microRNA-mRNA coexpression profiles correlate with platelet reactivity', *Blood*, 117(19), pp. 5189-5197.

Nassar, D., Letavernier, E., Baud, L., Aractingi, S. and Khosrotehrani, K. (2012) 'Calpain Activity Is Essential in Skin Wound Healing and Contributes to Scar Formation', *PLOS ONE*, 7(5), p. e37084.

Nemeth, K., Leelahavanichkul, A., Yuen, P.S., Mayer, B., Parmelee, A., Doi, K., Robey, P.G., Leelahavanichkul, K., Koller, B.H., Brown, J.M., Hu, X., Jelinek, I., Star, R.A. and Mezey, E. (2009) 'Bone marrow stromal cells attenuate sepsis via prostaglandin E(2)-dependent reprogramming of host macrophages to increase their interleukin-10 production', *Nat Med*, 15(1), pp. 42-9.

Newton, P.M., Watson, J.A., Wolowacz, R.G. and Wood, E.J. (2004) 'Macrophages restrain contraction of an in vitro wound healing model', *Inflammation*, 28(4), pp. 207-14.

Ng, M.R., Besser, A., Danuser, G. and Brugge, J.S. (2012) 'Substrate stiffness regulates cadherin-dependent collective migration through myosin-II contractility', *The Journal of Cell Biology*, 199(3), pp. 545-563.

Nielsen, J.S. and McNagny, K.M. (2008) 'Novel functions of the CD34 family', *Journal of Cell Science*, 121(22), pp. 3683-3692.

Niwa, M., Nagai, K., Oike, H. and Kobori, M. (2009) 'Evaluation of the Skin Irritation Using a DNA Microarray on a Reconstructed Human Epidermal Model', *Biological and Pharmaceutical Bulletin*, 32(2), pp. 203-208.

Nombela-Arrieta, C., Ritz, J. and Silberstein, L.E. (2011) 'The elusive nature and function of mesenchymal stem cells', *Nature Reviews. Molecular Cell Biology*, 12(2), pp. 126-131.

Noriyuki Morikawa, T.K.a.K.T. (2007) 'Assessment of the in vitro skin irritation of chemicals using the Vitrolife-Skin™ human skin model', *Proc. 6th World Congress on Alternatives & Animal Use in the Life Sciences*, AATEX 14(Special Issue), pp. 417-423.

Nuschke, A. (2014) 'Activity of mesenchymal stem cells in therapies for chronic skin wound healing', *Organogenesis*, 10(1), pp. 29-37.

Oda, Y., Tu, C.-L., Pillai, S. and Bikle, D.D. (1998) 'The Calcium Sensing Receptor and Its Alternatively Spliced Form in Keratinocyte Differentiation', *Journal of Biological Chemistry*, 273(36), pp. 23344-23352.

Odland, G. and Ross, R. (1968) 'HUMAN WOUND REPAIR', *I. Epidermal Regeneration*, 39(1), pp. 135-151.

Ornitz, D.M. and Itoh, N. (2001) 'Fibroblast growth factors', *Genome Biology*, 2(3), pp. reviews3005.1-reviews3005.12.

Ortiz, L.A., Dutreil, M., Fattman, C., Pandey, A.C., Torres, G., Go, K. and Phinney, D.G. (2007) 'Interleukin 1 receptor antagonist mediates the antiinflammatory and antifibrotic effect of mesenchymal stem cells during lung injury', *Proc Natl Acad Sci U S A*, 104(26), pp. 11002-7.

Ortiz, L.A., Gambelli, F., McBride, C., Gaupp, D., Baddoo, M., Kaminski, N. and Phinney, D.G. (2003) 'Mesenchymal stem cell engraftment in lung is enhanced in response to bleomycin exposure and ameliorates its fibrotic effects', *Proc Natl Acad Sci U S A*, 100(14), pp. 8407-11.

Oswald, J., Boxberger, S., Jorgensen, B., Feldmann, S., Ehninger, G., Bornhauser, M. and Werner, C. (2004) 'Mesenchymal stem cells can be differentiated into endothelial cells in vitro', *Stem Cells*, 22(3), pp. 377-84.

Otsuka, M., Zheng, M., Hayashi, M., Lee, J.-D., Yoshino, O., Lin, S. and Han, J. (2008) 'Impaired microRNA processing causes corpus luteum insufficiency and infertility in mice', *The Journal of Clinical Investigation*, 118(5), pp. 1944-1954.

Paladini, R.D., Takahashi, K., Bravo, N.S. and Coulombe, P.A. (1996) 'Onset of re-epithelialization after skin injury correlates with a reorganization of keratin filaments in wound edge keratinocytes: defining a potential role for keratin 16', *The Journal of Cell Biology*, 132(3), p. 381.

Pan, C., Kumar, C., Bohl, S., Klingmueller, U. and Mann, M. (2009) 'Comparative Proteomic Phenotyping of Cell Lines and Primary Cells to Assess Preservation of Cell Type-specific Functions', *Molecular & Cellular Proteomics*, 8(3), pp. 443-450.

Paquet-Fifield, S., Schluter, H., Li, A., Aitken, T., Gangatirkar, P., Blashki, D., Koelmeyer, R., Pouliot, N., Palatsides, M., Ellis, S., Brouard, N., Zannettino, A., Saunders, N., Thompson, N., Li, J. and Kaur, P. (2009) 'A role for pericytes as microenvironmental regulators of human skin tissue regeneration', *J Clin Invest*, 119(9), pp. 2795-806.

Parekkadan, B. and Milwid, J.M. (2010) 'Mesenchymal stem cells as therapeutics', *Annu Rev Biomed Eng*, 12, pp. 87-117.

Parenteau, N.L., Nolte, C.M., Bilbo, P., Rosenberg, M., Wilkins, L.M., Johnson, E.W., Watson, S., Mason, V.S. and Bell, E. (1991) 'Epidermis generated in vitro: practical considerations and applications', *Journal of Cellular Biochemistry*, 45(3), pp. 245-251.

Park, C.W., Kim, K.-S., Bae, S., Son, H.K., Myung, P.-K., Hong, H.J. and Kim, H. (2009) 'Cytokine Secretion Profiling of Human Mesenchymal Stem Cells by Antibody Array', *International Journal of Stem Cells*, 2(1), pp. 59-68.

Pastar, I., Khan, A.A., Stojadinovic, O., Lebrun, E.A., Medina, M.C., Brem, H., Kirsner, R.S., Jimenez, J.J., Leslie, C. and Tomic-Canic, M. (2012) 'Induction of Specific MicroRNAs Inhibits Cutaneous Wound Healing', *Journal of Biological Chemistry*, 287(35), pp. 29324-29335.

Pastar, I., Stojadinovic, O. and Tomic-Canic, M. (2008) 'Role of keratinocytes in healing of chronic wounds', *Surg Technol Int*, 17, pp. 105-12.

Pastar, I., Stojadinovic, O., Yin, N.C., Ramirez, H., Nusbaum, A.G., Sawaya, A., Patel, S.B., Khalid, L., Isseroff, R.R. and Tomic-Canic, M. (2014) 'Epithelialization in Wound Healing: A Comprehensive Review', *Advances in Wound Care*, 3(7), pp. 445-464.

Patel, D.M., Shah, J. and Srivastava, A.S. (2013) 'Therapeutic Potential of Mesenchymal Stem Cells in Regenerative Medicine', *Stem Cells International*, 2013, p. 15.

Peng, X., Cao, P., Li, J., He, D., Han, S., Zhou, J., Tan, G., Li, W., Yu, F., Yu, J., Li, Z. and Cao, K. (2015) 'MiR-1204 sensitizes nasopharyngeal carcinoma cells to paclitaxel both in vitro and in vivo', *Cancer Biology & Therapy*, 16(2), pp. 261-267.

Perin, L., Sedrakyan, S., Da Sacco, S. and De Filippo, R. (2008) 'Characterization of human amniotic fluid stem cells and their pluripotential capability', *Methods Cell Biol*, 86, pp. 85-99.

Petrie Aronin, C.E. and Tuan, R.S. (2010) 'Therapeutic potential of the immunomodulatory activities of adult mesenchymal stem cells', *Birth Defects Res C Embryo Today*, 90(1), pp. 67-74.

Phinney, D.G. and Prockop, D.J. (2007) 'Concise Review: Mesenchymal Stem/Multipotent Stromal Cells: The State of Transdifferentiation and Modes of Tissue Repair—Current Views', *STEM CELLS*, 25(11), pp. 2896-2902.

Pittenger, M.F., Mackay, A.M., Beck, S.C., Jaiswal, R.K., Douglas, R., Mosca, J.D., Moorman, M.A., Simonetti, D.W., Craig, S. and Marshak, D.R. (1999) 'Multilineage potential of adult human mesenchymal stem cells', *Science*, 284(5411), pp. 143-7.

Poli, G. (2000) 'Pathogenesis of liver fibrosis: role of oxidative stress', *Mol Aspects Med*, 21(3), pp. 49-98.

Poliseno, L., Salmena, L., Zhang, J., Carver, B., Haveman, W.J. and Pandolfi, P.P. (2010) 'A coding-independent function of gene and pseudogene mRNAs regulates tumour biology', *Nature*, 465(7301), pp. 1033-1038.

Polisetty, N., Fatima, A., Madhira, S.L., Sangwan, V.S. and Vemuganti, G.K. (2008) 'Mesenchymal cells from limbal stroma of human eye', *Mol Vis*, 14, pp. 431-42.

Polyzoidis, S., Koletsa, T., Panagiotidou, S., Ashkan, K. and Theoharides, T.C. (2015) 'Mast cells in meningiomas and brain inflammation', *Journal of Neuroinflammation*, 12, p. 170.

Popp, F.C., Eggenhofer, E., Renner, P., Slowik, P., Lang, S.A., Kaspar, H., Geissler, E.K., Piso, P., Schlitt, H.J. and Dahlke, M.H. (2008) 'Mesenchymal stem cells can induce long-term acceptance of solid organ allografts in synergy with low-dose mycophenolate', *Transpl Immunol*, 20(1-2), pp. 55-60.

Porter, A.M. (2001) 'Why do we have apocrine and sebaceous glands?', *J R Soc Med*, 94(5), pp. 236-7.

Portmann-Lanz, C.B., Schoeberlein, A., Portmann, R., Mohr, S., Rollini, P., Sager, R. and Surbek, D.V. (2010) 'Turning placenta into brain: placental mesenchymal stem cells

differentiate into neurons and oligodendrocytes', *Am J Obstet Gynecol*, 202(3), pp. 294 e1-294 e11.

Pöschl, E., Schlötzer-Schrehardt, U., Brachvogel, B., Saito, K., Ninomiya, Y. and Mayer, U. (2004) 'Collagen IV is essential for basement membrane stability but dispensable for initiation of its assembly during early development', *Development*, 131(7), p. 1619.

Posnett, J. and Franks, P.J. (2008) 'The burden of chronic wounds in the UK', *Nurs Times*, 104(3), pp. 44-5.

Poujade, M., Grasland-Mongrain, E., Hertzog, A., Jouanneau, J., Chavrier, P., Ladoux, B., Buguin, A. and Silberzan, P. (2007) 'Collective migration of an epithelial monolayer in response to a model wound', *Proceedings of the National Academy of Sciences of the United States of America*, 104(41), pp. 15988-15993.

Pravdyuk, A.I., Petrenko, Y.A., Fuller, B.J. and Petrenko, A.Y. (2013) 'Cryopreservation of alginate encapsulated mesenchymal stromal cells', *Cryobiology*, 66(3), pp. 215-222.

Pritchard, C.C., Cheng, H.H. and Tewari, M. (2012) 'MicroRNA profiling: approaches and considerations', *Nat Rev Genet*, 13(5), pp. 358-369.

Qin, J., Zhou, Z., Chen, W., Wang, C., Zhang, H., Ge, G., Shao, M., You, D., Fan, Z., Xia, H., Liu, R. and Chen, C. (2015) 'BAP1 promotes breast cancer cell proliferation and metastasis by deubiquitinating KLF5', *Nature Communications*, 6, p. 8471.

Qing, C. (2017) 'The molecular biology in wound healing & non-healing wound', *Chinese Journal of Traumatology*.

Qu-Petersen, Z., Deasy, B., Jankowski, R., Ikezawa, M., Cummins, J., Pruchnic, R., Mytinger, J., Cao, B., Gates, C., Wernig, A. and Huard, J. (2002) 'Identification of a novel population of muscle stem cells in mice', *potential for muscle regeneration*, 157(5), pp. 851-864.

Quent, V.M.C., Loessner, D., Friis, T., Reichert, J.C. and Hutmacher, D.W. (2010) 'Discrepancies between metabolic activity and DNA content as tool to assess cell proliferation in cancer research', *Journal of Cellular and Molecular Medicine*, 14(4), pp. 1003-1013.

Quirici, N., Scavullo, C., de Girolamo, L., Lopa, S., Arrigoni, E., Deliliers, G.L. and Brini, A.T. (2010) 'Anti-L-NGFR and -CD34 monoclonal antibodies identify multipotent mesenchymal stem cells in human adipose tissue', *Stem Cells Dev*, 19(6), pp. 915-25.

Quirici, N., Soligo, D., Bossolasco, P., Servida, F., Lumini, C. and Deliliers, G.L. (2002) 'Isolation of bone marrow mesenchymal stem cells by anti-nerve growth factor receptor antibodies', *Exp Hematol*, 30(7), pp. 783-91.

Rajkumar, V.S., Shiwen, X., Bostrom, M., Leoni, P., Muddle, J., Ivarsson, M., Gerdin, B., Denton, C.P., Bou-Gharios, G., Black, C.M. and Abraham, D.J. (2006) 'Platelet-Derived Growth Factor-β Receptor Activation Is Essential for Fibroblast and Pericyte Recruitment during Cutaneous Wound Healing', *The American Journal of Pathology*, 169(6), pp. 2254-2265.

Rani, S. and Ritter, T. (2015) 'The Exosome - A Naturally Secreted Nanoparticle and its Application to Wound Healing', *Advanced Materials*, pp. n/a-n/a.

Rasche, H. (2001) 'Haemostasis and thrombosis: an overview', *European Heart Journal Supplements*, 3(suppl Q), pp. Q3-Q7.

Rastegar, F., Shenaq, D., Huang, J., Zhang, W., Zhang, B.Q., He, B.C., Chen, L., Zuo, G.W., Luo, Q., Shi, Q., Wagner, E.R., Huang, E., Gao, Y., Gao, J.L., Kim, S.H., Zhou, J.Z., Bi, Y., Su, Y., Zhu, G., Luo, J., Luo, X., Qin, J., Reid, R.R., Luu, H.H., Haydon, R.C., Deng, Z.L. and He, T.C. (2010) 'Mesenchymal stem cells: Molecular characteristics and clinical applications', *World J Stem Cells*, 2(4), pp. 67-80.

Rea, S., Giles, N.L., Webb, S., Adcroft, K.F., Evill, L.M., Strickland, D.H., Wood, F.M. and Fear, M.W. (2009) 'Bone marrow-derived cells in the healing burn wound--more than just inflammation', *Burns*, 35(3), pp. 356-64.

Redd, M.J., Cooper, L., Wood, W., Stramer, B. and Martin, P. (2004) 'Wound healing and inflammation: embryos reveal the way to perfect repair', *Philos Trans R Soc Lond B Biol Sci*, 359(1445), pp. 777-84.

Rees, P.A., Greaves, N.S., Baguneid, M. and Bayat, A. (2015) 'Chemokines in Wound Healing and as Potential Therapeutic Targets for Reducing Cutaneous Scarring', *Advances in Wound Care*, 4(11), pp. 687-703.

Reif, A.E. and Allen, J.M.V. (1964) 'THE AKR THYMIC ANTIGEN AND ITS DISTRIBUTION IN LEUKEMIAS AND NERVOUS TISSUES', *The Journal of Experimental Medicine*, 120(3), pp. 413-433.

Reinke, J.M. and Sorg, H. (2012) 'Wound Repair and Regeneration', *European Surgical Research*, 49(1), pp. 35-43.

Renault, M.A., Roncalli, J., Tongers, J., Misener, S., Thorne, T., Jujo, K., Ito, A., Clarke, T., Fung, C., Millay, M., Kamide, C., Scarpelli, A., Klyachko, E. and Losordo, D.W. (2009) 'The Hedgehog transcription factor Gli3 modulates angiogenesis', *Circ Res*, 105(8), pp. 818-26.

Rennekampff, H.O., Hansbrough, J.F., Kiessig, V., Dore, C., Sticherling, M. and Schroder, J.M. (2000) 'Bioactive interleukin-8 is expressed in wounds and enhances wound healing', *J Surg Res*, 93(1), pp. 41-54.

Ridley, A.J., Schwartz, M.A., Burridge, K., Firtel, R.A., Ginsberg, M.H., Borisy, G., Parsons, J.T. and Horwitz, A.R. (2003) 'Cell Migration: Integrating Signals from Front to Back', *Science*, 302(5651), p. 1704.

Rittie, L., Sachs, D.L., Orringer, J.S., Voorhees, J.J. and Fisher, G.J. (2013) 'Eccrine sweat glands are major contributors to reepithelialization of human wounds', *Am J Pathol*, 182(1), pp. 163-71.

Ro, B.I. and Dawson, T.L. (2005) 'The role of sebaceous gland activity and scalp microfloral metabolism in the etiology of seborrheic dermatitis and dandruff', *J Investig Dermatol Symp Proc*, 10(3), pp. 194-7.

Roccaro, A.M., Sacco, A., Maiso, P., Azab, A.K., Tai, Y.T. and Reagan, M. (2013) 'BM mesenchymal stromal cell-derived exosomes facilitate multiple myeloma progression', *J Clin Invest*, 123.

Roggenkamp, D., Kopnick, S., Stab, F., Wenck, H., Schmelz, M. and Neufang, G. (2013) 'Epidermal nerve fibers modulate keratinocyte growth via neuropeptide signaling in an innervated skin model', *J Invest Dermatol*, 133(6), pp. 1620-8.

Rosen, E.M., Meromsky, L., Setter, E., Vinter, D.W. and Goldberg, I.D. (1990) 'Quantitation of cytokine-stimulated migration of endothelium and epithelium by a new assay using microcarrier beads', *Experimental Cell Research*, 186(1), pp. 22-31.

Rosenfeld, N., Aharonov, R., Meiri, E., Rosenwald, S., Spector, Y., Zepeniuk, M., Benjamin, H., Shabes, N., Tabak, S., Levy, A., Lebanony, D., Goren, Y., Silberschein, E., Targan, N., Ben-Ari, A., Gilad, S., Sion-Vardy, N., Tobar, A., Feinmesser, M., Kharenko, O., Nativ, O., Nass, D., Perelman, M., Yosepovich, A., Shalmon, B., Polak-Charcon, S., Fridman, E., Avniel, A., Bentwich, I., Bentwich, Z., Cohen, D., Chajut, A. and Barshack, I.

(2008) 'MicroRNAs accurately identify cancer tissue origin', *Nat Biotech*, 26(4), pp. 462-469.

Ross, R. (1994) 'The role of T lymphocytes in inflammation', *Proceedings of the National Academy of Sciences of the United States of America*, 91(8), p. 2879.

Rother, K., Kirschner, R., Sanger, K., Bohlig, L., Mossner, J. and Engeland, K. (2007) 'p53 downregulates expression of the G1/S cell cycle phosphatase Cdc25A', *Oncogene*, 26(13), pp. 1949-53.

Roy, S. and Sen, C.K. (2012) 'miRNA in Wound Inflammation and Angiogenesis', *Microcirculation*, 19(3), pp. 224-232.

Ruijtenberg, S. and van den Heuvel, S. (2016) 'Coordinating cell proliferation and differentiation: Antagonism between cell cycle regulators and cell type-specific gene expression', *Cell Cycle*, 15(2), pp. 196-212.

Ruszczak, Z. (2003) 'Effect of collagen matrices on dermal wound healing', *Advanced Drug Delivery Reviews*, 55(12), pp. 1595-1611.

Ruzehaji, N., Grose, R., Krumbiegel, D., Zola, H., Dasari, P., Wallace, H., Stacey, M., Fitridge, R. and Cowin, A.J. (2012) 'Cytoskeletal protein Flightless (Flii) is elevated in chronic and acute human wounds and wound fluid: neutralizing its activity in chronic but not acute wound fluid improves cellular proliferation', *Eur J Dermatol*, 22(6), pp. 740-50.

Ryan, M.O.C., Dinesh, S.R. and David, B. (2012) 'microRNA Regulation of Inflammatory Responses', *Annual Review of Immunology*, 30(1), pp. 295-312.

Sadler, T.W. (2010) 'The embryologic origin of ventral body wall defects', *Seminars in Pediatric Surgery*, 19(3), pp. 209-214.

Safari, M., Ghahari, L. and Zoroufchi, M.D. (2014) 'Effects of epidermal growth factor, platelet derived growth factor and growth hormone on cultured rat keratinocytes cells in vitro', *Pak J Biol Sci*, 17(7), pp. 931-6.

Safferling, K., Sütterlin, T., Westphal, K., Ernst, C., Breuhahn, K., James, M., Jäger, D., Halama, N. and Grabe, N. (2013) 'Wound healing revised: A novel reepithelialization mechanism revealed by in vitro and in silico models', *The Journal of Cell Biology*, 203(4), pp. 691-709.

Saint-Paul, L., Nguyen, C.-H., Buffière, A., de Barros, J.-P.P., Hammann, A., Landras-Guetta, C., Filomenko, R., Chrétien, M.-L., Johnson, P., Bastie, J.-N., Delva, L. and Quéré,

R. (2016) 'CD45 phosphatase is crucial for human and murine acute myeloid leukemia maintenance through its localization in lipid rafts', *Oncotarget*, 7(40), pp. 64785-64797.

Sánchez-Martín, L., Estecha, A., Samaniego, R., Sánchez-Ramón, S., Vega, M.Á. and Sánchez-Mateos, P. (2011) 'The chemokine CXCL12 regulates monocyte-macrophage differentiation and RUNX3 expression', *Blood*, 117(1), p. 88.

Sandell, L. and Sakai, D. (2008) 'Mammalian Cell Culture', in *Current Protocols Essential Laboratory Techniques*. John Wiley & Sons, Inc.

Santoro, M.M. and Gaudino, G. (2005) 'Cellular and molecular facets of keratinocyte reepithelization during wound healing', *Experimental Cell Research*, 304(1), pp. 274-286.

Sasaki, M., Abe, R., Fujita, Y., Ando, S., Inokuma, D. and Shimizu, H. (2008) 'Mesenchymal Stem Cells Are Recruited into Wounded Skin and Contribute to Wound Repair by Transdifferentiation into Multiple Skin Cell Type', *The Journal of Immunology*, 180(4), pp. 2581-2587.

Sato, K., Ozaki, K., Oh, I., Meguro, A., Hatanaka, K., Nagai, T., Muroi, K. and Ozawa, K. (2007) 'Nitric oxide plays a critical role in suppression of T-cell proliferation by mesenchymal stem cells', *Blood*, 109(1), pp. 228-34.

Schaffler, A. and Buchler, C. (2007) 'Concise review: adipose tissue-derived stromal cells--basic and clinical implications for novel cell-based therapies', *Stem Cells*, 25(4), pp. 818-27.

Scherer, W.F., Syverton, J.T. and Gey, G.O. (1953) 'STUDIES ON THE PROPAGATION IN VITRO OF POLIOMYELITIS VIRUSES', *The Journal of Experimental Medicine*, 97(5), pp. 695-710.

Schneider, M.R. (2012) 'MicroRNAs as novel players in skin development, homeostasis and disease', *British Journal of Dermatology*, 166(1), pp. 22-28.

Schnetkamp, T.G.K.P.P. (2016) 'Ca2+ Chemistry, Storage and Transport in Biologic Systems: An Overview', *Madame Curie Bioscience Database*.

Schnickmann, S., Camacho-Trullio, D., Bissinger, M., Eils, R., Angel, P., Schirmacher, P., Szabowski, A. and Breuhahn, K. (2009) 'AP-1-Controlled Hepatocyte Growth Factor Activation Promotes Keratinocyte Migration via CEACAM1 and Urokinase Plasminogen Activator/Urokinase Plasminogen Receptor', *Journal of Investigative Dermatology*, 129(5), pp. 1140-1148.

Schönfelder, U., Abel, M., Wiegand, C., Klemm, D., Elsner, P. and Hipler, U.-C. (2005) 'Influence of selected wound dressings on PMN elastase in chronic wound fluid and their antioxidative potential in vitro', *Biomaterials*, 26(33), pp. 6664-6673.

Schreier, T., Degen, E. and Baschong, W. (1993) *Fibroblast migration and proliferation during in vitro wound healing. A quantitative comparison between various growth factors and a low molecular weight blood dialysate used in the clinic to normalize impaired wound healing*.

Schultze-Mosgau, S., Wehrhan, F., Rodel, F., Amann, K., Radespiel-Troger, M. and Grabenbauer, G.G. (2003) 'Transforming growth factor-beta receptor-II up-regulation during wound healing in previously irradiated graft beds in vivo', *Wound Repair Regen*, 11(4), pp. 297-305.

Secunda, R., Vennila, R., Mohanashankar, A.M., Rajasundari, M., Jeswanth, S. and Surendran, R. (2015) 'Isolation, expansion and characterisation of mesenchymal stem cells from human bone marrow, adipose tissue, umbilical cord blood and matrix: a comparative study', *Cytotechnology*, 67(5), pp. 793-807.

Segre, J.A. (2006) 'Epidermal barrier formation and recovery in skin disorders', *Journal of Clinical Investigation*, 116(5), pp. 1150-1158.

Segrelles, C., Holguín, A., Hernández, P., Ariza, J.M., Paramio, J.M. and Lorz, C. (2011) 'Establishment of a murine epidermal cell line suitable for in vitro and in vivo skin modelling', *BMC Dermatology*, 11, pp. 9-9.

Semedo, P., Correa-Costa, M., Antonio Cenedeze, M., Maria Avancini Costa Malheiros, D., Antonia dos Reis, M., Shimizu, M.H., Seguro, A.C., Pacheco-Silva, A. and Saraiva Ĉamara, N.O. (2009) 'Mesenchymal Stem Cells Attenuate Renal Fibrosis Through Immune Modulation and Remodeling Properties in a Rat Remnant Kidney Model', *STEM CELLS*, 27(12), pp. 3063-3073.

Sen, C. and Roy, S. (2008) 'microRNA in Cutaneous Wound Healing', in Ying, S.-Y. (ed.) *Current Perspectives in microRNAs (miRNA)*. Springer Netherlands, pp. 349-366.

Sen, C.K. (2009) 'Wound Healing Essentials: Let There Be Oxygen', *Wound repair and regeneration : official publication of the Wound Healing Society [and] the European Tissue Repair Society*, 17(1), pp. 1-18.

Sen, C.K., Gordillo, G.M., Khanna, S. and Roy, S. (2009a) 'Micromanaging Vascular Biology: Tiny MicroRNAs Play Big Band', *Journal of vascular research*, 46(6), pp. 527-540.

Sen, C.K., Gordillo, G.M., Roy, S., Kirsner, R., Lambert, L., Hunt, T.K., Gottrup, F., Gurtner, G.C. and Longaker, M.T. (2009b) 'Human skin wounds: A major and snowballing threat to public health and the economy', *Wound Repair and Regeneration*, 17(6), pp. 763-771.

Senoo, M., Pinto, F., Crum, C.P. and McKeon, F. (2007) 'p63 Is Essential for the Proliferative Potential of Stem Cells in Stratified Epithelia', *Cell*, 129(3), pp. 523-536.

Shabbir, A., Cox, A., Rodriguez-Menocal, L., Salgado, M. and Badiavas, E.V. (2015) 'Mesenchymal Stem Cell Exosomes Induce Proliferation and Migration of Normal and Chronic Wound Fibroblasts, and Enhance Angiogenesis In Vitro', *Stem Cells and Development*, 24(14), pp. 1635-1647.

Sheng, G. (2015) 'The developmental basis of mesenchymal stem/stromal cells (MSCs)', *BMC Developmental Biology*, 15, p. 44.

Sheng, Z., Fu, X., Cai, S., Lei, Y., Sun, T., Bai, X. and Chen, M. (2009) 'Regeneration of functional sweat gland-like structures by transplanted differentiated bone marrow mesenchymal stem cells', *Wound Repair Regen*, 17(3), pp. 427-35.

Sherwood, E.R. and Toliver-Kinsky, T. (2004) 'Mechanisms of the inflammatory response', *Best Practice & Research Clinical Anaesthesiology*, 18(3), pp. 385-405.

Shi, R., Ge, L., Zhou, X., Ji, W.-J., Lu, R.-Y., Zhang, Y.-Y., Zeng, S., Liu, X., Zhao, J.-H., Zhang, W.-C., Jiang, T.-M. and Li, Y.-M. (2013) 'Decreased platelet miR-223 expression is associated with high on-clopidogrel platelet reactivity', *Thrombosis Research*, 131(6), pp. 508-513.

Shi, Y., Shu, B., Yang, R., Xu, Y., Xing, B., Liu, J., Chen, L., Qi, S., Liu, X., Wang, P., Tang, J. and Xie, J. (2015) 'Wnt and Notch signaling pathway involved in wound healing by targeting c-Myc and Hes1 separately', *Stem Cell Research & Therapy*, 6(1), p. 120.

Shilo, S., Roy, S., Khanna, S. and Sen, C.K. (2007) 'MicroRNA in cutaneous wound healing: a new paradigm', *DNA Cell Biol*, 26(4), pp. 227-37.

Shilo, S., Roy, S., Khanna, S. and Sen, C.K. (2008) 'Evidence for the Involvement of miRNA in Redox Regulated Angiogenic Response of Human Microvascular Endothelial Cells', *Arteriosclerosis, Thrombosis, and Vascular Biology*, 28(3), pp. 471-477.

Shimo, T., Nakanishi, T., Nishida, T., Asano, M., Kanyama, M., Kuboki, T., Tamatani, T., Tezuka, K., Takemura, M., Matsumura, T. and Takigawa, M. (1999) 'Connective tissue growth factor induces the proliferation, migration, and tube formation of vascular endothelial cells in vitro, and angiogenesis in vivo', *J Biochem*, 126(1), pp. 137-45.

Si, Y.L., Zhao, Y.L., Hao, H.J., Fu, X.B. and Han, W.D. (2011) 'MSCs: Biological characteristics, clinical applications and their outstanding concerns', *Ageing Res Rev*, 10(1), pp. 93-103.

Simmons, P.J. and Torok-Storb, B. (1991) 'Identification of stromal cell precursors in human bone marrow by a novel monoclonal antibody, STRO-1', *Blood*, 78(1), pp. 55-62.

Sims, G.P., Rowe, D.C., Rietdijk, S.T., Herbst, R. and Coyle, A.J. (2010) 'HMGB1 and RAGE in Inflammation and Cancer', *Annual Review of Immunology*, 28(1), pp. 367-388.

Sindrilaru, A., Peters, T., Schymeinsky, J., Oreshkova, T., Wang, H., Gompf, A., Mannella, F., Wlaschek, M., Sunderkötter, C., Rudolph, K.L., Walzog, B., Bustelo, X.R., Fischer, K.D. and Scharffetter-Kochanek, K. (2009) 'Wound healing defect of Vav3^{−/−} mice due to impaired β₂-integrin–dependent macrophage phagocytosis of apoptotic neutrophils', *Blood*, 113(21), pp. 5266-5276.

Smith, A.N., Willis, E., Chan, V.T., Muffley, L.A., Isik, F.F., Gibran, N.S. and Hocking, A.M. (2010) 'Mesenchymal stem cells induce dermal fibroblast responses to injury', *Exp Cell Res*, 316(1), pp. 48-54.

Song, Y.S., Lee, H.J., Park, I.H., Kim, W.K., Ku, J.H. and Kim, S.U. (2007) 'Potential differentiation of human mesenchymal stem cell transplanted in rat corpus cavernosum toward endothelial or smooth muscle cells', *Int J Impot Res*, 19(4), pp. 378-85.

Sonkoly, E., Ståhle, M. and Pivarcsi, A. (2008) 'MicroRNAs: novel regulators in skin inflammation', *Clinical and Experimental Dermatology*, 33(3), pp. 312-315.

Sotiropoulou, P.A., Perez, S.A., Gritzapis, A.D., Baxevanis, C.N. and Papamichail, M. (2006) 'Interactions between human mesenchymal stem cells and natural killer cells', *Stem Cells*, 24(1), pp. 74-85.

Spaeth, E., Klopp, A., Dembinski, J., Andreeff, M. and Marini, F. (2008) 'Inflammation and tumor microenvironments: defining the migratory itinerary of mesenchymal stem cells', *Gene Ther*, 15(10), pp. 730-8.

St. Hilaire, C., Carroll, S.H., Chen, H. and Ravid, K. (2009) 'Mechanisms of induction of adenosine receptor genes and its functional significance', *Journal of Cellular Physiology*, 218(1), pp. 35-44.

Stanley, P.E. (1986) 'Extraction of adenosine triphosphate from microbial and somatic cells', *Methods Enzymol*, 133, pp. 14-22.

Stone, R.C., Pastar, I., Ojeh, N., Chen, V., Liu, S., Garzon, K.I. and Tomic-Canic, M. (2016) 'Epithelial-Mesenchymal Transition in Tissue Repair and Fibrosis', *Cell and tissue research*, 365(3), pp. 495-506.

Stoppie, P., Borghgraef, P., De Wever, B., Geysen, J. and Borgers, M. (1993) 'The epidermal architecture of an in vitro reconstructed human skin equivalent (Advanced Tissue Sciences Skin2 Models ZK 1300/2000)', *Eur J Morphol*, 31(1-2), pp. 26-9.

Stott, N.S., Jiang, T.X. and Chuong, C.-M. (1999) 'Successive formative stages of precartilaginous mesenchymal condensations in vitro: Modulation of cell adhesion by Wnt-7A and BMP-2', *Journal of Cellular Physiology*, 180(3), pp. 314-324.

Straseski, J.A., Gibson, A.L., Thomas-Virnig, C.L. and Allen-Hoffmann, B.L. (2009) 'Oxygen deprivation inhibits basal keratinocyte proliferation in a model of human skin and induces regio-specific changes in the distribution of epidermal adherens junction proteins, aquaporin-3, and glycogen', *Wound repair and regeneration : official publication of the Wound Healing Society [and] the European Tissue Repair Society*, 17(4), pp. 606-616.

Strbo, N., Yin, N. and Stojadinovic, O. (2014) 'Innate and Adaptive Immune Responses in Wound Epithelialization', *Advances in Wound Care*, 3(7), pp. 492-501.

Streit, M., Velasco, P., Riccardi, L., Spencer, L., Brown, L.F., Janes, L., Lange-Asschenfeldt, B., Yano, K., Hawighorst, T., Iruela-Arispe, L. and Detmar, M. (2000) 'Thrombospondin-1 suppresses wound healing and granulation tissue formation in the skin of transgenic mice', *The EMBO Journal*, 19(13), pp. 3272-3282.

Strem, B.M., Hicok, K.C., Zhu, M., Wulur, I., Alfonso, Z., Schreiber, R.E., Fraser, J.K. and Hedrick, M.H. (2005) 'Multipotential differentiation of adipose tissue-derived stem cells', *Keio J Med*, 54(3), pp. 132-41.

Sun, C.Y., She, X.M., Qin, Y., Chu, Z.B., Chen, L., Ai, L.S., Zhang, L. and Hu, Y. (2013) 'miR-15a and miR-16 affect the angiogenesis of multiple myeloma by targeting VEGF', *Carcinogenesis*, 34(2), pp. 426-35.

Sun, X., Fu, X. and Sheng, Z. (2007) 'Cutaneous stem cells: something new and something borrowed', *Wound Repair and Regeneration*, 15(6), pp. 775-785.

Sundaram, G.M., Common, J.E.A., Gopal, F.E., Srikanta, S., Lakshman, K., Lunny, D.P., Lim, T.C., Tanavde, V., Lane, E.B. and Sampath, P. (2013) '/`See-saw/' expression of microRNA-198 and FSTL1 from a single transcript in wound healing', *Nature*, 495(7439), pp. 103-106.

Suzawa, K., Kobayashi, M., Sakai, Y., Hoshino, H., Watanabe, M., Harada, O., Ohtani, H., Fukuda, M. and Nakayama, J. (2007) 'Preferential induction of peripheral lymph node addressin on high endothelial venule-like vessels in the active phase of ulcerative colitis', *Am J Gastroenterol*, 102(7), pp. 1499-509.

Swirski, F.K., Nahrendorf, M., Etzrodt, M., Wildgruber, M., Cortez-Retamozo, V., Panizzi, P., Figueiredo, J.-L., Kohler, R.H., Chudnovskiy, A., Waterman, P., Aikawa, E., Mempel, T.R., Libby, P., Weissleder, R. and Pittet, M.J. (2009) 'Identification of Splenic Reservoir Monocytes and Their Deployment to Inflammatory Sites', *Science*, 325(5940), pp. 612-616.

Takeo, M., Lee, W., Rabbani, P., Sun, Q., Hu, H., Lim, Chae H., Manga, P. and Ito, M. (2016) 'EdnrB Governs Regenerative Response of Melanocyte Stem Cells by Crosstalk with Wnt Signaling', *Cell Reports*, 15(6), pp. 1291-1302.

Tamama, K. and Kerpedjieva, S.S. (2012) 'Acceleration of Wound Healing by Multiple Growth Factors and Cytokines Secreted from Multipotential Stromal Cells/Mesenchymal Stem Cells', *Adv Wound Care (New Rochelle)*, 1(4), pp. 177-182.

Tamama, K., Sen, C.K. and Wells, A. (2008) 'Differentiation of Bone Marrow Mesenchymal Stem Cells into the Smooth Muscle Lineage by Blocking ERK/MAPK Signaling Pathway', *Stem Cells and Development*, 17(5), pp. 897-908.

Taniguchi, K., Arima, K., Masuoka, M., Ohta, S., Shiraishi, H., Ontsuka, K., Suzuki, S., Inamitsu, M., Yamamoto, K.-i., Simmons, O., Toda, S., Conway, S.J., Hamasaki, Y. and Izuhara, K. (2014) 'Periostin Controls Keratinocyte Proliferation and Differentiation by

Interacting with the Paracrine IL-1α/IL-6 Loop', *Journal of Investigative Dermatology*, 134(5), pp. 1295-1304.

Tanner, K., Ferris, D.R., Lanzano, L., Mandefro, B., Mantulin, W.W., Gardiner, D.M., Rugg, E.L. and Gratton, E. (2009) 'Coherent Movement of Cell Layers during Wound Healing by Image Correlation Spectroscopy', *Biophysical Journal*, 97(7), pp. 2098-2106.

Tao, J., Liu, Z., Wang, Y., Wang, L., Yao, B., Li, Q., Wang, C., Tu, K. and Liu, Q. (2017) 'MiR-542-3p inhibits metastasis and epithelial-mesenchymal transition of hepatocellular carcinoma by targeting UBE3C', *Biomedicine & Pharmacotherapy*, 93, pp. 420-428.

Taub, R. (2004) 'Liver regeneration: from myth to mechanism', *Nat Rev Mol Cell Biol*, 5(10), pp. 836-847.

Tay, J.W., Romeo, G., Hughes, Q.W. and Baker, R.I. (2013) 'Micro-Ribonucleic Acid 494 regulation of protein S expression', *Journal of Thrombosis and Haemostasis*, 11(8), pp. 1547-1555.

Tedder, T.F. and Isaacs, C.M. (1989) 'Isolation of cDNAs encoding the CD19 antigen of human and mouse B lymphocytes. A new member of the immunoglobulin superfamily', *The Journal of Immunology*, 143(2), pp. 712-717.

Tenci, M., Rossi, S., Bonferoni, M.C., Sandri, G., Boselli, C., Di Lorenzo, A., Daglia, M., Icaro Cornaglia, A., Gioglio, L., Perotti, C., Caramella, C. and Ferrari, F. (2016) 'Particulate systems based on pectin/chitosan association for the delivery of manuka honey components and platelet lysate in chronic skin ulcers', *International Journal of Pharmaceutics*, 509(1), pp. 59-70.

Teruel-Montoya, R., Rosendaal, F.R. and Martínez, C. (2015) 'MicroRNAs in hemostasis', *Journal of Thrombosis and Haemostasis*, 13(2), pp. 170-181.

Teruel, R., Corral, J., Pérez-Andreu, V., Martínez-Martínez, I., Vicente, V. and Martínez, C. (2011a) 'Potential Role of miRNAs in Developmental Haemostasis', *PLoS ONE*, 6(3), p. e17648.

Teruel, R., PÉRez-SÁNchez, C., Corral, J., Herranz, M.T., PÉRez-Andreu, V., Saiz, E., GarcÍA-BarberÁ, N., MartÍNez-MartÍNez, I., RoldÁN, V., Vicente, V., LÓPez-Pedrera, C. and MartÍNez, C. (2011b) 'Identification of miRNAs as potential modulators of tissue factor expression in patients with systemic lupus erythematosus and antiphospholipid syndrome', *Journal of Thrombosis and Haemostasis*, 9(10), pp. 1985-1992.

Todaro, G.J., Lazar, G.K. and Green, H. (1965) 'The initiation of cell division in a contact-inhibited mammalian cell line', *Journal of Cellular and Comparative Physiology*, 66(3), pp. 325-333.

Toksoy, A., Müller, V., Gillitzer, R. and Goebeler, M. (2007) 'Biphasic expression of stromal cell-derived factor-1 during human wound healing', *British Journal of Dermatology*, 157(6), pp. 1148-1154.

Tokuda, Y., Crane, S., Yamaguchi, Y., Zhou, L. and Falanga, V. (2000) 'The levels and kinetics of oxygen tension detectable at the surface of human dermal fibroblast cultures', *Journal of Cellular Physiology*, 182(3), pp. 414-420.

Tomasz, M. (1995) 'Mitomycin C: small, fast and deadly (but very selective)', *Chemistry & Biology*, 2(9), pp. 575-579.

Tomic-Canic, M., Komine, M., Freedberg, I.M. and Blumenberg, M. (1998) 'Epidermal signal transduction and transcription factor activation in activated keratinocytes', *Journal of Dermatological Science*, 17(3), pp. 167-181.

Tondreau, T., Meuleman, N., Delforge, A., Dejeneffe, M., Leroy, R., Massy, M., Mortier, C., Bron, D. and Lagneaux, L. (2005) 'Mesenchymal stem cells derived from CD133-positive cells in mobilized peripheral blood and cord blood: proliferation, Oct4 expression, and plasticity', *Stem Cells*, 23(8), pp. 1105-12.

Tonnesen, M.G., Feng, X. and Clark, R.A.F. (2000) 'Angiogenesis in Wound Healing', *J Investig Dermatol Symp Proc*, 5(1), pp. 40-46.

Torsvik, A., Rosland, G.V., Svendsen, A., Molven, A., Immervoll, H., McCormack, E., Lonning, P.E., Primon, M., Sobala, E., Tonn, J.C., Goldbrunner, R., Schichor, C., Mysliwietz, J., Lah, T.T., Motaln, H., Knappskog, S. and Bjerkvig, R. (2010) 'Spontaneous malignant transformation of human mesenchymal stem cells reflects cross-contamination: putting the research field on track - letter', *Cancer Res*, 70(15), pp. 6393-6.

Trivanovic, D., Kocic, J., Mojsilovic, S., Krstic, A., Ilic, V., Djordjevic, I.O., Santibanez, J.F., Jovcic, G., Terzic, M. and Bugarski, D. (2013) 'Mesenchymal stem cells isolated from peripheral blood and umbilical cord Wharton's jelly', *Srp Arh Celok Lek*, 141(3-4), pp. 178-86.

Tsukahara, K., Takema, Y., Fujimura, T., Moriwaki, S. and Hattori, M. (2002) 'Quantitative two-dimensional analysis of facial wrinkles of Japanese women at various ages', *Int J Cosmet Sci*, 24(2), pp. 71-80.

Tu, C.-L., Chang, W. and Bikle, D.D. (2001) 'The Extracellular Calcium-sensing Receptor Is Required for Calcium-induced Differentiation in Human Keratinocytes', *Journal of Biological Chemistry*, 276(44), pp. 41079-41085.

Tuan, R.S., Boland, G. and Tuli, R. (2003) 'Adult mesenchymal stem cells and cell-based tissue engineering', *Arthritis Research & Therapy*, 5(1), pp. 32-45.

Turner, C.T., McInnes, S.J.P., Melville, E., Cowin, A.J. and Voelcker, N.H. (2017) 'Delivery of Flightless I Neutralizing Antibody from Porous Silicon Nanoparticles Improves Wound Healing in Diabetic Mice', *Advanced Healthcare Materials*, 6(2), pp. 1600707-n/a.

Ueno, K., Hirata, H., Shahryari, V., Chen, Y., Zaman, M.S., Singh, K., Tabatabai, Z.L., Hinoda, Y. and Dahiya, R. (2011) 'Tumour suppressor microRNA-584 directly targets oncogene Rock-1 and decreases invasion ability in human clear cell renal cell carcinoma', *British Journal of Cancer*, 104(2), pp. 308-315.

Usui, M.L., Mansbridge, J.N., Carter, W.G., Fujita, M. and Olerud, J.E. (2008a) 'Keratinocyte Migration, Proliferation, and Differentiation in Chronic Ulcers From Patients With Diabetes and Normal Wounds', *Journal of Histochemistry and Cytochemistry*, 56(7), pp. 687-696.

Usui, M.L., Mansbridge, J.N., Carter, W.G., Fujita, M. and Olerud, J.E. (2008b) 'Keratinocyte Migration, Proliferation, and Differentiation in Chronic Ulcers From Patients With Diabetes and Normal Wounds', *Journal of Histochemistry & Cytochemistry*, 56(7), pp. 687-696.

Usui, M.L., Underwood, R.A., Mansbridge, J.N., Muffley, L.A., Carter, W.G. and Olerud, J.E. (2005) 'Morphological evidence for the role of suprabasal keratinocytes in wound reepithelialization', *Wound Repair and Regeneration*, 13(5), pp. 468-479.

van de Kamp, J., Jahnen-Dechent, W., Rath, B., Knuechel, R. and Neuss, S. (2013) 'Hepatocyte growth factor-loaded biomaterials for mesenchymal stem cell recruitment', *Stem Cells Int*, 2013, p. 892065.

van Rooij, E., Sutherland, L.B., Thatcher, J.E., DiMaio, J.M., Naseem, R.H., Marshall, W.S., Hill, J.A. and Olson, E.N. (2008) 'Dysregulation of microRNAs after myocardial

infarction reveals a role of miR-29 in cardiac fibrosis', *Proceedings of the National Academy of Sciences of the United States of America*, 105(35), pp. 13027-13032.

Varkey, M., Ding, J. and Tredget, E.E. (2014) 'Superficial Dermal Fibroblasts Enhance Basement Membrane and Epidermal Barrier Formation in Tissue-Engineered Skin: Implications for Treatment of Skin Basement Membrane Disorders', *Tissue Engineering. Part A*, 20(3-4), pp. 540-552.

Varma, M.J., Breuls, R.G., Schouten, T.E., Jurgens, W.J., Bontkes, H.J., Schuurhuis, G.J., van Ham, S.M. and van Milligen, F.J. (2007) 'Phenotypical and functional characterization of freshly isolated adipose tissue-derived stem cells', *Stem Cells Dev*, 16(1), pp. 91-104.

Velnar, T., Bailey, T. and Smrkolj, V. (2009) 'The wound healing process: an overview of the cellular and molecular mechanisms', *J Int Med Res*, 37(5), pp. 1528-42.

Versteeg, H.H., Heemskerk, J.W.M., Levi, M. and Reitsma, P.H. (2013) 'New Fundamentals in Hemostasis', *Physiological Reviews*, 93(1), pp. 327-358.

Vishnubalaji, R., Manikandan, M., Al-Nbaheen, M., Kadalmani, B., Aldahmash, A. and Alajez, N. (2013) 'In vitro differentiation of human skin-derived multipotent stromal cells into putative endothelial-like cells', *BMC Developmental Biology*, 12(1), p. 7.

Visscher, M. and Narendran, V. (2014) 'Neonatal Infant Skin: Development, Structure and Function', *Newborn and Infant Nursing Reviews*, 14(4), pp. 135-141.

Viticchie, G., Lena, A.M., Cianfarani, F., Odorisio, T., Annicchiarico-Petruzzelli, M., Melino, G. and Candi, E. (2012) 'MicroRNA-203 contributes to skin re-epithelialization', *Cell Death Dis*, 3, p. e435.

Vitorino, P., Hammer, M., Kim, J. and Meyer, T. (2011) 'A Steering Model of Endothelial Sheet Migration Recapitulates Monolayer Integrity and Directed Collective Migration', *Molecular and Cellular Biology*, 31(2), pp. 342-350.

Vlahopoulos, S.A., Cen, O., Hengen, N., Agan, J., Moschovi, M., Critselis, E., Adamaki, M., Bacopoulou, F., Copland, J.A., Boldogh, I., Karin, M. and Chrousos, G.P. (2015) 'Dynamic aberrant NF-κB spurs tumorigenesis: A new model encompassing the microenvironment', *Cytokine & Growth Factor Reviews*, 26(4), pp. 389-403.

Vojtassak, J., Danisovic, L., Kubes, M., Bakos, D., Jarabek, L., Ulicna, M. and Blasko, M. (2006) 'Autologous biograft and mesenchymal stem cells in treatment of the diabetic foot', *Neuro Endocrinol Lett*, 27 Suppl 2, pp. 134-7.

Vörsmann, H., Groeber, F., Walles, H., Busch, S., Beissert, S., Walczak, H. and Kulms, D. (2013) 'Development of a human three-dimensional organotypic skin-melanoma spheroid model for in vitro drug testing', *Cell Death & Disease*, 4(7), p. e719.

Wagner, W., Wein, F., Seckinger, A., Frankhauser, M., Wirkner, U., Krause, U., Blake, J., Schwager, C., Eckstein, V., Ansorge, W. and Ho, A.D. (2005) 'Comparative characteristics of mesenchymal stem cells from human bone marrow, adipose tissue, and umbilical cord blood', *Exp Hematol*, 33(11), pp. 1402-16.

Walter, M.N., Wright, K.T., Fuller, H.R., MacNeil, S. and Johnson, W.E. (2010) 'Mesenchymal stem cell-conditioned medium accelerates skin wound healing: an in vitro study of fibroblast and keratinocyte scratch assays', *Exp Cell Res*, 316(7), pp. 1271-81.

Wang, G., Zhang, Q., Song, Y., Wang, X., Guo, Q., Zhang, J., Li, J., Han, Y., Miao, Z. and Li, F. (2015) 'PAK1 regulates RUFY3-mediated gastric cancer cell migration and invasion', *Cell Death & Disease*, 6(3), p. e1682.

Wang, L., Zhou, X., Zhou, T., Ma, D., Chen, S., Zhi, X., Yin, L., Shao, Z., Ou, Z. and Zhou, P. (2008) 'Ecto-5′-nucleotidase promotes invasion, migration and adhesion of human breast cancer cells', *Journal of Cancer Research and Clinical Oncology*, 134(3), pp. 365-372.

Wang, M.H., Zhou, Y.Q. and Chen, Y.Q. (2002) 'Macrophage-Stimulating Protein and RON Receptor Tyrosine Kinase: Potential Regulators of Macrophage Inflammatory Activities', *Scandinavian Journal of Immunology*, 56(6), pp. 545-553.

Wang, S., Qu, X. and Zhao, R. (2012a) 'Clinical applications of mesenchymal stem cells', *Journal of Hematology & Oncology*, 5(1), p. 19.

Wang, T., Feng, Y., Sun, H., Zhang, L., Hao, L., Shi, C., Wang, J., Li, R., Ran, X., Su, Y. and Zou, Z. (2012b) 'miR-21 Regulates Skin Wound Healing by Targeting Multiple Aspects of the Healing Process', *The American Journal of Pathology*, 181(6), pp. 1911-1920.

Wang, Z., Wang, Y., Farhangfar, F., Zimmer, M. and Zhang, Y. (2012c) 'Enhanced Keratinocyte Proliferation and Migration in Co-culture with Fibroblasts', *PLOS ONE*, 7(7), p. e40951.

Wawersik, M.J., Mazzalupo, S., Nguyen, D. and Coulombe, P.A. (2001) 'Increased Levels of Keratin 16 Alter Epithelialization Potential of Mouse Skin Keratinocytes In Vivo and Ex Vivo', *Molecular Biology of the Cell*, 12(11), pp. 3439-3450.

Wei, T., Orfanidis, K., Xu, N., Janson, P., Ståhle, M., Pivarcsi, A. and Sonkoly, E. (2010) 'The expression of microRNA-203 during human skin morphogenesis', *Experimental Dermatology*, 19(9), pp. 854-856.

Werner, S. (2011) 'A Novel Enhancer of the Wound Healing Process: The Fibroblast Growth Factor-Binding Protein', *The American Journal of Pathology*, 179(5), pp. 2144-2147.

Werner, S. and Grose, R. (2003) *Regulation of Wound Healing by Growth Factors and Cytokines*.

Wetzel, A., Chavakis, T., Preissner, K.T., Sticherling, M., Haustein, U.-F., Anderegg, U. and Saalbach, A. (2004) 'Human Thy-1 (CD90) on Activated Endothelial Cells Is a Counterreceptor for the Leukocyte Integrin Mac-1 (CD11b/CD18)', *The Journal of Immunology*, 172(6), pp. 3850-3859.

White, B. (2009) *National best practice and evidence based guidelines for wound management* (9781906218294). Health Service Executive Office of the Nursing Services: Health Service Executive (HSE) Services, H.S.E.O.o.t.N. [Online]. Available at: http://hdl.handle.net/10147/92646 (Accessed: 2010-02-22t16:38:10z).

Whitney, J.D. (2005) 'Overview: Acute and Chronic Wounds', *Nursing Clinics of North America*, 40(2), pp. 191-205.

Wickert, L.E., Pomerenke, S., Mitchell, I., Masters, K.S. and Kreeger, P.K. (2016) 'Hierarchy of cellular decisions in collective behavior: Implications for wound healing', 6, p. 20139.

Wienholds, E., Kloosterman, W.P., Miska, E., Alvarez-Saavedra, E., Berezikov, E., de Bruijn, E., Horvitz, H.R., Kauppinen, S. and Plasterk, R.H.A. (2005) 'MicroRNA Expression in Zebrafish Embryonic Development', *Science*, 309(5732), pp. 310-311.

Wozniak, M.A. and Keely, P.J. (2005) 'Use of three-dimensional collagen gels to study mechanotransduction in T47D breast epithelial cells', *Biol Proced Online*, 7, pp. 144-61.

Wright, H.L., Moots, R.J., Bucknall, R.C. and Edwards, S.W. (2010) 'Neutrophil function in inflammation and inflammatory diseases', *Rheumatology*, 49(9), pp. 1618-1631.

Wu, Y., Chen, L., Scott, P.G. and Tredget, E.E. (2007) 'Mesenchymal Stem Cells Enhance Wound Healing Through Differentiation and Angiogenesis', *Stem Cells*, 25(10), pp. 2648-2659.

Xie, Y., Rizzi, S.C., Dawson, R., Lynam, E., Richards, S., Leavesley, D.I. and Upton, Z. (2010) 'Development of a three-dimensional human skin equivalent wound model for investigating novel wound healing therapies', *Tissue Eng Part C Methods*, 16(5), pp. 1111-23.

Xu, S. and Chisholm, A.D. (2014) 'Methods for Skin Wounding and Assays for Wound Responses in C. elegans', *Journal of Visualized Experiments : JoVE*, (94), p. 51959.

Xu, W., Zhang, X., Qian, H., Zhu, W., Sun, X., Hu, J., Zhou, H. and Chen, Y. (2004) 'Mesenchymal stem cells from adult human bone marrow differentiate into a cardiomyocyte phenotype in vitro', *Exp Biol Med (Maywood)*, 229(7), pp. 623-31.

Yagi, H., Soto-Gutierrez, A., Parekkadan, B., Kitagawa, Y., Tompkins, R.G., Kobayashi, N. and Yarmush, M.L. (2010) 'Mesenchymal stem cells: Mechanisms of immunomodulation and homing', *Cell Transplant*, 19(6), pp. 667-79.

Yalvac, M.E., Yarat, A., Mercan, D., Rizvanov, A.A., Palotas, A. and Sahin, F. (2013) 'Characterization of the secretome of human tooth germ stem cells (hTGSCs) reveals neuro-protection by fine-tuning micro-environment', *Brain Behav Immun*, 32, pp. 122-30.

Yamaguchi, Y., Kubo, T., Murakami, T., Takahashi, M., Hakamata, Y., Kobayashi, E., Yoshida, S., Hosokawa, K., Yoshikawa, K. and Itami, S. (2005) 'Bone marrow cells differentiate into wound myofibroblasts and accelerate the healing of wounds with exposed bones when combined with an occlusive dressing', *Br J Dermatol*, 152(4), pp. 616-22.

Yan, T., Zhang, J., Tang, D., Zhang, X., Jiang, X., Zhao, L., Zhang, Q., Zhang, D. and Huang, Y. (2017) 'Hypoxia Regulates mTORC1-Mediated Keratinocyte Motility and Migration via the AMPK Pathway', *PLoS ONE*, 12(1), p. e0169155.

Yang, X., Wang, J., Guo, S.L., Fan, K.J., Li, J., Wang, Y.L., Teng, Y. and Yang, X. (2011) 'miR-21 promotes keratinocyte migration and re-epithelialization during wound healing', *Int J Biol Sci*, 7(5), pp. 685-90.

Yao, D., Ehrlich, M., Henis, Y.I. and Leof, E.B. (2002) 'Transforming Growth Factor-β Receptors Interact with AP2 by Direct Binding to β2 Subunit', *Molecular Biology of the Cell*, 13(11), pp. 4001-4012.

Yeum, C.E., Park, E.Y., Lee, S.B., Chun, H.J. and Chae, G.T. (2013) 'Quantification of MSCs involved in wound healing: use of SIS to transfer MSCs to wound site and quantification of MSCs involved in skin wound healing', *J Tissue Eng Regen Med*, 7(4), pp. 279-91.

Yew, T.L., Hung, Y.T., Li, H.Y., Chen, H.W., Chen, L.L., Tsai, K.S., Chiou, S.H., Chao, K.C., Huang, T.F., Chen, H.L. and Hung, S.C. (2011) 'Enhancement of wound healing by human multipotent stromal cell conditioned medium: the paracrine factors and p38 MAPK activation', *Cell Transplant*, 20(5), pp. 693-706.

Yi, R., Poy, M.N., Stoffel, M. and Fuchs, E. (2008) 'A skin microRNA promotes differentiation by repressing /`stemness/'', *Nature*, 452(7184), pp. 225-229.

Yoshida, S., Yamaguchi, Y., Itami, S., Yoshikawa, K., Tabata, Y., Matsumoto, K. and Nakamura, T. (2003) 'Neutralization of Hepatocyte Growth Factor Leads to Retarded Cutaneous Wound Healing Associated with Decreased Neovascularization and Granulation Tissue Formation', *Journal of Investigative Dermatology*, 120(2), pp. 335-343.

Yoshimura, H., Muneta, T., Nimura, A., Yokoyama, A., Koga, H. and Sekiya, I. (2007) 'Comparison of rat mesenchymal stem cells derived from bone marrow, synovium, periosteum, adipose tissue, and muscle', *Cell Tissue Res*, 327(3), pp. 449-62.

Young, H.E. (2004) 'Existence of reserve quiescent stem cells in adults, from amphibians to humans', *Curr Top Microbiol Immunol*, 280, pp. 71-109.

Yu Kan, L., Qiao Zhi, L., Rui, P., Hui Jiao, J., Guo Shun, Z., Xiao Li, Z., Rui Kang, T. and Ming, Z. (2009) 'The effect of extracellular calcium and inorganic phosphate on the growth and osteogenic differentiation of mesenchymal stem cells in vitro : implication for bone tissue engineering', *Biomedical Materials*, 4(2), p. 025004.

Zahorec, P., Koller, J., Danisovic, L. and Bohac, M. (2015) 'Mesenchymal stem cells for chronic wounds therapy', *Cell Tissue Bank*, 16(1), pp. 19-26.

Zanone, M.M., Favaro, E., Miceli, I., Grassi, G., Camussi, E., Caorsi, C., Amoroso, A., Giovarelli, M., Perin, P.C. and Camussi, G. (2010) 'Human mesenchymal stem cells modulate cellular immune response to islet antigen glutamic acid decarboxylase in type 1 diabetes', *J Clin Endocrinol Metab*, 95(8), pp. 3788-97.

Zhang, A., Wang, M.H., Dong, Z. and Yang, T. (2006) 'Prostaglandin E2 is a potent inhibitor of epithelial-to-mesenchymal transition: interaction with hepatocyte growth factor', *Am J Physiol Renal Physiol*, 291(6), pp. F1323-31.

Zhang, B., Wang, M., Gong, A., Zhang, X., Wu, X., Zhu, Y., Shi, H., Wu, L., Zhu, W., Qian, H. and Xu, W. (2015a) 'HucMSC-Exosome Mediated-Wnt4 Signaling Is Required for Cutaneous Wound Healing', *STEM CELLS*, 33(7), pp. 2158-2168.

Zhang, J., Guan, J., Niu, X., Hu, G., Guo, S., Li, Q., Xie, Z., Zhang, C. and Wang, Y. (2015b) 'Exosomes released from human induced pluripotent stem cells-derived MSCs facilitate cutaneous wound healing by promoting collagen synthesis and angiogenesis', *Journal of Translational Medicine*, 13(1), pp. 1-14.

Zhang, L., Stokes, N., Polak, L. and Fuchs, E. (2011a) 'Specific MicroRNAs Are Preferentially Expressed by Skin Stem Cells To Balance Self-Renewal and Early Lineage Commitment', *Cell stem cell*, 8(3), pp. 294-308.

Zhang, M., Sun, L., Wang, X., Chen, S., Jia, Q., Liu, N., Chen, Y., Kong, Y., Zhang, L. and Zhang, A.L. (2013) 'Activin B promotes BM-MSC-mediated cutaneous wound healing by regulating cell migration via the JNK-ERK signaling pathway', *Cell Transplant*.

Zhang, R., Leng, H., Huang, J., Du, Y., Wang, Y., Zang, W., Chen, X. and Zhao, G. (2014) 'miR-337 regulates the proliferation and invasion in pancreatic ductal adenocarcinoma by targeting HOXB7', *Diagnostic Pathology*, 9, p. 171.

Zhang, S., Cao, Z., Tian, H., Shen, G., Ma, Y., Xie, H., Liu, Y., Zhao, C., Deng, S., Yang, Y., Zheng, R., Li, W., Zhang, N., Liu, S., Wang, W., Dai, L., Shi, S., Cheng, L., Pan, Y., Feng, S., Zhao, X., Deng, H., Yang, S. and Wei, Y. (2011b) 'SKLB1002, a Novel Potent Inhibitor of VEGF Receptor 2 Signaling, Inhibits Angiogenesis and Tumor Growth In Vivo', *Clinical Cancer Research*, 17(13), p. 4439.

Zhang, S., Jin, J., Tian, X. and Wu, L. (2017) 'hsa-miR-29c-3p regulates biological function of colorectal cancer by targeting SPARC', *Oncotarget*, 8(61), pp. 104508-104524.

Zhang, X. and Mosser, D.M. (2008) 'Macrophage activation by endogenous danger signals', *The Journal of pathology*, 214(2), pp. 161-178.

Zhang, Z.-F., Zhang, J., Hui, Y.-N., Zheng, M.-H., Liu, X.-P., Kador, P.F., Wang, Y.-S., Yao, L.-B. and Zhou, J. (2011c) 'Up-Regulation of NDRG2 in Senescent Lens Epithelial Cells Contributes to Age-Related Cataract in Human', *PLoS ONE*, 6(10), p. e26102.

Zhao, S., Zhang, Y., Zheng, X., Tu, X., Li, H., Chen, J., Zang, Y. and Zhang, J. (2015) 'Loss of MicroRNA-101 Promotes Epithelial to Mesenchymal Transition in Hepatocytes', *J Cell Physiol*, 230(11), pp. 2706-17.

Zhou, S., Salisbury, J., Preedy, V.R. and Emery, P.W. (2013) 'Increased Collagen Synthesis Rate during Wound Healing in Muscle', *PLoS ONE*, 8(3), p. e58324.

Zhou, S., Zhang, Z., Zheng, P., Zhao, W. and Han, N. (2017) 'MicroRNA-1285-5p influences the proliferation and metastasis of non-small-cell lung carcinoma cells via downregulating CDH1 and Smad4', *Tumor Biology*, 39(6), p. 1010428317705513.

Zhu, N., Zhang, D., Chen, S., Liu, X., Lin, L., Huang, X., Guo, Z., Liu, J., Wang, Y., Yuan, W. and Qin, Y. (2011) 'Endothelial enriched microRNAs regulate angiotensin II-induced endothelial inflammation and migration', *Atherosclerosis*, 215(2), pp. 286-293.

Zhu, W., Xu, W., Jiang, R., Qian, H., Chen, M., Hu, J., Cao, W., Han, C. and Chen, Y. (2006) 'Mesenchymal stem cells derived from bone marrow favor tumor cell growth in vivo', *Exp Mol Pathol*, 80(3), pp. 267-74.

Zicha, D., Dunn, G.A. and Brown, A.F. (1991) 'A new direct-viewing chemotaxis chamber', *Journal of Cell Science*, 99(4), p. 769.

Zigmond, S.H. (1988) '[6] Orientation chamber in chemotaxis', *Methods in Enzymology*, 162, pp. 65-72.

Zuk, P.A., Zhu, M., Ashjian, P., De Ugarte, D.A., Huang, J.I., Mizuno, H., Alfonso, Z.C., Fraser, J.K., Benhaim, P. and Hedrick, M.H. (2002) 'Human adipose tissue is a source of multipotent stem cells', *Mol Biol Cell*, 13(12), pp. 4279-95.

Zuk, P.A., Zhu, M., Mizuno, H., Huang, J., Futrell, J.W., Katz, A.J., Benhaim, P., Lorenz, H.P. and Hedrick, M.H. (2001) 'Multilineage cells from human adipose tissue: implications for cell-based therapies', *Tissue Eng*, 7(2), pp. 211-28.

Zvaifler, N.J., Marinova-Mutafchieva, L., Adams, G., Edwards, C.J., Moss, J., Burger, J.A. and Maini, R.N. (2000) 'Mesenchymal precursor cells in the blood of normal individuals', *Arthritis Res*, 2(6), pp. 477-88.